UNIVERSIDAD COMPLUTENSE DE MADRID
FACULTAD DE GEOGRAFÍA E HISTORIA

TESIS DOCTORAL

El empleo de sistemas de información geográfica en la creación de herramientas para mejorar los planes de respuesta en emergencias nucleares y como ayuda en la toma de decisiones en áreas agrícolas

The use of geographic information systems in creating tools to improve nuclear emergency and response plans and as ab aid in the decision-making process for agricultural areas

MEMORIA PARA OPTAR AL GRADO DE DOCTOR

PRESENTADA POR

Blanca García Puerta

Directoras

María Pilar García Rodríguez
Cristina Trueba Alonso

Madrid

UNIVERSIDAD COMPLUTENSE DE MADRID

FACULTAD DE GEOGRAFÍA E HISTORIA

Departamento de Geografía

TESIS DOCTORAL

EL EMPLEO DE SISTEMAS DE INFORMACIÓN GEOGRÁFICA EN LA CREACIÓN DE HERRAMIENTAS PARA MEJORAR LOS PLANES DE RESPUESTA EN EMERGENCIAS NUCLEARES Y COMO AYUDA EN LA TOMA DE DECISIONES EN ÁREAS AGRÍCOLAS

THE USE OF GEOGRAPHIC INFORMATION SYSTEMS IN CREATING TOOLS TO IMPROVE NUCLEAR EMERGENCY AND RESPONSE PLANS AND AS AN AID IN THE DECISION-MAKING PROCESS FOR AGRICULTURAL AREAS

MEMORIA PARA OPTAR AL GRADO DE DOCTOR

PRESENTADA POR
Blanca García Puerta

DIRECTORES
María Pilar García Rodríguez
Cristina Trueba Alonso

Madrid, 2020

UNIVERSIDAD COMPLUTENSE DE MADRID

FACULTAD DE GEOGRAFÍA E HISTORIA

TESIS DOCTORAL

EL EMPLEO DE SISTEMAS DE INFORMACIÓN GEOGRÁFICA EN LA CREACIÓN DE HERRAMIENTAS PARA MEJORAR LOS PLANES DE RESPUESTA EN EMERGENCIAS NUCLEARES Y COMO AYUDA EN LA TOMA DE DECISIONES EN ÁREAS AGRÍCOLAS

THE USE OF GEOGRAFICAL INFORMATION SYSTEMS IN CREATING TOOLS TO IMPROVE NUCLEAR EMERGENCY AND RESPONSE PLANS AND AS AN AID IN THE DECISION-MAKING PROCESS FOR AGRICULTURAL AREAS

MEMORIA PARA OPTAR AL GRADO DE DOCTOR

PRESENTADA POR

Blanca García Puerta

DIRECTOR

María Pilar García Rodríguez
Cristina Trueba Alonso

A Ángel,

a mi madre y a mi padre

"*Nothing in life is to be feared, it is only to be understood.*
Now is the time to understand more, so that we may fear less"

Marie Curie (1867-1934)

ACKNOWLEDGEMENTS

I would like to thank all the people and organisms involved somehow in the development of this Doctoral Thesis, who have made it possible, technically or personally. My first words are dedicated to my Thesis directors:

To Cristina Trueba Alonso (Senior Scientist at Centro de Investigaciones Energéticas, Medioambientales y Tecnológicas – CIEMAT), thank you for willingly offering me your expertise, your valuable knowledge in Radiation Protection and for helping me to manage better the difficult situations that have arisen through these years. Also, my sincere thank you for all your efforts in helping me overcome the obstacles we faced, making it possible for me to attend all the courses, summits, meetings, etc., and because of that, I was able to achieve such priceless research stay abroad. Those experiences have allowed me to gain technical knowledge and to get acquainted with worldwide researchers in the Radiation Protection field.

To María Pilar García Rodríguez (Full Professor at Universidad Complutense de Madrid – UCM), thank you for sharing with me your wide knowledge in remote sensing and soils; for relying on my skills, for your unconditional support and for encouraging me from the beginning to the end. Also, for helping me with all the administrative issues I had in that process. In the 90's, when you were my Edaphology teacher, who would have thought that our paths were going to meet again!

Cristina, Pilar, thank you once again for offering your knowledge, for the effort and the time you have devoted to me, for your commitment, patience and, above all, for not letting me down.

This work would not have been possible without the contribution of Milagros Montero (Researcher at CIEMAT), who always tried to give another point of view of the subjects related to this Thesis which led me to find the best approach to reach the goals, bringing relevant improvements.

This Thesis has been developed in the Spanish research centre CIEMAT (Centro de Investigaciones Energéticas, Medioambientales y Tecnológicas), under the Ministry of Science and Innovation, more precisely in the Environmental Department. I would like to sincerely thank them for the opportunity that this organisation has given me as a researcher in training from 2016 to 2020, allowing me to benefit from its infrastructure and resources and for providing me with the financial support along the last four years. Special thanks to Yolanda Benito Moreno, Director of the Environmental Department for making every effort to enable me to undertake this work successfully.

I would also like to express my gratitude to the members of the Radiation Protection for the Public and the Environment Unit of CIEMAT, where I have been working over that time: Juan Carlos Mora, Danyl Pérez and Alla Dvorzhak, for offering me their help, to Alicia Escribano, for being my daily support since she arrived at the Unit and especially to the head of Unit, Almudena Real, for hosting me as just one more in the team. Thank you all for caring about me, for your support in difficult times and for being great colleagues.

Thank you also to Camino González Fernández (Professor at the Universidad Politécnica de Madrid – UPM), for her expert advice and for helping me to face some statistical approaches.

During this Thesis, I have been participating in the ANURE Project, carried out between the Joint Research Centre (JRC) and CIEMAT. This collaboration has been a magnificent experience which has given me new skills and knowledge about several technical aspects such as the JRodos system or Hysplit. Overall, the invaluable opportunity to share a common endeavour with a magnificent team. Thanks to Miguel Ángel Hernández Ceballos, Marco Sangiorgi and Luca De Felice from JRC, and, again, thanks to Cristina Trueba and Milagros Montero from CIEMAT.

It has been a great honour for me to have the opportunity in collaborating in the CONFIDENCE Project and all the activities organised in the frame of this European Project. I would like to address all my greetings to all the participants and, in particular to the Project Coordinator: Wolfgang Raskob (Coordinating Committee's member of the Center for Disaster Management and Risk Reduction Technology – CEDIM –Karlsruhe Institute of Technology, Germany), and again to Milagros Montero as leader of the Work Package 4,

for including me in this Project. Thanks to all the CONFIDENCE researches who showed interest in this work: Deborah Oughton (Director at CERAD, NFR CoE Environmental Radioactivity of the Norwegian University of Life Sciences), Catrinel Turcanu (Researcher at the Belgian Nuclear Research Centre SCK•CEN), Nick Beresford (Environmental Contaminants Group leader of the UK Centre for Ecology & Hydrology), Javier Guillén (Professor at Universidad de Extremadura) and, of course, Roser Sala (Researcher at the CISOT, Barcelona). Thank you all!

After many vicissitudes, as part of my research training, from February to April of 2019, I did a research stay in the Joint Research Centre (JRC) in Ispra, Italy. There I was hosted in the Disaster Risk Management Knowledge Centre (DRMKC), led by Montserrat Marín Ferrer who not only integrated me in the group but also offered me her help and enthusiasm. Thank you, Montse for your interest in this work and for giving visibility to what we have done in the ANURE Project. Thank you also to Francisco Ríos Díaz (Scientific/Technical Project Officer in the DRMKC) for being my mentor at the JRC. Also, thank you to Marc de Cort, the Radioactivity Environmental Monitoring group (REM) leader of the JRC, for letting me share his working space during my stay at the JRC – Ispra and for treating me as if I were part of his team. That stay was an amazing experience for me, there I found extraordinary people, such as Antofie Tiberiu Eugen and Stefano Luoni (both from the DRMKC) and Giorgia Cinelli (from REM). Thank you for their outstanding help and for offering me their time. This stay was partially supported by the ENEN+ project that has received funding from the Euratom research and training Work Programme 2016 – 2017 – 1 #755576.

To Inmaculada Sierra and Montserrat Moraleda, (Researchers at the CIEMAT), my lunchmates, together with Cristina and Milagros, thank you all for the enjoyable times during all these years, for waiting for me to finish my meal every day and, seriously, for worrying about me in tough times.

I cannot forget to mention the Doctorate Program Coordinators in Geography of the UCM: Julio Muñoz Jiménez, Javier Gutiérrez Puebla, David Palacios Estremera and Juan Carlos García Palomares. They have encouraged me and always have cleared my doubts regarding administrative issues.

I would never have even thought of starting a Thesis if I had not taken the Master TIG (Tecnologías de la Información Geográfica) of the UCM. That is the reason why I have to thank all the teachers of the Master during the course 2013-2014, where I have deepened my interest in GISs. My special thanks to Javier Gutiérrez Puebla, as Coordinator of the Master at that time, and to Nuria de Andrés, who was my Master thesis director. Thanks also to all my Master classmates, who built a fantastic group.

To all the team of the Medical Chemistry Lab of the UCM, led by María Luz López Rodríguez, thank you for always trusting and encouraging me in this Thesis.

To my parents, who instilled in me the values of hard work to reach my goals and to whom I have not devoted all the time I should. Thank you for believing in me. To my brother Carlos and to Maira, thanks and greetings from afar!

Last but not least, thank you to Ángel, my emotional support in any circumstances. Thank you for your wise and valuable tips, both technical and personal. I would not be able to complete this Doctoral Thesis without your help and support. Thank you for being my "amigo y compañero".

To all who were listed before and to those who I have not mentioned but at some point, were involved in one way or another and offered me their support, thanks a lot for being there!

INDEX

INDEX OF TABLES

INDEX OF FIGURES

LIST OF ABBREVIATIONS AND ACRONYMS

A	Activity
Ag	Silver
Am	Americium
BSS	Basic Safety Standard Directives
Ca	Calcium
$CaCO_3$	Calcium carbonate
CCFAC	Codex Committee on Food Additives and Contaminants
CEC	Cation-Exchange Capacity
CEDEX	Centro de Estudios y Experimentación de Obras Públicas
CIEMAT	Centro de Investigaciones Energéticas y Medioambientales
CHECIR	Chernobyl Centre for International Research Program
CLC	CORINE Land Cover (Co-ordination of Information on the Environment Program)
CRP	Coordinated Research Program (IAEA)
Cs	Caesium
Cs^+	Caesium cation
CSN	Nuclear Safety Council (In Spanish: Consejo de Seguridad Nuclear)
CSNI	Committee on the Safety of Nuclear Installations
C/N	C/N carbon/nitrogen
DB	Database
DEM	Digital Elevation Model
DEPOM	Deposition calculations for FDMT (JRODOS)
DRM	Disaster Risk Management
DRMKC	Disaster Risk Management Knowledge Centre
DSS	Decision Support System
EC	Electrical conductivity
ENRESA	Empresa Nacional de Residuos Radiactivos, S.A.
ENUSA	ENUSA INDUSTRIAS AVANZADAS, S.A., S.M.E.
EPR	Emergency Preparedness and Response
ESA	European Space Agency
ESDAC	European Soil Data Centre
EU	European Union
EURDEP	Radiological Data Exchange Platform
F	Infiltration Capacity of soils
FAO	Food and Agriculture Organisation of the United Nations
FDMT	Terrestrial Food Chain and Dose Module (JRODOS)
FES	Frayed Edges Site
F_v	Transfer factor from soil to plant.
G_Cs_Ing	Global Radiological Vulnerability Index for the ingestion pathway, regarding the radiocaesium
GFS	Global Forecast System

GIS	Geographic Information System
I_F	Infiltration Capacity index
I_H	Water Retention Capacity index
I_K	Potassium content index
I_{PQCs}	Physicochemical Caesium Retention Capacity index
I_Cs	Radiocaesium Reservoir Index
I_D	Deposition Index
I_K	Potassium Reservoir Index
I_P	Prioritisation Index
I_RV	Radiological Vulnerability Index
I_TF	Transfer Factor Index
IAEA	International Atomic Energy Agency
ICRP	International Commission on Radiological Protection
ICT	Information and Communication Technologies
IFIP	International Federation for Information Processing
ITL	Iberian Thermal Low
JRC	Joint Research Centre
K	Potassium
K^+	Potassium cation
KIT	Karlsruhe Institute of Technology
LAU	Local Administrative Units
LSMC	Local Scale transport and dispersion Modules Chain
MCA	Map of Crops and Utilisation of Spain (in Spanish: Mapa de Cultivos y Aprovechamientos
Mg	Magnesium
ML	Codex maximum level for a contaminant in a food or feed commodity (FAO-WHO, 1995)
Na	Sodium
NCDC	National Climatic Data Center of the United States
NCEP	National Centers for Environmental Prediction of the United States
NCGIA	National Center for Geographic Information and Analysis. University of California at Santa Barbara, USA.
NEA	Nuclear Energy Agency
NH^4	Ammonium
NOAA	National Oceanic and Atmosphere Administration of the United States
NORM	Naturally Occurring Radioactive Materials
NPP	Nuclear Power Plant
NRA	National Risk Assessment
NUT	Nomenclature des unités territoriales statistiques (in French)
OECD	Organisation for Economic Co-operation and Development
O.M.	Organic matter
P	Plutonium

PAMEN	Municipality action plans in nuclear emergency (in Spanish: “Planes de Actuación Municipal en Emergencia Nuclear”
PEI	Internal Emergency Plans (in Spanish: “Planes de Emergencia Interior”)
PEN	Internal Emergency Nuclear Plans (in Spanish: “Planes de Emergencia Nuclear Exterior”)
PENCA	Off-site nuclear emergency plan for the Almaraz (Cáceres) nuclear power plant. (In Spanish: “Plan de Emergencia Nuclear Exterior de la central nuclear de Almaraz – Cáceres”).
pH	Measure of the soil acidity
PLABEN	Nuclear Emergency Basic Plan (in Spanish: “Plan Básico de Emergencia Nuclear”)
PQ_{Cs}	Physicochemical Caesium Retention Capacity
PSA	Probabilistic safety assessment
PVRA	Surveillance network in the surroundings of nuclear power plants and nuclear fuel cycle facilities, (in Spanish: “Programa de Vigilancia Radiológica Ambiental”)
R	Water Retention Capacity
REE	Red Eléctrica Española
REM Group	Radiological Environmental Monitoring Group of the JRC
REM (Spanish)	Sampling stations network (in Spanish: “Red de Estaciones de Muestreo”)
REVIRA	National radiological surveillance network not associated with facilities (in Spanish: Red de Vigilancia Radiológica)
RIMPUFF	RIsø Mesoscale PUFF model
RIP	Radiocaesium Interception Potential
RP	Radiation Protection
S	Total exchangeable bases
SI	International System of Units (abbreviated from French Système international (d'unités))
SIOSE	Land Use Information System of Spain (in Spanish: Sistema de Información de Ocupación del Suelo en España)
SMU	Soil Mapping Unit
SOARCA	State-of-the-Art Reactor Consequence Analyses
STU	Soil Typological Unit
TARRAS	Transfer of Radionuclides in Soil – Plant Systems Project
TEMAS	Techniques and Management Strategies for Environmental Restoration and Their Ecological Consequences Project
TLS	Thermal Low System
U	Uranium
UCPM	Union Civil Protection Mechanism of the EU
UNDRR	United Nations Disaster office for Risk Reduction
UNESCO	United Nations Educational, Scientific and Cultural Organization
UNSCEAR	United nations Scientific Committee on the Effects of Atomic Radiation
V	Base saturation
WHO	World Health Organization
WNA	World Nuclear Association

ABSTRACT

TITLE: "THE USE OF GEOGRAPHIC INFORMATION SYSTEMS IN CREATING TOOLS TO IMPROVE NUCLEAR EMERGENCY AND RESPONSE PLANS AND AS AN AID IN THE DECISION-MAKING PROCESS FOR AGRICULTURAL AREAS"

Introduction

In the frame of the Radiation Protection (RP), Emergency Preparedness and Response (EPR) plans are fundamental in the effective management of an emergency situation related to the accidental release of radionuclides in a nuclear accident. These plans should be established in advance considering, as far as possible, the specificities of the potentially affected areas, which redounds in the success of the decision-making process for their application towards the recovery of the former living conditions.

In order to mitigate the harmful damages to the population derived from the entrance of the radionuclides released in the food chain through the ingestion exposure pathway, EPR plans must contemplate the implementation of recovery strategies in the agricultural areas, facing the long-term.

Therefore, in such a situation, it is essential to know the factors that condition that entrance. These are the type of radionuclides deposited (distinguishing those which pose a major radiological impact among the deposited material in the medium and long-term), the soil properties on which these are deposited, the radionuclides' behaviour in the soil, the mechanisms that condition the radionuclides' absorption by plants (closely related to the crop species), the own *transfer factors*, and the land use.

The Geographic Information Systems, used for processing, visualising and mapping the vast amount of input information and the outputs involved in analysing the soil-to-plant radionuclides' transfer, represent an undoubted and valuable aid to obtain useful tools for the EPR nuclear plans to manage a post-accident situation.

Objectives and Results

The general objective of this Thesis is to develop a methodology to assess the radiological vulnerability in mainland Spain affected by a ^{137}Cs contamination, regarding the ingestion pathway, and to provide aid tools to be used in the decision-making process of the EPR for the recovery of the areas of most concern, focusing on the mid and long-term.

The ultimate aim is to improve the planning of the recovery strategies to be applied in the agricultural areas affected by radioactive contamination in case a severe nuclear accident occurs, and once the exposure situation has moved from an *emergency* to an *existing exposure*.

These aid tools are maps representing the radiological vulnerability of peninsular Spain which categorise the territory according to the potential radiological impact for the population, through the food chain if a radioactive deposition occurs, from two different views. Both maps represent each corresponding five-category vulnerability index: *Minimum*, *Low*, *Medium*, *High,* and *Maximum* vulnerability.

The first one is the updated soils' radiological vulnerability map, which represents the potential of the Spanish soils to favour the transfer of radiocaesium to crops and, in turn, to the food chain. The result obtained is that the Spanish soils do not show any of the two extreme vulnerability indexes, and most of the territory is within the *Low vulnerability*.

The second radiological vulnerability map represents the susceptibility of the agricultural systems, potentially affected by a ^{137}Cs deposition, to transfer it to crops and therefore, to incorporate it to the food chain. Once the *representative crops* have been identified throughout the territory, the results show that the most widespread vulnerability category is the *Low* one, in which the main agricultural systems are comprised of olives for oil or wine grapes, grown in loamy soils. In this map, the agricultural areas of the most concern from the radiological vulnerability point of view (those with *Maximum* vulnerability) are highlighted.

That second map has been tested in a case study which assumes an accidental release from the Almaraz nuclear power plant. Thus, different deposition patterns have been obtained considering the average meteorological conditions along the year (annual and seasonal

conditions). Five prioritisation maps have been attained (with five prioritisation categories also) by combining the radiological vulnerability map of the agricultural systems and the deposition maps. These prioritisation maps represent the risk for the food chain regarding a ^{137}Cs deposition and could be used in the EPR to design the actions to be taken in the agricultural areas and the timing to be implemented, in order to limit the ^{137}Cs transfer to crops. For the case study designed, the prioritisation maps show summer as the worst scenario for an accident, related to the presence of the Thermal Low Systems, since it is when agricultural systems within *Maximum* and *High* prioritisation indexes are the largest, and therefore, the risk of the ^{137}Cs transfer to the food chain increases.

Conclusions

The Thesis fulfils the objectives proposed in providing useful tools to enhance the EPR plans after a nuclear emergency situation to aid in minimising the radiological consequences in agricultural systems in the long-term and, in turn, limiting the risk for the population through the ingestion pathway if an accident occurs. These tools could be used to identify and screen the areas that should need to be monitored, should facilitate the implementation of a structured response in applying countermeasures focused on recovering normal living conditions, and allow to identify and select the most concern areas for food contamination control campaigns over time, after an accident. Therefore, the response resources would be allocated more quickly and accurately, being focused on the specific selected areas, following the *optimisation* principle of the RP.

The methodology developed to perform the radiological vulnerability maps, the deposition pattern maps, and the prioritisation maps can be applied to obtain these maps in the rest of the Spanish and European sites, also considering more types of accidents.

RESUMEN

TÍTULO: "EL EMPLEO DE SISTEMAS DE INFORMACIÓN GEOGRÁFICA EN LA CREACIÓN DE HERRAMIENTAS PARA MEJORAR LOS PLANES DE RESPUESTA EN EMERGENCIAS NUCLEARES Y COMO AYUDA EN LA TOMA DE DECISIONES EN ÁREAS AGRÍCOLAS"

Introducción

En el marco de la Protección Radiológica (PR), los planes de Preparación y Respuesta en Emergencias (PRE) son fundamentales para la gestión eficaz de una emergencia relacionada con la liberación accidental de radionucleidos en un accidente nuclear. Estos planes deben estar definidos con antelación y deben considerar, en la medida de lo posible, las particularidades de las áreas potencialmente afectadas, lo cual redunda en el éxito del proceso de toma de decisiones para su aplicación en la recuperación de las anteriores condiciones de vida.

Para mitigar los daños a la población por la exposición a través de la ingestión, derivados de la entrada en la cadena alimentaria de los radionucleidos liberados, los planes de PRE deben contemplar la implementación de estrategias de recuperación en las áreas agrícolas, de cara al largo plazo.

Por lo tanto, en una situación como esa, es esencial conocer los factores que condicionan esa entrada; éstos son: el tipo de radionucleidos depositados (distinguiendo aquellos que suponen un mayor impacto radiológico en el medio y largo plazo), las propiedades de los suelos en los que se han depositado, el comportamiento de los radionucleidos en el suelo, los mecanismos que condicionan su absorción por las plantas (relacionados íntimamente con las especies de cultivos), los propios *factores de transferencia* y el uso del suelo.

Los Sistemas de Información Geográfica, utilizados en el procesamiento, visualización y para cartografiar la gran cantidad de información de entrada y de salida implicadas en el análisis de la transferencia de los radionucleidos del suelo a la planta, constituye una indudable y valiosa ayuda en la obtención de herramientas útiles para los planes de PRE nucleares, para gestionar una situación postaccidente.

Objetivos y Resultados

El objetivo general de esta Tesis es desarrollar una metodología para evaluar la vulnerabilidad radiológica en España relacionada con una contaminación por ^{137}Cs, por vía de la ingestión y proporcionar herramientas de ayuda para utilizarse en el proceso de toma de decisiones de la PRE para la recuperación de las zonas más problemáticas, de cara al medio y el largo plazo.

El objetivo final es mejorar la planificación de las estrategias de recuperación a aplicar en áreas agrícolas afectadas por una contaminación radioactiva en caso de que se produzca un accidente nuclear severo, una vez que la exposición ha pasado de *emergencia* a *exposición existente*.

Esas herramientas de ayuda son mapas que representan la vulnerabilidad radiológica de la España peninsular y categorizan el territorio según el potencial impacto radiológico para la población, a través de la cadena alimentaria, en caso de depósito. Esta se evalúa desde dos puntos de vista; sendos mapas representan la vulnerabilidad mediante su correspondiente índice, estableciendo cinco categorías: *Mínima*, *Baja*, *Media*, *Alta* y *Máxima*.

El primero de los mapas es el resultado de la actualización de los mapas de vulnerabilidad radiológica de los suelos, que representa la potencialidad de los suelos españoles para favorecer la transferencia del radiocesio a los cultivos y, de ahí, a la cadena alimentaria. El resultado obtenido es que los suelos españoles no presentan índices extremos de vulnerabilidad y que la mayor parte del territorio queda en la categoría de vulnerabilidad *Baja*.

El segundo mapa de vulnerabilidad radiológica representa la susceptibilidad de los sistemas agrícolas potencialmente afectados por un depósito de ^{137}Cs a transferir éste a los cultivos y, por tanto, a incorporarse a la cadena alimentaria. Una vez identificados los *cultivos representativos*, los resultados muestran que la categoría de vulnerabilidad más extensa es la *Baja*, siendo las aceitunas de almazara y las uvas para vinificación, cultivados en suelos francos los sistemas agrícolas principales en dicha categoría. En este mapa se destacan las áreas agrícolas más problemáticas desde el punto de vista radiológico (las de vulnerabilidad *Máxima*).

Este segundo mapa se ha probado en un caso estudio: una liberación accidental desde la central nuclear de Almaraz. Se han obtenido diferentes patrones de dispersión atendiendo a las condiciones meteorológicas medias a lo largo del año (anuales y estacionales). El resultado son cinco mapas de priorización (también con cinco categorías de priorización) que combinan la vulnerabilidad radiológica de los sistemas agrícolas y los mapas de depósito. Éstos representan el riesgo para la cadena alimentaria respecto a un depósito de ^{137}Cs y podrían utilizarse en la PRE para diseñar actuaciones en áreas agrícolas y para la organización temporal de su implementación, limitando así la transferencia del ^{137}Cs a los cultivos. Para el caso estudio, los mapas de priorización muestran que el verano, con la presencia de los Sistemas de Baja Térmica, es el peor escenario, pues es cuando la superficie de los sistemas agrícolas clasificados con *Máxima* y *Alta* priorización es mayor y el riesgo de transferencia del ^{137}Cs a la cadena alimentaria se incrementa.

Conclusiones

Esta Tesis cubre los objetivos propuestos para proporcionar herramientas útiles para mejorar los planes de PRE nuclear, para ayudar a minimizar las consecuencias radiológicas en los sistemas agrícolas en el largo plazo y para limitar el riesgo a la población respecto de la ingestión, en caso de accidente. Estas herramientas podrían usarse para identificar y seleccionar las zonas a ser monitoreadas, podrían facilitar la implementación de una respuesta estructurada en la aplicación de contramedidas enfocadas a recuperar las condiciones de vida normales, permiten identificar y seleccionar las zonas más problemáticas que requerirían campañas de control de alimentos a lo largo del tiempo, tras el accidente. Así, los recursos podrían localizarse de forma más rápida y precisa, focalizándose en las áreas seleccionadas, siguiendo el principio de *optimización* de la PR.

La metodología desarrollada para elaborar mapas de vulnerabilidad radiológica, de patrones de depósito y de priorización puede aplicarse para obtener estos mapas en el resto de los emplazamientos españoles y europeos, considerando más tipos de accidentes.

1 INTRODUCTION

This Thesis presents an integrated approach to evaluate the radiological vulnerability of soils and agricultural areas, focusing on peninsular Spain. It updates the existing analysis performed for the Spanish territory and develops a methodology to obtain useful tools to be used in the improvement of the nuclear Emergency Preparedness and Response (EPR) plans.

The radiological vulnerability of soils is defined as the potentiality to retain or to make bioavailable to crops the radionuclides deposited on them after an accidental release (Trueba, et al., 2000a). The capacity of the soil-plant system to transfer the radionuclides from soil to crops, giving rise to an exposure situation of the population through the food chain ingestion pathway, extends that definition to be applied to the radiological vulnerability of the soil-crop agricultural systems.

To know beforehand the behaviour of the radionuclides in the agricultural systems, a critical element in the definition of their radiological vulnerability, is of special importance in designing the emergency plans; that knowledge allows to classify the territory regarding the radiological risk potentially posed to the population.

The methodology here proposed provides maps as aid tools to be used in the decision-making process regarding the actions to be taken after an accidental radiological or nuclear release related to the agricultural sector. Thus, in the first stages of the emergency response (the urgent or early phase), taking into account the prevailing meteorological conditions in the release, these maps allow to identify those agricultural areas restricted for production, before the sampling campaigns are displayed.

As regards the mid and long-term, the recovery strategies for the contaminated areas should be planned oriented towards limiting the radiological exposure levels and return, to the extent possible, to the normal living conditions before the accident. The radiological vulnerability maps may allow to identify and locate the priority areas where to act, depending on the radiological risk, facilitating, jointly with the corresponding sampling campaigns to determine the contamination levels, the elaboration and implementation of the action plans for the recovery.

The emergency preparedness efforts have been mainly focused on the emergency exposure situation, during and immediately after an accident, implementing actions with the main aim of saving lives and protecting people as much as possible (IAEA, 2018b). However, once the radiation source is under control, the subsequent existing exposure situation requires actions to reduce the radiation levels in the affected areas, for the resumption of normal social and economic activity.

Taking into account the lessons learned from past emergency situations, recommendations and policies, such as the Council Directive 2013/59/EURATOM (EU, 2013), are now focussed in developing more integrated emergency plans including not only the *urgent* and *early phases* but also provision for the transition from an emergency exposure situation to an *existing exposure situation*.

Ultimately, the use of these type of maps is proposed as part of the radiological impact assessment. Precisely, this Thesis is framed in the contaminated agricultural areas after an emergency exposure situation, where the radioactive substances deposited on soils can affect the crops posing a risk for humans through the food chain exposure pathway. The categorisation of these areas according to their potential risk to the population will help to plan and implement the actions needed in the longer term, to recover the former normal living situation.

Several environmental data, georeferenced and non-georeferenced, are used to obtain the outputs in this Thesis. The treatment of different data formats and a great deal of information gathered on them requires the use of the appropriated software to manage all these data, held in different formats, and to perform the geoprocesses required in the vulnerability analysis of the agricultural areas and to define their prioritisation. That software is the Geographic Information Systems (GIS), which allows conducting spatial analysis counting on multiple information layers. The processing, visualising, and mapping capacities of GISs make them a useful software to be used in the management of extremely complex situations, as a nuclear accident, in which multiple parameters to be considered are involved. In fact, some of the utilities of that kind of software, such as the databases storage and the analysis of multiple layers, are included in the Decision Support Systems (DSS) developed in the field of the Radiation Protection (RP).

The use of a GIS software in this work enables to carry out the integrated approach designed to study the radiological vulnerability in Spain, which comprises the radiological vulnerability study of the soils and the agricultural areas and the definition of the prioritisation of the latter in a recovery intervention, taking into account the average meteorological conditions in the accidental nuclear event.

A description of the framework in which this Thesis is developed is shown in this section. A brief introduction about the radioactivity in history and its uses, what the ionising radiations are, and the importance of the Radiation Protection are depicted.

Besides, an insight of the EPR and the role of the DSSs in nuclear emergencies, as part of the background of this work are presented. A compilation of some of the applications of the GISs in this field is presented as well.

This section also includes the state-of-the-art regarding the factors considered along with this Thesis referred to the radionuclides' behaviour in soil and their transfer from soil-to-plant.

1.1 Framework in Radiation Protection

1.1.1 Ionising radiation

Since 1895, when Wilhelm Conrad Röntgen discovered X-Ray and since 1903, the date on which Antoine Henri Becquerel, Marie and Pierre Curie were awarded the Nobel Prize for Physics for discovering the radioactivity, ionisation radiation has been used along history for many purposes[1].

Radiation occurs when a source emits energy, then travels through a medium, such as air, until it is absorbed by matter. There are two types of radiation: non-ionizing, when radiation does not carry enough energy to ionize atoms or molecules and ionizing, when radiation has enough energy as to knock electrons out of their orbits around atoms, upsetting the electron/proton balance and giving the atom a positive charge. Electrically

[1] https://www.nrc.gov/about-nrc/radiation/around-us/uses-radiation.html

charged molecules and atoms are called ions. The main types of ionizing radiation are alpha radiation, beta radiation, gamma radiation, X-Ray and neutron radiation.

There are two type of sources of ionizing radiations, the natural background radiation, due to cosmic and terrestrial radiation and the artificial sources of radiation. The last ones come basically from the atmospheric testing, medical sources, industrial sources and the nuclear fuel cycle.

The atmospheric testing of atomic weapons released radioactive material, called fallout, into the air from the end of the Second World War until 1980 (González, 1998). As the fallout settled to the ground, it was incorporated into the environment. Much of the radionuclides released no longer exist due to their short half-lives but some other continue to decay to this day (Irlweck & Wallner, 2001; Bergan, 2002; Gabrieli, et al., 2011). Medical uses are widely known, from diagnosis (X-ray, computerized axial tomography, or computed tomography scanners) to nuclear medicine. Radioactive properties are also used in experimental research (such as dating or in X-ray application in art), in agriculture (to make plants more resistant) or in the industry (i.e. filling levels control, thickness measures control, determining of the humidity and density in soils, ionic smokes detectors, etc.) (CIEMAT, 2018).

Regarding the industrial uses, energy production in nuclear power plants (NPPs) is the most known; it is based on the nuclear fission (splitting the uranium atom) to produce the heat necessary to boil water, generate steam, and then to power a generator to produce electricity. During the fission process, ionising radiation is generated.

The measurement of the ionising radiation is based on the radioactive transformation, which is the mechanism through which the unstable nucleus emits the excess energy to decay in other stable or unstable element. That energy emission is measured in terms of *Activity* (A). *Activity* is defined as the expectation value of the number of spontaneous nuclear transformations from the given energy state in a time interval. According to the International System of Units (SI) the units of the activity is reciprocal second (s^{-1}), termed as becquerel (Bq) (IAEA, 2018a).

On the bases of the activity concept, the half-life is defined, for a radionuclide, as the time required for the activity to decrease, in a radioactive decay process, by half (IAEA, 2018a), and it is an inherent characteristic of each substance.

1.1.2 Exposure to ionising radiation

The human being is exposed to ionizing radiation from natural background and artificial sources. Although initially, as mentioned previously, the use of the latter was a great advance in the scientific development of society, the damage that its misuse could cause to health was soon revealed.

To assess the radiation exposures to humans, dosimetric quantities have been developed in order to describe dose-response relationships for radiation effects, providing the basis for risk estimation in RP. The *absorbed dose*, *D*, is the basic physical quantity, defined as "*the mean of the distribution of energy deposited in a tissue volume*" (ICRP, 2007). It is a measurable quantity (in $J \cdot kg^{-1}$, or its special name *Gray* (Gy)) and primary standards exist to determine its value.

However, to define the radiation risk derived from the radiation dose it is necessary to consider the differences among the biological effects depending on the radiation types and the sensitivity of organs and tissues to ionizing radiation (ICRP, 2007).

According to ICRP (2007), radiation exposure generates two kind of health damaging effects: *deterministic effects*, "*(harmful tissue reactions) due in large part to the killing/ malfunction of cells following high doses*" and *stochastic effects*, that is, "*cancer and heritable effects involving either cancer development in exposed individuals or heritable diseases in their offspring owing to mutation of reproductive (germ) cells*". In the former effects, a tissue loses its functionality due to "*serious malfunction or death*" of "*a critical population of cells*", which occurs over a threshold dose; above that, "*the severity of the injury increases with dose*." In the latter effects, the cellular repair mechanisms make them survive although genetic alterations may occur. PR conservatively considers that any dose poses a risk to health.

The definition of "*radiological protection quantities*" is based on the mean *absorbed dose* for each tissue or organ, since each tissue shows different sensitivity to different types of ionising radiation. Thus, the *equivalent dose, H,* is assessed by multiplying the *absorbed dose* by the corresponding quality factor for the type of radiation. Its units are $J \cdot kg^{-1}$, or its special name *Sievert* (Sv). For an individual, the *effective dose*, *E*, is assessed by summing the *equivalent doses* obtained for each tissue or organ, taking into account the radiation type (IAEA, 2019). The units for the *effective dose* are the same than for the *equivalent dose*. None of these two can be measured directly in body tissues but can be assessed from other operational quantities that can be measured (ICRP, 2007). There is a general acceptance of the utility of *effective dose* as the central quantity for dose assessments in radiological protection.

The radiological impact evaluations start from different radioactively contaminated scenarios and assess the different exposures pathways that will lead to doses to population. Among them, there are *external* and *internal radiation exposure* pathways. In the former, the radiation source is outside the body, while in the latter, the source is inside the body, being the intake by inhalation, ingestion or through the skin, the three internal exposure pathways. In the framework of this Thesis, the potential contamination of agricultural systems scenario after an accidental release focuses on the transfer of the radionuclides deposited on the soil to crops, and the ingestion of the edible parts by livestock or humans giving rise to internal exposure through the ingestion pathway[2].

1.1.3 Radiation Protection (RP)

The need to establish protection measures against the exposure to ionising radiation has given rise to the discipline called Radiation Protection (RP). It is a multidisciplinary activity, of a scientific and technical nature, which aims to protect people and the environment against the harmful effects that can result from exposure to ionising radiation.

Since 1928 there has been an independent international body, the International Commission on Radiological Protection (ICRP), which issues recommendations with scientific basis and advises on all aspects related to protection against ionising radiation.

[2] No external exposure pathway is considered.

These recommendations are the basis for the establishment of regulations and standards by international organizations and regional and national authorities.

The primary aim of the ICRP's Recommendations is "*to contribute to an appropriate level of protection for people and the environment against the detrimental effects of radiation exposure without unduly limiting the desirable human actions that may be associated with such exposure*" (ICRP, 2007).

The protection of the human health has as objectives: "*to manage and control exposures to ionising radiation so that deterministic effects are prevented, and the risks of stochastic effects are reduced to the extent reasonably achievable*". It is, therefore, "*the control (in the sense of restriction) of radiation doses that is important, no matter the source*". The protection measures can be focused on the source, the pathways or "*occasionally*" on the exposed population (ICRP, 2007).

The latest ICRP recommendations (ICRP, 2007) evolve from the previous process-based approach of practices[3] and interventions[4] to an approach based precisely on the characteristics of radiation exposure situations, which are the following:

- *Planned exposure situations*, which include situations that were previously categorised as *practices*.
- *Emergency exposure situations*, which are unexpected situations, i.e. during the operation of a *planned situation*, or from a malicious act, requiring urgent attention. In turn, it is divided into three phases "the *early phase*, the *intermediate phase* (which starts with the cessation of any release and regaining control of the source of releases), and the *late phase*" (ICRP, 2007); the two last phases are considered as *post-accident situation*. During all that sequence, the more information of the situation and the better knowledge of the affected area to manage the emergency by the decision-makes, the more effective protective measures will be.
- *Existing exposure situations*, which are exposure situations that exist when the control of radiation doses is decided to be implemented, such as those caused by

[3] *Practice*: "activity that causes an increase in exposure to radiation or in the risk of exposure to radiation". (ICRP, 2007).
[4] *Intervention* "*describe situations where actions are taken to reduce exposures*". (ICRP, 2007).

natural background radiation, "*including prolonged exposure situations after emergencies*" (ICRP, 2007).

Apart from the phases mentioned, the "*transition phase*" is defined in IAEA (2018b) referring to "*the process and the time period during which there is a progression to the point at which an emergency can be terminated*" (IAEA, 2018b).

To achieve the objectives established, Radiation Protection bases on three fundamental principles, gathered in ICRP (2007) which are the following:

- *The Principle of* Justification: Any decision that alters the radiation exposure situation should do more good than harm.
- *The Principle of Optimisation of Protection*: The likelihood of incurring exposure, the number of people exposed, and the magnitude of their individual doses should all be kept as low as reasonably achievable, taking into account economic and societal factors.
- *The Principle of Application of Dose Limits*: The total dose to any individual from regulated sources in planned exposure situations other than medical exposure of patients should not exceed the appropriate limits specified by the Commission. (p.14)

The two first principles apply in any exposure situation category while the third one applies only for planned exposure situations.

The *justification* and *optimisation principles* are fundamental in the application of the protection strategies and provide reference levels which aim to "*reduce all doses to levels that are as low as reasonably achievable*" (ICRP, 2007). However, as it was stated before, the *effective dose* used in the application of protection strategies is not a direct measurement; on the contrary, it has to be assessed.

For protecting to the "*members of the public*" ICRP (2007), establishes the use of the *justification principle:*

> where exposures can be controlled mainly by action to modify the pathways of exposure and not by acting directly on the source. […] Any decision taken to

> reduce doses, which always have some disadvantages, should be justified in the sense that they should do more good than harm. (p.90)

In that context, the ICRP (2017) defines the *decision-aiding techniques* for *optimisation* as a process that includes: defining the *exposure situation*, selecting the *"reference level"*[5], identifying the protective options and selecting the best one for the "*prevailing circumstances*" and implementing them.

The contribution to the optimisation of the *decision-aiding techniques* in the agricultural areas has inspired this Thesis.

1.1.3.1 International recommendations and regulatory frame

Radiation Protection regulations are continuously updated and enhanced. In that frame, the United Nations Scientific Committee on the Effects of Atomic Radiation (UNSCEAR)[6] is in charge of assessing and reporting "*levels and effects of exposure to ionizing radiation*". This information is used in radiation risk evaluations by governments and other organisms throughout the world, to establish protective measures.

Apart from the ICRP previously cited, different international organisations take into account the findings and results issued by UNSCEAR. The International Atomic Energy Agency (IAEA)[7], created in 1957 to promote safe, secure, and peaceful nuclear technologies, is one of those. IAEA focuses its efforts in developing and revising standard rules agreed by international consensus to serve as a reference for member states.

The guidelines and recommendations established by IAEA and ICRP, along with regional and sectorial recommendations from other international organisms, such as the World Health Organisation (WHO)[8] and Food and Agriculture Organisation of the United Nations (FAO)[9], as worldwide known organisation, or, in the particular nuclear field, the Nuclear

[5] Reference level: "*In emergency or existing controllable exposure situations, the reference levels represent the level of dose or risk, above which it is judged to be inappropriate to plan to allow exposures to occur* […], *and for which therefore protective actions should be planned and optimised*." (ICRP, 2007).
[6] https://www.unscear.org/
[7] https://www.iaea.org/
[8] https://www.who.int/
[9] http://www.fao.org/home/es/

Energy Agency (NEA)[10], are taken into consideration in the radiation protection regulation of the regulatory frame of each national legislation.

In case of European countries, EURATOM Directives reflect these recommendations and guides on its own frame to, in turn, be transposed to the member states' laws. European Atomic Energy Community (EAEC or Euratom) was established in 1957 as a treaty to promote research and disseminate technical information for setting uniform safety standards, to facilitate research and to ensure proper civil and military nuclear materials usage (EU, 2007). Since 1959, Basic Safety Standard Directives (BSS) have being adopted, focusing on ensuring "*the highest possible protection of workers and members of the public against the dangers arising from exposure to ionising radiation*" (EU, 2018). The Directives are regularly amended in accordance to the latest scientific findings and recommendations of the rest of the international organisations, being the EU (2013) the last update, which is entitled: "*laying down basic safety standards for protection against the dangers arising from exposure to ionising radiation*". It entered into force in February of 2014 and member states should have transposed by February the 6th of 2018.

The EU (2013) gathers considerations from past experiences and, for instance, in *section 5*: *Emergency exposure situations*, *Article 97*: *Emergency management system*, it is said:

> Member States shall ensure that account is taken of the fact that emergencies may occur on their territory and that they may be affected by emergencies occurring outside their territory. Member States shall establish an emergency management system and adequate administrative provisions to maintain such a system. (p. 36)

According to this Directive, the assessment of potential exposure situation and plans for the recovery and remediation to be addressed in the transition from an *emergency exposure situation* to an *existing exposure situation*, are two elements which shall be included in the emergency management system and in the Emergency Response Plans of the EU Members. This Thesis intends to perform that assessment.

[10] https://www.oecd-nea.org/

This Directive also contains the opinion of the European Economic and Social Committee and, for instance, in point 41 says:

> With regard to the management of emergency exposure situations, the current approach based on intervention levels should be replaced by a more comprehensive system comprising an assessment of potential emergency exposure situations, an overall emergency management system, emergency response plans, and pre-planned strategies for the management of each postulated event. (p. 5).

These considerations, among others included in the EU (2013), make it necessary to acquire as much as accurate knowledge as possible of the territory potentially affected and of the environmental conditions which govern the processes that could lead to harmful effects to the population related to the ionising radiation. That way, in a radiological or nuclear accidental situation, the authorities and the decision-makers may reach the decisions on the bases of specific necessities of each affected area, which results in an increase of the effectiveness of the implemented measures.

A specific Council Regulation regarding agricultural products, (EU, 2016), defines *maximum permitted levels* of radioactive contamination of food and feed following a nuclear accident or any other case of radiological emergency. This regulation lays down the contamination levels considering the sum of different radionuclides, for different foodstuffs (for infants and adults, following the criteria established CCFAC (2011)[11]) and feedstuffs.

The results obtained in this Thesis may be considered as a first step in the path of what needs to be included in an emergency management system, for instance, the assessment of potential *emergency exposure situations* and the *transition* from an *emergency exposure situation* to an *existing exposure situation*, including recovery and remediation; these may also be considered to help in the design of food contamination control campaigns.

[11] Originally defined in FAO-WHO (1995).

1.1.3.2 Radiation Protection in Spain

Currently there are 7 nuclear power reactors in Spain, located in 5 sites, among the 442 existing in the whole world (IAEA, 2020). The Spanish NPP to generate electricity are: Trillo, Almaraz (with 2 reactors), Cofrentes, Ascó (with 2 reactors) and Vandellós. Besides, there are 2 more NPP which are in permanent shutdown: José Cabrera-1 and Santa María de Garoña (Foro Nuclear, 2020). In 2019, the 7 reactors in operation generated 21,43% out of the total electric energy produced in the country (Foro Nuclear, 2020).

The Nuclear Safety Council (In Spanish Consejo de Seguridad Nuclear, CSN) is the "*sole safety and radiation protection authority in Spain*" [12] that is accountable directly to the Congress of Deputies and the Senate (CSN, 2020a). Among its responsibilities, defined in Ley 15-1980 and RD 1440/2010, it proposes radiation protection regulation to the government and adjusts national laws to comply with international legislation. Besides, CSN is in charge of monitoring the radiological levels for surveillance purposes[13].

The nuclear emergencies risk management is included in the National Security Strategy (Ley 17/2015)[14] which gathers the Civil Protection policies and services to be developed and implemented by the state in the emergency cycle processes (see Figure 1). The body that oversees citizens and goods protection in emergencies and catastrophes in Spain is the Directorate General for Civil Defence, being the one which takes the actions to be applied, following Emergency Preparedness and Response (EPR) plans, also for nuclear or radiological EPR plans.

[12] https://www.csn.es/en/home

[13] There are two surveillance networks in Spain. The first one, in the surroundings of NPPs and nuclear fuel cycle facilities, named PVRA (from the Spanish: "Programa de Vigilancia Radiológica Ambiental") and the second one, the national radiological surveillance network (not associated with facilities), named REVIRA (from the Spanish: "Red de Vigilancia Radiológica"). The last one includes the sampling stations network, named REM (from the Spanish: "Red de estaciones de muestreo") which collects both, the results from a wide variety of samples (water, air, food, deposition, sediments, etc.), and the automatic stations network, named REA (in Spanish: "Red de Estaciones Automáticas"), which reflects the daily and monthly gamma average dose rate (in µSv/h). REM and PVRA values are compiled in a web application for the consultation of the monitoring results (https://www.csn.es/kprgisweb2/index.html?lang=en) (CSN, 2020b). On the basis of EU (1987) and the EU (2000), the EU Members voluntarily share the results from their REA networks through the EUropean Radiological Data Exchange Platform (EURDEP) which publishes them in its web-mapping service for public consultation (https://remap.jrc.ec.europa.eu/Simple.aspx . Website hosted by JRC).

[14] The National Security Strategy (Ley 17/2015) consolidates the National Civil Protection System for the national emergency and disaster management (MPR, 2019) within the Sendai Framework.

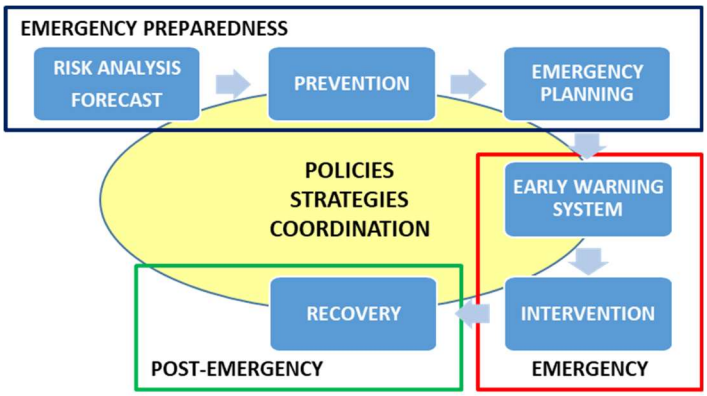

Figure 1. Emergency cycle process. Modified from MPR (2019).

The Nuclear Emergency Basic Plan (in Spanish: "Plan Básico de Emergencia Nuclear") (PLABEN, 2004) is the legal framework that regulates the preparedness and response system for nuclear accidents in the "*emergency phase*" (equivalent to the *early phase* established in ICRP (2007)). Nevertheless, in Annexe II it includes "*long-lasting measures*" focused on the "*recovery phase*" (which includes the intermediate and the late phases defined in ICRP (2007)) since they can be planned or even applied from the early phase. PLABEN comprises two plan categories: Interior Emergency Plans (in Spanish: "*Planes de Emergencia Interior*" – PEI – regulated in RD 1836/1999) and External Emergency Plans (in Spanish: "*Planes de Emergencia Nuclear Exterior*" – PEN[15]). The former depends on each NPP, while the latter falls in the competence of the central government of the country. According to the PLABEN, the actions to be taken in a nuclear emergency are implemented at municipality level, thus, the PEN plans involve, in turn, the Municipality Action Plans in Nuclear Emergency (in Spanish: "*Planes de Actuación Municipal en Emergencia Nuclear*" – PAMEN). Bearing that in mind, the assessments carried out in this Thesis reach that administrative level: the municipality. The hierarchical intervention plans to be implemented in a nuclear emergency in Spain, according to the PEI and the PEN, and the relations among them are shown in Figure 2, in which are identified the very first agent(s) involved.

[15] The Spanish off-site nuclear emergency plans for the NPPs in operational status are PENGUA (for Trillo NPP – Guadalajara), PENCA (for Almaraz NPP – Cáceres), PENTA (for Ascó and Vandellós NPPs – Tarragona), PENVA (for Cofrentes NPP – Valencia) and PENCRA (Central Level Response and Support Emergency Plan, as the support organisation for the organisations of the above plans.

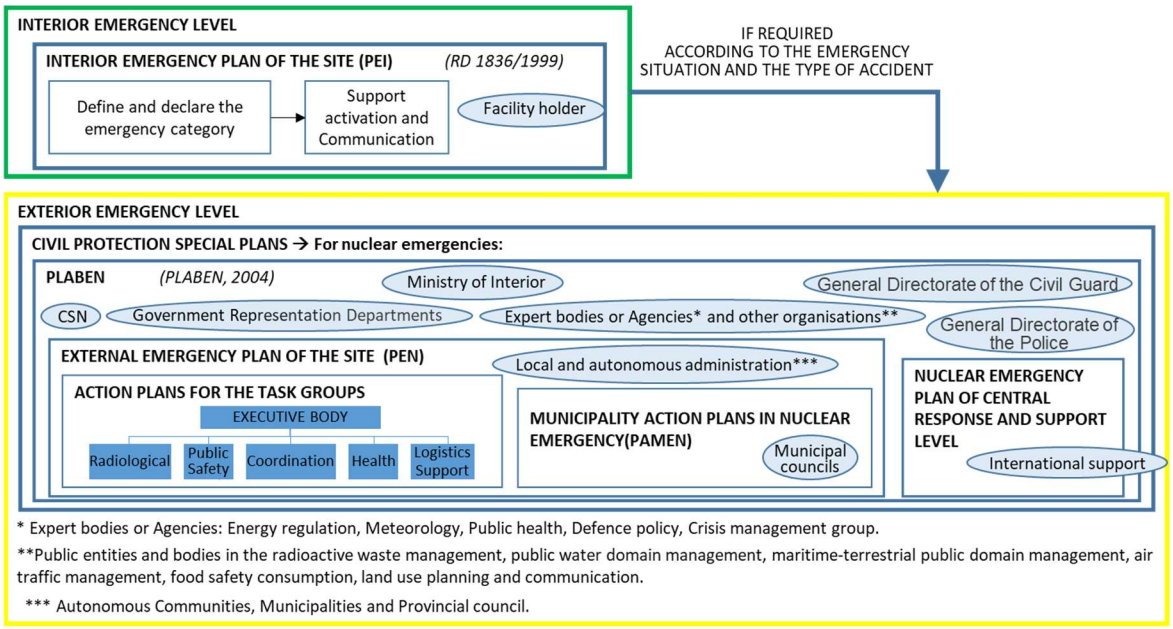

Figure 2. Scheme of the emergency levels and the corresponding plans developed in RD 1836/1999 and PLABEN (Nuclear Emergency Basic Plan - in Spanish: "Plan Básico de Emergencia Nuclear" (PLABEN, 2004)) to be developed and implemented in a nuclear emergency.

The plans shown in Figure 2 are coordinated according to the type of accident, depending on its severity and the amount of radioactive material that could be released to the exterior, and to the urgent protective measures required in each stage, which define the emergency situation (PLABEN, 2004).

1.2 Emergency Preparedness and Response (EPR)

Nowadays, EPR plans for NPPs are constantly being tested, updated and improved all around the world, because of the international organisms' initiatives, proposals and evaluations, materialised in the national efforts to implement the necessary technical, operational and regulatory changes. According to OECD-NEA (2018), in which lessons learnt to be applied in the nuclear field from non-nuclear events are evaluated, EPR is "*well-defined, well-practised*" in the 36 OECD countries[16] and "*no gaps are found*".

One example of those ongoing initiatives is the Strategic plan of the NEA countries 2017-2020. This plan intends "*to meet the evolving needs of member countries in the application and exploration of nuclear science and technology*". Regarding the radiological protection of public health and the environment, the aim of the plan is "*to assist member countries in*

[16] https://www.oecd.org/about/members-and-partners/

the regulation, implementation and further development of the system of radiological protection by identifying and effectively addressing conceptual, scientific, policy, regulatory, operational and societal issues".

Likewise, apart from the publication of the Safety standards on emergency preparedness and response (among other radiological and nuclear topics), IAEA regularly launches calls to its Coordinated Research Programs (CRP) for institutions to propose projects for research and development within different topic areas. The last CRP regarding EPR is the "*Effective Use of Dose Projection Tools in the Preparedness and Response to Nuclear and Radiological Emergencies*" program[17]. It has just started in 2020, will last until 2023 and involves a Spanish team led by TECNATOM[18] which includes CSN and CIEMAT (in Spanish Centro de Investigaciones Energéticas y Medioambientales), who are developing the project named "*Warnings, Best Practices and Recommendations on use of Software Tools for Making Decisions related to EPR*".

When a disaster occurs, regardless of the sort of calamity (natural, industrial, biological, Natech disasters[19], etc.) the strengthen of the EPR plans are put to the test on real-time, at that point, the reaction capabilities and the resources to mitigate the consequences may be insufficient, depending on the emergency scale. This fact appears to be more obvious if a wide territory is impacted, especially if it implies transboundary consequences.

A recent example is the coronavirus COVID-19 pandemic. That crisis put in evidence how important it is to define in advance the actions to be implemented to reduce the impacts in terms of public health and in socio-economic aspects, which may lead in loss of human lives. In March 12th of 2020, one day after the WHO had declared coronavirus COVID-19 a pandemic (WHO, 2020), the United Nations Disaster office for Risk Reduction (UNDRR) urged national management agencies of member states to include health emergencies as "*a top priority*" in developing their EPR capacities (UNDRR, 2020). At that point, the reaction capacity of the states was not enough to address the situation, and lots of human and

[17]https://www.iaea.org/newscenter/news/new-crp-effective-use-of-dose-projection-tools-in-the-preparedness-and-response-to-nuclear-and-radiological-emergencies-crp-j15002
[18] https://www.tecnatom.es/
[19] Natech disasters: "Technological accidents triggered by a natural hazard or disaster which result in consequences involving hazardous substances (e.g. fire, explosion, toxic release)" https://enatech.jrc.ec.europa.eu/

economic losses were being produced all around the world, resulting in a global health and economic crisis.

In this regard, there are several similarities among all fields (nuclear and non-nuclear) in EPR, lessons learnt, and good practices (OECD-NEA, 2018) should be considered in order to strengthen the action capabilities of the response systems to minimise any disaster damaging consequences. In that sense, OECD issues a major recommendation: to "*establish and promote a comprehensive, all-hazards and transboundary approach to country risk governance to serve as the foundation for enhancing national resilience and responsiveness*". In that context, European initiatives are being developed in order to have tools, repositories, databases and hubs available for all European Union (EU) Members, being the Risk Data Hub[20], developed by the Disaster Risk Management Knowledge Centre (DRMKC) under the JRC, the main European platform "*to improve the access and share EU-wide curated risk data for fostering Disaster Risk Management (DRM)*".

Regarding nuclear disasters, the two nuclear accidents with the largest consequences, from the radiological point of view, were the Chernobyl accident in Ukraine, in April 1986 and the Fukushima Daiichi accident in Japan, in March 2011. The first one, was a power-surge accident, caused by a "*failure of control of a fission chain reaction, which instantaneously destroyed the reactor and building*"; while the second one, Fukushima, "*was a loss-of-coolant accident in which the reactor cores of three units were melted by decay heat after losing the electricity supply*" (Imanaka, et al., 2015). Both accidents, together with the global fall out related to the atmospheric nuclear weapon testing, are the main sources of global environmental radioactive contamination, mainly ^{137}Cs. This radionuclide is considered the largest contributor to the external and internal exposure levels at contaminated areas from both accidents and from testing of nuclear weapons (Gupta & Walther, 2016).

By the time the Chernobyl nuclear accident occurred, the EPR plans were not so widely developed as they are nowadays. At that time, protocols for the early phase in an emergency situation were already designed; these were orientated to apply measures

[20] https://drmkc.jrc.ec.europa.eu/risk-data-hub

intended for people who lived close to the site, such as sheltering, evacuation, relocation, or iodine tablets intake. After that episode, national and international programs were developed in order to fill the gaps regarding EPR, "*especially in the areas of international communication and information exchange, and in harmonisation of response*" (NEA & OECD, 2002). The lessons learnt from that event encompassed several areas such as "*reactor safety and severe accident management, intervention criteria, emergency procedures, communication, medical treatment of irradiated persons, monitoring methods, radioecological processes, land and agricultural management, public information, etc.*" (NEA & OECD, 2002). These were the first steps for developing the tools to be applied in the planning phase, and in designing and implementing the actions to be taken in the recovery phase also.

Fukushima Daiichi nuclear disaster also revealed that there were aspects of the EPR to be enhanced such as those aspects related to communication, harmonisation and coordination issues regarding intervention levels for foodstuff or the importance of taking into account non-radiological aspects (social and economic) in such accidental scenarios. Regarding risk and safety assessments, the so-called "*stress tests*", started to be developed in European NPPs after that accident happened (EC, 2012). Besides, it was demonstrated the need for supporting tools to deal with all the issues caused by such magnitude situations, in that particular case oriented to aquatic environment simulations (KIT, 2017b).

Different international authorities developed several programs and initiatives as a response to that event, to improve the EPR for the future. One example of these protocols is the report: "Status of practice for Level 3 probabilistic assessments" (PSA) (NEA, 2018), in which is defined the procedure to assess off-site public risks for different scenarios derived from an accident in a nuclear site. That report, elaborated by the Committee on the Safety of Nuclear Installations (CSNI), is based on three progressive analysis levels. The last one, Level 3 PSA, includes the whole analysis: Level 1 PSA – "*a fuel damage accident or plant damage state frequency analysis*", plus Level 2 PSA – "*accident progression, containment performance, and radiological release frequency analysis*", plus "*off-site radiological consequence analysis*".

1.2.1 EPR stages in case of a nuclear accidental event

Emergency preparedness covers the planning and response to disasters, in this case, focusing on a nuclear accident.

The actions to be planned depend on the severity of the accident, the affected area and the derived consequences. According to (IAEA & OECD, 2008), there are seven levels in the International Nuclear and radiological Event Scale (INES) for a nuclear event, besides the level 0, which represents minor deviations (see Figure 3). In this logarithmic scale[21], events classified as "incidents" are from level 1 to level 3. Events upper 3 are considered accidents and offsite consequences (out of the NPP) are derived. Chernobyl and Fukushima Daiichi accidents both were classified as Level-7 in the INES scale range (Imanaka, et al., 2015).

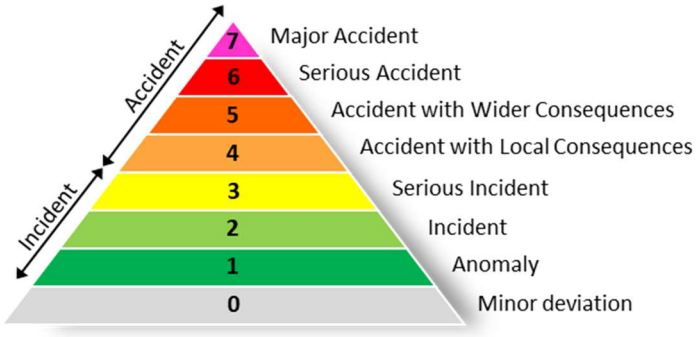

Figure 3. General criteria for rating events in INES. (IAEA & OECD, 2008)

The stage of the event in which actions have to be implemented (see 1.1.3) must be also taken into account. The definition for preparedness stage is the "*phase at which arrangements for an effective emergency response are established prior to a nuclear or radiological emergency*" (IAEA, 2015).

The temporal sequence of an accidental situation in a particular area or site can be outlined, as shown in Figure 4 (ICRP, 2018b).

[21] The severity of the of the events in the INES increase "*an order of magnitude for each increase of level on the scale*" (IAEA & OECD, 2008).

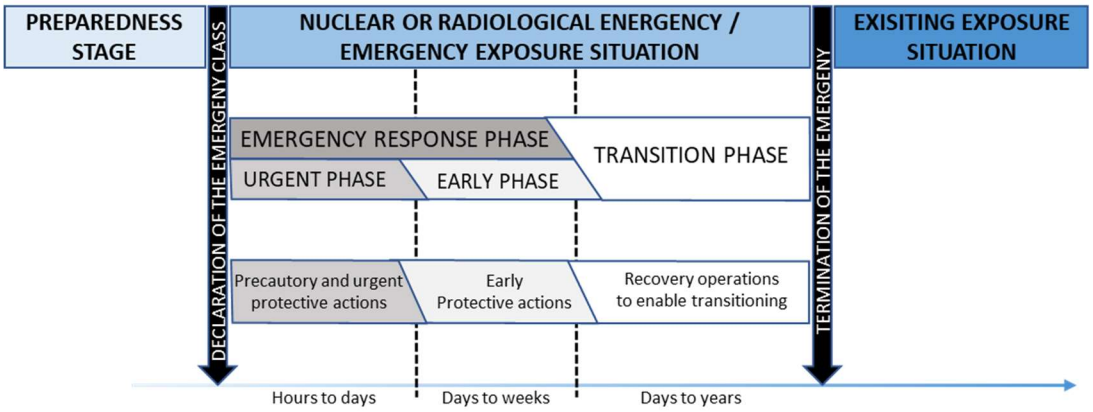

Figure 4. Scheme of the actions to be taken in the different phases and exposure situations of a radiological or nuclear accident (IAEA, 2018b).

In the *emergency response phase*, when the accident has been triggered, the release starts, and cloud dispersion and subsequent deposition of the contamination occurs; the cloud may affect the population via inhalation, or external irradiation, thus, early protective measures such as sheltering, evacuation or iodine prophylaxis must be executed; food or water consumption restrictions can also be implemented. In the Spanish case, in that phase (which may last from hours to days), according to the EPR management regulation in the country, the PLABEN must be applied. In the post-accident situation, the deposition is already complete, and the contamination pathways for the population may be related to inhalation (derived from resuspension of the radionuclides), ingestion (though food or water) or via external irradiation. The *intermediate phase* may last days, weeks or even months and response and/or recovery measures can be taken. In the *late phase*, which may last from weeks to years, also inhalation (due to resuspension) or ingestion are the main pathways to be considered. Decision-makers and stakeholders also should implement medium- or long-term protective measures at a certain point between the intermediate and the late phase, such as relocation of people (temporarily or permanently), apply food and/or water restrictions or starting the decontamination and the recovery.

Obviously, during the event there is not a predefined timing for the sequence processes occurring, because there are many variables involved. Therefore, as it is stated in (ICRP, 2007): "*an effective response must therefore be developed flexibly with regular review of its impact.*" That "*regular review*" is key in the decision-making prosses; thus, decisions should be supported by as many information as possible about the current situation. Therefore, regarding the intermediate and the late phases, it is important to develop

monitoring campaigns or environmental surveillance (depending on the stage of the event) and evaluate the effectiveness of the countermeasures implemented. These data should be useful to base the next decisions to be made.

In any case, developing a coordinated and organised EPR strategy by the authorities and the decision-makers, involving as much stakeholders as possible in the different stages of the EPR process, is the best way to be able to deal with the challenges faced in disaster event situations (OECD-NEA, 2006).

Regarding the countermeasures to be applied for the decontamination of areas affected by radiological or nuclear contamination facing the recovery, there are guidelines, recommendations and publications (IAEA & FAO, 1994; Nisbet, et al., 2009; Merkel & Hoyer, 2012; NGR, 2014; IAEA, 2015b; Nisbet, et al., 2017) which provide techniques or procedures for remediation[22], with information regarding efficiencies, costs, possible side effects, wastes generated, applicability conditions and residual doses. Remediation strategies are implemented according to the type of the radionuclides deposited, the activity concentration, the local specificities, etc.; the more accurate information about the contamination deposited and the characteristics of the area to be recovered, the higher the potential success in the recovery. *Justification* and *optimisation* principals should be applied in the recovery process also and, depending on the extension of the affected area, prioritisation should be considered taking into account the resources available (IAEA, 2015b).

The most studied countermeasures for recovering the contaminated agricultural systems, focused on minimising the transfer from soil to crops can be grouped in mechanical or physical technics (such as ploughing (deep, shallow or skim and burial ploughing), early removal of vegetation/crops or removal of topsoil) or chemical technics (fertilising with potassium or adding lime to soils) or change of the land use. A bunch of these were studied experimentally in Chernobyl in the framework of the RESSAC Program (L'Homme, et al., 1989) which led to other works, such as Maubert, et al. (1992) or Millán (1995). In another

[22] "*In terms of contamination of land by radioactive material, remediation is to be understood as any measure that may be carried out to reduce the radiation exposure from existing contamination of terrestrial areas through actions applied to the contamination itself (the source) or to the exposure pathways to humans*" (IAEA, 2015b).

experimental program, CHECIR[23], the CHECIR-4 project was developed to analyse, structure and model a real scenario, in Kirov (Belarus), to optimise the recovery strategies of the contaminated areas (Martí, et al., 1989). For the same reason, several investigations have addressed the remediation topic to facilitate the return of the agricultural soils affected by the Fukushima Daiichi accident, to the former farming husbandry practices (Vandenhove & Turcanu, 2011; Vandenhove & Sweeck, 2011).

However, there are other countermeasures, such as phytoremediation techniques[24] based on the use of specific plants that can absorb higher quantities of contaminants from soil (Nisbet, et al., 1993)[25].

Food processing for subsequent consumption or selection of edible crops that can be processed are also actions to reduce or dilute the concentration of radionuclides in food products.

1.2.2 Decision support systems (DSSs) in the Emergency Preparedness and Response (EPR)

Another example of the efforts to enhance the EPR was the development and the implementation of different decision support systems (DSSs) promoted by the European Commission, not only to be used in the European countries but also in other world regions, for instance in the Asian countries (EEAS, 2018).

The DSSs are used in several disciplines and involve computerised interactive systems oriented to support decision-making processes; for example, these are implemented in social science (Rushton, 2001), medicine and health (Al-Jumeily, et al., 2016) or business intelligence (Williams, 2016). DSSs are capable of managing a huge amount of "*data,*

[23] CHECIR Program: Chernobyl Centre for International Research.

[24] Phytoremediation seeks to increase the transfer from soil to plant. For radiocaesium contamination, the use of fertilisers which supply NH_4^+, aim plants to absorb it as much as possible to be reduced in soil (Nisbet, et al., 1993).

[25] Other technics that apply phytoremediation principles are being developed in DEMETERRES Project (Leonhardt & Chagvardieff, 2019) in which investigate the phytoextraction process in rice, based on the transport of radionuclides (radiocaesium and radiostrontium) in the plant, by applying gene-editing technologies such as CRISPR-Cas9 (Nieves-Cordones, 2017).

documents, knowledge, theories and/or models" to identify and solve different issues to be addressed (Ríos Insua, et al., 2005).

In the particular case of the management of an off-site nuclear emergency, the aim of a DSS is "*to provide consistent and comprehensive information at local, regional and national levels, during all phases of a real event and while preparing for a possible future event.*" (KIT, 2017b). The DSSs that are being used in the EU countries during the last three decades in the nuclear EPR field are the Realtime Online DecisiOn Support System, RODOS, (and its updated Java version, JRODOS) (KIT, 2017a), and the Accident Reporting and Guiding Operational System, ARGOS (PDC-ARGOS, 2014), the latter developed exclusively for the emergency phase management. Both JRODOS and ARGOS, are focused on contamination of terrestrial areas. On the contrary, the DSS MOIRA-PLUS (Monte, et al., 2009) evaluates the radionuclides' behaviour in contaminated freshwater bodies and its biota and provides comparative remediation strategies to reduce contamination levels.

TEMAS Project[26] (Montero, et al., 2001) performed a decision aiding computerised system (close to a DSS) to be applied in the restoration of contaminated areas by radiostrontium (^{90}Sr) and radiocaesium (^{134}Cs and ^{137}Cs) in a nuclear post-accidental situation, including urban, agricultural and forestry ecosystems. Regarding the crops contamination, that work assumes that the radionuclides uptake process by plants follows a logarithmic curve in a way that minimum radionuclide transfer from soil to plant occurs with a defined concentration of calcium for radiostrontium and of exchangeable potassium for radiocaesium[27] and, at that point, the transfer remains constant.

In this Thesis, JRODOS is the DSS used to perform a bunch of simulations of nuclear accidents according to the "*boundary conditions*" and the parameters considered in the selected case-study. That way, a probabilistic deposition analysis can be done to identify, in each spot, the most likely radioactive deposition (as the *prevailing* one), if a nuclear accident as the case-study designed occurs. JRODOS copes with off-site consequences derived from a nuclear accident, facing the emergency management in all its phases (early,

[26] TEMAS Project: Techniques and Management Strategies for Environmental Restoration and Their Ecological Consequences.

[27] 10 meq/100 g soil of exchangeable Ca for radiostrontium and 0,5 meq/100 g of the soil of exchangeable K for radiocaesium. (Montero, et al., 2001)

transition and long-term phases, see section 1.2.1) including the rehabilitation of the affected area.

1.2.3 Challenges to be faced in Radiation Protection regarding EPR

The European Radiation Protection research community, grouped currently in different platforms such as MELODI[28], ALLIANCE[29], NERIS[30], EURADOS[31] and EURAMED[32], performed a gap analysis of the radiation protection state-of-the-art (Vanhavere, 2018) in order to be addressed in further research programs[33]. The following are the research activities proposed to fill the gaps identified in that publication related to the scope of this Thesis:

- Vulnerability and risk assessment as a starting point for strategy development beyond simple dose or contamination criteria.
- Application of food chain models at the local level to derive sensible countermeasure strategies.
- Methods and guidance for optimisation (residual dose approach, temporal dynamics for the evolution of countermeasures, etc.)
- Advanced methods for data treatments to cope with the large amount of data available.
- Customisation of atmospheric, river, marine, brackish water, terrestrial and urban dispersion models, food chain models and dose assessment models.
- Mechanistic understanding of radionuclide dispersion in space and time, and transfer processes.

In the last gap analysis performed by the NERIS platform issued in November of 2019[34], the need of applying food chain models at the local level to derive sensible countermeasure strategies and the necessity to develop methods and guidance to optimise countermeasure

[28] MELODI: Multidisciplinary European Low Dose Initiative.
[29] The European Radioecology ALLIANCE.
[30] Network of European organisations involved in emergency and recovery preparedness and management.
[31] European Radiation Dosimetry Group.
[32] European Alliance for Medical Radiation Protection Research.
[33] That outcome, among many others, is the result of the participation of the cited platforms in the European Concerted Programme on Radiation Protection Research (CONCERT) included in the European funding program H2020.
[34] https://eu-neris.net/all-documents/sra-1/197-neris-research-priorities-nov-2019/file.html

strategies in agriculture were included as research activities to address the challenges in the field of EPR, including the recovery.

All these proposals reflect the concern of the nuclear research community with respect to agriculture and the importance to cope with the food chain issues derived from a nuclear or radiological emergency. These have been a motivation in developing this Thesis with the aim to enhance the EPR plans.

1.3 Background

1.3.1 Geographic Information Systems (GIS) in radiological or nuclear risk assessment

The Geographic Information Systems (GIS) are "*computer assisted systems for the capture, storage, retrieval, analysis and display of spatial data*." (Clarke, 1986). Currently, the scientific and technological developments have given rise to more sophisticated functionalities. According to ESRI, one of the most relevant enterprises in the GIS industry, a GIS "*analyses spatial location and organizes layers of information into visualizations using maps and 3D scenes. With this unique capability, GIS reveals deeper insights into data, such as patterns, relationships, and situations—helping users make smarter decisions*"[35].

The application of the Information and Communication Technologies (ICT), including GISs, in risk assessments has been analysed through the years by the International Federation for Information Processing (IFIP)[36], since it was founded in 1960 under the auspices of UNESCO[37]. In 2015, that organisation established the Domain Committee on Information Technology in Disaster Risk Reduction to provide disaster support to the international community. Several contributions presented in the Conference on Information Technology in Disaster Risk Reduction (ITDRR) held in 2017 highlighted the importance of GISs in disaster risk management (IFIP, 2019).

In radiological and nuclear risk assessments, as it does in many other disciplines, the use of GIS is key to manage, process, analyse lots of georeferenced and non-georeferenced data

[35] https://www.esri.com/en-us/what-is-gis/overview
[36] IFIP "is the global non-profit federation of societies of ICT professionals that aims at achieving a worldwide professional and socially responsible development and application of information and communication technologies." (IFIP, 2019).
[37] UNESCO: United Nations Educational, Scientific and Cultural Organization.

and to generate outputs (databases, maps, graphs, etc.) to be used for the decision-makers at different scales.

The GISs have been implemented in the DSSs (JRODOS, ARGOS or MOIRA-PLUS) to manage and analyse properties of the territory and features geographically referenced, in order to get a better knowledge of the studied area that can help in dealing with different situations related to a nuclear or radiological emergency, over time.

Regarding the agricultural systems management in nuclear or radiological emergencies, the Joint FAO/IAEA Division of Nuclear Techniques in Food and Agriculture [38] launched the CRP D1.50.15 on *Response to Nuclear Emergency affecting Food and Agriculture* (2013–2019), with the aim to "*develop innovative data collection, management and geovisualisation platforms that can be used both during routine monitoring and nuclear emergency situations*". In the frame of that CRP, several works were undertaken, and a specific publication with Technical Guidelines was launched (Lee Zhi Yi, A. & Dercon, G. (eds), 2019). These emphasise the importance of effective data management and show how data visualisation optimises response processes by using GISs and DSSs as vital resources in the decision-making in large-scale nuclear emergencies affecting agricultural systems.

The use of GISs in different radiological impact analysis has been crucial in the last decades. In the following, some examples of the usage of these are shown.

In Central Europe, many studies, and different approaches to identify the issues associated with real contamination related to radiological and nuclear impacts have been developed. One of the first studies carried out in which GIS was used as a fundamental tool is the "*Atlas of Caesium 137 deposition on Europe after the Chernobyl accident*" (De Cort, et al., 1998). In Figure 5, it is shown the activity concentration map of ^{137}Cs deposited in Europe just after the Chernobyl accident, performed in that work by using ARC/INFO version 6.1.[39].In De Cort, et al. (1998), the radionuclide studied was ^{137}Cs because, although some other

[38] The Joint FAO/IAEA Division of Nuclear Techniques in Food and Agriculture's mission is "to support and promote the safe and appropriate use of nuclear and related technologies by the FAO/IAEA Member States in food and agriculture and so contribute to peace, health and prosperity throughout the world, especially to global food security and sustainable agricultural development." http://www-naweb.iaea.org/nafa/joint-fao-iaea-50th-anniversary.html

[39] ESRI software.

radionuclides were released, it significantly contributed the most to the radiological impact from deposited material in the medium and long-term.

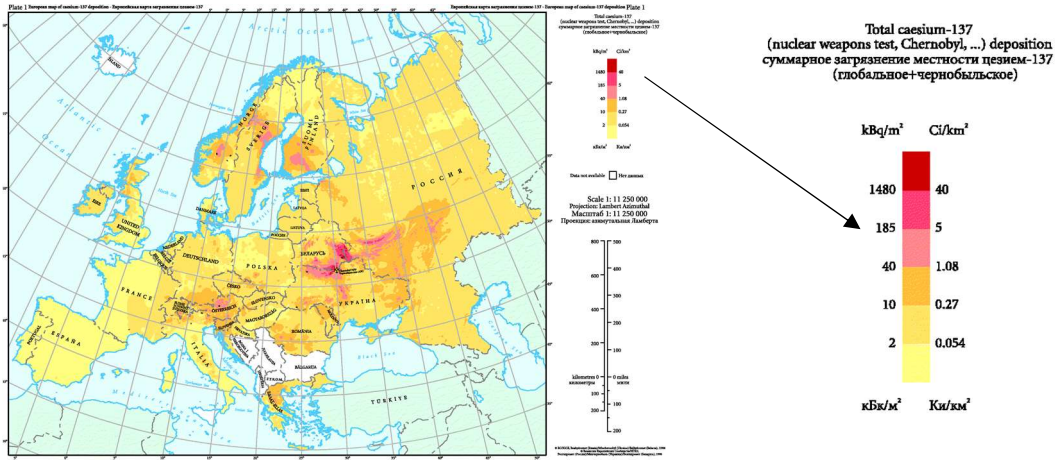

Figure 5. ^{137}Cs activity concentration in Europe immediately after the Chernobyl accident. (De Cort, et al., 1998)

The dispersion of the plume and the radioactive deposition in that accident did not affect the Iberian Peninsula (Legarda, et al., 2011) as it did in Central Europe, as seen in Figure 5. In that atlas, the existing contamination level maps in Europe before Chernobyl were also performed (see Figure 6). The source of that contamination was the global fall out related to the atmospheric nuclear weapon testing which took place between 1945 and 1980, although the radioactive depositions in Europe occurred most frequently in the mid-'50s and the early '60s (De Cort, et al., 1998). As seen in Figure 6, the Iberian Peninsula was not as much affected by those fallouts as the rest of Europe.

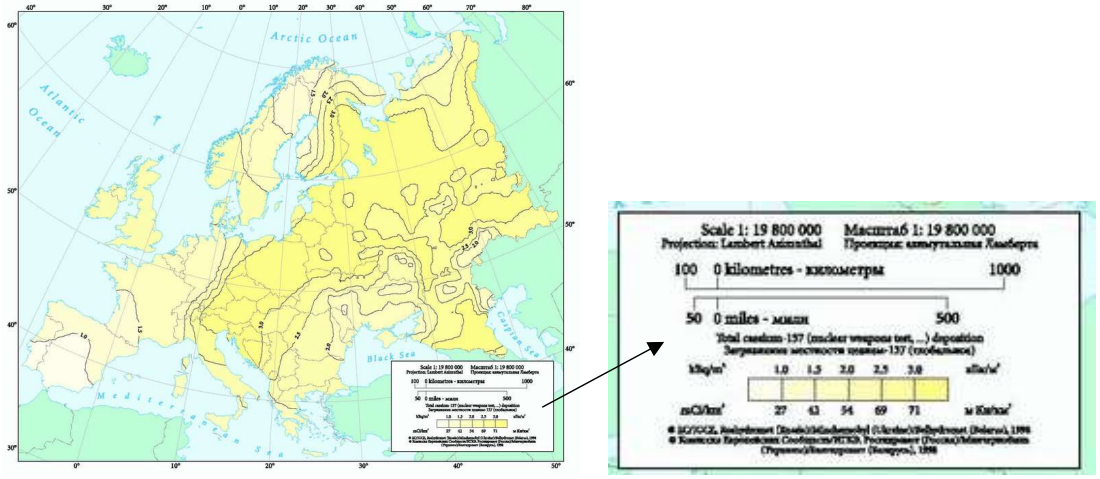

Figure 6. ^{137}Cs activity concentration deposition remained from the atmospheric testing of nuclear weapons, just before Chernobyl accident (in May 1986) (De Cort, et al., 1998).

Another example of the GIS use in radiological impact analysis in recent years is the In FlexRISK Project (Seibert, et al., 2015). In that project, a risk assessment of potential severe accidents in NPPs[40] and other nuclear sites in Europe for the Austrian decision-making process, was performed by means of a "*GIS-analysis*". The sites considered can be seen in Figure 7. A vast number of different meteorological conditions were taken into account to obtain a deposition map and other radiation dose maps. The results of this project are shown in http://flexrisk.boku.ac.at/en/results.html, where an interactive map is hosted.

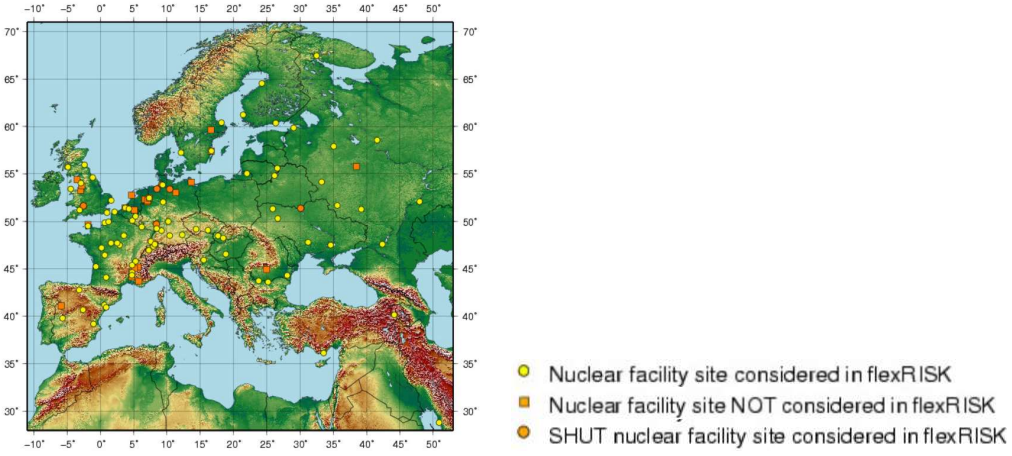

Figure 7. Nuclear Sites within the Domain of flexRISK. Source: http://flexrisk.boku.ac.at/en/site_map.html

Different examples of GIS usage can also be found in the publication: "Recommendations for National Risk Assessment for Disaster Risk Management in EU" (Poljanšek, et al., 2019). This report was issued by the EU Science Hub[41] as a guide for EU countries to fulfil the Union Civil Protection Mechanism (UCPM), established in the Decision No. 1313/2013/EU[42], in the periodical risk assessment. It gathers specific approaches to develop proper National Risk Assessment (NRA) in order to prevent risks in Europe; one of these is the nuclear risk (chapter 15), where a Spanish case-study is shown.

Other radiological impact studies at a more local scale have been carried out, in which the GIS usage is fundamental. Two examples are presented down below.

[40] An accident occurred in a NPP is defined as severe if it implies off-site consequences, which corresponds to levels between 4 to 7 in the International Nuclear and Radiological Event Scale (INES): https://www.iaea.org/resources/databases/international-nuclear-and-radiological-event-scale
[41] https://ec.europa.eu/jrc
[42] https://eur-lex.europa.eu/eli/dec/2013/1313/oj.

The European Atlas of Natural Radiation (REM Group. JRC-Ispra, 2019), is one of these relevant examples of the application of GIS in radiological research. That atlas includes maps regarding the radioactivity levels caused by different natural sources in Europe, such as uranium, thorium and potassium in soil, explained in Cinelli, et al. (2017) and Cinelli, et al. (2018) for Belgium.

An example of local radiological assessment that uses a GIS as fundamental software is Prister, et al. (2018). That work presents a "*methodology for assessing the radioecological criticality of a territory […] to strengthen effective emergency preparedness and response to severe nuclear emergencies at a nuclear power plant in all possible meteorological scenarios*". That study takes as background (among other publications) the first environmental study in which the concept of *radiological sensitivity* was defined[43] (Aarkrog, 1979), a concept that was subsequently analysed in Howard (2000), in which the *radiological sensitivity* was assessed considering critical loads[44], in the same way as it was established in the Vulnerability Forum (initiative promoted as a European Commission Concerted Action by EURATOM in the 5th European Framework Programme[45]). Howard (2000) begins by affirming:

> It is important to be able readily to identify major routes of exposure, the most highly exposed individuals or populations and the geographical areas of most concern arising from radioactive contamination. […] Prior identification of such areas and exposed individuals should improve the focus of emergency preparedness and planning and contribute to environmental impact assessment for future facilities. (p.1)

GIS tools are applied in the geoprocessing of all this information in that work, on the basis of Dubois, et al. (2004), where GISs are described as "*very valuable tools in radioecology*" to obtain "*thematic maps involved in radioecological modelling*". A ranking of the

[43] "The radioecological sensitivity is the infinite time-integrated radionuclide concentration in the environmental sample considered arising from a deposition of 1 mCi km^{-2} of the radionuclide in question. (Aarkrog, 1979)

[44] Critical load, referred to radioactive contamination, is the threshold that indicates the activity concentration deposited that is necessary to reach a defined activity concentration in foodstuff: the maximum permitted level.

[45] https://cordis.europa.eu/programme/id/EAEC_FWP_EAEC-FWP-EAEC-2C

radioecological "*criticality*" of each area is obtained as a notion of its risk from the contamination.

This Thesis delves deeper into the concepts of *geographical areas of most concern* and the *prior identification* of agricultural areas facing the EPR, using, soil properties, land use and type of plant species as base data (as in Prister, et al. – 2018), by means of a GIS.

1.3.2 Radioecological studies developed in characterising the Spanish territory

Several studies focused on analysing the Spanish territory from the Radiation Protection perspective have been conducted, in the last decades, some of these used a GIS to attain their outcomes.

An example of those which used a mapping software was the I+D Marna Project, an agreement between CSN and ENUSA[46], which started in 1991 (Suárez, et al., 2000), aimed to assess the natural gamma radiation rates to evaluate the radiation levels and the potential increase concerning the natural background[47]. The resulting rate exposure map of peninsular Spain, performed by using the software Golden Surfer[48], is shown in Figure 8.

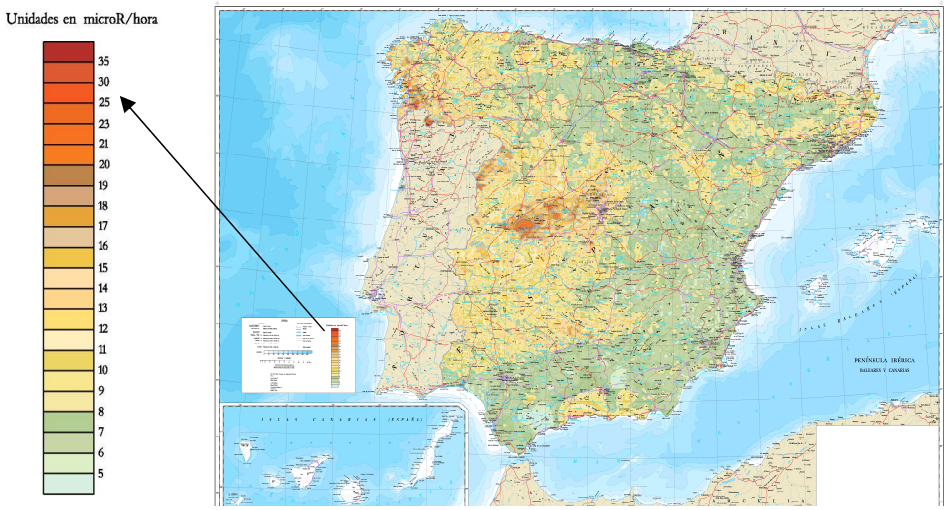

Figure 8. Map of the natural gamma radiation (µR/h)[49] in Spain. Scale 1/1000000. (MARNA Project)[50].

[46] http://www.enusa.es/
[47] https://www.csn.es/en/mapa-de-radiacion-gamma-natural-en-espana-marna
[48] https://www.goldensoftware.com/products/surfer
[49] Micro Roentgen a la hora. 100 µR/h = 1 µGy/h.
[50] https://www.csn.es/en/mapa-de-radiacion-gamma-natural-marna-mapa

Regarding natural radiation a local scale, for example, Baeza, et al. (1994) focused on that topic on Cáceres province and more recently Guillén, et al. (2014a) investigated it in commercial granites related to ^{40}K in Extremadura.

Some other studies conducted to analyse the Spanish territory from the Radiation Protection perspective were focused on evaluating the real consequences of radiological or nuclear accidents. Some of these are cited down below.

On January the 17th of 1996, in the morning, two aircraft, had an in-flight collision over Palomares (Almería province in the Southeast of Spain). As a consequence, aircraft's debris and four thermonuclear weapons[51] were dispersed over the land and the Mediterranean Sea. Two of the bombs "*suffered a conventional detonation*", generating the deposition of plutonium (Pu) and uranium (U) in about 2.3 km^2 (Sancho & García-Tenorio, 2019)[52]. CIEMAT[53] has been conducting continuous surveillance since then, both environmental and to the population also. Concerning the radiological characterisation of the site, a three-dimensional study of the affected area was carried out from 2007 to 2009, in which the GIS software ArcGIS 9.2 was used for analysis and mapping purposes (Sáez, 2008; Sáez, et al., 2009), showing the presence of different transuranic elements. Regarding the radiological risk due to the ingestion pathway of Pu and Americium (Am), no risk was observed related to meat or crops produced in the area while "*special attention should be paid to the consumption of wild terrestrial snails*" (Sancho & García-Tenorio, 2019).

In comparison with Central Europe, only a few have been carried out about severe nuclear accidents in Spain, because of the limited impact of those kinds of past events in Southwest Europe. That was the conclusion resulting in the works of Baeza, et al. (1991), focused on Extremadura and Valencia, Llaurado, et al. (1994) for northern Catalonia and in Navas, et al. (2007) for the central Ebro valley, which evaluated the activity concentration of the radiocaesium deposited on the soil after the Chernobyl accident.

The influence of the Chernobyl accident was also evaluated in Legarda, et al. (2011), in which a Spanish mainland map on the basis of the collected ^{137}Cs inventory was obtained

[51] Mk 28 FI type hydrogen bombs.
[52] A decontamination of the affected area was held in collaboration with the U.S. armed forces.
[53] http://www.ciemat.es/portal.do?IDM=112&NM=2

by using an interpolation method in a GIS; besides, the migration of ^{137}Cs was studied. This work concluded that the influence of the Chernobyl disaster on the caesium activity concentration was negligible in comparison to the nuclear weapons fallout contribution in the area.

Baeza, et al. (2012) analysed the environmental influence of the Fukushima accident in Spain taking into account the measurements from three monitoring stations of the REA (located in Cáceres, Barcelona and Sevilla), regarding a bunch of radionuclides[54]. The conclusion was that "*the associated fallout had negligible radiological consequences in Spain*".

Another group of works performed in the Spanish territory were focused on researching the radionuclides' behaviour in the Mediterranean ecosystems. Some examples are Sauras, et al. (1994), who studied the migration of ^{134}Cs, ^{85}Sr and ^{110m}Ag in the Mediterranean holm oak forest, an environment that was also analysed in Rauret, et al. (1994); Baeza, et al., (1996), in which the radon and thorium absorbed by *Cistus ladanifer*, a typical vegetation species in natural areas in Spain were analysed; the project: Study and impact evaluation due to non-nuclear industrial activities in the South of Spain[55], led by Professor Rafael García-Tenorio; a study of the temporal series of ^{137}Cs and ^{90}Sr in Tagus river (Miró, et al., 2012); the issue in which the migration of ^{137}Cs, ^{90}Sr and $^{239+240}$Pu in Mediterranean forest were analysed (Guillén, et al., 2015) or the publication previously cited Legarda, et al. (2011) which, regarding the mobility of ^{137}Cs, identified two different behaviours according to both soil groups, a first one: clay and loamy soils with lower mobility, and a second one which includes sandy soils with significantly higher mobility.

One last group of studies in the frame of the RP are focused on evaluating the radiological vulnerability of the Spanish soils, regarding the ^{137}Cs and ^{90}Sr. That concept was defined in Trueba, et al. (2000a) and used in Trueba (2004) *as "the potentiality to retain or to make bioavailable to the agricultural systems the radionuclides deposited on the soil*", attending

[54] ^{134}Cs, ^{136}Cs, ^{137}Cs, ^{131}I, and ^{132}Te.

[55] In Spanish: "Estudio y evaluación del impacto radiológico producido por las actividades de diversas industrias no nucleares del sur de España". University of Seville.

to the soil properties. To perform those vulnerability works, a soil profile compilation of the studied area was conducted, and a complete Spanish soil profile database (DB) was created. That DB has been an essential piece of information in this Thesis. The outputs are a bunch of radiological vulnerability maps regarding two different exposure pathways that may lead the radionuclides to affect the population: the external irradiation and the internal contamination, in particular by ingestion (through the food chain). The maps categorised the territory on the bases of the "*radiological vulnerability indexes*" and were attained by using the GIS software IDRISI for Windows, version 1.0. Subsequent updates of those maps (García-Puerta, 2014[56]; Trueba, et al., 2015) were performed by using ArcGIS desktop: Release 10.1. These works have been used as the starting point of this Thesis, which is the reason why these are described in more detail below.

Building on the previous work made in Trueba, et al. (2000a), a further step was taken in ATYCA Project (Trueba & Vallés, 2000) considering only the ingestion exposure pathway, by integrating the soil-to-crop transfer factors (*Fv*) (IAEA, 2010) for radiocaesium and radiostrontium. According to the content of the physic-chemical competitors of these radionuclides in the soil structure (potassium and calcium, respectively), the values of the F_vs, took from Nisbet & Woodman (2000), were adjusted. The main aim was to categorise the agricultural areas regarding the potentiality of the different peninsular soil types to transfer to crops.

Further attempts to consider in a global way the radiological vulnerability of the soil-crop systems in Spain were carried out in VULNES Project (Trueba, et al., 2003), in which the results of the radiological vulnerability of the Spanish soils obtained in Trueba, et al. (2000a) were combined with the main representative Spanish crops, distributed according to the land use defined in CEC (1993). That way, an association between soil type, radiological vulnerability of soil, land use, crop and F_v was carried out. The F_v values considered in that work were gathered from diverse sources in IAEA (2010),

[56] In that update a revision of the soil DB consisted of adjusting the reference coordinates of the soils' profiles, to harmonise them by using the European Terrestrial Reference System 1989 (ETRS89), as the official Geodetic Reference System in Spain to be used in geographic referencing for the Iberian Peninsula and Balearic Islands (RD 1071/2007).

which is the last updated F_v compilation database. Nevertheless, the outputs were obtained in tables but there were no georeferenced results in maps.

All the works listed in this section and those referred in the previous ones represent the bases on which this Thesis is founded.

1.4 State-of-the-art in researching the behaviour of ^{137}Cs in the soil-plant system

As said at the beginning of the Introduction, this Thesis is focused on analysing the radiological vulnerability of the peninsular Spain soils, regarding the ^{137}Cs deposited in agricultural areas.

Among the all the possible radionuclides to be deposited after an accidental release to the atmosphere, ^{137}Cs is selected for assessment purposes, because it can move easily through the air and be transported to relatively long distances (EPA, 2017), has a high solubility in water (Vandebroek, 2012), has a long half-live (30.07 years (ICRP, 2017)) and its entrance in the food chain may pose its accumulation in the human body causing sublethal and lethal ionising effects at the molecular level (Gupta & Walther, 2016). From the environmental point of view, its similar biochemical behaviour to potassium in soil (Vandebroek, 2012), a fundamental nutrient for plants with which it competes in the plants' root uptake process, could affect the crops production and the food chain in the long-term. This contamination scenario could generate a risk to the population, via the ingestion pathway if ^{137}Cs were incorporated in the body and distributed in the soft tissues, especially muscle tissues (Yamagata, 1962) (Leggett, et al., 2003). Besides, the ^{137}Cs contribution to the total radiation exposure after an accident in the long-term can reach relevant rates, as it occurred in Chernobyl, or, likewise for the case of the Fukushima accident it can become, along with ^{134}Cs, the main contribution in a quite shorter period, being almost the unique contributor 30 days after the accident (Imanaka, et al., 2015)[57].

In this section the existing knowledge in the literature with respect to the foundations on which this Thesis is based is described.

[57] The radiocaesium's contribution to the total radiation exposure in Chernobyl and Fukushima for the first year was 7.4 and 83 %, respectively. For 30 years after these accidents it has been calculated that 49 and 98 % of the total exposure was related to these radionuclides (Imanaka, et al., 2015).

1.4.1 Role of the soil's properties in the behaviour of ^{137}Cs in soil and its uptake by plants

Several processes govern the ions' balance in the soil, in their exchangeable and non-exchangeable forms, including for radionuclides. The soils' capability to bind the radionuclides deposited on it, depending on its properties, conditions the availability of the exchangeable radionuclides to be uptaken by plants.

Focusing on caesium, it is an alkali metal, and its oxidation state in solution is +1. However, it can be encountered in different chemical and physical forms, such as soluble inorganic salts (chloride or nitrate) or sulphates (ICRP, 2017). Among the 40 caesium radionuclides, ^{134}Cs and ^{137}Cs, which are fission products, produce significant environmental impacts in the mid and long-term[58]. ^{137}Cs is the one to be considered in this Thesis, as it is justified further on.

For both radionuclides, the soil properties that play a significant role in its behaviour within the soil are texture, clay content and clay types, pH, cation-exchange capacity (CEC), exchangeable potassium (K^+) content and organic matter content.

In general, sandy soil textures, low pH, high organic matter content or low CEC do not favour the fixation of ^{137}Cs in soil, while clayey soils (which have high CEC), low organic matter or high pH soils tend to fix the ^{137}Cs and to retain it in their structure, restricting the amount of bioavailable ^{137}Cs (Tarsitano, et al., 2011).

The exchangeable potassium content, which is mainly in soil solution, enhances the ^{137}Cs mobility since both compete for the clay's adsorption sites (Absalom, et al., 1999); however, although they have several physicochemical similarities, the ionic ratio of caesium (1.69 Å[59]) is slightly larger than the ionic ratio of potassium (1.33 Å). Thus, in the presence of exchangeable potassium, some clays' selective sites would be occupied by potassium, instead of radiocaesium. That is the reason why soil's capability to fix ^{137}Cs is also clay content dependent.

[58] ^{134}Cs half-life: 2.064 years. ^{137}Cs half-life: 30.167 years (ICRP, 2017).
[59] Å: Angstrom. 1 Å = $1.0 \cdot 10^{-10}$ m. https://www.lenntech.es/periodica/elementos/k.htm

To quantify the capacity of soils, or minerals in soils, to adsorb the radiocaesium the Radiocaesium Interception Potential (RIP) (mmol·kg-1) (Cremers, et al., 1988) was defined. The parameters to be considered in the RIP assessment are Frayed Edges Site (FES) (Francis & Brinkley, 1976), the Cs^+ to K^+ selectivity coefficient in FES, the ^{137}Cs fraction in soil and liquid coefficient, and the K^+ in the aqueous phase. FES are located at the layer edges of clay minerals (see Figure 9), most precisely in micaceous ones; these are able to selectively adsorb alkali ions (K^+, Rb^+, and Cs^+), increasing the CEC. RIP soil value is highly related to the mineralogical composition, besides the organic matter content in soil (Vandebroek et al, 2012; Uematsu et al., 2015). That way the type of clay minerals, mainly their charge characteristics, are a relevant factor to be considered: kaolinite (with low layer charge) has a small RIP, while vermiculite and illite (with high layer charge) have a large RIP (Nakao, et al., 2008). On the other hand, the higher the organic matter, the less the RIP (Fan, et al., 2014; Uematsu et al., 2015). Nevertheless, RIP is a very specific soils' parameter, which should be assessed under standardized experimental conditions (Wauters et al., 1996a; Wauters et al., 1996b) in soil samples to be contaminated with radiocaesium; thus it is not included as a common parameter in soil's studies (such as those consulted in this Thesis) but in radiological ones for specific contaminated sites.

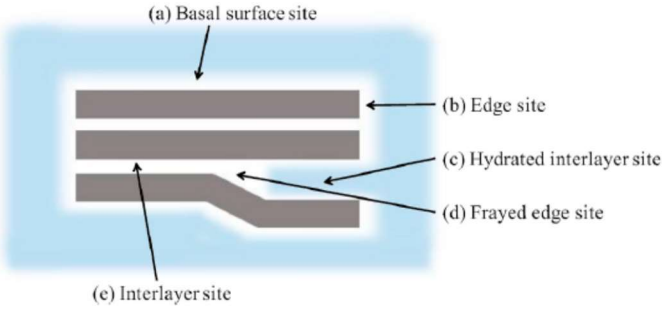

Figure 9. Adsorption sites on an illite particle according to the conceptual model shown in (Okumura, et al., 2018).

There are other particle adsorption sites in the complex clay structure apart from FES. For instance, in illites these sites are well defined in Okumura, et al. (2018); these are: basal surfaces, ("*fresh*") edge sites, hydrated interlayer sites and anhydrous interlayer sites (see Figure 9). The exitance of these sites, favours the ^{137}Cs binding in clayey soils.

In the view of the preceding, not only the clay content but the type of clay is also determinant in the process of the exchangeable potassium or caesium, since each one has different affinity by ^{137}Cs and by its competitor: potassium. For instance, biotite and illite

have similar properties, but biotite has a higher affinity for ^{137}Cs than illite (Okumura, et al., 2018; Ogasawara, et al., 2019) and weather biotite has even more affinity.

Regarding the organic matter in the behaviour of ^{137}Cs in soil, its role is highly complex. On one side, organic matter reduces the capability of clay to immobilise the ^{137}Cs by blocking the access to FES (Staunton, et al., 2002; Uematsu et al., 2015), which favours its bioavailability. However, soils with low Dissolved Organic Carbon (DOC) (an organic matter content indicator) are also influenced by temperature in a way that the higher the temperature, the more ^{137}Cs is in the liquid phase of soil (soil solution) (Staunton, et al., 2002). As an example in Mediterranean forest soils, (Llaurado, et al., 1994) was carried out to study in the Northeast of Spain, finding a significant positive correlation between ^{137}Cs activity concentration and the organic matter content in soils.

Nevertheless, in the novel approach developed in this Thesis, organic soils are not considered[60], because of their low representativeness in Spain, where mineral soils are the most widespread ones. According to the European soil map used as the base map in this Thesis (EC-ESBN, 2004), Dystric Histosols[61] are the only organic soils in the Iberian Peninsula, and they are located in a very few small spots in the Northwest (in Galicia and Asturias Spanish provinces, as it is described further on). However, mapping limitations associated mainly to the scale of representation do not allow to show, for instance, the Histosols associated with the alluvial plains such as the case of the Guadiana basin (García Rodríguez, 1996) at "Las Tablas de Daimiel" (González-Quiñones Ortas, 2006) (in Ciudad Real province). In any case, because of the limited general representativeness of the organic matter content in the Spanish soils and because of the complexity in the treatment of the organic matter as parameter in the novel methodology, it has not been considered.

Ammonium (NH_4^+) content and the presence of fungi and microorganisms in soil are also factors which influence the radiocaesium adsorption in soil.

NH_4^+ is another caesium competitor in occupying the selective clay minerals' sites, since caesium and ammonium are both cations with low hydration energy

[60] The map updating the Radiological Vulnerability of soils does not exclude the organic soils, following the same criteria as the one used in the original work, which is Trueba, et al., 2000a.
[61] Dystric Histosols (Od) (FAO-UNESCO, 1974).

(Ogasawara, et al., 2013). However, its presence in agricultural soils is not relevant among the inorganic nitrogen pool (Absalom, et al., 1999).

Due to the ^{137}Cs prevalent location in topsoil (Mahara, 1993) because of its limited mobility in soil (Legarda, et al., 2011; Dubchak, 2017), the presence of fungi or microorganisms also is another factor to be considered in the biogeochemical ^{137}Cs cycle, since these can modify the pH, the oxidation potential (eH), or the soil structure. Microorganisms are able also to vary the soil composition because of the microbial metabolism, by generating low molecular weight organic compounds or can even take up actively ^{137}Cs from soil solution (Tamponnet, et al., 2008). Besides, since the presence of microorganisms in soil is temperature-dependent (being optimum between 15 and 20 °C), again, also climatic conditions are a key factor to be considered in the ^{137}Cs-soil interaction (Tamponnet, et al., 2008). Therefore, although the existence of microorganisms could be considered for a local study, it exceeds the scope of this work.

Seasonal variations of the radionuclides air content near the soil surface, related to natural processes, such as soil erosion (Rubio-Delgado, et al., 2017) or resuspension of fine particles of soil (IAEA, 2009), or radon exhalation from ^{210}Pb in soil, have been observed. Specifically, for ^{137}Cs, a positive correlation with temperature is found, measuring maximum values of ^{137}Cs activity concentration in summer (Baeza, et al., 2016). Nevertheless, since equilibrium conditions have been considered in this Thesis, these facts are not taken into account.

1.4.2 Soil-to-plant transfer factors

The source of the radiological contamination in agricultural areas considered in this Thesis is related to a release to the atmosphere in which radionuclides, specifically ^{137}Cs, in the form of aerosols, are deposited on the ground. The most relevant chemical forms of ^{137}Cs are the water soluble and the exchangeable ones. Its entrance in soil occurs dissolved in water due to a wet deposition or a rain or irrigation episode after a dry deposit. Not all the deposited ^{137}Cs, is bioavailable to be uptaken by crops, and some are lost due to runoff and lixiviation processes.

A relevant aspect that influences the radiocaesium absorption by plants is, as it was previously mentioned, the bioavailable potassium content, in such a way that, potassium saturated soil solution avoids the caesium to be uptaken by plants. It is also important to state that the uptake process does not happen instantaneously once the deposition occurs, on the contrary, it may take a relatively large lapse of time, depending on several factors, which condition the ^{137}Cs bioavailability in soil (see section 1.4.1). Moreover, the velocity with which the processes govern the caesium bioavailability in soil decreases over time; this phenomenon is commonly known as "aging" (Absalom, et al., 1995; Smith, et al., 1999).

To quantify the radionuclides transfer from soil to plant, a parameter is defined: Transfer Factor (F_v) (as it is named in IAEA (2010) – concept already introduced in this work)[62]. F_vs are empirical values related to crops and soil parameters, no radiological ones, which have been measured in different types of experimental research that have taken place in field and laboratory conditions (including liximeters and pots experiments). A vast compilation of published F_v values have been gathered in (IAEA, 2010), unifying them attending to the experimental methods used. Therefore that F_v compilation represents the ratio of the dry weight concentration in plant, except for fruits for which fresh fruit weight is considered, to the dry weight concentration in soil (IAEA, 2010).

The radionuclides transfer from soil to plant is influenced by the deposited radionuclide itself (the chemical element and its form), the soil properties (included the soil texture, its fertility, etc.), the type of crop (related to the species, their vegetal physiology, the vegetative period and the roots' distribution in soil) and the agricultural management practices (IAEA, 2010; Guillén, et al., 2016). It is important also to take into account the hydrological and meteorological conditions when the deposition took place (Legarda, et al., 2011) which determines the wet or dry deposition and the time elapsed since the deposition occurred, because of the radionuclide's half-life and the physicochemical processes in soil (IAEA, 2010).

Some processes in soil lead to a reduction of the bioavailable radionuclides, such as fixation to soil minerals, incorporation by microorganisms or by plants through the root uptake

[62] There are some other ways to quantify the radionuclides transfer from soil to plant when a radioactive deposition occurs, from their activity concentration in soil (Guillén, et al., 2016).

(IAEA, 2009; IAEA, 2010). Nevertheless, regarding fixation, once ^{137}Cs enters the mineral soil phase, reversibility of the ^{137}Cs adsorption in the soil structure can take place; therefore, biological availability of radionuclides increases due to their reintegration in soil's liquid phase. In this work it is assumed that soil is in equilibrium conditions and the radionuclide fraction considered is the ^{137}Cs incorporated in the aqueous phase (a bioavailable form), because it is the fraction to be uptaken through roots.

On the other hand, as it occurs in the minerals' fixation process of the exchangeable potassium cations, their presence in soil reduces the transfer soil-to-plant, because potassium is a relevant nutrient for plants and both act as competitors in the plant uptake process. However, since potassium has a smaller ionic ratio (see section 1.4.1), it is easy for plants to be uptaken. Thus, the higher the soluble potassium content, the lower the ^{137}Cs plants' uptake.

In the compilation of transfer factor values previously mentioned, F_v is associated with climate conditions (IAEA, 2010); most of the studies related to that parameter are developed in North and Central Europe or most recently in Japan, because these regions were affected by global fallouts of nuclear weapon tests and nuclear accidents. However, as it was cited above, Spain, besides the nuclear weapons fallout, has not received significant radioactive deposition from past events and therefore not many studies related to the radionuclide behaviour in Mediterranean soils and their transfer to crops have been developed.

In the TARRAS Project (Transfer of Radionuclides in Soil – Plant Systems), experimental simulations of an accidental scenario in which the release of aerosols similar to those emitted in a severe accident from pressurised water reactors (PWRs), were carried out. A parametrisation of the deposition processes and the subsequent transfer of radionuclides of Sr, Cs and Ag to crops were performed taking into account the specificities of Mediterranean soils, such as the Spanish and French soils. The results obtained in that project were used in the RESSAC project cited previously (ENRESA, 1993).

Over the last few years, some research examples regarding this topic have been conducted for a typical Mediterranean ecosystem called "dehesa". For instance, in

Guillén, et al. (2018), stable elements are taken as a reference to define their corresponding radionuclides transfer to holm oaks, pine trees and wild grass. Some works related to transfer to mushrooms in that particular environmental conditions have also been performed (Guillén & Baeza, 2014b); however wild mushrooms, exposed to natural conditions, have not been considered as outdoor crops in this Thesis. Nevertheless, there are little data regarding the radionuclides transfer to specific Mediterranean agricultural species yet (Guillen, et al., 2019), and not at country scale. That is the reason why in this Thesis, F_vs for temperate climate have been considered (IAEA, 2010). Detailed information about all the considerations taken into account regarding the transfer factors database used in this work is given further on.

1.4.2.1 Soil-to-plant transfer models

The improvement of the knowledge about the caesium behaviour in soil and crops has been reflected in different models, developed to predict the caesium to be uptaken by plants. One example is the radioecological model ECOSYS (Müller & Pröhl, 1993), which is implemented in the FDMT module (Food chain and Dose Module for Terrestrial pathways) of the DSS RODOS. Among other assessments, it simulates the transfer of radionuclides to the food chain to calculate the individual and the collective doses (KIT, 2004). In Figure 10 the schematic workflow used in the FDMT model is shown. However, this model has been developed considering Central European conditions. Therefore, certain parameters such as atmospheric resistance of crops, times of harvest and yields, or season dependent growth dilution rates have been defined for that specific European region; some of them can be easily adapted to the Peninsular conditions, but not all of them.

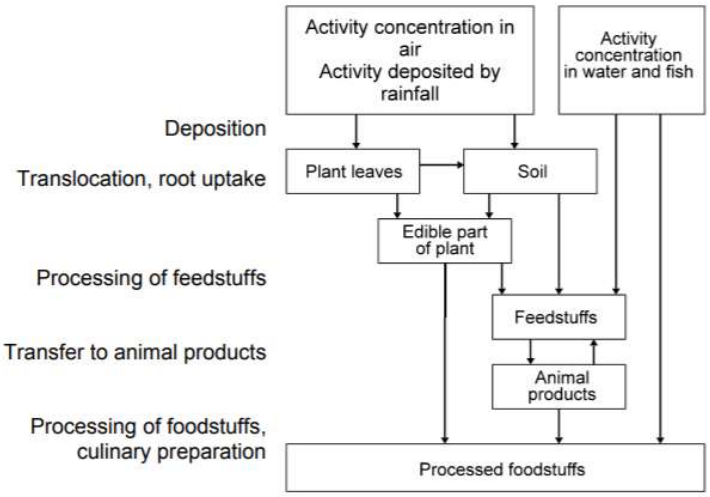

Figure 10. Steps of food chain transfer assessment in the FDMT module (based on ECOSYS model), included in RODOS (KIT, 2004).

Another example is the Absalom model (Absalom, et al., 1999) and its subsequent revisions (Absalom, et al., 2001), which have been widely implemented in Central European soils, initially to assess the radionuclides transfer to grass and afterwards for rice, wheat and barley. In Figure 11 the workflow developed for that model is shown. Lately, it has been simplified to reduce the complexity of the initial developments of the model, with the aim to eliminate what is named "*noise*" and redundancy (Tarsitano, et al., 2011). Thus, the following parameters are proposed to be eliminated from the original model: *Radiocaesium distribution coefficient for the humic soil fraction* (KD_{humus}) and *Cation exchange capacity on the humic soil fraction* (CEC_{humus}), *Concentration of Calcium and Magnesium ions in the soil solution* (m_{CaMg}) and *Proportion of labile radiocaesium adsorbed on the clay fraction* (KD_R). This model has been incorporated to the DSS ARGOS (www.pdc.dk/argos).

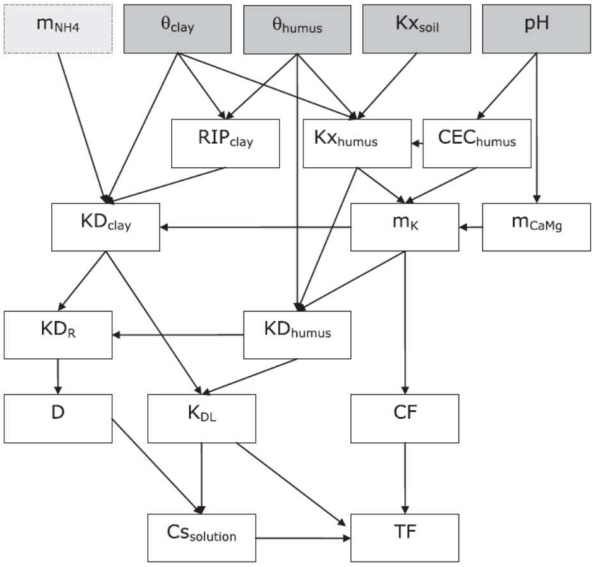

Being:
- m_{NH4}: Ammonium concentration in soil
- θ_{clay}: Gravimetric clay content
- θ_{humus}: Gravimetric humus content
- Kx_{soil}: Whole soil exchangeable potassium
- pH: Soil pH.
- RIP_{clay}:
- Kx_{humus}: Exchangeable potassium on the humic soil fraction
- CEC_{humus}: Cation exchange capacity on the humic soil fraction
- KD_{clay}: Radiocaesium distribution coefficient for the clay soil fraction
- KD_{humus}: Radiocaesium distribution coefficient for the humic soil fraction
- m_K: Concentration of K^+ in the soil solution
- m_{CaMg}: Concentration of Calcium and Magnesium ions in the soil solution
- KD_R: Proportion of labile radiocaesium adsorbed on the clay fraction
- D: Dynamic factor which describes the change in labile radiocaesium with time.
- K_{DL}: Whole soil labile radiocaesium distribution coefficient
- CF: Concentration factor for plant to soil solution radiocaesium concentration
- $Cs_{solution}$: Radiocaesium activity concentration in soil solution
- TF: Transfer factor, ratio of radiocaesium concentration in plant to whole soil

Figure 11. Absalom model. (Tarsitano, et al., 2011)

Nevertheless, there is not complete agreement on the processes which take place in certain soils related to kinetic and thermodynamic of ^{137}Cs for its binding in soil structure (Okumura, et al., 2018). That is the reason why, for instance, the Absalom model was not successful in the predictions made for Japanese soils (Almahayni, et al., 2019).

The radionuclides transfer from soil to plants and, then, to the food chain, are complex processes; that fact, linked to the variability in the factors to be taken into consideration, make these models are constantly evolving in search of higher accuracy and better adjustments to all the possible environmental conditions. For that purpose, ECOLEGO (ECOLEGO, 2012) was created as a useful software tool in the radiological risk assessment to develop new dynamic models and to perform deterministic[63] or probabilistic[64] simulations of the radionuclides transfer in a contaminated area. It has been used, for example, in IAEA (2016) to apply the mathematical approach of Pröhl, et al. (2004) in the

[63] Deterministic analysis: "Analysis using, for key parameters, single numerical values (taken to have a probability of 1), leading to a single value for the result." (IAEA, 2018a).

[64] Probabilistic analysis "is often taken to be synonymous with stochastic analysis. Strictly, however, 'stochastic' conveys directly the idea of randomness (or at least apparent randomness), whereas 'probabilistic' is directly related to probabilities, and hence only indirectly concerned with randomness." (IAEA, 2018a)

"*assessment of post-emplacement environmental and human health impacts of solid radioactive waste in purpose built repositories for solid radioactive waste*".

For the Spanish case, the scarcity of local parameters to implement these soil-to-plant transfer models could led to mask the truly transfer results.

1.5 Objectives

In the framework of the emergency preparedness and response (EPR) (IAEA, 2015a), this Thesis aims to provide useful tools to enhance the EPR plans after a radiological or nuclear emergency situation, in order to minimise the radiological consequences in the mid and long-term towards recovering, as much as possible, the former living conditions.

The ultimate aim is to improve the planification of the recovery strategies to be applied in the agricultural areas affected by a radioactive contamination, once the exposure situation has moved from an emergency to an existing one and in the transition of both stages.

The preparedness and response plans should be established in advance as set out in the EU (2013). Thus, the general objective of the present work is to develop a methodology to assess the radiological vulnerability of the Spanish agricultural systems affected by a ^{137}Cs contamination, providing, with the help of Geographical Information Systems (GIS), new tools for the EPR. The starting point has been the radiological vulnerability assessment of Spanish soils carried out some years ago (Trueba, et al., 2000a) to which the crop information and the soil to crop radionuclides transfer have been integrated. For this purpose, not only specific Spanish agricultural systems have been complied, but also the knowledge gained over the past years in the behaviour of radionuclides in soils and plants, reflected, for instance in Francis & Brinckley (1976), Cremers, et al. (1988), Mahara (1993), Tamponnet, et al. (2008), IAEA (2010), Baeza, et al. (2016), Rubio-Delgado, et al. (2017) or Guillén, et al. (2017) has been considered. The outputs will allow to identify in advance the agricultural areas of most concern, a valuable information to help in delineating the critical contaminated areas in case of a radiological deposition occurs, as it is established in the EU (2013) and, if necessary, in their recovery facing the subsequent growing seasons.

With the help of a GIS, the identification and categorization of the most radiologically vulnerable agricultural systems in peninsular Spain understood as those pairings soil – crop that, in case of an accidental release, could arise a higher risk to the population, is the main aim of the methodology applied in this Thesis. It has been tested in a case-study, which simulates a nuclear accident in Almaraz Nuclear Power Plant (NPP) with an off-site release of ^{137}Cs, among other radionuclides. The potential exposure to the ^{137}Cs deposition across the Iberian Peninsula is analysed, considering different average meteorological conditions throughout the year. That way, the most vulnerable agricultural systems are identified, delineated and categorised, allowing the prioritisation of the agricultural affected areas of most concern taking into account the meteorological seasons.

To achieve the general objective the following particular aims have been established:

- Updating the Spanish soil profile database[65] used to identify the soil properties that play a leading role in the processes that affect the behaviour of radionuclides, in this case, ^{137}Cs, in soils.
- To update the soil radiological vulnerability maps in the Spanish peninsula, defined as "*the qualitative soil potential to retain or make bioavailable for crop uptake the ^{137}Cs deposited in them*". For that purpose, the methodology designed in Trueba et al. (2000b), based on vulnerability indexes, is applied. The base map used is the last released version of the European soil map (EC-ESBN, 2004). The updated map of the *Global Radiological Vulnerability Index* for the ingestion pathway for radiocaesium is performed with the help of a GIS.
- To incorporate the crop type information and its distribution in mainland Spain. For that purpose, baseline data is used; the one related to the Spanish land use is gathered from the CORINE land cover (EEA, 2016)[66], MCA[67] (MAPA, 1980-1990; MAPA, 2000-2010) and IGN[68] (2005); the crop yield and surface occupancy are

[65] The soil classification used is FAO-UNESCO (1974).
[66] CORINE (Co-ordination of Information on the Environment Program) is managed by the European Environment Agency (EEA) and provides the land cover and land use classification for the European countries.
[67] MCA (Mapa de Cultivos y Aprovechamientos de España): Map of Crops and Utilisation of Spain.
[68] IGN (Instituto Geográfico Nacional): Spanish National Institute of Geography.

collected from MAGRAMA[69] (2016), and the Spanish administrative division is obtained from IGN (2008). A georeferenced crop type database is created to identify at each spot, the most *representative crop*, which corresponds to the one that occupies the largest cultivated area. In that task, a large amount of data must be managed, and several premises and assumptions should be defined; all of them are explained in detail in the following sections. The use of a GIS in that process is fundamental.

- The potential capacity of crops to uptake the bioavailable ^{137}Cs in soils is quantified by means of the soil-to-plant the transfer factor (F_v). The F_v values (IAEA, 2010) are considered in the methodology so that each area can be assigned its corresponding F_v value according to the topsoil properties, mainly the potassium and clay contents and the topsoil texture, and the *representative crop*. This way, the Spanish agricultural systems identification and mapping according to their radiological vulnerability, are performed. This output will allow the categorisation of the agricultural areas in those of most concern, helping decision-makers in the implementation of the recovery actions in a prioritised way. Again, the GIS software is critical in the management of all the data and in attaining the resulting maps.
- A case study based on a simulated nuclear accident in Almaraz NPP with an off-site release of ^{137}Cs is developed to test the methodology. This analysis is carried out with the results obtained from a bunch of hypothetical accident simulations along a five-year period (ANURE, 2017). These simulations have been used to map the most likely deposition pattern of ^{137}Cs and its severity, for the annual and seasonal average meteorological conditions. This task has been performed with the DSS JRODOS (KIT, 2017a) and a GIS (ESRI, 2016a). In the frame of the case study, the categorisation of the Spanish peninsular territory, in terms of the prioritised agricultural areas to act on for their recovery is obtained for annual and seasonal meteorological conditions. That categorisation seeks to focus actions in the areas of most concern to minimise the risk for the population to intake ^{137}Cs through the food chain ingestion pathway.

[69] MAGRAMA (Ministerio de Agricultura, Alimentación y Medio Ambiente): Ministry of Agriculture, Food and Environment.

2 METHODOLOGY

This chapter describes the methodology developed to assess the radiological vulnerability of the soils and the agricultural systems with respect to a ^{137}Cs contamination deposited on the ground.

The risk posed by that situation is the population exposure to ^{137}Cs internal contamination through the ingestion pathway. The methodology applied follows three main steps:

- First step: Study of the ^{137}Cs behaviour in soil to update the Soils' Radiological Vulnerability map. The first step aims to evaluate the potential of soils to make ^{137}Cs bioavailable to be uptaken by crops (Trueba, et al., 2000a; Trueba, 2004).
- Second step: Identification and distribution of crops. This step is focussed on identifying the different crop types and their distribution across peninsular Spain.
- Third step: Radiological Vulnerability assessment for the agricultural systems regarding ^{137}Cs. The categorisation and mapping of the radiological vulnerability of the Spanish agricultural systems is performed in the last step.

The results obtained from this methodology give a general overview of the different type of soils and soil – crops combinations (in the *agricultural areas*) that would be the most affected in case an accidental release and deposition of ^{137}Cs takes place in Spain or is received from abroad. Having this information in advance provides an excellent aid in the development of emergency response plans, allowing to locate and identify the agricultural areas of most concern. That should help decision-makers in the transition and the recovery phases to prioritise the remediation actions if required or establish food and/or drinking water restrictions, if needed, according to the EU (2013).

In the view of the above, the radiological vulnerability outputs for agricultural areas have been tested in a case study that emulates the deposition patterns through peninsular Spain, after a hypothetical release of ^{137}Cs from a Spanish NPP, taking into account the average seasonal meteorological conditions. Considering the *prevailing* deposition pattern of the release and the radiological vulnerability of the agricultural systems regarding ^{137}Cs, a categorisation of those of most concern allows the elaboration of prioritisation maps as a useful tool to aid in the decision-making process. These may be used in designing and in the application of the recovery strategies that will lead to minimising the radionuclide

transfer from soil to crops and, in turn, to reduce the exposure to the public to the radiological contamination and in the end, to establish "*living conditions that can be considered as normal*" (EU, 2013).

A detailed description of the methodology is developed in the following sections, including the design of the case study. All the features, databases and cartographic base maps (shapefiles and geodatabases (ESRI, 2016b)) used in each step are also described.

2.1 First step: Study of the ^{137}Cs behaviour in soil. Updating the Soils' Radiological Vulnerability map

The first step addressed in this Thesis has been the updating of the previous soils' radiological vulnerability maps performed for peninsular Spain (Trueba, et al., 2000a). The primary aim to perform that map was to assess the Mediterranean soil types role under a radiocaesium contamination event taking into account the soil processes that determine the behaviour of that radionuclide in soil, once it is deposited on them, and its potential entrance to the food chain (Trueba, et al., 2000a).

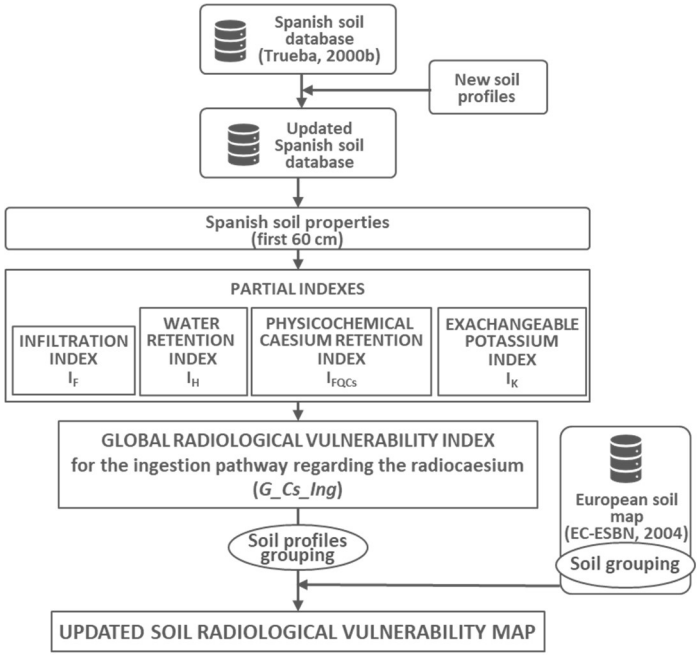

Figure 12. Workflow representing the first step of the methodology, in which the update of the existing Radiological Vulnerability maps of soils is performed.

The methodology followed uses as input data the values of the soil parameters given in the soil profiles collected in the Spanish soil database (DB) (Trueba, et al., 2000b) and requires

a soil cartographic base. In Figure 12, the methodology applied to reach that updating is reflected in a workflow.

The reasons for the current updating process have followed two main purposes. On the one hand, it was necessary to update the soil radiological vulnerability map according to the most recent European soil map (EC-ESBN, 2004). On the other hand, a thorough revision of the soil profile DB was needed to upgrade and enlarge, when possible, the profiles' density in those areas where it was insufficient.

The soil profile DB (Trueba, et al., 2000b) was performed after a huge bibliographic review of nearly 500 published references, allowing the compilation of 2176 soil profiles that included the parameters values of the soil properties at horizon level (Trueba, et al., 2000a). Unfortunately, not all of them had all the data needed for the radiological assessment purpose; nevertheless, 1655 profiles were considered as "*complete"*[70] ones for calculations. A subsequent revision of the mentioned database was done (García-Puerta, 2014)[71]; then, it was possible to recover two "complete" soil profiles which were initially excluded unintentionally, and to create a georeferenced database gathering the whole profiles set. It brought a total of 1657 "complete" and georeferenced soil profiles. That DB allowed to characterise the majority of the Spanish soil types included in the first two European soil maps used (CEC, 1985; EC, 1995). However, there were some areas in peninsular Spain with low soil profiles' density (Trueba, et al., 2015b), hindering the soil characterisation. Besides, some soil types included in the soil base map had none soil profiles in the soil DB to be linked to and vice versa (a link that is essential for the mapping purposes). That situation occurred for the 1985 European soil map version and, to a less extent, for its 1995 version. It is reasonable to think that this could be due to the map's scale, 1:1 million, in which detailed information cannot be represented and not forgetting that a map, in the end, is the result of a model which has its own uncertainties. These issues made necessary a new bibliographic revision with the intention of finding new "*complete*" soil profiles. This task has been carried out in this thesis.

[70] Soil profiles designed as "complete" are those with all the parameters necessary to perform the radiological vulnerability indexes (Trueba, et al., 2000a).

The methodology applied to evaluate the soils' radiological vulnerability takes into account a series of soil processes concerning to the food chain exposure pathway regarding radiocaesium: the soil capacity to infiltrate the water containing the radiocaesium (due to a wet deposition by rain or irrigation after a dry deposition), the soil capacity to retain water, the soil capacity to adsorb/desorb the radiocaesium in the soil matrix and the potassium nutrient capacity of soils. Radiocaesium desorption mechanisms are not considered. For this exposure pathway, the soil properties considered are those within the first 60 cm of the soil profile, as it is assumed that it is the layer where the roots are mainly developed (Trueba, et al., 2000a).

For each of these capacities, five categories showing a range of values of the soil properties involved, are defined. The influence of these categories on the behaviour of ^{137}Cs in the soil is defined qualitatively by means of indexes that determine the potentiality to make radiocaesium available.

Table 1. Soil capacities involved in the behaviour of ^{137}Cs, definition of categories for each of them and their radiological assessment.

Infiltration capacity: F		**Water retention capacity: H**		**Physicochemical retention capacity: FQ**		**Exchangeable K content: K**	
Categories of **F** (mm h^{-1})	Radiological index I_F	Categories of **R** (mm cm^{-1})	Radiological index I_H	Categories of **FQ:** soil type*	Radiological index I_{FQ}	Categories of exchangeable **K content** ($cmolkg^{-1}$)	Radiological index I_K
F≤1.0	1: Min.	R≤2.0	1: Min.	Clay 2:1 non expansive	1: Min.	K>1.0	1: Min.
1.0<F≤5.0	2: Low	2.0<R≤3.0	2: Low	Clay2:1 expansive	2: Low	0.50<K≤1.0	2: Low
5.0<F≤20.0	3: Medium	3.0<R≤4.0	3: Medium	Clay 1:1	3: Medium	0.25<K≤0.50	3: Medium
20.0<F≤50.0	4: High	4.0<R≤5.0	4: High	Peat	4: High	0.10<K≤0.25	4: High
F>50.0	5: Max.	R>5.0	5: Max.	Sand	5: Max.	K≤0.10	5: Max.

Min.: Minimum.
Max.: Maximum.
* Since the clay type is not indicated in the soil DB, the cation exchange capacity of the clays is assessed and from that, the clay type content is derived (Trueba, et al., 2000a).

Table 1 shows the categories defined for each soil capacity[72], their range values, the radiological vulnerability index associated and its meaning (Trueba, et al., 2000a).

The *Infiltration Capacity* (*F*) is defined in terms of water seep rate into the soil per time unit (Porta, et al., 2003). This soil property is mainly led by the soil texture, but also by its structure and its cation exchange capacity (CEC). A soil with a very high *F* will easily allow the entrance of the water containing the radiocaesium, reaching the rooting zone and giving rise to a maximum vulnerability index (I_F), that is the maximum potentiality to make radiocaesium available by crops.

The *Water Retention Capacity* (*R*) reflects the soil's water storage capacity within its pores. According to the methodology followed (Trueba, et al., 2000a), this soil property is assessed through the named "*water's maximum admissible reserve*", which considers the porosity, the field capacity and the soil permeability. In this case, high water retention capacity will favour the radiocaesium dissolved in it to be absorbed by the crops' roots giving rise to high vulnerability indexes (I_H).

The sorption/desorption of ^{137}Cs to the soil matrix is measured by the P*hysicochemical Caesium Retention Capacity* (FQ_{Cs}) that depends on its cation-exchange capacity, highly related to clay content and the type of clay. When the soil mineral phase shows a small number of exchange sites, the radionuclides remain free to be absorbed by the crop roots and the transfer potential of those soils increases, giving rise to maximum vulnerability indexes (I_{FQCs}). That is what usually occurs in low clay content soils, such as sandy soils. On the contrary, the higher the clay content, the higher the number of exchange sites and the greater the ability to fix the radionuclides in a more or less interchangeable manner and the lower their transfer potential, which leads to lower vulnerability indexes (I_{FQCs}). Regarding the clay types, the following are the clay structures ranked from higher to lower transfer potentiality: 1:1[73], 2:1 non-expansive and 2:1 expansive (Trueba, et al., 2000a).

[72] The soil capacities are identified with their corresponding abbreviation in Spanish.

[73] Clay structure types: i) 1:1: a tetrahedral layer linked to an octahedral (TO), for instance, kaolinite; ii) 2:1 one octahedral layer between two tetrahedral layers (TOT), such as illite, smectite and vermiculite (Ayala, et al., 1986).

Regarding the last soil capacity, the *Potassium Nutrient Capacity*, it refers to the similar behaviour of the exchangeable K and the radiocaesium on soils, as competitors for the exchange sites: the more exchangeable potassium content in the soil thickness considered, the lesser the competition for the root absorption of radiocaesium and the lesser its entrance to the plant, giving rise to minimum vulnerability indexes (I_K) (Trueba, et al., 2000a).

The indexes related to each one of these individual soil capacities were named "*partial soil radiological vulnerability indexes"*. Their combination to evaluate the full potential of soils to exhibit bioavailable ^{137}Cs to be uptaken by crops is defined as the *soil's* "*Global Radiological Vulnerability Index*" (*G_Cs_Ing*)[74]. This index is obtained from the sum of the four "partial indexes" and the reclassification of the resulting values in order to have, again, a five-category index (see Table 2) which represents the *Global Radiological Vulnerability Index* for the ingestion pathway regarding the radiocaesium.

Table 2. Categories of the radiological vulnerability index of soils (G_Cs_Ing[75]).

Index category description	G_Cs_Ing Index value	Colour mapping
Minimum	1	Dark blue
Low	2	Clair blue
Medium	3	Green
High	4	Yellow
Maximum	5	Red

The ranges given to this global index are shown in Table 3 and are interpreted as the potential of the soil (ranged from the minimum value (1) to the maximum (5)) to make the ^{137}Cs bioavailable to crops).

[74] The abbreviation of the partial indexes remained as they were initially defined (Trueba, et al., 2000a), although the global one has been identified differently in order to adapt it into English for a better understanding along with this Thesis. The original denomination of the *Global Radiological Vulnerability Index for the ingestion pathway regarding the radiocaesium* was *T_CA_Cs*, from the Spanish: *Índice Total para la Cadena Alimentaria respecto al Cesio*.

[75] The radiological vulnerability categories have been mapped preserving the original colours attributed in Trueba, et al., (2000a), in order to facilitate the comparison of the results with respect to the outcomes of the previous maps.

Table 3. Reclassification criteria to obtain the Global Radiological Vulnerability Index for the ingestion pathway for caesium (Trueba, et al., 2000a).

Global Radiological Vulnerability Index value for caesium and for ingestion (*G_Cs_Ing*)	**Ranges from the sum of the partial indexes**
1: Minimum	4 – 6
2: Low	7 – 9
3: Medium	10 – 12
4: High	13 – 16
5: Maximum	17 – 20

The assessment of the *G_Cs_Ing* index has been carried out for each soil profile contained in the updated DB (regardless of whether they can be mapped in the soil base map or not).

The partial and global indexes estimated for each soil profile individually do not give by themselves an overall idea of how the different peninsular soils are categorized concerning their radiological vulnerability to ^{137}Cs. These results need to be spatially distributed throughout peninsular Spain. In a first attempt to perform the updated map, interpolation methods were applied (García-Puerta, 2014). However, the lack of soil profiles in some large areas, in addition to the characteristics of the statistical distribution of some soil parameter values collected in the soil profile DB (which do not follow a normal or log-normal distribution), hinder to perform proper and continuous maps by interpolating the soil properties at a peninsular scale, for instance, by the kriging interpolation method (Oliver, 1990; Montero, et al., 2015).

This circumstance brings to follow the approach designed in Trueba, et al. (2000a) and Trueba, et al. (2004), also applied in García-Puerta (2014), in which a soil cartography support basis was used. For this purpose, it would have been more appropriated to use a specific Spanish soil map; however, such information was not available in the appropriate format at a national scale when the first radiological vulnerability maps were developed (Trueba, et al., 2000a), nor it is nowadays[76]. Indeed, the existing Spanish soil maps of the autonomous communities[77], when available, have partial information and not equivalent among each other or they are not digitalised. Instead, that lack of homogenized Spanish soil cartography regarding scale, soil classification, and format lead up to using the

[76] A Spanish soil map was issued in 2006 in paper format: *Mapa de suelos de España: Escala 1:1.000.000 [Material cartográfico] Instituto Geográfico Nacional; autor de la información temática, Vicente Gómez-Miguel (UPM); col. Área de Banco de Datos de la Naturaleza (Ministerio de Medio Ambiente). Escala 1:1.000.000 Instituto Geográfico Nacional, Madrid, 2006.*

[77] NUTs II (Eurostats, 2015).

European soil map in the first radiological vulnerability studies in Spain (Trueba, et al., 2000a; Trueba, 2004), in particular, the European soil map in force at the time the first maps were performed (CEC, 1985). In this Thesis, the last European soil map version (EC-ESBN, 2004) is the cartography adopted.

The approach designed in Trueba, et al.,(2000a) to represent the radiological vulnerability of soils consists in searching for a link between the soil profiles of the DB, on which the radiological vulnerability have been estimated, and the Soil Mapping Units (*SMU*s) included in the European soil map (EC-ESBN, 2004). To obtain that link, firstly, the soil profiles of the DB are grouped according to their soil classification (FAO-UNESCO, 1974). In turn, those groups comprised of soil profiles laid on a wide variety of bedrocks are split into separate groups according to their bedrocks. That way, different *soil groups* are obtained and their corresponding database is created. The same procedure is done with all the *SMU*s, regarding the classification of their dominant *Soil Typological Unit* (*STU*) (EC-ESBN, 2004) and their bedrock. A unique identifier (*ID*) is created for each pair: *soil type classification – bedrock*; thus, both: the soil groups DB and the base map can be linked through that *ID* to create, by using a GIS, a polygon feature or shapefile layer which contains the soil groups performed and their characteristic parameters associated.

As said before, the *Global Radiological Vulnerability Index* for the ingestion pathway regarding the radiocaesium (*G_Cs_Ing*) is assessed for each soil profile included in the soil DB considering the four partial indexes. The representative value of this index for each soil group is the mode value of the *G_Cs_Ing* indexes of the soil profiles included in each one. In case the mode value repeats in more than one index category, the highest index value is selected. A database gathering the *G_Cs_Ing* of the whole soil groups listed is created.

Using a GIS software (ESRI, 2016a), the *G_Cs_Ing* index can be represented by linking the soil groups' DB containing the vulnerability index value attributed to each soil group, with the European soil base map (EC-ESBN, 2004)[78], using the Join tool (ESRI, 2016a) through the common field *ID* (corresponding to the *soil type classification – bedrock* pair*)*. The resulting map is shown in section 3.1 (see Figure 30).

[78] The European soil base map (EC-ESBN, 2004) is a polygon shapefile (vector data format).

It is important to state that the soil groups' database connected to the updated radiological vulnerability map includes, besides the radiological vulnerability indexes that have been recalculated, the average soil parameter values of each soil type group. Thus, this new map is used as the base to assess the indexes needed to perform the last step of the methodology.

2.2 Second step: Identification and distribution of the crops throughout peninsular Spain

The identification and distribution of the agricultural systems in Spain and the assignation of a *representative crop* to each cultivated place constitutes the second step of the methodology proposed. That is an essential feature since the nutrients root uptake process for each plant species has its own metabolic mechanisms, which leads to different root uptake capacities, depending on the chemical element (Nishita, et al., 1961; Smolders & Shaw, 1995; Tamponnet, et al., 2008).

The workflow followed to perform the crops' distribution and, eventually, choose the representative crop, is shown in Figure 13.

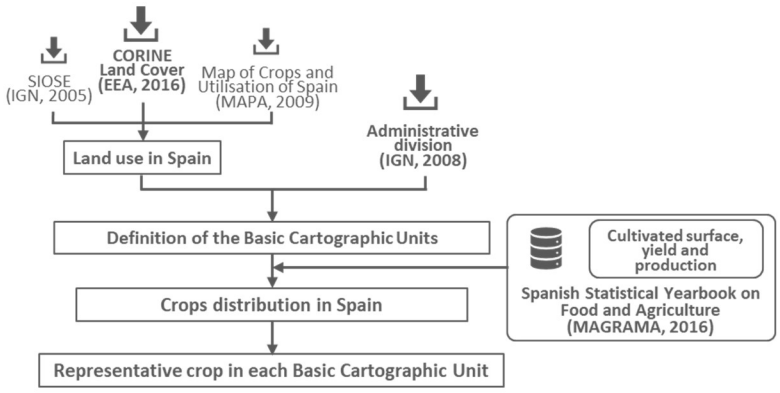

Figure 13. Workflow followed to perform the crops' distribution and to select the representative crop.

In the following subsections, the information needed to define the *representative crop* and the criteria used to choose it are developed.

2.2.1 Basic information data to perform the crops assignment

The crops' distribution is made on the base of the following data: i) the Spanish administrative division, ii) the land use, and iii) the Spanish crops classification.

i) Spanish administrative division

The geographical features used for the administrative divisions of peninsular Spain are included in a polygon shapefile obtained from the Spanish national cartographic base (IGN, 2008).

Apart from the three Territorial Units for Statistics levels (NUTs, abbreviated in French: Nomenclature des unités territoriales statistiques) (Eurostats, 2015)[79] (I: Autonomous Community Aggrupation, II: Autonomous Community (CA), III: Province), Spanish administrative division comprises two official lower levels: the municipalities[80], considered as Local Administrative Units (LAU) (Eurostats, 2015) and a specific Spanish administrative municipalities gathering: the rallied territories (in Spanish "terrenos mancomunados" (IGN, 2008)); two or more municipalities manage the latter. Both, municipalities, and rallied territories, have each particular unique identifier code, the Spanish five-figures code (INE, 2019)[80]. The territorial unit to be considered in this Thesis is the municipality since it is the administrative level on which the preparedness and response in an emergency situation is addressed in Spain (PLABEN, 2004). To avoid rallied territories to be excluded in the crop sharing, these have been included in the largest municipality which manages them. This inclusion can be done merging the main municipality and its corresponding rallied territory (Merge tool of (ESRI, 2016a)).

Thus, an administrative base map of peninsular Spain is obtained, in which the minimum unit corresponds to the municipalities.

The list of provinces (NUTs III) and the location of each one are shown in Annexe I.

[79] An updated version of the European administrative units' map entered into force on 08 August 2019. It includes the sixth regular amendment to the annexes adopted by Commission Delegated Regulation 2019/1755. https://ec.europa.eu/eurostat/web/nuts/nuts-maps

[80] The municipalities are encoded with their INE code, which is composed of five figures, where the first two correspond to the province code. For instance, the first listed municipality is Alegría-Dulantzi, in Alava province (province code: 01), and its code is 01001 (INE, 2019).

ii) Land use

Following the initial approach used in VULNES Project (Trueba, et al., 2003), this Thesis has used the Corine Land Cover (CLC)[81] map (EEA, 2016)[82] to identify the cultivated areas throughout peninsular Spain for the agricultural radiological vulnerability assessment. The objective is to list the different crops that are grown in each spot and, among them, identify the most representative one. The CLC was selected as the crop's distribution base map because as it is a European georeferenced database, the methodology developed in this Thesis may be applied all over the continental area; that way, homogeneous results throughout Europe can be obtained.

CLC classifies the European earth surface in five main classes (from 1 to 5) and these are, in turn, classified into two more levels of detail land use information; thus, there are 44 CLC classes in total. The first and the second land use classification levels for each of the five main classes are shown in Table 4. The classes included in the third land use level are exposed, exclusively for "*Agricultural areas*", in Table 5, and for "*Forest and semi-natural areas"*[83] in Table 6.

[81] CLC is a simplified representation of the territory, which reflects the landscape and the land use features interpreted at scale 1: 100 000 (with minimum mapping unit – MMU– 25 hectares and 100 m of minimum width for linear elements) by means the analysis of high-resolution satellite images (EEA, 2016). The images used to perform the 2016 version were provided by the European Space Agency (ESA) in 2011 and 2012 under the GIO Project (GIO, 2011).

[82] Although there is a recent version of the CLC map (EEA, 2019) all the work carried on has been done with the 2016 issue.

[83] "*Forest and semi-natural areas*" have been used in the crops' distribution, along with the "*Agricultural areas*".

Table 4. First and second information level for agricultural and forest land use. (EEA, 2016)

1 Artificial areas
Class 1.1 Urban fabric
Class 1.2 Industrial, commercial and transport units
Class 1.3 Mine, dump and construction sites
Class 1.4 Artificial non-agricultural vegetated areas
2 Agricultural areas
Class 2.1 Arable land
Class 2.2 Permanent crops
Class 2.3 Pastures
Class 2.4 Heterogeneous agricultural areas
3 Forest and semi-natural areas
Class 3.1 Forests
Class 3.2 Shrubs and/or herbaceous vegetation associations
Class 3.3 Open spaces with little or no vegetation
4 Wetlands
Class 4.1 Inland wetlands
Class 4.2 Coastal wetland
5 Water bodies
Class 5.1 Inland waters
Class 5.2 Marine waters

Table 5. Third information level for agricultural land use. (EEA, 2016)[84]

CLC code	Name
211	Non-irrigated arable land
212	Permanently irrigated land
213	Rice fields
221	Vineyards
222	Fruit trees and berry plantations
223	Olive groves
231	Pastures
241	Annual crops associated with permanent crops
242	Complex cultivation patterns
243	Land principally occupied by agriculture, with significant areas of natural vegetation
244	Agro-forestry areas

Table 6. Third information level for forest and semi-natural areas. (EEA, 2016)

CLC code	Name
311	Broad-leaved forest
312	Coniferous forest
313	Mixed forest
321	Natural grassland
322	Moors and heathland
323	Sclerophylous vegetation
324	Transitional woodland/shrub
331	Beaches, dunes, and sand plains
332	Bare rock
333	Sparsely vegetated areas
334	Burnt areas
335	Glaciers and perpetual snow

The crops potentially grown in each land use are assigned according to the specifications given in (EEA, 2016).

[84] In the mainland Spain, the cultivated surface, the one classified as "Agricultural area" (assigned in the first information level with number 2) (EEA, 2016) is around 232000 km^2, meaning a 47 % of the total Spanish peninsular surface area.

Nevertheless, there is some specific information in Spain regarding land use which is worth to be taken into account, i.e. the Map of Crops and Utilisation of Spain (in Spanish: Mapa de Cultivos y Aprovechamientos – MCA) (MAPA, 2000-2010) and the Land Use Information System of Spain (in Spanish: Sistema de Información de Ocupación del Suelo en España – SIOSE) (IGN, 2005).

Only "*Agricultural areas*" (land use class number 2) and, when necessary, "*Forest and semi-natural areas*" (land use class number 3) (EEA, 2016) are the categories in which crops have been distributed. Indeed, "*Agricultural areas*" should be the unique land use to be selected to allocate the representative crops, however, after comparing CLC (EEA, 2016) with SIOSE (IGN, 2005), and then with MCA (MAPA, 2000-2010), it was necessary to consider some "*Forest and semi-natural areas*" CLC classes. This comparison was made province by province, while the crops' sharing was conducted.

CLC (EEA, 2016) is presented as a polygon feature included in a geodatabase (ESRI, 2016b); thus, the land use can be managed as a single layer amongst the rest of the information considered with the GIS software used (ESRI, 2016b).

iii) Spanish crops classification

The Spanish Statistical Yearbook on Food and Agriculture (MAGRAMA, 2016)[85] is the database consulted to identify the cultivated crops in the country. It collects the agricultural information yearly including the cultivated area (in hectares), the production (in tonnes), and the yield (in Kg/ha), aggregated by province. However, it has no georeferenced data. Thus, it is necessary to treat this agricultural information to be georeferenced and what is more, to disaggregate it by municipalities. In order to do so, a management of the administrative, agricultural and land use data has been carried out.

Regarding the Spanish crops, the distribution process requires to perform a previous crops' codification; thus, each crop (MAGRAMA, 2016) has been encoded with a unique identifier

[85] The Spanish agricultural information is gathered in chapter 13: Food and Agriculture of the Statistical Yearbook, which is yearly issued, aggregated by province (NUTs III level).
By the time the tasks related to the agricultural information management had begun within this Thesis, the agricultural statistics available correspond to 2014 (MAGRAMA, 2016). The subsequent years the corresponding yearly statistics were launched.

named *IDentifier for Product* (*IDPR*). The *IDPR* reflects the general type of crop (arable: *A*, and non-arable: *W* (woody)) and the crop's group (MAGRAMA, 2016) it belongs. Table 7 shows a summary of the main crops' categorisation. Annexe II contains the whole list of crops in the statistics with its unique *IDPR* code.

Table 7. Main groups of crops included in the first level of the agricultural structure in Spain, gathered in the Statistical Yearbook on Food and Agriculture (MAGRAMA, 2016).

Crop type	First level of IDPR	Crops
Arable crops	A10000	Grain Cereals
	A20000	Grain Legumes
	A30000	Tubers
	A40000	Vegetables
	A50000	Industrial Crops
	A60000	Fodder Crops
Non arable crops (Woody)	W10000	Fruit Trees
	W20000	Vineyard
	W30000	Olive Grove
	W40000	Other Woody Crops

There are 133 different *IDPRs* all over Spain (MAGRAMA, 2016). Besides, depending on the crop type, several sub-classes according to the cultivation system (such as dry or irrigated land) are distinguished. The codes designed in this Thesis for the main sub-classes, based on the cultivated surface, separately for arable and for non-arable crops, are included in Table 8.

Table 8. Cultivated sub-classes surface area included in (MAGRAMA, 2016) for arable and for non-arable crop areas. Measure units are included.

MAGRAMA Crop Type (Code)	Cultivation System (CS)		IDentifier for the Cultivation System (IDCS)(1)	Units	Description
ARABLE (A)	Dry land	Harvested	DA/da	Ha.	Dry Area
		Grazed	DGA/dga	Ha.	Dry Grazed Area. (Only for fodder crops)
	Irrigated land	Free	FIA/fia	Ha.	Free Irrigated crop Area
		Sheltered(2)	SIA/sia	Ha.	Sheltered Irrigated crop Area
		Grazed	IGA/iga	Ha.	Irrigated Grazed Area. (Only for fodder crops)
	Total Area		TA/ta	Ha.	Total crop Area. (Only for rice crops)
NON-ARABLE (W)	Dry land		DRAP/drap	Ha.	Dry Regular plant Area, in Production
	Irrigated land		IRAP/irap	Ha.	Irrigated Regular plant Area, in Production
	Total Area		TRAP/trap	Ha.	Total Regular cultivated Area, in Production (Only for citrus fruit trees)
	Scattered trees		STP/stp	No. of trees	Scattered Trees, in Production

(1) *IDCS*, in capital letters, is used to identify crops in their corresponding provinces, according to MAGRAMA (2016) data and *idcs*, in lowercase letters, is reserved for the crops shared among the municipalities.
(2) Since the worst-case scenario has been considered for a direct deposition from a radioactive plume, sheltered crops have been regarded as non-sheltered ones.

It is important to state that for non-arable crops (woody crops) only the cultivated areas recognised as "productive"[86] (MAGRAMA, 2016) ones have been taken into consideration to perform the crops' distribution. That way, the production (kg or tn) is in accordance with the relation cultivated area– yield.

Eventually, considering the crops' classifications indicated above, 241 sub-classes for arable crops and 99 for non-arable crops are obtained. Each of them is encoded by using the *IDPR* followed by the *IDCS* (*IDPR*+*IDCS*). For instance, the codes for rainfed wheat and irrigated olives for oil correspond to *A11010DA* and *W31020IRA*, respectively (see Annexe II). All of these are the ones to be shared across the territory: initially within provinces (by using capital letters for each crop code) and then within municipalities (by using lowercases); for example, for the crops mentioned above their crop codes in the LAUs are *a11010da* and *w31020ira*, respectively.

2.2.2 Distribution of the crops and identification of the representative crop

Once all the necessary data is collected, the crops' distribution can be done with the eventual aim to identify the *representative crop* in each cultivated place.

CLC (EEA, 2016) has been used as the base map to distribute that wide variety of agricultural products within the peninsular provinces. The general correspondence between the Spanish crops (identified by its unique crop identifier code: *IDPR*+*IDCS*) and the land use classes where they can be grown is included in Annexe III[87]. This correspondence has been done following the criteria established in (EEA, 2016) for each land use category. As said before, the particular crops' assignment to each spot also takes into account the information provided in MCA (MAPA, 2000-2010) and SIOSE (IGN, 2005).

Because the Spanish crop database (MAGRAMA, 2016) has the information aggregated by province, the crop distribution is done province by province in such a way that each crop is associated with its corresponding land uses among the ones that exist in that NUT III administrative division.

[86] Productive crops are those trees plantations which, after their growing period, already produce fruits to be marketed.
[87] The land use codification, according to EEA (2016), is included in section 2.2.1.

In many cases, the same crop can be grown in different land uses, so a proportional distribution based on the cultivated surface in the province (MAGRAMA, 2016) and the different land uses' surface where it can be grown (EEA, 2016) is done. At the same time, several crops can be cultivated in the same land use. However, after directly applying a proportional surface distribution in the province's land uses, it frequently occurs that more cultivated hectares are associated with a land use than its own surface. On the other hand, there are some land uses in which natural vegetation is mixed with crops, such as those named as "*Land principally occupied by agriculture, with significant areas of natural vegetation*" (CLC code *243*) or in "*Agro-forestry areas*" (CLC code *244*) (EEA, 2016). In those areas, it may occur that, only a small proportion is cultivated; in these cases, the proportional sharing could lead to excessive crop allocation. Therefore, both factors should be taken into account to obtain a proper crops' distribution.

In order to avoid the over-occupancy of the land and an excessive allocation of crops in some land uses, the following general criteria are assumed to perform the provinces' crop distribution:

- On the one hand, the crops grouped in the *IDPR*s: *A10000*, *A20000*, *A30000*, *A50000* and *A60000*, (see Table 7) are, by far, the ones that cover most of the arable areas in the Spanish peninsular provinces. On the other hand, land uses coded as *211*[88] and *212*[89] correspond to the two largest areas for arable crops no mixed with woody ones. These cover 43 % and 10 % out of the total surface classified as agricultural in the Spanish Iberian Peninsula according to EEA (2016), respectively. Thus, 90% of the cultivated surface of the crops that proportionally would be linked to land uses different from *211* (non-irrigated) or *212* (irrigated), is added to them. Only 10 % of the surface attributed proportionally remains in the rest of the land uses in which they may be grown. This way the *211* and *212* CLCs, are filled as much as possible with arable crops; otherwise, these would be quite empty, while the rest of the arable crop's land uses would be extremely packed or even over-occupied. In case the 10 % remaining in the initially selected

[88] CLC 211: "*Non-irrigated arable land*".
[89] CLC 212: "*Permanently irrigated land*".

land use is under 5 ha, all the crop's surface is added to the *211* land use if it is a rainfed crop, or, if it is grown under irrigation, to the *212 CLC*.

- For Vegetables (*IDPR*: *A40000*), which have shorter cultivation periods and, usually, significatively smaller cultivation surface areas comparing to the rest of the arable crops, 1 ha is the minimum surface to remain within the land uses that would correspond them by a proportional distribution; smaller surfaces are added to *211* or *212*, as the case may be. That way, as is the case for the rest of the arable crops explained in the previous point, extremely small crops' surface to distribute among the municipalities is avoided.
- According to (MAPA, 1980-1990) around 43% of the *244*[90] land use which corresponds to "dehesas" in Spain (a typical Mediterranean ecosystem) is occupied by arable crops in Cáceres province. Thus, taking into consideration that this province has one of the largest *244* land use in Spain (440488.53 ha (EEA, 2016)), this ratio will be the value to consider as maximum for arable crops in this kind of land use.
- Land uses not specific for agricultural uses, such as *311*[91], *312*[92], *321*[93] and *324*[94] have been considered to be used for the general non-arable (W) crop-sharing, according to what is shown in SIOSE (IGN, 2005) and MCA (MAPA, 1980-1990; MAPA, 2000-2010). The most occupied non-agricultural land use is the one coded as *311;* walnuts and chestnuts are the main crops associated with that land use. The rest of the non-agricultural land uses are very occasionally occupied by crops; such is the case of the olives for oil[95], which has been associated with the land uses *312*, *321* and *324* in Tarragona province for the first one and Cáceres province for the last two land uses. Thus, cases like these are treated as exceptions.

Once these criteria are applied, it is checked that the total cultivated crops' surface associated with each land use class is not higher than its own surface within each province. If it occurred, proper adjustments in the crops' hectare rate must be made to eliminate the

[90] *CLC 244*: "*Agro-forestry areas*".
[91] *CLC 311*: "*Broad-leaved forest*".
[92] *CLC 312*: "Coniferous forest".
[93] *CLC 321*: "*Natural grassland*".
[94] *CLC 324*: "*Transitional woodland/shrub*".
[95] Olives for oil. *IDRP*: *W31020*.

over-occupation. That is performed by reducing the crops' percentage of the surface attributed to the saturated land use and increasing the crops' percentage in the rest of land uses where those crops can be grown[96].

The SIOSE (IGN, 2005) and MCA (MAPA, 1980-1990; MAPA, 2000-2010) maps have been consulted to identify specific crop's allocation; for instance, that is the case for cherries in Cáceres province which are in the areas classified as *311* in CLC.

Then, from the proportional crop distribution and the needed adjustments a new database which includes all the possible crops that can be grown in each land use category, within each province, is created.

As it was pointed out before, it is necessary to obtain the crops' distribution disaggregated by LAU: municipalities. Thus, the next step is to distribute the crops proportionally in each municipality (within each province), attending to their cultivated surface and the surface of the land use. Besides, there are small spots in which very local crops are grown, such as cherries in Caderechas Valley (in the North of Burgos province) or peppers to make paprika in La Vera region (in the Northeast of Cáceres province). By assigning these particular crops to their corresponding municipalities, local agricultural specificities are considered within each province.

This methodology provides a database that comprises all the possible crops potentially grown in each land use, at municipal level, in peninsular Spain.

In order to obtain the corresponding map to reflect the municipalities crop's distribution, the following steps have been taken. To automate these steps for all the provinces to be analysed, a geoprocessing workflow has been created by using Model Builder (ESRI, 2016c). The corresponding chart is shown in Figure 14, and hereafter the sequence of the geoprocesses to obtain the ultimate representative crop's map in peninsular Spain is described.

- First, CLC map (EEA, 2016) is clipped (using the "Clip" tool (ESRI, 2016a)) by the previously selected province (IGN, 2008) to be analysed. Then, the municipalities

[96] That adjustments have to be done province by province.

divisions map (IGN, 2008) and the CLC map (EEA, 2016) are overlapped, by using the "Identity" tool (ESRI, 2016a); this way, a new polygon vector layer is built. This layer is a single-part geometry feature class[97], where each feature (each polygon) corresponds to a municipality – land use class combination which is identified with a unique code-named "*mun_clc*". The "*mun_clc*" is considered as the *basic cartographic unit* in the municipality crops-sharing.

- The duplicated or useless attribute fields obtained as a result of the previous geoprocesses are removed from the associated table.
- A new field is added to build a unique identifier for the province – land use combination, named "*clc_pr*". The surface of these features is calculated by using the "Calculate Geometry" (Area) function in ArcMap (ESRI, 2016a). That surface (in hectares) is the one to be considered in the proportional crop sharing process for each province.
- The aim of the last set of geoprocesses is obtaining a multipart feature class with a unique identifier for each *basic cartographic unit* ("*mun_clc*"), in which the records of the multipart layer may contain information of several independent geometric entities (polygons with the same land use in the same municipality). To do that, first, the "Dissolve" tool (ESRI, 2016a) is used.
- Then the polygon set's surface of each record (each *basic cartographic unit* – "*mun_clc*") is calculated with the "Calculate Geometry" (Area) function in ArcMap (ESRI, 2016a), in a new field named "*Ha_mun_clc*", in hectares. This way, the extent of the land use in each municipality is attained, regardless of whether the land use class is distributed in several polygons.

[97] In a single-part polygon geometry feature class each set of attributes (a record) corresponds to a single polygon, while a multipart polygon geometry feature class is a feature in which one record references more than one polygon.

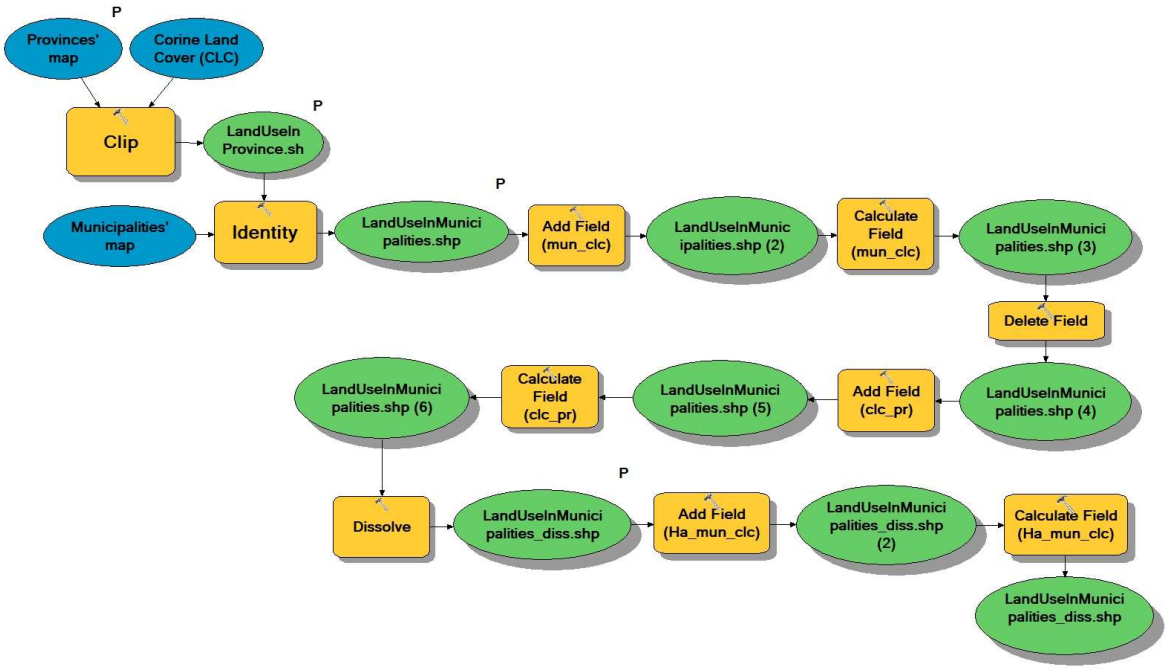

Figure 14. ModelBuilder (ESRI, 2016c) workflow designed to obtain a base map to be linked with the crops' distribution database.

Thus, the base map to represent the crops potentially grown in each municipality's land use is obtained, and the surface for each set of cartographic units, such as "*clc_pr*" (necessary to perform the crops' distribution along with the provinces) and the *basic cartographic units* (*mun_clc* – to distribute the crops into the municipalities) is known.

Once the surface area of each *clc_pr* feature is obtained, the proportional crop-sharing can be done in each province, applying the criteria described before; afterwards, the proportional distribution among its municipalities is carried out for each *mun_clc* feature. A database gathers the municipalities' crop-sharing for each province, in which each record corresponds to each *basic cartographic unit*.

In order to link the CLC base map and the database with the crops' distribution within the municipalities of each province, the "Join" tool (ESRI, 2016a) between both is applied by using the common field "*mun_clc*". The resulting feature (included in a geodatabase – ESRI, 2016b) and its associated attributes' table collect a bunch of different crops that may be grown in each land use within each municipality, in terms of potentiality: for each crop, a proportional cultivated surface in each land use within each municipality of the province is given. In order to obtain the *representative crop* within each "*mun-clc*", its assigned crops

are ranked by its shared cultivated surface, then, the crop with the largest one is chosen as the *representative crop* of the *basic cartographic unit*.

After carrying out this process province by province, a feature with the crop-sharing per province is obtained. In order to have a single feature class gathering all the crops across peninsular Spain, a feature in the geodatabase (ESRI, 2016b) is created by compiling the individual provinces ones; then a "*merge*" (ESRI, 2016a) is done with all of them. Thus, one feature class representing all the crops which are potentially grown in each *basic cartographic unit* across peninsular Spain and their *representative crop* is attained, as shown in Figure 34 included in section 3.2.

2.3 Third step: Radiological vulnerability assessment of the agricultural systems in peninsular Spain regarding ^{137}Cs

In this step, the radiological vulnerability assessment focuses on farming areas referred to the susceptibility of a cultivated area, potentially affected by a ^{137}Cs deposition, to transfer it to crops and therefore, to incorporate them into the human food chain. This methodological step combines the specific topsoil properties that influence the soil's capacity to store the ^{137}Cs with the crops' susceptibility to absorb that radionuclide through roots; in other words, it shows the behaviour of the ^{137}Cs in the soil-plant system.

The ^{137}Cs behaviour is key "*in understanding the risk of food-chain contamination*" (Vandebroek, 2012). According to Dubchak (2017), Cs^+ has limited vertical mobility; thus, it makes ^{137}Cs remain in the upper 5 or 20 cm soil's horizon, after its deposition, which coincides with the low vertical migration rates analysed in agricultural mineral soils (Almgren & Isaksson, 2006). Therefore, in this approach regarding the study of the radiological vulnerability of the Spanish agricultural systems, grown mainly in mineral soils, it has been assumed that the soil properties to be taken into account are those related to the first soil horizon (topsoil), where the plant's roots are mainly developed, especially for the arable crops and where the ^{137}Cs is mainly retained in soil (Legarda, et al., 2011).

Considering the assessment carried out in the first step of the methodology, the third step assumes that ^{137}Cs has already entered the soil and equilibrium or quasi-equilibrium conditions have been reached in the soil-plant system (IAEA, 2010).

The processes considered in this methodological step that take place in soil affecting the transfer of the radionuclides to crops are the radiocaesium soil sorption capacity and those related to the K nutrient status capacity. Therefore, the topsoil properties involved are the clay content, the exchangeable potassium content, and the soil texture.

As previously mentioned, the *representative crop*, defined as the one that occupies the largest surface area in each *basic cartographic unit*, will be taken as the characteristic of the agricultural system.

The radionuclides' transfer from soil to crops is quantified by means of the soil-to-plant transfer factor (F_v); this concept is based on the existence of a relationship between the contents of a radionuclide in the soil and in the plant, which depends on the type of radionuclide (^{137}Cs, in this Thesis), the soil type, and the crop type (IAEA, 2010).

From the soil side, the methodology developed in this Thesis assumes that a limited potassium reservoir in soils would eventually favour the presence of bioavailable ^{137}Cs over time, with whom it competes. This reservoir is determined by the K content, the clay content, and the soil texture. From the crop side, the *representative* one within each *basic cartographic unit*, jointly with the topsoil texture in which it grows, allows choosing the corresponding *transfer factor* value, according to (IAEA, 2010). For both features the corresponding indexes (intermediate indexes) are assessed by using numerical data, called respectively, *Radiocaesium Reservoir Index* (*I_Cs*) (obtained from the *Potassium Reservoir Index – I_K*), and *Transfer Factor Index* (*I_TF*). Thus, a semiquantitative analysis of the ^{137}Cs transfer from soil to crops is designed (quantitative parameter values are reclassified in qualitative indexes (Poljanšek, et al., 2017)). The combination of both allows identifying, categorising, and mapping the so-called *Radiological Vulnerability Index* of the agricultural systems (*I_RV*), which reflects the potential ^{137}Cs entrance to the food chain in the subsequent seasons after a deposition event.

The diagram corresponding to the workflow followed in the third step of the methodology to obtain the *Radiological Vulnerability of the agricultural systems* in Spain is shown in Figure 15, jointly with the two other methodological steps previously mentioned (in grey).

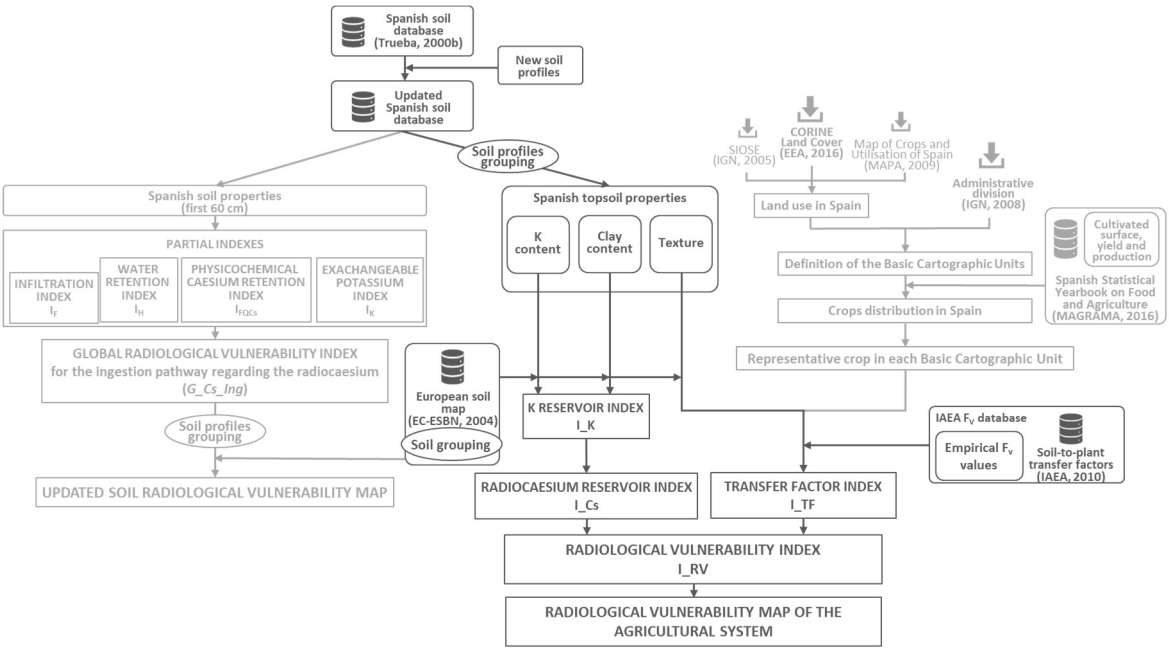

Figure 15. Workflow representing the third step of the methodology to obtain the Radiological Vulnerability Index of the agricultural systems and its mapping. First and second steps have been displayed in light grey, in order to show the link between those and the third step of the methodology.

Next sections describe the methodology applied to obtain the different intermediate indexes to define the eventual *Radiological Vulnerability* regarding ^{137}Cs for agricultural areas.

2.3.1 Definition of the Potassium Reservoir Index (I_K) and the corresponding Radiocaesium Reservoir Index (I_Cs)

As previously mentioned, due to their physicochemical similarities, radiocaesium competes with exchangeable K^+ for the clay binding sites (Absalom, et al., 1999) taking part in both, the adsorption/desorption in soil (being the desorption influenced by the strength of the fixation (Kirkby, et al., 2001) and the crop roots absorption/uptake processes. When the soil exhibits a high pool of exchangeable potassium within its mineral fraction (mainly clays), it is more likely to have a high concentration of this element in the soil solution, reducing the potential ^{137}Cs uptake by crops (Nisbet, et al., 1993).

The dominant type of clay gives the real measure of that behaviour as they show different exchange sites with different characteristics. However, this information is not available in the Spanish soil profile DB. Therefore, a relationship between average potassium and clay content of each soil group is used to classify the potential potassium pool or reserve in soils.

A categorisation based on the level of K soil fertility, considering its extraction within different clay contents (Domínguez Vivancos, 1997)[98] is set for that purpose. Table 9, collects the levels of exchangeable K content in soil (cmol·Kg^{-1}), depending on the clay percentage, which define the K soil fertility and are assumed to represent the potassium reserve in soils. That categorisation is used as the reference to establishing the *Potassium Reservoir Index* (*I_K*) in the topsoils and shows that the higher the clay content, the higher the amount of potassium needed to get the same potassium reserve in soil. The mean values of both topsoil parameters for each soil group (clay and potassium content), as well as the topsoil type[99] are included in Annexe IV, in which clay and potassium content are also represented in separate box-plots.

Table 9. Relationship between clay content in soil and bioavailable K^+ content, to define the categorisation of the Potassium Reservoir Index (I_K) (Domínguez Vivancos, 1997) and the Radiocaesium Reservoir Index (I_Cs).

Exchangeable K content in Soil (cmol·Kg^{-1}) depending on clay content				**Potassium Reservoir in Soil**	**Radiocaesium Reservoir Index**
Clay 0-10 %	**Clay >10-20 %**	**Clay >20-30 %**	**Clay >30 %**	**I_K**	**I_Cs**
>0,5	>0,8	>0,9	>1	Very High	**1: Minimum**
>0,4-0,5	>0,6-0,8	>0,7-0,9	>0,9-1	High	**2: Low**
>0,2-0,4	>0,5-0,6	>0,6-0,7	>0,7-0,9	Medium	**3: Medium**
>0,1-0,2	>0,3-0,5	>0,4-0,6	>0,5-0,7	Low	**4: High**
<=0,1	<=0,3	<=0,4	<=0,5	Very Low	**5: Maximum**

On the bases of the potassium reserve index categories, the *Radiocaesium Reservoir Index* (*I_Cs*) corresponds to a five classes discrete classification: from minimum to maximum caesium reservoir as shown in Table 9. In those soils with a very high potassium reserve, the radiocaesium will have less opportunity to occupy the clays binding sites, reducing its content in the soil in the mid and long-term and, thereby, limiting the crops uptake in the following growing seasons; those soils will show a minimum *Radiocaesium Reservoir Index*

[98] Domínguez Vivancos (1997) proposed the categorisation used to define the potassium reservoir in soil focusing on the fertilisation needs of the agricultural soils, in terms of potassium addition.

[99] Soil type criteria (IAEA, 2010) according to the mineral size fractions: sandy soils (sand fraction ≥ 65 % and clay fraction < 18%), clayey soils (clay fraction ≥ 35 %) and loamy soils (all other mineral soils). Organic soils are those with more than 20 % of organic matter content.
The arithmetic means of the granulometric fractions of the soil groups (the grain size particles: clay and sand) are the ones considered except for the soil groups No. 24 and No. 39: Humic Cambisols (Bh) and Ferric and Humic Podzols (Ph), respectively. For these two soil groups, the geometric mean gives rise to classify both as sandy soils, while considering the arithmetic mean result in loamy soils. That is justified by the fact that, in general, sandy soil textures are the ones which favour the most the radionuclides transfer from soil to plant in mineral soils.

(value set in 1). On the contrary, very low potassium pools in the soil will favour the availability of radiocaesium to take part in the soil sorption processes and, in turn, in future potential crop uptake, giving rise to the maximum *I_Cs* (value set in 5).

Considering the average topsoil properties for each soil group, the indexes *I_K* and *I_Cs* can be attained to be also mapped, using the European Soil map (EC-ESBN, 2004) as the base map, as it was described in section 2.1. The resulting I_Cs map is shown in Figure 36, in section 3.3.

2.3.2 Studying the soil-to-plant transfer factor (F_v) values and defining the *Transfer Factor Index* (*I_TF*)

Once the *representative crop* is identified for each *basic cartographic unit* (*mun_clc*) (see section 2.2.2), the soil-to-plant transfer factor (F_v) regarding ^{137}Cs (IAEA, 2010) can be assigned to each spot. Then, considering the topsoil type, the *Transfer Factor Index* (*I_TF*) is calculated.

2.3.2.1 Soil-to-plant Transfer factor (F_v) analysis

Soil-to-plant transfer factor values for ^{137}Cs are extracted from the compilation done by IAEA (2010) for temperate climates since this parameter has not been defined for a closer climate regime to the Spanish conditions (the Mediterranean, for most of the peninsular provinces) for many crops grown in the Spanish agricultural systems. In that reference, F_v values are provided for different plant groups (in some cases for different plant compartments) and different soil types: mineral soil textures and organic soils.

The compilation of the F_v values regarding ^{137}Cs (IAEA, 2010) is listed in Annexe V, including their geometrical mean, the standard deviation and the minimum and maximum empirical values for each plant group[100] – soil type pair. The assessment of the radiological vulnerability of the agricultural systems in this Thesis is focused on mineral soils, thus, only soil textures are considered in their vulnerability evaluation.

[100] When available, F_v for different plant's compartment are indicated.

The consulted F_v database for ^{137}Cs (IAEA, 2010) has some limitations, which condition the assessment methodology designed. These are listed below:

- the small number of samples for some crop species which implies reduced representativeness of the resulting transfer factor; for instance, the fruits of the herbaceous plants in sandy soils have only one empirical data,
- the lack of F_v values for crops not so widely cultivated in the world, compared to some other crops which have a quite sizeable experimental sampling, such as the grain of cereals grown in loamy soils, with 158 values,
- the grouping made for some crops, as is the case for the miscellaneous category called “other crops”, in which are included from walnuts to sunflowers; assigning the same F_v value to such different crops reflects a high uncertainty,
- the lack of crops’ transfer factor values for some crop – soil type combinations, as it occurs for shrubs’ fruits for sandy soils,
- there is a single value for some crops, regardless the soils type, as it occurs for stems and leaves of herbs and the miscellaneous class “other crops”.

A specific encoding has been designed in this Thesis to identify the plants’ group and its compartments which is shown in Table 10.

Table 10. Transfer factor (F_v) values for temperate climates in (IAEA, 2010).

Plant Group		Plant Compartment		Crop group ID_C
Plant	**ID_PG**	**Compartment**	**ID_PC**	
Cereals	ce	Grain	G	ceG
		Stems, shoots	S	ceS
Maize	ma	Grain	G	maG
		Stems, shoots	S	maS
Leafy vegetables	ly	Leaves	L	lyL
Non leafy vegetables	nl	Fruits, heads, berries, buds	F	nlF
Legume vegetables	lv	Seeds, Pods	S	lvS
Root crops	rc	Roots	R	rcR
		Leaves	L	rcL
Tubers	tb	Tubers	T	tbT
Grasses	gr	Stems, shoots	S	grS
Legume fodder	lf	Stems, shoots	S	lfS
Pasture	ps	Stems, shoots	S	psS
Herbs	he	Stems, leaves	X	heX
Other crops	oc	All	A	ocA
Woody trees	wt	Fruit	F	wtF
Shrubs	sh	Fruit	F	shF
Herbaceous plants	hp	Fruit	F	hpF

ID_PG: IDentification of the Plant's Group.
ID_PC: IDentification of the Plant's Compartment.
ID_C: IDentification of the Crop.

There is a wide variability of transfer factor values, not only among different crops but also for the different type of soils with respect to each crop (see Annexe V). What is more, there is a large range of values among the empirical results obtained for each crop– soil type pair (IAEA, 2010); that is the reason why the standard deviation is quite high in some cases. That variability is due to the wide variety of the environmental processes that influence that transfer (Guillén, et al., 2016), including the climate regime (Baeza, et al., 2001). In the present work, the geometric mean values given in IAEA (2010) for temperate climates are the ones to be used. In Figure 16, the F_v range values for each crop – soil combination is represented and also the mean value has been set.

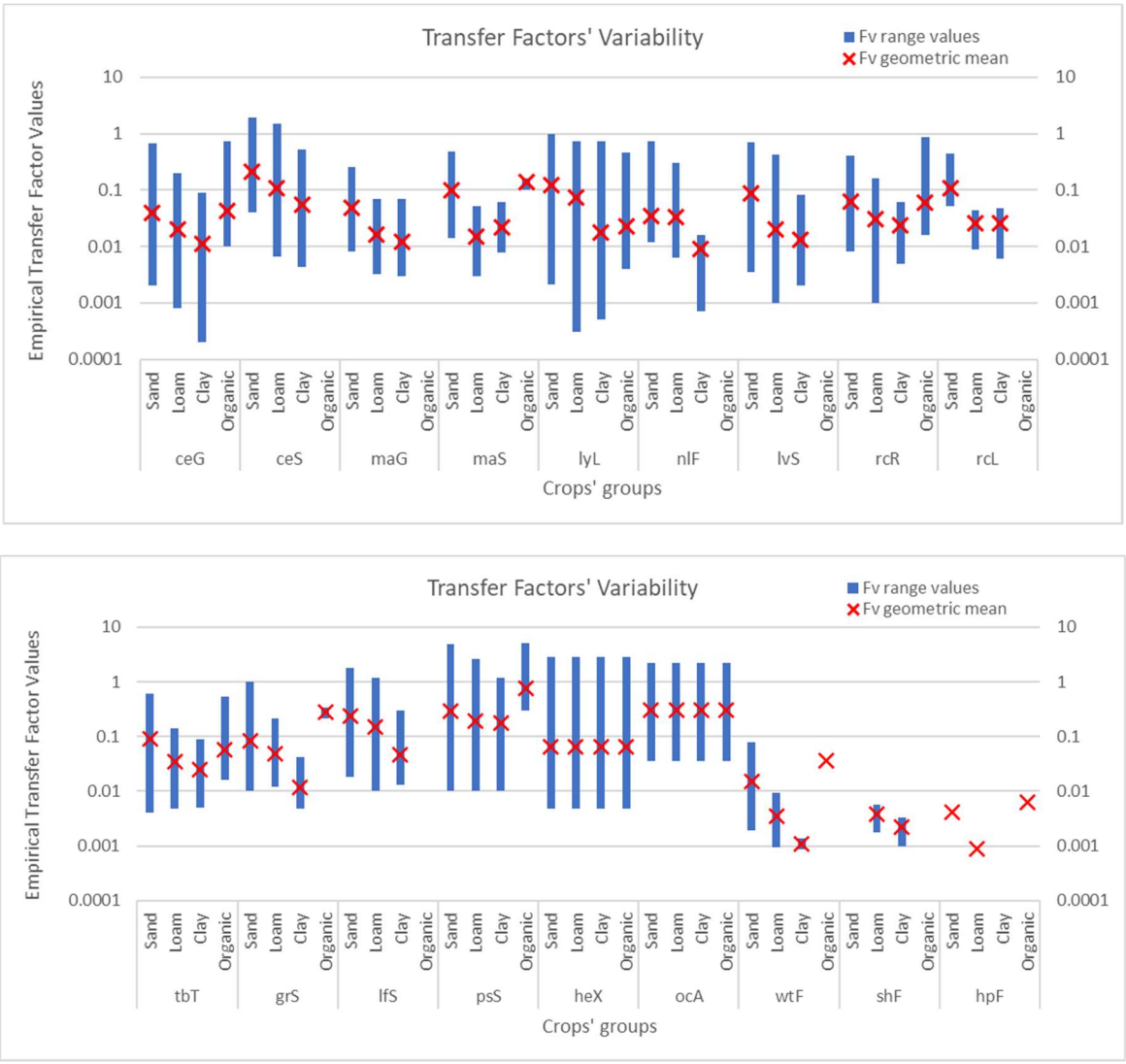

Figure 16. Charts representing the different empirical transfer factor values for each group of crops (and its compartments when corresponds) for each type of soil, in temperate climates, included in (IAEA, 2010). For herbaceous plants' group (heX) and for the "other crops" group there are no separated F_v data for each soil type; the mean F_v value of both crop groups, for all soil types, are 0.066 and 0.31, respectively, their minimum F_v values are 0.0048 and 0.036, respectively, and their maximum value are 2.8 and 2.2, respectively (IAEA, 2010).

As can be seen in Figure 16 and Annexe V, there are no F_v values for all crops – soil type combinations pairs. These cases are assumed as follows:

- As said before, for Herbs (*heX*) and Other crops (*ocA*) there are no F_v values for each soil type separately. Thus, the value indicated for all type of soils is considered for all of them individually. Therefore, in those areas in which the *representative crop* belongs to that crops' groups, it is not possible to evaluate the influence of the topsoil texture in the root uptake.
- For the shrubs' fruits (*shF*) there is no F_v value for sandy soils. Thus, the same F_v value as for loamy soils is attributed to sandy soils.

- For the herbaceous plants' fruits (*hpF*) there is no F_v value for clayey soils. Thus, the same F_v value as for loamy soils is attributed to clayey soils.

To assign a transfer factor value (IAEA, 2010) to each crop included in the Spanish agricultural structure (MAGRAMA, 2016), a correspondence between the Spanish crops classification and the crops' groups defined in (IAEA, 2010) has to be done. This correspondence is included in Annexe II. The criteria given in IAEA (2010) are the ones used to assign each Spanish crop (*IDPR*), extracted from MAGRAMA (2016), to each crop group (*ID_C*), defined in IAEA (2010). However, there are some Spanish crops which are not contemplated in IAEA (2010) and vice versa. Besides, there are several considerations to be done regarding some other specific crops. In this sense, the following assumptions are considered:

- The F_v values assigned to cereals and maize are the ones considered for the grain of cereals (*ID_C* as *ceG*) and maize (*ID_C* as *maG*), respectively.
- The crops included in Grain Legumes (MAGRAMA, 2016) (coded as *A20000*) have been considered as "seeds or pods" of "Legume vegetables" (*lvS* – as if all of them were for human consumption) and not taking into account the possible use for feedstuff (which would have been linked to the F_v for the "Legume fodder" plant group: *lfS*, as is the case for the crops within the *IDPR A60000*).
- In IAEA (2010) walnuts are included in the miscellaneous plants' group: "Other crops" (*oc*), where all compartment's plant (*A*) are considered (*ocA*); thus, by similarity, almonds (*W15010*), walnuts (*W15020*), hazelnuts (*W15030*), chestnut (*W15040*) and pistachio (*W15050*) are attributed the F_v for "Other crops" also. This assumption introduces a certain deviation of the results because in general, for ^{137}Cs, F_v value from soil to fruits is lower than the F_v value from soil to plants themselves (IAEA, 2010). That means that nuts are attributed a transfer factor between one and two orders of magnitude higher than, for example, apples, which are included in the crop group of fruits of woody trees (*wtF*) (see Figure 16 and Annexe V).
- Saffron (*IDPR*: *A54030*) has been considered as "Herbs" (*heX*).
- The Spanish crops classified as "Roots and Tubers" (*A64000*) (grouped in "Fodder crops" (MAGRAMA, 2016)), have been included in the crop's group of "Root crops"

(*rc*) (IAEA, 2010). For these crops, IAEA (2010) contemplates two plants' compartments: roots (*R*) and leaves (*L*). Taking into consideration that animals feed on both, the F_v value considered for these crops is the maximum between both plants' compartments according to the corresponding soil type in each particular *basic cartographic unit*.

- Regarding mushrooms, which are not included in IAEA (2010), they have not been considered because it has been assumed that agricultural industry grows them indoors.

Given the crop's sharing described in section 2.2.2, the crop group (*ID_C*) attributed to each *basic cartographic unit* (coded as "*mun_clc*") is done according to the *representative crop*: the most extent crop within each *mun_clc*.

To assign a soil-to-plant transfer factor value it is necessary to know, apart from the crop group, the soil type (the soil texture for mineral soils[101]). Then, the "*Identity*" tool (ESRI, 2016a) is used to overlap the topsoil properties and the crops maps. This way, the association between the topsoil texture and the *representative crop* (through the crop group to which it belongs to) is obtained and, therefore, the corresponding F_v can be assigned to each *basic cartographic unit*.

2.3.2.2 *Transfer Factor Index* (*I_TF*) definition

To consider the role of the transfer from soil-to-plant mechanisms in the Radiological Vulnerability of the agricultural systems, a *Transfer Factor Index* (*I_TF*) is built.

This index categorises each *basic cartographic unit* according to the F_v value, attributed to the *representative crop* and the soil type. As it was previously mentioned, organic soils are not taken into consideration due to their low representativeness in peninsular Spain; therefore, soil types are only referred to as the mineral soil texture. Besides, that soil texture is taken into account for the topsoil in which the crops' roots are developed.

[101] The topsoil texture map has been performed by using the European soil map (EC-ESBN, 2004) as the base map and the mean topsoil parameters of the soil groups, following the same mapping procedure described in section 2.1.

As can be seen in Figure 16 and Annexe V, F_v mean values are comprised in the range between $9.0 \cdot 10^{-4}$ (for herbaceous plants' fruits in loamy soils) and $3.1 \cdot 10^{-1}$ (for the crops grouped in the miscellaneous category so-called "other crops", for all plant's compartment, in non-specific soil type), which is an extremely wide range: tree orders of magnitude.

The *I_TF* is obtained from the transfer factor values in order to:

- obtain closer values (closer than the ones among the F_vs values themselves), avoiding differences in orders of magnitude,
- handle a range of values in a comparable scale to the *I_Cs*, with whom will be subsequently combined (as described further on) in order to characterise the radiological vulnerability in every *basic cartographic unit* in peninsular Spain, as a whole.

Taking into account the characteristics of the F_vs and their limitations (exposed in section 2.3.2.1), as well as the considerations made above, the *I_TF* is obtained applying the following expression:

$$I\_TF = 8 + Ln(F_v)$$

being:

- *I_TF*, is the *Transfer Factor Index*,
- *Ln* (F_v), corresponds to the natural logarithm of the transfer factor (F_v), which allows to reduce the range of values to work with, resulting between -7.01 to -1.17.
- In order to get positive values, 8 is added. This way, the minimum *I_TF* results in a continuous variable ranged from 1.0 to 6.8.

The correspondence between the transfer factor and the resulting *Transfer Factor Index* (*I_TF*) is shown in Table 11.

The assessment described requires to carry out a join between the crop groups' map (shown in Figure 35) and the soil map; that join was performed by using a GIS (ESRI, 2016a). The former contains, for each *basic cartographic unit*, the crop group to which the *representative crop* belongs. The latter, the soil map, gathers all the soil properties, including the topsoil type, of the soil group assigned to each *SMU* of the European soil base map (EC-ESBN, 2004), which is shown in section 3.3 (see Figure 37).

Table 11. In this table it is included: the soil-to-plant transfer factor values (F_v) for the different crops groups (Crops' code), grouped by topsoil texture (IAEA, 2010), the assessment done to obtain the Transfer Factor Index (I_TF) and all the possible combinations (multiplication) between the I_TF and the Radiocaesium Reservoir Index (I_Cs). The results from the multiplication are coloured according to the corresponding Radiological Vulnerability Index (I_RV) category, which are fixed by the percentiles P_{25}, P_{50}, P_{75} and P_{95} assessed from all the results. Five I_RV categories are obtained: I_RV 1: under 6.6; I_RV 2: 6.6 – 12.6; I_RV 3: 12.6 – 19.6; I_RV 4: 19.6 – 28.0; I_RV 5: over 28.0.

Topsoil texture	Crop code (ID_C)	Transfer Factor (F_v)	I_TF = 8+Ln (F_v)	I_RV				
				I_Cs=1	I_Cs=2	I_Cs=3	I_Cs=4	I_Cs=5
Sandy soils	ceG	**0.039**	**4.8**	4.8	9.5	14.3	19.0	23.8
	ceS	**0.21**	**6.4**	6.4	12.9	19.3	25.8	32.2
	maG	**0.049**	**5.0**	5.0	10.0	15.0	19.9	24.9
	maS	**0.1**	**5.7**	5.7	11.4	17.1	22.8	28.5
	lyL	**0.12**	**5.9**	5.9	11.8	17.6	23.5	29.4
	nlF	**0.035**	**4.6**	4.6	9.3	13.9	18.6	23.2
	lvS	**0.087**	**5.6**	5.6	11.1	16.7	22.2	27.8
	rcR	**0.062**	**5.2**	5.2	10.4	15.7	20.9	26.1
	rcL	**0.11**	**5.8**	5.8	11.6	17.4	23.2	29.0
	tbT	**0.093**	**5.6**	5.6	11.2	16.9	22.5	28.1
	grS	**0.084**	**5.5**	5.5	11.0	16.6	22.1	27.6
	lfS	**0.24**	**6.6**	6.6	13.1	19.7	26.3	32.9
	psS	**0.29**	**6.8**	6.8	13.5	20.3	27.0	33.8
	heX*	**0.066**	**5.3**	5.3	10.6	15.8	21.1	26.4
	ocA*	**0.31**	**6.8**	6.8	13.7	20.5	27.3	34.1
	wtF	**0.015**	**3.8**	3.8	7.6	11.4	15.2	19.0
	shF**	**0.0038**	**2.4**	2.4	4.9	7.3	9.7	12.1
	hpF	**0.0042**	**2.5**	2.5	5.1	7.6	10.1	12.6
Loamy soils	ceG	**0.02**	**4.1**	4.1	8.2	12.3	16.4	20.4
	ceS	**0.11**	**5.8**	5.8	11.6	17.4	23.2	29.0
	maG	**0.016**	**3.9**	3.9	7.7	11.6	15.5	19.3
	maS	**0.015**	**3.8**	3.8	7.6	11.4	15.2	19.0
	lyL	**0.074**	**5.4**	5.4	10.8	16.2	21.6	27.0
	nlF	**0.033**	**4.6**	4.6	9.2	13.8	18.4	22.9
	lvS	**0.02**	**4.1**	4.1	8.2	12.3	16.4	20.4
	rcR	**0.03**	**4.5**	4.5	9.0	13.5	18.0	22.5
	rcL	**0.026**	**4.4**	4.4	8.7	13.1	17.4	21.8
	tbT	**0.035**	**4.6**	4.6	9.3	13.9	18.6	23.2
	grS	**0.048**	**5.0**	5.0	9.9	14.9	19.9	24.8
	lfS	**0.15**	**6.1**	6.1	12.2	18.3	24.4	30.5
	psS	**0.19**	**6.3**	6.3	12.7	19.0	25.4	31.7
	heX*	**0.066**	**5.3**	5.3	10.6	15.8	21.1	26.4
	ocA*	**0.31**	**6.8**	6.8	13.7	20.5	27.3	34.1
	wtF	**0.0035**	**2.3**	2.3	4.7	7.0	9.4	11.7
	shF	**0.0038**	**2.4**	2.4	4.9	7.3	9.7	12.1
	hpF	**0.0009**	**1.0**	1.0	2.0	3.0	3.9	4.9
Clayey soils	ceG	**0.011**	**3.5**	3.5	7.0	10.5	14.0	17.5
	ceS	**0.056**	**5.1**	5.1	10.2	15.4	20.5	25.6
	maG	**0.012**	**3.6**	3.6	7.2	10.7	14.3	17.9
	maS	**0.022**	**4.2**	4.2	8.4	12.5	16.7	20.9
	lyL	**0.018**	**4.0**	4.0	8.0	11.9	15.9	19.9
	nlF	**0.0091**	**3.3**	3.3	6.6	9.9	13.2	16.5
	lvS	**0.013**	**3.7**	3.7	7.3	11.0	14.6	18.3
	rcR	**0.024**	**4.3**	4.3	8.5	12.8	17.1	21.4
	rcL	**0.026**	**4.4**	4.4	8.7	13.1	17.4	21.8
	tbT	**0.025**	**4.3**	4.3	8.6	12.9	17.2	21.6
	grS	**0.012**	**3.6**	3.6	7.2	10.7	14.3	17.9
	lfS	**0.046**	**4.9**	4.9	9.8	14.8	19.7	24.6
	psS	**0.18**	**6.3**	6.3	12.6	18.9	25.1	31.4
	heX*	**0.066**	**5.3**	5.3	10.6	15.8	21.1	26.4
	ocA*	**0.31**	**6.8**	6.8	13.7	20.5	27.3	34.1
	wtF	**0.0011**	**1.2**	1.2	2.4	3.6	4.8	5.9
	shF	**0.0022**	**1.9**	1.9	3.8	5.6	7.5	9.4
	hpF***	**0.0009**	**1.0**	1.0	2.0	3.0	3.9	4.9

*There is no data for the different soil textures, only for all together.
**There is no data for sandy soils. Those are assigned the loamy value.
*** There is no data for clayey soils. Those are assigned the loamy value.

Radiological Vulnerability Index (I_RV) Leyend

Minimum Vuln. I_RV=1 **Low Vuln. I_RV=2** **Medium Vuln. I_RV=3** **High Vuln. I_RV=4** **Maximum Vuln. I_RV=5**

Considering the F_v associated with each *basic cartographic unit*, and according to the expression defined to build the *Transfer factor Index* (*I_TF)*, the latter has been assessed and mapped for the CLC defined as "*Agricultural areas*" (EEA, 2016). The resulting *I_TF* map is shown in Figure 38 (section 3.3).

2.3.3 *Radiological Vulnerability Index* of agricultural systems regarding ^{137}Cs (*I_RV*)

The *Radiological Vulnerability Index* of the agricultural systems regarding ^{137}Cs is defined as the combination of the mineral soils' capacity to store that radionuclide and the soil-plant system's capacity to transfer it to crops, and therefore to the human food chain. That vulnerability may give rise to a risk exposure via ingestion in the long-term if a deposition occurs.

The *Radiocaesium Reservoir Index* (*I_Cs)* is the index built to reflect the topsoil capacity to storage radiocaesium in the soil's structure (focusing, in this case, on ^{137}Cs) which, over time may become bioavailable to crops (see 2.3.1). On the other hand, taking into account the *representative crop* and the topsoil texture in which it is grown, the *I_TF* is the index which quantifies the potential to transfer ^{137}Cs from soil to crop. As a result of the combination of both indexes, the *Radiological Vulnerability Index* (*I_RV*) of the agricultural systems is obtained. This combination is made multiplying them, using a risk matrix (Kolluru, et al., 1996; ISO/Guide 73:2009(en); Poljanšek, et al., 2017) where all the possible combinations between both are reflected. The matrix mentioned is included in the Table 11 previously cited.

To create the *Radiological Vulnerability Index (I_RV)*, the resulting values of multiplying the *I_Cs* by the *I_TF*, which range from 1 to 34.1, have been reclassified in five categories: from minimum to maximum radiological vulnerability. Addressing that categorisation has sought to highlight the agricultural areas of most concern; that aim has conditioned the reclassification of the results. That is the reason why the thresholds used to create the radiological vulnerability categories are the quartiles ($Q_1 = P_{25}$, $Q_2 = P_{50}$, and $Q_3 = P_{75}$) and the percentile P_{95} of the results of that calculation; that categorisation, using the P_{95}, allows to distinguish the areas of most concern from the rest of the uniformly distributed results. The latter percentile (P_{95}) has been chosen as a threshold precisely to highlight those areas

where the Radiological Vulnerability is definitely the highest; that way the most vulnerable areas are not covered up in a larger vulnerability category. Since limited areas are classified with the maximum radiological vulnerability, resources for the EPR can be assigned to the areas of most concern in a most direct determination. Then, a five-category index is obtained, according to an extended traffic lights colour coding, where blue and orange are included apart from the three basic colours: green, yellow and red. The final categorisation for the *I_RV* is shown in Table 12.

Table 12. Categorisation of the Radiological Vulnerability Index (I_RV) and colour coding for its categories.

Colour	Thresholds to define the I_RV categories	Radiological Vulnerability Index	
	Percentiles ranges obtained from the multiplication: I_Cs x I_TF	I_RV name	I_RV value
Blue	$< P_{25}$ → < 6.6	Minimum	1
Green	$P_{25} – P_{50}$ → 6.6 – 12.6	Low	2
Yellow	$P_{50} – P_{75}$ → 12.6 – 19.6	Medium	3
Orange	$P_{75} – P_{95}$ → 19.6 – 28 .0	High	4
Red	$> P_{95}$ → >28.0	Maximum	5

The *Radiological Vulnerability of the agricultural areas* can be mapped, by using a GIS (ESRI, 2016a). It is carried out by combining the *I_Cs* map and the *I_TF* map. That is done by overlapping both features (using the "*Identity*" tool (ESRI, 2016a)). In each resultant feature's polygon, a particular *I_Cs – I_TF* combination is attained, then both values can be multiplied; the outcome is reclassified to obtain the corresponding *I_RV* category according to the criteria given in Table 12. The final Radiological Vulnerability map, which shows the categorisation of the agricultural systems according to their potential to transfer the radiocaesium to the food chain, is shown in section 3.3 (Figure 42).

2.4 Application of the Radiological Vulnerability maps of the agricultural systems in the EPR

To validate the usefulness of the Radiological Vulnerability map of the agricultural systems to be use as a tool in the EPR, that map is tested in a case study that emulates a hypothetical nuclear accident with a ^{137}Cs release from Almaraz NPP. A deposition pattern of ^{137}Cs is estimated taking into account the seasonal meteorological conditions on which to apply the radiological vulnerability results of the agricultural systems. The objective is to identify those areas where actions need to be taken in a prioritised way in order to recover the

former living conditions. Figure 17 shows the workflow followed to attain the prioritisation maps in the case study designed to test the radiological vulnerability map.

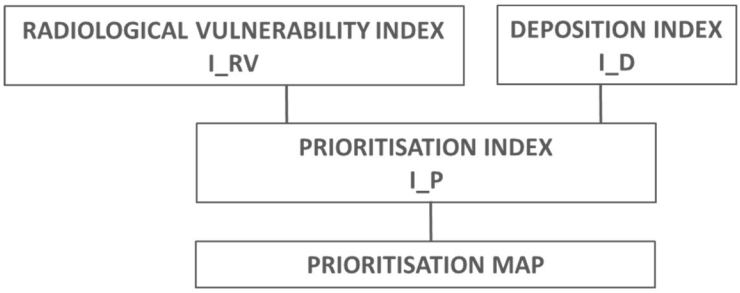

Figure 17. Workflow representing the methodology design to obtain the Prioritisation maps for the agricultural areas affected by a ^{137}Cs deposition in peninsular Spain.

To obtain the ^{137}Cs deposition data, many simulations of a hypothetical accident have been conducted. The selected case-study itself, the parameters considered to perform the accident simulations, the analysis of the simulations' outputs and the methodology designed to obtain the corresponding deposition maps are described in the next sections. Besides, the combination of the radiological vulnerability data and the deposition results, which leads to the *prioritisation* maps are explained further on.

2.4.1 Case-study presentation

The site chosen for the case-study is the Almaraz (NPP), located in Cáceres province (Extremadura, Spain) as shown in Figure 18.

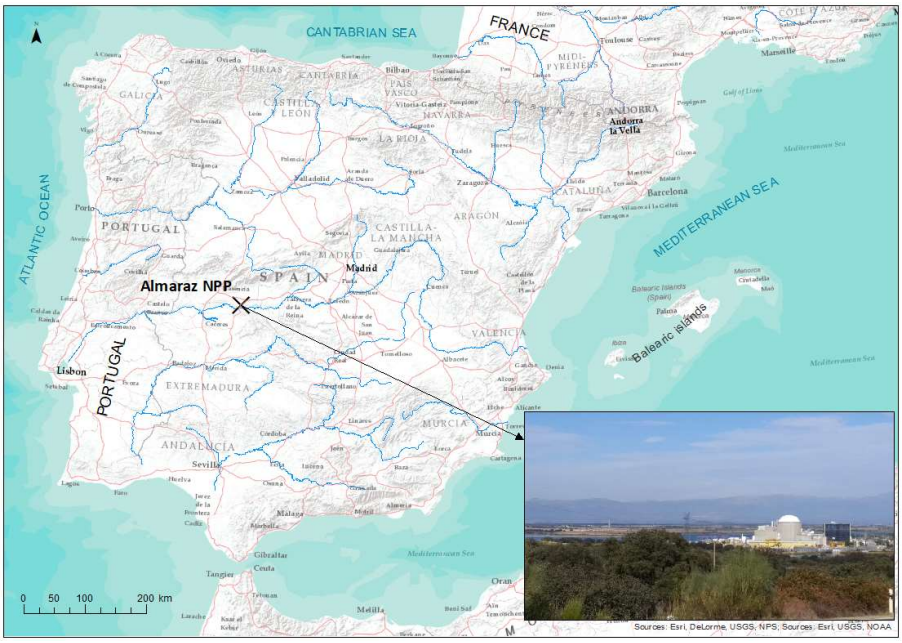

Figure 18. Almaraz NPP location. Projection WGS84. Source: ESRI map base. Picture taken by the author (October 2019).

The case-study assumes a hypothetical severe accident with offsite consequences due to an unintentional release from the selected site. The methodological approach is to generate dispersion plumes for many possible meteorological conditions, so those statistical results can reflect the characteristics of the dispersion and deposition patterns. Therefore, this kind of work must involve a large number of calculations with different meteorological scenarios.

The numerical dispersion calculations and the deposition prognosis have been carried out using the DSS JRODOS System (KIT, 2017a) for the defined accidental scenario. These simulations have been performed in the frame of the ANURE: "Assessment of the Nuclear Risk in Europe - A Case Study in the Almaraz Nuclear Power Plant (Spain)" Project (ANURE, 2017), carried out between the Joint Research Centre (JRC) and CIEMAT.

From the bunch of these simulations, a probabilistic assessment of the ^{137}Cs deposition is conducted, taking into account the deposition severity.

2.4.2 Baseline data and accident simulations

In order to attain a set of representative radionuclides deposition values across peninsular Spain, associated with a ^{137}Cs release from Almaraz NPP, a daily accident simulation has been performed through a five-year period, from 2012 to 2016. The start time for each simulation is randomly selected.

The radionuclides' dispersion and the deposition processes are clearly dependant on: i) the source term, ii) the dominant meteorological conditions, and iii) the orography. All these inputs, apart from land use, soil texture, and soil-to-plant transfer factor are stored in a PostgreSQL[102] database server connected to JRODOS. The simulations outputs are also stored in the PostgreSQL database, commonly used to store georeferenced data.

2.4.2.1 Source term

The source term determines the timing and the magnitude of the radioactive material released to the environment, emitted from a particular source, including the type and the

[102] https://www.postgresql.org/

quantity of the radionuclides released (NEA & OECD, 2002). It depends on the type of accident and, therefore, depends on the characteristics of the nuclear installation.

Almaraz NPP was built in 1973 and comprises two Pressurized light Water Reactors (PWR), model Westinghouse 3-loop, of 2947 thermal power (MWt), each of them with three cooling circuits. They were brought into commercial operation in 1983 and 1984, respectively (IAEA, 2020). Both units use as fuel, slightly enriched uranium oxide, and their electric power are 1049.43 MW and 1044.45 MW, respectively (CNAT, 2017). In Figure 19 a schema of the PWR type reactors is shown.

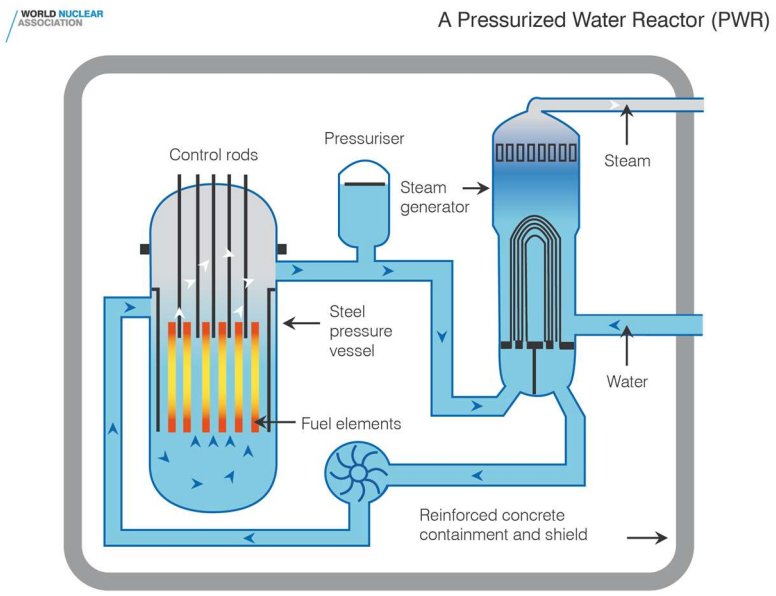

Figure 19. Schematic diagram of a Pressurized Water Reactor (PWR) (WNA, 2018). (Extracted from ANURE report)

The source term data have been derived from existing studies in order to provide, as much as possible, a realistic accident progression and off-site consequence release. Considering the characteristics of the Almaraz NPP, the Surry NPP (Virginia, USA) similar to it, has been chosen as a surrogate for source term estimation purposes. Surry NPP has been the object of integrated analysis, in the State-of-the-Art Reactor Consequence Analyses Project (SOARCA) (USNRC, 2012).

Within all the possible events and accidents considered in that integrated analysis two severe accidents were initially chosen to perform the case study: an interfacing systems loss-of-coolant accident (ISLOCA) initiated by an internal event caused by a rupture of low-head safety injection piping outside containment, and a long-term station blackout

(LTSBO), initiated by an external event resulting in loss of offsite and outside alternating current power. For the first type of accidental scenario, the radiological release time was 35 hours and for the second one 55 hours.

For this accident sequences, the source term for Almaraz has been obtained, from the given release fractions for the halogens, alkaline earths and alkali metals classes (USNRC, 2012), grouped on an hourly basis, to which the inventory[103] of ^{131}I, ^{90}Sr and ^{137}Cs of Almaraz NPP has been applied. Nevertheless, the deposition of ^{137}Cs is the one to be considered in the analysis.

In order to ensure that the total radionuclides released were fully deposited, the accidents' simulations considered 48 hours more once the release is over. Therefore, to obtain a proper deposition prognosis, each simulation lasts 83 hours in total for the ISCOLA accident and 103 hours for the LTSBO.

A probability analysis was developed to compare the simulations results obtained from both kind of accidents. As seen in Figure 20, according to the likelihood analysis of all the activity concentration ranges considered for the deposition, the ISLOCA accidental scenario would affect a larger area than the LTSBO scenario. Therefore, by assuming an ISLOCA accident, all the peninsular soils would be affected by a ^{137}Cs deposition and the whole radiological vulnerability map could be tested. That is the reason why the accident sequence chosen to perform the case study was the ISLOCA accident with the timing described before.

[103] Inventory definition: "*the amount of nuclear material present at a facility or a location outside facilities*". (IAEA, 2001)

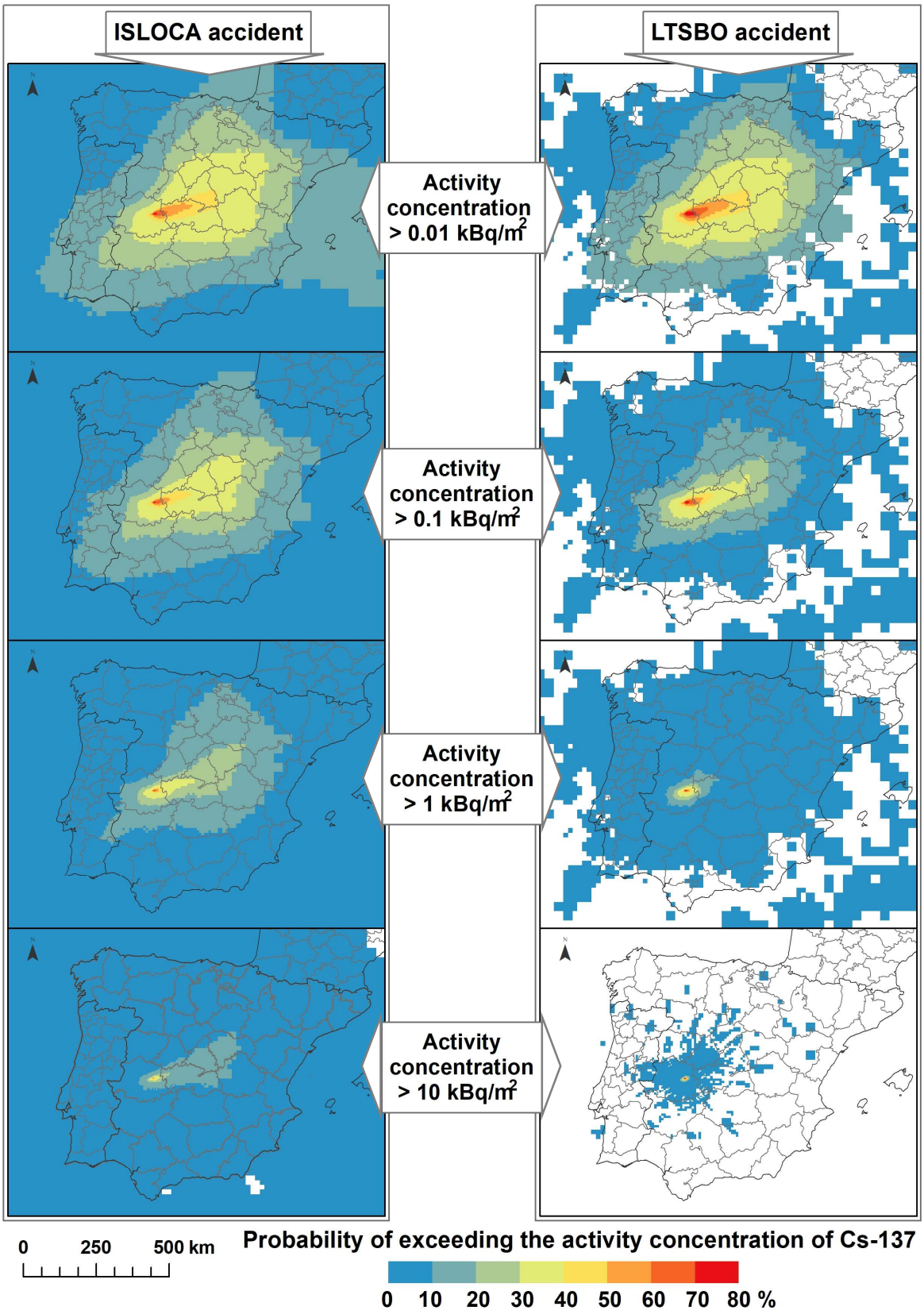

Figure 20. Probability analysis of the ^{137}Cs deposition derived from the simulations performed for an ISLOCA and a LTSBO accidental scenarios in Almaraz NPP. The ranges of activity concentration deposited on ground are, from top to bottom, over 0.01 kBq·m^{-2}, over 0.1 kBq·m^{-2}, over 1 kBq·m^{-2} and over 10 kBq·m^{-2}. Projection: UTM ETRS89 H30.

The release fractions of the radionuclides considered during the ISLOCA sequence accident is shown in Figure 21. The source term adapted to the Almaraz NPP, for the sequence accident, is shown in Annexe VI.

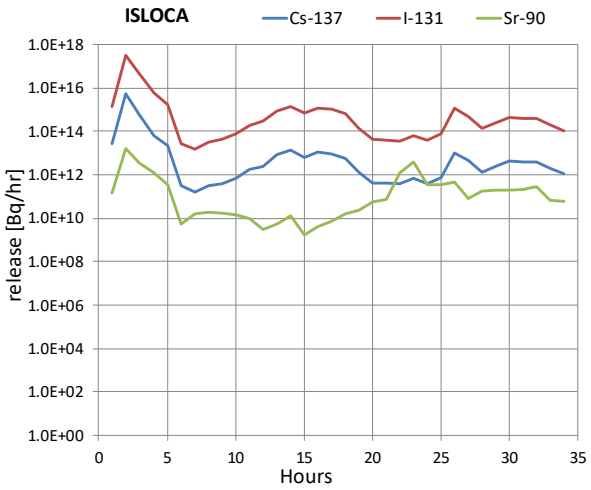

Figure 21. Release fractions of ^{131}I, ^{90}Sr and ^{137}Cs during the ISLOCA sequence accidents. (ANURE, 2017)

For this case study, as previously mentioned, only the release of ^{137}Cs will be considered. The contribution of this radionuclide to the ground contamination, has been estimated at 10^{-3} times with respect to the total gamma & beta activity concentration deposited.

2.4.2.2 Meteorological conditions

Once the radionuclides are released into the atmosphere, the meteorological conditions govern the dispersion and the ground deposition process (Hernández-Ceballos, et al., 2020). Wind direction determines the plume track and its velocity.

Rainfall is the main cause for the deposition, being in this case “wet deposition”, in contrast to the “dry deposition”. The latter occurs when the contaminants stick to the surfaces intersected by the plume along its path. Nevertheless, “wet deposition” occurs also due to irrigation practices or even to a later rainfall, which mobilises the previously deposited radionuclides. The run-off water also plays a role in carrying and spreading the radionuclides. However, only the meteorological conditions during the 83 hours simulations are considered and run-off consequences are not taken into account, since equilibrium conditions after the deposition are assumed.

The meteorological data are obtained from the Global Forecast System (GFS), produced by the National Climatic Data Center (NCDC), (one of the National Centers for Environmental Prediction (NCEP) of the United States) (NCEP-GFS, n.d.), attached to the National Oceanic and Atmosphere Administration (NOAA, n.d.). GFS is a weather forecast model which uses data on temperature, wind, precipitation, etc. for the entire globe, which are used to analyse and predict weather. The meteorological data for the five-year period considered for simulations was downloaded from the NOMADS website (https://nomads.ncdc.noaa.gov/data/gfsanl/[104]. The main characteristics of the dataset used are shown in Table 13.

Table 13. Main dataset characteristics obtained from the GFS.

Type of dataset/Model	Grid resolution	Period of record	Model cycle	Output time steps
Analysis / GFS-ANL	0.5°	01Jan2007–Present	4/day: 00, 06, 12, 18UTC	+00, (+03, +06 precipitation fields)

According to the JRODOS guides (KIT, 2017b), a five-year period to obtain statistically representative results in the whole set of simulations (see section 2.4.2.4) is an adequate length of time.

Theoretically, meteorological data are continuous however, the original files have some gaps which means a lack of meteorological information at certain points. While running a simulation in JRODOS, the missing data leads to stop it, and no valid deposition results are obtained for that precise simulation. This means that out of the 1853 possible simulation outputs (one per day in the five years), 1383 are the eventual valid deposition outcomes obtained from the whole set of releases simulated from Almaraz NPP, due to the simulations' failure.

2.4.2.3 Orography

The modelling of the dispersion and the deposition of the radionuclides released requires as input data a Digital Elevation Model (DEM) to consider the influence of the terrain's variations across the studied region.

[104] By the time the simulations were performed, meteorological data provided by the Spanish meteorological agency (AEMET) were no compatible with the JRODOS version.

The software used to perform the release and the deposition prognosis, JRODOS, includes a raster file (GeoTiff – *.tif) for the DEM (KIT, 2017d), with a resolution of 105.5 m, which is shown in Figure 22.

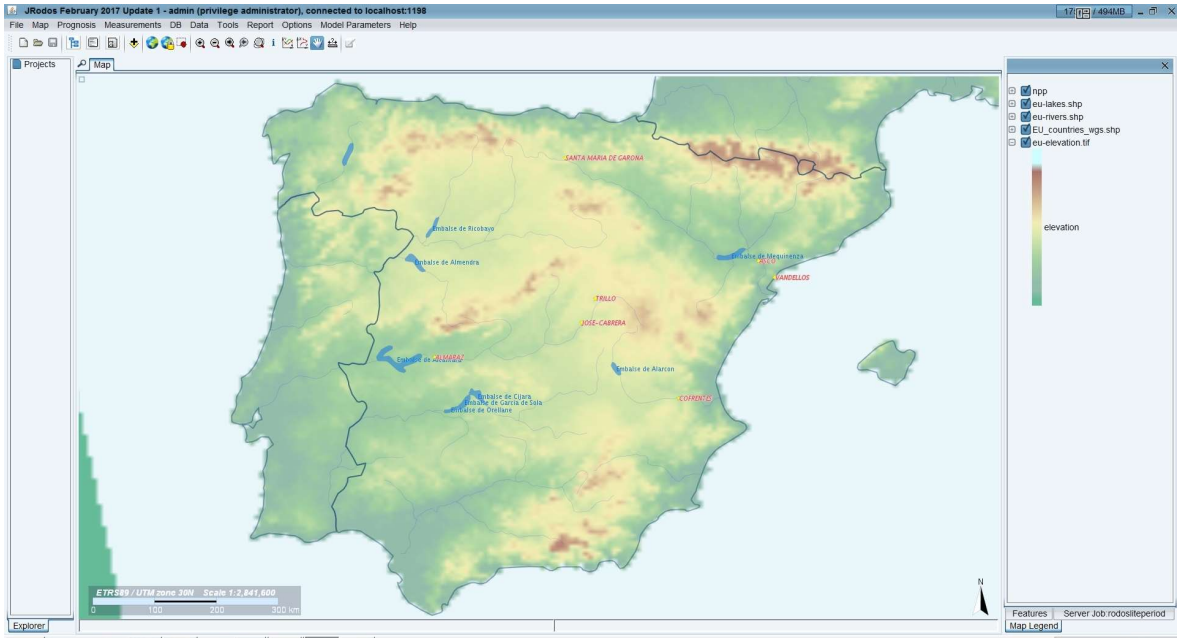

Figure 22. Default input DEM in JRODOS. Source: JRODOS software display.

2.4.2.4 Simulations to assess the ^{137}Cs deposition derived from an accidental release from Almaraz NPP

JRODOS (KIT, 2017a), as the software chosen to perform the accidental releases' simulations, includes different modules to obtain the ^{137}Cs activity concentration deposited on the ground for the daily simulations; these are the following (KIT, 2017c):

- The Local Scale transport and dispersion Modules Chain: LSMC, in which the Lagrangian mesoscale atmospheric dispersion puff model: RIMPUFF (RIsø Mesoscale PUFF model) (Thykier-Nielsen, et al., 1999) is implemented. The inputs used to run this module are the source term information regarding the radionuclides released and the meteorological data mentioned before.
- The DEPOsition Module DEPOM (Müller & Gering, 2002) estimates, among other outputs, the activity concentration deposited on ground (Bq/m^2), which is the result to be analysed. In further steps of the simulations this could be used to assess the root uptake to crops with the Food Chain and Dose Module for Terrestrial Pathways (FDMT) (Müller, et al., 2004).

The modules are run sequentially for each simulation starting from the LSMC module, for the transport and dispersion of the plume, followed by the DEPOM module. The whole sequence is carried out automatically along the five-year period, running the process by using the JRODOS Statistical tool (KIT, 2017a). It generates, the daily statistically distributed starting releases over the defined time interval (in this case from 2012 to 2016) to attain the corresponding outputs.

The outputs for each simulation are given for a grid with variable resolution distributed in five rings; cell size starts with 2 km wide from the grid centre ring and doubles with the distance, up to 50 km and again it doubles up to 100, 200, 400, and finally, up to 800 km far from the grid centre, where the cell size is 32 km wide. In total, the grid contains 8056 cells (numerated from 0 to 8055) and each cell is assigned the corresponding output deposition value for each simulation. The cell number distribution in the JRODOS output grid is included in Figure 23, where the five cell-size rings are represented in different colours.

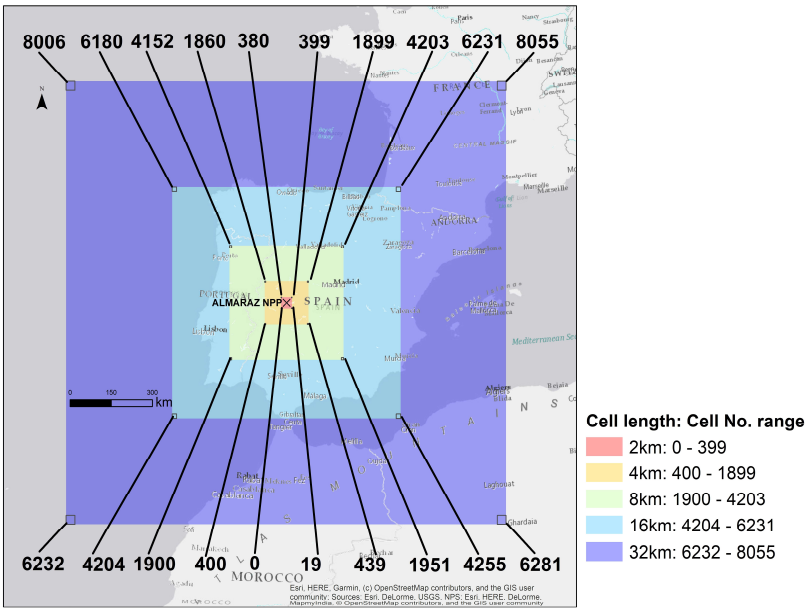

Figure 23. Cell number distribution in the JRODOS grid. Only the corner cells in each grid-sell size ring are identified. Base map source: OpenStreetMap taken from ESRI. Projection WGS84.

Each simulation output, in this case the ^{137}Cs activity concentration deposited on ground, is stored in the PostgreSQL database; it can be downloaded as text files (*.txt) or as shapefiles (ESRI, 2016a) (in which each cell corresponds to a polygon feature (KIT, 2017d)).

2.4.3 Deposition probabilistic assessment

The outputs from the 1383 simulations successfully performed for the five-year period, have been used to conduct a probabilistic assessment, considering the ^{137}Cs activity concentration deposited on the ground, for each of the 8056 grid cells. The aim is to map the average deposition pattern which reflects the deposition probability and its severity also. To do that, a five-category index, named *Deposition Index* (*I_D*) is created; it represents the deposition likelihood and the severity of the deposition, regarding the ^{137}Cs activity concentration deposited on the ground.

The annual average deposition pattern within the entire output grid is obtained using the whole bunch of simulations. In the same way, the seasonal average deposition pattern can be calculated by grouping the simulation outputs according to the release date; thus, the *prevailing* deposition patterns along the year are obtained. Annual and seasonal deposition maps have been performed following the procedure designed in ANURE (2017).

The total deposition values (dry and wet) of ^{137}Cs predicted at each grid cell at the end of each simulation, have been taken and grouped into contamination level categories. Being no categories of the kind available in Spanish regulation, the levels used as reference are those defined in the Nordic Guidelines and Recommendations 2014 (NGR, 2014) for strong gamma and beta emitters together. The classification of contamination levels chosen (NGR, 2014) comprises five ranges of activity concentration values from the total gamma and beta emitters; it defines the corresponding contamination levels regarding the radiation exposure severity, with the aim to evaluate the decontaminations needs in the environment (see Table 14).

Table 14. Contamination levels according to the activity concentration (kBq·m^{-2}) of strong gamma and beta emitters deposited on ground (NGR, 2014).

Contamination levels	**Strong gamma and beta emitters (kBq·m^{-2})**
Non-contaminated	No contamination at all or very low contamination
Slightly contaminated	<100
Contaminated	100 – 1000
Heavily contaminated	1000 – 10000
Extremely contaminated	>10000

That classification was adapted for methodological purposes to include one more class for non-impacted grid cells (0 $kBq \cdot m^{-2}$) and to modify the deposition ranges for the "*slightly contaminated*" and "*non-contaminated*" levels following an exponential progression for their activity concentration ranges, as it is shown in Table 15 (ANURE, 2017).

Table 15. Contamination levels modified from the original ones (ANURE, 2017).

Contamination levels	Strong gamma and beta emitters ($kBq \cdot m^{-2}$)
Non-impacted	0
Non-contaminated	0 – 10
Slightly contaminated	10 – 100
Contaminated	100 – 1000
Heavily contaminated	1000 – 10000
Extremely contaminated	>10000

As the activity concentration to be analysed corresponds only to ^{137}Cs, thus, it is necessary to consider the contribution of this radionuclide among all the gamma and beta emitters. This was assessed on the bases of the source term radionuclides, with a result of $1 \cdot 10^{-3}$ from the total activity concentration deposited from those emitters, as it was previously mentioned (see section 2.4.2.1). The corresponding ^{137}Cs activity concentration in soil for each contamination level is included in Table 16.

Table 16. ^{137}Cs activity concentration associated with the corresponding contamination level and the weight factor used to weight the probability of occurrence of each level by its severity. (ANURE, 2017)

Contamination levels (CL)	^{137}Cs activity concentration deposited ($kBq \cdot m^{-2}$)	Deposition Weighting Factor (DWF)
Non-impacted	0	1
Non-contaminated	0 – 0.01	10
Slightly contaminated	0.01 – 0.1	100
Contaminated	0.1 – 1	1000
Heavily contaminated	1 – 10	10000
Extremely contaminated	>10	100000

Firstly, for the annual average deposition pattern, a reclassification of the 1383 ^{137}Cs activity concentration values of each grid cell is done to define their contamination level. Then, the annual probability of occurrence of each contamination level is calculated in each grid cell.

Besides, a *Deposition Weight Factor* (*DWF*) is assigned to each level, starting from 1 for the "*non-impacted*" cells and increasing exponentially with the contamination level, as it does the activity concentration thresholds to define the contamination levels (see Table 16) (ANURE, 2017). This factor is applied to obtain the weighted deposition probability in each grid cell by multiplying the probability of occurrence of each contamination level by its

corresponding *DWF*. By introducing the *DWF*, the most potentially affected areas, in terms of probability of receiving a deposition and also in terms of deposition's severity (regarding the amount of activity concentration deposited) are highlighted. That way, given a probability of occurrence, the higher the contamination level the higher the *Deposition Index*[105].

In each grid cell, the sum of the multiplication of the probability of each deposition level by the corresponding deposition weighting factor is obtained, as it is shown in the following expression:

$$\sum_{i=0}^{8056} (P_i \times DWF_i)$$

Being:

i = cell grid number,

P: probability of occurrence of each deposition level,

DWF: *Deposition Weighting Factor*.

Percentiles P_{25}, P_{50}, P_{75} and P_{95} of that sum, considering all the grid cells, are calculated; this way, the entire simulation set (with the 1383 simulations) is taken into account. These percentiles are used as thresholds to create the five-category index named *Deposition Index (I_D)*. By considering the last percentile (P_{95}), those areas where the likelihood of being classified as *extremely contaminated* is the highest are highlighted (following the same criteria applied to define the *I_RV* – see section 2.3.3).

The process to assess the *I_D* is included in Figure 24.

[105] Since all the contamination levels are taken into account, each one has to be assigned a specific weighting factor to distinguish the contribution of one level from another; this is precisely the DWF.

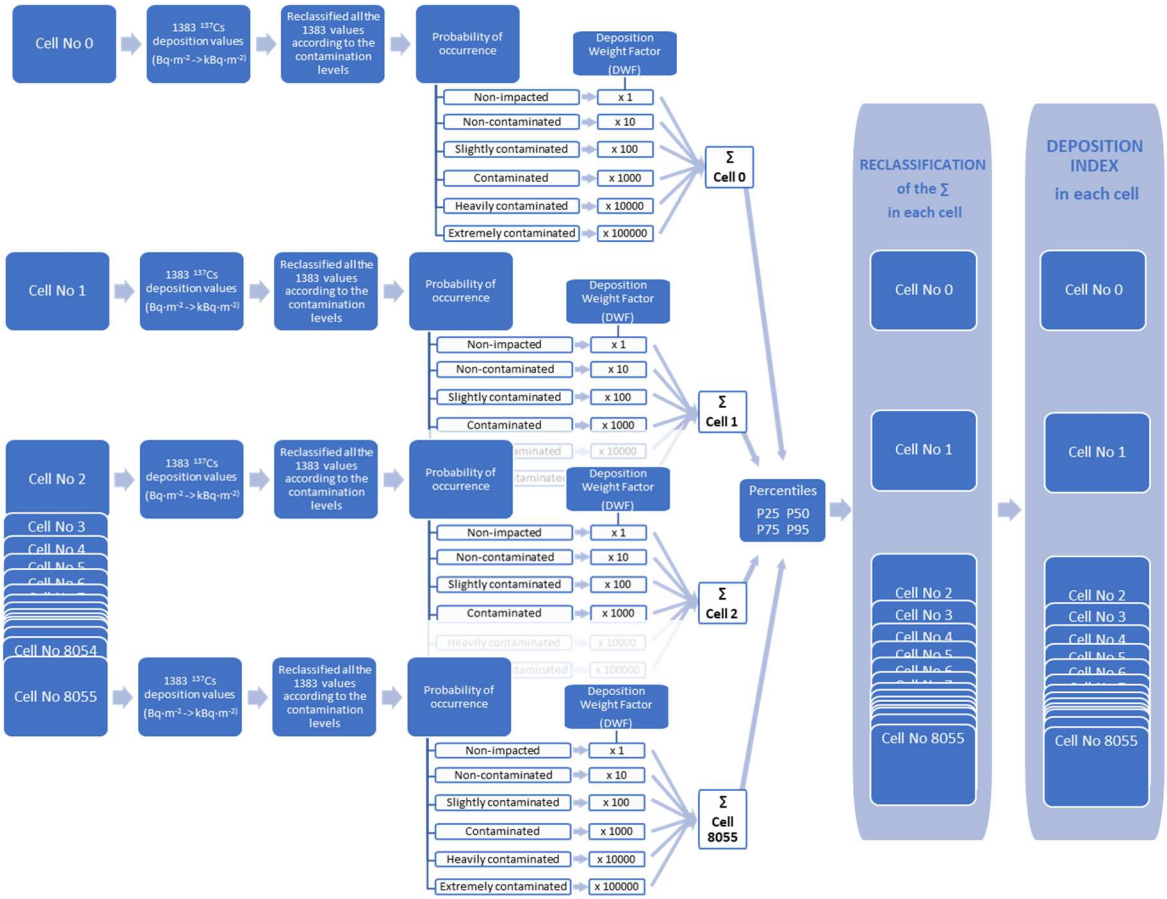

Figure 24. Workflow of the process to obtain the Deposition Index (I_D).

Having four thresholds (the four percentiles), five *Deposition Index* classes are obtained; these are assigned an integer number from 1, for the *Minimum I_D*, to 5, for the *Maximum I_D*. Each grid cell comes with its own *I_D* value, which is stored in a table (*.xlsx, *.csv or *.txt format). In Table 17 the thresholds used to identify the *I_D* and the *I_D* classes are shown.

Table 17. Thresholds to identify the Deposition Index (I_D), the derived I_D categories and the colours used to map it along the output simulations' grid.

Colour	Thresholds to define the I_D categories	Deposition Index
	Percentiles ranges obtained from the weighted deposition results in the whole 8056 cells: ∑ (P × DWF)	**I_D**
Blue	$< P_{25}$ → < 796.173	1: Minimum
Green	$P_{25} – P_{50}$ → 796.173 – 2962.621	2: Low
Yellow	$P_{50} – P_{75}$ → 2962.621– 6426.434	3: Medium
Orange	$P_{75} – P_{95}$ → 6426.434 – 15820.180	4: High
Red	$> P_{95}$ → > 15820.180	5: Maximum

Applying this methodology, the deposition pattern is obtained; it reflects the combination of the probability of ^{137}Cs deposition occurrence and its severity by means of the *Deposition Index*, thus, in each cell, the higher the hazard of being impacted, the higher the *Deposition Index* value.

To perform the Deposition map for each season, instead of considering the whole set of simulations (used to obtain the annual deposition map), only the simulations corresponding to each meteorological season's days[106] are taken into account. The percentiles to be considered to assess the thresholds for the annual and seasonal average conditions correspond to the percentiles calculated by using the whole set of simulations (the 1383 ^{137}Cs deposition values) (see Table 17). Therefore, the five deposition maps for the five different average meteorological situations (annual, spring, summer, autumn, and winter) are performed by using the same categorisation and the results obtained can be compared.

The output grid obtained from JRODOS is selected as a base to allocate the *I_D* value assessed as it is described above, for each cell. However, before combining both: the table with the cells' I_D and the grid, it is necessary to fix the latter, because in the JRODOS exporting process the shapefile gets some topological[107] issues: the polygons that correspond to several cells overlap each other in some spots across the grid and create gaps among the adjacent cells in other places. The proceeding to adjust all the shape file features was made in ArcMap. It starts by creating a geodatabase (ESRI, 2016b) to import the grid shapefile to be fixed, because, by definition, shapefiles do not store topological information (ESRI, 2016b). A new topology is created inside the new geodatabase with the rules to be fulfilled by the grid's polygons: "*must not overlap*" and "*must not have gaps*" (ESRI, 2016b). Having identified the topological errors, these can be solved by using the Topology toolbar (ESRI, 2016a) to edit the grid feature class, in order to obtain a proper one, without gaps or overlaps between polygons. In Figure 25 the output JRODOS grid (in red) and the fixed grid (in blue) are represented.

[106] The meteorological seasons are considered, thus, for instance, spring starts on the 1st of March and ends on 31st of May.
[107] Topology is a set of features (in this case, polygons) with a common geometry (ESRI, 2016a).

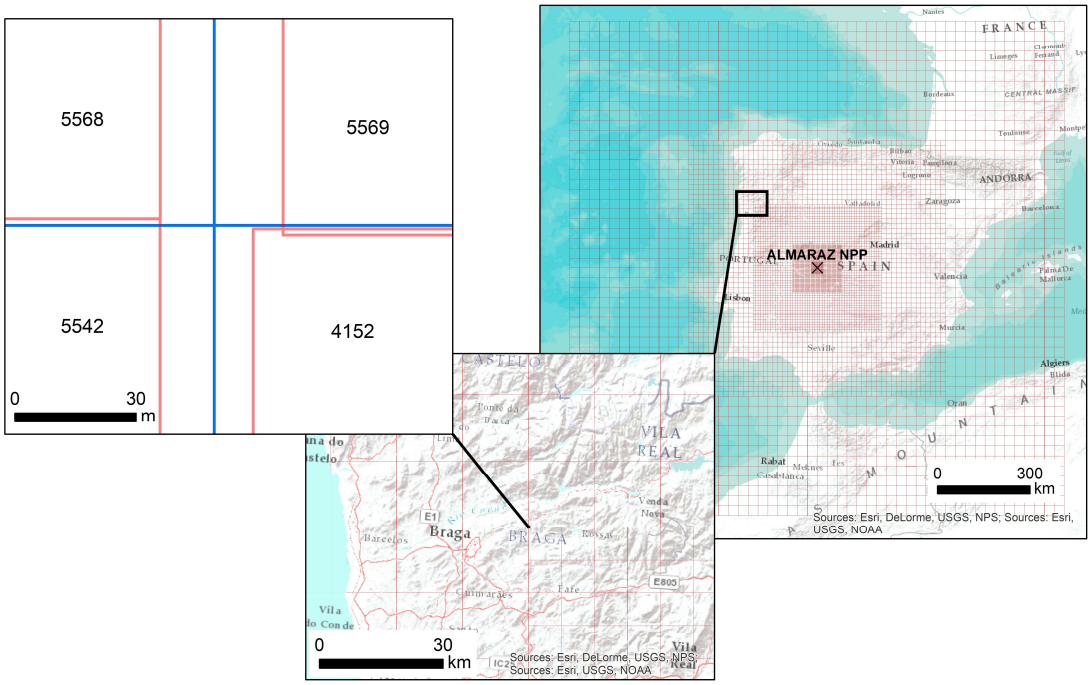

Figure 25. Detail of the JRODOS grid (in red) and the fixed one, without topological errors (in blue). As it can be seen, cell No. 5569 overlaps on 4152 and a gap exists between the cells to the right (5542 and 5568) and the cells to the left (4152 and 5569).

Once the fixed grid is obtained the assignment of the *I_D* to the grid cells is done by linking the grid feature with the output *I_D* values table (annual and seasonal), by their common cell number field, by using the Join tool in ESRI (2016). Thus, the Deposition Maps, representing the *prevailing* deposition, are attained for annual average meteorological conditions and for each seasonal average meteorological conditions. The five resulting Deposition maps are included in section 3.4.1 (Figure 54).

2.4.4 Prioritization maps

The combination of the Radiological Vulnerability map of the agricultural systems, with the ^{137}Cs Deposition maps obtained for this specific accidental scenario, allows the identification of those areas which imply a higher risk to the food chain contamination and for the ingestion exposure pathway. This information is essential to elaborate the response plans needed to face the mid and long-term for the recovery phase as they allow the categorization of the areas in which to implement recovery strategies in a prioritised way (ANURE, 2017). Then, a *Prioritisation Index* (*I_P*) is obtained and mapped for the agricultural mainland Spanish systems. The prioritization maps may be considered as risk maps which take into account both, the potential ^{137}Cs deposition in an agricultural system, and the

vulnerability of the agricultural areas to that phenomenon, focused on the human exposure to ^{137}Cs through the ingestion pathway. The process to obtain the prioritization maps is shown in the workflow included in Figure 17.

The combination of both parameters, the *Radiological Vulnerability* and the *Deposition* (annual or seasonal) is made by multiplying their corresponding indexes: *I_RV* (see section 2.3.3) and *I_D* (see section 2.4.3), as it is applied in the risks analysis methodologies (Kolluru, et al., 1996; ISO/Guide 73:2009(en); Poljanšek, et al., 2017). Both indexes have been assumed with the same weight factor (1), thus, none of them influence the most in the assessment. All the possible combinations between them are reflected in the matrix included in Figure 26.

Radiological Vulnerability Index / Deposition Index		Min. I_RV 1	Low I_RV 2	Med. I_RV 3	High I_RV 4	Max. I_RV 5
Minimum I_D	1	1	2	3	4	5
Low I_D	2	2	4	6	8	10
Medium I_D	3	3	6	9	12	15
High I_D	4	4	8	12	16	20
Maximum I_D	5	5	10	15	20	25

Prioritisation Index (I_P) Legend

Minimum Priority. I_P = 1 | Low Priority. I_P = 2 | Medium Priority. I_P = 3 | High Priority. I_P = 4 | Maximum Priority. I_P = 5

Figure 26. Matrix used to perform the combination between the Radiological vulnerability Index (I_RV) and the Deposition Index (I_D), in order to obtain the Prioritisation Index (I_P). The resulting categories according to the I_P values are shown in the key.

To obtain the *Prioritisation Index (I_P)*, the resulting combination values are grouped and reclassified into five categories, according to the named and colour classes shown in Table 18. This way, the potentially affected agricultural areas are classified into theses five-prioritisation categories.

Table 18. Prioritisation categories for the agricultural areas defined according to the I_RV and the I_D combination.

Colour	Range of the results of I_RV and I_D combination	Prioritisation Index I_P (Value and Category)
Blue	1 – 3	1: Minimum priority
Green	4 – 5	2: Low priority
Yellow	6 – 10	3: Medium priority
Orange	12 – 16	4: High priority
Red	20 – 25	5: Maximum priority

The priority categorisation of the agricultural areas for the case study designed, seeks to highlight fundamentally those with *Maximum Priority*, and also with *High Priority*, where to act on facing the recovery phase to apply the most effective and optimised measures on the frame of the EPR. The intention has been to avoid resulting extremely large areas, so that the actions to be taken for the recovery are affordable, particularly for the *Maximum I_P* category.

The combination of the I_RV map and the I_D map to obtain the *I_P* is done by overlapping both features (using the "*Identity*" tool (ESRI, 2016a)). Then, for each resultant polygon both indexes can be multiplied; the outcome is reclassified to obtain the corresponding *I_P* category according to the criteria given in Table 18. The five Prioritisation maps, for annual and seasonal average meteorological conditions, are included in section 3.4.2 (Figure 57).

3 RESULTS AND DISCUSION

Throughout this chapter, the results obtained following the methodologies described in section 2 are presented and discussed. These results, focused on mainland Spain, are grouped in the following:

- The *Radiological Vulnerability* regarding the soil potential to favour the bioavailability of ^{137}Cs to be uptaken by crops (which corresponds to the updated radiological vulnerability map).
- Identification and distribution of the crops throughout peninsular Spain. These results are related to the *representative crop* map, used to characterise the agricultural systems of most concern for the food chain exposure pathway, and the crop's group in which these are included according to (IAEA, 2010).
- The *Radiological Vulnerability of the agricultural areas*, which shows the capacity of the soil – plant system to transfer the ^{137}Cs from soil to crops.
- The results obtained from the case study tested in Almaraz NPP regarding: i) the ^{137}Cs deposition maps and ii) the categorisation of the agricultural areas attending to the need for prioritising where to implement recovery actions, addressing the EPR needs.

Nevertheless, before presenting the results of the three methodological steps, the results obtained regarding the Spanish soil profile database updating, on which are based the radiological vulnerability assessments in this Thesis, are presented. Subsequently, the resulting soil groups map (obtained by using the EC-ESBN (2004) as the base map to represent the Spanish soils' properties) is shown.

The Spanish soil DB has been enlarged with the addition of 26 new "*complete*" Spanish soil profiles (see Annexe VII). The general data of each one is structured in the heading of the corresponding sheets as shown in Figure 27 and the following soil properties are given for each horizon also: horizon type, upper limit (cm), thickness (cm), colour, texture, structure, compactation, root development, infiltration (mm h^{-1}), pH, EC (mS cm^{-1}), $CaCO_3$ (%), O.M. (%), C/N, gravel (%), coarse sand (%), fine sand (%), total sand (%), silt (%), clay (%), bulk density (g cm^{-3}), Ca (cmol kg^{-1}), Mg (cmol kg^{-1}), Na (cmol kg^{-1}), K (cmol kg^{-1}), S (cmol kg^{-1}),

CEC (cmol kg^{-1}), and V (%)[108]. Besides, indications about the location and the bedrock, as well as other general comments are included in the footer, if necessary. The soils' data shown in each sheet are organised following the same criteria (in terms of format, style and language) as it was designed for the original soil profile database (Trueba, et al., 2000b). Besides, the *Radiological Vulnerability Indexes of soils* (partial and global) are included.

PROFILE No.: xx	PROVINCE: xx	PROFILE CODE: xx	UTM COORDENATES. HUSE 30 (ETRS89): xx	MTN* SHEET: xx
MUNICIPALITY: xx			ELEVATION (m): xx	SLOPE (%): xx
LOCATION: xx				
LAND USE: xx			REFERENCE: xx	
USDA-SOIL TAXONOMY: xx				
FAO (1974) SOIL CLASIFICATION: xx			NUMBER OF HORIZONTS: xx	

*MTN: National Topographic Map (In Spanish: Mapa Topográfico Nacional)

Figure 27. Heading of each soil profile sheet.

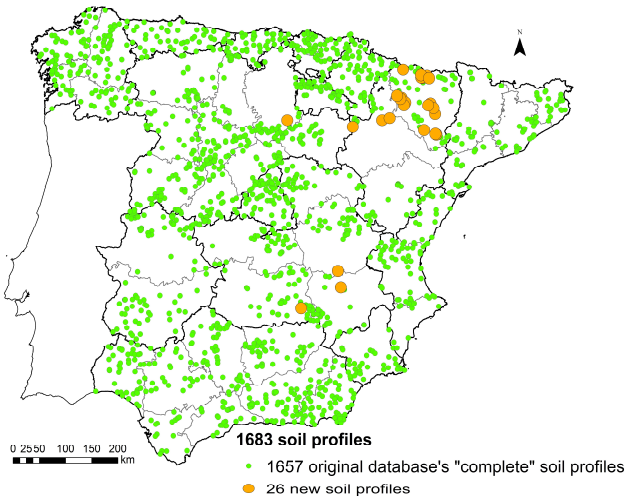

Figure 28. Soil profiles location through peninsular Spain. It can be distinguished the original "complete" ones and the 26 new ones. Projection UTM ETRS89-H30.

Despite the search that has been done in this Thesis to incorporate new "*complete*" soil profiles to the initial set (which brings the overall total of 1683 Spanish soil profiles in the *updated* Spanish soil database), that enlargement provides not enough information to characterise all the soil types included in EC-ESBN, (2004), as explained below. The spatial distribution of the soil profiles, distinguishing the new ones, can be seen in the map

[108] pH: soil acidity measured in water, EC: electrical conductivity, $CaCO_3$: calcium carbonate, O.M: organic matter, C/N carbon/nitrogen, Ca: calcium, Mg: magnesium, Na: sodium:, K: potassium, S: total exchangeable bases, CEC: Cation-exchange capacity, V: base saturation.

included in Figure 28, which has been performed by using GIS software (ESRI, 2016a), according to their coordinates.

The soil profile compilation that has been done has enlarged and improved the original database, mainly in Huesca province (with 18 more profiles) and in Zaragoza (with 4 more) and in Albacete, Burgos, Ciudad Real and Cuenca (with one more profile in each). However, as it is shown in Figure 28, despite of the increase in the number of soil profiles, there are some spots not properly characterised yet. That occurs in the provinces of Burgos, Zaragoza, Albacete, Cáceres, León, Palencia, half South of Cuenca or within a considerable extension of Teruel, Lérida or Murcia. Nevertheless, the soil database compiles an enormous amount of information about the vast majority of the soil types in Spain.

Regarding the most recent European soil map used in this Thesis as the base map (EC-ESBN, 2004), it contains the same features as the one used in the first updating of the Radiological Vulnerability of the Spanish soils (García-Puerta, 2014), the EC (1995). However, both have some differences in comparison with CEC (1985). A most considerable variety of soil types are distinguished in the two latest issues for peninsular Spain; specifically, 9 more STUs (36 instead of 27 STUs), allocated in 10 more SMU added (72 instead of 62 *SMU*s). Therefore, several soil types[109] of which there were soil profiles in the DB have representation in these two last versions (in contrast to the 1985 European soil map), such as Calcaric Fluvisols (Jc), Dystric Regosols (Rd), Rendzinas (E), Gleyic Acrisols (Ag), Orthic Solonchak (Zo), Eutric Regosols (Re), Calcaric Regosols (Rc), Chromic Cambisols (Bc), Orthic Podzols (Po), Gleyic Luvisols (Lg), Chromic Luvisols (Lc) and Rhodo-Chromo-Calcic Luvisols (Lkcr). However, the soil profiles classified as Gleyic Cambisols (Bg) and Dystric Planosols (Wd) have lost their representation in the two last map versions (EC, 1995; EC-ESBN, 2004) in contrast with the first one (CEC, 1985). On the other hand, Ochric Andosol (To), Calcaro-Chromic Cambisol (Bcc) and Ferric Luvisol (Lf), although having representation in the soil base map cannot be characterised because of the lack of these soil types in the soil DB. The first one is situated in Gerona province, the second one is allocated in one spot in Badajoz, just in the Portuguese border, and the third one is also along the Portuguese border: one spot in

[109] Soil type referred to the soil classification (FAO-UNESCO, 1974).

Palencia, one in Cáceres and another one in Badajoz. These three soil types (To, Bcc and Lf, respectively) sum slightly over 130 km^2, which is a minimal surface.

The enhancement of the base map used (EC-ESBN, 2004) in comparison with the 1985 issue, added to the enlargement of the soil DB with 26 more "*complete*" soil profiles, enables to use a total of 1410 "*complete*" soil profiles in the assessing of the radiological vulnerability in peninsular Spain, instead of the 1060 profiles used in the first two issues, in 2000 and 2004. In total, 44 soil groups which can be linked to the soil base map (EC-ESBN, 2004) have arisen from the soil DB.

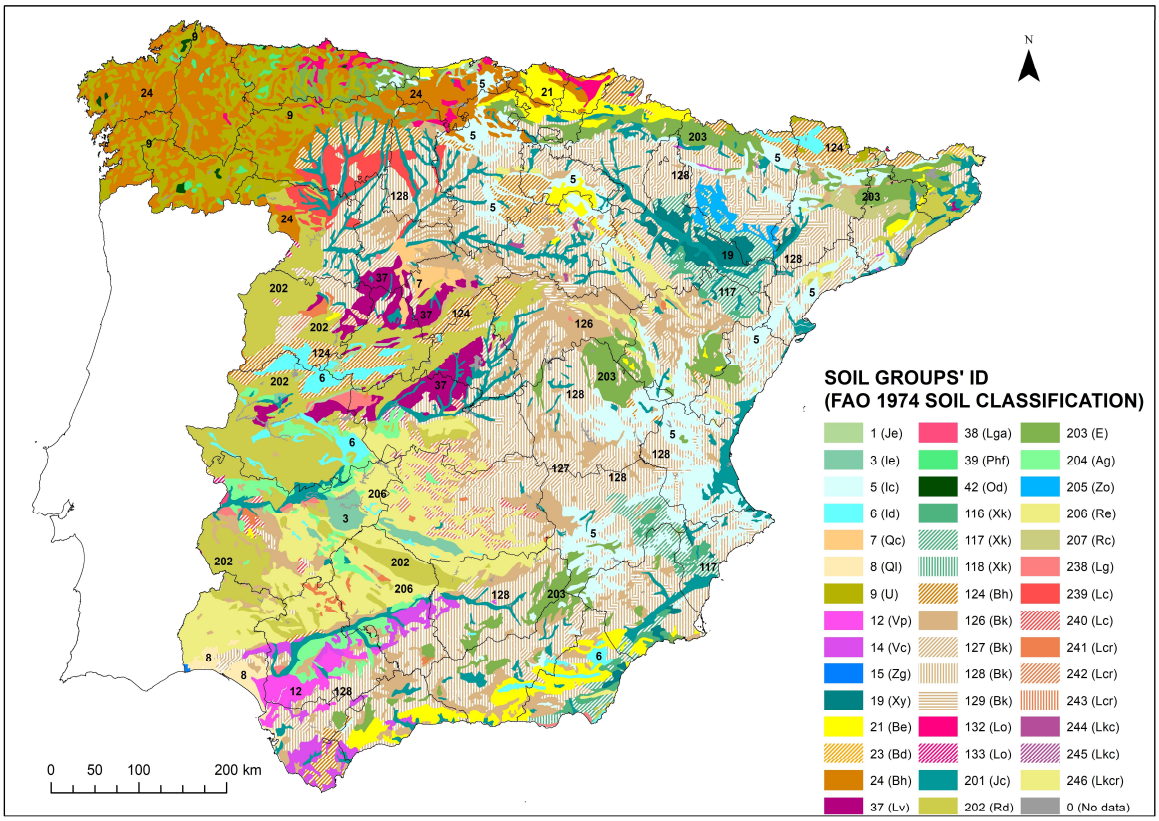

Figure 29. Distribution of the soil groups in peninsular Spain. Their corresponding ID number and the soil classification according to FAO-UNESCO 1974 is shown. Projection UTM ETRS89 H30.

The map with the soil groups' distribution that has been used to represent the Radiological Vulnerability in peninsular Spain all along this Thesis is included in Figure 29, and the list of

the soil groups made from the updated soil DB, which have representation in the soil base map (EC-ESBN, 2004) is included in Annexe IV[110].

However, as it occurred in the previous works, there are some soil groups which do not have representation in the base map (EC-ESBN, 2004). For the current version, there are 40 soil groups which cannot be mapped; these are the ones encoded with the numbers 22, *25*, 40, *41, 208, 209* and those over the code *1000* (see Annexe VIII[111]). It is important to state that the soil groups number 25 and 41, comprised of Gleyic Cambisols[112] and Dystric Planosols[113], respectively, have lost their representation in the two last soil map versions (EC, 1995); (EC-ESBN, 2004), in contrast with the first one (CEC, 1985).

3.1 Results of studying the ^{137}Cs behaviour in soil. The updated Soils' Radiological Vulnerability map

The *Global Radiological Vulnerability* index (*G_Cs_ing*) represents the potential of the soils to favour the transfer of radiocaesium to crops and the food chain, giving rise to a risk to the population due to the ingestion exposure pathway, according to Trueba, et al. (2000a). Following that methodological approach, five categories for the vulnerability of soils regarding the potential availability of ^{137}Cs for crops are considered. The resulting map for mainland Spain is shown in Figure 30.

[110] The following is the information included in Annexe IV regarding the soil groups: ID, soil type code and classification, bedrock codification, number of soil profiles included from the updated Spanish soil DB, topsoil clay content, topsoil texture and topsoil potassium content.
[111] Annexe VIII gathers the results of the partial and global indexes of each soil group for the assessment of the Radiological Vulnerability of the soils, whether it has correspondence with the map or not. These results are explained in detail in section 3.1.
[112] Gleyic Cambisols (Bg).
[113] Dystric Planosols (Wd).

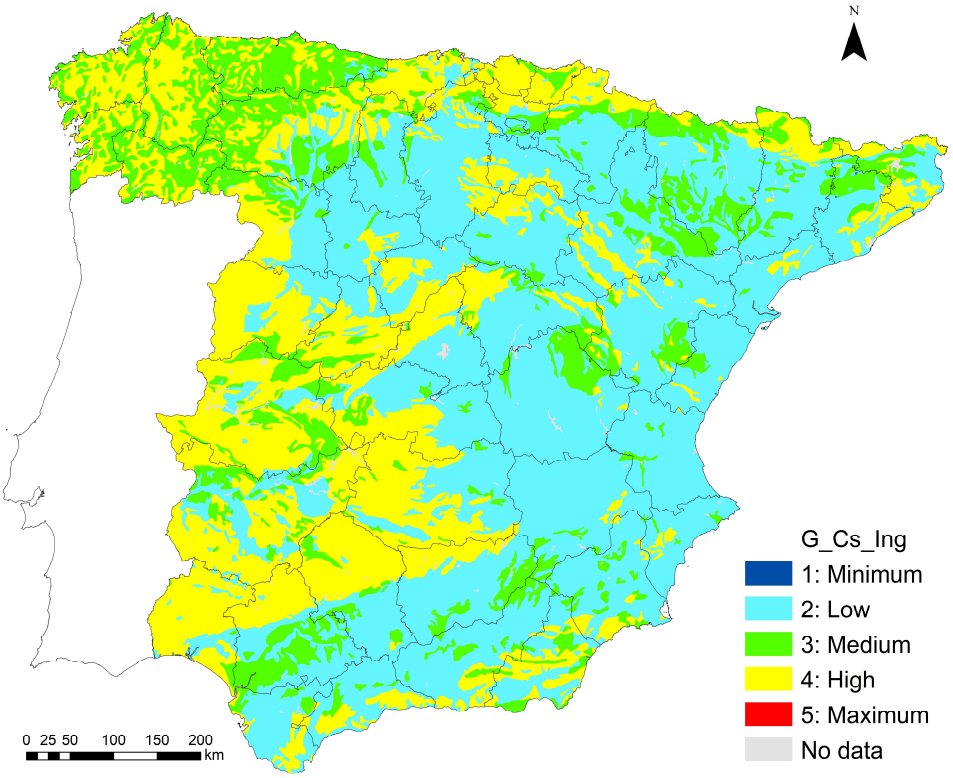

Figure 30. Updated version of the Global Radiological Vulnerability map for radiocaesium, regarding the ingestion pathway (G_Cs_Ing). Projection: UTM ETRS89 H30.

In the light of the resulting radiological vulnerability map, the following considerations can be stated:

- There are no areas where soils are classified with the *Maximum* (value of 5) or *Minimum Global radiological vulnerability* indexes (value equals to 1).
- The highest *G_Cs_Ing* index value in peninsular Spain is equal to 4 (in yellow), meaning high potential to transfer ^{137}Cs to crops. It is associated with soil groups located mainly in mountainous areas and on igneous or metamorphic acid bedrock, with significant organic matter content (compared to the rest of the soil groups), such is the case for Humic Cambisols on acid crystalline rocks (included granite)[114] or District Histosols[115] in Galicia, in the Pyrenees or in other ranges, such as Sistema Ibérico and in the Sistema Central. It also appears in Regosols (both Dystric[116] or Eutric[117]), located mainly in the West of Spain and for those soil groups with a clearly sandy texture, with relatively low potassium content such as the Cambic

[114] Humic Cambisols on acid crystalline rocks (included granite) (Bh) (No. 124)
[115] District Histosols (No. 42)
[116] Dystric Regosols (No. 202)
[117] Eutric Regosols (No. 206)

Arenosols[118] in Valladolid and Segovia provinces, or the Luvic Arenosols[119] in Huelva. It represents just over the 33 % of peninsular Spain surface.

- The *Medium Global Radiological Vulnerability* index, with a value of 3 and mapped in green, is assigned to different soil types located in a wide variety of landscapes and bedrocks all around peninsular Spain, although it is the less widely spread of the *G_Cs_Ing* index's values, with slightly over 17 % of the total surface area. The most representative soil groups within this vulnerability are the Ranker[120] soils on igneous bedrock located in Galicia[121], which are sandy soils with low pH and limited potassium but with relatively high organic matter, the Rendzinas[122] on limestones in sub-mountainous areas, which are alkaline soils with significant organic matter content, the clayey soils such as Pellic Vertisols[123] in the Guadalquivir basin, and the saline soils as Gypsic Xerosols[124] in the Ebro basin. The last two soil groups compensate their maximum and medium water retention capacity, respectively, which increase the radiological vulnerability for the ingestion pathway, with their high pH and limited infiltration rate, which reduce it.
- The surface area occupied by the *G_Cs_Ing* index value equals to 2 (in light blue) corresponds to the half of the entire mainland Spain surface. Soils widely distributed all around Spain, such as Calcic Cambisols on Quaternary materials[125], on marls[126] or limestones[127], Calcaric Fluvisols[128] or Calcic Lithosols[129] in the mid-East of the country, among other minority soils, are classified with this low radiological vulnerability regarding radiocaesium for the ingestion pathway. The common feature of these areas is the dominance of detrital and calcareous sedimentary formations. These soils generally have low infiltration rates, taking time for the

[118] Cambic Arenosols (No. 7)
[119] Luvic Arenosols (No. 8)
[120] Ranker (No. 9)
[121] Galicia corresponds to a NUTs II located in the Northwest of Spain and comprises A Coruña, Lugo, Ourense and Pontevedra provinces.
[122] Rendzinas (No. 203)
[123] Pellic Vertisols (No. 12)
[124] Gypsic Xerosols (No. 19)
[125] Calcic Cambisols on Quaternary materials (No. 127)
[126] Calcic Cambisols on marls (No. 128)
[127] Calcic Cambisols on limestones (No. 126)
[128] Calcaric Fluvisols (No. 201)
[129] Calcic Lithosols (No. Ic)

water containing the radiocaesium in solution to reach the root zone. In addition, the presence of clay can make the potassium reserve in the soil high enough to inhibit the radiocaesium availability to the root uptake.

To analyse the improvement of this updated version of the soil vulnerability map it is necessary to compare it with its first version (Trueba, et al., 2000a). Thus, it can be seen the influence of the cartography base map on the spatial distribution of the vulnerability indexes and also the new soil profiles added to the DB. Figure 31 shows the first *global radiological vulnerability* map (Trueba, et al., 2000a; Trueba, 2004), elaborated considering the vulnerability indexes obtained from the original soil profile DB which uses, as cartography support basis, the 1985 version of the European soil map (CEC, 1985).

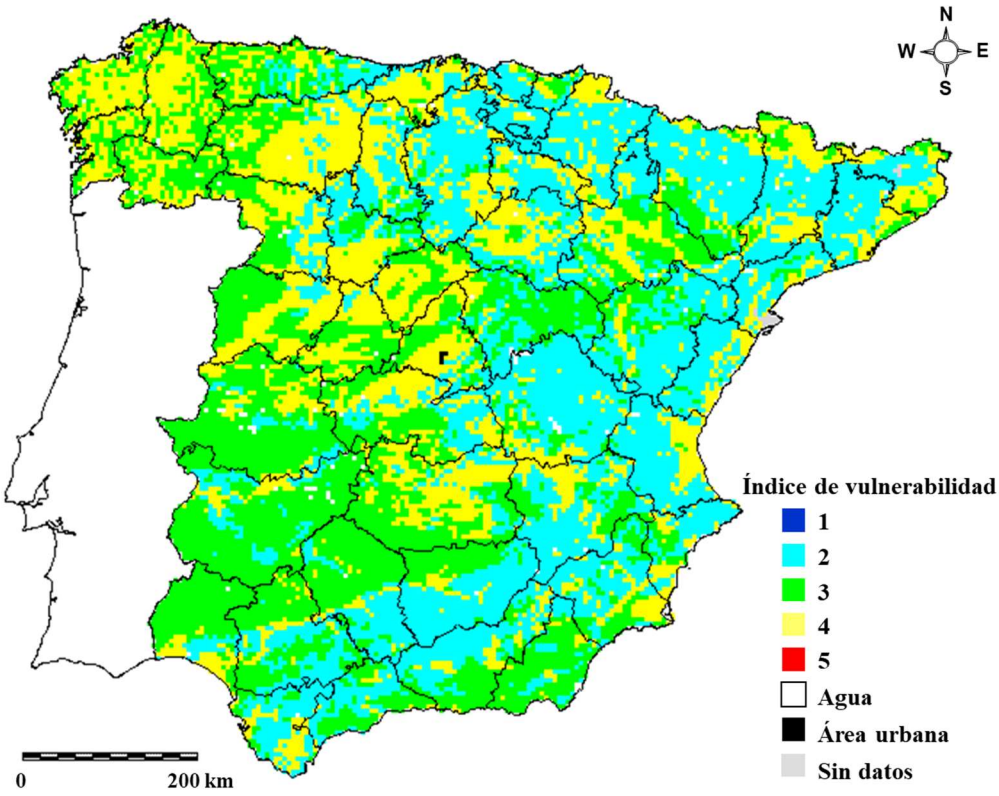

Figure 31. First version of the Global Radiological Vulnerability map for radiocaesium, regarding the ingestion pathway. Legend: Minimum vulnerability: dark blue; Low vulnerability: pale blue; Medium vulnerability: green; High vulnerability: yellow; Maximum vulnerability: red; Water bodies: black; Urban areas: grey; Other areas without soil's properties data in the European soil map used as base map: white. Projection no identified. (Trueba, et al., 2000a).

As it is not possible to identify the location of the soil groups in the vulnerability map obtained in Trueba, et al. (2000a) due to the absence of the original map file, the comparison between this and the updated one can be done exclusively visualising both maps in plain sight. It is not possible to refer those differences to the soil groups themselves

either, just to the images of both vulnerability maps' versions. Having this in mind can be seen that the trend shown in the updated map follows the results of the first one. The extreme vulnerability index categories (*minimum* and *maximum*) are not represented in any maps' version. In general, the Northwest, North of Castilla y León, Cantabria, La Rioja, Aragón, and the Pyrenees, keep the same distribution and values as the original map. However, a large area that originally showed *medium* values of vulnerability, now shows *high* values. This mainly occurs in the Western part of Spain, along the border with Portugal and Central Spain, increasing the percentage of soils that have *high* potentiality to transfer radiocaesium to crops. On the contrary, some soils having originally *medium* values of vulnerability, the updated results assign them *low* potentialities to transfer radiocaesium; this occurs primarily in Central East Spain in soils developed on calcareous bedrocks, associated with where there are Calcic Cambisols in the current soil map version.

The updated results, in particular the increase of *high* and *low vulnerability indexes* at the expense of the *medium* values, can derive from several reasons. The main factor that influences over that variation lies in the differences between the European soil map used as the base map, which, in turn, implies some variations in the gathering of the soil profiles to create the soil groups (García-Puerta, 2014). On the other hand, the existence of 26 more soil profiles in the updated DB, jointly with the assessment method to obtain the *G_Cs_Ing* of each soil group, leads also to the resulting differences. As the soil vulnerability index corresponds to the indexes' mode value of the soil profiles belonging to each soil group, even by adding only one more soil profile to a group, this group is subject to change its *Global Radiological Vulnerability Index*.

A first update of the *Global Radiological Vulnerability* map of the Spanish soils regarding radiocaesium for the food chain pathway was performed in (García-Puerta, 2014), included also in (Trueba, et al., 2015). That update was carried out with the aim to represent the *G_Cs_Ing* by using, as the base map, a most current version of the European soil map (EC, 1995) and to use the soil profile properties of the original soil DB (Trueba, et al., 2000b). The resulting map is shown in Figure 32.

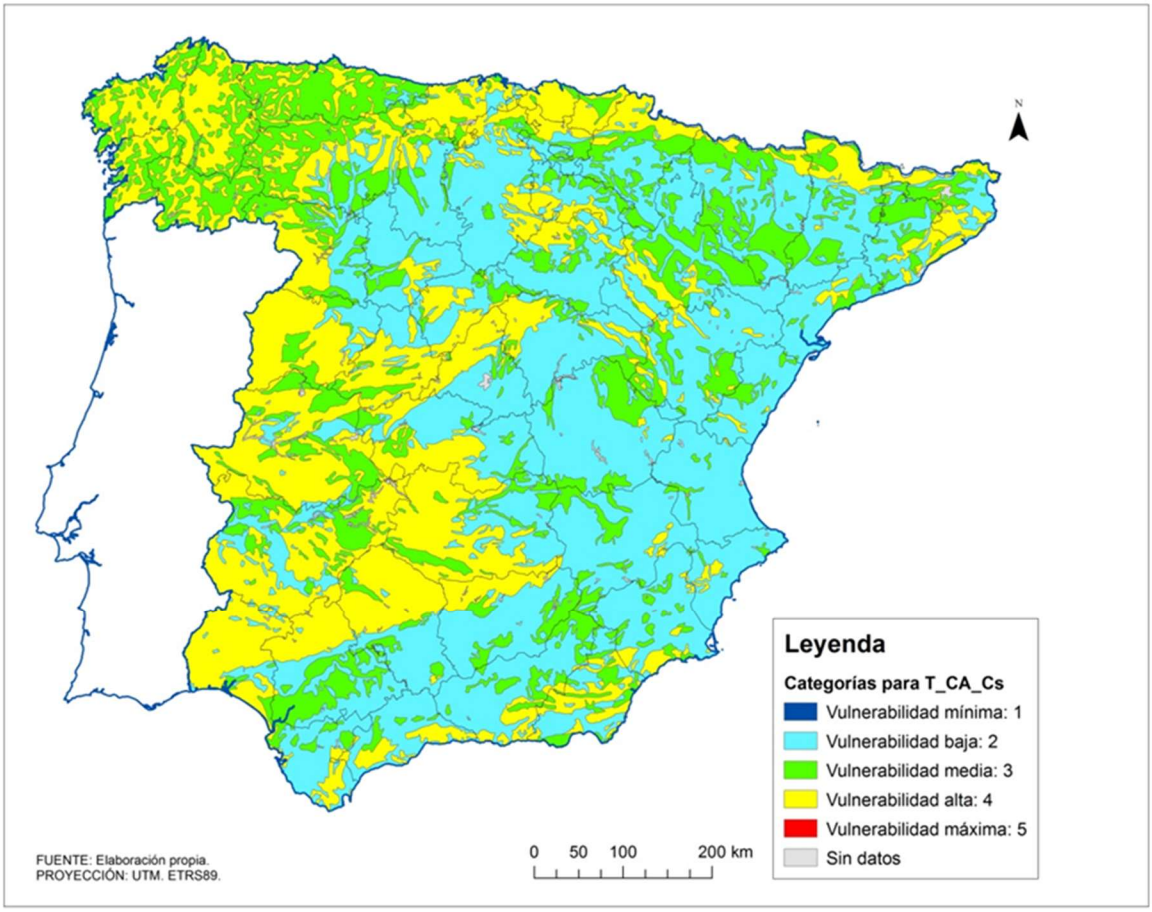

Figure 32. Global Radiological Vulnerability map for radiocaesium, regarding the ingestion pathway (García-Puerta, 2014). Legend: Minimum vulnerability: dark blue; Low vulnerability: pale blue; Medium vulnerability: green; High vulnerability: yellow; Maximum vulnerability: red. Projection: UTM ETRS89 H30. (García-Puerta, 2014).

A comparison between the 2014 radiological vulnerability map version and the update performed in this Thesis can be done. Although two different soil base maps had been used in the mapping of the *G_Cs_Ing* index – CEC (1985) and EC (1995) – these have no cartographic variations in Spain, therefore, the only differentiating factor is the update performed in the soil profile DB. The value changes obtained for the *partial* (I_F, I_H, I_{FQCs} and I_K) and *global* (*G_Cs_Ing*) indexes in both versions for the Spanish soils are shown in Annexe VIII. In that Annexe the following information is also provided: the identifier number of each soil group, the total number of soil profiles included in each one (according to the grouping criteria stablished in Trueba, et al. (2000a), adapted to the newest soil map (García-Puerta, 2014))[130], the resulting soils' radiological vulnerability indexes values for

[130] When corresponds, the number of new soil profiles added to each group is specified.

the partial and global indexes and the difference between the index values obtained in (García-Puerta, 2014) and in this Thesis[131].

Only 7 soil groups (out of the 44 total groups which have correspondence between their soil type classification (FAO-UNESCO, 1974) and the dominant *STU* in the *SMU*s of the soil base map (EC-ESBN, 2004)) have modified at least one of their indexes with respect to García-Puerta (2014). These soil groups are listed in Table 19.

Table 19. Soil groups which have different radiological vulnerability indexes values with respect to the previous radiological assessments.

Soil type classification (code) (FAO-UNESCO, 1974)	**Soil group number (No.)**	**Indexes which have different value in the updated radiological vulnerability map**
Eutric Lithosols (Ie)	3	I_K and G_Cs_Ing
Gypsic Xerosols (Xy)	19	I_F
Eutric Cambisols (Be)	20	I_H
Dystric Cambisols (Bd)	23	I_{FQCs}
Calcic Xerosol (Xk)	116	I_k
Calcic Cambisols (Bk)	127	G_Cs_Ing
Chromo-calcic Luvisols (Lkc)	244	G_Cs_Ing

For Eutric Lithosols[132] on shales, the *partial* index (I_K) and the *global* index (*G_Cs_Ing*) have been modified, for the rest of the soil groups only one index has changed (see Table 19). The former soil group and Calcic Cambisols on Quaternary sediments have reduced one level the *global* index regarding the ingestion pathway for ^{137}Cs, both from *medium* (with a value of 3) to *low radiological vulnerability* (2). Chromo-calcic Luvisols on Quaternary sediments are the only group which have increased the *G_Cs_Ing* index, specifically it has passed from *low* vulnerability (2) in the previous map version to *medium* (3) in the last update. The location of the three soil groups mentioned is shown in Figure 33. Some of the rest soil groups have differences exclusively in the *partial* indexes but not in the *global* one.

[131] The soil groups are shown separately, depending on whether they have correspondence in the base map (EC-ESBN, 2004) or not.

[132] The list of the soil groups, including their soils' classification (according to the legend (FAO-UNESCO, 1974) and the bedrock is included in Annexe IV.

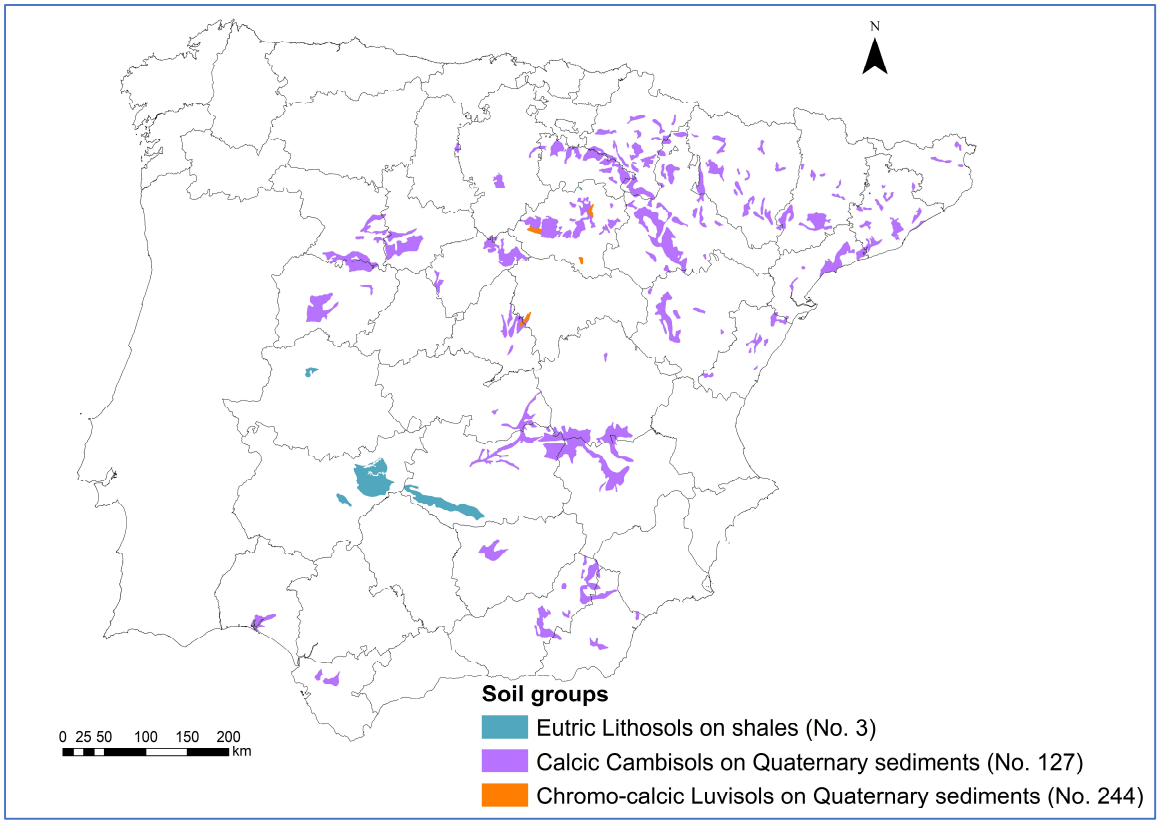

Figure 33. Location of the Eutric Lithosols on shales (soil group number 3) and Calcic Cambisols on Quaternary sediments (soil group number 127), which have reduced the G_Cs_Ing index in the present version with respect the previous one, and Chromo-calcic Luvisols on Quaternary sediments (soil group number 244) which have increased the G_Cs_Ing index (Trueba, et al., 2015). Projection ETRS 89 H30.

Regarding the non-mapped soil groups, only for Orthic Solontez soils[133] two *partial* indexes are different in the updated assessment as seen in Annexe VIII.

These few differences in the indexes values resulting in some soil groups, are related to having updated the soil profile DB and with the methodology to obtain them, based on assessing the mode among all the soil profiles belonging to this group. That way, by including just one more soil profile in a soil group, this statistical value may change, as is the case for the soil groups previously mentioned.

Besides, although the Spanish soil database gathers a relevant amount of soil profiles, it is important to take into account that some soil groups do not have a wide number of soil profiles (such as Dystric Histosols[134], with only two soil profiles); this may limit the

[133] Orthic Solontez soils (No. 1029).
[134] Dystric Histosols (Od) (No. 42).

representativeness of the indexes' values in some cases. That consideration is applicable to the different radiological vulnerability assessments performed in this Thesis.

The use of the (EC-ESBN, 2004) map, which is a more detailed soil map than the (CEC, 1985), jointly with the updated soil profile DB is considered an improvement in the identification of the radiological vulnerability of the Spanish soils, regarding their potential to favour the bioavailability of ^{137}Cs to be uptaken by crops.

3.2 Identification and distribution of the crops and the agricultural systems throughout peninsular Spain

According to the crops' distribution performed by using the CLC land use (EC-ESBN, 2004), the Spanish agricultural statistics (MAGRAMA, 2016), and the administrative division (IGN, 2008), the *representative crops*' map has been obtained (see Figure 34). As it can be seen in the legend of the map included in Figure 34, 45 out of the 133 *IDPRs*[135] in peninsular Spain become a *representative crop*.

The *representative crops*' map obtained depicts the *basic cartographic units* in which these are the most extended crops[136]; however, the precise location where they are grown within the *basic cartographic units* cannot be obtained.

[135] The *representative crop* is identified with the crops' codification, which represents the *Identification of the PRoduct* (*IDPR*), plus the *Identification of the Cultivation System* (*IDCS*): *IDPR+IDCS*.

[136] It is important to clarify that sheltered crops (crops encoded with the *IDCS* as "*SIA*" for the province sharing and as "*sia*" for the municipalities sharing – see Table 8 in section 2.2.1) are the most representative ones in two Andalusian provinces such as Huelva and Almería; strawberries (in the former) and tomatoes (in the latter), are grown in greenhouses. However, since the worst-case scenario has been considered for a direct deposition from a radioactive plume, these sheltered crops have been regarded as non-sheltered ones.

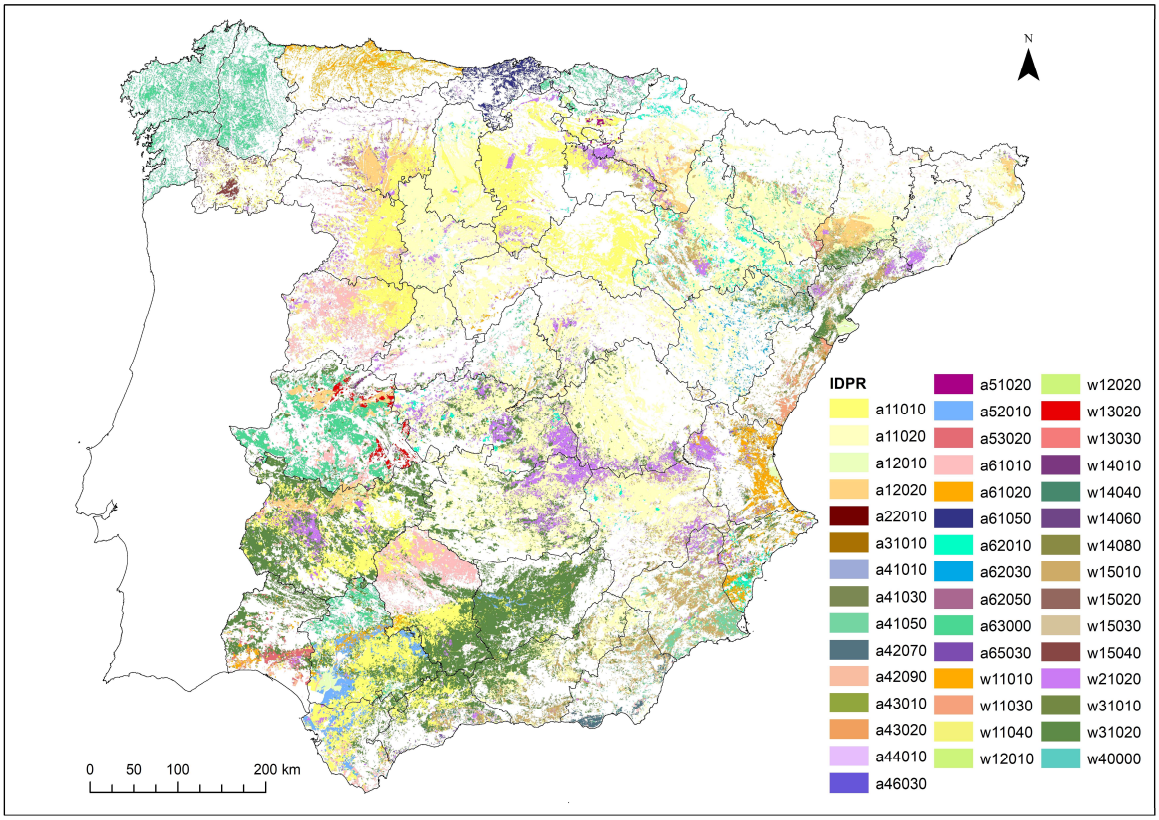

a110xx: Winter cereals	a460xx: Other vegetables	w110xx: Citrus fruit trees
a120xx: Spring cereals	a510xx: Sugar Crops	w120xx: Pome fruit
a220xx: Legumes. Group II	a520xx: Textile Crops	w130xx: Stone fruit (drupe)
a310xx: Tubers	a530xx: Oilseed Crops	w140xx: Fleshy fruit
a410xx: Leafy vegetables	a610xx: Gramineous	w150xx: Nut
a420xx: Fruit vegetables	a620xx: Legumes	W210xx: Vineyard
a430xx: Flower vegetables	a630xx: Meadows	W310xx: Olive grove
a440xx: Root vegetables	a650xx: Other fodder crops	W400xx: Other crops

Figure 34. Representative crops' map (mapping exclusively the IDPR) according to the crops' distribution by municipalities in the "Agricultural areas" (EEA, 2016). Projection UTM ETRS89 H30. A brief summarise of the IDPR code is included. The complete IDPR code correspondence with the crops can be seen in Annexe II. (IDPR: IDentifier of PRoduct).

Moreover, the cultivated surface of the *representative crop* is not the surface of the *basic cartographic unit* which it is linked to since it is only one of the possible crops to be grown in it, although the largest. However, the transfer parameters from soil to crop to be considered for each *basic cartographic unit* as a whole are those associated with the *representative crop* (see section 2.3.2). Due to that simplification, throughout this Thesis, when naming *agricultural surface area* or *agricultural affected area*, it refers to the surface of the whole set of *basic cartographic units* analysed at that point, not to the cultivated area which has been distributed in the territory by municipalities.

This work is focused on studying the ^{137}Cs transfer from soil to crops in order to define the potential risk for the population through the ingestion pathway, due to the entrance of that

radionuclide in the food chain in case of deposition of that radionuclide occurs. However, the Spanish agricultural system comprises certain industrial crops (MAGRAMA, 2016), included in the *IDPR* crop group *A50000* (see the attached key for Figure 34 and Annexe II) which are not edible ones. It was necessary to consider them in the crops sharing to obtain a realistic distribution and are also included in the vulnerability analysis of the agricultural system; however, these are considered separately.

Each *representative crop* has been included in its corresponding crop group (IAEA, 2010) (coded as *ID_C*[137]) (see section 2.2.1 and Annexe II), to obtain a crop groups map. That crop groups map is shown in Figure 35.

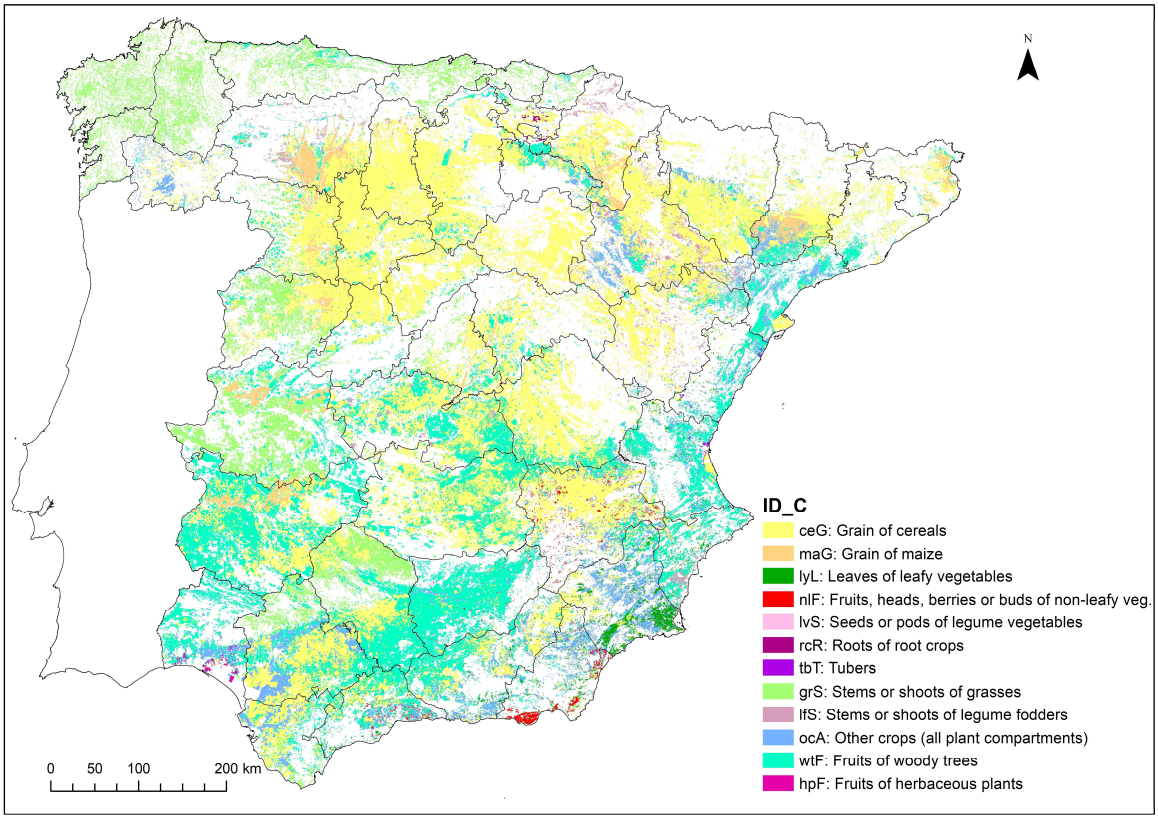

Figure 35. Crop groups' map (pairing plant group – plant compartment (IAEA, 2010)), coded as ID_C, to which each representative crop is associated with the "Agricultural areas" (EEA, 2016). Projection UTM ETRS89 H30.

Along this document, *agricultural surface area* or *agricultural affected area* refer exclusively to the land uses belonging to the class number 2 of CORINE´s first level of land uses' classification (EEA, 2016), named as: "*Agricultural areas*". Although some non-agricultural land uses have been utilised to distribute the crops cultivated in Spain

[137] *ID_C*: IDentifier of crop, built from the crops' groups defined in IAEA (2010).

(MAGRAMA, 2016)[138], such as those included in the land use class number 3 of the CORINE's first information level (which includes "Forest and semi-natural areas") (EEA, 2016), these areas have not been considered to assess their Radiological Vulnerability. The reason for this has to do with the distribution of the forestry areas within CORINE land uses. Areas with these CLCs class were needed to host some crops, fundamentally woody crops and more specifically the nuts[139] crops, according to what is represented in MAPA (1980-1990), MAPA (2000-2010) and in (IGN, 2005), in order to have a more realistic crop distribution. That proceeding also helps to avoid the overload of agricultural land uses (land use class number 2 of the CORINE's first information level (EEA, 2016)). It is important to state that those forestry areas are relatively vast (summing around 36300 km^2 in the whole Peninsular Spain), although a small percentage its cultivated. In turn, according to the methodology designed and to the crops' distribution performed in this Thesis, the crop which occupies the largest surface in each *basic cartographic unit* is the crop to be used to estimate the radiological vulnerability of the whole unit: the *representative crop*, representing the entire agricultural system in the area. Thus, if the forestry areas are considered in the vulnerability assessment, a huge surface would be characterised with a *I_RV* index value, which would neither be a very realistic representation nor a practical result from the EPR point of view.

Regarding the nut crops, which are included in the "*other crops*" group, the F_v attributed to them is the highest transfer factor from soil to plant value (IAEA, 2010). That transfer factor assignment not only is a quite significant simplification, but it also brings an important deviation, because, as it is generally assumed, woody crops transfer relatively little radionuclides from soil to their fruits, comparing to the radionuclides' absorption of the rest of crops (IAEA, 2010).

Taking into account the considerations above mentioned if "*Forest and semi-natural areas*" were included in the assessment of the *radiological vulnerability of the agricultural areas*, the F_v attributed to those would lead to obtaining elevated *I_RV* index values in that little

[138] The forest and semi-natural areas (EEA, 2016) considered to host woody crops are the land uses coded 311, 312, 321 and 324.

[139] Very sporadically, other crops have been associated with the forest and seminatural areas such as cherries in Cáceres.

occupied, but vast surface. Therefore, to address a useful radiological impact assessment, the forestry areas are not considered, in order to avoid highlighting zones where little surface area is occupied by crops, which, in turn, would have been attributed overestimated F_vs values.

The assumptions regarding the *agricultural surface area* and the *representative crop* intend to be a simplification, needed to deal with the complexity of the agricultural systems. In the same sense, the soil map performed and the transfer factor assignment to the crop groups are also a streamlining, necessary to carry out the radiological vulnerability assessment of the agricultural areas in Spain.

The following are the results obtained regarding the crop – soil texture pairing throughout the territory, which, in turn, influence on the *Radiological Vulnerability of the agricultural areas*, according to the crops distribution that has been performed:

- According to the crops distribution performed in this Thesis from the data published in MAGRAMA (2016) and considering the crops grouping (IAEA, 2010), cereals (*ceG*) are, by far, the most widespread ones in the peninsular Spain, with almost 50 % of the agricultural areas as shown in Table 20; almost a half of them correspond to rainfed barley[140] and a third are rainfed wheat[141] as main *representative crops*. The second crop group, according to its surface, are fruits of woody trees (*wtF*), with over a quarter of the total agricultural area in peninsular Spain; olives for oil[142] (about two thirds of the *wtF* group) and wine grapes[143] (with a 23.8 %), both rainfed, are the *representative crops* most widely distributed. Grass (*grS*), which includes different rainfed and irrigated fodder crops[144] is the third most widely distributed crop group (see Table 20). These three crop groups cover more than 86 % of the agricultural surface area in the territory being studied.

[140] Rainfed barley. *IDPR+IDCS*: *a11020da*.
[141] Rainfed wheat. *IDPR+IDCS*: *a11010da*.
[142] Olives for oil. *IDPR+IDCS*: *w31020drap*.
[143] Wine grapes. *IDPR+IDCS*: *w21020drap*.
[144] Fodder crops. *IDPR*: *a60000*. Fodder crops, included grass, might be not eaten as such but can enter the food chain through animal feeding.

Table 20. Surface area occupied by the crop groups identified in peninsular Spain.

Crop Group (ID_C)	Surface area within the agricultural areas (km^2)	Surface area (%)
Cereals (grain) - ceG	110825.52	47.74%
Woody trees (fruits) - wtF	58952.49	25.40%
Grasses - grS	29874.17	12.87%
Other crops - ocA	15447.11	6.65%
Maize (grain) - maG	7980.02	3.44%
Legume fodder - lfS	4128.16	1.78%
Leafy vegetables (leaves) - lyL	2987.32	1.29%
Non-leafy vegetables - nlF	1399.73	0.60%
Herbaceous plants (fruits) - hpF	233.87	0.10%
Tubers - tbT	137.60	0.06%
Root crops - rcR	121.05	0.05%
Legume vegetables - lvS	33.97	0.01%
Total	232121.01	100.00%

The resultant *representative crops*' map (see Figure 34) and the derived crops' groups map (see Figure 35) show a lack of spatial continuity in the border of some provinces, where a sudden change of crops occurs. This would go against what the Tobler's first law of geography defined in Tobler (1970): "*everything is related to everything else, but near things are more related than distant things*". It becomes more evident between Cáceres and Badajoz, between the latter and Córdoba or between Murcia and Alicante province. In the first example, grass is the main crops' group assigned to the *basic cartographic units* in Cáceres (the Northern province), while in Badajoz the *representative crops* are fruits from woody trees. In the second case, the same circumstance appears, being the North of Córdoba where grasses are assigned to, in contrast to the woody trees' fruits of Badajoz. In the third provinces pair, leafy vegetables and the "*other crops*" are the crops groups assigned to the Western province (Murcia) while woody trees are the *representative crops* in the Eastern one (Alicante). In these regions, that fact redounds in a sudden change in the resulting *Radiological Vulnerability Index* values.

Two main factors led to that sudden change. The first one is related to the *basic cartographic unit*, a multipart feature in which is not possible to allocate the representative crops accurately; thus, it may be possible that the assigned *representative crop* occupies only part of the features included in each *basic cartographic unit*. The second one is related to the crops' information and their handling. On the one hand, the raw data are aggregated by province; then, it had to be distributed through the municipalities, which is a

simplification of the real agricultural systems. On the other hand, only one crop was chosen to characterise each *basic cartographic unit*, which contributes to that simplification even more.

3.3 Results of the radiological vulnerability assessment for the agricultural systems regarding ^{137}Cs

Once the behaviour of ^{137}Cs in the soil is analysed, a step further has been given by incorporating the cultivated crops' role across mainland Spain and the behaviour of that radionuclide in the soil – plant system. That way, the *Radiological Vulnerability of the agricultural systems* is defined as the combination of the mineral soils' capacity to store ^{137}Cs and the soil-plant system's potential to transfer it to crops and therefore to the human food chain in the long-term. Depending on the vulnerability of the agricultural systems, if a deposition of ^{137}Cs occurs, it may pose to a risk exposure via ingestion in the subsequent growing seasons.

As it was previously mentioned in section 2.3.3, the *Radiological Vulnerability of the agricultural systems* (*I_RV*) is assessed regarding the following features:

- The topsoil properties, according to the updated Spanish soil database, such as clay and exchangeable potassium contents, used to assess the *Radiocaesium Reservoir Index* (*I_Cs*). Figure 36 shows the representation of the *I_Cs* index in the whole territory.

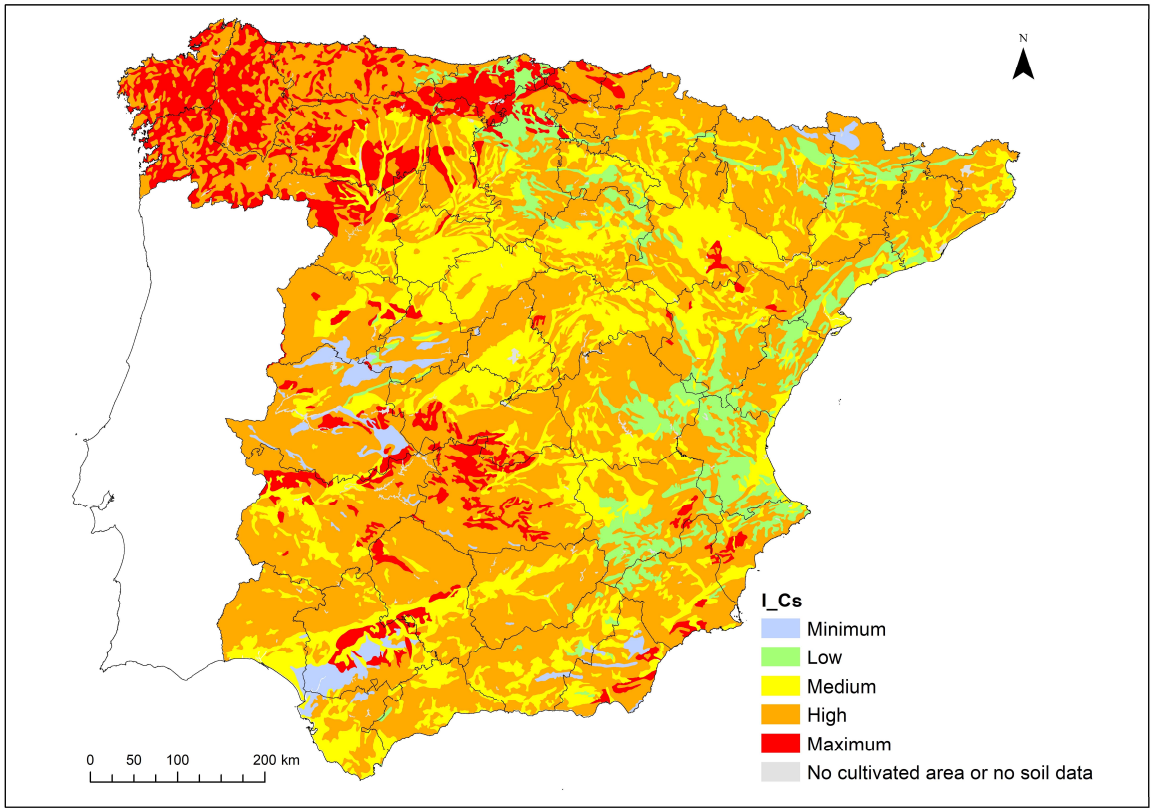

Figure 36. Radiocaesium Reservoir Index (I_Cs) map of peninsular Spain. Projection UTM ETRS89 H30.

- The crop group (IAEA, 2010) (coded as ID_C[145]) to which the *representative crop* (coded with the *IDPR+IDCS*[146]) of each *basic cartographic unit*[147].
- The ^{137}Cs transfer factor (F_v) from soil to plant, assigned to the crop group – topsoil texture pair (see section 2.3.2.1), to assess the *Transfer Factor Index* (*I_TF*), as explained in section 2.3.2.2. The topsoil texture map obtained can be seen in Figure 37. The resulting *I_TF* map is shown in Figure 38.

[145] *ID_C*: IDentifier of crop, built from the crops' groups defined in IAEA (2010).
[146] The *representative crop* is identified with the crops' codification which represents the *Identification of the PRoduct* (*IDPR*). Besides, it is disaggregated according to the *Identification of the Cultivation System* (*IDCS*). See section 2.2.1.
[147] The *Basic cartographic unit* is each multipart feature with the same CORINE's land use within each municipality. It is coded as "*mun_clc*".

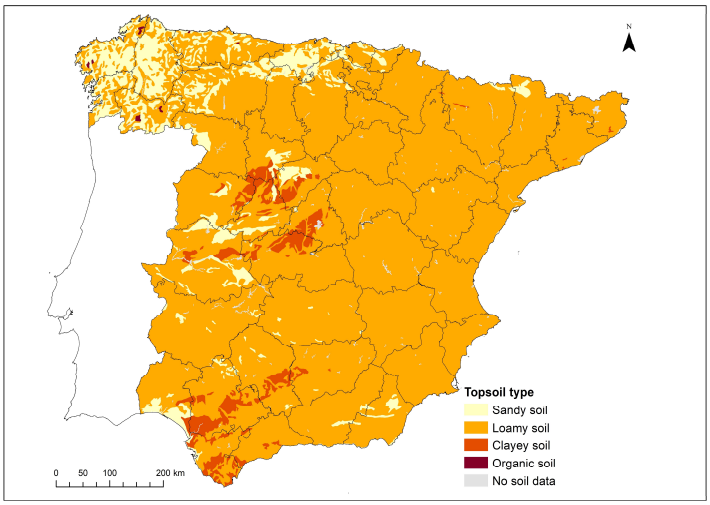

Figure 37. Topsoil type (soil mineral texture or organic soil) of the soil groups, according to (IAEA, 2010) criteria, on bases of the updated soil profile database (Annexe IV). Projection UTM ETRS89 H30.

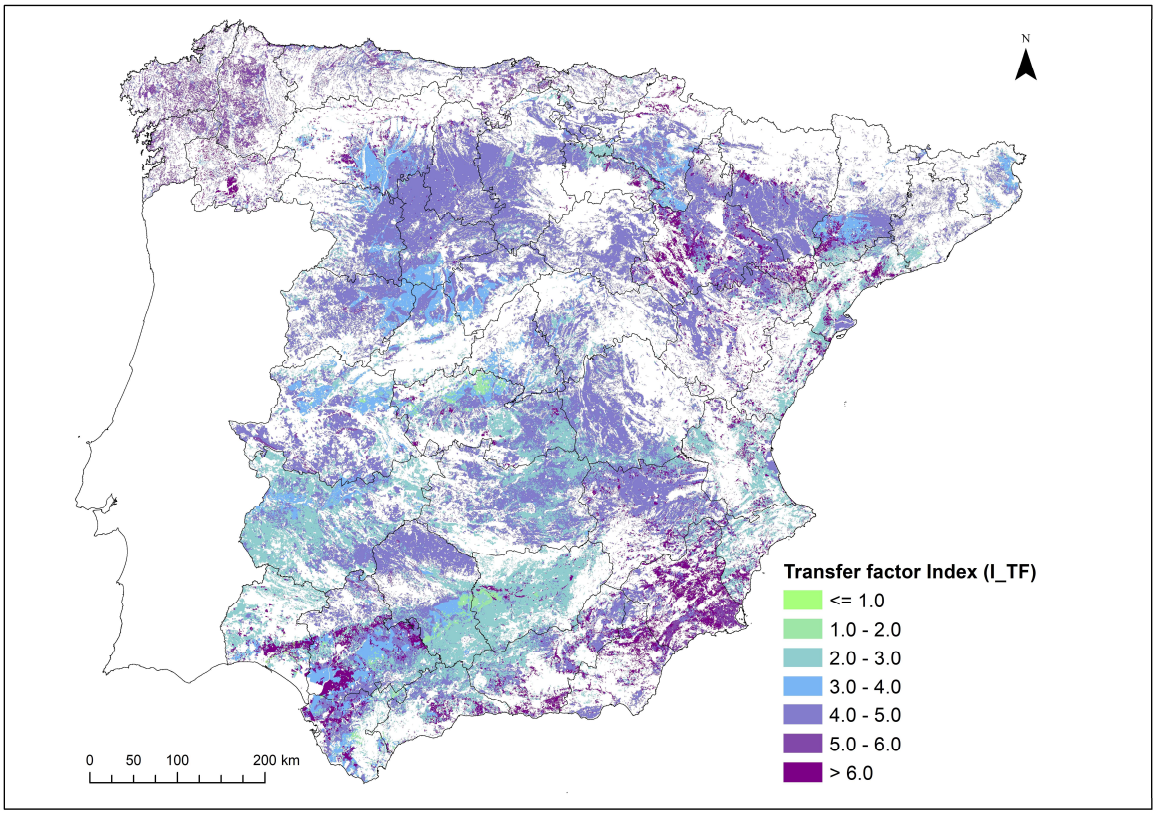

Figure 38. Transfer Factor Index (I_TF) map of peninsular Spain, according to the formula: $I\_TF = 8 + Ln(F_v)$. *Only "Agricultural areas" (EEA, 2016) are mapped. Projection UTM ETRS89 H30.*

Applying the methodology designed, the *Radiological Vulnerability Index* (*I_RV*) for the agricultural areas is obtained and assigned to each *basic cartographic unit*. This index categorises the radiological vulnerability in five classes according to the criteria shown in Table 12 (in section 3.3.3), in which the radiological vulnerability identification, the index value, and the mapping colours are included.

According to the topsoil texture[148] map (see the corresponding map in Figure 37), loamy topsoils are the most widespread ones in mainland Spain (with more than 88 % of the whole territory). Thus, in general, the crop group – loamy soil combinations are the most representative ones as they are also for whatever *I_RV* index category except for the *Minimum* one. That prevalence of loamy soils conditions their categorisation regarding the *Radiocaesium Reservoir* and the *Transfer Factor Index* (both texture dependent) and, in turn, the *Radiological Vulnerability* results for the agricultural areas. The most representative soil group with loamy topsoil texture is Calcic Cambisols on marls[149]; these occupy more than 28 % of the agricultural areas. To provide context to the importance of that soil group, it should be stated that the second loamy soil group in occupancy is the one comprised of Calcaric Fluvisols[150], which represents only 8.2 % of the total with that topsoil texture. Regarding sands, the soil group most widely distributed with that topsoil texture is comprised of Humic Cambisols on acid crystalline rocks[151] (3.7 % of the whole agricultural area). Vertic Luvisols[152] are the representative ones for clayey soils (2.9 % of the whole agricultural area). The occupancy percentages of the soil groups, gathered by their topsoil texture, are shown in Figure 39.

[148] It is important to keep in mind that all the soil properties considered for the *Radiological Vulnerability* assessment for the agricultural areas are referred exclusively to the topsoil.
[149] Calcic Cambisol on marls (Bk) (No. 128). The list of the soil groups, including their soils' classification, according to the legend (FAO-UNESCO, 1974) and their bedrock is included in Annexe IV.
[150] Calcaric Fluvisols (Jc) (No. 201).
[151] Humic Cambisols on acid crystalline rocks (included granite) (Bh) (No. 24).
[152] Vertic Luvisols (Lv) (No. 37).

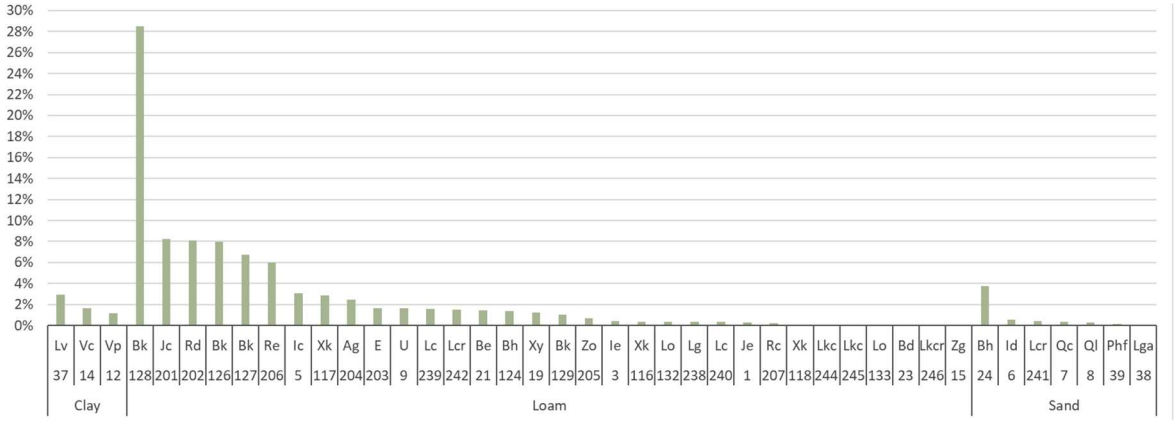

Figure 39. Percentage of the agricultural surface area with each soil group, grouped by the topsoil texture. The abscissa axis shows the soil classification (FAO-UNESCO, 1974) followed by the soil group, and the topsoil texture. For loamy textures, the soil groups classified as Je Rc Xk, Lkc, Lo, Bd, Lkcr and Zg occupy less than 0.3 % each. For sandy textures, Ql, Phf and Lga are the soil groups which occupy less than 0.3 % of the area.

With respect to the intermediate indexes defined to assess the *Radiological Vulnerability* of the agricultural areas, the *Radiocaesium Reservoir Index* (*I_Cs*) and the *Transfer Factor Index* (*I_TF*), the following are the main results attained:

- With regard to the *Radiocaesium Reservoir Index* (resulting from the relation between the clay fraction content and exchangeable potassium content of soils (Domínguez Vivancos, 1997) – see section 2.3.1[153]), the soil groups with loamy topsoil texture show the whole possible *Radiocaesium Reservoir Indexes* except the *Minimum* (equals to 1). Sandy soils result with all the *I_Cs* except with the *Low* category (equals to 2), and clayey soils are exclusively classified with *Minimum* or *Medium I_Cs* (equal to 1 and 3, respectively). Therefore, clayey soils result in a much higher potassium relative reserve than loamy or sandy soils, which redounds in a lower ^{137}Cs reserve in soil, limiting its potential transfer to crops and reducing the risk for the food chain. The relatively small surface area of sandy soils and the limited ^{137}Cs reservoir capacity of the clayey soils make loamy soils the ones that condition the most the radiological vulnerability in peninsular Spain. In Figure 40, it is shown the percentage of the agricultural surface area with each soil group, gathered by the topsoil texture and by the *Radiocaesium Reservoir Index* (*I_Cs*), assessed by each soil group, according to the clay and potassium content.

[153] The relation between clay and potassium content is based on (Domínguez Vivancos, 1997).

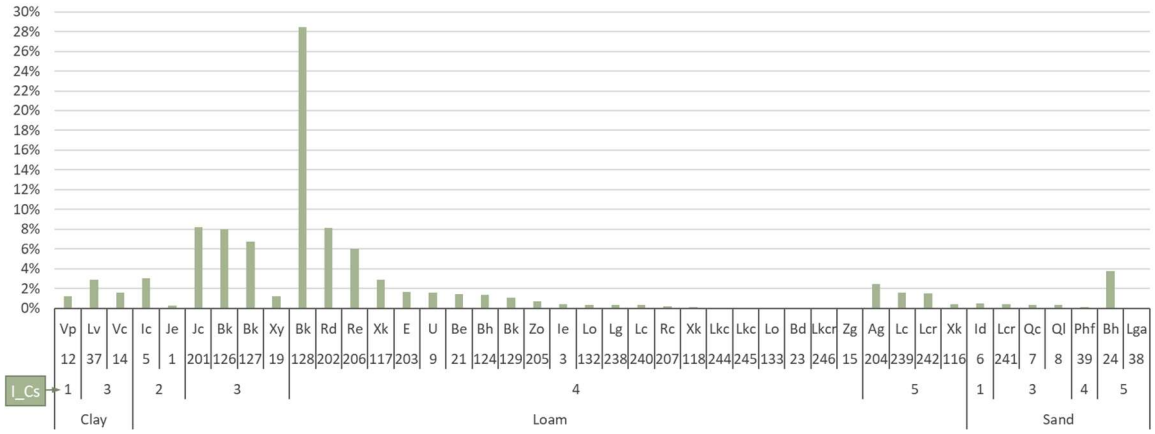

Figure 40. Percentage of the agricultural surface area with each soil group, gathered by the topsoil texture and by the Radiocaesium Reservoir Index (I_Cs). The abscissa axis shows the soil classification (FAO-UNESCO, 1974) followed by the soil group, the resulting I_Cs index value and the topsoil texture. For loamy textures, the soil groups classified as Rc, Xk, Lkc, Lkc, Lo, Bd, Lkcr and Zg occupy less than 0.3 % each. For sandy textures, Phf and Lga are the soil groups which occupy less than 0.3 % of the area.

- Taking into account the most widespread *representative crop* in each *basic cartographic unit*, the crop group to which it belongs to and considering the topsoil texture (IAEA, 2010), the corresponding F_v is assigned. Then, the resulting *Transfer Factor Index* (*I_TF*) is attained. The crop group – topsoil combinations most distributed in the agricultural areas resulted for cereals on loamy soils (43.2% of the total surface) with an *I_TF* equals to 4.09, followed by fruits of woody trees on loamy soils (23.7 %) with an *I_TF* equals to 2.35 and by grasses on loamy soils with a *I_TF* equals to 4.96 (occupying 9.1 % of the agricultural surface area), as shown in Figure 41. It might be said that the first and the third crop – soil combinations give rise to a relatively high *Transfer Factor Index* (intimately related to their F_v values: $2.0 \cdot 10^{-2}$ and $4.8 \cdot 10^{-2}$, respectively (IAEA, 2010)), therefore these contribute significantly to increase the radiological risk for the food chain, while the second one results in a considerably lower *I_TF* (which is attributed a F_v of $3.5 \cdot 10^{-3}$ (IAEA, 2010), one order of magnitude lower than the others), then, comparatively, fruits of woody trees on loamy soils do not pose a risk as high as the other two pairs if a deposition of ^{137}Cs occurs.

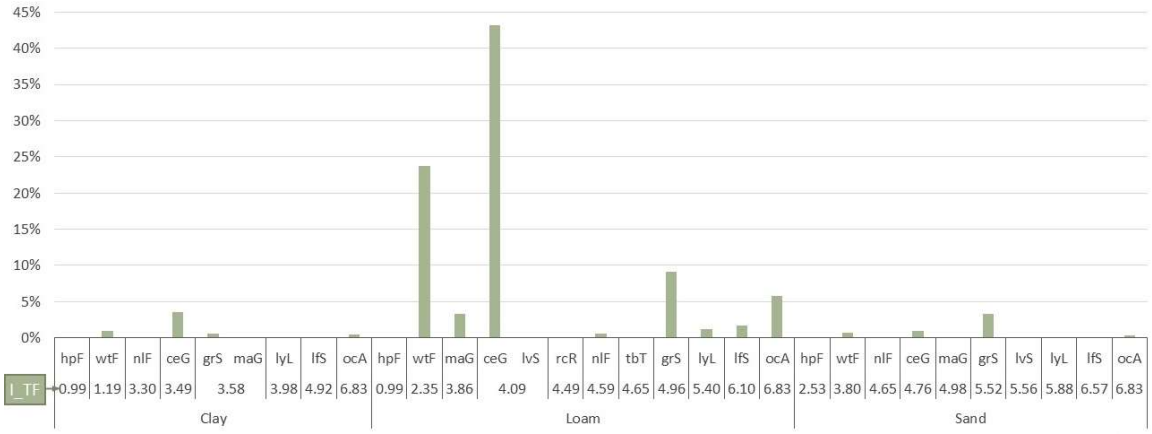

Figure 41. Percentage of the agricultural surface area in which each crop group is grown, gathered by the topsoil texture and by the Transfer Factor Index (I_TF). The abscissa axis shows the crop group (IAEA, 2010) (named ID_C), followed by the resulting I_TF index value (sorted by the lowest to the highest) and the topsoil texture. For sandy soils, only grasses occupy more than 3% of the agricultural surface. For loamy textures, cereals, fruits of woody trees, grasses, "other crops" and maize occupy more than 3 % of the surface. In case of clayey textures, only cereals occupy more than 3 % of the total surface area.

In order to show the figures relative to the *agricultural surface area* affected by each *Radiological Vulnerability Index* (obtained taking into account the *I_Cs* and *I_TF* indexes), besides the spatial distribution through peninsular Spain shown in Figure 42, different tables and charts have been elaborated. These tables, together with the Radiological Vulnerability map, should help to understand the *Radiological Vulnerability of the agricultural systems* in the studied area. Annexe IX collects part of them, including the following:

- Table with the affected surface by each *Radiological Vulnerability* category (in km^2) in every single peninsular Spain's province,
- a chart representing the *agricultural affected area* within each *I_RV* index value (in km^2), by province,
- five graphs, one per *I_RV* category independently, representing the *agricultural affected area* within each Radiological vulnerability index (in km^2), by province,
- a table including the percentage of the *agricultural surface area* within each *I_RV* category, with respect to the whole *agricultural surface area* in each province, and its corresponding chart,
- one more table and its corresponding chart showing the percentage of the *agricultural surface area* within each *I_RV* category, with respect to the whole *agricultural surface* in mainland Spain.

The rest of the results are gathered in Annexe X, where three tables are included per each *Radiological Vulnerability Index* (stating from *I_RV* equals to 5) showing:

- Surface of the agricultural areas affected by each *Radiological Vulnerability Index*, disaggregated by crop group, then by topsoil texture and finally by soil group. The corresponding *Transfer Factor Index* (*I_TF*) for each *agricultural system* (crop group – soil texture combination) and the *Radiocaesium Reservoir Index* (*I_Cs*) of each soil group (derived from their clay and potassium content) are also included.
- Agricultural areas' surface within each *I_RV* considering the *representative crop*.
- Agricultural areas' surface within each *I_RV* considering the crop group to which the *representative crop* belongs.

Nevertheless, although the *basic cartographic units* are referred to the municipalities, it is not possible to carry out such a detailed description to show their vulnerability results.

The resulting map that shows the *Radiological Vulnerability of the agricultural systems* in mainland Spain, regarding the ^{137}Cs, can be seen in Figure 42.

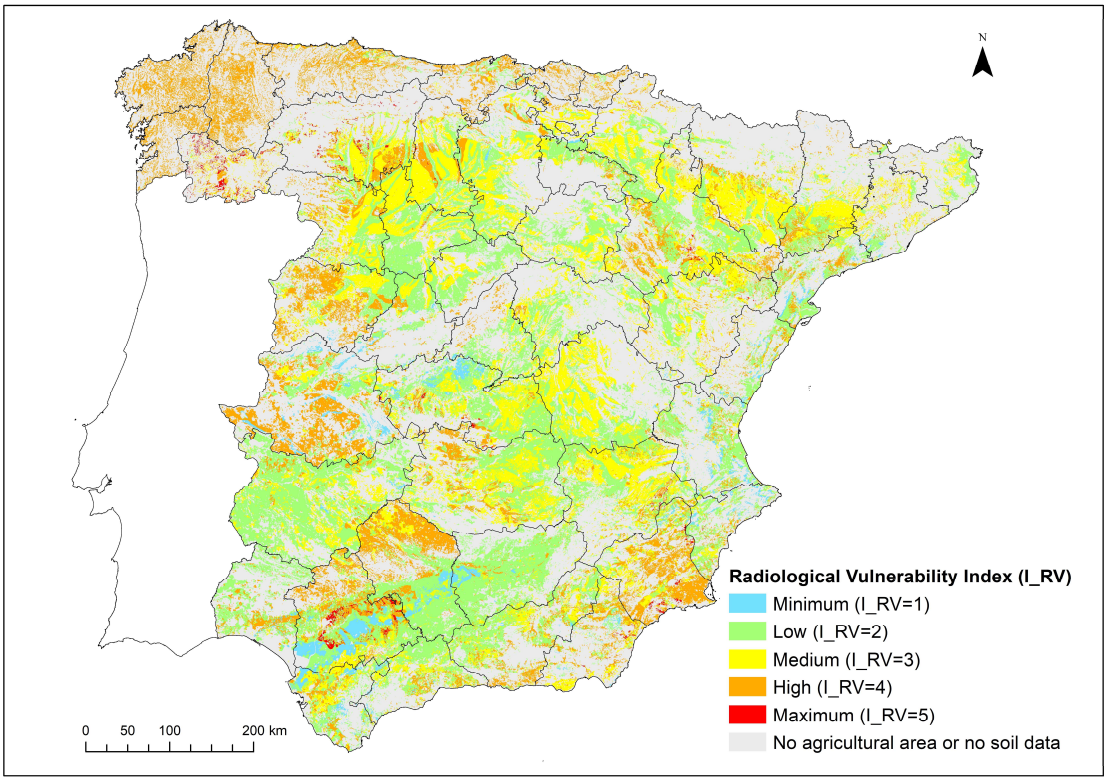

Figure 42. Radiological vulnerability map of the agricultural systems in peninsular Spain, regarding the ^{137}Cs. Within this map the five categories of the I_RV index are represented: I_RV = 1: Minimum Radiological Vulnerability; I_RV = 2: Low Radiological Vulnerability; I_RV = 3: Medium Radiological Vulnerability; I_RV = 4: High Radiological Vulnerability; I_RV = 5: Maximum Radiological Vulnerability. Projection: UTM ETRS89 H30.

As shown in Figure 42, limited agricultural areas are affected by the two extreme *I_RV* indexes. As seen in Figure 43, in which the percentage of the *agricultural surface* affected by each *Radiological Vulnerability Index* value in peninsular Spain is plotted, the crop – soil type combinations with *Minimum* and *Maximum* potential exposure through the food chain are only 3.08 and 0.56 %, respectively.

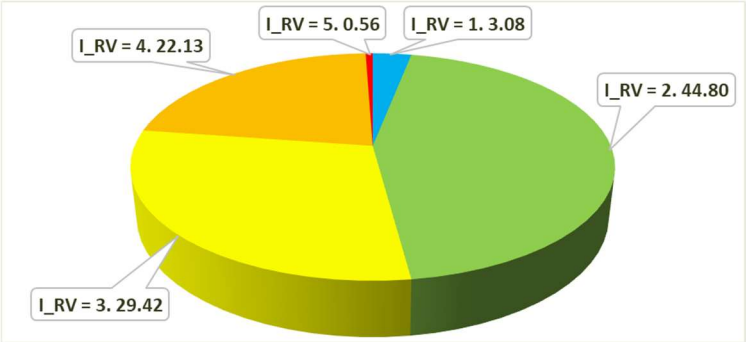

Figure 43. Percentage of the agricultural surface area in peninsular Spain affected by each radiological vulnerability index value (I_RV), with respect to the total agricultural surface area (232121 km²). Maximum I_RV in red, has 1305.65 km²; High I_RV in orange, has 51379.74 km²; Medium I_RV in yellow, has 68285.51 km²; Low I_RV in green, has 103999.90 km²; Minimum I_RV in blue, has 7150.21 km².

Regarding the *Maximum I_RV*, its significantly lower surface in comparison with the rest of the vulnerability categories is related to, apart from the factors involved in the vulnerability assessment, to the upper threshold used to perform the categorisation of that index. That threshold corresponds to the percentile P_{95} of the multiplication of the *Radiocaesium Reservoir Index* by the *Transfer Factor Index*. That way, it has been accomplished to highlight those zones with the highest *Radiological Vulnerability* within an area affordable to be evaluated for recovery actions firstly. Sandy and loamy soils, combined with *representative crops* to which high transfer factors from soil to plant, such as "other crops" and legume fodder, give rise to that *Radiological Vulnerability* category.

On the contrary, the agricultural areas within *Minimum I_RV*, located in the West and South of Spain, are related to all kind of soils, but mainly to those with clayey textures, implying lower F_v and, in turn, lower a *Transfer Factor Index*, and in general to soils with *Very High Potassium Reservoir Index*, which implies *Minimum Radiocaesium Reservoir Index*. Besides, the most widespread *representative crops* within this *I_RV* are grouped as woody trees fruits, which have the lowest ^{137}Cs transfer from soil to plant (IAEA, 2010).

The *agricultural areas* affected by the three highest *Radiological Vulnerability* values sum a surface area which corresponds to the 52.11 % of the total (as shown in Figure 43). Those agricultural systems should be the ones to focus on to identify the potential risk for the food chain. While the *Maximum* vulnerability affects mainly to very specific areas, more precisely in the West of Spain, the *High Radiological Vulnerability* index covers all peninsular provinces to a greater or lesser degree as it occurs for the *Medium I_RV*.

As seen in Figures 38 and 43, the most widely spread *I_RV* corresponds to the *Low* one, occupying the 44,8 % of the agricultural area. It is distributed all around the country except for the Northern stretch. Loamy soils are the prevailing soil types which, although these have a relatively reduced potassium content, leading to an elevated *Radiocaesium Reservoir Index*, are cultivated with *representative crops* grouped into the woody trees (again, with the lowest F_v (IAEA, 2010)); that fact balances the eventual vulnerability result.

The following subsections discuss the main results obtained in the *Radiological Vulnerability* assessment for each *I_RV* index value through peninsular Spain, starting with the *Maximum I_RV* and following the description in descending indexes order.

3.3.1 Maximum Radiological Vulnerability

The *Maximum Radiological Vulnerability* represents those agricultural systems where the crop type – topsoil texture pair shows the worst radiological situation, that is, the soil has a high potential to store ^{137}Cs and the associated crops show a high root absorption capacity. It is assigned a *I_RV* index value of 5. The location of the areas with this *I_RV* are shown in Figure 42 and, detached from the rest of the *I_RV* values, in Figure 44. The total surface area resulting in this *I_RV* index value in peninsular Spain is 1305.65 km^2, which represents less than 1 % of the agricultural areas (see Figure 43).

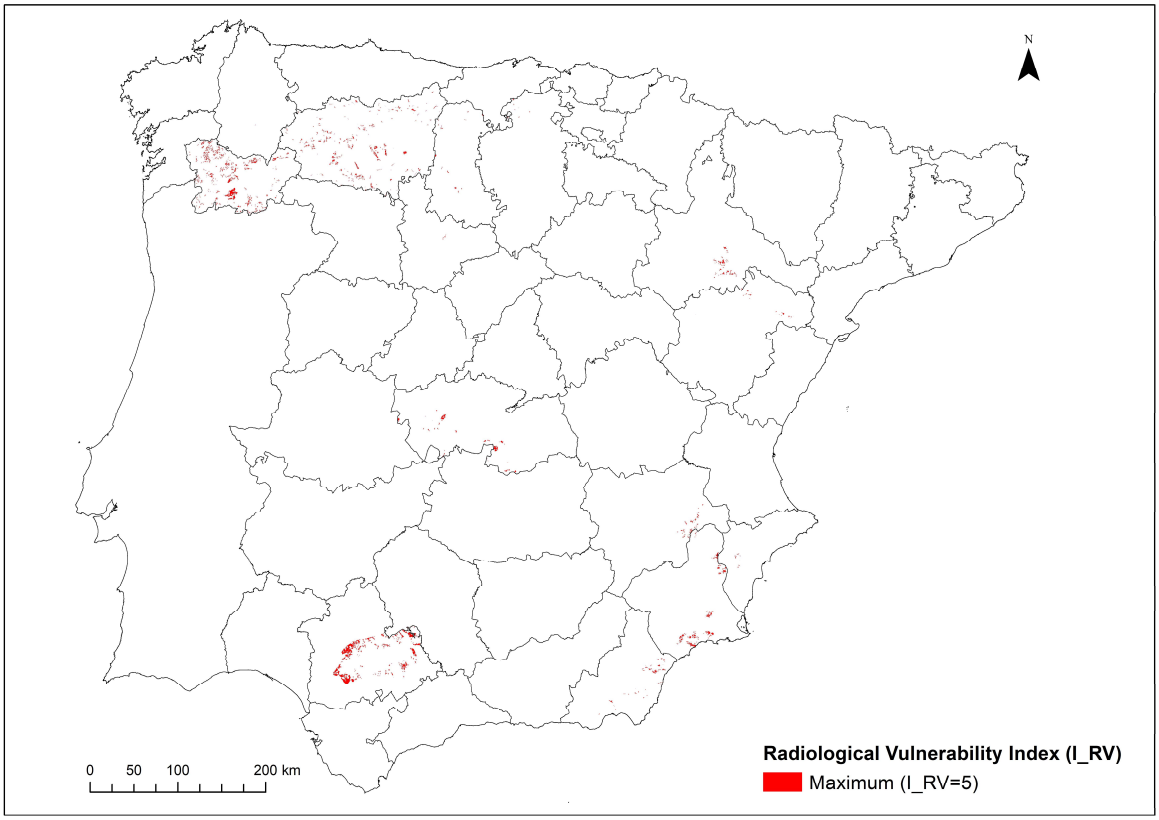

Figure 44. Agricultural areas in peninsular Spain with Maximum Radiological vulnerability (I_RV equals to 5). Projection: UTM ETRS89 H30.

As can be seen in the Radiological Vulnerability map (Figures 42 and 44) and in the charts included in Annexe IX, the *agricultural affected areas* with this index value are located in very specific spots within Sevilla, Ourense, León, Murcia, Toledo, Zaragoza, and other nine more Eastern provinces but with much less representativeness. This distribution can also be seen in the chart included in Figure 45, which shows the percentage of the surface area of the peninsular Spanish provinces with *Maximum I_RV* to the total agricultural surface in the whole mainland country area.

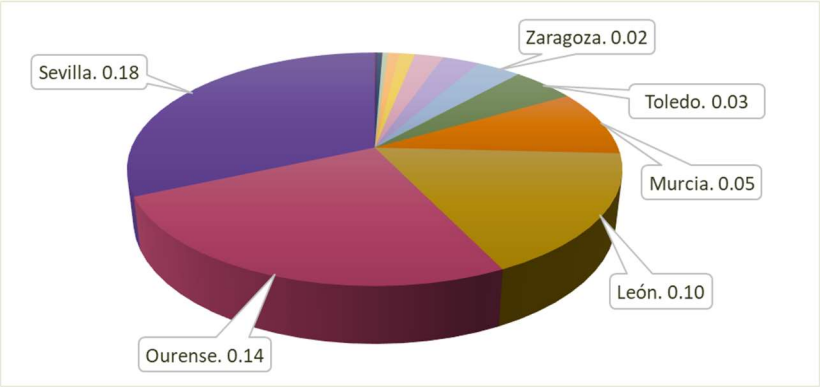

Figure 45. Chart representing the percentage of the agricultural surface areas within I_RV equals to 5, by peninsular Spanish province. A total of fifteen provinces are affected by the Maximum I_RV. Only provinces over 0.02% are labelled.

All the soils within the *Maximum I_RV* have a *Very Low Potassium Reserve* (*I_K*) due to the relation between clay content and potassium content (see section 2.3.1); that redounds in a *Maximum Radiocaesium Reserve* (*I_Cs*), meaning that the topsoil exhibits free binding sites in which ^{137}Cs can be adsorbed, being included in the crystal lattice, which may become bioavailable for crops over time.

Besides, the affected agricultural areas are characterised by the crop groups – soil textures combinations with the highest F_v values (over $1.2 \cdot 10^{-1}$ (IAEA, 2010)); that fact gives rise to *Transfer Factor Index* values (*I_TF*) equal or higher than 5.9 (the highest in the whole country's territory); therefore, these agricultural systems have a very high capacity to transfer the bioavailable ^{137}Cs in soil to the crops. These pairs, included in Annexe X and summarised in Table 21, are the following:

- "other crops" (ocA) or legume fodder (lfS) grown mainly in loamy soils, such as Gleyic Acrisols[154], Calcic Xerosols on calcareous sandstones[155], Rhodo-Chromic Luvisols on shales[156] or Chromic Luvisols on river alluvium[157] (the latter only associated with legume fodder),
- legume fodder, "other crops" or leafy vegetables (lyL) (the latter quite negligible) grown in Humic Cambisols on acid crystalline rocks[158], classified as sandy soils.

Table 21. Crop group – soil texture combinations within Maximum I_RV, sorted by surface area occupancy (in descending order). Transfer factor value (F_v) (IAEA, 2010) and the corresponding I_TF are included.

Crop group (ID_C) - Soil texture	Transfer factor soil-to-plant Fv	Transfer Factor Index I_TF	Surface of I_RV = 5 (km^2)
Other crops (ocA)-Loam	0.31	6.8	608.28
Other crops (ocA)-Sand	0.31	6.8	334.74
Legume fodder (lfS)-Loam	0.15	6.1	223.83
Legume fodder (lfS)-Sand	0.24	6.6	138.79
Leafy vegetables (leaves) (lyL)-Sand	0.12	5.9	0.01

[154] Gleyic Acrisols (Ag) (No. 204). The list of the soil groups, including their soils' classification, according to the legend (FAO-UNESCO, 1974) and their bedrock is included in Annexe IV.
[155] Calcic Xerosols on calcareous sandstones (Xk) (No. 116).
[156] Rhodo-Chromic Luvisols on shales (Lcr) (No. 242).
[157] Chromic Luvisols on river alluvium (Lc) (No. 239).
[158] Humic Cambisols on acid crystalline rocks (included granite) (Bh) (No. 24). The list of the soil groups, including their soils' classification, according to the legend (FAO-UNESCO, 1974) and their bedrock is included in Annexe IV.

The edible *representative crops* included in the crop's groups mentioned are the rainfed chestnuts[159] (located mainly in Galicia[160]) with more than 25 % of the surface, the rainfed vetch[161] (in León) with a 17 %, and the rainfed almonds[162] with almost the 15 % (distributed in the Southeast of Spain and, occasionally, in other central areas) as seen in the tables included in Annexe X for the *Maximum I_RV*. Irrigated lucerne[163], rainfed grazed sainfoin[164], irrigated walnut[165] and rainfed brassica[166] are the rest of the edible representative crops affected, which sum less than 11 % of the area within *maximum* vulnerability index. Irrigated cotton[167], as a non-edible crop, is the most widespread *representative crop*, with almost a third of the total area within this index (all in Sevilla province).

More than 72 % of the crops affected by *Maximum Radiological Vulnerability* are grouped on the "*other crops*" group (IAEA, 2010) as seen in Annexe X, more than 40 % not counting the non-edible crops. Therefore, the fact that some *representative crops* were included on the miscellaneous group, with a generic F_v value and not a particular one, which in turn is the highest (IAEA, 2010), generates a certain via and uncertainty in the results obtained for the *Radiological Vulnerability* assessment of the agricultural areas within *Maximum* value.

It is important to remark that none of the agricultural areas affected by *I_RV* equals to 5 include clayey soils. It is due to two main factors. The first one is that the clay and potassium contents rate (Domínguez Vivancos, 1997) of the clayey topsoils give rise to a *Medium Radiocaesium Reservoir Index*, as highest (as seen in Figure 40) which is not enough to reach the *Maximum* vulnerability. The second one is that, as a general trend, the transfer factor attributed to those agricultural areas grown in clayey soils are lower than in any other soil's texture (IAEA, 2010). Therefore, the combination of these two factors prevents the clayey topsoil to result in this *Radiological Vulnerability* category.

[159] Chestnuts (IDPR: *w15040*).
[160] Galicia (NUTs II) comprises four provinces: A Coruña, Lugo, Orense and Pontevedra.
[161] Vetch (*IDPR*: *a62050*).
[162] Almonds (*IDPR*: *w15010*).
[163] Lucerne (*IDPR*: *a62010*).
[164] Sainfoin (*IDPR*: *a62030*).
[165] Walnut (*IDPR*: *w15020*).
[166] Brassica (*IDPR*: *a41010*).
[167] Cotton seed (*IDPR*: *a52010*).

The low exchangeable potassium content in the topsoil in relation to the potential binding sites of the topsoil's clay fraction, linked to the relevant role of the topsoil texture, are reflected as critical factors in the areas classified with the *Maximum I_RV* index in peninsular Spain. At the same time, the F_v value introduces particular distortion in the resulting map associated, in this case, to nuts, as described above. Therefore, it has been shown the importance of the transfer factor in the methodology designed and the necessity of having proper F_v values for the *representative crops* identified in the Spanish agricultural system, as it was stated in section 2.3.2.1.

Apart from the vias introduced by the miscellaneous crop group (see section 3.2), the agricultural systems within *Maximum Radiological Vulnerability*: legume fodders and leafy vegetables cultivated in the loamy soils above mentioned, should be, a priori, the ones of most concern in case of an accidental release of ^{137}Cs occurs, facing the recovery. Nevertheless, the recovery measures should also consider the real ^{137}Cs deposition, based on surveillance and monitoring campaigns.

3.3.2 High Radiological Vulnerability

The next radiological vulnerability category to take concern of is the *High I_RV*, which is assigned an index value equals to 4. It is widely distributed in peninsular Spain, as seen in Figures 42 and 46. It occupies 51379.74 km^2 (see Annexes IX and X), which is the 22.13 % (as shown in Figure 43) of the total agricultural area in mainland Spain. In Figure 46 it is shown the spatial distribution of the *High radiological vulnerability* throughout peninsular Spain.

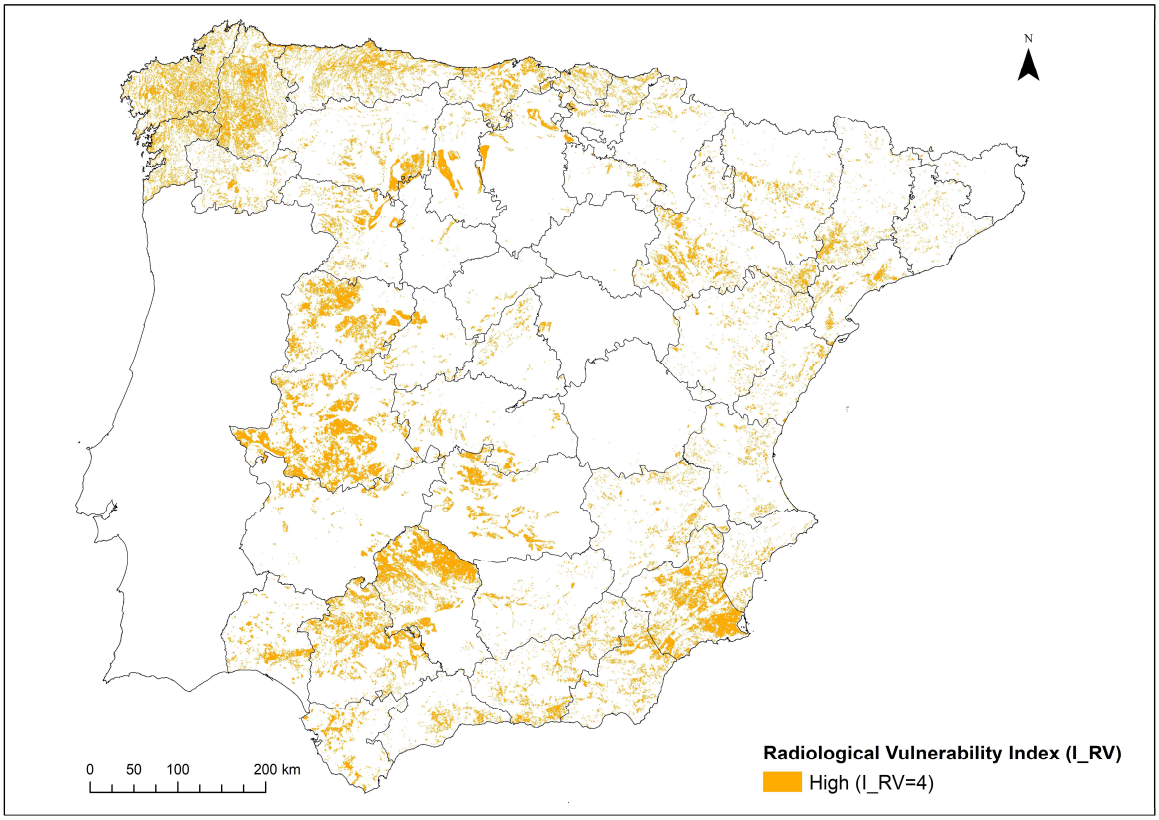

Figure 46. Agricultural areas in peninsular Spain with High Radiological Vulnerability (I_RV equals to 4). Projection: UTM ETRS89 H30.

The provinces with the largest *High I_RV* surface are, in this order: Cáceres, Córdoba, Murcia, Lugo, Sevilla and Salamanca, among others (see Annexe IX and Figure 47).

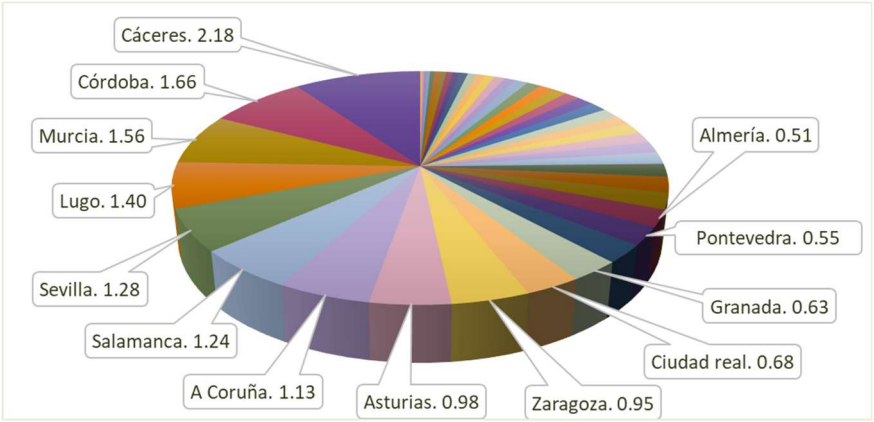

Figure 47. Chart representing the percentage of the agricultural surface areas within I_RV equals to 4, by peninsular Spanish province. Only provinces over 0.5 % are labelled.

The largest agricultural systems affected by *High Radiological Vulnerability* are those where the *representative crop* belongs to the grass crop group (grS), being almost the 51 % of the total within this *I_RV* index, of which about 74 % are grown in loamy soils and the rest are grown in sandy soils, as seen in Annexe X. The relation between the clay and potassium

content leads to a *Radiocaesium Reservoir* in soil ranged from *High* to *Maximum*. That fact means that the binding sites of clays are not occupied by enough potassium to block the ^{137}Cs adsorption, then, its entrance in the soil structure could result in bioavailable ^{137}Cs for crops to be uptaken in the subsequent seasons. That *I_Cs* index, combined with the *Transfer Factor Index* (equals to 5.0) assessed from the corresponding F_v of grass cultivated in loamy soils (IAEA, 2010), derive in the *High I_RV* (see Table 22). That relatively high F_v values, redound in certain ability of the system to transfer the ^{137}Cs from soil to crop. Transfer factor values associated with all possible crop group – soil texture combinations obtained in mainland Spain with *High I_RV*, are listed in Table 22, sorted in descending order of surface.

The *representative crops* included in that agricultural system (grasses on loamy soils) are principally meadows[168] and winter cereals for foodstuff[169]. These are mainly grown in Dystric Regosols[170], Rankers[171] and Eutric Regosols[172], all of them developed from acid crystalline rocks or metamorphic rocks such as schists or shales.

Table 22. Crop group – soil texture combinations within High I_RV, sorted by surface area occupancy (in descending order). Transfer factor value (F_v) (IAEA, 2010) and the corresponding I_TF are included.

Crop group (ID_C) - Soil texture	Soil-to-plant Transfer factor Fv (IAEA, 2010)	Transfer Factor Index I_TF	Surface of I_RV = 4 (km^2)
Grasses (grS)-Loam	0.048	5.0	19329.71
Other crops (ocA)-Loam	0.31	6.8	12056.23
Cereals (grain) (ceG)-Loam	0.02	4.1	7128.04
Grasses (grS)-Sand	0.084	5.5	6828.69
Legume fodder (lfS)-Loam	0.15	6.1	2239.00
Leafy vegetables (leaves) (lyL)-Loam	0.074	5.4	2005.93
Cereals (grain) (ceG)-Sand	0.039	4.8	1024.51
Other crops (ocA)-Clay	0.31	6.8	424.90
Other crops (ocA)-Sand	0.31	6.8	220.95
Maize (grain) (maG)-Sand	0.049	5.0	55.67
Non-leafy vegetables (nlF)-Loam	0.033	4.6	37.16
Legume fodder (lfS)-Sand	0.24	6.6	18.02
Legume vegetables (leaves) (lvS)-Sand	0.087	5.6	10.94

[168] Meadows (*IDPR*: *a63000*).
[169] Winter cereals (*IDPR*: *a61010*).
[170] Dystric Regosols (Rd) (No. 202).
[171] Rankers (U) (No. 9).
[172] Eutric Regosols (Re) (No. 206).

The second largest agricultural system within *I_RV* equals to 4 corresponds to the "other crops" group (IAEA, 2010) (ocA) in loamy soils (as shown in Table 22 and Annexe X), with slightly less than 25 % of the total *High Radiological Vulnerability* surface area in mainland Spain. The soil type in which these crops are grown are mainly Calcic Cambisols (Bk) on marls[173], with a *High Radiocaesium Reservoir Index*. The *Transfer Factor Index* for the "other crops" group is 6.8, the highest of all, since these are attributed the highest F_v (IAEA, 2010). That *I_TF* value combined with the *I_Cs* results described above for that crop – soil combination leads to the same *I_RV* than the former agricultural system (grasses on loamy soils); in this case, the most widespread *representative crops* are, by far, almond trees[174].

There are some other crop groups – soil type combinations affected by *High Radiological Vulnerability* but less relevant in terms of surface, as seen in Table 22 and Annexe X, such as grasses (grS) or maize (maG) on sands, cereals (ceG), legume fodder (lfS) or leafy vegetables (lyL) on loamy or sandy soils and non-leafy vegetables (nlF) on loamy soils. A negligible surface area of the agricultural systems is comprised of "other crops" (ocA) cultivated in clayey or sandy soils; however, it is important to remind that for this crop group there are not different F_v values to be assigned to each soil texture, therefore, all the *representative crops* gathered on it are characterised with the same F_v and, in turn, with the same *Transfer Factor Index* (*I_TF*), which introduces certain distortion in the vulnerability results.

To conclude, fodder crops such as meadows and winter cereals, cultivated in loamy soils are the most widespread crop – soil texture combination with *High Radiological Vulnerability*. Although the influence of having a miscellaneous crop group such as "other crops" (ocA), is not as decisive as for the *Maximum I_RV*, this group affects to the *Radiological Vulnerability* definition for a significant part of the Spanish territory.

[173] Calcic Cambisol on marls (Bk) (No. 128).
[174] Almonds (*IDPR*: *w15010*).

Apart from the consideration stated above, the agricultural areas affected by *High I_RV* should be areas to be concern of in case of an accidental release occurs, regarding a deposition of ^{137}Cs.

3.3.3 Medium Radiological Vulnerability

The *Medium Radiological Vulnerability* (index value equals to 3) is the second vulnerability category most widely spread in peninsular Spain and represents a total surface of 68285.51 km^2, almost the 30 % of the total agricultural areas as seen in Figure 43. Its geographical distribution can be seen in Figures 42 and 48 also; it is mainly associated with plain and extent arable lands in the inland provinces, although a coastal area such as the South of Almería province also stands out.

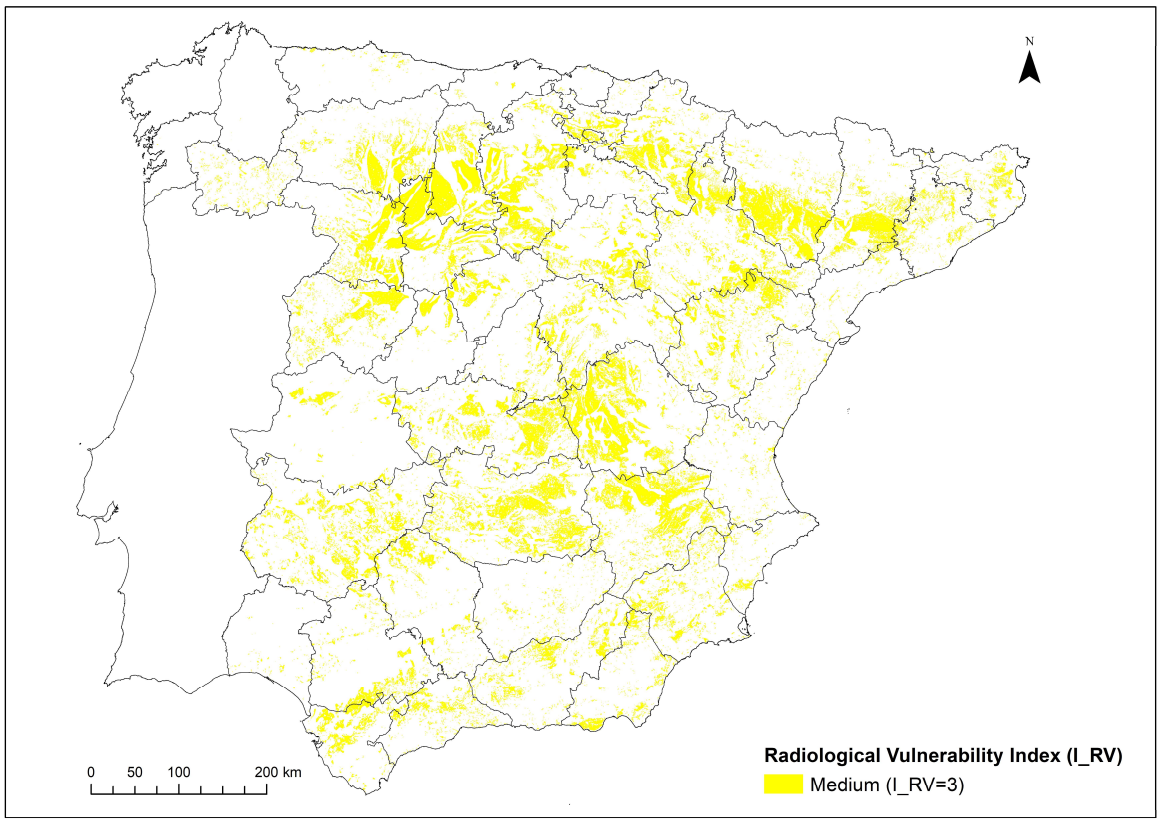

Figure 48. Agricultural areas in peninsular Spain with Medium Radiological vulnerability (I_RV equals to 3). Projection: UTM ETRS89 H30.

Cuenca is the province that shows the largest surface within this *Radiological Vulnerability* index (4974.66 km^2), followed by Ciudad Real, Albacete, Huesca, Zaragoza and Burgos (see Figure 49 and Annexe IX).

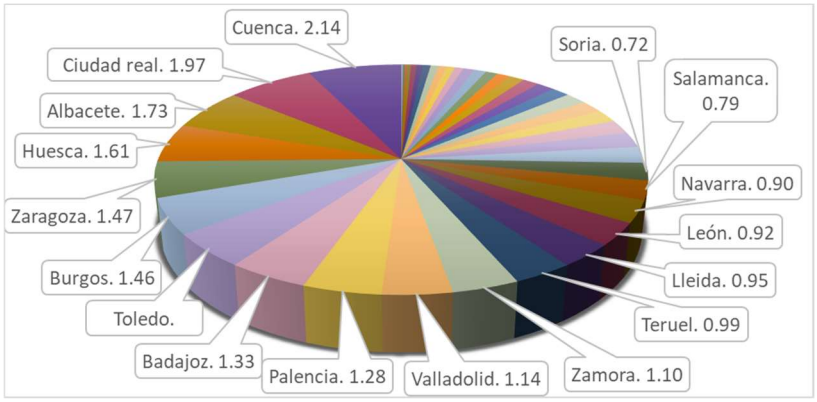

Figure 49. Chart representing the percentage of the agricultural surface areas within I_RV equals to 3, by peninsular Spanish province. Only provinces over 0.7 % are labelled.

In general, the most representative soil group with *Medium I_RV* index is, by far the Calcic Cambisol on marls[175], which occupies more than the 56 % of the surface; the other 37 affected soil groups account for less than 7 % each, as seen in Table 23.

Table 23. Soil groups affected with the Medium Radiological Vulnerability through peninsular Spain sorted in decreasing order according to the affected surface area.

No. Soil Group	Soil Classification (FAO-UNECO, 1974)	Surface of I_RV = 3 (km²)	Surface % of I_RV = 3
128	Bk	38270.23	56.04%
206	Re	4586.72	6.72%
117	Xk	3896.62	5.71%
202	Rd	3786.57	5.55%
129	Bk	1925.29	2.82%
203	E	1907.99	2.79%
201	Jc	1437.38	2.10%
205	Zo	1389.23	2.03%
124	Bh	1348.62	1.97%
239	Lc	917.64	1.34%
5	Ic	885.48	1.30%
7	Qc	800.23	1.17%
127	Bk	745.20	1.09%
126	Bk	727.04	1.06%
3	Ie	629.86	0.92%
241	Lcr	627.78	0.92%
21	Be	603.20	0.88%
19	Xy	565.60	0.83%
24	Bh	506.29	0.74%
240	Lc	434.62	0.64%
238	Lg	427.07	0.63%
207	Rc	418.01	0.61%
9	U	398.20	0.58%
204	Ag	238.45	0.35%
118	Xk	194.68	0.29%
244	Lkc	171.08	0.25%
8	Ql	101.24	0.15%
245	Lkc	89.37	0.13%
132	Lo	80.80	0.12%
37	Lv	55.05	0.08%
38	Lga	32.14	0.05%
39	Phf	29.37	0.04%
23	Bd	25.05	0.04%
242	Lcr	17.35	0.03%
133	Lo	14.69	0.02%
15	Zg	0.71	<0.01%
14	Vc	0.69	<0.01%
Total		68285.5	100.0

[175] Calcic Cambisol on marls (Bk) (No. 128).

Sandy soils and particularly clayey soils are negligible in the agricultural areas within *Medium Radiological Vulnerability Index*, as it occurs in the upper *I_RV* indexes (see tables in Annexe X).

The agricultural systems within *Medium Radiological Vulnerability* include, cereals (ceG) as the most widespread crop group, being the main *representative crops* barley[176] and wheat[177]. This crop group occupies more than 85 % of the whole agricultural areas classified with this vulnerability[178]. Although there is a wide variety of crop group – topsoil texture combinations, as seen in Table 24 and Annexe X, others than cereals on loamy soils, these are far less common in this radiological vulnerability category.

The relation between clay content and potassium content in the topsoil of that most widespread agricultural system results in *High Radiocaesium Reservoir* (equals to 4); therefore, binding sites of clays could be occupied by ^{137}Cs in case a deposition occurs, which could become bioavailable for crops over time. The *Transfer Factor Index* assessed for that crop group – topsoil texture combination is 4.1 (see Table 24 and Annexe X); thus, these systems show certain capacity to transfer the ^{137}Cs from soil to plant. As a result, the High *I_Cs* and the intermedium *I_TF* give rise to a *Medium Radiological Vulnerability*.

Regarding the singular area previously mentioned, located in the South of Almería, its main agricultural system is comprised of non-leafy vegetables (nlF), principally tomatoes[179] as *representative crop*, grown in Calcic Cambisols on marls[180] or Calcic Xerosols on marls or Quaternary sediments[181]. The *Radiocaesium Reservoir index* is also *High* and the *Transfer Factor Index*, according to the corresponding F_v is 4.6, which combined, result also in the *I_RV* equals to 3.

[176] Barley (*IDPR*: *a11020*).
[177] Wheat (*IDPR*: *a11010*).
[178] For this particular agricultural system, Calcic Cambisol on marls are also the soil group most representative.
[179] Tomatoes (*IDPR*: *a42070*). These are sheltered crops; however, these are considered as if they were non-sheltered as worst scenario (see 2.2.1).
[180] Calcic Cambisol on marls (Bk) (No. 128).
[181] Calcic Xerosols on marls or on Quaternary sediments (Xk) (No. 117 and 118, respectively).

Table 24. Crop group – soil texture combinations within Medium I_RV, sorted by surface area occupancy (in descending order). Transfer factor value (Fv) (IAEA, 2010) and the corresponding I_TF are included.

Crop group (ID_C) - Soil texture	Soil-to-plant Transfer factor Fv (IAEA, 2010)	Transfer Factor Index I_TF	Surface of I_RV = 3 (km^2)
Cereals (grain) (ceG)-Loam	0.02	4.1	57139.27
Maize (grain) (maG)-Loam	0.016	3.9	3524.42
Legume fodder (lfS)-Loam	0.15	6.1	1327.76
Non-leafy vegetables (nlF)-Loam	0.033	4.6	1200.46
Cereals (grain) (ceG)-Sand	0.039	4.8	1191.31
Grasses (grS)-Loam	0.048	5.0	1152.11
Other crops (ocA)-Loam	0.31	6.8	885.48
Leafy vegetables (leaves) (lyL)-Loam	0.074	5.4	644.27
Woody trees (fruits) (wtF)-Sand	0.015	3.8	551.52
Grasses (grS)-Sand	0.084	5.5	315.82
Root crops (rcR)-Loam	0.03	4.5	120.66
Tubers (tbT)-Loam	0.035	4.6	115.70
Legume fodder (lfS)-Clay	0.046	4.9	55.74
Maize (grain) (maG)-Sand	0.049	5.0	38.40
Legume vegetables (lvS)-Loam	0.02	4.1	22.59

The agricultural systems resulting in *Medium Radiological Vulnerability Index* should be considered as areas of relative concern in case an accidental release of ^{137}Cs takes place. Depending on the deposition occurred, the prioritisation to take recovery actions should be analysed.

3.3.4 Low Radiological Vulnerability

The *Low radiological vulnerability*, with an index value of 2, is the most widespread one, covering a surface area about 104000 km^2 in mainland Spain. The agricultural areas with *Low I_RV* are represented in Figures 42 and 50.

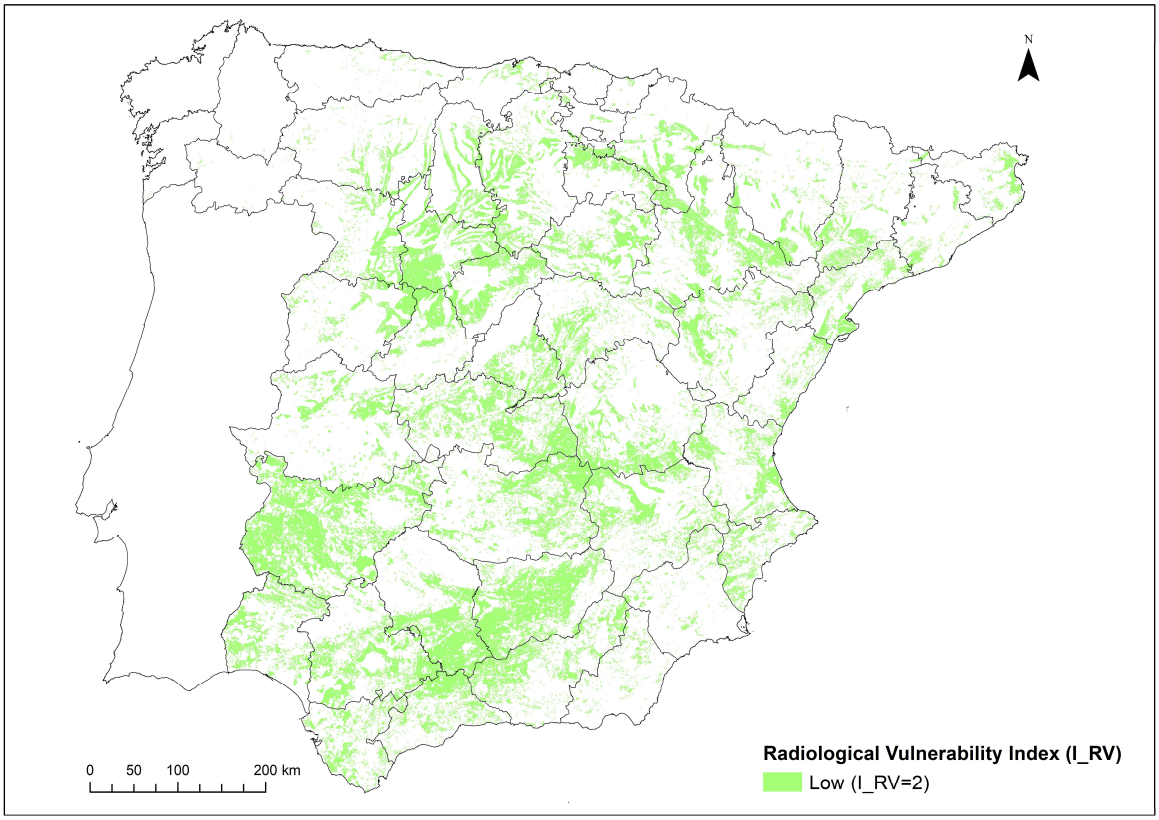

Figure 50. Agricultural areas in peninsular Spain with Low Radiological vulnerability (I_RV equals to 2). Projection: UTM ETRS89 H30.

Its geographical distribution covers all the provinces except A Coruña, being Badajoz, Jaén, Toledo, Ciudad Real, Córdoba and Sevilla those with the largest surface within this vulnerability category, as seen in the chart included in Figure 51.

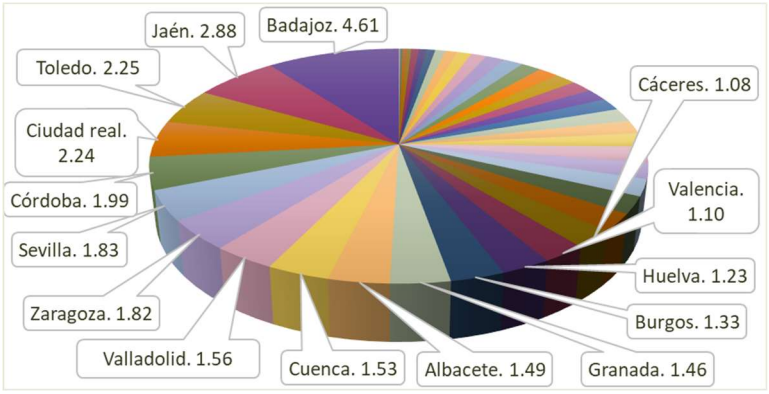

Figure 51. Chart representing the percentage of the agricultural surface areas within I_RV equals to 2, by peninsular Spanish province. Only provinces over 1.0 % are labelled.

The *Low I_RV* has been obtained in 39 existing soil groups out of the 44 in peninsular Spain. The most representative ones are Calcic Cambisols on marls[182], on limestones[183] or Quaternary sediments[184], and Calcaric Fluvisols[185] (each of them occupy over 13 % of the agricultural areas within this vulnerability category); all sum a total over the 64 % of the affected surface. The complete set of soil groups' surface in the *Low radiological vulnerability* class is included in Table 25.

Table 25. Soil groups affected with Low Radiological Vulnerability through peninsular Spain sorted in decreasing order according to the affected surface area.

No. Soil Group	Soil Classification (FAO-UNECO, 1974)	Surface of I_RV = 2 (km^2)	Surface percentage of I_RV = 2
128	Bk	20324.65	19.54%
126	Bk	16836.96	16.19%
201	Jc	16045.04	15.43%
127	Bk	13441.24	12.92%
202	Rd	6143.14	5.91%
206	Re	6036.91	5.80%
37	Lv	5861.62	5.64%
5	Ic	4364.91	4.20%
14	Vc	2125.88	2.04%
19	Xy	2044.91	1.97%
204	Ag	1907.82	1.83%
117	Xk	1211.22	1.16%
203	E	943.03	0.91%
242	Lcr	939.16	0.90%
12	Vp	738.65	0.71%
21	Be	697.31	0.67%
124	Bh	621.79	0.60%
1	Je	576.85	0.55%
8	Ql	483.27	0.46%
3	Ie	412.61	0.40%
240	Lc	336.41	0.32%
241	Lcr	316.73	0.30%
239	Lc	269.60	0.26%
238	Lg	249.92	0.24%
9	U	198.31	0.19%
116	Xk	187.83	0.18%
129	Bk	180.67	0.17%
6	Id	177.88	0.17%
132	Lo	99.93	0.10%
205	Zo	65.48	0.06%
133	Lo	52.15	0.05%
245	Lkc	33.27	0.03%
7	Qc	26.79	0.03%
23	Bd	23.01	0.02%
246	Lkcr	12.16	0.01%
244	Lkc	8.26	0.01%
15	Zg	2.38	0.00%
207	Rc	2.06	0.00%
118	Xk	0.10	0.00%
Total		103999.9	100.00%

These four soil groups result in *Medium* or *High Radiocaesium Reservoir* category (see Annexe X). However, that relatively high *I_Cs* indexes are compensated with the *Transfer*

[182] Calcic Cambisols on marls (Bk) (No. 128).
[183] Calcic Cambisols on limestones (Bk) (No. 126).
[184] Calcic Cambisols on Quaternary sediments (Bk) (No. 127).
[185] Calcaric Fluvisols (Jc) (No. 201).

Factor Index because the *representative crops* grown in these loamy soils belong to crop groups with relatively low F_v values. The most widespread crops groups within that *I_RV* category, as shown in Table 26, are fruits of woody trees (wtF), more precisely olives for oil[186] and wine grapes[187] and secondly, cereals (ceG), specifically barley[188], all of them rainfed crops.

Table 26. Crop group – soil texture combinations within Low I_RV, sorted by surface area occupancy (in descending order). Transfer factor value (F_v) (IAEA, 2010) and the corresponding I_TF are included.

Crop group (ID_C) - Soil texture	Soil-to-plant Transfer factor Fv (IAEA, 2010)	Transfer Factor Index I_TF	Surface of I_RV = 2 (km^2)
Woody trees (fruits) (wtF)-Loam	0.0035	2.3	52999.19
Cereals (grain) (ceG)-Loam	0.02	4.1	36044.94
Cereals (grain) (ceG)-Clay	0.011	3.5	6466.66
Maize (grain) (maG)-Loam	0.016	3.9	4086.96
Grasses (grS)-Clay	0.012	3.6	1211.32
Other crops (ocA)-Clay	0.31	6.8	738.65
Woody trees (fruits) (wtF)-Sand	0.015	3.8	658.12
Grasses (grS)-Loam	0.048	5.0	585.24
Maize (grain) (maG)-Clay	0.012	3.6	269.07
Leafy vegetables (leaves) (lyL)-Loam	0.074	5.4	259.49
Other crops (ocA)-Sand	0.31	6.8	177.88
Herbaceous plants (fruits) (hpF)-Sand	0.0042	2.5	168.67
Non-leafy vegetables (nlF)-Loam	0.033	4.6	145.52
Legume fodder (lfS)-Loam	0.15	6.1	125.02
Leafy vegetables (leaves) (lyL)-Clay	0.018	4.0	25.93
Tubers (tbT)-Loam	0.035	4.6	21.89
Non-leafy vegetables (nlF)-Clay	0.0091	3.3	14.52
Legume vegetables (lvS)-Loam	0.02	4.1	0.44
Root crops (rcR)-Loam	0.03	4.5	0.39

The main factor that makes fruits of woody trees having such a limited *I_RV* index value is the reduced *Transfer Factor Index*, since the corresponding F_v is significantly low (see Annexe V). At the same time, for cereals, the *I_Cs* is the index that contributes the most to reduce their vulnerability (see Annexe X), due to the limited capacity to store radiocaesium.

It is important to note the appearance of a third agricultural system in terms of occupancy, characterised by another soil type different from loamy soils; that is the cereals (ceG) on clayey soils (see Table 26). The soil groups included in that system correspond to Vertic Luvisols[189] and Chromic Vertisols[190] as shown in Annexe X. Their clay – potassium content

[186] Olives for oil (*IDPR*: *w31020*).
[187] Wine grapes (*IDPR*: *w21020*).
[188] Barley (*IDPR*: *a11020*).
[189] Vertic Luvisols (Lv) (No. 37).
[190] Chromic Vertisols (Vc) (No. 14).

relation gives rise to an *I_Cs* index value equals to 3.5, which is relatively low; that means that the binding sites of clays would be mostly occupied by potassium and soil would not have significant capacity to store ^{137}Cs to become bioavailable for crops. Considering the crop group – topsoil texture pair it results in intermedium *I_TF*, therefore cereals would have a certain capacity to uptake the ^{137}Cs in case it becomes bioavailable. The combination of these indexes results in the *Low I_RV* in which it is included, showing that both indexes are relatively compensated.

In any case, the potential entrance of ^{137}Cs in the food chain associated with all these agricultural systems is lower than the one associated with the agricultural systems included in the previous subsections.

3.3.5 Minimum Radiological Vulnerability

The *Minimum radiological vulnerability index* (*I_RV* equal 1) is the second less represented in peninsular Spain in terms of affected area, with 7150.21 km^2, as it is shown in the corresponding chart included in Annexe X. The spatial distribution throughout the studied area can be seen in Figures 42 and 52.

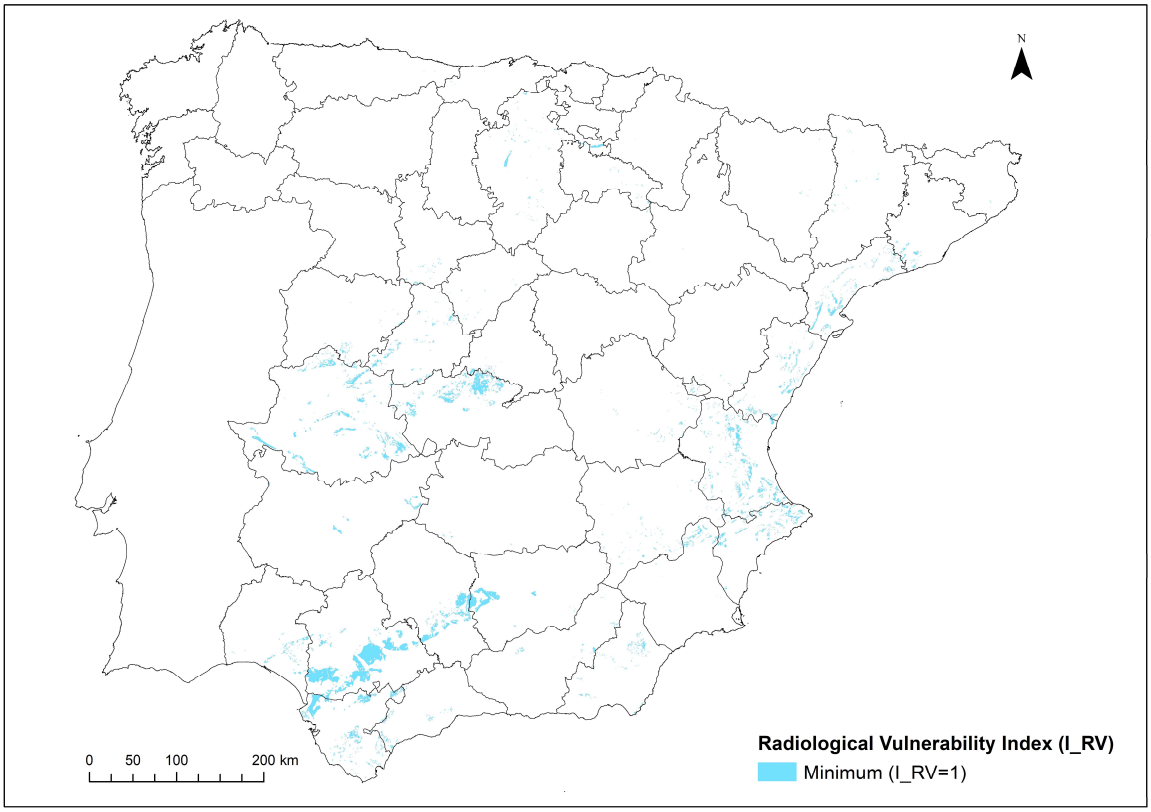

Figure 52. Agricultural areas in peninsular Spain with Minimum Radiological vulnerability (I_RV equals to 1). Projection: UTM ETRS89 H30.

The province of Sevilla has, by far, the largest area with *Minimum Radiological Vulnerability*, followed by Cáceres, Toledo and Valencia, among others (see Annexe IX). In Figure 53, a chart representing the surface area of the peninsular Spanish provinces with *Minimum I_RV*, with respect the total of the agricultural surface, is shown.

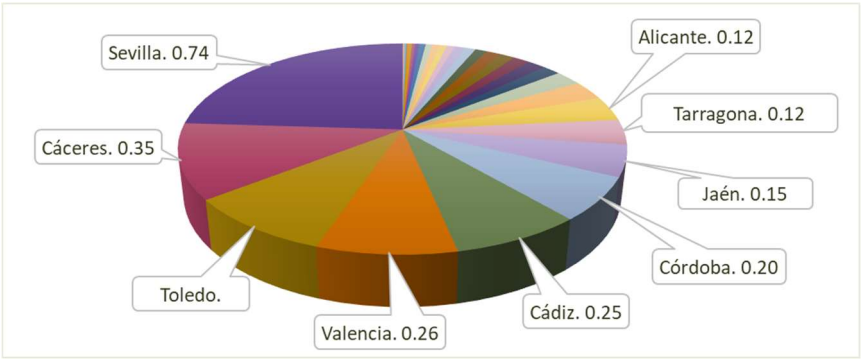

Figure 53. Chart representing the percentage of the agricultural surface areas within I_RV equals to 1, by peninsular Spanish province. Only provinces over 0.1 % are labelled.

There is a number of agricultural systems within the *Minimum I_RV*, but the most widely spread ones are those comprised of fruits of woody trees (wtF) grown in all topsoil textures, followed by the cereals (ceG) grown in clayey or sandy soils (see Annexe X).

The first agricultural system, fruits of woody trees, occupies more than two thirds of the whole agricultural area within this vulnerability category in peninsular Spain, of which almost a half are grown in clayey soils (mainly Chromic Vertisols[191] and Vertic Luvisols[192]), about 42 % are grown in loamy soils (principally Calcaric Lithosols[193]) and the rest on sandy soils (Dystric Lithosols[194]) (see Annexe X). The *Radiocaesium Reserve Index* of the referred clayey soils is classified as *Medium* (equals 3), due to their high clay content combined with a relatively limited potassium content; that leads to exhibit free binding sites in which ^{137}Cs can be adsorbed.

The fruits of woody trees grown in clayey soils, are attributed a *I_TF* index equals to 1.19 (as shown in Annexe X), due to their low F_v (which is nearly the lowest compared with the other crop groups (IAEA, 2010) as shown in Annexe V) which compensates the *I_Cs* to give rise to the *Minimum I_RV*. The *representative crops* mainly cultivated on these agricultural systems are olives for oil[195] and wine grapes[196] (see Annexe X).

The second agricultural system with *Minimum Radiological Vulnerability*, cereals in clayey or sandy soils are comprised of Pellic Vertisols[197] and Dystric Lithosols[194], respectively; they occupy more than a quarter of the agricultural areas within this *I_RV* (as shown in Annexe X). In this case, the *I_Cs* is equal to 1, meaning a minimum capacity to retain ^{137}Cs in the topsoil because of the potassium content. On the other hand, *I_TF* ranges from 3.49 to 4.76, which is relatively high meaning that this system shows certain capacity to transfer ^{137}Cs from soil to plants; however, both indexes compensate for one another.

There are some other agricultural systems comprised by grass (grS), fruits of herbaceous plants (hpF), leafy vegetables (lyL), maize (maG) and non-leafy vegetables (nlF) but these occupy slightly over 8 % of the total agricultural systems with *Minimum Radiological Vulnerability*.

[191] Chromic Vertisols (Vc) (No. 14).
[192] Vertic Luvisols (Lv) (No.37).
[193] Calcaric Lithosols (Ic) (No. 5).
[194] Dystric Lithosols (Id) (No. 6).
[195] Olives for oil (*IDPR*: *w31020*).
[196] Wine grapes (*IDPR*: *w21020*).
[197] Pellic Vertisols (Vp) (No. 12).

Having that *Radiological Vulnerability Index*, in case of a ^{137}Cs deposition, these areas would be, a priori, the ones of less concern, in comparison with the agricultural systems analysed in the previous subsections.

3.3.6 General considerations regarding the Radiological Vulnerability results

According to the detailed analysis carried out in the previous subsections a summary with the general considerations regarding the *Radiological Vulnerability of the agricultural systems* in peninsular Spain can be stated, according to the results obtained in the assessment performed, resulting in the map shown in Figure 42 and in the figures included in Annexes IX and X:

- Derived from the crops sharing performed, a lack of spatial continuity results in mapping the *Radiological Vulnerability indexes* in some regions throughout the peninsula. This occurs in the border of some provinces, where a sudden change of the *I_RV* value is obtained. Such is the case for the Extremadura's provinces (Cáceres and Badajoz), between Badajoz and Córdoba and between Murcia and Alicante. That fact is related to the crops' distribution performed, as explained in section 3.2.
- The agricultural surface area in peninsular Spain according to (EEA, 2016) (in which there is soil data[198]) is 232121 km^2. The most represented radiological vulnerability category in that territory is the *Low I_RV* (equal to 2), approximately half the agricultural surface. That means that most of the Spanish agricultural systems (crop group – topsoil texture combination) show low potential to transfer ^{137}Cs from soil to crops over time, in case an accidental release occurs and, in turn, the potential entrance of ^{137}Cs in the food chain is low, according to the criteria used in the categorisation of the vulnerability of these systems. As seen in Figures 42, 50 and 51, it is relatively uniformly distributed in mainland Spain, except in the Northern strip. The main agricultural system within that I_RV is the one comprised of olives for oil and wine grapes grown in loamy soils.

[198] Areas with soil information are the ones in which the soil properties gathered in the updated Spanish soil database can be represented in (EC-ESBN, 2004).

- The two extreme radiological vulnerability indexes (*Maximum* and *Minimum*) occupy the lowest surface, partially owing, for the former, to the categorisation criteria followed. The agricultural systems most representative are chestnuts grown in loamy soils for the *Maximum I_RV*, and olives and grapes grown in clayey soils for the *Minimum I_RV*.
- The other two *radiological vulnerability indexes* affect feedstuff as grasses for *High Radiological Vulnerability* and cereals for *Medium Radiological Vulnerability*, both grown in loamy soils.

3.4 Results obtained in the case study to apply the Radiological Vulnerability map of the agricultural systems in the EPR

The radiological vulnerability map of the agricultural areas with respect to their potential transfer of ^{137}Cs to the food chain has been tested in a case study. It contemplates a hypothetical severe accident in Almaraz NPP.

The development of a case study serves to illustrate the usefulness of knowing in advance the radiological vulnerability of Spanish agricultural systems for the EPR. The combination of the radiological vulnerability of the territory with a scenario of soil contamination with ^{137}Cs, allows the categorisation and mapping of the affected areas of most concern, in order to prioritise where to take actions in the recovery phase to recover the normal living conditions. That map can be used as a tool in the decision-making process for the recovery facing the mid and long-term, aiming to minimise the exposure of the public through the ingestion pathway.

In the subsequent sections the deposition maps with the results of the simulated ^{137}Cs deposition and the prioritisation maps of the agricultural systems for the case study considered are described.

3.4.1 Case study results: Deposition probability assessment

The case study considers a severe accident with offsite consequences caused by an unintentional release of ^{137}Cs from the selected site, Almaraz NPP. To map the most probable deposition patterns derived from an ISLOCA accident (see section 2.4.3), a bunch

of daily release simulations are performed taking into account the meteorological data from 2012 to 2016 (ANURE, 2017). A statistical assessment from these simulations is done to obtain the *prevailing* deposition patterns.

The ^{137}Cs Deposition map considering the complete release simulations dataset is used to obtain the annual average deposition pattern. Besides, the seasonal deposition maps are performed on the basis of the simulations starting in those days belonging to each meteorological season[199].

In the resulting deposition maps the deposition patterns of the ^{137}Cs for the annual, spring, summer, autumn and winter average meteorological conditions are obtained. These maps show the probability of the deposition throughout peninsular Spain and its severity, also. Both factors are united to create an index named *^{137}Cs Deposition Index* (*I_D*), representing the deposition probability weighted by its severity, which reflects the activity concentration range deposited. The *I_D* index has five categories, from minimum (which is assigned a value of 1) to maximum (with a value of 5). It is assessed and assigned to each calculation grid cell by applying the methodology described in section 2.4.3.

From the resulting Deposition maps (see Figure 54) it is clear that the dispersion of ^{137}Cs and its deposition in the Iberian Peninsula is highly influenced by the prevailing winds which range from West to West-South-West along the year, although these are less effective in terms of dispersion during summer. This fact, studied in ANURE (2017), is related to the geographic location of the Iberian Peninsula and the air masses that affect it (Hernández-Ceballos, et al., 2020) and to the location of Almaraz NPP, in particular. On one side, maritime Western air masses are generated by the combination of the semi-permanent Azores high-pressure and the Icelandic low-pressure systems located in the North Atlantic Ocean (Lorente-Plazas, et al., 2015). On the other side, the Tajo river basin, where Almaraz NPP is located, determines the channelling of winds in that area of mainland Spain. However, several differences can be observed among the five deposition average tendencies shown in Figure 54.

[199] The 1st of March is taken as first day for spring.

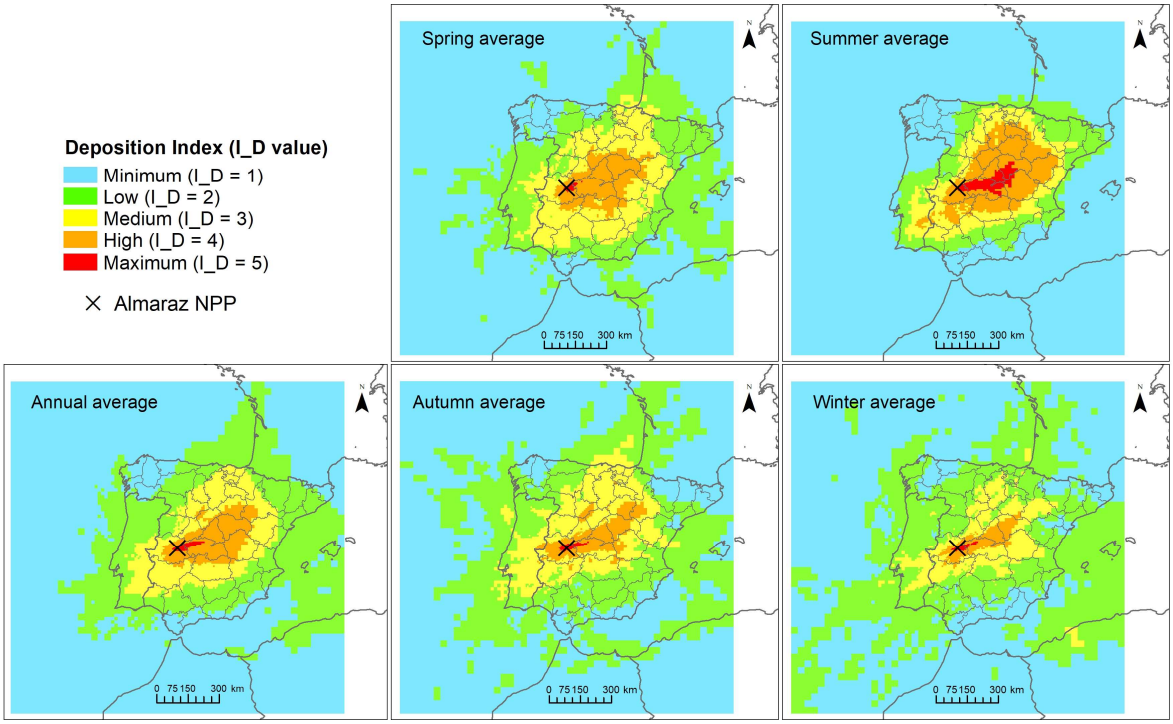

Figure 54. Annual and seasonal ^{137}Cs Deposition index average maps along 2012 – 2016 period. Projection: UTM ETRS89 H30.

In general, de deposition maps obtained for spring and autumn correspond to intermediate meteorological situations between the two extreme ones in the Iberian Peninsula, which occur in summer, with long stagnant situations, and in winter, with significant atmospheric dispersion conditions.

Taking into account exclusively the deposition results obtained in mainland Spain, the *Low deposition* category (with an *I_D* value equals to 2) is the most widespread one for annual average conditions, as well as for autumn and winter (see Table 27), with an impacted surface ranged between 36.5 % and 49.3 %, as seen in Figure 55. In these periods, the most representative values of the weighted deposition probability correspond to those included in the P_{25} – P_{50} interval (see Table 17 in section 2.4.3).

Table 27. Surface area affected by each I_D class in the annual average deposition map and in the corresponding seasonal average deposition maps, in peninsular Spain (km²).

Period	Deposition Index (I_D)				
	Minimum Deposition I_D = 1	Low Deposition I_D = 2	Medium Deposition I_D = 3	High Deposition I_D = 4	Maximum Deposition I_D = 5
Annual	64175.00	182735.30	163402.71	79744.61	3671.93
Spring	61780.68	143586.92	200963.12	85642.69	1756.13
Summer	94930.61	129670.39	116252.06	134015.21	18861.29
Autumn	81100.64	180329.23	170074.29	59281.13	2944.28
Winter	97426.67	243516.03	119372.67	31146.05	2268.12

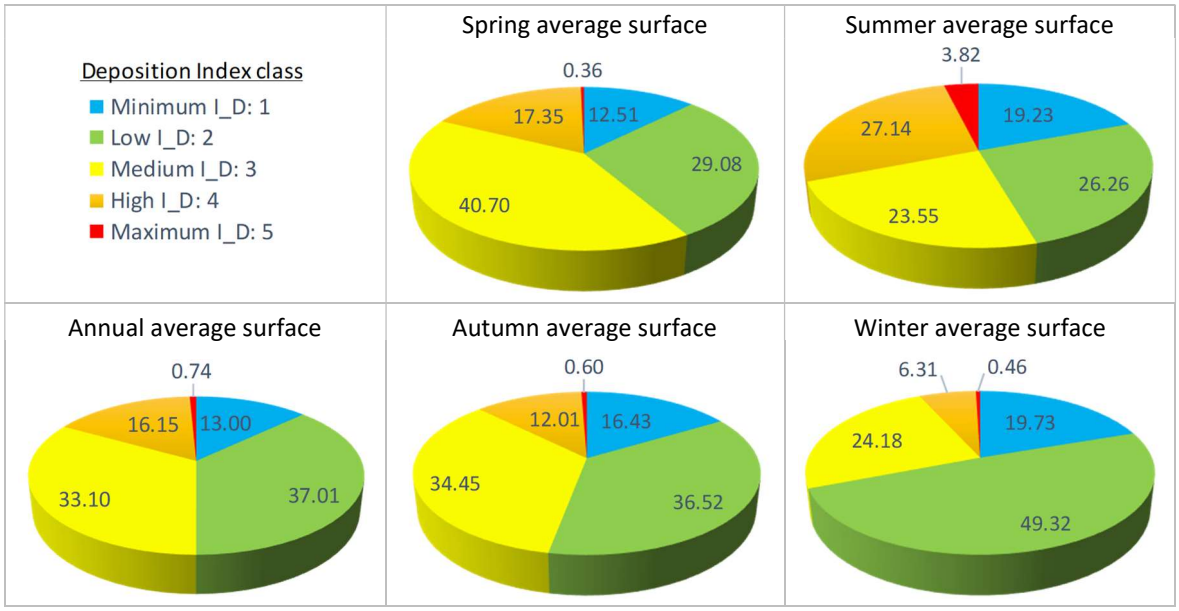

Figure 55. Percentage of peninsular Spain surface affected by the five Deposition Index classes considering the annual and seasonal average meteorological conditions.

In spring and summer, the most representative *deposition indexes* are, for the former, the *Medium I_D* (equals to 3), with almost 41 % of the total surface, and, for the latter, the *High deposition* index (*I_D* equals 4), with about 27 %, which is really closed to the 26.26 % of the area within the *Low deposition* index (see Figure 55).

For autumn average meteorological conditions *Medium* and *Low Deposition Indexes*, as the two most widespread ones, affect almost the same surface area: nearly a 34 % the former and slightly over 36 % the latter, quite similar to the surfaces resulting within both *I_D*s for annual average conditions, as shown in Figure 55.

Summer, apart from having the most extensive area with *High I_D*, shows the largest surface for the *Maximum Deposition Index* (*I_D* equal to 5) among all the seasons. Although in all

the periods less than 1 % of mainland Spain results affected by *Maximum I_D*, in summer it reaches about 4 %. In any case, these are reduced extensions which are highly related to the methodology applied, in which the threshold considered to assign the *Maximum I_D* category is the percentile P_{95} of the weighted deposition probability. This treatment has allowed to highlight those areas where the most severe deposition is the most likely within the ones resulting in *High I_D* throughout the year (see Table 17 in section 2.4.3). That way, the resulting affected surface to be considered in a prioritised recovery of the contaminated areas is delimited.

The surface affected by *Medium*, *High*, and *Maximum Deposition Indexes* from winter to summer shows a gradual, but relevant increase of ^{137}Cs deposition probability and severity, related to the particular meteorological configurations taking place in the Iberian Peninsula during summer. According to Millán & Artiñano (1992): "*The formation of a thermal low over the Iberian Peninsula on summer days forces the atmospheric convergence of surface winds from the coastal areas towards the central plateau*". These Thermal Low Systems (TLS) are well reflected in the summer average Deposition map (ANURE, 2017), in which the *Deposition indexes* over the *Minimum* are concentrated in the inland (see Figure 54). This meteorological situation forces the contamination plume to stay over the inland and reduces the effectiveness of the Western winds which, in turn, does not favour the contaminants' dispersion; thus, a higher activity concentration remains in the stable atmosphere and then, the deposition probability, besides its severity, increases in the centre of the Peninsula.

Therefore, in summer, the deposition pattern reflects that ^{137}Cs concentrates in inland Spain which gives rise to lower *deposition indexes* in the Northwest of the country, while the more effective prevailing winds favour the dispersion and make the ^{137}Cs deposition to be more widely spread in winter. Therefore, the winter meteorological configuration gives rise to lower *deposition indexes* values in the majority of the Spanish provinces (as seen in Annexe XI), reducing the deposition severity.

Once the general deposition pattern in the whole peninsular Spain has been analysed, the figures referred exclusively to the agricultural areas are shown in Table 28.

Table 28. Agricultural surface area occupied by each I_D class considering annual and seasonal average conditions, in the Spanish (km^2).

Period	Deposition Index (I_D)				
	Minimum Deposition I_D = 1	Low Deposition I_D = 2	Medium Deposition I_D = 3	High Deposition I_D = 4	Maximum Deposition I_D = 5
Annual	22553.46	82363.36	86782.97	38489.46	1931.76
Spring	19221.95	63708.01	105665.58	42748.70	776.77
Summer	36577.66	57510.36	61795.68	64504.45	11732.87
Autumn	28818.71	82969.67	89074.02	29613.75	1644.86
Winter	35735.74	115816.20	63821.93	15651.96	1095.19

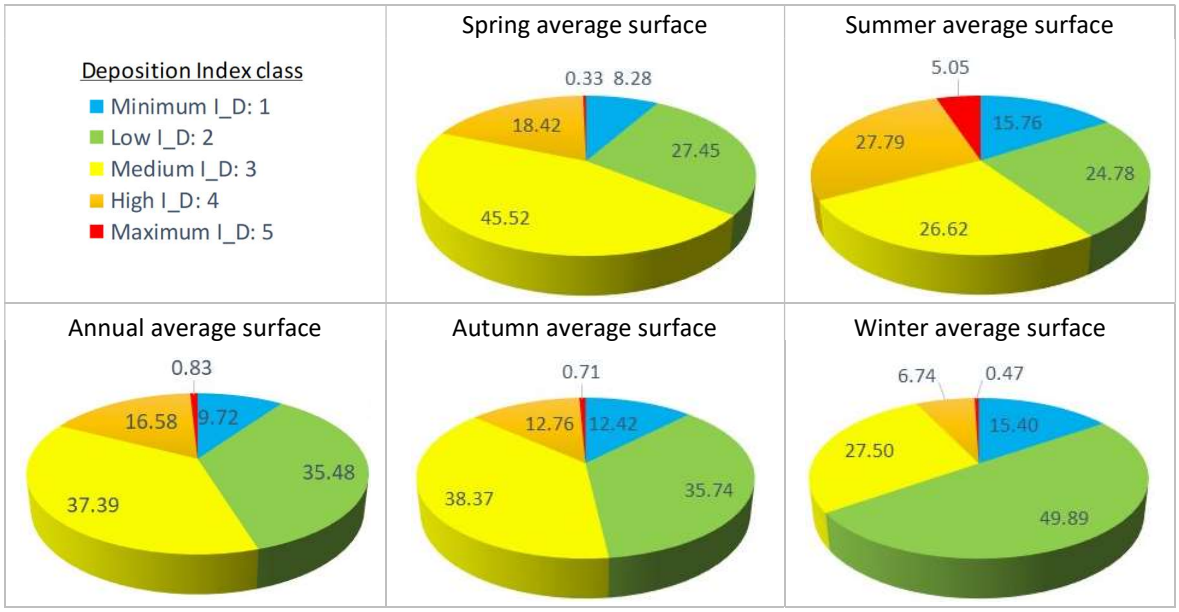

Figure 56. Percentage of the agricultural areas' surface in peninsular Spain affected by the five Deposition Index classes, considering the annual and seasonal average meteorological conditions.

Although the trend of the surfaces of the agricultural areas affected by each *I_D* along the year is quite similar to the ones affecting the entire territory, some differences in terms of percentage have been obtained, as can be seen in Figure 56, in comparison with the percentages shown in Figure 55.

Taking into account exclusively the agricultural areas, again, the *Low Deposition Index* occupies the largest surface in winter. However, although the percentages do not experience meaningful change compared to the surface for the whole country, it has been enough so that for annual and autumn average conditions, *Low I_D* is not the most widespread one but the *Medium I_D*. The latter *Deposition index* class remains the largest for spring conditions, as it occurs with the *High I_D* for summer. Regarding summer, it is

remarkable that the agricultural area affected by the *Maximum Deposition Index* corresponds to more than 5 % of the total.

Considering that percentages, summer appears to be the most problematic season due to the particular meteorological configuration which takes place in the region, related to the TLS. Indeed, the agricultural areas of six Spanish provinces are affected by the *Maximum Deposition Inde*x in summer (see Annexe XI), while during the rest of the year only Cáceres and Toledo are impacted (as it occurs, for annual average conditions).

In the light of the average deposition pattern results obtained from the release and deposition simulations along the five-year period, the worst-case scenario is the summer situation, because at that season areas affected by the Maximum and *High Deposition Indexes* are the largest, and more provinces are within these index values, as it is shown in Annexe XI.

3.4.2 Case study results: Prioritisation maps

According to the methodology described in section 2.4.4, the *Prioritization Index* (coded as *I_P*) results from the combination of the *Radiological Vulnerability Index* of the agricultural areas, regarding ^{137}Cs (*I_RV*) with the *Deposition Index* (*I_D*). *I_P Index* represents the risk of each agricultural area to transfer the ^{137}Cs deposited on the ground from soil to crops in the root uptake process, derived from a hypothetical nuclear accident with similar characteristics as the case study. Hence, the higher the *I_P* index, ranged between 1 to 5, the higher the risk of ^{137}Cs transfer to food, for human beings, or feed, for farm animals and the higher the risk exposure via ingestion in the mid and long-term for a specific contaminated scenario. From the Radiation Protection point of view, the categorisation of the areas of most concern regarding the population exposure allows the identification of the zones where the actions to minimise that risk must be taken in a prioritised way.

To obtain the *Prioritisation Index* the combination of both indexes: *I_RV* and *I_D*, is carried out by using a risk matrix (see Figure 26). The resulting five *I_P* index categories are set out in *Table 18*. As it was previously mentioned (see section 2.4.4), the *Radiological Vulnerability Index* and the *Deposition Index* have been assumed with the same weight factor (1).

It can be stated that neither *Minimum radiological vulnerability* (*I_RV* equals to 1) implies a *Minimum* prioritisation, nor *Maximum radiological vulnerability* (*I_RV* equals 5) leads always to *Maximum* prioritisation. On the contrary, the eventual Priority classification depends on the probability of the deposition and the activity concentration deposited in these areas, which is defined with the *Deposition Index* (*I_D*). Therefore, a categorisation of the territory is done with the aim to prioritise the agricultural areas to act on facing their recovery, taking into account the *prevailing* ^{137}Cs deposition pattern. In this work, the prioritisation results obtained refer exclusively to the case-study.

The geographical representation corresponds to the Prioritisation maps made for annual and seasonal meteorological conditions. As it is explained in section 2.4.4, these maps, shown in Figure 57, are obtained by overlapping the radiological vulnerability of agricultural systems map and the deposition map for each period of time considered.

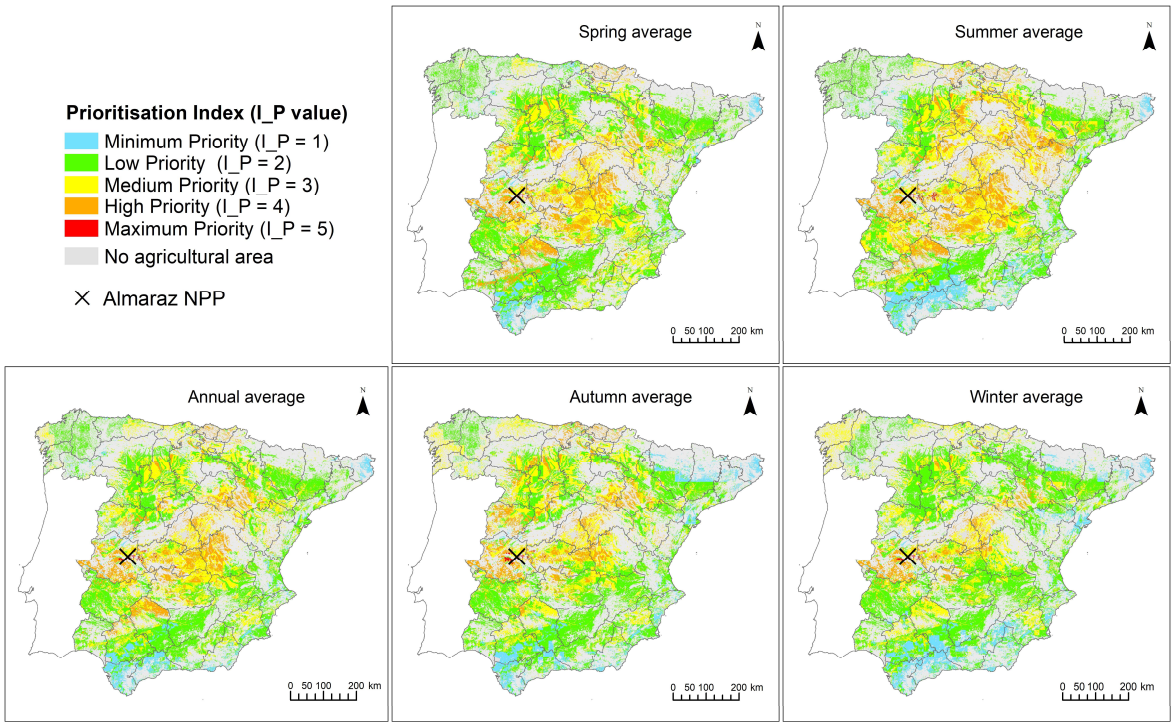

Figure 57. Annual and seasonal Prioritisation maps regarding the ^{137}Cs deposited on agricultural peninsular Spain soils, according the case study focusing on Almaraz NPP. Projection: UTM ETRS89 H30.

The resulting maps and the databases associated can be easily managed and consulted by using a GIS; however, in a paper-based result like this, it is necessary to summarise the information mapped. Therefore, a bunch of tables and charts have been elaborated to

show the *Prioritisation Index* results throughout the territory (as it was performed to present the vulnerability results regarding the agricultural areas). These are the following:

- In Table 30 it is included the surface of the five *I_P* classes in each period of time (annual and seasonal average), which are plotted all together in Figure 58, so the surface differences among seasons can be seen.

Table 29. Surface area corresponding to each Prioritisation class (I_P) in the annual Prioritisation map and in the seasonal Prioritisation maps, in the Spanish (km²).

Period	Prioritisation Index (I_P)				
	Minimum Priority I_P = 1	Low Priority I_P = 2	Medium Priority I_P = 3	High Priority I_P = 4	Maximum Priority I_P = 5
Annual	15192.21	114132.01	70734.52	31626.27	436.01
Spring	12475.90	110873.77	69815.44	38691.16	264.74
Summer	23690.24	86721.57	73601.11	47506.37	601.73
Autumn	21446.46	112977.77	68822.89	28374.36	499.52
Winter	27657.06	130573.61	59234.27	14276.72	379.34

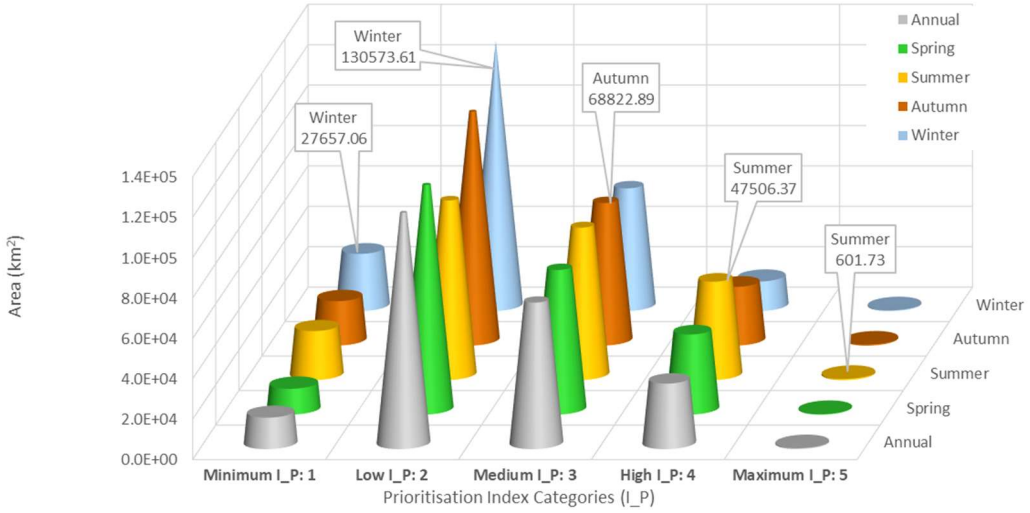

Figure 58. Chart representing the surface area occupied by each Prioritisation index considering the annual average meteorological conditions and each average seasonal meteorological conditions, regarding the ^{137}Cs deposited on agricultural soils in peninsular Spain, according to the case study centred in Almaraz NPP. The season in which the largest surface is obtained for each I_P value is tagged.

- The pie charts gathered in Figure 59 represent those surface areas as percentage of the whole Spanish agricultural areas for each period of time separately.

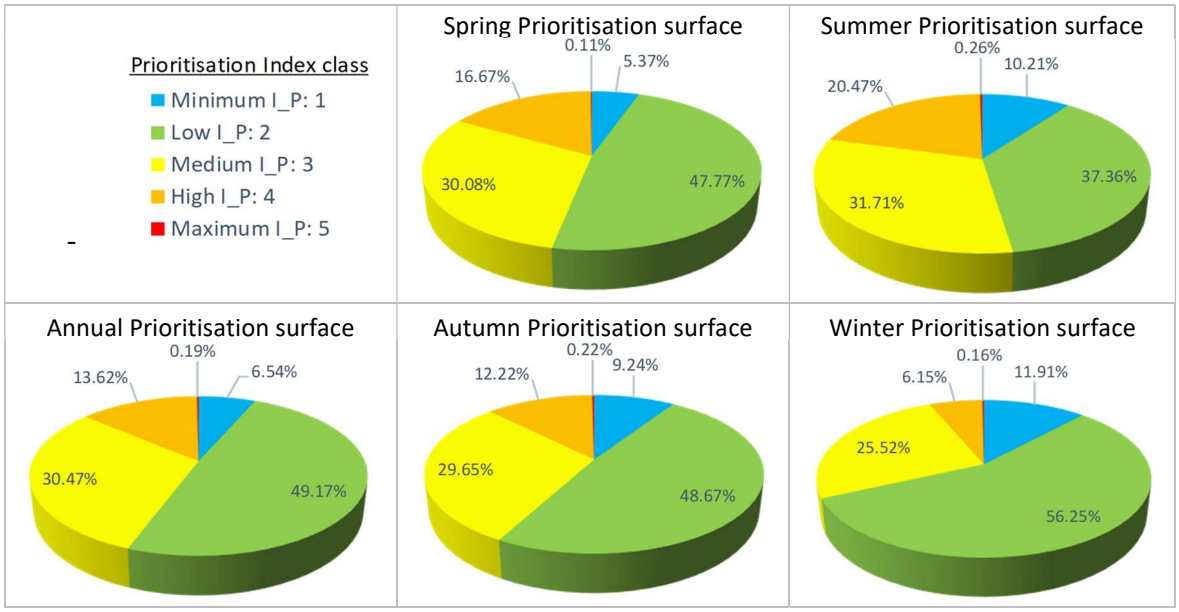

Figure 59. Pie charts representing the percentage surface area occupied by each Prioritisation index considering the annual average meteorological conditions and each seasonal average meteorological conditions, regarding the ^{137}Cs deposited on the agricultural peninsular Spain soils, according to the case study centred in Almaraz NPP.

- The surface area derived from all the *I_RV – I_D* combinations are shown in the matrixes, gathered in Annexe XII, one per each period of time. In these matrixes the surface is expressed both in km^2 and as a percentage of the whole agricultural areas in peninsular Spain.
- Annexe XIII includes the tables and charts representing the surface area by each *I_P* category, disaggregated by province (in km^2 and in percentage also) for annual average conditions and for seasonal average conditions.
- The surface area of the crop groups affected by each *Prioritisation Index*, for the different average meteorological conditions are included in Annexe XIV.

Following the criteria established in section 2.4.4, (see Figure 26), areas with high probability to be classified as extremely contaminated[200] (resulting in *Maximum Deposition Index – I_D* equals to 5), which also show significant potential to transfer ^{137}Cs to crops in the mid and long-term (with High or *Maximum Radiological Vulnerability Index – I_RV* equals to 4 and 5, respectively), will clearly need to be considered as priority areas. Actions should be taken in these areas first, in order to minimise the food chain exposure pathway to population. However, areas with *Maximum* deposition index values, where the potential to transfer ^{137}Cs is lower (from *Low* to *Minimum Radiological Vulnerability*), require not so

[200] Contamination levels defined according to *Table 16* in section 2.4.3.

priority nor immediate actions, they can be modulated in time. This scheme, can be followed regarding all the deposition categories, modulating the urgency and priority of actions in regard to the potential to transfer ^{137}Cs shown by the agricultural areas.

In terms of the surface area affected by each *I_RV – I_D* pair to give rise to the *Prioritisation Index* in the case study, as can be seen in see Annexe XII, the indexes combination which affects the largest surface is *Low Radiological Vulnerability* Index (2) and *Medium Deposition Index* (3) for annual, spring and autumn conditions (ranging from over 14 % to about 23 % of the total agricultural area). In summer, the most widespread combination is *Low Radiological Vulnerability* Index (2) with *High Deposition Index* (4) (being the 14.3 % of the total). For winter average conditions the indexes combination that gives rise to the largest area is *Low Radiological Vulnerability Index* (2) and *Low Deposition Index* (2) (with the 20.61 %). Although the I_RV index remains low in all the periods, the deposition index varies, giving rise to *Low Priority index* (2), except for summer, when the most spread combination results in *Medium Priority Index* (3). For the case study, these facts show the influence of the meteorological conditions throughout mainland Spain along the year, being summer the worst-case scenario, related to the Iberian Thermal Low (ITL) (Millán & Artiñano, 1992; Hoinka & Castro, 2003), while winter is the opposite scenario, due to the existence of more effective dispersion because of the presence of prevailing West winds (Maya-Manzano, et al., 2016).

As seen in Table 30 and Figures 58 and 59, the *Maximum* priority class is the less spread one within the agricultural areas among the results obtained for this case study which is highly related to the criteria used to define the *Maximum* categories for the *Deposition Index* and the *Radiological Vulnerability Index* as it was revealed in sections 3.4.1 and 3.3, respectively. It is also conditioned by the assumption conducted to define the *I_RV – I_D* combinations resulting in the eventual *I_P* shown in the matrix included in Figure 26 (section 2.4.4). These criteria seek to obtain distributed categories to highlight the agricultural areas with *Maximum Priority* to act on and, at the same time, that these are not extremely large so that the actions to be taken first are affordable.

Nevertheless, attending to the criteria stablished in this Thesis, summing the surface affected by the *High* and *Maximum Prioritisation* classes the resulting area is the second

less large in all the periods analysed except in winter, when is the smallest. Besides, the sum of the two lowest *I_P* classes, are over 50 % of the agricultural areas except in summer, when it is slightly under 48 %, which implies that, considering the case study, if an accidental release of ^{137}Cs occurs in summer, the risk of its transfer to the food chain increases. The *Low Priority*, individually, is the most widespread one in all the periods, followed by the *Medium*. Winter is the only season when the two highest *I_P* classes are the fifth and fourth less widespread ones, showing that, in the case study, the risk for a radiological contamination regarding ^{137}Cs through ingestion is the lowest.

Therefore, the worst situation occurs during the summer season mainly due to the extension of the two highest prioritisation classes (*I_P* equals to 4 and 5); then is when about 602 km^2 result affected by *Maximum I_P*, mostly in Toledo (half of that surface), followed by Cáceres (with a third), among other four provinces with minor agricultural surface area affected, as shown in Annexe XIII. Areas showing *High Priority Indexes*, those which must be intervened in a second most priority phase, are more spread than the former ones and, again, the worst situation occurs during summer. In that season, 47.506,37 km^2 (more than 20 % of the total surface, as shown in Table 30, and Figures 58 and 59) affect mainly Cuenca, Cáceres and Ciudad Real (see Annexe XIII); that surface is more than three times larger than in winter for this case study.

Undoubtedly, in case a recovery strategy has to be designed and implemented, these designated areas (with *Maximum* and *High Priority Index*) should be the first ones on which to decide the actions to be taken.

Regarding the characteristics of the agricultural systems within the *Maximum Priority*, grasses (grS) are the crop group most widely distributed in whatever season (see Annexe XIV), covering at least 70 %, except in summer when, although being the most widespread one, that crop group is grown in less than 37 % of the total *I_P* equals 5. The main crop included in that crops group are meadows[201] followed by winter cereals[202], principally grown in Dystric Regosols[203]. The second most relevant crop group within *Maximum*

[201] Meadows (*IDPR*: *a63000*).
[202] Winter cereals (*IDPR*: *a61010*).
[203] Dystric Regosols (Rd) (No. 202).

Priority in summer is legume fodder (lfS), mainly lucerne[204], also on loamy soils such as Rhodo-Chromic Luvisol on shales[205] or Calcic Xerosols on calcareous sandstones[206] as the most representative ones.

The main agricultural systems within *High Priority* throughout all seasons are comprised of cereals (crop group ceG), as shown in Annexe XIV; that crop group occupies a surface ranged from 47 % of that prioritisation class in winter, to almost 63 % in summer. Among cereals, barley[207] is the most affected crop, cultivated in Calcic Cambisols on marls[208].

Around 50 % of the agricultural areas classified within *Medium Priority* are cultivated with cereals (ceG) in every season (see Annexe XIV). Again, barley[207] grown in loamy soils, principally Calcic Cambisols (among them mainly those developed on marls[208]) is the most characteristic crop – soil type combination in the agricultural systems within that priority class.

A wider variety of crop groups are gathered in areas classified as *Low* and *Minimum Priority* (Annexe XIV), including fruits of woody trees[209] and herbaceous plants[210], while these are missing in areas within *Maximum I_P* and relatively limited for High and *Medium Priority Indexes* (depending on each season's deposition pattern). Cereals (ceG), mainly barley[211] in Calcic Cambisols developed on different bedrocks[212] are the most representative ones in *Low Priority* areas in every season except in summer (when it is the second crop group by surface). Agricultural areas with olives for oil[213] (included in the crop group for fruits of woody trees – wtF) are the largest in summer (also grown in Calcic Cambisols[212]); olives are the second most widely spread crop in the rest of the seasons. Agricultural systems within *Minimum Priority* have fruits of woody crops (wtF) and cereals (ceG), in that order, as the

[204] Lucerne (*IDPR*: *a62010*).
[205] Rhodo-Chromic Luvisol on shales (Lcr) (No. 242).
[206] Calcic Xerosols on calcareous sandstones (Xk) (No. 116).
[207] Barley (*IDPR*: *a11020*).
[208] Calcic Cambisols on marls (Bk) (No. 128).
[209] Fruits of woody trees (*ID_C*: wtF).
[210] Herbaceous plants (*ID_C*: hpF).
[211] Barley (*IDPR*: *a11020*).
[212] Calcic Cambisols (Bk) on limestones (No. 126), on Quaternary sediments (No. 127) on marls (No. 128) and gypseous marls (No. 129).
[213] Olives for oil (*IDPR*: *w31020*).

most representative crop groups, except in autumn when wtF follow to ceG, both grown in loamy soils, mainly Calcic Cambisols on marls[212].

3.4.3 Discussion regarding the prioritisation maps

Once having the overall view, the decision-makers may design in advance the corresponding preventive measures regarding the preparedness stage of the EPR. These actions can be focused on the public health safety (facing radiological issues) and the socio-economic impact also (facing non-radiological issues) at different scales: municipality, province, or country. On one the hand, knowing the potential agricultural affected surface and the production potentially impacted may help to choose the appropriated measures which may avoid, as much as possible, a ^{137}Cs transfer to the food chain, on the bases of the prioritisation information. On the other hand, that knowledge is also useful to forecast the potential social and economic consequences in case of an accidental radioactive deposition occurs. In any case, the optimal bunch of actions can be planned with well-thought-out strategies according to the specificities of each region.

Facing the recovery of the affected areas regarding the long-term, transfer reduction could be achieved by applying one or several countermeasures; ultimately, different techniques may be implemented in order to minimise the radionuclides transfer to the food chain (see section 1.2.1).

The nutrients' absorption by crops show different ratios according to the plants' growing stage; therefore, that stage should be taken into account also when deciding the recovery strategies to be implemented for best management. In that sense, in case of an accidental release takes place in summer (defined previously as the worst-case scenario in the case study presented), it should be essential to distinguish the areas which could have been already harvested, for instance those cultivated with cereals included in agricultural areas with *Maximum*, *High* and even *Medium Priority* or lucerne in the former class. The same concern should be determined for those areas included in *Maximum Priority* where grasses (meadows) were cultivated as mentioned above, not only regarding their growing stage but also taking into account whether livestock was grazing on them when the event occurred. Nevertheless, those concerns would be pondered regarding the season when the

accident occurs (in terms of harvesting season) and the approach designed deals with the mid and long term.

Hence, the most suitable remediation strategies may be selected and prepared in advance, attending to the local specificities of the affected areas using, as decision-making tools, the prioritisation maps previously exposed, which would be suitable for a scenario with the same characteristics as the case study designed, in order to reduce reaction timing for the recovery. To define the prioritisation maps for a different source term or a different site, a particular case study should be performed.

On the other hand, in the decision-making process, some areas may be considered as exclusion zones, which is another strategy in order to derive resources to those contaminated zones where the countermeasures may be most effective, applying the *optimisation* principle.

Facing the food sector, all the possible countermeasures to be adopted in the agricultural environment (see section 1.2.1) should be oriented to reduce as much as possible the consumers' exposure through the ingestion pathway. The aim would be to ensure the foodstuffs do not reach the Codex maximum level (ML) (FAO-WHO, 1995)[214], in this case for ^{137}Cs. Those ML values must be taken into account in all the emergency phases. For the early phase food (or water) restrictions can be adopted, depending on the deposition pattern, however, for the mid and long-term after the accident, the recovery of the agricultural areas shall[215] be faced; both decisions shall be taken on the bases of the *justification* principle. The EPR plans, according to the EU (2013), shall also include the measures needed to be adopted in the transition phase "*from an emergency exposure situation to an existing exposure situation*". Afterwards, areas with long-lasting

[214] According to (FAO-WHO, 1995), "the Codex maximum level (ML) for a contaminant in a food or feed commodity is the maximum concentration of that substance recommended by the Codex Alimentarius Commission to be legally permitted in that commodity". For radionuclides, among other contaminants, a Guideline level (GL) is defined. "The GL is the maximum level of a substance in a food or feed commodity which is recommended by the Codex Alimentarius Commission to be acceptable for commodities moving in international trade". GL for ^{137}Cs are included in pages 50 and 54, being 1000 Bq/kg. (FAO-WHO, 1995).

[215] Council Directive 2013/59/EURATOM (EU, 2013) uses "*shall*" as the modal verb to refer the measures to be adopted by the Member States.

contamination should be delineated, following the cited Directive regarding the existing exposure situations, and the restrictions or the recovery measures shall be contemplated.

Therefore, the application of the above-mentioned countermeasures in the agricultural systems, should be oriented to minimise the radionuclides transfer from soil to crops for the subsequent harvest seasons to minimise the ^{137}Cs entrance in the food chain.

4 CONCLUSIONS

This multidisciplinary Thesis fulfils in providing useful tools to enhance the EPR plans after a radiological or nuclear emergency situation to aid in minimising the radiological consequences in agricultural systems in the mid and long-term, considering the *prevailing circumstances*.

The inclusion of this tools in the EPR plans could improve the recovery strategies to be applied in the agricultural areas affected by radioactive contamination, and once the exposure situation has moved from an emergency to an existing one, by means of *decision-aiding techniques*.

The conclusions obtained are summarised in the next points. One last point is included in this section to describe possible further researches to continue this work.

- **Conclusions regarding the methodological approaches**

An integrated approach based on the application of different steps to study the radiological vulnerability of the Spanish agricultural system has been applied. This approach analyses the main environmental factors that imply major radiological impact to the public through the ingestion pathway in case a ^{137}Cs deposition occurs, derived from a radiological or nuclear accident. The integrated approach includes the design of a case study to test the Radiological Vulnerability map of the agricultural systems affected by a ^{137}Cs deposition from a hypothetical severe accident occurred in Almaraz NPP. Within the case study, a prioritisation of the agricultural areas affected is performed to identify those where the recovery actions should be applied first to reduce the risk for the population to intake the ^{137}Cs through the food chain ingestion pathway. Along with the methodological steps, a GIS software (ArcMap from ESRI) has been an essential software to manage the vast amount of information required to perform the corresponding geoprocessing and to attain the maps and their associated databases. These resulting maps are the tools proposed to enhance the EPR plans.

- Regarding the soils' information in peninsular Spain

The Spanish soil database has been updated by including 26 more soil profiles, gathered from the bibliography. These new profiles are located in those areas within mainland Spain in which there was low soil profiles density, according to the original DB.

The upgraded Spanish soil DB, which provides extended soils information, jointly with the use of the last European soil base map, which is a more detailed soil map than the version used in the first Spanish radiological vulnerability works, has increased the number of soil groups to be characterised and mapped.

That improvement has allowed a thorough characterisation of the different Spanish soil types which has redounded in the enhancement of the radiological vulnerability classification for the Spanish soils. Nevertheless, it is important to take into account that some soil groups are still not properly characterised because of their short number of soil profiles; that may limit the representativeness of the indexes' values in some cases. The extreme case is for those areas of the base map in which the dominant *STU*s are classified as Ochric Andosol, Calcaro-Chromic Cambisol or Ferric Luvisol (which occupy slightly over 130 km^2) because none of the soil profiles in the updated Spanish DB is classified as them.

- Regarding the Radiological Vulnerability of soils

Concerning the Radiological Vulnerability of the Spanish soils regarding radiocaesium and the ingestion pathway, the corresponding five-category index, *G_Cs_Ing*, is updated. It shows an overview of the general ^{137}Cs behaviour in soil and allows its categorisation, ranged from *Minimum* to *Maximum*, in mainland Spain according to their capacity to favour the presence of bioavailable ^{137}Cs to be absorbed by crops.

The resulting map completes the first step of the integrated approach defined in the methodology.

- Regarding the crops' distribution

A proportional crops' distribution, disaggregated by municipalities and considering the land use, is conducted on the basis of the official Spanish agricultural statistics which contains

detailed local crops' data by province (cultivated area, production, yield and cultivation regime).

The result is a crop's geodatabase with the agricultural information regarding all the possible crops grown in each *basic cartographic unit* (municipality – CLC land use pair). The *representative crop* (the one that covers the largest extension) is assigned to each *basic cartographic unit* to perform a crops' map to accomplish the second step of the methodology.

The *representative crops*' map reflects a lack of spatial continuity along the border of some provinces where a sudden change of crop types and then of crops' groups appears. It is related to the crop sharing constraints and to the assignment of a *representative crop* to each *basic cartographic unit* (a multipart feature of the geodatabase), which, in turn, depends on the CLC land use. That fact influences on assessing and mapping the *Radiological Vulnerability of the agricultural systems*.

- Regarding the Radiological Vulnerability of the agricultural systems

In the third step of the integrated approach, the *Radiological Vulnerability index of the agricultural systems* (*I_RV*) is assessed to define the susceptibility of the agricultural areas potentially affected by a deposition of ^{137}Cs, to transfer it to crops and therefore, to incorporate it in the human food chain.

This five-category index (ranged from *Minimum* to *Maximum* vulnerability) takes into account, firstly, the main topsoil properties that influence the radiocaesium entrance into the crystal lattice of clay minerals, which are potassium and clay content. Secondly, it considers the parameters that condition the potential of the agricultural systems to transfer the exchangeable ^{137}Cs from soil to plant. These are the crop type, the soil texture and the corresponding transfer factor (F_v) from soil-to-plant.

The Radiological Vulnerability map of the agricultural systems in peninsular Spain is attained by representing the *I_RV* index (ranged, in the same way as the *G_Cs_Ing* index, from *Minimum* to *Maximum*), on the bases of the soils' map and the crop groups' map, by using a GIS. The resulting map classifies the soil – crop parings according to the radiological

impact pose to the population through the ingestion pathway for the mid and long-term, in case of ^{137}Cs contamination.

- **Conclusions regarding the Radiological Vulnerability results**

- Regarding the Radiological Vulnerability of soils: *G_Cs_Ing Index*

The updated soil's Radiological Vulnerability map regarding the radiocaesium (representing the *G_Cs_Ing* index) shows no extreme categories; the highest potential of soils to favour the bioavailability of ^{137}Cs is the *High G_Cs_Ing index* (with a value of 4). The soils classified with this index value have significant organic matter content, have clearly sandy texture and/or their exchangeable potassium content is limited. These usually match with mountainous regions and with areas in which bedrock are igneous or metamorphic. That is the case of the Western Spain, including part of the Galician soils, the Pyrenees, the Sistema Ibérico and the Sistema Bético. The main affected soil groups are Humic Cambisols on acid crystalline rocks (included granite), District Histosols, Regosols, Cambic Arenosols or Luvic Arenosols. Areas within this index represent around 32 % of peninsular Spain surface.

Medium Global Radiological Vulnerability index results mainly for sandy and acid soils such as Ranker, for alkaline soils such as Rendzinas on limestones in sub-mountainous areas (both with significant infiltration capacity and limited water retention capacity), for clayey soils such as Pellic Vertisols of the Guadalquivir river, or even for saline soils such as Gypsic Xerosols of the Ebro's basin (the latter two with the opposite characteristics than the former two). The soils within that vulnerability represent about 17 % of peninsular Spain.

The *Low Radiological Vulnerability index* (*G_Cs_Ing* equals to 2), is the most widely spread category, occupying about 50 % of the total surface. The main common characteristics of the soils with this index (the lowest in the whole territory) are low water retention rates and/or low water retention capacity or the presence of clays to bind the radiocaesium; all of these will lead to a lesser bioavailable radiocaesium ratio and a limited crops' root uptake rate. The most representative soil groups within this index category are Calcic Cambisols on limestones, marls or Quaternary sediments, located in the centre and the Eastern half of Spain, Vertic Luvisols in the centre and Calcaric Fluvisols associated with the river beds.

These results of the updated map follow the trend shown in the two previous versions, i.e. (Trueba, et al., 2000a) and (García-Puerta, 2014). However, some differences have been revealed.

The fact that influences the most significant changes concerning the first map version is related to the European soil map used as a base map because more soil groups can be characterised and mapped in the updated soil base map. The changes are located in the Western part of Spain, along the border with Portugal and in Central Spain, where a large area that originally showed *Medium* vulnerability values now shows *High* values; that fact increases the area with significant potential to transfer radiocaesium to crops. On the contrary, primarily in Central East Spain where there are soils developed on calcareous bedrocks according to the current European soil map, such as Calcic Cambisols, originally had *Medium vulnerability index* values, and now those result within *Low* potential to transfer radiocaesium. The Northern strip keeps the same distribution and values as the original map.

The differences regarding the second map's version are related to the updated Spanish soil DB and with the fact that the *G_Cs_Ing* index of each soil group is obtained by assessing the mode value of the soil profiles' index belonging to each one; therefore, adding just one soil profile to a soil group may lead to a different index's value. That is the case for 3 soil groups, i.e., Eutric Lithosols (in Badajoz and Ciudad Real), Calcic Cambisols on Quaternary sediments (widely distributed except in the Northwest and Southwest) and Chromo-calcic Luvisols on Quaternary sediments (in Guadalajara and Soria). The first two soil groups have reduced their *G_Cs_Ing* index by one while the third has increased its *G_Cs_Ing* index by one.

- Regarding the Radiological Vulnerability of the agricultural systems: *I_RV* index

The map representing the *Radiological Vulnerability of the agricultural systems* shows *Maximum I_RV* (equals to 5) only in the 0.56 % of the agricultural areas. Such a limited affected surface is related to the upper threshold used to perform the categorisation of that index, derived from the combination of the *Radiocaesium Reservoir Index* and the *Transfer Factor Index,* apart from the factors involved in the vulnerability assessment (the

topsoil and agricultural system properties). That way, those zones with the highest *Radiological Vulnerability* are highlighted.

The agricultural systems affected by the *Maximum Radiological Vulnerability* are comprised of crops grouped in the "*other crops*" class and, to a lesser extent, in leguminous fodders and leafy vegetables. These are mainly grown in Humic Cambisols on acid crystalline rocks or Gleyic Acrisols, giving rise to significant *Radiocaesium Reservoir* (*I_Cs*) and *Transfer Factor* (*I_TF*) indexes. Agricultural systems within that *I_RV* show the highest potential to transfer to crops the highly stored ^{137}Cs in the soil in the mid and long-term.

It is important to state that, in general, the "*other crops*" group introduces certain distortion in the results because this is assigned the highest transfer factor value (independently to the soil texture), added to the fact that this miscellaneous group includes very different type of crops (from nuts to sunflower).

Over 22 % of the agricultural area results in *High Radiological Vulnerability* (*I_RV* equals 4); these areas are spread all around peninsular Spain and are related to a wide variety of soils. These have a clay – potassium combination which gives rise to a *Radiocaesium Reservoir Index* from *Medium* to *Maximum*. The main crop – soil pair in areas within this *I_RV* index value is grass grown in loamy soils, which result in a *Transfer Factor index* relatively high.

The following *Radiological Vulnerability Index* values (3, 2 and 1) comprise a wider range of soil types. For these, the *Radiocaesium Reservoir Index* is compensated at a certain point with the transfer factor value assigned to the *representative crops* throughout the territory. Thus, it results in lower *Radiological Vulnerability Indexes*: *Medium*, *Low* and *Minimum*, being *Low I_RV* the most widespread in peninsular Spain, representing about 45 % of the agricultural surface. The main agricultural systems within the *Low Radiological Vulnerability Index* are comprised of olives for oil or wine grapes (both grouped in fruits of woody trees crops) grown in loamy soils, primarily in Calcic Cambisols on marls.

Regarding the transfer factor values compiled from the literature for temperate climates, it is relevant to remark the necessity to count on that parameter for the Mediterranean climate, which is the most representative in peninsular Spain. Besides, apart from the F_v values assigned to the "*other crops*" group, there are some other groups which do not have

F_v values for all the soil textures, and in some others, the number of samples used to define their mean value is quite low. These are limitations related to a lack of specific transfer factor data for the Spanish conditions.

- **Conclusions regarding the results obtained for the case study**

The conclusions arise from the case study design to test the *Radiological Vulnerability of the agricultural systems* are presented hereafter.

- Regarding the deposition probability assessment

Considering the type of accident, the source term, and the release location considered, five deposition pattern maps for average meteorological conditions, annual and seasonal, have been obtained. These represent the Deposition Index (*I_D*), ranged from *Minimum* to *Maximum*. The resulting deposition maps show the probability weighted by the severity (in terms of activity concentration) of a ^{137}Cs deposition as a result of an accidental release from Almaraz NPP, taking into account the seasonal variations.

The prevailing winds, ranged from West to West-South-West, are shown in all of the deposition maps. In winter, these prevailing winds are more effective (dispersion increases), and the ^{137}Cs deposition reaches further areas, although the activity concentration deposited decreases significantly near the source.

However, in summer, the presence of the Thermal Low Systems (TLS), a frequent meteorological phenomenon during that season over the Iberian Peninsula, gives rise to less dispersion and therefore to a higher deposition probability and a higher deposition severity in inland Spain in comparison to the coastal areas. As a result, six Spanish provinces are affected by the *Maximum Deposition Index* (equals to 5) in summer, while during the rest of the seasons only Cáceres and Toledo are impacted by that *I_D* category. Regarding the *High I_D* (equals to 4), summer is also the season with the largest affected area along the year.

The *Low Deposition Index* (with an *I_D* value equals to 2) is the most widely spread category in the agricultural areas for winter average meteorological conditions. In contrast, for annual, spring and autumn average conditions the *Medium Deposition Index* (*I_D* equals to

3) is the one that occupies the largest surface, while in summer the *High I_D* (equals to 4) is the most widespread deposition category. Regarding summer, it is remarkable that the agricultural area affected by the *Maximum Deposition Index* corresponds to more than 5 % of the total. These results reveal that, in general, the summer average meteorological situation is the worst accidental case scenario.

Besides to the meteorological conditions, the limited area resulted for the *Maximum I_D* is related to the fact that the threshold used to define the last deposition category is the percentile P_{95} of the weighted deposition probability. This way, it has been accomplished to highlight the extremely contaminated areas with the highest probability of occurrence throughout the year.

- Regarding the Prioritisation maps

The Prioritisation maps highlight those agricultural areas of most concern from the radiological vulnerability point of view and also considers the probability of being affected by a ^{137}Cs deposition, i.e. the most radiologically vulnerable areas plus the highest potentiality to receive a ^{137}Cs deposition. The rest of the possible combinations of radiological vulnerability and the potential deposition exposure are ranked to define the prioritisation of the whole agricultural lands to take actions for the recovery.

As it has been exposed in this Thesis, the accidental sequence chosen for the case study does not appear to have a major generalised impact in the agricultural areas of peninsular Spain, and a moderated risk for these areas is attained. Therefore, according to the results obtained in the Prioritisation maps, in this case, the emergency response to take actions to limit the ^{137}Cs transfer to crops may be modulated in time.

Considering the *Maximum Priority* category (*I_P* equals to 5), Toledo and Cáceres rank consistently in the topmost affected provinces by surface area throughout the year, being the only ones for summer average meteorological conditions. It also occurs regarding the *High Priority* category (*I_P* equals to 4) but, in this case, some other provinces, i.e. Ciudad Real, Córdoba, Cuenca or Zaragoza, have also affected significant surface.

The *Low Priority Index* is the most widespread category at any period, followed by the *Medium* and by the *High I_P* categories, while the less represented *I_P* index class is the *Maximum* at any season. Partly, this is related to the methodological approach designed to obtain the *Radiological Vulnerability Index* and the *Deposition Index*. In both, at a certain point of the assessment, the percentile P_{95} is used to distinguish their upper class. The purpose to do so is to highlight the areas of most concern in which to act primarily to minimise the ^{137}Cs transfer to the food chain.

The worst situation occurs in summer, because the largest surface area with *Maximum* and *High Priority* appear, due to the influence of the TLS in the average meteorological conditions, which implies less dispersion and makes the deposition concentrates in the inland. Taking into consideration that summer is when many crops are harvested in Spain, if an accidental release occurs, depending on the moment, the harvest could not be affected at all, or it could be lost entirely[216]. In any case, the recovery measures, if needed, would benefit the subsequent harvest seasons.

Regarding grazed crops (such as grass), it should be noticed that in the summertime livestock is kept outdoors. That fact would make it necessary to stable the livestock and not feed the animals with fodder harvested after the event. These measures should last longer depending on the contamination deposited on each area, and the countermeasures adopted for the recovery.

- **Conclusions regarding the applicability of the resulting maps in the frame of the Emergency Preparedness and Response (EPR)**

In every stage of a nuclear emergency, all the information about the actual situation at any time must be gathered and analysed. Facing the mid and long term, when the emergency phase finalises, the radiological impact evaluation might be carried out; then, all the aid tools should be ready to be used to decide the measures to be applied in order to minimise population exposure. That way, informed decisions can be made bearing in mind the *optimisation* and *justification* principles of the EPR.

[216] Nevertheless, those concerns would be pondered regarding the short term, but the approach designed deals with the mid and long term.

In this regard, the resulting maps performed in this Thesis and their corresponding associated databases are useful tools to be taken into consideration in designing EPR plans and for its implementation if necessary, from the transition phase.

The Radiological Vulnerability map of peninsular Spain's soils can be used to know the soil groups which show the highest capability to make ^{137}Cs bioavailable beforehand, useful information in planning the recovery and to be considered in land use planning changes.

The crops' distribution map, jointly with its associated database, is a fundamental tool in the EPR since the identification, in advance, of such a local agricultural specificity would redound in the resources' optimisation of the recovery requirements of the agricultural systems if an emergency occurs. This feature could also be used with different purposes regarding diverse kind of studies, including other risk assessments.

The Radiological Vulnerability map of the agricultural systems is a helpful tool for designing and implementing recovery measures required in case a radiological o nuclear accident, having in advance the knowledge about the ^{137}Cs transfer potential from soil to crops and, therefore, to the food chain. Therefore, if necessary, the resources for the recovery may be allocated to the selected areas more quickly and accurately, increasing their effectiveness. That aid map should facilitate the implementation of a structured response, focused on recovering normal living conditions.

It also may be an aid in the task of selecting the areas to collect prioritised samples to measure the fraction of the ^{137}Cs transfer to crops concerning the deposition after an accidental event, once the situation is under control, i.e. since the transition phase. Those agricultural systems which most favour that transfer would be the areas of most concern.

The vulnerability maps and the prioritisation maps can also be used to choose the placement of the automatic and sampling stations of the exiting radioactivity monitoring included in the National Radiological Surveillance Network, in case the surveillance infrastructure were to be extended or modified. In a real accident situation (comparable with the one considered in the case study concerning the site, the source term and the type of accident), the deposition maps presented could be an aid for the surveillance purposes

to manage the mobile units for the environmental radiological measurement campaigns, not only for the agricultural areas but for the whole affected territory.

For the nuclear EPR, considering an event with the same characteristics as the ones assumed in the simulations, the Priority maps may be used, in advance, firstly, to identify the agricultural areas of most concern with respect to the potential ^{137}Cs transfer from soil to crops and, secondly, to prepare, beforehand, the best strategies to reduce the radiological vulnerability in those agricultural areas where the radiological impact would be worst, in terms of production surface, economic impact, strategic crop, etc.; thus, the radiological and non-radiological consequences derived from a hypothetical accident like that would be reduced in those areas. For the mid and long-term, the Priority maps may help decision-makers in the recovery phase to prioritise the recovery actions of the agricultural areas if required and also to define which one is more effective or even excluding those areas to be considered as non-liveable at the moment. Therefore, the process of achieving normal living conditions could be optimised.

In the intermediate and late phases of the accident, these prioritisation tools also could be used to design the adequate food and feed control campaigns, in the frame of the EU (2004) and EU (2016), to ensure that the commercialised products do not exceed the permissible levels (Codex maximum level – ML) (FAO-WHO, 1995) defined in the regulation in force (CCFAC, 2011).

Therefore, by using all these maps in the EPR plans, countermeasures to be applied would be more effective because local parameters would be considered. Moreover, the resources for recovery purposes would be allocated more accurately, being focused on the specific selected areas, following the *optimisation* principle of the Radiation Protection. The aim of reducing the contamination through the application of the countermeasures would be achieved gradually in the subsequent growing seasons.

Therefore, regarding the results obtained in the case study, those could help to enhance the Spanish External Emergency Plans (PEN) of Almaraz NPP (Cáceres) (PENCA), included in the PLABEN, for the municipality action plans in a nuclear emergency (PAMEN). The local specificities of the potentially affected areas defined in the deposition maps and the

agricultural areas of most concern obtained from the prioritisation maps could be considered for the transition and the late phases, facing the recovery.

If an accident were to happen, the methodology designed could also be applied to obtain the proper deposition and prioritisation map once the contamination data are collected. That way a specific prioritisation of the affected agricultural areas for actions to be taken for the recovery could be established; these maps would improve even more the decision-making since more specific information and real data of the accident were considered.

These maps address the new BSS requirements (EU, 2013) according to what is stated in *Article 97: Emergency management system*, regarding the assessment of potential exposure situations and the enhancement of the existing plans for recovery and remediation in the transition and recovery phases. The development of the Radiological Vulnerability and Prioritisation maps for the agricultural areas as aid tools in the EPR also follows the line of what is outlined by the European Economic and Social Committee in points 41 and 42 of the last BSS issue, since those maps represent a different approach on the assessment of potential emergency exposure situations, in contrast to the current one based on intervention level. Besides, these maps contribute to delineate areas of most concern as it is stated in *Article 73: Contaminated areas* of the cited Directive.

Therefore, the methodology designed offers an integrated approach in providing different aid tools to be used in the *decision-aiding techniques* within the EPR for the *prevailing circumstances*, in case a severe nuclear accident with offsite consequences, due to a ^{137}Cs release contaminates the agricultural systems. The design of this methodology is an innovative contribution to the EPR, mainly regarding the data processing to obtain the maps of the Radiological Vulnerability of the agricultural systems and the Prioritisation of these areas.

- **Further research**

According to the conclusions reached in this Thesis, some future works are proposed. These could be developed in order to improve the results obtained in this Thesis and to enlarge the tools to be applied in the Emergency Preparedness and Response regarding a severe nuclear accident in Spain and Europe, facing the requirements established in the BSS (EU, 2013).

The assessment of the *Radiological Vulnerability of the agricultural systems* performed in this Thesis is focused on the ingestion pathway and radiocaesium, however, ^{90}Sr is the other radionuclide which contributes most to the dose through the food chain. Therefore, performing radiological vulnerability maps of the agricultural systems for ^{90}Sr and together for ^{137}Cs and ^{90}Sr would be a valuable improvement.

A relevant downside in the analysis of the *Radiological Vulnerability* (both of soils and agricultural systems) has been found. It is related to the lack of information about the type of the clay minerals contained in soil in the soil DB used. That key feature is a major factor in the bioavailable ^{137}Cs exchange between soil and plants that should be addressed in future researches with respect to the soil-to-plant transfer.

The *Radiological Vulnerability* assessments carried out in this Thesis use the updated Spanish soil DB information to be represented in the European soil map (used as a base map). However, not every soil type in the DB has its corresponding entry in this base map, and others represented on it cannot be characterised by using that DB (although a minority). In this sense, a study of different mapping solutions could be done. Being aware of the difficulties of that task, the different European soil properties maps published by the European Soil Data Centre (ESDAC)[217] (Ballabio, et al., 2016), including the ones regarding topsoil chemical properties issued recently (Ballabio, et al., 2019), could be used in the radiological vulnerability indexes assessment for the whole EU.

[217] https://esdac.jrc.ec.europa.eu/

Nevertheless, a European radiological vulnerability assessment for the agricultural systems should incorporate the role of the organic matter since those soils are representative in that region of the world.

For further results at European level concerning the representative crops map, an adequate approach should be considered since the crops' distribution performed in this Thesis corresponds to a proportional disaggregation of the raw data which exclusively extracts Spanish agricultural information yearly. Therefore, the elaboration of the European agricultural systems' maps should take into consideration a common criterion for all the EU countries. Besides, to improve the applicability of the prioritisation maps (also for the Spanish ones), the identification of the growing stage of each crop might be addressed. It could be performed by reflecting the sowing and harvesting periods of each crop. Therefore, those maps could provide a decisive help for planning and implementing protective measures in the short term also.

The Radiological Vulnerability map of the agricultural systems could be a valuable starting point to evaluate the local specificities for the non-radiological consequences analysis, considering the socio-economic aspects if a severe accident occurs.

The *Transfer Factor Index* designed in this Thesis to classify the agricultural systems could be applied to the rest of the European territory, considering the transfer factors from soil to plant values (F_v) used in this work. Maybe some assumptions, in the line of those made in this Thesis, should be previously adopted regarding those cases with no values for certain soil textures or for the miscellaneous crops group which includes quite different types of crops.

Another consideration that should be done is related to the climate conditions in the EU countries. The lack of F_v values for many crops for climates other than for temperate in the literature (including the Mediterranean climate) would make it necessary to consider the climate conditions as one more factor to be added in the radiological vulnerability assessment.

Regarding the study about the deposition patterns, a wider vision could be obtained by performing the deposition maps for all the NPPs in Spain and Europe. These results could

be included in the specific EPR plans of each NPP. For each site, the input information layers used in the release and deposition simulations should be customised in the DSS JRODOS, attending to the local specificities. Besides, different accidental situations (apart from the ISLOCA accident simulated in this Thesis) should be considered, in order to analyse the diverse deposition patterns derived from different types of accidental releases. That way, critical areas in terms of the probability of occurrence of a radioactive deposition in case of hypothetical severe accidents and their severity would be identified in the whole territory.

Thus, the methodology designed in this Thesis could be used to create Prioritisation maps for the rest of the Spanish sites, and those located in other European regions, addressing the "*transboundary approach*" recommended by OECD-NEA (2018). These maps might be a decision-making aid tool in the European EPR in the transition phase and the recovery phase after a severe accidental release.

Therefore, since the methodologies applied in this Thesis to define the radiological vulnerability of the soils and the agricultural systems in Spain, to identify the prevailing deposition patterns and to perform the prioritisation maps of the agricultural areas are scalable, applicable in the rest of the European countries, its implementation in the EU would provide a global vision for the whole region. That way, a European atlas for the agricultural systems could be elaborated as a standard European tool for the EPR, focused on minimising the radionuclides transfer to the food chain.

5 REFERENCES

Aarkrog, A., 1979. *Environmental studies on radioecological sensitivity and variability with special emphasis on the fallout nuclides Sr-90 and Cs-137*. Roskilde, Denmark: Risø National Laboratory, DK-4000.

Absalom, J.P., Young, S. & Crout, N., 1995. *Radio-caesium fixation dynamics: measurement in six Cumbrian soils*. Eur. J. Soil Sci., 46, 461-469.

Absalom, J.P, Young, S.D., Crout, N.M.J., Nisbet, A.F., Woodman, R.F.M., Smolders, E., Gillett, A.G., 1999. *Predicting Soil to Plant Transfer of Radiocesium Using Soil Characteristics*. Environ. Sci. Technol., 33(8), 1218-1223.

Absalom, J.P., Young, S.D., Crout, N.M.J., Sanchez, A.L., Wright, S.M., Smolders, E., Nisbet, A., Gillet, A.G., 2001. *Predicting the transfer of radiocaesium from organic soils to plants using soil characteristics*. J. Environ. Radioact., 52, 31-43.

Al-Jumeily, D., Hussain, A., Mallucci, C. & Oliver, C. eds., 2016. *Introduction*. *In Emerging Topics in Computer Science and Applied Computing, Applied Computing in Medicine and Health.* Waltham, MA 02451, USA: Morgan Kaufmann, xxxvii-xlviii.

Almahayni, T., Beresford, N., Crout, N. & Sweeck, L., 2019. *Fit-for-purpose modelling of radiocaesium soil-to-plant transfer for nuclear emergencies: a review*. J. Environ. Radioact., 201, 58-66.

Almgren, S. & Isaksson, M., 2006. *Vertical migration studies of ^{137}Cs from nuclear weapons fallout and the Chernobyl accident*. J. Environ. Radioact., 91, 90-102.

ANURE, 2017. Specific Agreement between JRC-CIEMAT. Joint Project ANURE "*Assessment of the Nuclear Risk in Europe. A Case Study in the Almaraz Nuclear Power Plant (Spain)*" Ref. CIEMAT 7551/2016.

Ayala, F., Ferrer, M., Oteo, C. & Salinas, J., 1986. *Mapa Previsor de Riesgos por Expansividad de Arcillas en España a Escala 1:1.000.000*. IGME.

Baeza, A., Del Rio, L. M., Miró, C., Paniagua, J.M. & Navarro, E., 1991. *Radiological impact of the Chernobyl nuclear power plant accident on two regions of Spain – Extremadura and Valencia*. In: M. García-León & G. Madurga, eds. *Low-level measurements of man-made radionuclides in the environment*. World Scientific, 416-424.

Baeza, A., Del Rio, M., Miro, C. & Paniagua, J., 1994. *Natural radionuclide distribution in soils of Cáceres (Spain): Dosimetry implications*. J. Environ. Radioact., 23, 19-37.

Baeza, A., Paniagua, J., Rufo, M. & Barandica, J., 1996. *Bio-availability and transfer of natural radionuclides in a mediterranean ecosystem*. Appl. Radiat. Isot*.,* 47(9-10), 939-945.

Baeza, A., J., Paniagua, Rufo, M., Guillén, J., Sterling, A., 2001. *Seasonal variation in radionuclide transfer in Mediterranean grazing-land ecosystem*. J. Environ Radioact, 55, 283-302.

Baeza, A., Corbacho, J.A., Rodríguez, A., Galván, J., García-Tenorio, R., Manjón, G., Mantero, J., Vioque, I., Arnold, D., Grossi, C., Serrano, I., Vallés, I., Vargas, A., 2012. *Influence of the Fukushima Dai-ichi nuclear accident on Spanish environmental radioactivity levels radioactivity levels*. J. Environ. Radioact., 114, 138-145.

Baeza, A., Rodríguez-Perulero, A. & Guillén, J., 2016. *Anthropogenic and naturally occurring radionuclide content in near surface air in Cáceres (Spain)*. J. Environ. Radioact., 165, 24-31.

Ballabio, C., Panagos, P. & Montanarella, L., 2016. *Mapping topsoil physical properties at European scale using the LUCAS database*. Geoderma, 261, 110-123.

Ballabio, C., Lugato, E., Fernández-Ugalde, O., Orgiazzi, A., Jones, A., Borrelli, P., Montanarella, L., Panagos, P., 2019. *Mapping LUCAS topsoil chemical properties at European scale using Gaussian process regression*. Geoderma, 355, Article 113912.

Bergan, T., 2002. *Radioactive fallout in Norway from atmospheric nuclear weapons tests*. J. Environ. Radioact., 60(1-2), 189-208.

Böhm, W., 1979. *Methods of studing root systems*. Berlin, Germany: Springer - Verlag.

Codex Committee on Food Additives and Contaminants (CCFAC), 2011. *Fact sheet on Codex Guideline Levels for radionuclides in food contaminated following a nuclear or radiologycal emergency* – prepared by Codex Secretariat FAO-WHO (2 May 2011).

Commission of the European Communities (CEC), 1985. *Soil map of the European Communities 1:1 million*. Luxembourg: Office for the Official Publications of the European Communities.

Commission of the European Communities (CEC), 1993. *CORINE Land Cover, guide technique*. Report EU 12585EN, Luxemburg: Office for Publications of the European Communities.

Centrales Nucleares Almaraz-Trillo (CNAT), 2017. Homepage. [Online] Available at: https://www.cnat.es/ [Accessed 21 11 2019].

CIEMAT, 2018. *Curso de Técnico Experto en Protección Radiológica: Instalaciones radiactivas*. Madrid, España: CIEMAT - Aula vitual.

Cinelli, G., Tondeur, F., Dehandschutter, B., Bossew, P., Tollefsen, T., De Cort, M., 2017. *Mapping uranium concentration in soil: Belgian experience towards a European map*. J. Environ. Radioact., 166, 220-234.

Cinelli, G., Tondeur, F. & Dehandschutter, B., 2018. *Mapping potassium and thorium concentrations in Belgian soils*. J. Environ. Radioact., 184-185, 127-139.

Clarke, K.C., 1986. *Advances in Geographic Information Systems*. Comput. Environ. Urban, 10 (3-4), 175-184.

Cremers, A., Elsen, A., Depreter, P. & Maes, A., 1988. *Quantitative-analysis of radiocesium retention in soils*. Nature, 35, 247-249.

Consejo de Seguridad Nuclear (CSN), 2020a. Homepage [Online] Available at: https://www.csn.es/en/home [Accessed 23 03 2020].

Consejo de Seguridad Nuclear (CSN), 2020b. *Environmental Radiological Surveillance in Spain*. [Online] Available at: https://www.csn.es/en/sistema-de-vigilancia-ambiental-en-espana [Accessed 06 04 2020].

De Cort, M., Dubois, G., Fridman, S.D., Germenchuk, M.G., Izrael, Y.A., Janssens, A., Jones, A., Kelly, G.N., Kvasnikova, E., Matveenko, I.I., Nazarov, I.M., Pokumeiko, Y.M., Sitak, V.A., Stukin, E.D., Tabachny, L.Y., Tsaturov, Y.S., Avdyushin, S.I., 1998. *Atlas of Caesium deposition on Europe after the Chernobyl accident. EUR 1673 EN/RU.* Copyright: EC/IGCE, Roshydromet/Minchernobyl (UA)/Belhydromet, 1998 ed. Brussels - Luxembourg: Office for Official Publications of the European Communities.

Domínguez Vivancos, A., 1997. *Tratado de Fertilización*. Madrid, España: Mundi-Prensa. Page 161.

Dubchak, S., 2017. *Distribution of caesium in soil and its uptake by plants.* In: Gupta D. & Walther, C. eds. Impact of Cesium on Plants and the Environment. Hannover, Germany: Springer Cham, 1-18.

Dubois, G., Tollefsen, T., Bossew, P. & De Cort, M., 2004. *GIS and radioecology: a data perspective*. In: 10th EC GI & GIS Workshop, ESDI State of the Art. Warsaw, Poland: 23-25 June 2004.

European Commission (EC), 1995. *Soil Geographical Data Base of Europe, version 3, scale 1:1 million.* European Commission.

European Commission (EC), 2012. *Communication from the Commission to the Council and the European Parliament on the comprehensive risk and safety assessments ("stress tests") of nuclear power plants in the European Union and related activities,* Brussels.

European Commission - European Soil Databases (EC-ESBN), 2004. *The European Soil Database distribution version 2.0*, European Commission and the European Soil Bureau Network, CD-ROM, EUR 19945 EN.

ECOLEGO, 2012. *Ecolego Version 6.2*, http://ecolego.facilia.se/ecolego/show/HomePage. Stockholm, Sweden.

European Environment Agency (EEA) 2016. *Corine Land Cover 2012 seamless vector data. 2016. Version 18_5.* [Online] Available at: http://land.copernicus.eu/pan-european/corine-land-cover/clc-2012 [Accessed 6 2 2017].

European Environment Agency (EEA) 2019. *Corine Land Cover 2018. Version 20*. [Online] Available at: https://land.copernicus.eu/pan-european/corine-land-cover/clc2018?tab=download [Accessed 17 02 2020].

European External Action Service (EEAS), 2018. *Enhancing Emergency Preparedness and Response in ASEAN: Technical Support for Decision Making*. [Online] Available at: https://eeas.europa.eu/headquarters/headquarters-homepage/39692/enhancing-emergency-preparedness-and-response-asean-technical-support-decision-making_en [Accessed 25 11 2019].

ENRESA, 1993. *Segundo plan de investigación y desarrollo (1991-1995). Informe anual,* Madrid, España.

ESRI, 2016a. *ArcGIS Desktop: Release 10.5*. Environmental Systems Research Institute, Redlands, CA.

ESRI, 2016b. *An overview of the geodatabase*. [Online] Available at: https://desktop.arcgis.com/en/arcmap/10.5/manage-data/geodatabases/what-is-a-geodatabase.htm [Accessed 8 11 2019].

ESRI, 2016c. *What is ModelBuilder?* [Online] Available at: https://desktop.arcgis.com/en/arcmap/10.5/analyze/modelbuilder/what-is-modelbuilder.htm [Accessed 12 11 2019].

European Union (EU), 1987. *Council decision 87/600/Euratom: on Community arrangements for the early exchange of information in the event of a radiological emergency*.

European Union (EU), 2000. *Commission Recommendation 2000/473/ Euratom*: *on the application of Article 36 of the Euratom Treaty concerning the monitoring of the levels of radioactivity in the environment for the purpose of assessing the exposure of the population as a whole.*

European Union (EU), 2004. *Corrigendum to Regulation (EC) No 882/2004 of the European Parliament and of the Council of 29 April 2004 on official controls performed to ensure the verification of compliance with feed and food law, animal health and animal welfare rules*.

European Union (EU), 2007. *Treaty establishing the European Atomic Energy Community (Euratom). The Publications Office of the European Union.* [Online] Available at: https://eur-lex.europa.eu/legal-content/EN/TXT/HTML/?uri=LEGISSUM:xy0024&from=EN [Accessed 23 03 2020].

European Union (EU), 2013. *Council Directive 2013/59/EURATOM of 5 December of 2013: laying down basic safety standards for protection against the dangers arising from exposure to ionising radiation*. Directorate - General for Energy (European Commission).

European Union (EU), 2016. *Council Regulation (Euratom) 2016/52 of 15 January 2016 laying down maximum permitted levels of radioactive contamination of food and feed following a nuclear accident or any other case of radiological emergency, and repealing Regulation*. No 3954.

European Union (EU), 2018. *Publications Office of the EU*. *Basic Safety Standards Directive. Better radiation protection*. [Online] Available at: https://op.europa.eu/en/publication-detail/-/publication/293b4d07-74fd-11e8-9483-01aa75ed71a1 Directorate - General for Energy (European Commission) [Accessed 23 03 2020].

Eurostats, 2015. *Nomenclature of Territorial Units for Statistics (NUTS) 2013 - Statistical Units - Data set.* [Online] Available at: http://ec.europa.eu/eurostat/web/gisco/geodata/reference-data/administrative-units-statistical-units/nuts [Accessed 04 04 2018].

Fan, Q. Yamaguchi, N., Tanaka, M., Tsukada, H., Takahashi, Y., 2014. *Relationship between the adsorption species of cesium and radiocesium interception potential in soils and minerals: an EXAFS study*. J. Environ. Radioacti., 138, 92-100.

FAO-UNESCO, 1974. *Soil map of the world, 1:50,000,000. Volume 1. Legend.* Paris, France: UNESCO.

FAO-WHO, 1995. *Codex Alimentarius. International food standards. General standard for contaminants and toxins in food and feed* (CODEX STAN 193-1995).

Foro Nuclear, 2020. *Energía nuclear en España*. [Online] Available at: https://www.foronuclear.org/es/energia-nuclear/energia-nuclear-en-espana [Accessed 30 03 2020].

Francis, C. & Brinkley, F., 1976. *Preferential adsorption of Cs-137 to micaceous minerals in contaminated freshwater sediment*. Nature, 260, 511-513.

Gabrieli, J. Cozzi, G., Vallelonga, P., Schwikowski, M., Sigl, M., Eickenberg, J., Wacker, L., Boutron, C., Gäggeler, H., Cescon, P., Barbante, C., 2011. *Contamination of Alpine snow and ice at Colle Gnifetti, Swiss/Italian Alps, from nuclear weapons tests*. Atmos. Environ., 45, 587-593.

García-Puerta, B., 2014. *Actualización de la Representación de los Índices de Vulnerabilidad Radiológica de los Suelos de la Península Ibérica*. [Master Thesis, Universidad Complutense de Madrid, Spain.] https://eprints.ucm.es/26765/

García Rodríguez, M., 1996. *Hidrogeología de las Tablas de Daimiel y de los Ojos del Guadiana. Bases hidrogeológicas para una clasificación funcional de humedales ribereños*. [Doctoral dissertation, Universidad Complutense de Madrid, Spain].

GIO, 2011. *GIO land monitoring 2011-2015: Project Implementation Plan (abbreviated as PIP), Continental and Local Component*. European Environment Agency.

González, A., 1998. *Radioactive residues of the Cold War period: a radiological legacy*. Vienna, Austria: IAEA BULLETIN, 40/4/1998.

González-Quiñones Ortas, V., 2006. *Metodología, formulación y aplicación de un índice de calidad de suelos con fines agrícolas para Castilla-La Mancha*. [Doctoral dissertation, Universidad Universidad Autónoma de Madrid, Spain].

Guillén, J., Tejado, J.J., Baeza, A., Corbacho, J.A., Muñoz, J.G., 2014a. *Assessment of radiological hazard of commercial granites from Extremadura (Spain)*. J. Environ. Radioact., 132, 81-88.

Guillén, J. & Baeza, A., 2014b. *Radioactivity in mushrooms: A health hazard?* Food Chem., 154, 14-25.

Guillén, J., Baeza, A., Corbacho, J. & Muñoz-Muñoz, J., 2015. *Migration of ^{137}Cs, ^{90}Sr, and $^{239+240}$Pu in Mediterranean forests: influence of bioavailability and association with organic acids in soil*. J. Environ. Radioact., 144, 96-102.

Guillén, J., Baeza, A., Salas, A., Muñoz-Muñoz, J.G., Muñoz-Serrano, A., 2016. *Factors Influencing the Soil to Plant Transfer of Radiocaesium*. In: Gupta K.D. and Walther, C. ed. *Impact of Cesium on Plants and the Environment*. Hannover, Germany: Springer International Publishing, 19-34.

Guillén, J., Beresford, N.A., Baeza, A., Izquierdo, M., Wood, M.D., Salas, A., Muñoz-Serrano, A., Corrales-Vázquez, J.M., Muñoz-Muñoz, J.G., 2018. *Transfer parameters for ICRP's Reference Animals and Plants in a terrestrial Mediterranean ecosystem*. J. Environ. Radioact., 186, 9-22.

Guillen, J., Gómez Polo, F., Baeza, A. & Ontalba, M., 2019. *Transfer parameters for radionuclides and radiologically significant stable elements to foodstuffs in Spain*. NERC Environmental Information Data Centre. [Online] Available at: https://doi.org/10.5285/48d5395e-e9fb-45ed-b69f-1ea0d2d36be6 [Accessed 23 03 2020].

Gupta, D. & Walther, C. eds., 2016. *Preface*. In: *Impact of cesium on plants and the environment.* ed. Hannover, Germany: Springer International Publishing, pp. v-vii.

Hernández-Ceballos, M.A., Sangiorgi, M., García-Puerta, B., Montero, M., Trueba, C., 2020. *Dispersion and ground deposition of radioactive material according to airflow patterns for enhancing the preparedness to N/R emergencies*. J. Environ. Radioact., 216. Article 106178.

Hoinka, K. & Castro, M., 2003. *The Iberian Peninsula Thermal Low*. Q. J. Roy. Meteor. Soc., 129(590), 1491-1511.

Howard, B., 2000. *The concept of radioecological sensitivity*. Radiat. Prot. Dosim., 92(1-3), 29-34.

IAEA, 2001. *Safeguards glossary*. ISBN 92–0–111902–X ed. Vienna, Austria: International Atomic Energy Agency.

IAEA, 2009. *Quantification of radionuclide transfer in terrestrial and freshwater environments for radiological assessments*. *IAEA-TECDOC-1616*, Vienna, Austria: International Atomic Energy Agency.

IAEA, 2010. *Handbook of Parameter Values for the Prediction of Radionuclide Transfer in Terrestrial and Freshwater Environments. Technical reports series no. 472*, Vienna, Austria: International Atomic Energy Agency.

IAEA, 2015. *Preparedness and Response for a nuclear or radiological emergency. General safety requirements. No. GSR Part 7*, Vienna, Austria: International Atomic Energy Agency.

IAEA, 2015b. *Policy and Strategies for Environmental Remediation. IAEA Nuclear Emergency Series*. *No. NW-G-3.1*, Vienna, Austria: International Atomic Energy Agency.

IAEA, 2016. *Environmental change in post-closure safety assessment of solid radioactive waste repositories. Report of working group 3. Reference models for waste disposal of EMRAS II topical heading reference approaches for human dose assessment*. *IAEA-TECDOC-1799*, Vienna, Austria: International Atomic Energy Agency.

IAEA, 2018a. *IAEA Safety Glossary. Terminology Used in Nuclear Safety*, Vienna, Austria: International Atomic Energy Agency.

IAEA, 2018b. *Arrangements for the termination of a nuclear or radiological emergency. IAEA Safety Standards series No. GSG-11*, Vienna, Austria: International Atomic Energy Agency.

IAEA, 2019. *Glossary of Terms in PRIS Reports*. [Online] Available at: https://pris.iaea.org/pris/Glossary.aspx [Accessed 14 11 2019].

IAEA, 2020. *Power Reactor Information System (PRIS)*. [Online] Available at: https://pris.iaea.org/pris/CountryStatistics/CountryDetails.aspx?current=ES [Accessed 04 03 2020].

IAEA & FAO, 1994. *Guidelines for Agricultural Countermeasures following an accidental release of radionuclides*. *Technical Reports Series No. 363,* Vienna, Austria: International Atomic Energy Agency.

IAEA & OECD, 2008. *INES. The international nuclear and radiological event scale. User's manual*, Vienna, Austria: International Atomic Energy Agency.

ICRP, 2007. *The 2007 Recommendations of the International Commission on Radiological Protection*. ICRP Publication 103. Ann. ICRP 37(2–4).

ICRP, 2017. *Occupational intakes of radionuclides: Part 3*. ICRP Publication 137. Ann. ICRP 46(3/4).

International Federation for Information Processing (IFIP), 2019. Murayama, Y., Velev, D., Zlateva, P. eds. *Information technology in disaster risk reduction - Second IFIP TC 5 DCITDRR International Conference, ITDRR*. Sofia, Bulgaria, October 25-27, 2017. Revised Selected Papers. IFIP Advances in Information and Communication Technology 516, Springer 2019.

IGN, 2005. *Centro Nacional de Descargas del Centro Nacional de Información Geográfica: SIOSE*. [Online] Available at: http://centrodedescargas.cnig.es/CentroDescargas/buscadorCatalogo.do?codFamilia=SIOSE [Accessed 27 1 2017].

IGN, 2008. *Base Cartográfica Nacional a escala 1:200.000. BCN200. Version 4.0*. Instituto Geográfico Nacional. [Online] Available at: http://centrodedescargas.cnig.es/CentroDescargas/ [Accessed 05 05 2011].

Imanaka, T., Hayashi, G. & Endo, S., 2015. *Comparison of the accident process, radioactivity release and ground contamination between Chernobyl and Fukushima-1*. Radiat. Res., 56 (Spetial issue - Fukushima), i56-i61.

Instituto Nacional de Estadísitica (INE), 2019. *Códigos INE* [Online] Available at: https://www.ine.es/daco/daco42/codmun/codmunmapa.htm

Irlweck, K. & Wallner, G., 2001. *Reinvestigation of airborne Pb-210, Cs-137 and Bi-207 in Viena (Austria) after atmospheric nuclear weapons tests*. J. Environ. Radioact., 55, 61-69.

ISO/Guide 73:2009(en), 2009. *Risk management — Vocabulary*. Technical Management Board – groups.

Kirkby, E., Kosegarten, H., Mengel, K. & Thomas, A., 2001. *Principles of plant nutrition*. 5th ed. London: Kluwer Academic.

KIT, 2004. *Model Description of the Terrestrial Food Chain and Dose Module FDMT in RODOS PV6.0. Version 1.1*, Karlsruhe, Germany.

KIT, 2017a. *JRodos, Java based RODOS version*. [Online] Available at: https://resy5.iket.kit.edu/JRODOS/ [Accessed 25 11 2019].

KIT, 2017b. *JRodos: An off-site emergency management system for nuclear accidents*, Karlsruhe, Germany: Karlsruhe Institute of Technology.

KIT, 2017c. *JRodos User Guide. Version 3.0.*, Karlsruhe, Germany: Karlsruhe Institute of Technology.

KIT, 2017d. *JRodos Customization Guide. Version 3.0.,* Karlsruhe, Germany: Karlsruhe Institute of Technology.

Kolluru, R., Bartell, S., Pitblado, R. & Stricoff, S., 1996. *Risk assessment and management hand book.* New York, USA: McGraw-Hill.

Lee Zhi Yi, A. & Dercon, G. (eds), 2019. *Data management and visualisation in response to large-scale nuclear emergencies affecting food and agriculture*. Vienna, Austria, FAO/IAEA.

Legarda, F., Romero, L.M., Herranz, M., Barrera, M., Idoeta, R. , Valiño, F., Olondo, C., Caro, A., 2011. *Inventory and vertical migration of 137Cs in Spanish mainland soils*. J. Environ. Radioact., 102, 589-597.

Leonhardt, N. & Chagvardieff, P., 2019. *DEMETERRES Project. An innovative project for the: Development of bio-and eco-technologies for farmland soil remediation in support to a restauration strategy following a nuclear accident*. [Online] Available at: https://public.weconext.eu/demeterres/index-fr.html [Accessed 18 03 2020].

Ley 15/1980, de 22 de abril, *de creación del Consejo de Seguridad Nuclear*. (BOE nº 100, de 25 de abril de 1980. Ref. BOE-A-1980-8650).

Ley 17/2015, de 9 de julio, del Sistema Nacional de Protección Civil. (BOE nº 164, de 10 de julio de 2015. Ref. BOE-A-2015-7730)

L'Homme, A., Parmentier, N., Legrand, B. & Fache, P., 1989. *RESSAC Program. Presentation of the Rehabilitation of Soils and Surfaces after an ACciden*t. Rapport DAS/661. Vienne, Austria: IAEA.

Llauradó, M., Vidal, M., Rauret, G., Roca, C., Fons, J., Vallejo, V.R., 1994. *Radiocaesium behaviour in Mediterranean conditions*. J. Environ. Radioact., 23, 81-100.

Lorente-Plazas, R., Montávez, J.P., Jimenez, P.A., Jerez, S., Gómez-Navarro, J.J., García-Valero, A., Jimenez-Guerrero, P., 2015. *Characterization of surface winds over the Iberian Peninsula*. Int. J. Climatol*.,* 35, 1007–1026.

MAGRAMA, 2016. *Avance Anuario de Estadística 2015. Tercera parte: Estadísticas agrarias y de alimentación. Capítulo 13: Superficie y producciones de cultivo*, Madrid, Spain: Ministerio de Agricultura, Alimentación y Medio Ambiente.

Mahara, Y., 1993. *Storage and migration of fallout strontium-90 and caesium-137 for over 40 years in the surface soil of Nagasaki*. J. Environ. Qual., 22, 722-730.

MAPA, 1980-1990. *Mapa de Cultivos y Aprovechamientos de España a escala 1:50.000.* Hojas: 597, 597, 599, 600, 6001, 623, 624, 625, 626, 650, 651, 652, 653, 654, 678, 679, 680, 681, 682, 704, 705, 706, 707, 708. Madrid, Spain: Ministerio de Agricultura Pesca y Alimentación.

MAPA, 2000-2010. *Mapa de Cultivos y Aprovechamientos de España 2000-2010, a escala 1:50.000*. Ministerio de Agricultura Pesca y Alimentación. [Online] WMS service: https://wms.mapama.gob.es/sig/Agricultura/MapaCultivos2000-2010/wms.aspx?request=GetCapabilities&service=WMS.

Martí, J., Arapis, G. & Iranzo, E., 1989. *Evaluation of the countermeasures applied against contamination of land,* Madrid, Spain: CIEMAT/GIT/M5A03/-1/89.

Maubert, H., Jouve, A., Mary, N. & Millán-Gómez, R., 1992. *Agricultural soils decontamination techniques, methods and results of tests released near Chernobyl. FRIBOUR5.DOC*

Maya-Manzano, J.A., Fernández-Rodríguez, S., Smith, M., Tormo-Molina, R., Reynolds, A.M., Silva-Palacios, I., Gonzalo-Garijo, A., Sadys, M., 2016. *Airborne Quercus pollen in SW Spain: Identifying favourable conditions for atmospheric transport and potential source areas*. Sci. Total Environ., 571, 1037-1047.

Merkel, B. & Hoyer, M., 2012. *Remediation of sites contaminated by radionuclides*. In: *Radionuclide Behaviour in the Natural Environment: Science, Implications and Lessons for the Nuclear Industry*. Poinssot C. & Geckeis H. (eds.): Woodhead Publishing Series in Energy, 601-645.

Millán, M. & Artiñano, B., 1992. *Meso-meteorological cycles of air pollution in the iberian peninsula, (MECAPIP), Contract EV4V-0097-E, Air Pollution Research Report 44, (Eur No. 14834) CEC-DG XII/E-1*, Valencia, Spain: CEAM.

Millán, R., 1995. *Metodologías aplicables para la recuperación de áreas en situación postaccidente nuclear.* [Doctoral dissertation, Universidad Autónoma de Madrid. Dpto. de Química Agrícola]. Madrid, Spain.

Miró, C., Baeza, A., Madruga, M. & Periañez, R., 2012. *Caesium-137 and Strontium-90 temporal series in the Tagus River: experimental results and a modelling study*. J. Environ. Radioact., 113, 21-31.

Monte, L., Brittain, J.E., Gallego, E., Håkanson, L., Hofman, D., Jiménez, A., 2009. *MOIRA-PLUS: A Decision Support System for the management of complex fresh water ecosystems contaminated by radionuclides and heavy metals*. Comput. GeosciUK, 35(5), 880-896.

Montero, M., Moraleda, M., Claver, F., Vazquez, C., Gutierrez, J., 2001. *Methodology for decision making in environmental restoration after nuclear accidents: TEMAS system (version 2.1)*, Madrid, Spain: CIEMAT.

Montero, J.M., Fernández-Avilés, G. & Mateu, J., 2015. *Spatial and spatio-temporal geostatistical modeling and kriging*, Chichester (West Sussex), UK: John Wiley and Sons.

MPR (Ministerio de Presidencia, Relaciones con las Cortes e Igualdad), 2019. *Estrategia Nacional de Protección Civil*.

Müller, H. & Pröhl, G., 1993. ECOSYS-87: *A Dynamic Model for Assessing Radiological Consequences of Nuclear Accidents*. Health Phys., 3(64), 232-252.

Müller, H. & Gering, F., 2002. *User Guide for the Deposition Module DepoM of RODOS PV5.0. Version 1.1 (final),* Karlsruhe, Germany: KIT, Karlsruhe Institute of Technology.

Müller, H., Gering, F. & Pröhl, G., 2004. *Model Description of the Terrestrial Food Chain and Dose Module. FDMT in RODOS PV6.0. RODOS(RA3)-TN(03)06. Version 1.1.*, Neuherberg, Germany: GSF - Institut für Strahlenschutz.

Nakao, A., Thiry, Y., Funakawa, S. & Kosaki, T., 2008. *Characterization of the frayed edge site of micaceous minerals in soil clays influenced by different pedogenetic conditions in Japan and northern Thailand*. J. Soil Sci. Plant Nutr., 54, 479-489.

Navas, A., Walling, D.E., Quine, T.A., Machín Gayarre, J., Soto, J., Domenech, S., López-Vicente, M., López-Vicente, M., 2007. *Variability in 137Cs inventories and potential climatic and lithological controls in the central Ebro valley, Spain*. J. Radioanal. Nucl. Chem., 274(2), 331-339.

NCEP-GFS, n.d. *Global Forecast System produced by the National Centers for Environmental Prediction (NCEP)*. [Online] Available at: https://www.ncdc.noaa.gov/data-access/model-data/model-datasets/global-forcast-system-gfs [Accessed 21 11 2019].

NEA & OECD, 2002. *Chernobyl, Assessment of Radiological and Health Impacts. Update of Chernobyl: Ten Tears On*, Paris, France: OECD.

NEA, 2018. *Status of practice for Level 3 probabilistic assessments. Nuclear Safety. NEA/CSNI/R(2018)1*, Paris, France: OECD.

Nieves-Cordones, M., 2017. *La técnica CRISPR permite obtener cultivos resistentes a la contaminación radiactiva*. Investigación y Ciencia, Septiembre, pp. 10-12.

Nisbet, A., Konoplev, A.V., Shaw, G., Lembrechts, J.F., Merckx, R., Smolders, E., Vandecasteele, C.M., Lönsjö, H., Carini, F., Burton, O., 1993. *Application of fertilisers and ameliorants to reduce soil to plant transfer of radiocaesium and radiostrontium in the medium to long term – a summary*. Sci Total Environ, 137, 173-182.

Nisbet, A. & Woodman, R., 2000. *Soil-to-Plant Transfer Factors for Radiocaesium and Radiostrontium in Agricultural Systems*. Health Phys., 78(3), pp. 279-288.

Nisbet, A., Jones, A.L., Turcanu, C., Camps, J., Andersson, K.G., Hänninen, R., Rantavaara, A., Solatie, D., Kostiainen, E., Jullien, T., Pupin, V., Ollagnon, H., Papachristodoulou, C., Ioannides, K., Oughton, D., 2009. *Generic handbook for assisting in the management of contaminated food production systems in Europe following a radiological emergency. Integrated Project FI6R-CT-2004-508843. EURANOS(CAT1)-TN(09)-01. European approach to nuclear and radiological emergency management and rehabilitation strategies (EURANOS)*. UK: Health Protection Agency (HPA).

Nisbet, A., Charnock, T. & Watson, S., 2017. *HARMONE Guidance Handbook for Recovery after a Radiological Incident. Deliverable D5.55*. OPERRA Project. A project within the EC 7th Framework Programme.

Nishita, H., Romney, E. & Larson, K., 1961. *Uptake of radioactive fission products by crop plants*. J. Agric. Food Chem., 9, 101-106.

NOAA, n.d. *National Centers of Information.* [Online] Available at: https://www.ncdc.noaa.gov/ [Accessed 21 11 2019].

Nordic Guidelines and Recommendations (NGR), 2014. *Protective Measures in Early and Intermediate Phases of a Nuclear Or Radiological Emergency*. Beredskabsstyrelsen (Denmark), Sundhedsstyrelsen (Denmark), Geislavarnir Rikisins (Iceland), Stuk (Finland), Statens Stralevern (Norway), Stral Sakerhets Myndigheten (Sweden).

OECD-NEA, 2006. *Stakeholders and Radiological Protection: Lessons from Chernobyl 20 years after. NEA 6170*. Nuclear Energy Agency.

OECD-NEA, 2018. *Towards an all-hazards approach to emergency preparedness and response. Lessons learnt from non-nuclear events, NEA No. 7308*. Nuclear Energy Agency.

Ogasawara, S., Nakao, A. & Yanai, J., 2013. *Radiocesium interception potential (RIP) of smectite and kaolin reference minerals containing illite (micaceous mineral) as impurity*. J. Soil Sci. Plant Nutr., 59, 852-857.

Ogasawara, S., Eguchi, T., Nakao, A., Fujimura, S., Takahashi, Y., Matsunami, H., Tsukada, H., Yanai, J., Shinano, T., 2019. *Phytoavailability of ^{137}Cs and stable Cs in soils from different parent materials in Fukushima, Japan*. J. Environ. Radioact., 198, 117-125.

Okumura, M., Kerisit, S., Bourg, I.C, Lammers, L.N., Ikeda, T., Sassi, M., Rosso, K.M., Machida, M., 2018. *Radiocesium interaction with clay minerals: Theory and simulation advances Post-Fukushima*. J Environ. Radioact., 210, 105809.

Oliver, M., 1990. *Kriging: A method of interpolation for Geographical Information Systems*. Int. J. Geogr. Inf. Sci., 4, 313-332.

PDC-ARGOS, A., 2014. Homepage [Online] Available at: https://pdc-argos.com/index.html [Accessed 25 11 2019].

PLABEN, 2004. Real Decreto 1546/2004, de 25 de junio, *por el que se aprueba el Plan Básico de Emergencia Nuclear*. (BOE nº 169, de 14 de julio de 2004. BOE-A-2004-13061).

Poljanšek, K., Casajus Valles, A., Marin Ferrer, M., De Jager, A., Dottori, F., Galbusera, L., Garcia Puerta, B., Giannopoulos, G., Girgin, S., Hernandez Ceballos, M., Iurlaro, G., Karlos, V., Krausmann, E., Larcher, M., Lequarre, A., Theocharidou, M., Montero Prieto, M., Naumann, G., Necci, A., Salamon, P., Sangiorgi, M., Sousa, M. L, Trueba Alonso, C., Tsionis, G., Vogt, J., and Wood, M., 2019. *Recommendations for National Risk Assessment for Disaster Risk Management in EU , EUR 29557 EN*, Publications Office of the European Union, Luxembourg, 2019, ISBN 978-92-79-98366-5 (online), doi:10.2760/084707 (online), JRC114650.

Porta, J., López-Acevedo, M. & Roquero, C., 2003. *Edafología para la Agricultura y Medio Ambiente*. 3rd ed. Madrid, Spain: Mundi-Prensa.

Prister, B.S., Vinogradskaya, V.D., Lev, T., Talerko, M.M., Garger, E.K., Onishi, Y., Tischenko, O.G., 2018. *Preventive radioecological assessment of optimization of monitoring and countermeasures after radiation accidents*. J. Environ. Radioact., 184-185, 140-151.

Pröhl, G., Olyslaegers, G., Zeevaert, T., Kanyar, B., Pinedo, P., Simón. I., Bergström, U., Hallberg, B., Mobbs, S., Chen, Q., Kowe, R., 2004. *BIOMOSA: Biosphere models for safety assessment of radioactive waste disposal based on the application of the Reference Biosphere Methodology*. A project within the EC 5th Framework Programme.

Rauret, G., Llauradó, M., Tent, J., Rigol, A., Alegre, L.H., Utrillas, M.J., 1994. *Deposition on holm oak leaf surfaces of accidentally released*. Sci. Total Environ., 157, 7-16.

Real Decreto (RD) 1836/1999, de 3 de diciembre, por el que se aprueba el Reglamento sobre instalaciones nucleares y radiactivas. (BOE nº 313 de 31 de diciembre de 1999. BOE-A-1999-24924).

Real Decreto (RD) 1071/2007, de 27 de julio, *por el que se regula el sistema geodésico de referencia oficial en España*. (BOE nº 207 de 29 de agosto de 2007. BOE-A-2007-15822).

Real Decreto (RD) 1440-2010, de 5 de noviembre, *por el que se aprueba el Estatuto del Consejo de Seguridad Nuclear*. (BOE nº 282 de 22 de noviembre de 2010. BOE-A-2010-17861).

REM Group. JRC-Ispra, 2019. *Atlas of Natural Radiation*. [Online] Available at: https://remon.jrc.ec.europa.eu/About/Atlas-of-Natural-Radiation [Accessed 02 03 2019].

Ríos Insua, S., Jiménez Martín, A. & Mateos Caballero, A., 2005. *Los Sistemas de Ayuda a la Decisión*. Anales de la Real Academia de Doctores de España. ISSN: 1138-2414, 9, 161-177.

Rubio-Delgado, J., Guillén, J., Corbacho, J.A., Gómez-Gutiérrez, Á., Baeza, A., Schnabel, S., 2017. *Comparison of two methodologies used to estimate erosion rates in Mediterranean ecosystems: ^{137}Cs and exposed tree roots*. Sci. Total Environ., 605-606, 541-550.

Rushton, G., 2001. *Spatial Decision Support Systems*. In: Smelser N.J., & Baltes, P.B. eds. International Encyclopedia of the Social & Behavioral Sciences. Oxford, UK: Pergamon Press, 14785-14788.

Sáez, J., 2008. *Mapa radiológico tridimensional de Palamares. Informe al Consejo de Seguridad Nuclear. Segundo semestre 2007. Caracterización radiológica superficial intensiva. CIEMAT Report DG/PRP-01/08*, Madrid, Spain: CIEMAT.

Sáez, J., Correa, E., Burgos, D. & Lanzas, R., 2009. *Three-dimensional Radiological Map of Palomares final report. CIEMAT report SG/PIEM-VR-01/09*, Madrid. Spain: CIEMAT.

Sancho, C. & García-Tenorio, R., 2019. *Radiological evaluation of the transuranic remaining contamination in Palomares (Spain): A historical review*. J. Environ. Radioact., 203, 55-70.

Sauras, T., Roca, M.C., Tent, J., Llauradó, M., Vidal, M., Rauret, G., Vallejo, V.R., 1994. *Migration study of radionuclides in a Mediterranean forest soil using synthetic aerosols*. Sci. Total Environ., 157, 231-238.

Seibert, P., Arnold, D., Arnold, N., Gufler, K., Kromp-Kolb, H., Mraz, G., Wenisch, A., 2015. *Flexible Tools for Assessment of Nuclear Risk in Europe. BOKU-Met Report 23*. Project financed by the programme "New Energies 2020" of the Austrian Climate and Energy Fund (KLI.EN). Vienna, Austria: Institut für Meteorologie (BOKU-Met), Department Wasser – Atmosphäre – Umwelt. Universität für Bodenkultur Wien.

Smith, J.T., Fesenko, S.V., Howard, B.J., Horrill, A.D., Sanzharova, N.I., Alexakhin, R.M., Elder, D.G., Naylor, C., 1999. *Temporal Change in Fallout ^{137}Cs in Terrestrial and Aquatic Systems: A Whole Ecosystem Approach*. Environ. Sci. Technol., 33(1), 49-54.

Smolders, E. & Shaw, G., 1995. *Changes in radiocaesium uptake and distribution in wheat during plant development: a solution culture study*. Plant and Soil, 176, 1-6.

Staunton, S., Dumat, C. & Zsolnay, A., 2002. *Possible role of organic matter in radiocaesium adsorption in soils*. J. Environ. Radioact., 58, 163-173.

Suárez, E., Fernández, J.A., Baeza, A., Moro, M.C., García Pomar, D., Moreno, J., Lanaja, J.M., 2000. *Proyecto Marna. Mapa de radiación gamma natural. Colección Informes técnicos 5.2000*, Madrid, España: Consejo de Seguridad Nuclear.

Tamponnet, C., Martin-Garin, A., Gonze, M.A., Parekh, N., Vallejo, R., Sauras-Yera, T., Casadesus, J., Plassard, C., Staunton, S., Norden, M., Avila, R., Shaw, G., 2008. *An overview of BORIS: Bioavailability of Radionuclides in Soils.* J. Environ. Radioact., 99, 820-830.

Tarsitano, D., Crout, N. & Young, S., 2011. *Evaluating and reducing a model of radiocaesium soil-plant uptake*. J. Environ. Radioact., 102, 262-269.

Thykier-Nielsen, S., Deme, S. & Mikkelsen, T., 1999. *Description of the Atmospheric Dispersion Module RIMPUFF*, Roskilde (Denmark) - Budapest (Hungary): Risø National Laboratory and Atomic Energy Research Institute.

Tobler, W., 1970. *A computer movie simulating urban growth in the Detroit region*. *Econ. Geogr.,* 46. Supplement: Proceedings. International Geographical, 234-240.

Trueba, C. & Vallés, O., 2000. *Evaluación de la Vulnerabilidad Radiológica de los suelos españoles para la recuperación ambiental tras accidente nuclear. Proyecto ATYCA*. Madrid, Spain: CIEMAT.

Trueba, C., Millán, R., Schmid, T. & Lago, C., 2000a. *Estimación de Índices de Vulnerabilidad Radiológica para los Suelos Peninsulares Españoles*. Madrid, Spain: CIEMAT.

Trueba, C., Millán, R., Schmid, T. & Lago, C., 2000b. *Base de Datos de Propiedades Edafológicas de los Suelos Españoles*. Madrid, Spain: CIEMAT.

Trueba, C., Millán, R. & Schmid, T., 2003. *Vulnerabilidad específica de los sistemas agrícolas españoles (VULNES). CIEMAT/DIAE/51630/01-03*. Madrid, Spain: CIEMAT.

Trueba, C., 2004. *Metodología para evaluar la sensibilidad radiológica de suelos y su aplicación a los suelos peninsulares españoles*. [Doctoral dissertation. Departamento de Ingeniería Nuclear. Escuela Técnica Superior de Ingenieros Industriales. Universidad Politécnica de Madrid]. Madrid, Spain.

Trueba, C., Montero, M. & García-Puerta, B., 2015. *Mapas de vulnerabilidad radiológica. Actualización al nuevo mapa europeo de suelos.* ISBN: 978-84-7834-749-0. Madrid, Spain: CIEMAT.

Trueba, C., Montero, M. & García-Puerta, B., 2015b. *La Vulnerabilidad radiológica del suelo como herramienta en la preparación local para la recuperación posaccidente. Actualización de los mapas nacionales*. Revista Radioprotección, 81, 32-38.

Uematsu, S., Smolders, E., Sweeck, L., Wannijn, J., Van Hees, M., Vandenhove, H., 2015. *Predicting radiocaesium sorption characteristics with soil chemical properties for Japanese soils*. Sci. Total Environ., 524-525, 148-156.

USNRC, 2012. *State-of-the-Art Reactor Consequence Analyses (SOARCA) Project. NUREG-1935*, (NUREG/CR-7110, Volume 2, Revision 1), Albuquerque, New Mexico 87185, USA: Department of Energy. Office of Nuclear Regulatory Research.

UNDRR, 2020. *UNDRR News*. [Online] Available at: https://www.undrr.org/news/undrr-urges-disaster-management-agencies-prioritize-biological-hazards [Accessed 22 03 2020].

Vandebroek, L., Van Hees, M., Delvaux, B., Spaargaren, O., Thiry, Y., 2012. *Relevance of radiocaesium interception potential (RIP) on a worldwide scale to assess soil vulnerability to Cs-137 contamination*. J. Environ. Radioact., 104, 87-93.

Vandenhove, H., Sweeck, L., 2011. *Soil Vulnerability for Cesium Transfer*. Integr. Environ. Asses. 7(3), 374-378.

Vandenhove, H., Turcano, C., 2011. *Agricultural Land Management Options Following Large-Scale Environmental Contamination*. Integr. Environ. Asses. 7(3), 385-387.

Vanhavere, F., 2018. *Third Annual Joint priority list. Deliverable D3.3*. EJP-CONCERT. Ref. Ares(2018)1177391 - 02/03/2018.

Wauters, J. Elsen, A., Cremers, A., Konoplev, A.V., Bulgakov, A.A., Comans, R.N.J., 1996a. *Prediction of solid/liquid distribution coefficients of radiocaesium in soils and sediments. Part one: a simplified procedure for the solid phase characterization*. Appl. Geochem., 11, 589-594.

Wauters, J. Elsen, A., Cremers, A., Konoplev, A.V., Bulgakov, A.A., Comans, R.N.J., 1996b. *Prediction of solid/liquid distribution coefficients of radiocaesium in soils and sediments. Part two: a new procedure for solid phase speciation of radiocaesium*. Appl. Geochem., 11, 595-599.

WHO, 2020. *WHO Director-General's opening remarks at the media briefing on COVID-19 - 11 March 2020*. [Online] Available at: https://www.who.int/dg/speeches/detail/who-director-general-s-opening-remarks-at-the-media-briefing-on-covid-19---11-march-2020 [Accessed 22 03 2020].

Williams, S., 2016. *Chapter 6 - Leveraging BI for performance management, process improvement, and decision support*. In: *Business intelligence strategy and big data analytics A general management perspective*. Cambridge, MA 02139, USA: Morgan Kaufmann, 99-150.

World Nuclear Association (WNA), 2018. *Nuclear Power Reactors*. [Online] Available at: https://www.world-nuclear.org/information-library/nuclear-fuel-cycle/nuclear-power-reactors/nuclear-power-reactors.aspx [Accessed 14 11 2019].

ANNEXES

ANNEXE I: LIST AND LOCATION OF THE PENINSULAR SPAIN PROVINCES

Province code	Province name
01	Álava
02	Albacete
03	Alicante
04	Almería
05	Ávila
06	Badajoz
07	Illes Balears[1]
08	Barcelona
09	Burgos
10	Cáceres
11	Cádiz
12	Castellón
13	Ciudad real
14	Córdoba
15	A Coruña
16	Cuenca
17	Girona
18	Granada
19	Guadalajara
20	Guipúzcoa
21	Huelva
22	Huesca
23	Jaén
24	León
25	Lleida
26	La Rioja

Province code	Province name
27	Lugo
28	Madrid
29	Málaga
30	Murcia
31	Navarra
32	Ourense
33	Asturias
34	Palencia
35	Las Palmas[1]
36	Pontevedra
37	Salamanca
38	Santa Cruz de Tenerife[1]
39	Cantabria
40	Segovia
41	Sevilla
42	Soria
43	Tarragona
44	Teruel
45	Toledo
46	Valencia
47	Valladolid
48	Vizcaya
49	Zamora
50	Zaragoza
51	Ceuta[2]
52	Melilla[2]

[1] Non peninsular Spanish provinces. [2] Autonomous cities located in African continent. SOURCE:

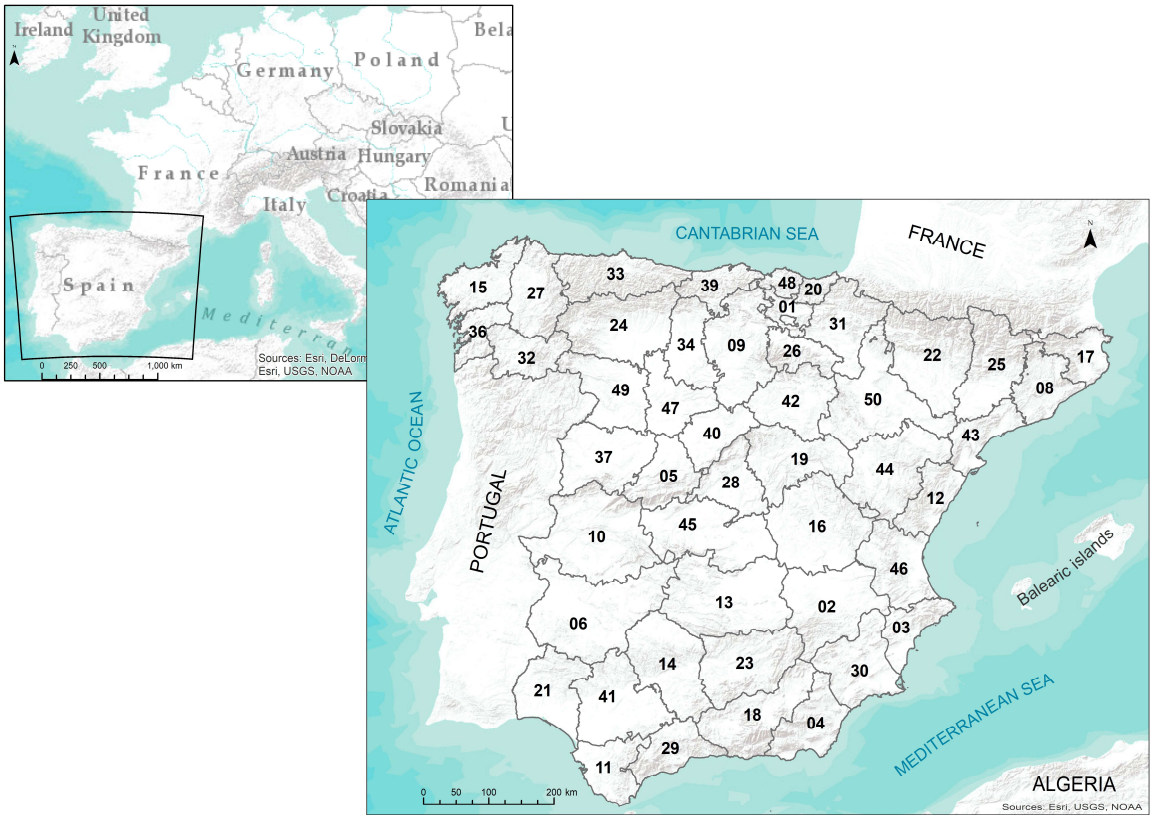

Peninsular Spain provinces

ANNEXE II: LIST OF CROPS GROWN IN THE SPANISH AGRICULTURAL SYSTEM (MAGRAMA, 2015) AND THEIR CORRESPONDING CODIFICATION (IDPR). CORRESPONDENCE BETWEEN CROP'S CODE AND THE GROUP OF PLANTS - PLANT'S COMPARTMENT PAIR (ID_C) (IAEA, 2010)

ID_C	IDPR	CROP (in English)	CULTIVO (in Spanish)
	A10000	CEREALS	CEREALES EN GRANO
	A11000	WINTER CEREALS	CEREALES DE INVIERNO
ceG	A11010	WHEAT Total	TRIGO TOTAL
ceG	A11020	BARLEY Total	CEBADA TOTAL
ceG	A11030	OATS	AVENA
ceG	A11040	RYE	CENTENO
ceG	A11050	TRITICALE	TRITICALE
	A12000	SPRING CEREALS	CEREALES DE PRIMAVERA
ceG	A12010	RICE	ARROZ
maG	A12020	MAIZE	MAÍZ
ceG	A12030	SORGHUM	SORGO
ceG	A12040	WHEAT Total	TRIGO TOTAL
ceG	A12041	Durum Wheat	Trigo duro
ceG	A12042	Common Wheat	Trigo blando
ceG	A12050	RYE	CENTENO
ceG	A13000	OTHER CEREALS	OTROS CEREALES
	A20000	LEGUMES/PULSES	LEGUMINOSAS EN GRANO
	A21000	GROUP I	LEGUM. EN GRANO GRUPO I
lvS	A21010	CHICKPIES	GARBANZOS
lvS	A21020	DRY PEAS	GUISANTES SECOS
	A22000	GROUP II	LEGUM. EN GRANO GRUPO II
lvS	A22010	DRY BEANS	JUDÍAS SECAS
lvS	A22020	DRY BROAD BEANS	HABAS SECAS
	A23000	GROUP III	LEGUM. EN GRANO GRUPO III
lvS	A23010	LENTIL	LENTEJAS
lvS	A23020	VETCH	VEZA
lvS	A23030	LUPINE	ALTRAMUZ
	A24000	GROUP IV	LEGUM. EN GRANO GRUPO IV
lvS	A24010	VETCHLING	ALMORTAS
lvS	A24020	CAROB	ALGARROBAS
lvS	A24030	LENTILS	YEROS
lvS	A25000	OTHER PULSES	OTRAS LEGUMINOSAS
	A30000	TUBERS	TUBÉRCULOS
	A31000	TUBERS	TUBÉRCULOS
tbT	A31010	POTATOES Total	PATATA Total
tbT	A31020	SWEET POTATO	BATATA
tbT	A31030	YAM	BONIATO
tbT	A31040	TIGER NUT	CHUFA

ID_C	IDPR	CROP (in English)	CULTIVO (in Spanish)
	A40000	VEGETABLES	HORTALIZAS
	A41000	LEAFY VEGETABLES	DE HOJA O TALLO
lyL	A41010	BRASSICA	COL
lyL	A41020	GREEN CABBAGE	BERZA
lyL	A41030	ASPARAGUS	ESPÁRRAGO
lyL	A41040	CELERY	APIO
lyL	A41050	LETTUCE	LECHUGA
lyL	A41060	ENDIVE	ESCAROLA
lyL	A41070	SPINACH	ESPINACA
lyL	A41080	CHARD	ACELGA
lyL	A41090	THISTLE	CARDO
lyL	A41100	OTHER LEAFY VEGETABLES	OTRAS HORTALIZAS DE HOJA
	A42000	FRUIT VEGETABLES	DE FRUTO
hpF	A42010	WATERMELON	SANDÍA
hpF	A42020	MELON	MELÓN
nlF	A42030	PUMPKIN	CALABAZA
nlF	A42040	COURGETTE	CALABACIN
nlF	A42050	CUCUMBER	PEPINO
nlF	A42060	AUBERGINE	BERENJENA
nlF	A42070	TOMATO	TOMATE
nlF	A42080	PEPPER	PIMIENTO
hpF	A42090	STRAWBERRY	FRESA Y FRESÓN
	A43000	FLOWER VEGETABLES	DE FLOR
lyL	A43010	ARTICHOKE	ALCACHOFA
lyL	A43020	BROCCOLI	BROCOLI
lyL	A43030	CAULIFLOWER	COLIFLOR
	A44000	ROOT VEGETABLES	RAICES Y BULBOS
nlF	A44010	GARLIC	AJO
nlF	A44020	ONION	CEBOLLA
nlF	A44030	SPRING ONION	CEBOLLETA
lyL	A44040	LEEK	PUERRO
rcR	A44050	RED BEET	REMOLACHA DE MESA
rcR	A44060	CARROT	ZANAHORIA
rcR	A44070	RADISH	RÁBANO
rcR	A44080	TURNIP	NABO
	A45000	GREEN LEGUMES	LEGUMINOSAS
lvS	A45010	GREEN BEAN	JUDÍAS VERDES
lvS	A45020	GREEN PEAS	GUISANTES VERDES
lvS	A45030	BEANS	HABAS VERDES
	A46000	OTHER VEGETABLES	OTROS VEGETALES
-	A46010	MUSHROOMS/CHAMPIGNON	CHAMPIÑÓN
-	A46020	MUSHROOMS/WILD PRODUCTS	SETAS
lyL	A46030	OTHER VEGETABLES	OTRAS HORTALIZAS

ID_C	IDPR	CROP (in English)	CULTIVO (in Spanish)
	A50000	INDUSTRIAL CROPS	CULTIVOS INDUSTRIALES
	A51000	SUGAR CROPS	PLANTAS AZUCARERAS
ocA	A51010	SUGAR CANE	CAÑA DE AZÚCAR
rcR	A51020	SUGAR BEET	REMOLACHA AZUCARERA
	A52000	TEXTILE CROPS	PLANTAS TEXTILES
ocA	A52010	COTTON SEED	ALGODÓN
ocA	A52020	FLAX	LINO
ocA	A52030	HEMP	CÁÑAMO
	A53000	OILSEED CROPS	PLANTAS OLEAGINOSAS
ocA	A53010	PEANUT	CACAHUETE
ocA	A53020	SUNFLOWER SEED	GIRASOL
ocA	A53030	SAFFLOWER	CÁRTAMO
lvS	A53040	SOYA BEAN	SOJA
ocA	A53050	RAPE	COLZA
	A54000	CONDIMENT /FLAVORING	CONDIMENTO
nlF	A54010	PAPRIKA	PIMIENTO PARA PIMENTÓN
ocA	A54020	ANISE	ANÍS
heX	A54030	SAFFRON	AZAFRÁN
ocA	A54040	CUMIN	COMINOS
	A55000	INDUSTRIAL CROPS	PLANTAS INDUSTRIALES
ocA	A55010	TOBACCO	TABACO
ocA	A55020	HOP	LÚPULO
ocA	A55030	LAVENDER	LAVANDA
	A56000	OTHER INDUSTRIAL CROPS	OTROS CULT. INDUSTRIALES
	A60000	FODDER CROPS	CULTIVOS FORRAJEROS
	A61000	GRAMINEOUS	GRAMÍNEAS
grS	A61010	WINTER CEREALS	CEREALES DE INVIERNO
grS	A61020	MAIZE FOR STOCKFEEDING	MAÍZ FORRAJERO
grS	A61030	SORGHUM FOR STOCKFEEDING	SORGO FORRAJERO
grS	A61040	RYEGRASS	BALLICO
grS	A61050	OTHER GRAMINEOUS	OTRAS GRAMÍN. PARA FORRAJE
	A62000	LEGUMES	LEGUMINOSAS
lfS	A62010	LUCERNE	ALFALFA
lfS	A62020	CLOVER	TRÉBOL
lfS	A62030	SAINFOIN	ESPARCETA
lfS	A62040	SULLA	ZULLA
lfS	A62050	VETCH	VEZA
lfS	A62060	OTHER LEGUMES	OTRAS LEGUM. PARA FORRAJE
grS	A63000	MEADOWS	PRADERAS POLIFITAS
	A64000	ROOTS AND TUBERS	RAÍCES Y TUBÉRCULOS
rcR/rcL	A64010	TURNIP FOR STOCKFEEDING	NABO FORRAJERO
rcR/rcL	A64020	FODDER BEET	REMOLACHA FORRAJERA
rcR/rcL	A64030	CARROT FOR STOCKFEEDING	ZANAHORIA FORRAJERA
	A65000	OTHER FODDER CROPS	FORRAJERAS VARIAS
lyL	A65010	FODDER KALE	COL FORRAJERA
nlF	A65020	PUMPKIN FOR STOCKFEEDING	CALABAZA FORRAJERA
lyL	A65030	OTHER CROPS FOR STOCKFEEDING	CARDO Y OTROS FORRAJES

ID_C	IDPR	CROP (in English)	CULTIVO (in Spanish)
	W10000	FRUIT TREES	FRUTALES
	W11000	CITRUS FRUIT TREES	FRUTALES CÍTRICOS
wtF	W11010	SWEET ORANGE	NARANJO DULCE
wtF	W11020	SOUR ORANGE	NARANJO AMARGO
wtF	W11030	MANDARIN ORANGES	MANDARINO
wtF	W11040	LEMON	LIMONERO
wtF	W11050	GRAPEFRUIT	POMELO
wtF	W11060	OTHERS	OTROS CÍTRICOS
	W12000	POME FRUIT	FRUTALES DE PEPITA
wtF	W12010	APPLE	MANZANA
wtF	W12020	PEAR	PERA
wtF	W12030	QUINCE	MEMBRILLERO
wtF	W12040	MEDLAR	NÍSPERO
wtF	W12050	OTHERS	OTROS FRUTALES DE PEPITA
	W13000	STONE FRUIT (DRUPE)	FRUTALES DE HUESO
wtF	W13010	APRICOT	ALBARICOQUERO
wtF	W13020	CHERRY	CEREZAS Y GUINDAS
wtF	W13030	PEACH	MELOCOTONERO
wtF	W13040	PLUM	CIRUELO
	W14000	FLESHY FRUIT	FRUTALES DE FRUTO CARNOSO
wtF	W14010	FIG TREE	HIGUERA
wtF	W14020	CHERIMOYA	CHIRIMOYO
wtF	W14030	POMEGRANATE	GRANADO
wtF	W14040	AVOCADO	AGUACATE
wtF	W14050	BANANA	PLATANERA
wtF	W14060	DATE PALM	PALMERA DATILERA
shF	W14070	CHUMBERA	CHUMBERA
wtF	W14080	KIWI	KIWI
shF	W14090	RASPBERRY	FRAMBUESO
wtF	W14100	OTHERS	OTROS FRUTALES CARNOSOS
	W15000	NUT	FRUTALES DE FRUTO SECO
ocA	W15010	ALMOND	ALMENDRO
ocA	W15020	WALNUT	NOGAL
ocA	W15030	HAZELNUT	AVELLANO
ocA	W15040	CHESTNUT	CASTAÑO
ocA	W15050	PISTACHIO	PISTACHO
	W20000	VINEYARD	VIÑEDO
	W21000	VINEYARD	VIÑEDO
wtF	W21010	TABLE GRAPES	VIÑEDO UVA DE MESA
wtF	W21020	WINE GRAPES	VIÑEDO UVA VINIFICACIÓN
wtF	W21030	RAISINS	VIÑEDO UVA PASIFICACIÓN
	W30000	OLIVE GROVE	OLIVAR
	W31000	OLIVE GROVE	OLIVAR
wtF	W31010	TABLE OLIVES	ACEITUNA DE MESA
wtF	W31020	OLIVES FOR OIL	ACEITUNA DE ALMAZARA
wtF	W40000	OTHER WOODY CROPS	OTROS CULTIVOS LEÑOSOS

ID_C: IDentification for the Crop Group. Built from the plant groups and compartments (IAEA, 2010)

IDPR: IDentification for the Crop. Built from the Spanish agricultural structure. (MAGRAMA, 2015)

ANNEXE III: CORRESPONDENCE BETWEEN THE CROPS CULTIVATED IN SPAIN (MAGRAMA, 2015) AND THE LAND USE IN WHICH THEY MAY BE GROWN (EEA, 2016)

Crop code	CLC land use							
IDPR+IDCS	**211**	**212**	**213**	**222**	**241**	**242**	**243**	**244**
A11000D	✓	-	-	-	✓	✓	✓	-
A11000FI	-	✓	-	-	✓	✓	✓	-
A12010T	-	-	✓	-	✓	✓	✓	-
A12020D	✓	-	-	-	✓	✓	✓	-
A12030D	-	✓	-	-	✓	✓	✓	-
A13000D	✓	-	-	-	✓	✓	✓	-
A13000FI	-	✓	-	-	✓	✓	✓	-
A20000D	✓	-	-	-	✓	✓	✓	-
A20000FI	-	✓	-	-	✓	✓	✓	-
A30000D	✓	-	-	-	✓	✓	✓	-
A30000FI	-	✓	-	-	✓	✓	✓	-
A40000D	✓	-	-	-	-	✓	✓	-
A40000FI	-	✓	-	-	-	✓	✓	-
A40000SI	-	✓	-	-	-	✓	-	-
A50000D*	✓	-	-	-	✓	✓	✓	-
A55020D	✓	-	-	✓	✓	✓	✓	-
A50000FI*	-	✓	-	-	✓	✓	✓	-
A55020FI	-	✓	-	✓	✓	✓	✓	-
A61000D	✓	-	-	-	✓	✓	✓	✓
A61000FI	-	✓	-	-	✓	✓	✓	✓
A62000D	✓	-	-	-	✓	✓	✓	✓
A62000FI	-	✓	-	-	✓	✓	✓	✓
A63000D	✓	-	-	-	✓	✓	✓	✓
A63000FI	-	✓	-	-	✓	✓	✓	✓
A64000D	✓	-	-	-	✓	✓	✓	-
A64000FI	-	✓	-	-	✓	✓	✓	-
A65000D	✓	-	-	-	✓	✓	✓	-
A65000FI	-	✓	-	-	✓	✓	✓	-

*Except for the crops included in this group specified in the following row/s.

IDPR: IDentifier of the Product built considering the Spanish agricultural structure.
IDCS: IDentifier of the Cultivation System.
✓ means that that crop (IDPR+IDCS) is associated to a CLC land use.

Crop code	CLC land use							
IDPR+IDCS	221	222	223	241	242	243	244	311
W11000TR	-	✓	-	✓	✓	-	-	-
W11000ST	-	-	-	✓	✓	-	-	-
W12000D	-	✓	-	✓	✓	-	-	-
W12000I	-	✓	-	✓	✓	-	-	-
W12000ST	-	-	-	✓	✓	-	-	-
W13000D	-	✓	-	✓	✓	-	-	-
W13000I	-	✓	-	✓	✓	-	-	-
W13000ST	-	-	-	✓	✓	-	-	-
W14000D*	-	✓	-	✓	✓	-	-	-
W14060D	-	✓	-	✓	✓	-	✓	-
W14000I*	-	✓	-	✓	✓	-	-	-
W14060I	-	✓	-	✓	✓	-	✓	-
W14000ST*	-	-	-	✓	✓	-	-	-
W14060ST	-	-	-	✓	✓	-	✓	-
W15000D*	-	✓	-	✓	✓	-	-	-
W15020D	-	✓	-	✓	✓	-	-	✓
W15040D	-	✓	-	✓	✓	-	-	✓
W15000I*	-	✓	-	✓	✓	-	-	-
W15020I	-	✓	-	✓	✓	-	-	✓
W15040I	-	✓	-	✓	✓	-	-	✓
W15000ST*	-	-	-	✓	✓	-	-	-
W15020ST	-	-	-	✓	✓	-	-	✓
W15040ST	-	-	-	✓	✓	-	-	✓
W20000	✓	✓	-	✓	✓	✓	-	-
W30000D	-	-	✓	✓	✓	-	✓	-
W30000I	-	-	✓	✓	✓	-	✓	-
W30000ST	-	-	-	✓	✓	-	✓	-
W40000D**	-	✓	-	✓	✓	-	✓	✓
W40000I**	-	-	-	✓	✓	-	✓	✓
W40000ST**	-	-	-	✓	✓	-	✓	✓

*Except for the crops included in this group specified in the following row/s.

**W40000 gathers the following crop groups included in (MAGRAMA, 2016) (in Spanish in parenthesis): Carob (Algarrobo), Caper (Alcaparra), Coffee plant (Cafeto), Common cane (Caña vulgar), Reed (Mimbrera), Mulberry and others (Morera y otros), Agave and pita (Agave y pita) and the miscellaneous group: “Other woody crops”.

✓ means that that crop (IDPR+IDCS) is associated to a CLC land use.

ANNEXE IV: LIST OF THE SOIL GROUPS WITH REPRESENTATION IN THE EUROPEAN SOIL MAP (EC-ESBN, 2004) AND SOME OF THEIR AVERAGE TOPSOIL PROPERTIES

SOIL GROUP ID	CODE (FAO 74)	SOIL TYPE (FAO-UNESCO, 1974)	BEDROCK CODE[1]	TOTAL SOIL PROFILES NUMBER[2]	TOPSOIL CLAY CONTENT[3] (%)	TOPSOIL TYPE[4]	TOPSOIL POTASSIUM CONTENT[3] ($cmol \cdot kg^{-1}$)
1	Je	FLUVISOL EUTRICO	110, 113	16	14.45	Loam	0.61
3	Ie	LITOSOL EUTRICO	743	4 (1)	15.59	Loam	0.34
5	Ic	LITOSOL CALCICO	210, 451	8	17.07	Loam	0.62
6	Id	LITOSOL DISTRICO	711	3	14.09	Sand	0.99
7	Qc	ARENOSOL CAMBICO	430, 442	27	3.89	Sand	0.26
8	Ql	ARENOSOL LUVICO	430	5	3.06	Sand	0.36
9	U	RANKER	710, 711	77	14.64	Loam	0.32
12	Vp	VERTISOL PELLICO	110, 230, 712	3	55.77	Clay	1.31
14	Vc	VERTISOL CROMICO	230, 722	25	45.63	Clay	0.72
15	Zg	SOLONCHAK GLEICO	110, 120	9	17.02	Loam	0.39
19	Xy	XEROSOL GIPSICO	233	4 (1)	34.26	Loam	0.86
21	Be	CAMBISOL EUTRICO	454, 711, 743	86 (1)	16.68	Loam	0.38
22	Bd	CAMBISOL DISTRICO	711	74	16.03	Loam	0.38
23	Bd	CAMBISOL DISTRICO	456, 730, 731	16 (1)	16.54	Loam	0.41
24	Bh	CAMBISOL HUMICO	710, 711	54	12.88	Sand	0.30
37	Lv	LUVISOL VERTICO	610, 712	5	35.37	Clay	0.76
38	Lga	LUVISOL ALBICO	453	1	10.30	Sand	0.10
39	Phf	PODZOL FERRICO Y HUMICO	711	15	10.58	Sand	0.36
40	We	PLANOSOL EUTRICO	340	4	14.27	Loam	0.72
42	Od	HISTOSOL DISTRICO	910	2	15.18	Organic	0.47
116	Xk	XEROSOL CALCICO	451	3 (1)	20.11	Loam	0.36
117	Xk	XEROSOL CALCICO	230	18 (1)	23.55	Loam	0.45
118	Xk	XEROSOL CALCICO	100	6 (2)	16.11	Loam	0.44
124	Bh	CAMBISOL HUMICO	454, 740, 743	67 (2)	17.13	Loam	0.33
126	Bk	CAMBISOL CALCICO	210	74	22.26	Loam	0.60
127	Bk	CAMBISOL CALCICO	100, 110	30 (4)	23.69	Loam	0.66
128	Bk	CAMBISOL CALCICO	230	85	23.88	Loam	0.57
129	Bk	CAMBISOL CALCICO	233	16 (1)	26.89	Loam	0.56
132	Lo	LUVISOL ORTICO	210, 521	41	14.21	Loam	0.33
133	Lo	LUVISOL ORTICO	712, 743	75	12.17	Loam	0.31
201	Jc	FLUVISOL CALCAREO	110, 232	57	19.49	Loam	0.54
202	Rd	REGOSOL DISTRICO	711, 740, 743	22 (1)	13.24	Loam	0.31
203	E	RENDZINA	210	42 (3)	20.64	Loam	0.52
204	Ag	ACRISOL GLEICO	640	14	21.75	Loam	0.19
205	Zo	SOLONCHAK ORTICO	230	18 (1)	19.65	Loam	0.31
206	Re	REGOSOL EUTRICO	740, 743	47 (2)	15.53	Loam	0.34
207	Rc	REGOSOL CALCAREO	232	99	20.53	Loam	0.45
208	Bc	CAMBISOL CROMICO	452	30	19.05	Loam	0.31
209	Po	PODZOL ORTICO	414	14	7.56	Sand	0.26
238	Lg	LUVISOL GLEICO	610	26	12.85	Loam	0.33
239	Lc	LUVISOL CROMICO	110	23 (1)	17.33	Loam	0.28
240	Lc	LUVISOL CROMICO	230	58	23.92	Loam	0.55
241	Lcr	LUVISOL RHODO-CROMICO	610	9	9.81	Sand	0.21
242	Lcr	LUVISOL RHODO-CROMICO	743	16	20.55	Loam	0.38
243	Lcr	LUVISOL RHODO-CROMICO	730	21	18.13	Loam	0.38
244	Lkc	LUVISOL CROMO-CALCICO	112	19 (1)	21.65	Loam	0.47
245	Lkc	LUVISOL CROMO-CALCICO	610	4	26.70	Loam	0.47
246	Lkcr	LUVISOL RHODO-CROMO-CALCICO	215	38	23.86	Loam	0.59

[1]Bedrock codes are listed hereunder.
[2]In parenthesis are included the number of new soil profiles added to each soil group, if corresponds. The soil groups comprised of Gleyic Cambisols (No. 25) and Orthic Solonetz (No. 1029), with no representation in the soil base map (EC-ESBN, 2004) were increased by one soil profile each.
[3]Topsoil clay and potassium content are plotted further on.
[4]Soil type according to IAEA, 2010.

BEDROCK (EC-ESBN, 2004):

BEDROCK CODE	LITHOLOGICAL DESCRIPTION
100	UNDIFFERENTIATED ALLUVIAL DEPOSITS (OR GLACIAL DEPOSITS)
110	RIVER ALLUVIUM
111	OLD FLUVIATILE DEPOSIT (TERTIARY)
112	TERRACES
113	LACUSTROFLUVIAL ALLUVIUM
120	ESTUARINE/MARINE ALLUVIUM
130	GLACIOFLUVIAL DEPOSITS
131	TILL
140	GLACIOFLUVIAL DRIFT
150	COLLUVIUM
200	CALCAREOUS ROCKS
209	RESIDUUM FROM CALCAREOUS ROCKS
210	LIMESTONE
211	PRIMARY LIMESTONE (CARBONIFEROUS)
212	SECONDARY LIMESTONE
213	TERTIARY LIMESTONE
214	FERRUGINEOUS LIMESTONE
215	HARD LIMESTONE
216	SOFT LIMESTONE
217	MARLY LIMESTONE
218	CHALKY LIMESTONE
219	DETRITAL LIMESTONE
220	SECONDARY CHALK
230	MARL
231	SECONDARY MARL
232	TERTIARY MARL
233	GYPSEOUS MARL
234	SCHISTOSE MARL
240	GYPSUM
250	DOLOMITE
300	CLAYEY MATERIALS
310	OLD CLAYEY SEDIMENTARY DEPOSITS
311	PRIMARY CLAY AND SANDSTONE
312	SECONDARY CLAY
313	TERTIARY CLAY
314	PLEISTOCENE CLAY
319	RESIDUUM FROM OLD CLAYEY SEDIMENTARY DEPOSITS
320	ALLUVIAL OR GLACIOFLUVIAL CLAY
321	TERTIARY ALLUVIAL CLAY
322	GLACIAL CLAY (TERTIARY AND QUATERNARY)
323	GRAVELLY CLAY
324	BOULDER CLAY
330	RESIDUAL CLAY FROM CALCAREOUS ROCKS
331	CLAY-WITH-FLINTS
332	SIDEROLITH FORMATIONS
333	CALCAREOUS DECALCIFICATION CLAY
340	CLAYSTONE, MUDSTONE
350	CALCAREOUS CLAY
400	SANDY MATERIALS
410	OLD SANDY SEDIMENTARY DEPOSITS
411	SECONDARY SANDS
412	TERTIARY SANDS
413	FLINT SANDS
414	PLEISTOCENE SANDS
419	RESIDUUM FROM OLD SANDY SEDIMENTARY DEPOSITS
420	ALLUVIAL OR GLACIOFLUVIAL SANDS
421	GLACIAL SANDS
422	SANDY GRAVELLY MATERIALS
429	RESIDUUM FROM ALLUVIAL OR GLACIOFLUVIAL SANDS
430	EOLIAN SANDS
431	LOCALLY SANDCOVER
440	COASTAL SANDS (DUNE SANDS)
441	SHELLY COASTAL SANDS
442	NON CALCAREOUS COASTAL SANDS
450	SANDSTONE
451	CALCAREOUS SANDSTONE (MACIGNO)
452	FERRUGINEOUS SANDSTONE (OLD RED SANDSTONE)
453	CLAYEY SANDSTONE
454	SOFT QUARTZY SANDSTONE
455	HARD QUARTZY SANDSTONE
456	QUARTZITE
457	SCHISTOSE SANDSTONE
459	RESIDUUM FROM SANDSTONE
500	LOAMY MATERIALS
510	RESIDUAL LOAM
511	OLD LOAM (TOUYAS)
512	STONY LOAM
513	CLAY LOAM
514	SANDY LOAM
520	EOLIAN LOAM
521	LOESS
522	THIN LOESS COVER
523	SANDY LOESS
530	SILTSTONE
539	RESIDUUM FROM SILTSTONE
514	SANDY LOAM

BEDROCK CODE	LITHOLOGICAL DESCRIPTION	BEDROCK CODE	LITHOLOGICAL DESCRIPTION
600	DETRITAL FORMATIONS	800	VOLCANIC ROCKS
610	ARKOSE	809	RESIDUUM FROM VOLCANIC ROCKS
620	BRECCIA AND PUDDINGSTONE	810	ACID VOLCANIC ROCKS
630	FLYSCH AND MOLASSE	819	RESIDUUM FROM ACID VOLCANIC ROCKS
640	RANAS	820	BASIC VOLCANIC ROCKS
700	CRYSTALLINE ROCKS AND MIGMATITES	821	PHONOLITES
709	RESIDUUM FROM CRYSTALLINE ROCKS AND MIGMATITES	822	BASALT
710	ACID CRYSTALLINE ROCKS (AND MIGMATITES)	823	ANDESITE
711	GRANITE	824	RHYOLITE
712	DIORITE, QUARTZODIORITE	825	VOLCANIC TUFF
719	RESIDUUM FROM ACID CRYSTALLINE ROCKS	830	VOLCANIC SLAG
720	NON ACID CRYSTALLINE ROCKS (AND MIGMATITES)	900	OTHER ROCKS
721	SYENITE	901	SEDIMENTARY ROCKS
722	GABBRO	902	SEDIMENTARY, METAMORPHIC AND ERUPTIVE ROCKS
723	SERPENTINE	910	ORGANIC MATERIALS
730	CRYSTALLINE METAMORPHIC ROCKS		
731	GNEISS		
732	EMBRECHITES		
739	RESIDUUM FROM CRYSTALLINE METAMORPHIC ROCKS		
740	SCHISTS		
741	MICASCHISTS		
742	SLATES		
743	SHALES		
744	CALCSCHISTS		
745	GREEN SCHISTS		
749	RESIDUUM FROM SCHISTS		
750	OTHER METAMORPHIC ROCKS		

The bedrock list has been elaborated from the MAT1 field extracted from the European soil map (EC-ESBN, 2004)

TOPSOIL CLAY AND POTASSIUM CONTENT:

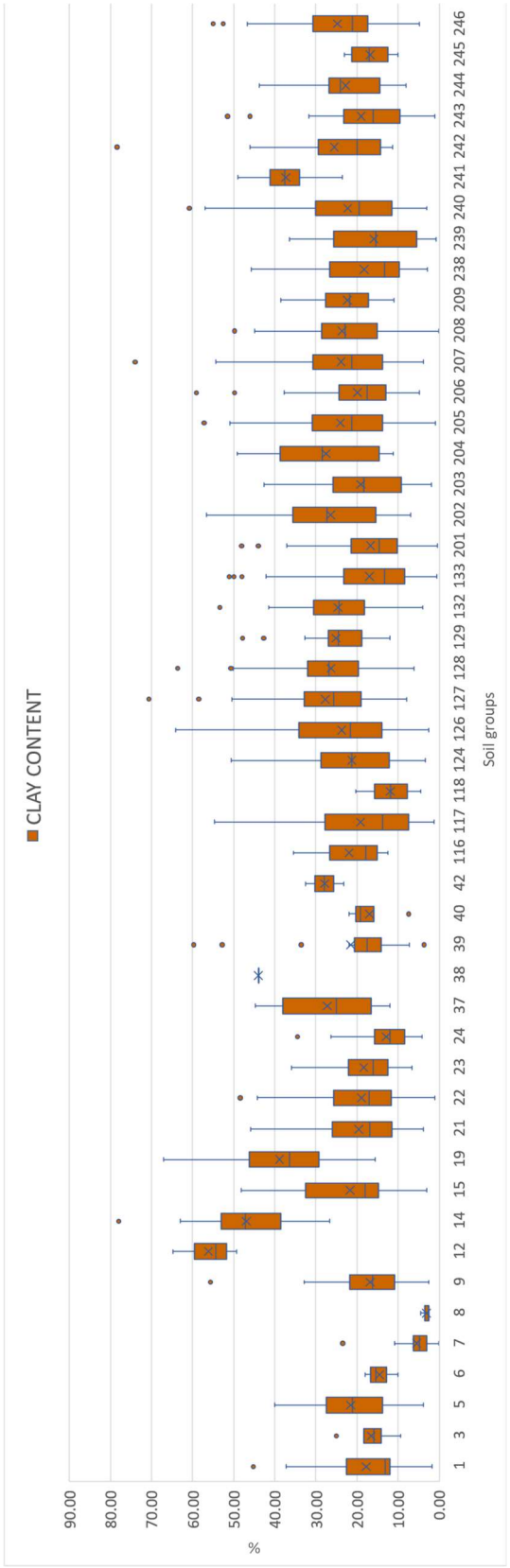

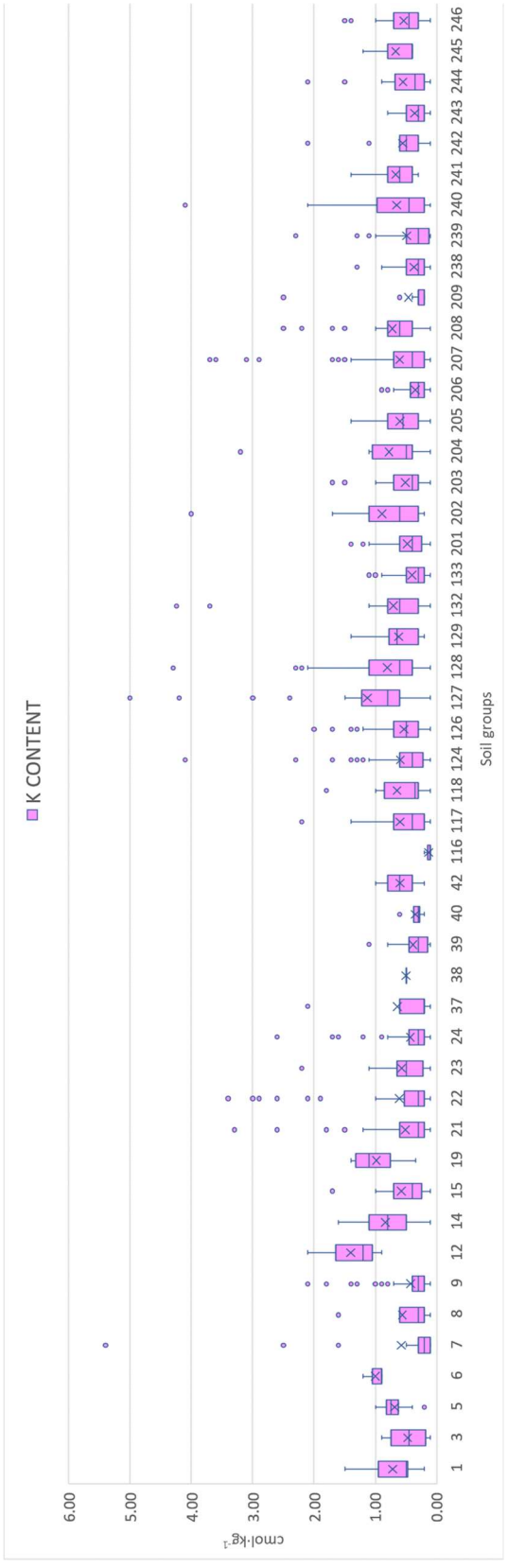

ANNEXE V: TRANSFER FACTOR FROM SOIL TO PLANT (Fv) VALUES FOR ^{137}Cs CONSIDERING THE CROP TYPE, THE PLANT COMPARTMENT AND THE TOPSOIL TEXTURE FOR TEMPERATE CLIMATES. (IAEA, 2010)

Plant Group	ID_PG	Plant Compartment	ID_PC	ID_C	Soil Group	ID_tx	ID_F_V	N	G. Mean	GSD_SD	Minimum	Maximum
Cereals	ce	Grain	G	ceG	All	0	Cs_ceG_0	470	$2.90\cdot10^{-2}$	$4.10\cdot10^{1}$	$2.00\cdot10^{-4}$	$9.00\cdot10^{-1}$
Cereals	ce	Grain	G	ceG	Sand	1	Cs_ceG_1	156	$3.90\cdot10^{-2}$	$3.30\cdot10^{1}$	$2.00\cdot10^{-3}$	$6.60\cdot10^{-1}$
Cereals	ce	Grain	G	ceG	Loam	2	Cs_ceG_2	158	$2.00\cdot10^{-2}$	$4.10\cdot10^{1}$	$8.00\cdot10^{-4}$	$2.00\cdot10^{-1}$
Cereals	ce	Grain	G	ceG	Clay	4	Cs_ceG_4	110	$1.10\cdot10^{-2}$	$2.70\cdot10^{1}$	$2.00\cdot10^{-4}$	$9.00\cdot10^{-2}$
Cereals	ce	Grain	G	ceG	Organic	8	Cs_ceG_8	28	$4.30\cdot10^{-2}$	$2.70\cdot10^{1}$	$1.00\cdot10^{-2}$	$7.30\cdot10^{-1}$
Cereals	ce	Stems, shoots	S	ceS	All	0	Cs_ceS_0	130	$1.50\cdot10^{-1}$	$5.00\cdot10^{1}$	$4.30\cdot10^{-3}$	$3.70\cdot10^{1}$
Cereals	ce	Stems, shoots	S	ceS	Sand	1	Cs_ceS_1	35	$2.10\cdot10^{-1}$	$3.30\cdot10^{1}$	$4.10\cdot10^{-2}$	$1.90\cdot10^{1}$
Cereals	ce	Stems, shoots	S	ceS	Loam	2	Cs_ceS_2	36	$1.10\cdot10^{-1}$	$4.50\cdot10^{1}$	$6.50\cdot10^{-3}$	$1.50\cdot10^{1}$
Cereals	ce	Stems, shoots	S	ceS	Clay	4	Cs_ceS_4	37	$5.60\cdot10^{-2}$	$3.70\cdot10^{1}$	$4.30\cdot10^{-3}$	$5.30\cdot10^{-1}$
Maize	ma	Grain	G	maG	All	0	Cs_maG_0	67	$3.30\cdot10^{-2}$	$3.00\cdot10^{1}$	$3.00\cdot10^{-3}$	$2.60\cdot10^{-1}$
Maize	ma	Grain	G	maG	Sand	1	Cs_maG_1	47	$4.90\cdot10^{-2}$	$2.40\cdot10^{1}$	$8.00\cdot10^{-3}$	$2.60\cdot10^{-1}$
Maize	ma	Grain	G	maG	Loam	2	Cs_maG_2	14	$1.60\cdot10^{-2}$	$2.70\cdot10^{1}$	$3.20\cdot10^{-3}$	$7.00\cdot10^{-2}$
Maize	ma	Grain	G	maG	Clay	4	Cs_maG_4	11	$1.20\cdot10^{-2}$	$3.30\cdot10^{1}$	$3.00\cdot10^{-3}$	$7.00\cdot10^{-2}$
Maize	ma	Stems, shoots	S	maS	All	0	Cs_maS_0	101	$7.30\cdot10^{-2}$	$3.00\cdot10^{1}$	$3.00\cdot10^{-3}$	$4.90\cdot10^{-1}$
Maize	ma	Stems, shoots	S	maS	Sand	1	Cs_maS_1	77	$1.00\cdot10^{-1}$	$2.30\cdot10^{1}$	$1.40\cdot10^{-2}$	$4.90\cdot10^{-1}$
Maize	ma	Stems, shoots	S	maS	Loam	2	Cs_maS_2	10	$1.50\cdot10^{-2}$	$2.50\cdot10^{1}$	$3.00\cdot10^{-3}$	$5.20\cdot10^{-2}$
Maize	ma	Stems, shoots	S	maS	Clay	4	Cs_maS_4	11	$2.20\cdot10^{-2}$	$2.10\cdot10^{1}$	$7.80\cdot10^{-3}$	$6.00\cdot10^{-2}$
Maize	ma	Stems, shoots	S	maS	Organic	8	Cs_maS_8	3	$1.40\cdot10^{-1}$	$1.30\cdot10^{1}$	$1.00\cdot10^{-1}$	$1.60\cdot10^{-1}$
Leafy veg.	ly	Leaves	L	lyL	All	0	Cs_lyL_0	290	$6.00\cdot10^{-2}$	$6.00\cdot10^{1}$	$3.00\cdot10^{-4}$	$9.80\cdot10^{-1}$
Leafy veg.	ly	Leaves	L	lyL	Sand	1	Cs_lyL_1	96	$1.20\cdot10^{-1}$	$4.10\cdot10^{1}$	$2.10\cdot10^{-3}$	$9.80\cdot10^{-1}$
Leafy veg.	ly	Leaves	L	lyL	Loam	2	Cs_lyL_2	119	$7.40\cdot10^{-2}$	$5.00\cdot10^{1}$	$3.00\cdot10^{-4}$	$7.30\cdot10^{-1}$
Leafy veg.	ly	Leaves	L	lyL	Clay	4	Cs_lyL_4	67	$1.80\cdot10^{-2}$	$6.70\cdot10^{1}$	$5.00\cdot10^{-4}$	$7.20\cdot10^{-1}$
Leafy veg.	ly	Leaves	L	lyL	Organic	8	Cs_lyL_8	7	$2.30\cdot10^{-2}$	$7.40\cdot10^{1}$	$4.00\cdot10^{-3}$	$4.60\cdot10^{-1}$
Non leafy veg.	nl	Fruits, heads, berries, buds	F	nlF	All	0	Cs_nlF_0	38	$2.10\cdot10^{-2}$	$4.10\cdot10^{1}$	$7.00\cdot10^{-4}$	$7.30\cdot10^{-1}$
Non leafy veg.	nl	Fruits, heads, berries, buds	F	nlF	Sand	1	Cs_nlF_1	17	$3.50\cdot10^{-2}$	$4.10\cdot10^{1}$	$1.20\cdot10^{-2}$	$7.30\cdot10^{-1}$
Non leafy veg.	nl	Fruits, heads, berries, buds	F	nlF	Loam	2	Cs_nlF_2	5	$3.30\cdot10^{-2}$	$5.50\cdot10^{1}$	$6.30\cdot10^{-3}$	$3.00\cdot10^{-1}$
Non leafy veg.	nl	Fruits, heads, berries, buds	F	nlF	Clay	4	Cs_nlF_4	14	$9.10\cdot10^{-3}$	$2.20\cdot10^{1}$	$7.00\cdot10^{-4}$	$1.60\cdot10^{-2}$
Legumes veg.	lv	Seeds, Pods	S	lvS	All	0	Cs_lvS_0	126	$4.00\cdot10^{-2}$	$3.70\cdot10^{1}$	$1.00\cdot10^{-3}$	$7.10\cdot10^{-1}$
Legumes veg.	lv	Seeds, Pods	S	lvS	Sand	1	Cs_lvS_1	66	$8.70\cdot10^{-2}$	$2.50\cdot10^{1}$	$3.50\cdot10^{-3}$	$7.10\cdot10^{-1}$
Legumes veg.	lv	Seeds, Pods	S	lvS	Loam	2	Cs_lvS_2	42	$2.00\cdot10^{-2}$	$3.30\cdot10^{1}$	$1.00\cdot10^{-3}$	$4.20\cdot10^{-1}$
Legumes veg.	lv	Seeds, Pods	S	lvS	Clay	4	Cs_lvS_4	18	$1.30\cdot10^{-2}$	$3.00\cdot10^{1}$	$2.00\cdot10^{-3}$	$8.10\cdot10^{-2}$
Root crops	rc	Roots	R	rcR	All	0	Cs_rcR_0	81	$4.20\cdot10^{-2}$	$3.00\cdot10^{1}$	$1.00\cdot10^{-3}$	$8.80\cdot10^{-1}$
Root crops	rc	Roots	R	rcR	Sand	1	Cs_rcR_1	37	$6.20\cdot10^{-2}$	$2.50\cdot10^{1}$	$8.00\cdot10^{-3}$	$4.00\cdot10^{-1}$
Root crops	rc	Roots	R	rcR	Loam	2	Cs_rcR_2	21	$3.00\cdot10^{-2}$	$3.70\cdot10^{1}$	$1.00\cdot10^{-3}$	$1.60\cdot10^{-1}$
Root crops	rc	Roots	R	rcR	Clay	4	Cs_rcR_4	17	$2.40\cdot10^{-2}$	$2.20\cdot10^{1}$	$5.00\cdot10^{-3}$	$6.00\cdot10^{-2}$
Root crops	rc	Roots	R	rcR	Organic	8	Cs_rcR_8	5	$5.90\cdot10^{-2}$	$5.00\cdot10^{1}$	$1.60\cdot10^{-2}$	$8.80\cdot10^{-1}$
Root crops	rc	Leaves	L	rcL	All	0	Cs_rcL_0	12	$3.50\cdot10^{-2}$	$3.00\cdot10^{1}$	$6.00\cdot10^{-3}$	$4.50\cdot10^{-1}$
Root crops	rc	Leaves	L	rcL	Sand	1	Cs_rcL_1	3	$1.10\cdot10^{-1}$	$3.30\cdot10^{1}$	$5.10\cdot10^{-2}$	$4.50\cdot10^{-1}$
Root crops	rc	Leaves	L	rcL	Loam	2	Cs_rcL_2	2	$2.60\cdot10^{-2}$		$9.00\cdot10^{-3}$	$4.30\cdot10^{-2}$
Root crops	rc	Leaves	L	rcL	Clay	4	Cs_rcL_4	7	$2.60\cdot10^{-2}$	$2.10\cdot10^{1}$	$6.00\cdot10^{-3}$	$4.70\cdot10^{-2}$
Tubers	tb	Tubers	T	tbT	All	0	Cs_tbT_0	138	$5.60\cdot10^{-2}$	$3.00\cdot10^{1}$	$4.00\cdot10^{-3}$	$6.00\cdot10^{-1}$
Tubers	tb	Tubers	T	tbT	Sand	1	Cs_tbT_1	69	$9.30\cdot10^{-2}$	$3.00\cdot10^{1}$	$4.00\cdot10^{-3}$	$6.00\cdot10^{-1}$

Plant Group	ID_PG	Plant Compartment	ID_PC	ID_C	Soil Group	ID_tx	ID_F_V	N	G. Mean	GSD_SD	Minimum	Maximum
Tubers	tb	Tubers	T	tbT	Loam	2	Cs_tbT_2	40	$3.50\cdot10^{-2}$	$2.30\cdot10^{1}$	$4.80\cdot10^{-3}$	$1.40\cdot10^{-1}$
Tubers	tb	Tubers	T	tbT	Clay	4	Cs_tbT_4	21	$2.50\cdot10^{-2}$	$2.20\cdot10^{1}$	$5.00\cdot10^{-3}$	$9.00\cdot10^{-2}$
Tubers	tb	Tubers	T	tbT	Organic	8	Cs_tbT_8	7	$5.80\cdot10^{-2}$	$3.70\cdot10^{1}$	$1.60\cdot10^{-2}$	$5.40\cdot10^{-1}$
Grasses	gr	Stems, shoots	S	grS	All	0	Cs_grS_0	64	$6.30\cdot10^{-2}$	$3.66\cdot10^{1}$	$4.80\cdot10^{-3}$	$9.90\cdot10^{-1}$
Grasses	gr	Stems, shoots	S	grS	Sand	1	Cs_grS_1	41	$8.40\cdot10^{-2}$	$3.30\cdot10^{1}$	$1.00\cdot10^{-2}$	$9.90\cdot10^{-1}$
Grasses	gr	Stems, shoots	S	grS	Loam	2	Cs_grS_2	10	$4.80\cdot10^{-2}$	$2.30\cdot10^{1}$	$1.20\cdot10^{-2}$	$2.10\cdot10^{-1}$
Grasses	gr	Stems, shoots	S	grS	Clay	4	Cs_grS_4	9	$1.20\cdot10^{-2}$	$2.10\cdot10^{1}$	$4.80\cdot10^{-3}$	$4.30\cdot10^{-2}$
Grasses	gr	Stems, shoots	S	grS	Organic	8	Cs_grS_8	4	$2.80\cdot10^{-1}$	$1.20\cdot10^{1}$	$2.10\cdot10^{-1}$	$3.40\cdot10^{-1}$
Legume fodder	lf	Stems, shoots	S	lfS	All	0	Cs_lfS_0	85	$1.60\cdot10^{-1}$	$3.30\cdot10^{1}$	$1.00\cdot10^{-2}$	$1.80\cdot10^{1}$
Legume fodder	lf	Stems, shoots	S	lfS	Sand	1	Cs_lfS_1	29	$2.40\cdot10^{-1}$	$3.70\cdot10^{1}$	$1.80\cdot10^{-2}$	$1.80\cdot10^{1}$
Legume fodder	lf	Stems, shoots	S	lfS	Loam	2	Cs_lfS_2	51	$1.50\cdot10^{-1}$	$3.00\cdot10^{1}$	$1.00\cdot10^{-2}$	$1.20\cdot10^{1}$
Legume fodder	lf	Stems, shoots	S	lfS	Clay	4	Cs_lfS_4	4	$4.60\cdot10^{-2}$	$4.10\cdot10^{1}$	$1.30\cdot10^{-2}$	$3.00\cdot10^{-1}$
Pasture	ps	Stems, shoots	S	psS	All	0	Cs_psS_0	401	$2.50\cdot10^{-1}$	$4.10\cdot101$	$1.00\cdot10^{-2}$	$5.00\cdot10^{1}$
Pasture	ps	Stems, shoots	S	psS	Sand	1	Cs_psS_1	169	$2.90\cdot10^{-1}$	$4.10\cdot10^{1}$	$1.00\cdot10^{-2}$	$4.80\cdot10^{1}$
Pasture	ps	Stems, shoots	S	psS	Loam	2	Cs_psS_2	124	$1.90\cdot10^{-1}$	$4.10\cdot10^{1}$	$1.00\cdot10^{-2}$	$2.60\cdot10^{1}$
Pasture	ps	Stems, shoots	S	psS	Clay	4	Cs_psS_4	75	$1.80\cdot10^{-1}$	$3.70\cdot10^{1}$	$1.00\cdot10^{-2}$	$1.20\cdot10^{1}$
Pasture	ps	Stems, shoots	S	psS	Organic	8	Cs_psS_8	31	$7.60\cdot10^{-1}$	$2.20\cdot10^{1}$	$3.00\cdot10^{-1}$	$5.00\cdot10^{1}$
Herbs	he	Stems, leaves	X	heX	All	0	Cs_heX_0	4	$6.60\cdot10^{-2}$	$1.49\cdot10^{1}$	$4.80\cdot10^{-3}$	2.80
Other crops	oc	All	A	ocA	All	0	Cs_ocA_0	9	$3.10\cdot10^{-1}$	$4.50\cdot10^{1}$	$3.60\cdot10^{-2}$	2.20
Woody trees	wt	Fruit	F	wtF	All	0	Cs_wtF_0	15	$5.80\cdot10^{-3}$	$1.50\cdot10^{1}$	$8.60\cdot10^{-4}$	$8.00\cdot10^{-2}$
Woody trees	wt	Fruit	F	wtF	Sand	1	Cs_wtF_1	4	$1.50\cdot10^{-2}$	$1.60\cdot10^{1}$	$1.90\cdot10^{-3}$	$8.00\cdot10^{-2}$
Woody trees	wt	Fruit	F	wtF	Loam	2	Cs_wtF_2	5	$3.50\cdot10^{-3}$	$8.80\cdot10^{-1}$	$9.40\cdot10^{-4}$	$9.20\cdot10^{-3}$
Woody trees	wt	Fruit	F	wtF	Clay	4	Cs_wtF_4	2	$1.10\cdot10^{-3}$		$8.80\cdot10^{-4}$	$1.40\cdot10^{-3}$
Woody trees	wt	Fruit	F	wtF	Organic	8	Cs_wtF_8	1	$3.70\cdot10^{-2}$			
Woody trees	wt	Fruit	F	wtF	Unspecified	-1	Cs_wtF_-1	3	$6.00\cdot10^{-3}$	$1.70\cdot10^{1}$	$8.60\cdot10^{-4}$	$1.90\cdot10^{-2}$
Shrubs	sh	Fruit	F	shF	All	0	Cs_shF_0	6	$2.10\cdot10^{-3}$	$8.10\cdot10^{-1}$	$6.90\cdot10^{-4}$	$5.70\cdot10^{-3}$
Shrubs	sh	Fruit	F	shF	Loam	2	Cs_shF_2	2	$3.80\cdot10^{-3}$		$1.80\cdot10^{-3}$	$5.70\cdot10^{-3}$
Shrubs	sh	Fruit	F	shF	Clay	4	Cs_shF_4	2	$2.20\cdot10^{-3}$		$9.80\cdot10^{-4}$	$3.30\cdot10^{-3}$
Shrubs	sh	Fruit	F	shF	Unspecified	-1	Cs_shF_-1	2	$2.00\cdot10^{-3}$		$6.90\cdot10^{-4}$	$3.30\cdot10^{-3}$
Herb. plants	hp	Fruit	F	hpF	All	0	Cs_hpF_0	8	$2.90\cdot10^{-3}$	$3.30\cdot10^{-3}$	$4.10\cdot10^{-4}$	$8.90\cdot10^{-3}$
Herb. plants	hp	Fruit	F	hpF	Sand	1	Cs_hpF_1	1	$4.20\cdot10^{-3}$			
Herb. plants	hp	Fruit	F	hpF	Loam	2	Cs_hpF_2	1	$9.00\cdot10^{-4}$			
Herb. plants	hp	Fruit	F	hpF	Organic	8	Cs_hpF_8	1	$6.40\cdot10^{-3}$			
Herb. plants	hp	Fruit	F	hpF	Unspecified	-1	Cs_hpF_-1	5	$1.00\cdot10^{-3}$	$1.30\cdot10^{1}$	$4.10\cdot10^{-4}$	$8.90\cdot10^{-3}$

ID_PG: IDentification for the Plant's Group.
ID_PC: IDentification for the Plant's Compartment.
ID_C: IDentification for the Crop.
ID_tx: IDentification for the soil texture.
ID_F_V: IDentification for the radionuclide to be transfer, the plant group and the plant compartment to uptake the
N: Number of empirical data used to define the F_V.
G_Mean: Geometric mean.
GSD_SD: Standard deviation.
Minimum: Minimum empirical data used to define the F_V.
Maximum: Maximum empirical data used to define the F_V.

ANNEXE VI: ^{131}I, ^{90}Sr AND ^{137}Cs RELEASED ACCORDING TO THE SOURCE TERM CONSIDERED IN THE CASE-STUDY

Source term for an ISLOCA accident (Interfacing System Loss of Coolant Accident), applied to the Almaraz NPP inventory			
Time (Hour since the failure)	**Activity of the released radionuclides that are considered in the simulations (Bq)**		
	^{131}I	**^{90}Sr**	**^{137}Cs**
13	$1.35 \cdot 10^{15}$	$1.49 \cdot 10^{11}$	$2.52 \cdot 10^{13}$
14	$3.10 \cdot 10^{17}$	$1.57 \cdot 10^{13}$	$5.32 \cdot 10^{15}$
15	$4.30 \cdot 10^{16}$	$3.32 \cdot 10^{12}$	$5.60 \cdot 10^{14}$
16	$5.64 \cdot 10^{15}$	$1.16 \cdot 10^{12}$	$6.57 \cdot 10^{13}$
17	$1.72 \cdot 10^{15}$	$3.44 \cdot 10^{11}$	$2.21 \cdot 10^{13}$
18	$2.56 \cdot 10^{13}$	$5.13 \cdot 10^{9}$	$3.24 \cdot 10^{11}$
20	$1.48 \cdot 10^{13}$	$1.51 \cdot 10^{10}$	$1.65 \cdot 10^{11}$
21	$3.06 \cdot 10^{13}$	$1.95 \cdot 10^{10}$	$2.96 \cdot 10^{11}$
22	$4.13 \cdot 10^{13}$	$1.76 \cdot 10^{10}$	$3.87 \cdot 10^{11}$
23	$7.51 \cdot 10^{13}$	$1.45 \cdot 10^{10}$	$6.90 \cdot 10^{11}$
24	$1.91 \cdot 10^{14}$	$9.31 \cdot 10^{9}$	$1.73 \cdot 10^{12}$
25	$2.49 \cdot 10^{14}$	$3.15 \cdot 10^{9}$	$2.27 \cdot 10^{12}$
26	$8.77 \cdot 10^{14}$	$5.38 \cdot 10^{9}$	$7.97 \cdot 10^{12}$
27	$1.44 \cdot 10^{15}$	$1.28 \cdot 10^{10}$	$1.31 \cdot 10^{13}$
28	$7.11 \cdot 10^{14}$	$1.64 \cdot 10^{9}$	$6.45 \cdot 10^{12}$
29	$1.17 \cdot 10^{15}$	$3.92 \cdot 10^{9}$	$1.06 \cdot 10^{13}$
30	$9.90 \cdot 10^{14}$	$7.07 \cdot 10^{9}$	$8.96 \cdot 10^{12}$
31	$6.25 \cdot 10^{14}$	$1.48 \cdot 10^{10}$	$5.65 \cdot 10^{12}$
32	$1.37 \cdot 10^{14}$	$2.32 \cdot 10^{10}$	$1.26 \cdot 10^{12}$
33	$4.29 \cdot 10^{13}$	$5.20 \cdot 10^{10}$	$4.10 \cdot 10^{11}$
34	$3.91 \cdot 10^{13}$	$7.47 \cdot 10^{10}$	$4.01 \cdot 10^{11}$
35	$3.53 \cdot 10^{13}$	$1.24 \cdot 10^{12}$	$3.92 \cdot 10^{11}$
36	$6.10 \cdot 10^{13}$	$3.64 \cdot 10^{12}$	$6.81 \cdot 10^{11}$
37	$4.04 \cdot 10^{13}$	$3.49 \cdot 10^{11}$	$3.92 \cdot 10^{11}$
38	$7.83 \cdot 10^{13}$	$3.42 \cdot 10^{11}$	$7.57 \cdot 10^{11}$
39	$1.13 \cdot 10^{15}$	$4.50 \cdot 10^{11}$	$1.04 \cdot 10^{13}$
40	$4.84 \cdot 10^{14}$	$8.24 \cdot 10^{10}$	$4.43 \cdot 10^{12}$
41	$1.32 \cdot 10^{14}$	$1.69 \cdot 10^{11}$	$1.29 \cdot 10^{12}$
42	$2.38 \cdot 10^{14}$	$1.84 \cdot 10^{11}$	$2.29 \cdot 10^{12}$
43	$4.36 \cdot 10^{14}$	$1.98 \cdot 10^{11}$	$4.11 \cdot 10^{12}$
44	$4.06 \cdot 10^{14}$	$2.20 \cdot 10^{11}$	$3.85 \cdot 10^{12}$
45	$4.01 \cdot 10^{14}$	$2.77 \cdot 10^{11}$	$3.88 \cdot 10^{12}$
46	$2.05 \cdot 10^{14}$	$6.77 \cdot 10^{10}$	$1.97 \cdot 10^{12}$
47	$1.01 \cdot 10^{14}$	$6.10 \cdot 10^{10}$	$1.04 \cdot 10^{12}$
Total release	$3.72 \cdot 10^{17}$	$2.83 \cdot 10^{13}$	$6.09 \cdot 10^{15}$

ANNEXE VII: SHEETS OF THE NEW SPANISH SOIL PROFILES INCLUDED IN THE UPDATED DATABASE

Nº DE ORDEN:	PROVINCIA:	CÓDIGO PERFIL:	COORDENADAS UTM. HUSO 30 (ETRS89):		HOJA_MTN:
2001	ALBACETE	AB101	X: 578300,000	Y: 4323700,000	765

TÉRM. MUNICIPAL: ALBACETE **ALTITUD (m):** **PENDIENTE (%):** 0

SITUACIÓN: CARRETERA DE LA GINETA A BARRAX, 9,5 KM A LA IZQUIERDA. ALBACETE

USO: AGRÍCOLA DE REGADÍO **REFERENCIA:** GONZÁLEZ-QUIÑONES06, P

USDA-SOIL TAXONOMY (1975): CALCIXEREPT PETROCÁLCICO

LEYENDA FAO (1974): Xk XEROSOL CALCICO **Nº HORIZONTES:** 6

HORIZONTES:

0 cm	Ap1	Textura:	FCL	Elem. gruesos (%):		Ca (cmol/Kg):	19,7
		Estructura:	B	Arena gruesa (%):		Mg (cmol/Kg):	5,5
		Compactación:	F	Arena fina (%):		Na (cmol/Kg):	1,9
		Raíces:	MP	Arena total (%):	13,4	K (cmol/Kg):	0,2
		Color:	7,5YR4/4	Limo (%):	48,9	S (cmol/Kg):	27,3
		pH (H2O):	8,1	Arcilla (%):	37,7	CIC (cmol/Kg):	27,8
		CE (mS/cm):	0,3	C/N:	6,9	V = S/CIC (%):	98
		Caliza (%):	2,6	D. aparente (g/cm3):	1,4		
		Materia Orgánica (%):	1,6	Infiltración (mm/h):			
15 cm	Ap2	Textura:	FC	Elem. gruesos (%):		Ca (cmol/Kg):	22,6
		Estructura:	B	Arena gruesa (%):		Mg (cmol/Kg):	2,7
		Compactación:	F	Arena fina (%):		Na (cmol/Kg):	0,8
		Raíces:	MP	Arena total (%):	16,7	K (cmol/Kg):	0,3
		Color:	7,5YR4/4	Limo (%):	45,4	S (cmol/Kg):	26,4
		pH (H2O):	7,9	Arcilla (%):	37,9	CIC (cmol/Kg):	26,5
		CE (mS/cm):	0,5	C/N:	7,0	V = S/CIC (%):	100
		Caliza (%):	4,2	D. aparente (g/cm3):	1,4		
		Materia Orgánica (%):	1,2	Infiltración (mm/h):			
38 cm	Bk	Textura:	FC	Elem. gruesos (%):		Ca (cmol/Kg):	16,2
		Estructura:	B	Arena gruesa (%):		Mg (cmol/Kg):	1,3
		Compactación:	F	Arena fina (%):		Na (cmol/Kg):	0,3
		Raíces:	MP	Arena total (%):	22,8	K (cmol/Kg):	0,2
		Color:	7,5YR5/6	Limo (%):	46,4	S (cmol/Kg):	18,0
		pH (H2O):	8,0	Arcilla (%):	30,8	CIC (cmol/Kg):	17,9
		CE (mS/cm):	0,4	C/N:	6,3	V = S/CIC (%):	100
		Caliza (%):	9,8	D. aparente (g/cm3):	1,5		
		Materia Orgánica (%):	0,9	Infiltración (mm/h):			
63 cm	2Cmk	Textura:		Elem. gruesos (%):		Ca (cmol/Kg):	
		Estructura:	L	Arena gruesa (%):		Mg (cmol/Kg):	
		Compactación:	EF	Arena fina (%):		Na (cmol/Kg):	
		Raíces:	N	Arena total (%):		K (cmol/Kg):	
		Color:		Limo (%):		S (cmol/Kg):	
		pH (H2O):		Arcilla (%):		CIC (cmol/Kg):	
		CE (mS/cm):		C/N:		V = S/CIC (%):	
		Caliza (%):		D. aparente (g/cm3):			
		Materia Orgánica (%):		Infiltración (mm/h):			
67 cm	2Bk	Textura:		Elem. gruesos (%):		Ca (cmol/Kg):	
		Estructura:	B	Arena gruesa (%):		Mg (cmol/Kg):	
		Compactación:	F	Arena fina (%):		Na (cmol/Kg):	
		Raíces:	N	Arena total (%):		K (cmol/Kg):	
		Color:	7,5YR6/6	Limo (%):		S (cmol/Kg):	
		pH (H2O):		Arcilla (%):		CIC (cmol/Kg):	
		CE (mS/cm):		C/N:		V = S/CIC (%):	
		Caliza (%):		D. aparente (g/cm3):			
		Materia Orgánica (%):		Infiltración (mm/h):			

96 cm		Textura:	Elem. gruesos (%):	Ca (cmol/Kg):
	2R	Estructura:	Arena gruesa (%):	Mg (cmol/Kg):
		Compactación:	Arena fina (%):	Na (cmol/Kg):
		Raíces:	Arena total (%):	K (cmol/Kg):
		Color:	Limo (%):	S (cmol/Kg):
		pH (H2O):	Arcilla (%):	CIC (cmol/Kg):
		CE (mS/cm):	C/N:	V = S/CIC (%):
		Caliza (%):	D. aparente (g/cm3):	
		Materia Orgánica (%):	Infiltración (mm/h):	

ÍNDICES DE VULNERABILIDAD RADIOLÓGICA DEL PERFIL:

CODSUELO	PARCIALES						TOTALES	
116	Infiltración	Retención Hídrica	Retención Físico-Química Cs	Retención Físico-Química Sr	Contenido en K	Contenido en Ca	Total al Cs	Total al Sr
CADENA ALIMENTARIA	3	2	2	1	4	1	3	2
IRRADIACIÓN EXTERNA	4	2	4	5	-	-	4	4

OBSERVACIONES: MATERIAL ORIGINAL: CALIZAS DETRÍTICAS (TERCIARIO SUPERIOR).

Nº DE ORDEN:	PROVINCIA:	CÓDIGO PERFIL:	COORDENADAS UTM. HUSO 30 (ETRS89):		HOJA_MTN:
2002	BURGOS	BU101	X: 475836,731	Y: 4640775,671	315

TÉRM. MUNICIPAL: PINILLA DE LOS BARRUECOS **ALTITUD (m):** 1020 **PENDIENTE (%):**

SITUACIÓN: EN EL KM 0.900 DE LA CARRETERA LOCAL A LA GENERAL BURGOS-SORIA

USO: MONTE DE ROBLE **REFERENCIA:** JUNTACL88, PAG. 59

USDA-SOIL TAXONOMY (1975):

LEYENDA FAO (1974): Lc LUVISOL CROMICO **Nº HORIZONTES:** 5

HORIZONTES:

0 cm	A	Textura:	FA	Elem. gruesos (%):		Ca (cmol/Kg):	8,0
		Estructura:		Arena gruesa (%):	37,8	Mg (cmol/Kg):	3,0
		Compactación:	FR	Arena fina (%):	41,7	Na (cmol/Kg):	0,2
		Raíces:	A	Arena total (%):	79,5	K (cmol/Kg):	0,2
		Color:	10YR3/2	Limo (%):	8,5	S (cmol/Kg):	11,4
		pH (H2O):	6,6	Arcilla (%):	12,0	CIC (cmol/Kg):	15,9
		CE (mS/cm):		C/N:	15,5	V = S/CIC (%):	72
		Caliza (%):		D. aparente (g/cm3):	1,5		
		Materia Orgánica (%):	5,3	Infiltración (mm/h):			
8 cm	Bw	Textura:	FA	Elem. gruesos (%):		Ca (cmol/Kg):	2,0
		Estructura:		Arena gruesa (%):	37,4	Mg (cmol/Kg):	1,2
		Compactación:	FR	Arena fina (%):	38,9	Na (cmol/Kg):	0,2
		Raíces:	A	Arena total (%):	76,3	K (cmol/Kg):	0,1
		Color:	7,5YR5/6	Limo (%):	10,6	S (cmol/Kg):	3,5
		pH (H2O):	5,6	Arcilla (%):	13,1	CIC (cmol/Kg):	6,3
		CE (mS/cm):		C/N:	13,5	V = S/CIC (%):	55
		Caliza (%):		D. aparente (g/cm3):	1,5		
		Materia Orgánica (%):	0,9	Infiltración (mm/h):			
40 cm	Bt/Cl	Textura:	C	Elem. gruesos (%):		Ca (cmol/Kg):	3,9
		Estructura:		Arena gruesa (%):	8,3	Mg (cmol/Kg):	6,5
		Compactación:	F	Arena fina (%):	26,4	Na (cmol/Kg):	0,3
		Raíces:	A	Arena total (%):	34,7	K (cmol/Kg):	0,1
		Color:	2,5YR4/6	Limo (%):	24,9	S (cmol/Kg):	10,8
		pH (H2O):	4,8	Arcilla (%):	40,4	CIC (cmol/Kg):	20,7
		CE (mS/cm):		C/N:	8,0	V = S/CIC (%):	52
		Caliza (%):		D. aparente (g/cm3):	1,2		
		Materia Orgánica (%):	0,5	Infiltración (mm/h):			
65 cm	Cl	Textura:	FC	Elem. gruesos (%):		Ca (cmol/Kg):	3,9
		Estructura:		Arena gruesa (%):	1,0	Mg (cmol/Kg):	2,5
		Compactación:	F	Arena fina (%):	39,0	Na (cmol/Kg):	0,2
		Raíces:	A	Arena total (%):	40,0	K (cmol/Kg):	0,1
		Color:	2,5YR4/6	Limo (%):	24,5	S (cmol/Kg):	6,7
		pH (H2O):	4,5	Arcilla (%):	35,5	CIC (cmol/Kg):	18,8
		CE (mS/cm):		C/N:	6,8	V = S/CIC (%):	36
		Caliza (%):		D. aparente (g/cm3):	1,2		
		Materia Orgánica (%):	0,5	Infiltración (mm/h):			
95 cm	C	Textura:	FCA	Elem. gruesos (%):		Ca (cmol/Kg):	1,9
		Estructura:	L	Arena gruesa (%):	2,5	Mg (cmol/Kg):	1,6
		Compactación:	MF	Arena fina (%):	58,0	Na (cmol/Kg):	0,2
		Raíces:	A	Arena total (%):	60,5	K (cmol/Kg):	0,1
		Color:	10R3/6	Limo (%):	18,0	S (cmol/Kg):	3,8
		pH (H2O):	4,5	Arcilla (%):	21,5	CIC (cmol/Kg):	10,7
		CE (mS/cm):		C/N:	2,9	V = S/CIC (%):	35
		Caliza (%):		D. aparente (g/cm3):	1,2		
		Materia Orgánica (%):	0,1	Infiltración (mm/h):			

ÍNDICES DE VULNERABILIDAD RADIOLÓGICA DEL PERFIL:

CODSUELO	PARCIALES						TOTALES	
239	Infiltración	Retención Hídrica	Retención Físico-Química Cs	Retención Físico-Química Sr	Contenido en K	Contenido en Ca	Total al Cs	Total al Sr
CADENA ALIMENTARIA	2	1	1	3	4	3	2	2
IRRADIACIÓN EXTERNA	2	1	5	4	-	-	3	3

OBSERVACIONES: GEOLOGÍA: JURÁSICO. CUARZARENITAS Y ARCILLAS ARENOSAS. TOPOGRAFÍA: LADERA SUAVE. DRENAJE: EXTERNO, BUENO. INTERNO, BUENO.

Nº DE ORDEN:	PROVINCIA:	CÓDIGO PERFIL:	COORDENADAS UTM. HUSO 30 (ETRS89):		HOJA_MTN:
2003	CIUDAD REAL	CR101	X: 502318,550	Y: 4284475,050	813

TÉRM. MUNICIPAL: VILLANUEVA DE LOS INFANTES **ALTITUD (m):** 842 **PENDIENTE (%):** 1

SITUACIÓN: CERRO CERCA DEL KM 4 DE LA CM-3127 DE VILLANUEVA DE LOS INFANTES A MONTIEL. CAMINO MARGEN DERECHO (FE

USO: PASTIZAL/ERIAL **REFERENCIA:** GONZÁLEZ-QUIÑONES06, P

USDA-SOIL TAXONOMY (1975): XERORTHENT LÍTICO

LEYENDA FAO (1974): Ie LITOSOL **Nº HORIZONTES:** 2

HORIZONTES:

0 cm	Ap	Textura:	FA	Elem. gruesos (%):		Ca (cmol/Kg):	18,6
		Estructura:	B	Arena gruesa (%):		Mg (cmol/Kg):	0,8
		Compactación:	FR	Arena fina (%):		Na (cmol/Kg):	1,1
		Raíces:	F	Arena total (%):	73,8	K (cmol/Kg):	0,9
		Color:	10R5/6	Limo (%):	16,8	S (cmol/Kg):	21,4
		pH (H2O):	7,9	Arcilla (%):	9,4	CIC (cmol/Kg):	13,2
		CE (mS/cm):	0,2	C/N:	17,4	V = S/CIC (%):	100
		Caliza (%):	0,0	D. aparente (g/cm3):	1,7		
		Materia Orgánica (%):	3,6	Infiltración (mm/h):			
12 cm	R	Textura:		Elem. gruesos (%):		Ca (cmol/Kg):	
		Estructura:		Arena gruesa (%):		Mg (cmol/Kg):	
		Compactación:		Arena fina (%):		Na (cmol/Kg):	
		Raíces:		Arena total (%):		K (cmol/Kg):	
		Color:		Limo (%):		S (cmol/Kg):	
		pH (H2O):		Arcilla (%):		CIC (cmol/Kg):	
		CE (mS/cm):		C/N:		V = S/CIC (%):	
		Caliza (%):		D. aparente (g/cm3):			
		Materia Orgánica (%):		Infiltración (mm/h):			

ÍNDICES DE VULNERABILIDAD RADIOLÓGICA DEL PERFIL:

CODSUELO	PARCIALES						TOTALES	
3	Infiltración	Retención Hídrica	Retención Físico-Química Cs	Retención Físico-Química Sr	Contenido en K	Contenido en Ca	Total al Cs	Total al Sr
CADENA ALIMENTARIA	2	3	2	1	2	1	2	2
IRRADIACIÓN EXTERNA	2	2	4	5	-	-	3	3

OBSERVACIONES: MATERIAL ORIGINAL: ARENISCAS DEL TRIAS (BUNDSANDSTEIN). SE APORTA VALOR DEL PORCENTAJE DE CALIZA ACTIVA.

Nº DE ORDEN:	PROVINCIA:	CÓDIGO PERFIL:	COORDENADAS UTM. HUSO 30 (ETRS89):		HOJA_MTN:
2004	CIUDAD REAL	CU101	X: 572600,000	Y: 4354500,000	717

TÉRM. MUNICIPAL: CASAS DE GUIJARRO **ALTITUD (m):** **PENDIENTE (%):** 0

SITUACIÓN: CARRETERA DE LA RODA A POZO AMARGO. CUENCA

USO: VIÑEDO EN SECANO **REFERENCIA:** GONZÁLEZ-QUIÑONES06, P

USDA-SOIL TAXONOMY (1975): RHODOXERAF PETROCÁLCICO

LEYENDA FAO (1974): Xk XEROSOL CÁLCICO **Nº HORIZONTES:** 3

HORIZONTES:

0 cm		Textura:	AF	Elem. gruesos (%):		Ca (cmol/Kg):	2,8
	Ap	Estructura:	GS	Arena gruesa (%):		Mg (cmol/Kg):	0,5
		Compactación:	MF	Arena fina (%):		Na (cmol/Kg):	0,5
		Raíces:	F	Arena total (%):	80,0	K (cmol/Kg):	0,4
		Color:	7,5YR4/4	Limo (%):	16,0	S (cmol/Kg):	4,2
		pH (H2O):	8,3	Arcilla (%):	4,0	CIC (cmol/Kg):	4,2
		CE (mS/cm):	0,2	C/N:	8,0	V = S/CIC (%):	100
		Caliza (%):	3,1	D. aparente (g/cm3):	1,7		
		Materia Orgánica (%):	0,7	Infiltración (mm/h):			
35 cm		Textura:	C	Elem. gruesos (%):		Ca (cmol/Kg):	21,1
	2Bt	Estructura:	B	Arena gruesa (%):		Mg (cmol/Kg):	1,7
		Compactación:	F-P	Arena fina (%):		Na (cmol/Kg):	0,4
		Raíces:	F	Arena total (%):	44,2	K (cmol/Kg):	0,8
		Color:	2,5YR3/6	Limo (%):	0,0	S (cmol/Kg):	24,0
		pH (H2O):	7,9	Arcilla (%):	55,8	CIC (cmol/Kg):	24,0
		CE (mS/cm):	0,2	C/N:	6,7	V = S/CIC (%):	100
		Caliza (%):	2,4	D. aparente (g/cm3):	1,2		
		Materia Orgánica (%):	0,3	Infiltración (mm/h):			
75 cm		Textura:	FA	Elem. gruesos (%):		Ca (cmol/Kg):	4,4
	2Ck/2Ckm	Estructura:	N	Arena gruesa (%):		Mg (cmol/Kg):	0,5
		Compactación:	F	Arena fina (%):		Na (cmol/Kg):	0,6
		Raíces:	MP	Arena total (%):	72,1	K (cmol/Kg):	0,3
		Color:	7,5YR6/8	Limo (%):	12,0	S (cmol/Kg):	5,8
		pH (H2O):	8,7	Arcilla (%):	16,0	CIC (cmol/Kg):	5,7
		CE (mS/cm):	0,3	C/N:	3,3	V = S/CIC (%):	100
		Caliza (%):	15,7	D. aparente (g/cm3):	1,5		
		Materia Orgánica (%):	0,2	Infiltración (mm/h):			

ÍNDICES DE VULNERABILIDAD RADIOLÓGICA DEL PERFIL:

CODSUELO	PARCIALES						TOTALES	
118	Infiltración	Retención Hídrica	Retención Físico-Química Cs	Retención Físico-Química Sr	Contenido en K	Contenido en Ca	Total al Cs	Total al Sr
CADENA ALIMENTARIA	2	1	2	1	2	1	2	1
IRRADIACIÓN EXTERNA	1	1	4	5	-	-	2	3

OBSERVACIONES: MATERIAL ORIGINAL: ARENAS, GRAVAS, ARCILLAS Y CANTOS DEL SISTEMA ALUVIAL DEL RÍO JÚCAR. SE APORTA VALOR DEL PORCENTAJE DE CALIZA ACTIVA.

Nº DE ORDEN:	PROVINCIA:	CÓDIGO PERFIL:	COORDENADAS UTM. HUSO 30 (ETRS89):		HOJA_MTN:
2005	HUESCA	HU101	X: 737229,000	Y: 4621753,000	357

TÉRM. MUNICIPAL: CASTEJÓN DE MONEGROS **ALTITUD (m):** 230 **PENDIENTE (%):** 1

SITUACIÓN: PUYAROLLOS

USO: MAIZAL (RIEGO POR ASPERSIÓN) **REFERENCIA:** BADIA11

USDA-SOIL TAXONOMY (1975):

LEYENDA FAO (1974): Re REGOSOL EUTRICO **Nº HORIZONTES:** 6

HORIZONTES:

0 cm	Ap1	Textura:	FL	Elem. gruesos (%):	1	Ca (cmol/Kg):	41,0
		Estructura:	B	Arena gruesa (%):		Mg (cmol/Kg):	1,6
		Compactación:	S	Arena fina (%):		Na (cmol/Kg):	0,3
		Raíces:	F	Arena total (%):	28,4	K (cmol/Kg):	0,5
		Color:	10YR4,5/4	Limo (%):	53,6	S (cmol/Kg):	43,5
		pH (H2O):	8,2	Arcilla (%):	18,0	CIC (cmol/Kg):	14,9
		CE (mS/cm):	0,2	C/N:		V = S/CIC (%):	100
		Caliza (%):		D. aparente (g/cm3):	1,1		
		Materia Orgánica (%):	1,6	Infiltración (mm/h):			
20 cm	Ap2	Textura:	FL	Elem. gruesos (%):	<1	Ca (cmol/Kg):	44,4
		Estructura:	B	Arena gruesa (%):		Mg (cmol/Kg):	1,9
		Compactación:	S	Arena fina (%):		Na (cmol/Kg):	0,3
		Raíces:	P	Arena total (%):	27,8	K (cmol/Kg):	0,3
		Color:	10YR4,5/4	Limo (%):	54,3	S (cmol/Kg):	46,9
		pH (H2O):	8,3	Arcilla (%):	17,9	CIC (cmol/Kg):	12,7
		CE (mS/cm):	0,2	C/N:		V = S/CIC (%):	100
		Caliza (%):		D. aparente (g/cm3):	1,2		
		Materia Orgánica (%):	1,4	Infiltración (mm/h):			
40 cm	AC	Textura:	FL	Elem. gruesos (%):	13,4	Ca (cmol/Kg):	43,4
		Estructura:	B	Arena gruesa (%):		Mg (cmol/Kg):	4,6
		Compactación:	S	Arena fina (%):		Na (cmol/Kg):	0,3
		Raíces:	P	Arena total (%):	30,2	K (cmol/Kg):	0,2
		Color:	10YR4,5/4	Limo (%):	50,8	S (cmol/Kg):	48,6
		pH (H2O):	8,2	Arcilla (%):	19,0	CIC (cmol/Kg):	11,7
		CE (mS/cm):	0,2	C/N:		V = S/CIC (%):	100
		Caliza (%):		D. aparente (g/cm3):	1,1		
		Materia Orgánica (%):	1,2	Infiltración (mm/h):			
70 cm	C1	Textura:	F-FL	Elem. gruesos (%):	<1	Ca (cmol/Kg):	
		Estructura:	B	Arena gruesa (%):		Mg (cmol/Kg):	
		Compactación:	S	Arena fina (%):		Na (cmol/Kg):	
		Raíces:	MP	Arena total (%):	33,9	K (cmol/Kg):	
		Color:	10YR4,5/4	Limo (%):	50,0	S (cmol/Kg):	
		pH (H2O):	8,2	Arcilla (%):	16,1	CIC (cmol/Kg):	
		CE (mS/cm):	0,2	C/N:		V = S/CIC (%):	
		Caliza (%):		D. aparente (g/cm3):	1,2		
		Materia Orgánica (%):	0,6	Infiltración (mm/h):			
100 cm	2C	Textura:	FA	Elem. gruesos (%):	<1	Ca (cmol/Kg):	
		Estructura:	N	Arena gruesa (%):		Mg (cmol/Kg):	
		Compactación:	S	Arena fina (%):		Na (cmol/Kg):	
		Raíces:	MP	Arena total (%):	57,1	K (cmol/Kg):	
		Color:	10YR4,5/4	Limo (%):	33,1	S (cmol/Kg):	
		pH (H2O):	8,3	Arcilla (%):	9,8	CIC (cmol/Kg):	
		CE (mS/cm):	0,2	C/N:		V = S/CIC (%):	
		Caliza (%):		D. aparente (g/cm3):	1,1		
		Materia Orgánica (%):	0,5	Infiltración (mm/h):			

130 cm		Textura:	FA	Elem. gruesos (%):	<1	Ca (cmol/Kg):	
	3C	Estructura:	N	Arena gruesa (%):		Mg (cmol/Kg):	
		Compactación:	S	Arena fina (%):		Na (cmol/Kg):	
		Raíces:	N	Arena total (%):	68,5	K (cmol/Kg):	
		Color:	10YR4,5/4	Limo (%):	25,6	S (cmol/Kg):	
		pH (H2O):	8,3	Arcilla (%):	5,9	CIC (cmol/Kg):	
		CE (mS/cm):	0,1	C/N:		V = S/CIC (%):	
		Caliza (%):		D. aparente (g/cm3):	1,2		
		Materia Orgánica (%):	0,2	Infiltración (mm/h):			

ÍNDICES DE VULNERABILIDAD RADIOLÓGICA DEL PERFIL:

CODSUELO	PARCIALES						TOTALES	
206	Infiltración	Retención Hídrica	Retención Físico-Química Cs	Retención Físico-Química Sr	Contenido en K	Contenido en Ca	Total al Cs	Total al Sr
CADENA ALIMENTARIA	2	2	2	1	3	1	2	1
IRRADIACIÓN EXTERNA	2	3	4	5	-	-	3	4

OBSERVACIONES: MATERIAL ORIGINAL: MATERIAL DETRÍTICO FINO.

Nº DE ORDEN:	PROVINCIA:	CÓDIGO PERFIL:	COORDENADAS UTM. HUSO 30 (ETRS89):		HOJA_MTN:
2006	HUESCA	HU102	X: 694241,000	Y: 4683807,000	247

TÉRM. MUNICIPAL: LOARRE **ALTITUD (m):** 685 **PENDIENTE (%):** 2

SITUACIÓN: LA ESPLANETA. COMARCA: HOYA DE HUESCA

USO: ALMENDROS EN SECANO **REFERENCIA:** BADIA11

USDA-SOIL TAXONOMY (1975):

LEYENDA FAO (1974): Lk LUVISOL CALCICO **Nº HORIZONTES:** 4

HORIZONTES:

0 cm	Ap	Textura:	FC	Elem. gruesos (%):	36,3	Ca (cmol/Kg):	33,6
		Estructura:	B	Arena gruesa (%):	8,1	Mg (cmol/Kg):	0,4
		Compactación:	F	Arena fina (%):	28,3	Na (cmol/Kg):	0,1
		Raíces:	MP	Arena total (%):	36,3	K (cmol/Kg):	0,5
		Color:	5YR3/4	Limo (%):	29,7	S (cmol/Kg):	34,5
		pH (H2O):	7,7	Arcilla (%):	34,0	CIC (cmol/Kg):	23,8
		CE (mS/cm):	0,6	C/N:		V = S/CIC (%):	100
		Caliza (%):		D. aparente (g/cm3):	1,2		
		Materia Orgánica (%):	1,4	Infiltración (mm/h):			
40 cm	Bt	Textura:	C	Elem. gruesos (%):	11,7	Ca (cmol/Kg):	33,1
		Estructura:	B	Arena gruesa (%):	8,5	Mg (cmol/Kg):	0,6
		Compactación:	F	Arena fina (%):	22,8	Na (cmol/Kg):	0,1
		Raíces:	MP	Arena total (%):	31,3	K (cmol/Kg):	0,3
		Color:	2,5YR3/4	Limo (%):	27,0	S (cmol/Kg):	34,1
		pH (H2O):	7,8	Arcilla (%):	41,6	CIC (cmol/Kg):	25,4
		CE (mS/cm):	0,6	C/N:		V = S/CIC (%):	100
		Caliza (%):		D. aparente (g/cm3):	1,4		
		Materia Orgánica (%):	1,2	Infiltración (mm/h):			
70 cm	Bkc	Textura:	F	Elem. gruesos (%):	58	Ca (cmol/Kg):	37,4
		Estructura:	B	Arena gruesa (%):	14,0	Mg (cmol/Kg):	0,6
		Compactación:	F	Arena fina (%):	27,5	Na (cmol/Kg):	0,1
		Raíces:	N	Arena total (%):	41,5	K (cmol/Kg):	0,2
		Color:	7,5YR4/6	Limo (%):	35,4	S (cmol/Kg):	38,4
		pH (H2O):	8,5	Arcilla (%):	23,1	CIC (cmol/Kg):	20,5
		CE (mS/cm):	1,1	C/N:		V = S/CIC (%):	100
		Caliza (%):		D. aparente (g/cm3):	1,4		
		Materia Orgánica (%):	0,4	Infiltración (mm/h):			
120 cm	Ckm	Textura:		Elem. gruesos (%):		Ca (cmol/Kg):	
		Estructura:		Arena gruesa (%):		Mg (cmol/Kg):	
		Compactación:		Arena fina (%):		Na (cmol/Kg):	
		Raíces:		Arena total (%):		K (cmol/Kg):	
		Color:		Limo (%):		S (cmol/Kg):	
		pH (H2O):		Arcilla (%):		CIC (cmol/Kg):	
		CE (mS/cm):		C/N:		V = S/CIC (%):	
		Caliza (%):		D. aparente (g/cm3):			
		Materia Orgánica (%):		Infiltración (mm/h):			

ÍNDICES DE VULNERABILIDAD RADIOLÓGICA DEL PERFIL:

CODSUELO	PARCIALES						TOTALES	
244	Infiltración	Retención Hídrica	Retención Físico-Química Cs	Retención Físico-Química Sr	Contenido en K	Contenido en Ca	Total al Cs	Total al Sr
CADENA ALIMENTARIA	2	3	2	1	3	1	3	2
IRRADIACIÓN EXTERNA	2	4	4	5	-	-	4	4

OBSERVACIONES: MATERIAL ORIGINAL: DETRÍTICO FINO (<2 M) SOBRE GRUESO (2M).

Nº DE ORDEN:	PROVINCIA:	CÓDIGO PERFIL:	COORDENADAS UTM. HUSO 30 (ETRS89):		HOJA_MTN:
2007	HUESCA	HU103	X: 760790,420	Y: 4613130,540	386

TÉRM. MUNICIPAL: BALLOBAR **ALTITUD (m):** 255 **PENDIENTE (%):** 1

SITUACIÓN: PARAJE: EL BASAL. COMARCA: BAJO CINCA

USO: GANADERO OCASIONAL **REFERENCIA:** BADIA11

USDA-SOIL TAXONOMY (1975):

LEYENDA FAO (1974): So SOLONETZ ORTICO **Nº HORIZONTES:** 4

HORIZONTES:

0 cm	Ahz	Textura:	FCL	Elem. gruesos (%):	0	Ca (cmol/Kg):	13,8
		Estructura:	L	Arena gruesa (%):	0,7	Mg (cmol/Kg):	6,3
		Compactación:	F	Arena fina (%):	7,2	Na (cmol/Kg):	10,8
		Raíces:	MP	Arena total (%):	7,9	K (cmol/Kg):	0,3
		Color:	10YR5/3,5	Limo (%):	65,4	S (cmol/Kg):	31,1
		pH (H2O):	8,1	Arcilla (%):	26,7	CIC (cmol/Kg):	12,3
		CE (mS/cm):	35,6	C/N:		V = S/CIC (%):	100
		Caliza (%):	26,0	D. aparente (g/cm3):	1,2		
		Materia Orgánica (%):	1,1	Infiltración (mm/h):			
26 cm	Btnz	Textura:	FCL	Elem. gruesos (%):	0	Ca (cmol/Kg):	11,7
		Estructura:	P	Arena gruesa (%):	0,2	Mg (cmol/Kg):	5,1
		Compactación:	MF	Arena fina (%):	3,3	Na (cmol/Kg):	12,4
		Raíces:	MP	Arena total (%):	3,5	K (cmol/Kg):	0,2
		Color:	5YR5/6	Limo (%):	57,6	S (cmol/Kg):	29,4
		pH (H2O):	8,8	Arcilla (%):	38,9	CIC (cmol/Kg):	15,2
		CE (mS/cm):	16,1	C/N:		V = S/CIC (%):	100
		Caliza (%):	31,9	D. aparente (g/cm3):	1,2		
		Materia Orgánica (%):	0,4	Infiltración (mm/h):			
50 cm	Cyz	Textura:	F	Elem. gruesos (%):	17	Ca (cmol/Kg):	
		Estructura:	N	Arena gruesa (%):	13,4	Mg (cmol/Kg):	
		Compactación:	F	Arena fina (%):	14,3	Na (cmol/Kg):	
		Raíces:	N	Arena total (%):	27,7	K (cmol/Kg):	
		Color:	10YR5/4	Limo (%):	46,5	S (cmol/Kg):	
		pH (H2O):	8,3	Arcilla (%):	25,8	CIC (cmol/Kg):	
		CE (mS/cm):	22,6	C/N:		V = S/CIC (%):	
		Caliza (%):	10,6	D. aparente (g/cm3):	1,4		
		Materia Orgánica (%):	0,1	Infiltración (mm/h):			
80 cm	R	Textura:		Elem. gruesos (%):		Ca (cmol/Kg):	
		Estructura:		Arena gruesa (%):		Mg (cmol/Kg):	
		Compactación:		Arena fina (%):		Na (cmol/Kg):	
		Raíces:		Arena total (%):		K (cmol/Kg):	
		Color:		Limo (%):		S (cmol/Kg):	
		pH (H2O):		Arcilla (%):		CIC (cmol/Kg):	
		CE (mS/cm):		C/N:		V = S/CIC (%):	
		Caliza (%):		D. aparente (g/cm3):			
		Materia Orgánica (%):		Infiltración (mm/h):			

ÍNDICES DE VULNERABILIDAD RADIOLÓGICA DEL PERFIL:

CODSUELO	PARCIALES						TOTALES	
1029	Infiltración	Retención Hídrica	Retención Físico-Química Cs	Retención Físico-Química Sr	Contenido en K	Contenido en Ca	Total al Cs	Total al Sr
CADENA ALIMENTARIA	2	2	1	1	4	1	2	1
IRRADIACIÓN EXTERNA	2	2	5	5	-	-	3	3

OBSERVACIONES: MATERIAL ORIGINAL: CALIZAS Y MARGAS. OLIGOCENO. SE APORTA VALOR DEL PORCENTAJE DE CALIZA TOTAL; LOS VALORES DE CALIZA ACTIVA EN LOS TRES PRIMEROS HORIZONTES SON: 8,2%, 8,0% Y 11,6%.

Nº DE ORDEN:	PROVINCIA:	CÓDIGO PERFIL:	COORDENADAS UTM. HUSO 30 (ETRS89):		HOJA_MTN:
2008	HUESCA	HU104	X: 701400,000	Y: 4675200,000	247

TÉRM. MUNICIPAL: LA SOTONERA **ALTITUD (m):** 484 **PENDIENTE (%):** 1

SITUACIÓN: GUADASESPE-1. COMARCA: HOYA DE HUESCA

USO: CEREAL EN SECANO **REFERENCIA:** BADIA11

USDA-SOIL TAXONOMY (1975):

LEYENDA FAO (1974): Xk XEROSOL CALCICO **Nº HORIZONTES:** 5

HORIZONTES:

0 cm	Ap1	Textura:	FC	Elem. gruesos (%):	<1	Ca (cmol/Kg):	48,6
		Estructura:	B-G	Arena gruesa (%):	5,1	Mg (cmol/Kg):	1,3
		Compactación:	F	Arena fina (%):	20,7	Na (cmol/Kg):	0,2
		Raíces:	A	Arena total (%):	25,8	K (cmol/Kg):	0,5
		Color:	2,5Y4/1	Limo (%):	45,5	S (cmol/Kg):	50,6
		pH (H2O):	8,0	Arcilla (%):	28,7	CIC (cmol/Kg):	27,5
		CE (mS/cm):	1,6	C/N:	13,2	V = S/CIC (%):	100
		Caliza (%):	54,5	D. aparente (g/cm3):	1,2		
		Materia Orgánica (%):	5,8	Infiltración (mm/h):			
20 cm	Ap2	Textura:	FC	Elem. gruesos (%):	<1	Ca (cmol/Kg):	41,5
		Estructura:	B-G	Arena gruesa (%):	4,8	Mg (cmol/Kg):	4,0
		Compactación:	F	Arena fina (%):	16,3	Na (cmol/Kg):	0,3
		Raíces:	MP	Arena total (%):	21,1	K (cmol/Kg):	0,2
		Color:	2,5Y4,5/1	Limo (%):	46,3	S (cmol/Kg):	45,9
		pH (H2O):	7,9	Arcilla (%):	32,6	CIC (cmol/Kg):	25,7
		CE (mS/cm):	1,9	C/N:	10,2	V = S/CIC (%):	100
		Caliza (%):	54,8	D. aparente (g/cm3):	1,2		
		Materia Orgánica (%):	3,8	Infiltración (mm/h):			
40 cm	Ckcg	Textura:	FCL	Elem. gruesos (%):	14,5	Ca (cmol/Kg):	32,8
		Estructura:	B-G	Arena gruesa (%):	1,1	Mg (cmol/Kg):	2,9
		Compactación:	F	Arena fina (%):	4,7	Na (cmol/Kg):	0,2
		Raíces:	MP	Arena total (%):	5,7	K (cmol/Kg):	0,1
		Color:	2,5Y7/1	Limo (%):	62,6	S (cmol/Kg):	35,9
		pH (H2O):	8,0	Arcilla (%):	31,7	CIC (cmol/Kg):	19,7
		CE (mS/cm):	1,9	C/N:	7,5	V = S/CIC (%):	100
		Caliza (%):	74,9	D. aparente (g/cm3):	1,2		
		Materia Orgánica (%):	2,0	Infiltración (mm/h):			
65 cm	R1	Textura:		Elem. gruesos (%):		Ca (cmol/Kg):	
		Estructura:		Arena gruesa (%):		Mg (cmol/Kg):	
		Compactación:		Arena fina (%):		Na (cmol/Kg):	
		Raíces:		Arena total (%):		K (cmol/Kg):	
		Color:		Limo (%):		S (cmol/Kg):	
		pH (H2O):		Arcilla (%):		CIC (cmol/Kg):	
		CE (mS/cm):		C/N:		V = S/CIC (%):	
		Caliza (%):		D. aparente (g/cm3):			
		Materia Orgánica (%):		Infiltración (mm/h):			
100 cm	R2	Textura:		Elem. gruesos (%):		Ca (cmol/Kg):	
		Estructura:		Arena gruesa (%):		Mg (cmol/Kg):	
		Compactación:		Arena fina (%):		Na (cmol/Kg):	
		Raíces:		Arena total (%):		K (cmol/Kg):	
		Color:		Limo (%):		S (cmol/Kg):	
		pH (H2O):		Arcilla (%):		CIC (cmol/Kg):	
		CE (mS/cm):		C/N:		V = S/CIC (%):	
		Caliza (%):		D. aparente (g/cm3):			
		Materia Orgánica (%):		Infiltración (mm/h):			

ÍNDICES DE VULNERABILIDAD RADIOLÓGICA DEL PERFIL:

CODSUELO	PARCIALES						TOTALES	
118	Infiltración	Retención Hídrica	Retención Físico-Química Cs	Retención Físico-Química Sr	Contenido en K	Contenido en Ca	Total al Cs	Total al Sr
CADENA ALIMENTARIA	2	2	2	1	4	1	3	1
IRRADIACIÓN EXTERNA	2	1	4	5	-	-	3	3

OBSERVACIONES: MATERIAL ORIGINAL: DETRÍTICO FINO DEL HOLOCENO. SE APORTA VALOR DEL PORCENTAJE DE CALIZA TOTAL.

Nº DE ORDEN:	PROVINCIA:	CÓDIGO PERFIL:	COORDENADAS UTM. HUSO 30 (ETRS89):		HOJA_MTN:
2009	HUESCA	HU105	X: 759059,820	Y: 4614462,900	386

TÉRM. MUNICIPAL: ONTIÑENA **ALTITUD (m):** 247 **PENDIENTE (%):** 3

SITUACIÓN: PARAJE MOLUNA BAJA. CORRAL DE REINÉ. COMARCA: BAJO CINCA

USO: ALTERNANCIA DE BARBECHO CON CEBADA. NO ADMITE LEGU **REFERENCIA:** BADIA11

USDA-SOIL TAXONOMY (1975):

LEYENDA FAO (1974): Xk XEROSOL CÁLCICO FASE SALINA **Nº HORIZONTES:** 5

HORIZONTES:

0 cm	ApZ1	Textura:	FCL	Elem. gruesos (%):	1,1	Ca (cmol/Kg):	11,4
		Estructura:	B	Arena gruesa (%):	0,5	Mg (cmol/Kg):	2,1
		Compactación:	FR	Arena fina (%):	10,0	Na (cmol/Kg):	3,6
		Raíces:	P	Arena total (%):	10,5	K (cmol/Kg):	0,3
		Color:		Limo (%):	60,7	S (cmol/Kg):	17,5
		pH (H2O):	8,6	Arcilla (%):	28,7	CIC (cmol/Kg):	13,8
		CE (mS/cm):	8,5	C/N:		V = S/CIC (%):	100
		Caliza (%):	22,1	D. aparente (g/cm3):	1,2		
		Materia Orgánica (%):	1,4	Infiltración (mm/h):			
20 cm	Apz2	Textura:	FCL	Elem. gruesos (%):	1	Ca (cmol/Kg):	12,6
		Estructura:	B	Arena gruesa (%):	0,3	Mg (cmol/Kg):	3,1
		Compactación:	F	Arena fina (%):	6,5	Na (cmol/Kg):	6,1
		Raíces:	P	Arena total (%):	6,8	K (cmol/Kg):	0,3
		Color:		Limo (%):	56,8	S (cmol/Kg):	22,1
		pH (H2O):	8,4	Arcilla (%):	36,5	CIC (cmol/Kg):	15,8
		CE (mS/cm):	14,5	C/N:		V = S/CIC (%):	100
		Caliza (%):	25,2	D. aparente (g/cm3):	1,2		
		Materia Orgánica (%):	1,1	Infiltración (mm/h):			
40 cm	ACz	Textura:	FCL	Elem. gruesos (%):	1,1	Ca (cmol/Kg):	
		Estructura:	B	Arena gruesa (%):	0,4	Mg (cmol/Kg):	
		Compactación:	F	Arena fina (%):	6,8	Na (cmol/Kg):	
		Raíces:	MP	Arena total (%):	7,2	K (cmol/Kg):	
		Color:		Limo (%):	55,3	S (cmol/Kg):	
		pH (H2O):	8,3	Arcilla (%):	37,5	CIC (cmol/Kg):	15,3
		CE (mS/cm):	25,3	C/N:		V = S/CIC (%):	
		Caliza (%):	28,1	D. aparente (g/cm3):	1,2		
		Materia Orgánica (%):	0,7	Infiltración (mm/h):			
60 cm	Ckcz	Textura:	FC	Elem. gruesos (%):	<1	Ca (cmol/Kg):	
		Estructura:	B	Arena gruesa (%):	2,2	Mg (cmol/Kg):	
		Compactación:	F	Arena fina (%):	18,5	Na (cmol/Kg):	
		Raíces:	MP	Arena total (%):	20,7	K (cmol/Kg):	
		Color:		Limo (%):	52,6	S (cmol/Kg):	
		pH (H2O):	8,4	Arcilla (%):	26,8	CIC (cmol/Kg):	10,7
		CE (mS/cm):	29,3	C/N:		V = S/CIC (%):	
		Caliza (%):	41,8	D. aparente (g/cm3):	1,2		
		Materia Orgánica (%):	0,4	Infiltración (mm/h):			
92 cm	R	Textura:		Elem. gruesos (%):		Ca (cmol/Kg):	
		Estructura:		Arena gruesa (%):		Mg (cmol/Kg):	
		Compactación:		Arena fina (%):		Na (cmol/Kg):	
		Raíces:		Arena total (%):		K (cmol/Kg):	
		Color:		Limo (%):		S (cmol/Kg):	
		pH (H2O):		Arcilla (%):		CIC (cmol/Kg):	
		CE (mS/cm):		C/N:		V = S/CIC (%):	
		Caliza (%):		D. aparente (g/cm3):			
		Materia Orgánica (%):		Infiltración (mm/h):			

ÍNDICES DE VULNERABILIDAD RADIOLÓGICA DEL PERFIL:

CODSUELO	PARCIALES						TOTALES	
117	Infiltración	Retención Hídrica	Retención Físico-Química Cs	Retención Físico-Química Sr	Contenido en K	Contenido en Ca	Total al Cs	Total al Sr
CADENA ALIMENTARIA	2	2	2	1	3	1	2	1
IRRADIACIÓN EXTERNA	2	2	4	5	-	-	3	3

OBSERVACIONES: MATERIAL ORIGINAL: CALIZAS Y MARGAS POLICROMAS OLIGOCENAS. SE APORTA VALOR DEL PORCENTAJE DE CALIZA TOTAL; LOS VALORES DE CALIZA ACTIVA EN LOS CUATRO PRIMEROS HORIZONTES SON: 7,3%, 7,90%, 9,5% Y 8,8%.

Nº DE ORDEN:	PROVINCIA:	CÓDIGO PERFIL:	COORDENADAS UTM. HUSO 30 (ETRS89):		HOJA_MTN:
2010	HUESCA	HU106	X: 698900,000	Y: 4670005,000	247

TÉRM. MUNICIPAL: LUPIÑÉN-ORTILLA **ALTITUD (m):** 490 **PENDIENTE (%):** 10

SITUACIÓN: RIPAS DE LIPIÑÉN. COMARCA: HOYA DE HUESCA

USO: ESPARTAL O ALBARDINAR **REFERENCIA:** BADIA11

USDA-SOIL TAXONOMY (1975):

LEYENDA FAO (1974): Zo SOLONCHAK ORTICO **Nº HORIZONTES:** 3

HORIZONTES:

0 cm	Ah	Textura:	F	Elem. gruesos (%):	1	Ca (cmol/Kg):	35,4
		Estructura:	B	Arena gruesa (%):	3,3	Mg (cmol/Kg):	0,6
		Compactación:	S	Arena fina (%):	35,9	Na (cmol/Kg):	2,3
		Raíces:	A	Arena total (%):	39,2	K (cmol/Kg):	0,5
		Color:	10YR4/4	Limo (%):	42,0	S (cmol/Kg):	38,8
		pH (H2O):	8,6	Arcilla (%):	18,8	CIC (cmol/Kg):	22,3
		CE (mS/cm):	0,4	C/N:	8,2	V = S/CIC (%):	100
		Caliza (%):	38,6	D. aparente (g/cm3):	1,4		
		Materia Orgánica (%):	1,6	Infiltración (mm/h):			
25 cm	Cnz1	Textura:	FC	Elem. gruesos (%):	<1	Ca (cmol/Kg):	42,3
		Estructura:	L	Arena gruesa (%):	0,5	Mg (cmol/Kg):	1,4
		Compactación:	F	Arena fina (%):	11,8	Na (cmol/Kg):	14,5
		Raíces:	F	Arena total (%):	12,3	K (cmol/Kg):	0,3
		Color:	10YR5/4	Limo (%):	51,0	S (cmol/Kg):	58,5
		pH (H2O):	9,3	Arcilla (%):	36,7	CIC (cmol/Kg):	20,5
		CE (mS/cm):	5,6	C/N:	8,7	V = S/CIC (%):	100
		Caliza (%):	38,4	D. aparente (g/cm3):	1,2		
		Materia Orgánica (%):	0,8	Infiltración (mm/h):			
60 cm	Cnz2	Textura:	FL	Elem. gruesos (%):	<1	Ca (cmol/Kg):	16,1
		Estructura:	L	Arena gruesa (%):	2,2	Mg (cmol/Kg):	0,9
		Compactación:	F	Arena fina (%):	31,6	Na (cmol/Kg):	18,2
		Raíces:	MP	Arena total (%):	33,8	K (cmol/Kg):	0,2
		Color:	10YR6/4	Limo (%):	55,3	S (cmol/Kg):	35,4
		pH (H2O):	9,5	Arcilla (%):	10,9	CIC (cmol/Kg):	18,5
		CE (mS/cm):	7,2	C/N:	7,5	V = S/CIC (%):	100
		Caliza (%):	39,6	D. aparente (g/cm3):	1,4		
		Materia Orgánica (%):	0,5	Infiltración (mm/h):			

ÍNDICES DE VULNERABILIDAD RADIOLÓGICA DEL PERFIL:

CODSUELO	PARCIALES						TOTALES	
205	Infiltración	Retención Hídrica	Retención Físico-Química Cs	Retención Físico-Química Sr	Contenido en K	Contenido en Ca	Total al Cs	Total al Sr
CADENA ALIMENTARIA	2	1	2	1	3	1	2	1
IRRADIACIÓN EXTERNA	1	1	4	5	-	-	2	3

OBSERVACIONES: MATERIAL ORIGINAL: DETRÍTICO FINO DEL HOLOCENO SUPERIOR (CON RESTOS CERÁMICOS DE LA EDAD DEL BRONCE A MEDIEVAL). SE APORTA VALOR DEL PORCENTAJE DE CALIZA TOTAL.

Nº DE ORDEN:	PROVINCIA:	CÓDIGO PERFIL:	COORDENADAS UTM. HUSO 30 (ETRS89):		HOJA_MTN:
2011	HUESCA	HU107	X: 758440,890	Y: 4652921,800	325

TÉRM. MUNICIPAL: BARBASTRO **ALTITUD (m):** 405 **PENDIENTE (%):** 4

SITUACIÓN: TORRE FIERRO (LAS ALMUNIETAS)

USO: VIÑEDO CON RIEGO LOCALIZADO **REFERENCIA:** BADIA11

USDA-SOIL TAXONOMY (1975):

LEYENDA FAO (1974): Bk CAMBISOL CALCICO **Nº HORIZONTES:** 5

HORIZONTES:

0 cm	Ap	Textura:	FL	Elem. gruesos (%):	14,6	Ca (cmol/Kg):	54,8
		Estructura:	B	Arena gruesa (%):	2,5	Mg (cmol/Kg):	2,2
		Compactación:	F	Arena fina (%):	14,0	Na (cmol/Kg):	0,6
		Raíces:	A	Arena total (%):	16,5	K (cmol/Kg):	4,2
		Color:	10YR4/3	Limo (%):	59,2	S (cmol/Kg):	61,8
		pH (H2O):	7,8	Arcilla (%):	24,3	CIC (cmol/Kg):	29,7
		CE (mS/cm):	1,7	C/N:		V = S/CIC (%):	100
		Caliza (%):	16,3	D. aparente (g/cm3):	1,4		
		Materia Orgánica (%):	4,4	Infiltración (mm/h):			
30 cm	Bk	Textura:	FCL	Elem. gruesos (%):	7,2	Ca (cmol/Kg):	58,8
		Estructura:	B	Arena gruesa (%):	1,7	Mg (cmol/Kg):	1,1
		Compactación:	MF	Arena fina (%):	14,5	Na (cmol/Kg):	0,3
		Raíces:	A	Arena total (%):	16,2	K (cmol/Kg):	0,7
		Color:	10YR4/4	Limo (%):	54,5	S (cmol/Kg):	60,8
		pH (H2O):	7,9	Arcilla (%):	29,2	CIC (cmol/Kg):	25,8
		CE (mS/cm):	2,4	C/N:		V = S/CIC (%):	100
		Caliza (%):	24,6	D. aparente (g/cm3):	1,2		
		Materia Orgánica (%):	2,5	Infiltración (mm/h):			
50 cm	Bwkc	Textura:	FL	Elem. gruesos (%):	<1	Ca (cmol/Kg):	199,5
		Estructura:	B	Arena gruesa (%):	4,4	Mg (cmol/Kg):	1,3
		Compactación:	FR	Arena fina (%):	3,7	Na (cmol/Kg):	0,5
		Raíces:	MP	Arena total (%):	8,1	K (cmol/Kg):	0,2
		Color:	2,5Y5,5/4	Limo (%):	72,9	S (cmol/Kg):	201,4
		pH (H2O):	8,0	Arcilla (%):	19,0	CIC (cmol/Kg):	24,2
		CE (mS/cm):	2,7	C/N:		V = S/CIC (%):	100
		Caliza (%):	31,1	D. aparente (g/cm3):	1,4		
		Materia Orgánica (%):	1,4	Infiltración (mm/h):			
90 cm	Cy	Textura:	F	Elem. gruesos (%):	<1	Ca (cmol/Kg):	201,6
		Estructura:	B	Arena gruesa (%):	15,5	Mg (cmol/Kg):	1,1
		Compactación:	FR	Arena fina (%):	22,4	Na (cmol/Kg):	4,0
		Raíces:	N	Arena total (%):	37,9	K (cmol/Kg):	0,1
		Color:	2,5Y7/3	Limo (%):	47,3	S (cmol/Kg):	203,2
		pH (H2O):	7,7	Arcilla (%):	14,9	CIC (cmol/Kg):	23,1
		CE (mS/cm):	2,0	C/N:		V = S/CIC (%):	100
		Caliza (%):	3,4	D. aparente (g/cm3):	1,4		
		Materia Orgánica (%):	0,6	Infiltración (mm/h):			
120 cm	R	Textura:		Elem. gruesos (%):		Ca (cmol/Kg):	
		Estructura:		Arena gruesa (%):		Mg (cmol/Kg):	
		Compactación:		Arena fina (%):		Na (cmol/Kg):	
		Raíces:		Arena total (%):		K (cmol/Kg):	
		Color:		Limo (%):		S (cmol/Kg):	
		pH (H2O):		Arcilla (%):		CIC (cmol/Kg):	
		CE (mS/cm):		C/N:		V = S/CIC (%):	
		Caliza (%):		D. aparente (g/cm3):			
		Materia Orgánica (%):		Infiltración (mm/h):			

ÍNDICES DE VULNERABILIDAD RADIOLÓGICA DEL PERFIL:

CODSUELO	PARCIALES						TOTALES	
129	Infiltración	Retención Hídrica	Retención Físico-Química Cs	Retención Físico-Química Sr	Contenido en K	Contenido en Ca	Total al Cs	Total al Sr
CADENA ALIMENTARIA	2	2	2	1	1	1	2	1
IRRADIACIÓN EXTERNA	2	2	4	5	-	-	3	3

OBSERVACIONES: MATERIAL ORIGINAL: YESO MIOCENO. SE APORTA VALOR DEL PORCENTAJE DE CALIZA TOTAL.

Nº DE ORDEN:	PROVINCIA:	CÓDIGO PERFIL:	COORDENADAS UTM. HUSO 30 (ETRS89):		HOJA_MTN:
2012	HUESCA	HU108	X: 732703,000	Y: 4722649,000	178

TÉRM. MUNICIPAL: TORLA **ALTITUD (m):** 1193 **PENDIENTE (%):** 45

SITUACIÓN: CAMINO AL SOASO DE LINÁS DE BROTO. COMARCA: SOBRARBE

USO: QUEJIGAR CON BOJ, TOMILLOS Y ALIAGAS **REFERENCIA:** BADIA11

USDA-SOIL TAXONOMY (1975):

LEYENDA FAO (1974): E RENDSINA **Nº HORIZONTES:** 3

HORIZONTES:

0 cm	Ah1	Textura:	FC	Elem. gruesos (%):	36,5	Ca (cmol/Kg):	42,6
		Estructura:	G	Arena gruesa (%):	10,6	Mg (cmol/Kg):	0,9
		Compactación:	S	Arena fina (%):	19,0	Na (cmol/Kg):	0,1
		Raíces:	A	Arena total (%):	29,6	K (cmol/Kg):	0,8
		Color:	10YR4/2	Limo (%):	38,5	S (cmol/Kg):	44,4
		pH (H2O):	8,1	Arcilla (%):	32,0	CIC (cmol/Kg):	26,5
		CE (mS/cm):		C/N:	12,2	V = S/CIC (%):	100
		Caliza (%):	6,9	D. aparente (g/cm3):	1,2		
		Materia Orgánica (%):	7,8	Infiltración (mm/h):			
20 cm	Ah2	Textura:	F	Elem. gruesos (%):	70,1	Ca (cmol/Kg):	35,1
		Estructura:	G	Arena gruesa (%):	15,4	Mg (cmol/Kg):	0,6
		Compactación:	F	Arena fina (%):	25,0	Na (cmol/Kg):	0,1
		Raíces:	F	Arena total (%):	40,3	K (cmol/Kg):	0,4
		Color:	10YR5/3	Limo (%):	48,5	S (cmol/Kg):	36,1
		pH (H2O):	8,1	Arcilla (%):	11,2	CIC (cmol/Kg):	15,5
		CE (mS/cm):		C/N:	9,9	V = S/CIC (%):	100
		Caliza (%):	12,4	D. aparente (g/cm3):	1,4		
		Materia Orgánica (%):	2,3	Infiltración (mm/h):			
40 cm	R	Textura:		Elem. gruesos (%):		Ca (cmol/Kg):	
		Estructura:		Arena gruesa (%):		Mg (cmol/Kg):	
		Compactación:		Arena fina (%):		Na (cmol/Kg):	
		Raíces:		Arena total (%):		K (cmol/Kg):	
		Color:		Limo (%):		S (cmol/Kg):	
		pH (H2O):		Arcilla (%):		CIC (cmol/Kg):	
		CE (mS/cm):		C/N:		V = S/CIC (%):	
		Caliza (%):		D. aparente (g/cm3):			
		Materia Orgánica (%):		Infiltración (mm/h):			

ÍNDICES DE VULNERABILIDAD RADIOLÓGICA DEL PERFIL:

CODSUELO	PARCIALES						TOTALES	
203	Infiltración	Retención Hídrica	Retención Físico-Química Cs	Retención Físico-Química Sr	Contenido en K	Contenido en Ca	Total al Cs	Total al Sr
CADENA ALIMENTARIA	1	2	1	1	2	1	1	1
IRRADIACIÓN EXTERNA	1	2	5	5	-	-	3	3

OBSERVACIONES: MATERIAL ORIGINAL: TURBIDITAS EOCÉNICAS (ALTERNANCIA DE MARGAS Y CALCARENITAS). SE APORTA VALOR DEL PORCENTAJE DE CALIZA TOTAL.

Nº DE ORDEN:	PROVINCIA:	CÓDIGO PERFIL:	COORDENADAS UTM. HUSO 30 (ETRS89):		HOJA_MTN:
2013	HUESCA	HU109	X: 743000,000	Y: 4725000,000	178

TÉRM. MUNICIPAL: TORLA **ALTITUD (m):** 1420 **PENDIENTE (%):** 40

SITUACIÓN: ESBARRE A LA CUEVA. COMARCA: SOBRARBE

USO: HAYEDO CON BOJ **REFERENCIA:** BADIA11

USDA-SOIL TAXONOMY (1975):

LEYENDA FAO (1974): Bh CAMBISOL HUMICO **Nº HORIZONTES:** 6

HORIZONTES:

0 cm	Ah1	Textura:	FA	Elem. gruesos (%):	63,9	Ca (cmol/Kg):	49,1
		Estructura:	G	Arena gruesa (%):	19,5	Mg (cmol/Kg):	3,3
		Compactación:	S	Arena fina (%):	37,3	Na (cmol/Kg):	0,1
		Raíces:	A	Arena total (%):	56,8	K (cmol/Kg):	0,2
		Color:	10YR3/1	Limo (%):	29,4	S (cmol/Kg):	52,7
		pH (H2O):	7,8	Arcilla (%):	13,8	CIC (cmol/Kg):	25,3
		CE (mS/cm):		C/N:	14,7	V = S/CIC (%):	100
		Caliza (%):	3,7	D. aparente (g/cm3):	1,5		
		Materia Orgánica (%):	8,5	Infiltración (mm/h):			
20 cm	Ah2	Textura:	FA	Elem. gruesos (%):	74,4	Ca (cmol/Kg):	32,2
		Estructura:	G	Arena gruesa (%):	15,0	Mg (cmol/Kg):	4,5
		Compactación:	S	Arena fina (%):	37,1	Na (cmol/Kg):	0,1
		Raíces:	A	Arena total (%):	52,1	K (cmol/Kg):	0,1
		Color:	10YR3/2	Limo (%):	44,1	S (cmol/Kg):	36,9
		pH (H2O):	7,9	Arcilla (%):	3,9	CIC (cmol/Kg):	24,6
		CE (mS/cm):		C/N:	12,4	V = S/CIC (%):	100
		Caliza (%):	6,0	D. aparente (g/cm3):	1,5		
		Materia Orgánica (%):	5,8	Infiltración (mm/h):			
40 cm	Bw1	Textura:	FA	Elem. gruesos (%):	78,9	Ca (cmol/Kg):	21,0
		Estructura:	G	Arena gruesa (%):	18,5	Mg (cmol/Kg):	2,0
		Compactación:	S	Arena fina (%):	38,3	Na (cmol/Kg):	0,1
		Raíces:	F	Arena total (%):	56,8	K (cmol/Kg):	0,0
		Color:	10YR4/3	Limo (%):	39,8	S (cmol/Kg):	23,1
		pH (H2O):	8,1	Arcilla (%):	3,5	CIC (cmol/Kg):	16,8
		CE (mS/cm):		C/N:	12,5	V = S/CIC (%):	100
		Caliza (%):	51,2	D. aparente (g/cm3):	1,5		
		Materia Orgánica (%):	2,3	Infiltración (mm/h):			
70 cm	Bw2	Textura:	FA	Elem. gruesos (%):	67,5	Ca (cmol/Kg):	22,7
		Estructura:	B	Arena gruesa (%):	12,9	Mg (cmol/Kg):	1,8
		Compactación:	S	Arena fina (%):	39,1	Na (cmol/Kg):	0,1
		Raíces:	F	Arena total (%):	52,0	K (cmol/Kg):	0,1
		Color:	10YR4/3	Limo (%):	46,3	S (cmol/Kg):	24,6
		pH (H2O):	8,1	Arcilla (%):	1,8	CIC (cmol/Kg):	15,5
		CE (mS/cm):		C/N:	12,4	V = S/CIC (%):	100
		Caliza (%):	53,8	D. aparente (g/cm3):	1,5		
		Materia Orgánica (%):	1,9	Infiltración (mm/h):			
115 cm	C1	Textura:	FA	Elem. gruesos (%):	80,1	Ca (cmol/Kg):	23,7
		Estructura:	N	Arena gruesa (%):	42,2	Mg (cmol/Kg):	0,6
		Compactación:	S	Arena fina (%):	25,4	Na (cmol/Kg):	0,1
		Raíces:	P	Arena total (%):	67,6	K (cmol/Kg):	0,0
		Color:	10YR5/2	Limo (%):	29,7	S (cmol/Kg):	24,4
		pH (H2O):	8,3	Arcilla (%):	2,7	CIC (cmol/Kg):	11,2
		CE (mS/cm):		C/N:	9,9	V = S/CIC (%):	100
		Caliza (%):	72,1	D. aparente (g/cm3):	1,5		
		Materia Orgánica (%):	1,2	Infiltración (mm/h):			

150 cm		Textura:	FA	Elem. gruesos (%):	80,6	Ca (cmol/Kg):	17,4
	C2	Estructura:	N	Arena gruesa (%):	43,1	Mg (cmol/Kg):	0,4
		Compactación:	S	Arena fina (%):	20,4	Na (cmol/Kg):	0,1
		Raíces:	N	Arena total (%):	63,5	K (cmol/Kg):	0,0
		Color:	10YR5,5/2	Limo (%):	33,9	S (cmol/Kg):	18,0
		pH (H2O):	8,4	Arcilla (%):	2,6	CIC (cmol/Kg):	9,9
		CE (mS/cm):		C/N:	9,8	V = S/CIC (%):	100
		Caliza (%):	69,0	D. aparente (g/cm3):	1,5		
		Materia Orgánica (%):	0,8	Infiltración (mm/h):			

ÍNDICES DE VULNERABILIDAD RADIOLÓGICA DEL PERFIL:

CODSUELO	PARCIALES						TOTALES	
124	Infiltración	Retención Hídrica	Retención Físico-Química Cs	Retención Físico-Química Sr	Contenido en K	Contenido en Ca	Total al Cs	Total al Sr
CADENA ALIMENTARIA	1	1	2	1	5	1	2	1
IRRADIACIÓN EXTERNA	1	2	4	5	-	-	3	3

OBSERVACIONES: MATERIAL ORIGINAL: TILLS. SE APORTA VALOR DEL PORCENTAJE DE CALIZA TOTAL.

Nº DE ORDEN:	PROVINCIA:	CÓDIGO PERFIL:	COORDENADAS UTM. HUSO 30 (ETRS89):		HOJA_MTN:
2014	HUESCA	HU110	X: 733737,000	Y: 4721817,000	178

TÉRM. MUNICIPAL: TORLA **ALTITUD (m):** 1230 **PENDIENTE (%):** 2

SITUACIÓN: SIERRA VIU. COMARCA: SOBRARBE

USO: DEPÓSITO MORRÉNICO (TILLS) **REFERENCIA:** BADIA11

USDA-SOIL TAXONOMY (1975):

LEYENDA FAO (1974): Re REGOSOL EUTRICO **Nº HORIZONTES:** 4

HORIZONTES:

0 cm	Ah	Textura:	F	Elem. gruesos (%):	36,5	Ca (cmol/Kg):	42,2
		Estructura:	G	Arena gruesa (%):	20,2	Mg (cmol/Kg):	1,0
		Compactación:	S	Arena fina (%):	24,8	Na (cmol/Kg):	0,2
		Raíces:	A	Arena total (%):	45,0	K (cmol/Kg):	0,8
		Color:	10YR3/2	Limo (%):	35,7	S (cmol/Kg):	44,1
		pH (H2O):	7,8	Arcilla (%):	19,3	CIC (cmol/Kg):	27,4
		CE (mS/cm):		C/N:	12,2	V = S/CIC (%):	100
		Caliza (%):	16,5	D. aparente (g/cm3):	1,4		
		Materia Orgánica (%):	8,5	Infiltración (mm/h):			
25 cm	2C1	Textura:	FA	Elem. gruesos (%):	86,5	Ca (cmol/Kg):	20,7
		Estructura:	N	Arena gruesa (%):	31,8	Mg (cmol/Kg):	0,9
		Compactación:	S	Arena fina (%):	20,4	Na (cmol/Kg):	0,1
		Raíces:	F	Arena total (%):	52,2	K (cmol/Kg):	0,2
		Color:	2,5Y4/3	Limo (%):	31,4	S (cmol/Kg):	21,9
		pH (H2O):	8,5	Arcilla (%):	16,4	CIC (cmol/Kg):	12,9
		CE (mS/cm):		C/N:	10,9	V = S/CIC (%):	100
		Caliza (%):	34,2	D. aparente (g/cm3):	1,5		
		Materia Orgánica (%):	1,8	Infiltración (mm/h):			
60 cm	2C2	Textura:	FA	Elem. gruesos (%):	70,5	Ca (cmol/Kg):	18,1
		Estructura:	N	Arena gruesa (%):	49,7	Mg (cmol/Kg):	0,6
		Compactación:	S	Arena fina (%):	16,9	Na (cmol/Kg):	0,1
		Raíces:	F	Arena total (%):	66,6	K (cmol/Kg):	0,1
		Color:	2,5Y4/2,5	Limo (%):	18,3	S (cmol/Kg):	18,8
		pH (H2O):	8,5	Arcilla (%):	15,1	CIC (cmol/Kg):	12,5
		CE (mS/cm):		C/N:	6,0	V = S/CIC (%):	100
		Caliza (%):	36,3	D. aparente (g/cm3):	1,5		
		Materia Orgánica (%):	0,6	Infiltración (mm/h):			
90 cm	3C	Textura:	FA	Elem. gruesos (%):	46,8	Ca (cmol/Kg):	22,0
		Estructura:	N	Arena gruesa (%):	37,2	Mg (cmol/Kg):	0,4
		Compactación:	F	Arena fina (%):	36,0	Na (cmol/Kg):	0,1
		Raíces:	P	Arena total (%):	73,2	K (cmol/Kg):	0,2
		Color:	2,5Y5/3	Limo (%):	10,4	S (cmol/Kg):	22,7
		pH (H2O):	8,5	Arcilla (%):	16,5	CIC (cmol/Kg):	16,5
		CE (mS/cm):		C/N:	7,1	V = S/CIC (%):	100
		Caliza (%):	31,5	D. aparente (g/cm3):	1,5		
		Materia Orgánica (%):	0,7	Infiltración (mm/h):			

ÍNDICES DE VULNERABILIDAD RADIOLÓGICA DEL PERFIL:

CODSUELO	PARCIALES						TOTALES	
206	Infiltración	Retención Hídrica	Retención Físico-Química Cs	Retención Físico-Química Sr	Contenido en K	Contenido en Ca	Total al Cs	Total al Sr
CADENA ALIMENTARIA	1	1	2	1	3	1	2	1
IRRADIACIÓN EXTERNA	2	1	4	5	-	-	3	3

OBSERVACIONES: MATERIAL ORIGINAL: DEPÓSITO MORRÉNICO (TILLS). SE APORTA VALOR DEL PORCENTAJE DE CALIZA TOTAL.

Nº DE ORDEN:	PROVINCIA:	CÓDIGO PERFIL:	COORDENADAS UTM. HUSO 30 (ETRS89):		HOJA_MTN:
2015	HUESCA	HU111	X: 731914,000	Y: 4722407,000	178

TÉRM. MUNICIPAL: TORLA **ALTITUD (m):** 1230 **PENDIENTE (%):** 3

SITUACIÓN: COMUNAL DE LINÁS DE BROTO. COMARCA: SOBRARBE

USO: PASTO **REFERENCIA:** BADIA11

USDA-SOIL TAXONOMY (1975):

LEYENDA FAO (1974): Bg CAMBISOL GLEICO **Nº HORIZONTES:** 6

HORIZONTES:

0 cm	Ah1	Textura:	FC	Elem. gruesos (%):	2,1	Ca (cmol/Kg):	21,1
		Estructura:	G	Arena gruesa (%):	8,1	Mg (cmol/Kg):	1,3
		Compactación:	S	Arena fina (%):	26,4	Na (cmol/Kg):	0,1
		Raíces:	A	Arena total (%):	34,5	K (cmol/Kg):	0,6
		Color:	10YR3/2	Limo (%):	35,9	S (cmol/Kg):	23,1
		pH (H2O):	6,0	Arcilla (%):	29,6	CIC (cmol/Kg):	25,3
		CE (mS/cm):		C/N:	10,3	V = S/CIC (%):	91
		Caliza (%):	0,0	D. aparente (g/cm3):	1,2		
		Materia Orgánica (%):	9,4	Infiltración (mm/h):			
10 cm	Ah2	Textura:	F	Elem. gruesos (%):	43,1	Ca (cmol/Kg):	11,8
		Estructura:	G	Arena gruesa (%):	15,6	Mg (cmol/Kg):	0,4
		Compactación:	S	Arena fina (%):	30,9	Na (cmol/Kg):	0,1
		Raíces:	F	Arena total (%):	46,5	K (cmol/Kg):	0,5
		Color:	10YR3,5/3	Limo (%):	31,1	S (cmol/Kg):	12,7
		pH (H2O):	6,1	Arcilla (%):	22,4	CIC (cmol/Kg):	17,8
		CE (mS/cm):		C/N:	8,9	V = S/CIC (%):	72
		Caliza (%):	0,0	D. aparente (g/cm3):	1,4		
		Materia Orgánica (%):	4,4	Infiltración (mm/h):			
34 cm	Bw	Textura:	F	Elem. gruesos (%):	72,4	Ca (cmol/Kg):	7,4
		Estructura:	B	Arena gruesa (%):	20,2	Mg (cmol/Kg):	0,2
		Compactación:	S	Arena fina (%):	26,3	Na (cmol/Kg):	0,1
		Raíces:	F	Arena total (%):	46,5	K (cmol/Kg):	0,3
		Color:	10YR4/3	Limo (%):	30,2	S (cmol/Kg):	8,0
		pH (H2O):	6,5	Arcilla (%):	23,3	CIC (cmol/Kg):	12,0
		CE (mS/cm):		C/N:	4,9	V = S/CIC (%):	66
		Caliza (%):	0,0	D. aparente (g/cm3):	1,4		
		Materia Orgánica (%):	1,3	Infiltración (mm/h):			
70 cm	C	Textura:	FCA	Elem. gruesos (%):	78,1	Ca (cmol/Kg):	9,8
		Estructura:	N	Arena gruesa (%):	30,2	Mg (cmol/Kg):	0,3
		Compactación:	S	Arena fina (%):	24,4	Na (cmol/Kg):	0,1
		Raíces:	P	Arena total (%):	54,6	K (cmol/Kg):	0,3
		Color:	10YR4,5/3	Limo (%):	24,3	S (cmol/Kg):	10,4
		pH (H2O):	6,8	Arcilla (%):	21,1	CIC (cmol/Kg):	11,6
		CE (mS/cm):		C/N:	4,0	V = S/CIC (%):	90
		Caliza (%):	0,0	D. aparente (g/cm3):	1,2		
		Materia Orgánica (%):	0,6	Infiltración (mm/h):			
120 cm	2Ckg	Textura:	FA	Elem. gruesos (%):	86,2	Ca (cmol/Kg):	24,4
		Estructura:	N	Arena gruesa (%):	34,9	Mg (cmol/Kg):	0,2
		Compactación:	S	Arena fina (%):	23,8	Na (cmol/Kg):	0,1
		Raíces:	N	Arena total (%):	58,7	K (cmol/Kg):	0,1
		Color:	2,5Y5/3	Limo (%):	21,4	S (cmol/Kg):	24,8
		pH (H2O):	8,1	Arcilla (%):	19,9	CIC (cmol/Kg):	11,2
		CE (mS/cm):		C/N:		V = S/CIC (%):	100
		Caliza (%):	21,5	D. aparente (g/cm3):	1,5		
		Materia Orgánica (%):	0,3	Infiltración (mm/h):			

160 cm		Textura:	AF	Elem. gruesos (%):	66,4	Ca (cmol/Kg):	25,3
	3Ckg	Estructura:	N	Arena gruesa (%):	63,1	Mg (cmol/Kg):	0,1
		Compactación:	S	Arena fina (%):	17,5	Na (cmol/Kg):	0,1
		Raíces:	N	Arena total (%):	80,6	K (cmol/Kg):	0,1
		Color:	2,5Y5/3	Limo (%):	11,8	S (cmol/Kg):	25,6
		pH (H2O):	8,7	Arcilla (%):	7,6	CIC (cmol/Kg):	9,5
		CE (mS/cm):		C/N:		V = S/CIC (%):	100
		Caliza (%):	33,2	D. aparente (g/cm3):	1,7		
		Materia Orgánica (%):	0,2	Infiltración (mm/h):			

ÍNDICES DE VULNERABILIDAD RADIOLÓGICA DEL PERFIL:

CODSUELO	PARCIALES						TOTALES	
25	Infiltración	Retención Hídrica	Retención Físico-Química Cs	Retención Físico-Química Sr	Contenido en K	Contenido en Ca	Total al Cs	Total al Sr
CADENA ALIMENTARIA	2	1	1	3	3	1	2	2
IRRADIACIÓN EXTERNA	3	1	5	3	-	-	3	3

OBSERVACIONES: MATERIAL ORIGINAL: DEPÓSITO DETRÍTICO GRUESO (GRAVAS Y CANTOS CON MATRIZ ARENOSA) DE ORIGEN GLACIO-LACUSTRE, DEL PLEISTOCENO SUPERIOR (50.000 AÑOS). SE APORTA VALOR DEL PORCENTAJE DE CALIZA TOTAL.

Nº DE ORDEN:	PROVINCIA:	CÓDIGO PERFIL:	COORDENADAS UTM. HUSO 30 (ETRS89):		HOJA_MTN:
2016	HUESCA	HU112	X: 749686,700	Y: 4673092,060	249

TÉRM. MUNICIPAL: ALQUEZAR **ALTITUD (m):** 670 **PENDIENTE (%):** 60

SITUACIÓN: CAMINO A LA ERMITA SAN GREGORIO. COMARCA: SOMONTANO

USO: CARRASCAL CON BOJ **REFERENCIA:** BADIA11

USDA-SOIL TAXONOMY (1975):

LEYENDA FAO (1974): E RENDSINA **Nº HORIZONTES:** 3

HORIZONTES:

0 cm	Ah	Textura:	FA	Elem. gruesos (%):		Ca (cmol/Kg):	28,6
		Estructura:	G	Arena gruesa (%):	20,1	Mg (cmol/Kg):	0,6
		Compactación:	F	Arena fina (%):	18,6	Na (cmol/Kg):	0,1
		Raíces:	A	Arena total (%):	38,7	K (cmol/Kg):	0,6
		Color:	5YR3/3	Limo (%):	29,8	S (cmol/Kg):	29,9
		pH (H2O):	7,3	Arcilla (%):	31,5	CIC (cmol/Kg):	23,2
		CE (mS/cm):		C/N:	14,3	V = S/CIC (%):	100
		Caliza (%):	2,0	D. aparente (g/cm3):	1,5		
		Materia Orgánica (%):	5,5	Infiltración (mm/h):			
20 cm	C/R	Textura:	FA	Elem. gruesos (%):		Ca (cmol/Kg):	49,3
		Estructura:	G	Arena gruesa (%):	19,9	Mg (cmol/Kg):	0,3
		Compactación:	F	Arena fina (%):	16,4	Na (cmol/Kg):	0,1
		Raíces:	F	Arena total (%):	36,3	K (cmol/Kg):	0,4
		Color:	5YR4/4	Limo (%):	29,1	S (cmol/Kg):	50,1
		pH (H2O):	7,5	Arcilla (%):	34,6	CIC (cmol/Kg):	16,8
		CE (mS/cm):		C/N:	9,9	V = S/CIC (%):	100
		Caliza (%):	10,7	D. aparente (g/cm3):	1,5		
		Materia Orgánica (%):	2,2	Infiltración (mm/h):			
40 cm	R	Textura:		Elem. gruesos (%):		Ca (cmol/Kg):	
		Estructura:		Arena gruesa (%):		Mg (cmol/Kg):	
		Compactación:		Arena fina (%):		Na (cmol/Kg):	
		Raíces:		Arena total (%):		K (cmol/Kg):	
		Color:		Limo (%):		S (cmol/Kg):	
		pH (H2O):		Arcilla (%):		CIC (cmol/Kg):	
		CE (mS/cm):		C/N:		V = S/CIC (%):	
		Caliza (%):		D. aparente (g/cm3):			
		Materia Orgánica (%):		Infiltración (mm/h):			

ÍNDICES DE VULNERABILIDAD RADIOLÓGICA DEL PERFIL:

CODSUELO	PARCIALES						TOTALES	
203	Infiltración	Retención Hídrica	Retención Físico-Química Cs	Retención Físico-Química Sr	Contenido en K	Contenido en Ca	Total al Cs	Total al Sr
CADENA ALIMENTARIA	1	2	1	2	2	1	1	1
IRRADIACIÓN EXTERNA	1	2	5	4	-	-	3	3

OBSERVACIONES: MATERIAL ORIGINAL: CALIZAS. SE APORTA VALOR DEL PORCENTAJE DE CALIZA TOTAL.

Nº DE ORDEN:	PROVINCIA:	CÓDIGO PERFIL:	COORDENADAS UTM. HUSO 30 (ETRS89):		HOJA_MTN:
2017	HUESCA	HU113	X: 755248,250	Y: 4664688,240	287

TÉRM. MUNICIPAL: SALAS BAJAS **ALTITUD (m):** 450 **PENDIENTE (%):** 2

SITUACIÓN: CABAÑERA. CAMINO DE SALAS BAJAS A BARBASTRO

USO: OLIVAR Y VIÑEDO EN SECANO **REFERENCIA:** BADIA11

USDA-SOIL TAXONOMY (1975):

LEYENDA FAO (1974): Bk CAMBISOL CALCICO **Nº HORIZONTES:** 5

HORIZONTES:

0 cm	Ap	Textura:	F	Elem. gruesos (%):	14,8	Ca (cmol/Kg):	39,7
		Estructura:	B	Arena gruesa (%):	15,2	Mg (cmol/Kg):	1,3
		Compactación:	S	Arena fina (%):	27,9	Na (cmol/Kg):	0,5
		Raíces:	F	Arena total (%):	43,1	K (cmol/Kg):	4,3
		Color:	7,5YR4/4	Limo (%):	35,8	S (cmol/Kg):	45,7
		pH (H2O):	8,2	Arcilla (%):	21,1	CIC (cmol/Kg):	24,5
		CE (mS/cm):		C/N:	9,4	V = S/CIC (%):	100
		Caliza (%):	15,6	D. aparente (g/cm3):	1,4		
		Materia Orgánica (%):	2,7	Infiltración (mm/h):			
40 cm	Bw	Textura:	FC	Elem. gruesos (%):	10,9	Ca (cmol/Kg):	30,0
		Estructura:	B	Arena gruesa (%):	14,9	Mg (cmol/Kg):	1,3
		Compactación:	F	Arena fina (%):	21,1	Na (cmol/Kg):	0,2
		Raíces:	F	Arena total (%):	36,0	K (cmol/Kg):	7,7
		Color:	7,5YR4,5/4	Limo (%):	34,5	S (cmol/Kg):	39,2
		pH (H2O):	8,0	Arcilla (%):	29,6	CIC (cmol/Kg):	25,3
		CE (mS/cm):		C/N:	8,5	V = S/CIC (%):	100
		Caliza (%):	14,3	D. aparente (g/cm3):	1,2		
		Materia Orgánica (%):	1,6	Infiltración (mm/h):			
80 cm	Bkc	Textura:	FC	Elem. gruesos (%):	79,3	Ca (cmol/Kg):	35,8
		Estructura:	B	Arena gruesa (%):	17,1	Mg (cmol/Kg):	0,7
		Compactación:	MF	Arena fina (%):	23,9	Na (cmol/Kg):	0,2
		Raíces:	P	Arena total (%):	41,0	K (cmol/Kg):	5,6
		Color:	7,5YR6/6	Limo (%):	31,3	S (cmol/Kg):	42,3
		pH (H2O):	8,6	Arcilla (%):	27,8	CIC (cmol/Kg):	24,5
		CE (mS/cm):		C/N:	8,4	V = S/CIC (%):	100
		Caliza (%):	20,6	D. aparente (g/cm3):	1,2		
		Materia Orgánica (%):	1,1	Infiltración (mm/h):			
100 cm	Ck	Textura:	FC	Elem. gruesos (%):	26,2	Ca (cmol/Kg):	39,8
		Estructura:	N	Arena gruesa (%):	12,9	Mg (cmol/Kg):	0,5
		Compactación:	MF	Arena fina (%):	21,8	Na (cmol/Kg):	0,2
		Raíces:	MP	Arena total (%):	34,7	K (cmol/Kg):	0,1
		Color:	10YR6/6	Limo (%):	37,5	S (cmol/Kg):	40,6
		pH (H2O):	8,7	Arcilla (%):	27,8	CIC (cmol/Kg):	24,8
		CE (mS/cm):		C/N:	6,8	V = S/CIC (%):	100
		Caliza (%):	49,8	D. aparente (g/cm3):	1,2		
		Materia Orgánica (%):	0,6	Infiltración (mm/h):			
140 cm	2C	Textura:	FL	Elem. gruesos (%):	0	Ca (cmol/Kg):	44,6
		Estructura:	N	Arena gruesa (%):	0,7	Mg (cmol/Kg):	3,5
		Compactación:	MF	Arena fina (%):	8,2	Na (cmol/Kg):	0,2
		Raíces:	N	Arena total (%):	8,9	K (cmol/Kg):	0,1
		Color:	10YR6/6	Limo (%):	69,8	S (cmol/Kg):	48,5
		pH (H2O):	8,4	Arcilla (%):	21,3	CIC (cmol/Kg):	23,2
		CE (mS/cm):		C/N:	6,7	V = S/CIC (%):	100
		Caliza (%):	33,8	D. aparente (g/cm3):	1,4		
		Materia Orgánica (%):	0,8	Infiltración (mm/h):			

ÍNDICES DE VULNERABILIDAD RADIOLÓGICA DEL PERFIL:

CODSUELO	PARCIALES						TOTALES	
127	Infiltración	Retención Hídrica	Retención Físico-Química Cs	Retención Físico-Química Sr	Contenido en K	Contenido en Ca	Total al Cs	Total al Sr
CADENA ALIMENTARIA	2	1	2	1	1	1	1	1
IRRADIACIÓN EXTERNA	2	1	4	5	-	-	3	3

OBSERVACIONES: MATERIAL ORIGINAL: DEPÓSITO DETRÍTICO FINO SOBRE MARGAS MIOCENAS. SE APORTA VALOR DEL PORCENTAJE DE CALIZA TOTAL.

Nº DE ORDEN:	PROVINCIA:	CÓDIGO PERFIL:	COORDENADAS UTM. HUSO 30 (ETRS89):		HOJA_MTN:
2018	HUESCA	HU114	X: 745075,000	Y: 4669875,000	287

TÉRM. MUNICIPAL: SASO DE ADAHUESCA **ALTITUD (m):** 615 **PENDIENTE (%):** 2

SITUACIÓN: ADAHUESCA

USO: VIÑEDO EN SECANO **REFERENCIA:** BADIA11

USDA-SOIL TAXONOMY (1975):

LEYENDA FAO (1974): Be CAMBISOL EUTRICO **Nº HORIZONTES:** 5

HORIZONTES:

0 cm	Ap	Textura:	F	Elem. gruesos (%):	10,5	Ca (cmol/Kg):	19,3
		Estructura:	B	Arena gruesa (%):	25,3	Mg (cmol/Kg):	1,5
		Compactación:	F-MF	Arena fina (%):	9,1	Na (cmol/Kg):	0,1
		Raíces:	F	Arena total (%):	34,4	K (cmol/Kg):	0,5
		Color:	7,5YR4/6	Limo (%):	38,2	S (cmol/Kg):	21,3
		pH (H2O):	6,8	Arcilla (%):	27,5	CIC (cmol/Kg):	20,3
		CE (mS/cm):		C/N:	8,1	V = S/CIC (%):	100
		Caliza (%):		D. aparente (g/cm3):	1,4		
		Materia Orgánica (%):	1,5	Infiltración (mm/h):			
20 cm	Bw	Textura:	FC	Elem. gruesos (%):	10,2	Ca (cmol/Kg):	22,7
		Estructura:	B	Arena gruesa (%):	20,4	Mg (cmol/Kg):	1,5
		Compactación:	F-MF	Arena fina (%):	6,9	Na (cmol/Kg):	0,1
		Raíces:	P	Arena total (%):	27,3	K (cmol/Kg):	0,4
		Color:	5YR4/6	Limo (%):	40,5	S (cmol/Kg):	24,6
		pH (H2O):	7,3	Arcilla (%):	32,3	CIC (cmol/Kg):	20,3
		CE (mS/cm):		C/N:	6,7	V = S/CIC (%):	100
		Caliza (%):		D. aparente (g/cm3):	1,2		
		Materia Orgánica (%):	1,1	Infiltración (mm/h):			
45 cm	Bt	Textura:	C	Elem. gruesos (%):	8,5	Ca (cmol/Kg):	32,3
		Estructura:	B	Arena gruesa (%):	9,8	Mg (cmol/Kg):	1,8
		Compactación:	MF	Arena fina (%):	8,6	Na (cmol/Kg):	0,2
		Raíces:	P	Arena total (%):	18,4	K (cmol/Kg):	0,6
		Color:	2,5YR4/4	Limo (%):	33,6	S (cmol/Kg):	34,8
		pH (H2O):	7,3	Arcilla (%):	48,0	CIC (cmol/Kg):	26,5
		CE (mS/cm):		C/N:	5,7	V = S/CIC (%):	100
		Caliza (%):		D. aparente (g/cm3):	1,2		
		Materia Orgánica (%):	0,8	Infiltración (mm/h):			
70 cm	Bkm	Textura:		Elem. gruesos (%):		Ca (cmol/Kg):	
		Estructura:		Arena gruesa (%):		Mg (cmol/Kg):	
		Compactación:		Arena fina (%):		Na (cmol/Kg):	
		Raíces:		Arena total (%):		K (cmol/Kg):	
		Color:		Limo (%):		S (cmol/Kg):	
		pH (H2O):		Arcilla (%):		CIC (cmol/Kg):	
		CE (mS/cm):		C/N:		V = S/CIC (%):	
		Caliza (%):		D. aparente (g/cm3):			
		Materia Orgánica (%):		Infiltración (mm/h):			
170 cm	Ck	Textura:		Elem. gruesos (%):		Ca (cmol/Kg):	
		Estructura:		Arena gruesa (%):		Mg (cmol/Kg):	
		Compactación:		Arena fina (%):		Na (cmol/Kg):	
		Raíces:		Arena total (%):		K (cmol/Kg):	
		Color:		Limo (%):		S (cmol/Kg):	
		pH (H2O):		Arcilla (%):		CIC (cmol/Kg):	
		CE (mS/cm):		C/N:		V = S/CIC (%):	
		Caliza (%):		D. aparente (g/cm3):			
		Materia Orgánica (%):		Infiltración (mm/h):			

ÍNDICES DE VULNERABILIDAD RADIOLÓGICA DEL PERFIL:

CODSUELO	PARCIALES						TOTALES	
21	Infiltración	Retención Hídrica	Retención Físico-Química Cs	Retención Físico-Química Sr	Contenido en K	Contenido en Ca	Total al Cs	Total al Sr
CADENA ALIMENTARIA	3	1	2	2	3	1	2	2
IRRADIACIÓN EXTERNA	2	1	4	4	-	-	3	3

OBSERVACIONES: MATERIAL ORIGINAL: MATERIAL DETRÍTICO, RUBEFACTADO; (GLACIS PLEISTOCENO).

Nº DE ORDEN:	PROVINCIA:	CÓDIGO PERFIL:	COORDENADAS UTM. HUSO 30 (ETRS89):		HOJA_MTN:
2019	HUESCA	HU115	X: 691828,000	Y: 4682233,000	247

TÉRM. MUNICIPAL: AYERBE **ALTITUD (m):** 598 **PENDIENTE (%):** 1

SITUACIÓN: SASO DE AYERBE. COMARCA: HOYA DE HUESCA

USO: VIÑEDO EN SECANO, EN MOSAICO CON ALMENDROS Y CEREA **REFERENCIA:** BADIA11

USDA-SOIL TAXONOMY (1975):

LEYENDA FAO (1974): Bk CAMBISOL CÁLCICO **Nº HORIZONTES:** 6

HORIZONTES:

0 cm	Ap1	Textura:	F	Elem. gruesos (%):	17,1	Ca (cmol/Kg):	40,1
		Estructura:	B	Arena gruesa (%):	14,2	Mg (cmol/Kg):	0,9
		Compactación:	S	Arena fina (%):	16,5	Na (cmol/Kg):	0,1
		Raíces:	MP	Arena total (%):	30,7	K (cmol/Kg):	0,6
		Color:	7,5YR4/6	Limo (%):	47,7	S (cmol/Kg):	41,7
		pH (H2O):	8,4	Arcilla (%):	21,6	CIC (cmol/Kg):	26,3
		CE (mS/cm):		C/N:	9,7	V = S/CIC (%):	100
		Caliza (%):	33,0	D. aparente (g/cm3):	1,4		
		Materia Orgánica (%):	2,4	Infiltración (mm/h):			
10 cm	Ap2	Textura:	F	Elem. gruesos (%):	17,2	Ca (cmol/Kg):	45,0
		Estructura:	B	Arena gruesa (%):	10,4	Mg (cmol/Kg):	0,4
		Compactación:	F-FR	Arena fina (%):	24,7	Na (cmol/Kg):	0,1
		Raíces:	MP	Arena total (%):	35,1	K (cmol/Kg):	0,4
		Color:	7,5YR4/6	Limo (%):	45,7	S (cmol/Kg):	45,9
		pH (H2O):	8,2	Arcilla (%):	19,2	CIC (cmol/Kg):	23,5
		CE (mS/cm):		C/N:	10,1	V = S/CIC (%):	100
		Caliza (%):	36,7	D. aparente (g/cm3):	1,4		
		Materia Orgánica (%):	1,9	Infiltración (mm/h):			
40 cm	Bwkc	Textura:	F	Elem. gruesos (%):	19,4	Ca (cmol/Kg):	45,9
		Estructura:	B	Arena gruesa (%):	10,4	Mg (cmol/Kg):	0,6
		Compactación:	F-FR	Arena fina (%):	18,3	Na (cmol/Kg):	0,1
		Raíces:	N	Arena total (%):	28,7	K (cmol/Kg):	0,1
		Color:	10YR5/6	Limo (%):	47,0	S (cmol/Kg):	46,7
		pH (H2O):	8,4	Arcilla (%):	24,3	CIC (cmol/Kg):	21,5
		CE (mS/cm):		C/N:	7,1	V = S/CIC (%):	100
		Caliza (%):	49,3	D. aparente (g/cm3):	1,4		
		Materia Orgánica (%):	1,0	Infiltración (mm/h):			
80 cm	BCkc	Textura:	F	Elem. gruesos (%):	18,7	Ca (cmol/Kg):	42,9
		Estructura:	B	Arena gruesa (%):	11,8	Mg (cmol/Kg):	1,0
		Compactación:	F-FR	Arena fina (%):	18,6	Na (cmol/Kg):	0,1
		Raíces:	N	Arena total (%):	30,4	K (cmol/Kg):	0,1
		Color:	10YR5,5/6	Limo (%):	50,9	S (cmol/Kg):	44,2
		pH (H2O):	8,5	Arcilla (%):	18,7	CIC (cmol/Kg):	21,6
		CE (mS/cm):		C/N:	8,5	V = S/CIC (%):	100
		Caliza (%):	49,1	D. aparente (g/cm3):	1,4		
		Materia Orgánica (%):	0,6	Infiltración (mm/h):			
110 cm	Ckc	Textura:	F	Elem. gruesos (%):	15,7	Ca (cmol/Kg):	46,3
		Estructura:	B	Arena gruesa (%):	10,9	Mg (cmol/Kg):	0,7
		Compactación:	F-FR	Arena fina (%):	20,0	Na (cmol/Kg):	0,1
		Raíces:	N	Arena total (%):	30,9	K (cmol/Kg):	0,1
		Color:	10YR6/6	Limo (%):	48,4	S (cmol/Kg):	47,3
		pH (H2O):	8,6	Arcilla (%):	20,7	CIC (cmol/Kg):	20,6
		CE (mS/cm):		C/N:	7,0	V = S/CIC (%):	100
		Caliza (%):	38,3	D. aparente (g/cm3):	1,4		
		Materia Orgánica (%):	0,5	Infiltración (mm/h):			

150 cm		Textura:	FA	Elem. gruesos (%):	85,8	Ca (cmol/Kg):	22,0
	2Ck	Estructura:	N	Arena gruesa (%):	18,0	Mg (cmol/Kg):	0,6
		Compactación:	F-FR	Arena fina (%):	35,5	Na (cmol/Kg):	0,1
		Raíces:	N	Arena total (%):	53,5	K (cmol/Kg):	0,1
		Color:	10YR5/4	Limo (%):	33,6	S (cmol/Kg):	22,8
		pH (H2O):	8,7	Arcilla (%):	12,9	CIC (cmol/Kg):	12,2
		CE (mS/cm):		C/N:	6,7	V = S/CIC (%):	100
		Caliza (%):	35,3	D. aparente (g/cm3):	1,5		
		Materia Orgánica (%):	0,3	Infiltración (mm/h):			

ÍNDICES DE VULNERABILIDAD RADIOLÓGICA DEL PERFIL:

CODSUELO	PARCIALES						TOTALES	
127	Infiltración	Retención Hídrica	Retención Físico-Química Cs	Retención Físico-Química Sr	Contenido en K	Contenido en Ca	Total al Cs	Total al Sr
CADENA ALIMENTARIA	1	1	2	1	3	1	2	1
IRRADIACIÓN EXTERNA	2	1	4	5	-	-	3	3

OBSERVACIONES: MATERIAL ORIGINAL: DETRÍTICO FINO. SE APORTA VALOR DEL PORCENTAJE DE CALIZA TOTAL.

Nº DE ORDEN:	PROVINCIA:	CÓDIGO PERFIL:	COORDENADAS UTM. HUSO 30 (ETRS89):		HOJA_MTN:
2020	HUESCA	HU116	X: 697200,000	Y: 4737200,000	144

TÉRM. MUNICIPAL: AISA **ALTITUD (m):** 1830 **PENDIENTE (%):** 2

SITUACIÓN: IZAGRA

USO: PASTOS SUPRAFORESTALES **REFERENCIA:** BADIA11

USDA-SOIL TAXONOMY (1975):

LEYENDA FAO (1974): E RENDSINA **Nº HORIZONTES:** 3

HORIZONTES:

0 cm	Ah1	Textura:	FC	Elem. gruesos (%):	10	Ca (cmol/Kg):	3,2
		Estructura:	G	Arena gruesa (%):	1,7	Mg (cmol/Kg):	0,4
		Compactación:		Arena fina (%):	31,6	Na (cmol/Kg):	0,0
		Raíces:	A	Arena total (%):	33,4	K (cmol/Kg):	0,3
		Color:	2,5Y3/2	Limo (%):	31,4	S (cmol/Kg):	19,8
		pH (H2O):	5,4	Arcilla (%):	34,2	CIC (cmol/Kg):	19,8
		CE (mS/cm):		C/N:	7,8	V = S/CIC (%):	100
		Caliza (%):		D. aparente (g/cm3):	1,5		
		Materia Orgánica (%):	8,3	Infiltración (mm/h):			
20 cm	Ah2	Textura:	FC	Elem. gruesos (%):	15	Ca (cmol/Kg):	1,8
		Estructura:	G	Arena gruesa (%):	2,1	Mg (cmol/Kg):	0,2
		Compactación:		Arena fina (%):	30,9	Na (cmol/Kg):	0,0
		Raíces:	F	Arena total (%):	33,0	K (cmol/Kg):	0,1
		Color:	2,5Y4/4	Limo (%):	31,1	S (cmol/Kg):	18,7
		pH (H2O):	5,7	Arcilla (%):	35,6	CIC (cmol/Kg):	11,1
		CE (mS/cm):		C/N:		V = S/CIC (%):	100
		Caliza (%):		D. aparente (g/cm3):	2,5		
		Materia Orgánica (%):	2,7	Infiltración (mm/h):			
35 cm	R	Textura:		Elem. gruesos (%):		Ca (cmol/Kg):	
		Estructura:		Arena gruesa (%):		Mg (cmol/Kg):	
		Compactación:		Arena fina (%):		Na (cmol/Kg):	
		Raíces:		Arena total (%):		K (cmol/Kg):	
		Color:		Limo (%):		S (cmol/Kg):	
		pH (H2O):		Arcilla (%):		CIC (cmol/Kg):	
		CE (mS/cm):		C/N:		V = S/CIC (%):	
		Caliza (%):		D. aparente (g/cm3):			
		Materia Orgánica (%):		Infiltración (mm/h):			

ÍNDICES DE VULNERABILIDAD RADIOLÓGICA DEL PERFIL:

CODSUELO	PARCIALES						TOTALES	
203	Infiltración	Retención Hídrica	Retención Físico-Química Cs	Retención Físico-Química Sr	Contenido en K	Contenido en Ca	Total al Cs	Total al Sr
CADENA ALIMENTARIA	4	4	1	4	3	3	3	4
IRRADIACIÓN EXTERNA	4	4	5	2	-	-	5	4

OBSERVACIONES: MATERIAL ORIGINAL: CALIZAS, LUTITAS Y ARENISCAS EOCENAS.

Nº DE ORDEN:	PROVINCIA:	CÓDIGO PERFIL:	COORDENADAS UTM. HUSO 30 (ETRS89):		HOJA_MTN:
2021	HUESCA	HU117	X: 731400,000	Y: 4726800,000	178

TÉRM. MUNICIPAL: TORLA **ALTITUD (m):** 1723 **PENDIENTE (%):** 40

SITUACIÓN: SOASO. LINÁS DE BROTO

USO: PRADO ALPINO DE LA ALIANZA NARDION ESTRICTAE **REFERENCIA:** BADIA11

USDA-SOIL TAXONOMY (1975):

LEYENDA FAO (1974): Bd CAMBISOL DISTRICO **Nº HORIZONTES:** 4

HORIZONTES:

0 cm	Ah	Textura:	FC	Elem. gruesos (%):	20,3	Ca (cmol/Kg):	2,8
		Estructura:		Arena gruesa (%):		Mg (cmol/Kg):	0,7
		Compactación:		Arena fina (%):		Na (cmol/Kg):	0,1
		Raíces:	A	Arena total (%):	28,1	K (cmol/Kg):	0,4
		Color:	2,5Y3/3	Limo (%):	36,0	S (cmol/Kg):	4,0
		pH (H2O):	4,9	Arcilla (%):	35,9	CIC (cmol/Kg):	15,0
		CE (mS/cm):		C/N:	12,1	V = S/CIC (%):	29
		Caliza (%):		D. aparente (g/cm3):	0,7		
		Materia Orgánica (%):	7,4	Infiltración (mm/h):			
20 cm	ABw	Textura:	FC	Elem. gruesos (%):	23,9	Ca (cmol/Kg):	2,0
		Estructura:	G	Arena gruesa (%):		Mg (cmol/Kg):	0,4
		Compactación:		Arena fina (%):		Na (cmol/Kg):	0,1
		Raíces:	A	Arena total (%):	27,7	K (cmol/Kg):	0,3
		Color:		Limo (%):	40,4	S (cmol/Kg):	2,8
		pH (H2O):	5,0	Arcilla (%):	31,9	CIC (cmol/Kg):	12,2
		CE (mS/cm):		C/N:	7,6	V = S/CIC (%):	25
		Caliza (%):		D. aparente (g/cm3):	1,2		
		Materia Orgánica (%):	4,1	Infiltración (mm/h):			
40 cm	Bw	Textura:	FC	Elem. gruesos (%):	28	Ca (cmol/Kg):	1,4
		Estructura:	G	Arena gruesa (%):		Mg (cmol/Kg):	0,2
		Compactación:		Arena fina (%):		Na (cmol/Kg):	0,1
		Raíces:	P	Arena total (%):	31,2	K (cmol/Kg):	0,2
		Color:		Limo (%):	37,8	S (cmol/Kg):	1,9
		pH (H2O):	5,1	Arcilla (%):	31,1	CIC (cmol/Kg):	9,6
		CE (mS/cm):		C/N:	5,2	V = S/CIC (%):	23
		Caliza (%):		D. aparente (g/cm3):	1,2		
		Materia Orgánica (%):	1,8	Infiltración (mm/h):			
60 cm	C	Textura:	F	Elem. gruesos (%):	35,4	Ca (cmol/Kg):	1,2
		Estructura:		Arena gruesa (%):		Mg (cmol/Kg):	0,2
		Compactación:		Arena fina (%):		Na (cmol/Kg):	0,1
		Raíces:	N	Arena total (%):	43,9	K (cmol/Kg):	0,2
		Color:		Limo (%):	33,0	S (cmol/Kg):	1,7
		pH (H2O):	5,1	Arcilla (%):	24,1	CIC (cmol/Kg):	7,8
		CE (mS/cm):		C/N:	5,4	V = S/CIC (%):	24
		Caliza (%):		D. aparente (g/cm3):	1,4		
		Materia Orgánica (%):	1,0	Infiltración (mm/h):			

ÍNDICES DE VULNERABILIDAD RADIOLÓGICA DEL PERFIL:

CODSUELO	PARCIALES						TOTALES	
23	Infiltración	Retención Hídrica	Retención Físico-Química Cs	Retención Físico-Química Sr	Contenido en K	Contenido en Ca	Total al Cs	Total al Sr
CADENA ALIMENTARIA	1	2	3	4	3	3	2	3
IRRADIACIÓN EXTERNA	1	1	3	2	-	-	2	1

OBSERVACIONES: MATERIAL ORIGINAL: DEPÓSITO DETRÍTICO FINO (COLUVIO) DE LUTITAS Y ARENISCAS.

Nº DE ORDEN:	PROVINCIA:	CÓDIGO PERFIL:	COORDENADAS UTM. HUSO 30 (ETRS89):		HOJA_MTN:
2022	HUESCA	HU118	X: 746918,940	Y: 4720959,630	178

TÉRM. MUNICIPAL: FANLO **ALTITUD (m):** 1930 **PENDIENTE (%):** 10

SITUACIÓN: CUELLO ARENAS, RIPALÉS (ORDESA)

USO: PASTOS **REFERENCIA:** BADIA11

USDA-SOIL TAXONOMY (1975):

LEYENDA FAO (1974): Bh CAMBISOL HUMICO **Nº HORIZONTES:** 3

HORIZONTES:

0 cm	Ah	Textura:	FC	Elem. gruesos (%):	4,34	Ca (cmol/Kg):	21,7
		Estructura:	G	Arena gruesa (%):	3,2	Mg (cmol/Kg):	1,0
		Compactación:		Arena fina (%):	13,6	Na (cmol/Kg):	0,0
		Raíces:	A	Arena total (%):	16,8	K (cmol/Kg):	0,4
		Color:	2,5Y3/3	Limo (%):	43,2	S (cmol/Kg):	23,0
		pH (H2O):	7,1	Arcilla (%):	40,0	CIC (cmol/Kg):	23,1
		CE (mS/cm):		C/N:	9,6	V = S/CIC (%):	100
		Caliza (%):		D. aparente (g/cm3):	0,6		
		Materia Orgánica (%):	11,9	Infiltración (mm/h):			
20 cm	Bw	Textura:	C	Elem. gruesos (%):	23,56	Ca (cmol/Kg):	15,2
		Estructura:	B	Arena gruesa (%):	0,5	Mg (cmol/Kg):	0,6
		Compactación:		Arena fina (%):	16,6	Na (cmol/Kg):	0,0
		Raíces:	F	Arena total (%):	17,1	K (cmol/Kg):	0,1
		Color:	2,5Y4/3	Limo (%):	38,3	S (cmol/Kg):	15,9
		pH (H2O):	7,3	Arcilla (%):	44,7	CIC (cmol/Kg):	16,5
		CE (mS/cm):		C/N:		V = S/CIC (%):	97
		Caliza (%):		D. aparente (g/cm3):	1,0		
		Materia Orgánica (%):	5,8	Infiltración (mm/h):			
50 cm	C	Textura:	FC	Elem. gruesos (%):	61,21	Ca (cmol/Kg):	11,9
		Estructura:	B	Arena gruesa (%):	5,7	Mg (cmol/Kg):	0,5
		Compactación:		Arena fina (%):	19,7	Na (cmol/Kg):	0,0
		Raíces:	F	Arena total (%):	25,4	K (cmol/Kg):	0,1
		Color:	2,5Y4/3,5	Limo (%):	39,5	S (cmol/Kg):	12,6
		pH (H2O):	7,4	Arcilla (%):	35,1	CIC (cmol/Kg):	12,8
		CE (mS/cm):		C/N:		V = S/CIC (%):	98
		Caliza (%):		D. aparente (g/cm3):	1,5		
		Materia Orgánica (%):	1,9	Infiltración (mm/h):			

ÍNDICES DE VULNERABILIDAD RADIOLÓGICA DEL PERFIL:

CODSUELO	PARCIALES						TOTALES	
124	Infiltración	Retención Hídrica	Retención Físico-Química Cs	Retención Físico-Química Sr	Contenido en K	Contenido en Ca	Total al Cs	Total al Sr
CADENA ALIMENTARIA	2	2	4	2	4	1	3	2
IRRADIACIÓN EXTERNA	2	2	2	4	-	-	2	3

OBSERVACIONES: MATERIAL ORIGINAL: LUTITAS, LIMOLITAS.

Nº DE ORDEN:	PROVINCIA:	CÓDIGO PERFIL:	COORDENADAS UTM. HUSO 30 (ETRS89):		HOJA_MTN:
2023	ZARAGOZA	Z101	X: 685737,000	Y: 4687853,000	247

TÉRM. MUNICIPAL: MURILLO DE GÁLLEGO **ALTITUD (m):** 505 **PENDIENTE (%):** 1

SITUACIÓN: TERRAZAS DEL GÁLLEGO (Tb). REINO DE MALLOS. COMARCA: HOYA DE HUESCA

USO: VIÑEDO, CON RIEGO A GOTEO **REFERENCIA:** BADIA11

USDA-SOIL TAXONOMY (1975):

LEYENDA FAO (1974): Bk CAMBISOL CALCICO **Nº HORIZONTES:** 6

HORIZONTES:

0 cm	Ap1	Textura:	FC	Elem. gruesos (%):	58,5	Ca (cmol/Kg):	45,9
		Estructura:	N	Arena gruesa (%):	35,5	Mg (cmol/Kg):	0,3
		Compactación:	FR	Arena fina (%):	8,0	Na (cmol/Kg):	0,1
		Raíces:	MP	Arena total (%):	43,6	K (cmol/Kg):	0,7
		Color:	7,5YR4/4	Limo (%):	25,8	S (cmol/Kg):	47,0
		pH (H2O):	7,9	Arcilla (%):	30,6	CIC (cmol/Kg):	24,6
		CE (mS/cm):	0,5	C/N:		V = S/CIC (%):	100
		Caliza (%):		D. aparente (g/cm3):	1,1		
		Materia Orgánica (%):	2,4	Infiltración (mm/h):			
10 cm	Ap2	Textura:	FC	Elem. gruesos (%):	47,1	Ca (cmol/Kg):	44,9
		Estructura:	B	Arena gruesa (%):	35,7	Mg (cmol/Kg):	0,3
		Compactación:	F	Arena fina (%):	8,8	Na (cmol/Kg):	0,1
		Raíces:	MP	Arena total (%):	44,5	K (cmol/Kg):	0,6
		Color:	7,5YR4/4	Limo (%):	21,9	S (cmol/Kg):	45,8
		pH (H2O):	7,9	Arcilla (%):	33,7	CIC (cmol/Kg):	23,8
		CE (mS/cm):	0,6	C/N:		V = S/CIC (%):	100
		Caliza (%):		D. aparente (g/cm3):	1,3		
		Materia Orgánica (%):	1,9	Infiltración (mm/h):			
30 cm	Bw	Textura:	FC	Elem. gruesos (%):	43,5	Ca (cmol/Kg):	36,3
		Estructura:	B	Arena gruesa (%):	32,7	Mg (cmol/Kg):	0,3
		Compactación:	F	Arena fina (%):	9,9	Na (cmol/Kg):	0,1
		Raíces:	MP	Arena total (%):	42,6	K (cmol/Kg):	0,7
		Color:	5YR4/6	Limo (%):	23,1	S (cmol/Kg):	37,3
		pH (H2O):	7,9	Arcilla (%):	34,3	CIC (cmol/Kg):	24,6
		CE (mS/cm):	0,6	C/N:		V = S/CIC (%):	100
		Caliza (%):		D. aparente (g/cm3):	1,3		
		Materia Orgánica (%):	1,7	Infiltración (mm/h):			
50 cm	BCk	Textura:	FC	Elem. gruesos (%):	74,1	Ca (cmol/Kg):	48,4
		Estructura:	B	Arena gruesa (%):	32,8	Mg (cmol/Kg):	0,5
		Compactación:	F	Arena fina (%):	11,3	Na (cmol/Kg):	0,1
		Raíces:	N	Arena total (%):	44,0	K (cmol/Kg):	0,6
		Color:	7,5YR4/6	Limo (%):	24,9	S (cmol/Kg):	49,6
		pH (H2O):	7,8	Arcilla (%):	31,1	CIC (cmol/Kg):	21,2
		CE (mS/cm):	1,1	C/N:		V = S/CIC (%):	100
		Caliza (%):		D. aparente (g/cm3):	1,4		
		Materia Orgánica (%):	1,2	Infiltración (mm/h):			
90 cm	Ck	Textura:	FA	Elem. gruesos (%):	84	Ca (cmol/Kg):	31,6
		Estructura:	N	Arena gruesa (%):	42,0	Mg (cmol/Kg):	0,2
		Compactación:	S	Arena fina (%):	16,5	Na (cmol/Kg):	0,1
		Raíces:	N	Arena total (%):	58,5	K (cmol/Kg):	0,2
		Color:	7,5YR5/4	Limo (%):	26,4	S (cmol/Kg):	32,1
		pH (H2O):	8,1	Arcilla (%):	15,0	CIC (cmol/Kg):	12,9
		CE (mS/cm):	1,1	C/N:		V = S/CIC (%):	100
		Caliza (%):		D. aparente (g/cm3):	1,5		
		Materia Orgánica (%):	0,7	Infiltración (mm/h):			

110 cm		Textura:		Elem. gruesos (%):	Ca (cmol/Kg):
	Ckm	Estructura:		Arena gruesa (%):	Mg (cmol/Kg):
		Compactación:		Arena fina (%):	Na (cmol/Kg):
		Raíces:		Arena total (%):	K (cmol/Kg):
		Color:		Limo (%):	S (cmol/Kg):
		pH (H2O):	8,2	Arcilla (%):	CIC (cmol/Kg):
		CE (mS/cm):		C/N:	V = S/CIC (%):
		Caliza (%):		D. aparente (g/cm3):	
		Materia Orgánica (%):		Infiltración (mm/h):	

ÍNDICES DE VULNERABILIDAD RADIOLÓGICA DEL PERFIL:

CODSUELO	PARCIALES						TOTALES	
127	Infiltración	Retención Hídrica	Retención Físico-Química Cs	Retención Físico-Química Sr	Contenido en K	Contenido en Ca	Total al Cs	Total al Sr
CADENA ALIMENTARIA	1	1	2	1	2	1	1	1
IRRADIACIÓN EXTERNA	1	2	4	5	-	-	3	3

OBSERVACIONES: MATERIAL ORIGINAL: MATERIAL ALUVIAL (GRAVAS Y CANTOS CON MATRIZ ARENOSA) DEL PLEISTOCENO SUPERIOR

Nº DE ORDEN:	PROVINCIA:	CÓDIGO PERFIL:	COORDENADAS UTM. HUSO 30 (ETRS89):		HOJA_MTN:
2024	ZARAGOZA	Z102	X: 657107,000	Y: 4640818,000	322

TÉRM. MUNICIPAL: TAUSTE **ALTITUD (m):** 425 **PENDIENTE (%):** 5

SITUACIÓN: EL PINADILLO

USO: PINAR QUEMADO (8/2008), CON SOTOBOSQUE **REFERENCIA:** BADIA11

USDA-SOIL TAXONOMY (1975):

LEYENDA FAO (1974): Xy XEROSOL GIPSICO **Nº HORIZONTES:** 4

HORIZONTES:

0 cm		Textura:	F	Elem. gruesos (%):	6,2	Ca (cmol/Kg):	190,8
	Ahy1	Estructura:	G	Arena gruesa (%):	7,5	Mg (cmol/Kg):	0,6
		Compactación:	FR	Arena fina (%):	41,1	Na (cmol/Kg):	0,9
		Raíces:	A	Arena total (%):	48,6	K (cmol/Kg):	0,3
		Color:	10YR5/3	Limo (%):	35,9	S (cmol/Kg):	192,7
		pH (H2O):	8,0	Arcilla (%):	15,5	CIC (cmol/Kg):	6,3
		CE (mS/cm):	2,8	C/N:	12,0	V = S/CIC (%):	100
		Caliza (%):	21,1	D. aparente (g/cm3):	1,0		
		Materia Orgánica (%):	6,0	Infiltración (mm/h):			
25 cm		Textura:	F	Elem. gruesos (%):	1,4	Ca (cmol/Kg):	189,0
	Ahy2	Estructura:	G	Arena gruesa (%):	18,1	Mg (cmol/Kg):	2,5
		Compactación:	S	Arena fina (%):	21,4	Na (cmol/Kg):	1,0
		Raíces:	F	Arena total (%):	39,5	K (cmol/Kg):	0,3
		Color:	10YR5/4	Limo (%):	39,1	S (cmol/Kg):	192,8
		pH (H2O):	8,0	Arcilla (%):	21,4	CIC (cmol/Kg):	5,9
		CE (mS/cm):	3,0	C/N:	11,2	V = S/CIC (%):	100
		Caliza (%):	21,5	D. aparente (g/cm3):	1,2		
		Materia Orgánica (%):	5,0	Infiltración (mm/h):			
50 cm		Textura:	F	Elem. gruesos (%):	0,4	Ca (cmol/Kg):	189,1
	By	Estructura:	M	Arena gruesa (%):	8,8	Mg (cmol/Kg):	0,1
		Compactación:	MF	Arena fina (%):	41,0	Na (cmol/Kg):	0,9
		Raíces:	MP	Arena total (%):	49,8	K (cmol/Kg):	0,1
		Color:	10YR7/2	Limo (%):	33,5	S (cmol/Kg):	190,1
		pH (H2O):	8,0	Arcilla (%):	16,7	CIC (cmol/Kg):	1,2
		CE (mS/cm):	2,5	C/N:	10,6	V = S/CIC (%):	100
		Caliza (%):	6,5	D. aparente (g/cm3):	1,2		
		Materia Orgánica (%):	1,3	Infiltración (mm/h):			
100 cm		Textura:	F	Elem. gruesos (%):	25,3	Ca (cmol/Kg):	190,7
	Cy	Estructura:	N	Arena gruesa (%):	16,0	Mg (cmol/Kg):	0,3
		Compactación:	MF	Arena fina (%):	26,3	Na (cmol/Kg):	1,1
		Raíces:	MP	Arena total (%):	42,3	K (cmol/Kg):	0,1
		Color:	10YR8/2	Limo (%):	39,3	S (cmol/Kg):	41,7
		pH (H2O):	8,1	Arcilla (%):	18,4	CIC (cmol/Kg):	3,2
		CE (mS/cm):	2,5	C/N:	9,4	V = S/CIC (%):	100
		Caliza (%):	10,4	D. aparente (g/cm3):	1,2		
		Materia Orgánica (%):	0,7	Infiltración (mm/h):			

ÍNDICES DE VULNERABILIDAD RADIOLÓGICA DEL PERFIL:

CODSUELO	PARCIALES						TOTALES	
19	Infiltración	Retención Hídrica	Retención Físico-Química Cs	Retención Físico-Química Sr	Contenido en K	Contenido en Ca	Total al Cs	Total al Sr
CADENA ALIMENTARIA	1	2	4	1	3	1	3	1
IRRADIACIÓN EXTERNA	1	2	2	5	-	-	2	3

OBSERVACIONES: MATERIAL ORIGINAL: YESO MIOCENO. SE APORTA VALOR DEL PORCENTAJE DE CALIZA TOTAL.

Nº DE ORDEN:	PROVINCIA:	CÓDIGO PERFIL:	COORDENADAS UTM. HUSO 30 (ETRS89):		HOJA_MTN:
2025	ZARAGOZA	Z103	X: 671532,000	Y: 4644951,000	322

TÉRM. MUNICIPAL: ZUERA **ALTITUD (m):** 630 **PENDIENTE (%):** 35

SITUACIÓN: LOMA DE BAILO. VAL DE ISA

USO: PINAR QUEMADO (8/2008) **REFERENCIA:** BADIA11

USDA-SOIL TAXONOMY (1975):

LEYENDA FAO (1974): Bk CAMBISOL CALCICO **Nº HORIZONTES:** 5

HORIZONTES:

0 cm	Ah	Textura:	FC	Elem. gruesos (%):	18,7	Ca (cmol/Kg):	48,0
		Estructura:	G	Arena gruesa (%):	9,9	Mg (cmol/Kg):	2,5
		Compactación:	F	Arena fina (%):	12,5	Na (cmol/Kg):	0,2
		Raíces:	A	Arena total (%):	22,4	K (cmol/Kg):	1,5
		Color:	10YR5/1	Limo (%):	43,4	S (cmol/Kg):	52,2
		pH (H2O):	8,0	Arcilla (%):	34,2	CIC (cmol/Kg):	27,7
		CE (mS/cm):	1,9	C/N:	15,9	V = S/CIC (%):	100
		Caliza (%):	49,0	D. aparente (g/cm3):	0,9		
		Materia Orgánica (%):	9,8	Infiltración (mm/h):			
30 cm	ABk	Textura:	FCL	Elem. gruesos (%):	14,7	Ca (cmol/Kg):	43,4
		Estructura:	B	Arena gruesa (%):	6,3	Mg (cmol/Kg):	1,8
		Compactación:	F	Arena fina (%):	9,5	Na (cmol/Kg):	0,4
		Raíces:	F	Arena total (%):	15,8	K (cmol/Kg):	0,6
		Color:	10YR3,5/1	Limo (%):	46,3	S (cmol/Kg):	46,3
		pH (H2O):	8,0	Arcilla (%):	37,9	CIC (cmol/Kg):	17,6
		CE (mS/cm):	2,6	C/N:	13,3	V = S/CIC (%):	100
		Caliza (%):	55,0	D. aparente (g/cm3):	1,0		
		Materia Orgánica (%):	4,1	Infiltración (mm/h):			
60 cm	Bwk	Textura:	FCL	Elem. gruesos (%):	17	Ca (cmol/Kg):	40,3
		Estructura:	B	Arena gruesa (%):	5,1	Mg (cmol/Kg):	1,8
		Compactación:	F	Arena fina (%):	12,7	Na (cmol/Kg):	0,4
		Raíces:	F	Arena total (%):	17,8	K (cmol/Kg):	0,5
		Color:	10YR4/2	Limo (%):	44,5	S (cmol/Kg):	43,0
		pH (H2O):	8,2	Arcilla (%):	37,7	CIC (cmol/Kg):	11,5
		CE (mS/cm):	1,8	C/N:	13,2	V = S/CIC (%):	100
		Caliza (%):	66,0	D. aparente (g/cm3):	1,1		
		Materia Orgánica (%):	2,5	Infiltración (mm/h):			
90 cm	BCk	Textura:	FCL	Elem. gruesos (%):	13,7	Ca (cmol/Kg):	38,9
		Estructura:	B	Arena gruesa (%):	4,8	Mg (cmol/Kg):	2,0
		Compactación:	MF	Arena fina (%):	15,1	Na (cmol/Kg):	0,4
		Raíces:	F	Arena total (%):	19,9	K (cmol/Kg):	0,4
		Color:	10YR6/2	Limo (%):	45,6	S (cmol/Kg):	41,7
		pH (H2O):	8,4	Arcilla (%):	34,5	CIC (cmol/Kg):	8,9
		CE (mS/cm):	1,2	C/N:	10,9	V = S/CIC (%):	100
		Caliza (%):	68,0	D. aparente (g/cm3):	1,1		
		Materia Orgánica (%):	1,7	Infiltración (mm/h):			
110 cm	C	Textura:	FC	Elem. gruesos (%):	67,8	Ca (cmol/Kg):	39,7
		Estructura:	N	Arena gruesa (%):	6,8	Mg (cmol/Kg):	3,3
		Compactación:	MF	Arena fina (%):	15,6	Na (cmol/Kg):	0,5
		Raíces:	F	Arena total (%):	22,4	K (cmol/Kg):	0,4
		Color:	10YR6/2	Limo (%):	44,1	S (cmol/Kg):	43,9
		pH (H2O):	8,4	Arcilla (%):	33,5	CIC (cmol/Kg):	8,4
		CE (mS/cm):	1,3	C/N:	8,7	V = S/CIC (%):	100
		Caliza (%):	72,0	D. aparente (g/cm3):	1,2		
		Materia Orgánica (%):	1,3	Infiltración (mm/h):			

ÍNDICES DE VULNERABILIDAD RADIOLÓGICA DEL PERFIL:

CODSUELO	PARCIALES						TOTALES	
127	Infiltración	Retención Hídrica	Retención Físico-Química Cs	Retención Físico-Química Sr	Contenido en K	Contenido en Ca	Total al Cs	Total al Sr
CADENA ALIMENTARIA	1	2	2	1	1	1	1	1
IRRADIACIÓN EXTERNA	1	2	4	5	-	-	3	3

OBSERVACIONES: MATERIAL ORIGINAL: DEPÓSITO DETRÍTICO FINO. SE APORTA VALOR DEL PORCENTAJE DE CALIZA TOTAL.

Nº DE ORDEN:	PROVINCIA:	CÓDIGO PERFIL:	COORDENADAS UTM. HUSO 30 (ETRS89):		HOJA_MTN:
2026	ZARAGOZA	Z104	X: 601146,000	Y: 4627798,000	352

TÉRM. MUNICIPAL: TRASMOZ **ALTITUD (m):** 1018 **PENDIENTE (%):** 30

SITUACIÓN: ROBLEDAL, MONTE LA MATA CTRA. VERA A AGRAMONTE (ZF-0251), KM 9

USO: ROBLE ALBAR, DE REBROTE, CON HIEDRA, GRAMÍNEAS, MUSG **REFERENCIA:** BADIA11

USDA-SOIL TAXONOMY (1975):

LEYENDA FAO (1974): Rd REGOSOL DISTRICO **Nº HORIZONTES:** 4

HORIZONTES:

0 cm	Ah	Textura:	F	Elem. gruesos (%):	59,1	Ca (cmol/Kg):	4,3
		Estructura:	G	Arena gruesa (%):	13,5	Mg (cmol/Kg):	1,1
		Compactación:	S	Arena fina (%):	34,7	Na (cmol/Kg):	0,2
		Raíces:	A	Arena total (%):	48,2	K (cmol/Kg):	0,6
		Color:	10YR3/2	Limo (%):	42,2	S (cmol/Kg):	6,1
		pH (H2O):	5,5	Arcilla (%):	9,6	CIC (cmol/Kg):	16,9
		CE (mS/cm):		C/N:	10,0	V = S/CIC (%):	36
		Caliza (%):		D. aparente (g/cm3):	1,4		
		Materia Orgánica (%):	5,2	Infiltración (mm/h):			
30 cm	C	Textura:	F	Elem. gruesos (%):	81,6	Ca (cmol/Kg):	1,4
		Estructura:	N	Arena gruesa (%):	14,4	Mg (cmol/Kg):	0,0
		Compactación:	S	Arena fina (%):	33,1	Na (cmol/Kg):	0,1
		Raíces:	F	Arena total (%):	47,5	K (cmol/Kg):	0,2
		Color:	10YR6/3	Limo (%):	41,1	S (cmol/Kg):	1,8
		pH (H2O):	5,1	Arcilla (%):	11,5	CIC (cmol/Kg):	5,5
		CE (mS/cm):		C/N:	3,4	V = S/CIC (%):	32
		Caliza (%):		D. aparente (g/cm3):	1,4		
		Materia Orgánica (%):	0,7	Infiltración (mm/h):			
100 cm	R	Textura:		Elem. gruesos (%):		Ca (cmol/Kg):	
		Estructura:		Arena gruesa (%):		Mg (cmol/Kg):	
		Compactación:		Arena fina (%):		Na (cmol/Kg):	
		Raíces:		Arena total (%):		K (cmol/Kg):	
		Color:		Limo (%):		S (cmol/Kg):	
		pH (H2O):		Arcilla (%):		CIC (cmol/Kg):	
		CE (mS/cm):		C/N:		V = S/CIC (%):	
		Caliza (%):		D. aparente (g/cm3):			
		Materia Orgánica (%):		Infiltración (mm/h):			

ÍNDICES DE VULNERABILIDAD RADIOLÓGICA DEL PERFIL:

CODSUELO	PARCIALES						TOTALES	
202	Infiltración	Retención Hídrica	Retención Físico-Química Cs	Retención Físico-Química Sr	Contenido en K	Contenido en Ca	Total al Cs	Total al Sr
CADENA ALIMENTARIA	1	2	2	4	3	3	2	3
IRRADIACIÓN EXTERNA	1	2	4	2	-	-	3	2

OBSERVACIONES: MATERIAL ORIGINAL: COLUVIO DE ARENISCAS CUARCÍTICAS. BUNDSANSTEIN (TRIÁSICO). EXISTE UN HORIZONTE ORGÁNICO (OL=Oi) DE HOJARASCA FRESCA DE 1 CM DE ESPESOR.

REFERENCES OF THE SOIL PROFILES

JUNTACL88	José Forteza Bonnin et al., 1987. MAPA DE SUELOS DE CASTILLA Y LEÓN. Dirección General de Medio Ambiente y Urbanismo. Servicio de Ordenación del Territorio y Cartografía. Junta de Castilla y León. Pag. 59.
GONZÁLEZ-QUIÑONES06	Vanesa Gonzáles-Quiñones, 2006. METODOLOGÍA, FORMULACIÓN Y APLICACIÓN DE UN ÍNDICE DE CALIDAD DE SUELOS CON FINES AGRÍCOLAS PARA CASTILLA-LA MANCHA (Tesis doctoral). Pag. 100.
BADÍA11	David Badía, 2011. iARASOL, PROGRAMA INTERACTIVO PARA EL ESTUDIO Y CLASIFICACIÓN DE SUELOS DE ARAGÓN (http://www.suelosdearagon.com/)

ANNEXE VIII: PARTIAL AND GLOBAL RADIOLOGICAL VULNERABILITY INDEXES OF SOILS IN THE PENINSULAR SPAIN. RESULTS AND DIFFERENCES BETWEEN THE RESULTS OBTAINED IN (TRUEBA, 2000) AND IN THIS UPDATE

SOIL GROUPS WITH REPRESENTATION IN THE EUROPEAN SOIL MAP, IN THE PENINSULAR SPAIN		Values of the Radiological Vulnerability Indexes regarding radiocaesium for the ingestion patway					Differences between the Partial Indexes in García-Puerta, 2014 and the new ones				
SOIL GROUP	SOIL TYPE FAO85 [No. SOIL PROFILES]	I_F	I_H	I_{FQCs}	I_K	G_Cs_Ing	I_F	I_H	I_{FQCs}	I_K	G_Cs_Ing
1	Je FLUVISOL EUTRICO_1 [n=16]	4	2	5	3	4					
3	Ie LITOSOL EUTRICO_3 [n=4]	3	2	1	2	2				-3	-1
5	Ic LITOSOL CALCICO_5 [n=8]	3	1	2	2	2					
6	Id LITOSOL DISTRICO_6 [n=3]	4	1	5	2	3					
7	Qc ARENOSOL CAMBICO_7 [n=27]	4	1	5	4	4					
8	Ql ARENOSOL LUVICO_8 [n=5]	4	1	5	3	4					
9	U RANKER_9 [n=77]	4	2	5	5	3					
12	Vp VERTISOL PELLICO_12 [n=3]	1	5	2	2	3					
14	Vc VERTISOL CROMICO_14 [n=25]	1	3	2	2	2					
15	Zg SOLONCHAK GLEICO_15 [n=9]	1	1	5	4	2					
19	Xy XEROSOL GIPSICO_19 [n=4]	1	3	1	2	3	-3				
21	Be CAMBISOL EUTRICO_21 [n=86]	4	1	5	4	4		-1			
23	Bd CAMBISOL DISTRICO_23 [n=16]	4	2	2	4	4			-3		
24	Bh CAMBISOL HUMICO_24 [n=54]	4	2	5	5	4					
37	Lv LUVISOL VERTICO_37 [n=5]	1	4	1	2	2					
38	Lga LUVISOL ALBO-GLEICO_38 [n=1]	2	2	3	4	3					
39	Phf PODZOL FERRICO Y HUMICO_39 [n=15]	4	3	5	4	4					
42	Od HISTOSOL DISTRICO_42 [n=2]	4	5	4	4	4					
116	Xk XEROSOL CALCICO_116 [n=3]	4	2	5	4	4				1	
117	Xk XEROSOL CALCICO_117 [n=18]	3	1	1	3	2					
118	Xk XEROSOL CALCICO_118 [n=6]	4	2	2	3	3					
124	Bh CAMBISOL HUMICO_124 [n=67]	4	3	2	5	4					
126	Bk CAMBISOL CALCICO_126 [n=74]	4	1	2	3	2					
127	Bk CAMBISOL CALCICO_127 [n=30]	2	2	2	3	2					-1
128	Bk CAMBISOL CALCICO_128 [n=85]	3	2	2	2	2					
129	Bk CAMBISOL CALCICO_129 [n=16]	3	2	2	3	3					
132	Lo LUVISOL ORTICO_132 [n=41]	4	1	2	4	3					
133	Lo LUVISOL ORTICO_133 [n=75]	4	1	5	4	4					
201	Jc FLUVISOL CALCAREO_201 [n=57]	4	1	1	3	2					
202	Rd REGOSOL DISTRICO_202 [n=22]	4	2	5	3	4					
203	E RENDZINA_203 [n=42]	4	1	2	3	3					
204	Ag ACRISOL GLEICO_204 [n=14]	3	2	1	5	3					
205	Zo SOLONCHAK ORTICO_205 [n=18]	2	2	2	3	3					
206	Re REGOSOL EUTRICO_206 [n=47]	4	1	5	4	4					
207	Rc REGOSOL CALCAREO_207 [n=99]	3	1	2	3	2					
238	Lg LUVISOL GLEICO_238 [n=26]	4	1	2	4	3					
239	Lc LUVISOL CROMICO_239 [n=23]	4	1	2	4	3					
240	Lc LUVISOL CROMICO_240 [n=58]	4	3	2	3	3					
241	Lcr LUVISOL RHODO-CROMICO_241 [n=9]	4	2	3	4	4					
242	Lcr LUVISOL RHODO-CROMICO_242 [n=16]	4	3	2	4	4					
243	Lcr LUVISOL RHODO-CROMICO_243 [n=21]	4	2	2	4	3					
244	Lkc LUVISOL CROMO-CALCICO_244 [n=19]	3	2	2	3	3					1
245	Lkc LUVISOL CROMO-CALCICO_245 [n=4]	1	4	1	2	4					
246	Lkcr LUVISOL RHODO-CROMO-CALCICO_246 [n=38]	3	2	2	2	3					

INDEXES LEGEND

- 1 Minimum index value
- 2 Low index value
- 3 Medium index value
- 4 High index value
- 5 Maximum index value

DIFFERENCE LEGEND

- -X Index value has decreased *x* points in the updated map with respect the one issued in 2015.
- X Index value has increased *x* points in the updated map with respect the one issued in 2015.

Blank cells reflect no difference between both versions.

SOIL GROUPS WITH NO REPRESENTATION IN THE EUROPEAN SOIL MAP, IN THE PENINSULAR SPAIN		Values of the Radiological Vulnerability Indexes regarding radiocaesium for the ingestion patway					Differences between the Partial Indexes in García-Puerta, 2014 and the new ones				
SOIL GROUP	SOIL TYPE FAO85 [No. SOIL PROFILES]	I_F	I_H	I_{FQCs}	I_K	G_Cs_Ing	I_F	I_H	I_{FQCs}	I_K	G_Cs_Ing
22*	Bd CAMBISOL DISTRICO_22 [n=74]	4	2	2	4	3					
25	Bg CAMBISOL GLEICO_25 [n=32]	4	2	2	4	4					
40*	We PLANOSOL EUTRICO_40 [n=4]	3	2	1	2	3					
41	Wd PLANOSOL DISTRICO_41 [n=1]	1	3	2	3	2					
208*	Bc CAMBISOL CROMICO_208 [n=30]	4	2	2	4	3					
209*	Po PODZOL ORTICO_209 [n=14]	4	2	5	5	4					
1001	Ah ACRISOL HUMICO_1001 [n=44]	4	2	5	3	4					
1002	Ao ACRISOL ORTICO_1002 [n=38]	4	2	3	4	3					
1003	Th ANDOSOL HUMICO_1003 [n=3]	1	3	5	3	3					
1004	Tm ANDOSOL MOLLICO_1004 [n=1]	3	1	5	2	3					
1005	Qa ARENOSOL ALBICO_1005 [n=5]	5	1	5	5	4					
1006	Bv CAMBISOL VERTICO_1006 [n=8]	1	4	1	3	2					
1007	Ch CHERNOZEM HAPLICO_1007 [n=3]	4	3	5	4	4					
1008	Jd FLUVISOL DISTRICO_1008 [n=12]	4	2	5	4	4					
1009	Jt FLUVISOL TIONICO_1009 [n=2]	2	3	5	2	3					
1010	Gc GLEYSOL CALCAREO_1010 [n=4]	2	2	5	3	4					
1011	Gd GLEYSOL DISTRICO_1011 [n=4]	3	3	1	5	3					
1012	Ge GLEYSOL EUTRICO_1012 [n=7]	4	3	4	1	3					
1013	Gh GLEYSOL HUMICO_1013 [n=14]	4	2	1	5	3					
1014	Gm GLEYSOL MOLLICO_1014 [n=3]	4	3	5	3	4					
1015	Kk KASTANOZEM CALCICO_1015 [n=15]	4	1	2	3	3					
1016	Kh KASTANOZEM HAPLICO_1016 [n=7]	3	2	2	4	3					
1017	Kl KASTANOZEM LUVICO_1017 [n=4]	1	2	2	5	4					
1018	Hc PHAEOZEM CALCAREO_1018 [n=15]	1	2	2	2	2					
1019	Hg PHAEOZEM GLEICO_1019 [n=2]	4	2	5	4	4					
1020	Hh PHAEOZEM HAPLICO_1020 [n=19]	4	2	5	2	3					
1021	Hl PHAEOZEM LUVICO_1021 [n=5]	4	3	3	2	3					
1022	Wm PLANOSOL MOLLICO_1022 [n=1]	3	4	3	4	4					
1023	Pg PODZOL GLEICO_1023 [n=2]	4	4	5	5	4					
1024	Pl PODZOL LEPTICO_1024 [n=1]	4	1	5	4	4					
1025	Pp PODZOL PLACICO_1025 [n=1]	4	1	5	3	4					
1026	Dd PODZOLUVISOL DISTRICO_1026 [n=1]	4	2	4	1	3					
1027	SOLONCHAK MOLLICO_1027 [n=1]	1	3	2	1	2					
1028	Sg SOLONETZ GLEICO_1028 [n=1]	1	2	2	3	2					
1029	So SOLONETZ ORTICO_1029 [n=10]	3	2	5	5	4		-1	2		
1030	Xk XEROSOL HAPLICO_1030 [n=2]	5	4	3	3	4					
1031	Xk XEROSOL LUVICO_1031 [n=1]	4	3	2	1	3					
1032	YERMOSOL CALCICO_1032 [n=2]	3	3	2	5	3					
1033	YERMOSOL HAPLICO_1033 [n=1]	1	2	2	3	2					
1034	YERMOSOL LUVICO_1034 [n=1]	3	2	1	3	2					

* Soil groups associated to SMUs with Portuguese code and with representation only in Portugal.

INDEXES LEGEND

1 Minimum index value
2 Low index value
3 Medium index value
4 High index value
5 Maximum index value

DIFFERENCE LEGEND

- X Index value has decreased *x* points in the updated map with respect the one issued in 2015.
X Index value has increased *x* points in the updated map with respect the one issued in 2015.

Blank cells reflect no difference between both versions.

ANNEXE IX: TABLES AND CHARTS OF THE *AGRICULTURAL AREAS* WITHIN EACH RADIOLOGICAL VULNERABILITY INDEX (I_RV) CATEGORY, BY PROVINCE, IN THE PENINSULAR SPAIN

Peninsular Spain Province	Province Code	Radiological Vulnerability Index (I_RV) Surface [km²]				
		I_RV = 1	I_RV = 2	I_RV = 3	I_RV = 4	I_RV = 5
Álava	1	38.93	345.87	627.79	134.37	
Albacete	2	67.81	3465.95	4023.12	871.65	29.25
Alicante	3	271.41	1509.58	319.03	384.71	4.75
Almería	4	110.62	610.58	920.49	1189.40	37.48
Ávila	5	164.82	1699.26	446.88	347.95	
Badajoz	6	90.80	10696.06	3093.45	601.90	
Barcelona	8	63.54	619.31	968.43	262.50	
Burgos	9	90.69	3093.15	3388.56	560.03	5.58
Cáceres	10	823.63	2507.79	684.89	5066.45	
Cádiz	11	572.95	1769.12	1236.93	742.78	
Castellón	12	209.69	954.21	202.17	411.41	
Ciudad real	13	8.18	5199.08	4565.39	1578.82	
Córdoba	14	469.34	4608.44	1128.22	3858.05	
A Coruña	15				2629.00	
Cuenca	16	41.67	3561.62	4974.66	38.17	
Girona	17	2.20	708.88	614.73	32.76	
Granada	18	44.86	3382.96	1484.56	1458.72	
Guadalajara	19		2265.75	1593.79	87.69	
Guipúzcoa	20		48.16	39.01	320.65	
Huelva	21	110.62	2844.25	90.18	926.59	
Huesca	22	4.42	1574.01	3743.75	768.07	
Jaén	23	341.50	6674.22	460.94	352.43	
León	24	0.28	1253.91	2135.18	1278.83	221.90
Lleida	25	19.27	1637.90	2212.97	805.50	
La Rioja	26	16.12	1173.03	421.43	222.78	
Lugo	27		7.45	1.67	3253.07	0.32
Madrid	28	44.45	1942.80	640.52	279.62	
Málaga	29	73.13	2272.99	871.76	531.52	
Murcia	30	102.11	825.66	1330.01	3614.59	119.15
Navarra	31	0.52	2004.29	2086.63	248.83	
Ourense	32		29.19	416.53	737.50	334.35
Asturias	33	0.84	202.51	127.27	2274.83	
Palencia	34		1775.70	2971.86	677.55	15.83
Pontevedra	36		4.42	4.07	1267.10	
Salamanca	37	48.27	1731.85	1828.22	2888.49	
Cantabria	39	1.59	338.77	46.06	1116.61	
Segovia	40	12.00	2403.01	823.32	101.51	
Sevilla	41	1716.51	4239.01	1205.80	2967.27	412.65
Soria	42	2.28	2475.79	1672.12	1.21	
Tarragona	43	277.32	1608.95	307.35	619.34	
Teruel	44	9.10	2358.39	2291.89	692.47	11.70
Toledo	45	662.08	5224.33	3238.09	659.34	64.69
Valencia	46	609.39	2549.28	423.97	547.05	
Valladolid	47	26.40	3613.50	2642.58	181.15	2.73
Vizcaya	48		31.69	12.49	442.15	0.08
Zamora	49		1929.49	2547.27	1142.91	
Zaragoza	50	0.86	4227.72	3419.50	2204.44	45.20
Total I_RV surface		**7150.21**	**103999.90**	**68285.51**	**51379.74**	**1305.65**

Blank cells mean no affected surface.

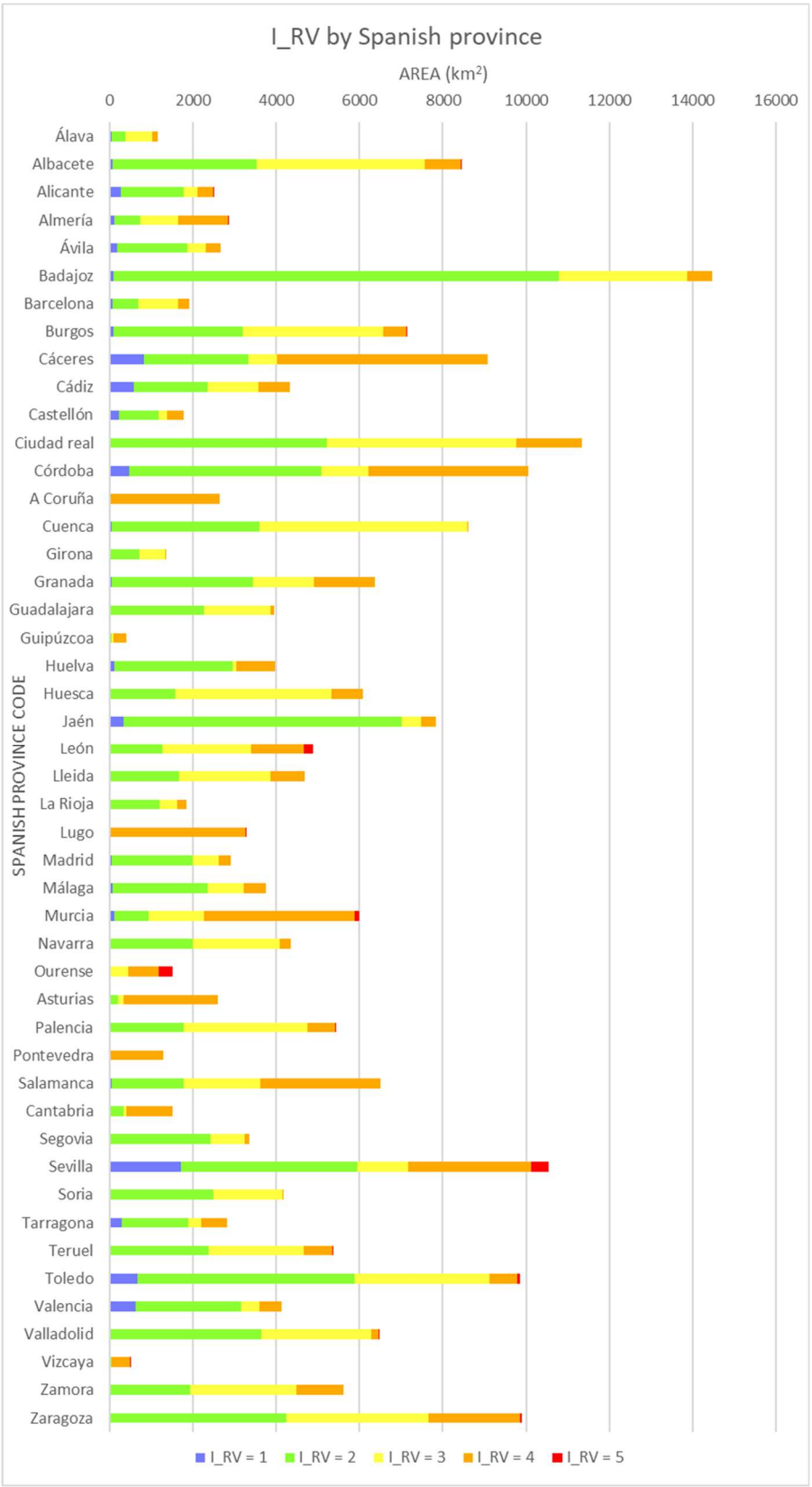

Radiological vulnerability indexes surface (km^2), by province: I_RV=1, Minimum Radiological Vulnerability, in blue; I_RV=2, Minimum Radiological Vulnerability, in green; I_RV=3, Medium Radiological Vulnerability, in yellow; I_RV=4, High Radiological Vulnerability, in orange; I_RV=5, Maximum Radiological Vulnerability, in red.

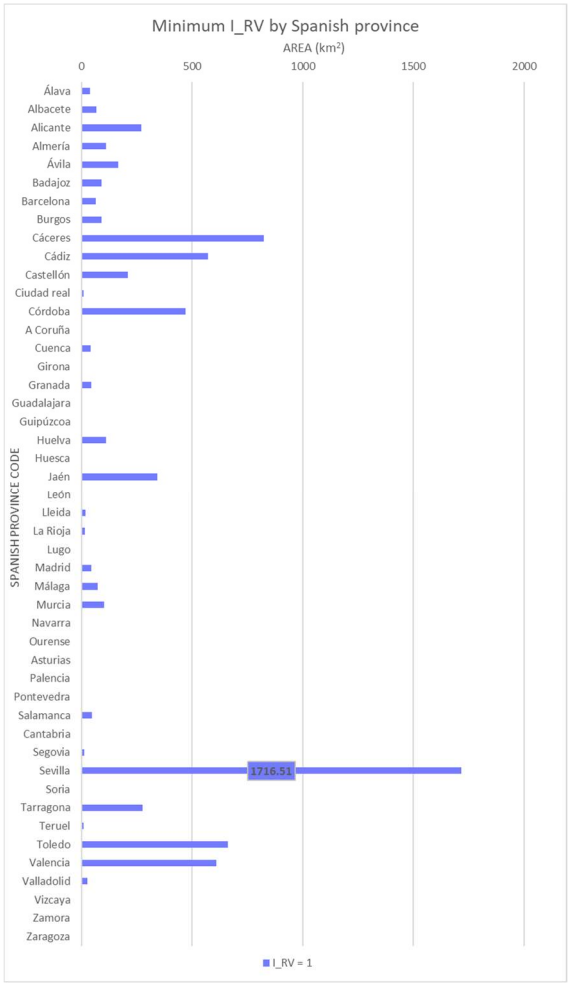
Minimum I_RV by Spanish province
AREA (km²)
0
500
1000
1500
2000
SPANISH PROVINCE CODE
Álava
Albacete
Alicante
Almería
Ávila
Badajoz
Barcelona
Burgos
Cáceres
Cádiz
Castellón
Ciudad real
Córdoba
A Coruña
Cuenca
Girona
Granada
Guadalajara
Guipúzcoa
Huelva
Huesca
Jaén
León
Lleida
La Rioja
Lugo
Madrid
Málaga
Murcia
Navarra
Ourense
Asturias
Palencia
Pontevedra
Salamanca
Cantabria
Segovia
Sevilla
Soria
Tarragona
Teruel
Toledo
Valencia
Valladolid
Vizcaya
Zamora
Zaragoza
1716.51
I_RV = 1

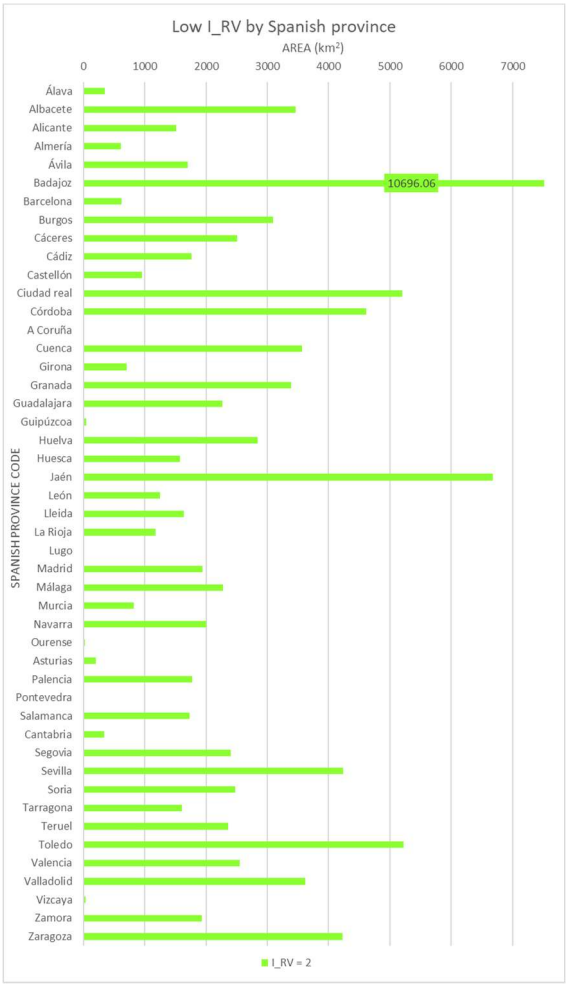
Low I_RV by Spanish province
AREA (km²)
0
1000
2000
3000
4000
5000
6000
7000
SPANISH PROVINCE CODE
Álava
Albacete
Alicante
Almería
Ávila
Badajoz
Barcelona
Burgos
Cáceres
Cádiz
Castellón
Ciudad real
Córdoba
A Coruña
Cuenca
Girona
Granada
Guadalajara
Guipúzcoa
Huelva
Huesca
Jaén
León
Lleida
La Rioja
Lugo
Madrid
Málaga
Murcia
Navarra
Ourense
Asturias
Palencia
Pontevedra
Salamanca
Cantabria
Segovia
Sevilla
Soria
Tarragona
Teruel
Toledo
Valencia
Valladolid
Vizcaya
Zamora
Zaragoza
10696.06
I_RV = 2

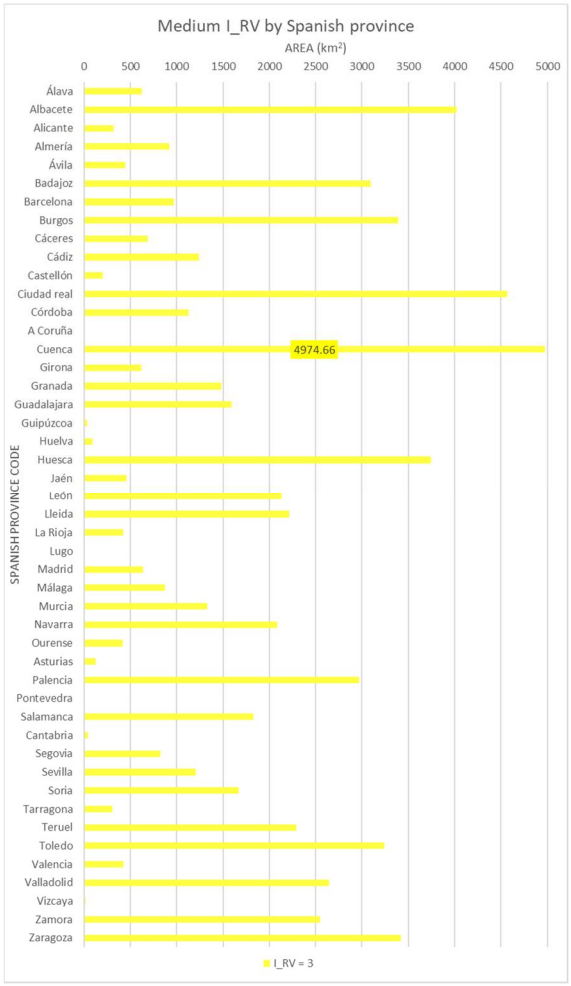
Medium I_RV by Spanish province
AREA (km²)
0
500
1000
1500
2000
2500
3000
3500
4000
4500
5000
SPANISH PROVINCE CODE
Álava
Albacete
Alicante
Almería
Ávila
Badajoz
Barcelona
Burgos
Cáceres
Cádiz
Castellón
Ciudad real
Córdoba
A Coruña
Cuenca
Girona
Granada
Guadalajara
Guipúzcoa
Huelva
Huesca
Jaén
León
Lleida
La Rioja
Lugo
Madrid
Málaga
Murcia
Navarra
Ourense
Asturias
Palencia
Pontevedra
Salamanca
Cantabria
Segovia
Sevilla
Soria
Tarragona
Teruel
Toledo
Valencia
Valladolid
Vizcaya
Zamora
Zaragoza
4974.66
I_RV = 3

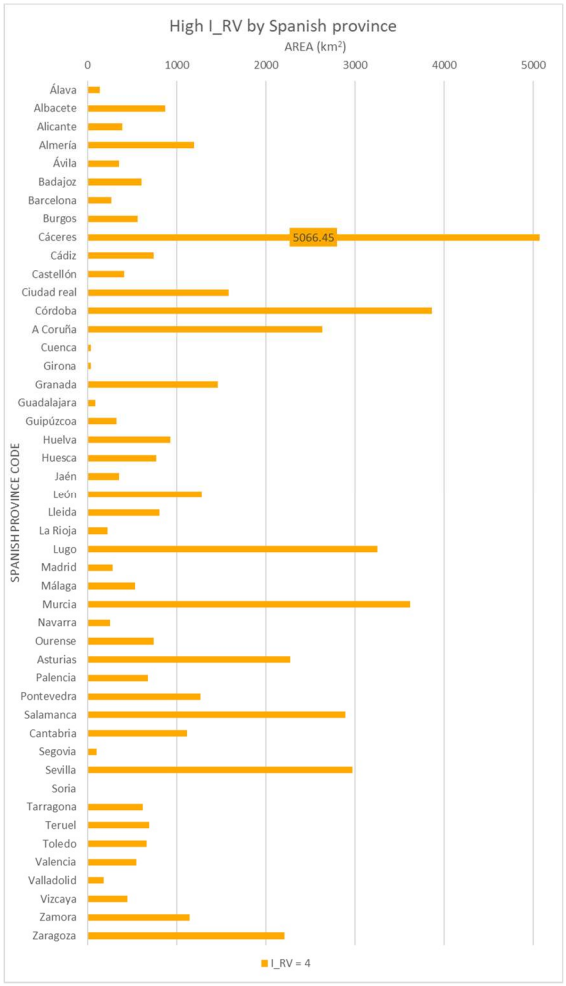
High I_RV by Spanish province
AREA (km²)
0
1000
2000
3000
4000
5000
SPANISH PROVINCE CODE
Álava
Albacete
Alicante
Almería
Ávila
Badajoz
Barcelona
Burgos
Cáceres
Cádiz
Castellón
Ciudad real
Córdoba
A Coruña
Cuenca
Girona
Granada
Guadalajara
Guipúzcoa
Huelva
Huesca
Jaén
León
Lleida
La Rioja
Lugo
Madrid
Málaga
Murcia
Navarra
Ourense
Asturias
Palencia
Pontevedra
Salamanca
Cantabria
Segovia
Sevilla
Soria
Tarragona
Teruel
Toledo
Valencia
Valladolid
Vizcaya
Zamora
Zaragoza
5066.45
I_RV = 4

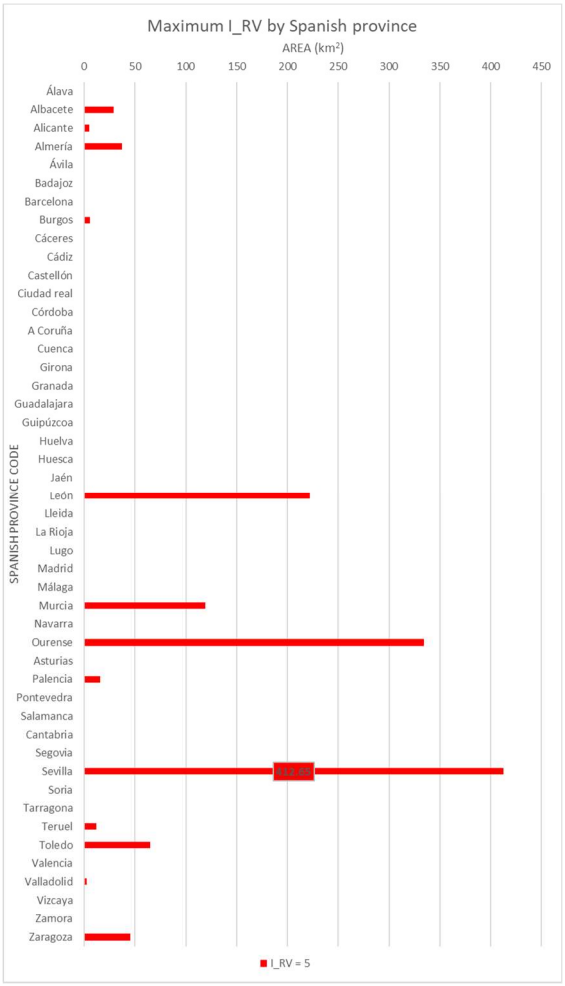
Maximum I_RV by Spanish province
AREA (km²)
0
50
100
150
200
250
300
350
400
450
SPANISH PROVINCE CODE
Álava
Albacete
Alicante
Almería
Ávila
Badajoz
Barcelona
Burgos
Cáceres
Cádiz
Castellón
Ciudad real
Córdoba
A Coruña
Cuenca
Girona
Granada
Guadalajara
Guipúzcoa
Huelva
Huesca
Jaén
León
Lleida
La Rioja
Lugo
Madrid
Málaga
Murcia
Navarra
Ourense
Asturias
Palencia
Pontevedra
Salamanca
Cantabria
Segovia
Sevilla
Soria
Tarragona
Teruel
Toledo
Valencia
Valladolid
Vizcaya
Zamora
Zaragoza
I_RV = 5

Peninsular Spain Province	Province Code	Percentage of Surface of each Radiological Vulnerability Index (I_RV) by Province, with respect to the Total *Agricultural Surface Area* in the Province				
		I_RV = 1	I_RV = 2	I_RV = 3	I_RV = 4	I_RV =
Álava	1	3.3943	30.1555	54.7346	11.7155	
Albacete	2	0.8017	40.9795	47.5671	10.3059	0.3458
Alicante	3	10.9021	60.6384	12.8153	15.4533	0.1909
Almería	4	3.8563	21.2853	32.0886	41.4633	1.3065
Ávila	5	6.1987	63.9082	16.8068	13.0863	
Badajoz	6	0.6270	73.8565	21.3604	4.1562	
Barcelona	8	3.3202	32.3605	50.6030	13.7163	
Burgos	9	1.2705	43.3336	47.4721	7.8457	0.0781
Cáceres	10	9.0681	27.6105	7.5405	55.7809	
Cádiz	11	13.2573	40.9349	28.6210	17.1868	
Castellón	12	11.7972	53.6832	11.3740	23.1457	
Ciudad real	13	0.0721	45.8009	40.2185	13.9085	
Córdoba	14	4.6636	45.7911	11.2104	38.3350	
A Coruña	15				10.0000	
Cuenca	16	0.4837	41.3367	57.7366	0.4430	
Girona	17	0.1620	52.1784	45.2482	2.4113	
Granada	18	0.7041	53.0986	23.3014	22.8959	
Guadalajara	19		57.4010	40.3774	2.2216	
Guipúzcoa	20		11.8098	9.5648	78.6254	
Huelva	21	2.7851	71.6141	2.2705	23.3302	
Huesca	22	0.0726	25.8447	61.4711	12.6115	
Jaén	23	4.3619	85.2491	5.8875	4.5015	
León	24	0.0058	25.6418	43.6632	26.1514	4.5378
Lleida	25	0.4122	35.0305	47.3298	17.2275	
La Rioja	26	0.8793	63.9826	22.9867	12.1514	
Lugo	27		0.2284	0.0512	99.7107	0.0097
Madrid	28	1.5289	66.8228	22.0306	9.6177	
Málaga	29	1.9505	60.6227	23.2507	14.1760	
Murcia	30	1.7043	13.7805	22.1982	60.3284	1.9886
Navarra	31	0.0119	46.1789	48.0762	5.7330	
Ourense	32		1.9238	27.4473	48.5969	22.0320
Asturias	33	0.0321	7.7726	4.8847	87.3106	
Palencia	34		32.6359	54.6204	12.4527	0.2910
Pontevedra	36		0.3465	0.3189	99.3346	
Salamanca	37	0.7430	26.6568	28.1403	44.4600	
Cantabria	39	0.1057	22.5393	3.0642	74.2908	
Segovia	40	0.3594	71.9497	24.6515	3.0394	
Sevilla	41	16.2838	40.2136	11.4389	28.1492	3.9146
Soria	42	0.0549	59.6375	40.2785	0.0290	
Tarragona	43	9.8586	57.1979	10.9261	22.0174	
Teruel	44	0.1696	43.9707	42.7309	12.9107	0.2181
Toledo	45	6.7226	53.0468	32.8789	6.6948	0.6568
Valencia	46	14.7564	61.7305	10.2664	13.2467	
Valladolid	47	0.4083	55.8816	40.8666	2.8014	0.0421
Vizcaya	48		6.5145	2.5677	90.9017	0.0161
Zamora	49		34.3345	45.3277	20.3377	
Zaragoza	50	0.0087	42.7141	34.5483	22.2722	0.4567
Total I_RV surface		**7150.21**	**103999.90**	**68285.51**	**51379.74**	**1305.65**
		232121.01				

Blank cells mean no affected surface.

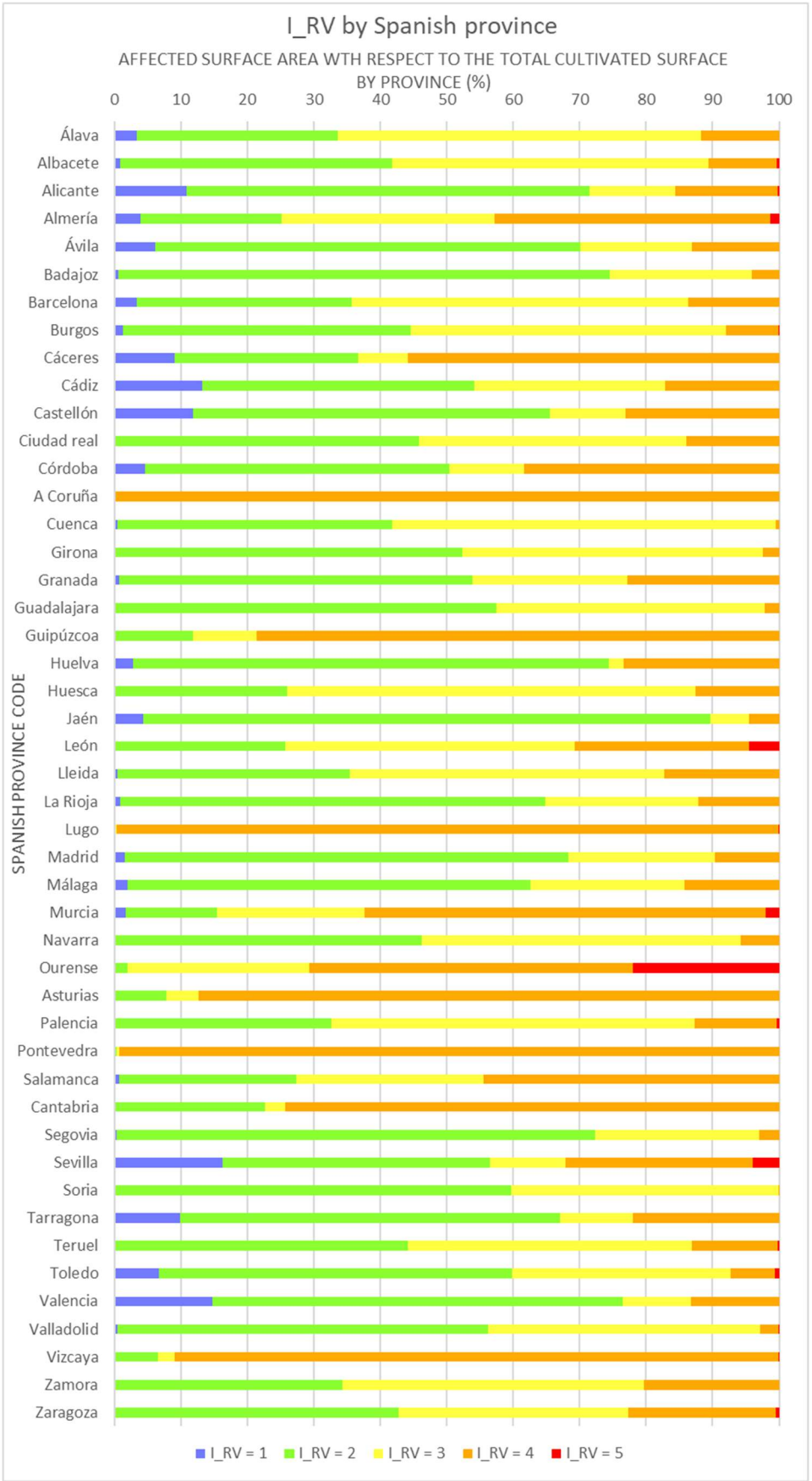
I_RV by Spanish province
AFFECTED SURFACE AREA WTH RESPECT TO THE TOTAL CULTIVATED SURFACE BY PROVINCE (%)
0
10
20
30
40
50
60
70
80
90
100
SPANISH PROVINCE CODE
Álava
Albacete
Alicante
Almería
Ávila
Badajoz
Barcelona
Burgos
Cáceres
Cádiz
Castellón
Ciudad real
Córdoba
A Coruña
Cuenca
Girona
Granada
Guadalajara
Guipúzcoa
Huelva
Huesca
Jaén
León
Lleida
La Rioja
Lugo
Madrid
Málaga
Murcia
Navarra
Ourense
Asturias
Palencia
Pontevedra
Salamanca
Cantabria
Segovia
Sevilla
Soria
Tarragona
Teruel
Toledo
Valencia
Valladolid
Vizcaya
Zamora
Zaragoza
I_RV = 1
I_RV = 2
I_RV = 3
I_RV = 4
I_RV = 5

Peninsular Spain Province	Province Code	Percentage of Surface of each Radiological Vulnerability Index (I_RV) by Province, with respect to the Total *Agricultural Surface Area* in the Peninsular Spain					
		I_RV = 1	I_RV = 2	I_RV = 3	I_RV = 4	I_RV = 5	Total percentage
Álava	1	0.0168	0.1490	0.2705	0.0579		0.49
Albacete	2	0.0292	1.4932	1.7332	0.3755	0.0126	3.64
Alicante	3	0.1169	0.6503	0.1374	0.1657	0.0020	1.07
Almería	4	0.0477	0.2630	0.3966	0.5124	0.0161	1.24
Ávila	5	0.0710	0.7321	0.1925	0.1499		1.15
Badajoz	6	0.0391	4.6080	1.3327	0.2593		6.24
Barcelona	8	0.0274	0.2668	0.4172	0.1131		0.82
Burgos	9	0.0391	1.3326	1.4598	0.2413	0.0024	3.08
Cáceres	10	0.3548	1.0804	0.2951	2.1827		3.91
Cádiz	11	0.2468	0.7622	0.5329	0.3200		1.86
Castellón	12	0.0903	0.4111	0.0871	0.1772		0.77
Ciudad real	13	0.0035	2.2398	1.9668	0.6802		4.89
Córdoba	14	0.2022	1.9854	0.4860	1.6621		4.34
A Coruña	15				1.1326		1.13
Cuenca	16	0.0180	1.5344	2.1431	0.0164		3.71
Girona	17	0.0009	0.3054	0.2648	0.0141		0.59
Granada	18	0.0193	1.4574	0.6396	0.6284		2.74
Guadalajara	19		0.9761	0.6866	0.0378		1.70
Guipúzcoa	20		0.0207	0.0168	0.1381		0.18
Huelva	21	0.0477	1.2253	0.0388	0.3992		1.71
Huesca	22	0.0019	0.6781	1.6128	0.3309		2.62
Jaén	23	0.1471	2.8753	0.1986	0.1518		3.37
León	24	0.0001	0.5402	0.9199	0.5509	0.0956	2.11
Lleida	25	0.0083	0.7056	0.9534	0.3470		2.01
La Rioja	26	0.0069	0.5054	0.1816	0.0960		0.79
Lugo	27		0.0032	0.0007	1.4015	0.0001	1.41
Madrid	28	0.0191	0.8370	0.2759	0.1205		1.25
Málaga	29	0.0315	0.9792	0.3756	0.2290		1.62
Murcia	30	0.0440	0.3557	0.5730	1.5572	0.0513	2.58
Navarra	31	0.0002	0.8635	0.8989	0.1072		1.87
Ourense	32		0.0126	0.1794	0.3177	0.1440	0.65
Asturias	33	0.0004	0.0872	0.0548	0.9800		1.12
Palencia	34		0.7650	1.2803	0.2919	0.0068	2.34
Pontevedra	36		0.0019	0.0018	0.5459		0.55
Salamanca	37	0.0208	0.7461	0.7876	1.2444		2.80
Cantabria	39	0.0007	0.1459	0.0198	0.4810		0.65
Segovia	40	0.0052	1.0352	0.3547	0.0437		1.44
Sevilla	41	0.7395	1.8262	0.5195	1.2783	0.1778	4.54
Soria	42	0.0010	1.0666	0.7204	0.0005		1.79
Tarragona	43	0.1195	0.6932	0.1324	0.2668		1.21
Teruel	44	0.0039	1.0160	0.9874	0.2983	0.0050	2.31
Toledo	45	0.2852	2.2507	1.3950	0.2841	0.0279	4.24
Valencia	46	0.2625	1.0983	0.1827	0.2357		1.78
Valladolid	47	0.0114	1.5567	1.1384	0.0780	0.0012	2.79
Vizcaya	48		0.0137	0.0054	0.1905		0.21
Zamora	49		0.8312	1.0974	0.4924		2.42
Zaragoza	50	0.0004	1.8213	1.4732	0.9497	0.0195	4.26
Total I_RV surface area percentage		**3.08**	**44.80**	**29.42**	**22.13**	**0.56**	**100.00**

Blank cells mean no affected surface.

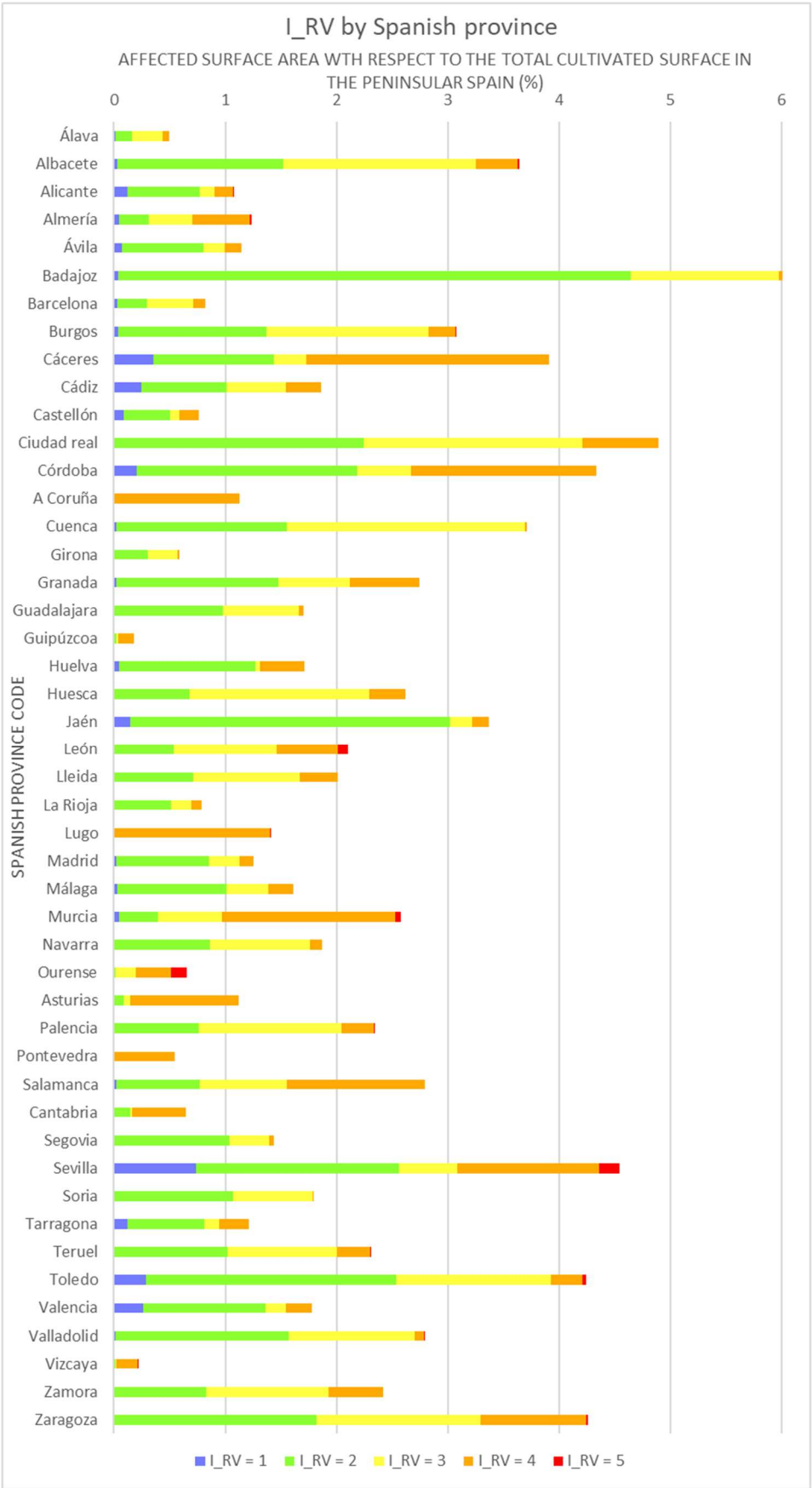
I_RV by Spanish province
AFFECTED SURFACE AREA WTH RESPECT TO THE TOTAL CULTIVATED SURFACE IN THE PENINSULAR SPAIN (%)
0
1
2
3
4
5
6
SPANISH PROVINCE CODE
Álava
Albacete
Alicante
Almería
Ávila
Badajoz
Barcelona
Burgos
Cáceres
Cádiz
Castellón
Ciudad real
Córdoba
A Coruña
Cuenca
Girona
Granada
Guadalajara
Guipúzcoa
Huelva
Huesca
Jaén
León
Lleida
La Rioja
Lugo
Madrid
Málaga
Murcia
Navarra
Ourense
Asturias
Palencia
Pontevedra
Salamanca
Cantabria
Segovia
Sevilla
Soria
Tarragona
Teruel
Toledo
Valencia
Valladolid
Vizcaya
Zamora
Zaragoza
I_RV = 1
I_RV = 2
I_RV = 3
I_RV = 4
I_RV = 5

ANNEXE X: SURFACE OF THE AGRICULTURAL AREAS AFFECTED BY EACH RADIOLOGICAL VULNERABILITY INDEX, DISAGGREGATED BY CROP GROUP, TOPSOIL TEXTURE AND SOIL TYPE (FAO-UNESCO 1974) AND A SUMMARY INCLUDING THE SURFACE OF THE AGRICULTURAL AREAS CONSIDERING THEIR REPRESENTATIVE CROPS AND THE CROP GROUPS TO WHICH THEY BELONG TO

In this Annexe it is included the following data referred to each *Radiological Vulnerability Index* (*I_RV*), in descending order, gathered in tables:

- Surface of the agricultural areas affected by each *Radiological Vulnerability Index*, disaggregated by crop group, topsoil texture and soil type (FAO-UNESCO 1974), in km^2 and in percentage,
- Agricultural areas surface considering their *representative crops*, in km^2 and in percentage,
- Agricultural areas surface considering the crop group to which the *representative crop* of the *basic cartographic units* belongs to, in km^2 and in percentage.

Surface of the agricultural areas affected by the *Maximum Radiological Vulnerability Index* (*I_RV* equal to 5), disaggregated by crop group, topsoil texture and soil group according to the soil type (FAO-UNESCO 1974):

Rad. Vuln. Index I_RV	Crop group (IAEA, 2010) ID_C	Soil texture	Transfer Factor Index I_TF	Soil class. (FAO-UNESCO, 1974)	No. soil group	Clay content (%)	K content (cmol·kg^{-1})	RCs Reserv. Index I_Cs	Surface area of the soil groups (km^2)	Crop Group area grown in each soil texture (%)	Crop group area with each I_RV (%)
5	**ocA**	**Loam**	6.83	Ag	204	21.75	0.19	5	412.84		
				Xk	116	20.11	0.36	5	192.66		
				Lcr	242	20.55	0.38	5	2.78		
		Total Loam							**608.28**	**64.5%**	
		Sand	6.83	Bh	24	12.88	0.30	5	334.74		
		Total Sand							**334.74**	**35.5%**	
	Total ocA								**943.02**	100.0%	**72.23%**
	lfS	**Loam**	6.10	Lc	239	17.33	0.28	5	107.25		
				Xk	116	20.11	0.36	5	54.71		
				Lcr	242	20.55	0.38	5	41.45		
				Ag	204	21.75	0.19	5	20.42		
		Total Loam							**223.83**	**61.7%**	
		Sand	6.57	Bh	24	12.88	0.30	5	138.79		
		Total Sand							**138.79**	**38.3%**	
	Total lfS								**362.62**	100.0%	**27.77%**
	lyL	**Sand**	5.88	Bh	24	12.88	0.30	5	0.01		
		Total Sand							**0.01**	**100.0%**	
	Total lyL								**0.01**	100.0%	**0.001%**
Total 5									**1305.65**		100.0%

Agricultural areas surface within the *Maximum Radiological Vulnerability* considering the representative crop, in km^2 and in percentage:

Affected crops in areas within I_RV = 5				
Crop code	**Crop**	**Crop group code**	**Surface (km^2)**	**Surface percentage**
a52010fia	Irrigated cotton seed	ocA	412.65	31.60
w15040drap	Rainfed chestnut	ocA	334.67	25.63
a62050da	Rainfed vetch	lfS	221.90	17.00
w15010drap	Rainfed almond	ocA	195.63	14.98
a62010fia	Irrigated lucerne	lfS	131.96	10.11
a62030dga	Rainfed grazed sainfoin	lfS	8.76	0.67
w15020drap	Irrigated walnut	ocA	0.07	0.01
a41010da	Rainfed brassica	lyL	0.01	<0.01
Total			1305.65	100%

Agricultural areas surface within the *Maximum Radiological Vulnerability* considering the crop group to which the *representative crop* of the *basic cartographic units* belongs to, in km^2 and in percentage:

Affected crops groups in areas within I_RV = 5			
Crop group code	**Crop group – Plant compartment**	**Surface (km^2)**	**Surface percentage**
ocA	Other crops (all plant's compartments)	943.02	72.23%
lfS	Legume fodder's stems and shoots	362.62	27.77%
lyL	Leafy vegetables' leaves	0.01	<0.01%

Surface of the agricultural areas affected by the *High Radiological Vulnerability Index* (*I_RV* equal to 4), disaggregated by crop group, topsoil texture and soil group according to the soil type (FAO-UNESCO 1974):

Rad. Vuln. Index I_RV	Crop group (IAEA, 2010) ID_C	Soil texture	Transfer Factor Index I_TF	Soil class. (FAO-UNESCO, 1974)	No. soil group	Clay content (%)	K content (cmol·kg^{-1})	RCs Reserv. Index I_Cs	Surface area of the soil groups (km^2)	Crop Group area grown in each soil texture (%)	Crop group area with each I_RV (%)
4	**grS**	**Loam**	4.96	Rd	202	13.24	0.31	4	8830.53		
				U	9	14.64	0.32	4	2814.63		
				Re	206	15.53	0.34	4	2746.89		
				Be	21	16.68	0.38	4	766.64		
				Bh	124	17.13	0.33	4	753.62		
				Ag	204	21.75	0.19	5	737.68		
				Bk	128	23.88	0.57	4	675.11		
				Lo	132	14.21	0.33	4	673.68		
				E	203	20.64	0.52	4	605.04		
				Lcr	242	20.55	0.38	5	202.98		
				Xk	117	23.55	0.45	4	143.79		
				Lc	239	17.33	0.28	5	119.87		
				Lg	238	12.85	0.33	4	79.77		
				Zo	205	19.65	0.31	4	69.83		
				Rc	207	20.53	0.45	4	56.18		
				Bk	129	26.89	0.56	4	28.24		
				Xk	118	16.11	0.44	4	7.39		
				Xk	116	20.11	0.36	5	7.01		
				Ie	3	15.59	0.34	4	5.96		
				Lo	133	12.17	0.31	4	3.30		
				Lc	240	23.92	0.55	4	0.73		
				Zg	15	17.02	0.39	4	0.50		
				Bd	23	16.54	0.41	4	0.33		
				Lkcr	246	23.86	0.59	4	0.00		
		Total Loam							**19329.71**	**73.9%**	
		Sand	5.52	Bh	24	12.88	0.30	5	6643.61		
				Phf	39	10.58	0.36	4	185.08		
		Total Sand							**6828.69**	**26.1%**	
	Total grS								**26158.39**	100.0%	**50.91%**
	ocA	**Loam**	6.83	Bk	128	23.88	0.57	4	4774.02		
				Jc	201	19.49	0.54	3	1640.56		
				Bk	127	23.69	0.66	3	1444.37		
				Bk	126	22.26	0.60	3	978.48		
				Be	21	16.68	0.38	4	941.27		
				Xk	117	23.55	0.45	4	720.39		
				Re	206	15.53	0.34	4	465.42		
				Bk	129	26.89	0.56	4	259.53		
				U	9	14.64	0.32	4	246.17		
				Xy	19	34.26	0.86	3	187.97		
				E	203	20.64	0.52	4	150.36		
				Bh	124	17.13	0.33	4	113.41		
				Rd	202	13.24	0.31	4	60.64		
				Zo	205	19.65	0.31	4	56.83		
				Lg	238	12.85	0.33	4	7.07		
				Xk	118	16.11	0.44	4	3.54		
				Zg	15	17.02	0.39	4	2.75		
				Lo	132	14.21	0.33	4	1.97		
				Rc	207	20.53	0.45	4	1.21		
				Lkc	245	26.70	0.47	4	0.28		
		Total Loam							**12056.23**	**94.9%**	
		Clay	6.83	Vc	14	45.63	0.72	3	424.28		
				Lv	37	35.37	0.76	3	0.62		
		Total Clay							**424.90**	**3.3%**	
		Sand	6.83	Ql	8	3.06	0.36	3	148.12		
				Phf	39	10.58	0.36	4	72.33		
				Lcr	241	9.81	0.21	3	0.50		
		Total Sand							**220.95**	**1.7%**	
	Total ocA								**12702.07**	100.0%	**24.72%**

Rad. Vuln. Index I_RV	Crop group (IAEA, 2010) ID_C	Soil texture	Transfer Factor Index I_TF	Soil class. (FAO-UNESCO, 1974)	No. soil group	Clay content (%)	K content (cmol·kg^{-1})	RCs Reserv. Index I_Cs	Surface area of the soil groups (km^2)	Crop Group area grown in each soil texture (%)	Crop group area with each I_RV (%)
4	**ceG**	**Loam**	4.09	Ag	204	21.75	0.19	5	2316.65		
				Lc	239	17.33	0.28	5	2258.13		
				Lcr	242	20.55	0.38	5	2237.57		
				Xk	116	20.11	0.36	5	315.70		
		Total Loam							**7128.04**	**87.4%**	
		Sand	4.76	Bh	24	12.88	0.30	5	1006.94		
				Lga	38	10.30	0.10	5	17.57		
		Total Sand							**1024.51**	**12.6%**	
	Total ceG								**8152.55**	100.0%	**15.87%**
	lfS	**Loam**	6.10	Bk	128	23.88	0.57	4	826.72		
				Xk	117	23.55	0.45	4	450.31		
				Bh	124	17.13	0.33	4	315.81		
				E	203	20.64	0.52	4	179.31		
				Re	206	15.53	0.34	4	111.29		
				Be	21	16.68	0.38	4	106.28		
				U	9	14.64	0.32	4	89.60		
				Rd	202	13.24	0.31	4	57.83		
				Lg	238	12.85	0.33	4	39.91		
				Zo	205	19.65	0.31	4	33.21		
				Lo	132	14.21	0.33	4	23.17		
				Lkc	245	26.70	0.47	4	3.66		
				Bk	129	26.89	0.56	4	1.91		
		Total Loam							**2239.00**	**99.2%**	
		Sand	6.57	Qc	7	3.89	0.26	3	12.78		
				Lcr	241	9.81	0.21	3	2.95		
				Phf	39	10.58	0.36	4	2.29		
		Total Sand							**18.02**	**0.8%**	
	Total lfS								**2257.03**	100.0%	**4.39%**
	lyL	**Loam**	5.40	Bk	128	23.88	0.57	4	1196.54		
				Xk	117	23.55	0.45	4	305.53		
				Be	21	16.68	0.38	4	282.51		
				Xk	116	20.11	0.36	5	92.85		
				E	203	20.64	0.52	4	52.27		
				Bk	129	26.89	0.56	4	48.06		
				Re	206	15.53	0.34	4	15.13		
				Xk	118	16.11	0.44	4	6.65		
				Bh	124	17.13	0.33	4	3.82		
				Lg	238	12.85	0.33	4	1.20		
				Rd	202	13.24	0.31	4	1.07		
				Lo	132	14.21	0.33	4	0.32		
		Total Loam							**2005.93**	**100.0%**	
	Total lyL								**2005.93**	100.0%	**3.90%**
	maG	**Sand**	4.98	Bh	24	12.88	0.30	5	50.99		
				Lga	38	10.30	0.10	5	4.23		
				Phf	39	10.58	0.36	4	0.46		
		Total Sand							**55.67**	**100.0%**	
	Total maG								**55.67**	100.0%	**0.11%**
	nlF	**Loam**	4.59	Xk	116	20.11	0.36	5	37.16		
		Total Loam							**37.16**	**100.0%**	
	Total nlF								**37.16**	100.0%	**0.07%**
	lvS	**Sand**	5.56	Bh	24	12.88	0.30	5	10.94		
		Total Sand							**10.94**	**100.0%**	
	Total lvS								**10.94**	100.0%	**0.02%**
Total 4									**51379.74**		100.0%

Agricultural areas surface within the *High Radiological Vulnerability* considering the *representative crop*, in km^2 and in percentage:

Affected crops in areas within I_RV = 4				
Crop code	**Crop**	**Crop group code**	**Surface (km^2)**	**Surface percentage**
w15010drap	Rainfed almond	ocA	10014.49	19.49
a61010da	Rainfed winter cereals	grS	8548.51	16.64
a63000da	Rainfed meadows	grS	8210.26	15.98
a11010da	Rainfed wheat total	ceG	4456.64	8.67
a63000iga	Irrigated grazed meadows	grS	3905.09	7.60
a11020da	Rainfed barley total	ceG	3066.38	5.97
a61020da	Rainfed maize for stock feeding	grS	2274.83	4.43
a63000dga	Rainfed grazed meadows	grS	1963.60	3.82
a52010fia	Irrigated cotton seed	ocA	1597.80	3.11
a62010fia	Irrigated lucerne	lfS	1375.15	2.68
a41050fia	Irrigated lettuce	lyL	1310.89	2.55
a61050da	Rainfed other gramineous	grS	1109.31	2.16
a53020da	Rainfed sunflower seed	ocA	738.38	1.44
a62030dga	Rainfed grazed sainfoin	lfS	546.83	1.06
a62050da	Rainfed vetch	lfS	335.05	0.65
w15040drap	Rainfed chestnut	ocA	318.49	0.62
a11010fia	Irrigated wheat total	ceG	290.41	0.57
a11020fia	Irrigated barley total	ceG	262.12	0.51
a41030fia	Irrigated asparagus	lyL	210.91	0.41
a43020fia	Irrigated broccoli	lyL	182.44	0.36
a46030fia	Irrigated other vegetables	lyL	148.76	0.29
a43010fia	Irrigated artichoke	lyL	109.84	0.21
a61020fia	Irrigated maize for stock feeding	grS	101.51	0.20
a12010ta	Total rice	ceG	77.00	0.15
a12020fia	Irrigated maize	maG	55.67	0.11
a63000fia	Irrigated meadows	grS	43.97	0.09
a65030da	Rainfed other crops for stock feeding	lyL	42.19	0.08
w15010irap	Irrigated almond	ocA	24.18	0.05
a42070sia	Sheltered tomato	nlF	22.84	0.04
a44010fia	Irrigated garlic	nlF	14.31	0.03
a22010da	Irrigated meadows	lvS	10.94	0.02
w15030drap	Rainfed hazelnut	ocA	4.17	0.01
w15020drap	Rainfed walnut	ocA	2.62	0.01
w15020irap	Irrigated walnut	ocA	1.94	<0.01
a61050iga	Irrigated grazed other gramineous	grS	1.30	<0.01
a41050da	Rainfed lettuce	lyL	0.59	<0.01
a41010da	Rainfed brassica	lyL	0.32	<0.01
Total			51379.74	100%

Agricultural areas within the *High Radiological Vulnerability* surface considering the crop group to which the *representative crop* of the *basic cartographic units* belongs to, in km^2 and in percentage:

Affected crops groups in areas within I_RV = 4			
Crop group code	**Crop group – Plant compartment**	**Surface (km^2)**	**Surface percentage**
grS	Grasses' stems and shoots	26158.39	50.91%
ocA	Other crops (all plant's compartments)	12702.07	24.72%
ceG	Cereals' grain	8152.55	15.87%
lfS	Legume fodder's stems and shoots	2257.03	4.39%
lyL	Leafy vegetables' leaves	2005.93	3.90%
maG	Maize's grain	55.67	0.11%
nlF	Non-leafy vegetables' fruit, heads, berries and buds	37.16	0.07%
lvS	Legume vegetables' seeds and pods	10.94	0.02%

Surface of the agricultural areas affected by the *Medium Radiological Vulnerability Index* (*I_RV* equal to 3), disaggregated by crop group, topsoil texture and soil group according to the soil type (FAO-UNESCO 1974):

Rad. Vuln. Index I_RV	Crop group (IAEA, 2010) ID_C	Soil texture	Transfer Factor Index I_TF	Soil class. (FAO-UNESCO, 1974)	No. soil group	Clay content (%)	K content (cmol·kg^{-1})	RCs Reserv. Index I_Cs	Surface area of the soil groups (km^2)	Crop Group area grown in each soil texture (%)	Crop group area with each I_RV (%)
3	**ceG**	**Loam**	4.09	Bk	128	23.88	0.57	4	36961.03		
				Re	206	15.53	0.34	4	4527.68		
				Xk	117	23.55	0.45	4	3690.87		
				Rd	202	13.24	0.31	4	3418.68		
				E	203	20.64	0.52	4	1784.95		
				Bk	129	26.89	0.56	4	1538.72		
				Zo	205	19.65	0.31	4	1329.29		
				Bh	124	17.13	0.33	4	1154.02		
				Ie	3	15.59	0.34	4	544.64		
				Be	21	16.68	0.38	4	415.65		
				Rc	207	20.53	0.45	4	415.62		
				Lc	240	23.92	0.55	4	411.44		
				U	9	14.64	0.32	4	384.47		
				Lg	238	12.85	0.33	4	193.63		
				Lkc	244	21.65	0.47	4	170.73		
				Lkc	245	26.70	0.47	4	89.37		
				Lo	132	14.21	0.33	4	70.17		
				Bd	23	16.54	0.41	4	23.07		
				Lo	133	12.17	0.31	4	14.54		
				Zg	15	17.02	0.39	4	0.71		
		Total Loam							**57139.27**	**98.0%**	
		Sand	4.76	Qc	7	3.89	0.26	3	794.59		
				Lcr	241	9.81	0.21	3	312.02		
				Ql	8	3.06	0.36	3	68.42		
				Phf	39	10.58	0.36	4	16.29		
		Total Sand							**1191.31**	**2.0%**	
	Total ceG								**58330.58**	100.0%	**85.42%**
	maG	**Loam**	3.86	Lc	239	17.33	0.28	5	917.64		
				Bk	128	23.88	0.57	4	901.74		
				Bk	129	26.89	0.56	4	382.71		
				Rd	202	13.24	0.31	4	364.36		
				Ag	204	21.75	0.19	5	238.45		
				Bh	124	17.13	0.33	4	193.79		
				Lg	238	12.85	0.33	4	189.20		
				Ie	3	15.59	0.34	4	85.21		
				Zo	205	19.65	0.31	4	59.95		
				Re	206	15.53	0.34	4	53.39		
				E	203	20.64	0.52	4	52.59		
				Be	21	16.68	0.38	4	24.51		
				Lc	240	23.92	0.55	4	23.17		
				Lcr	242	20.55	0.38	5	17.35		
				U	9	14.64	0.32	4	13.73		
				Rc	207	20.53	0.45	4	2.39		
				Bd	23	16.54	0.41	4	1.98		
				Lo	132	14.21	0.33	4	1.78		
				Lkc	244	21.65	0.47	4	0.35		
				Lo	133	12.17	0.31	4	0.14		
		Total Loam							**3524.42**	**98.9%**	
		Sand	4.98	Lcr	241	9.81	0.21	3	38.40		
		Total Sand							**38.40**	**1.1%**	
	Total maG								**3562.82**	100.0%	**5.22%**

Rad. Vuln. Index I_RV	Crop group (IAEA, 2010) ID_C	Soil texture	Transfer Factor Index I_TF	Soil class. (FAO-UNESCO, 1974)	No. soil group	Clay content (%)	K content (cmol·kg^{-1})	RCs Reserv. Index I_Cs	Surface area of the soil groups (km^2)	Crop Group area grown in each soil texture (%)	Crop group area with each I_RV (%)
3	**grS**	**Loam**	4.96	Bk	127	23.69	0.66	3	501.74		
				Jc	201	19.49	0.54	3	413.63		
				Bk	126	22.26	0.60	3	184.53		
				Xy	19	34.26	0.86	3	52.21		
		Total Loam							**1152.11**	**78.5%**	
		Sand	5.52	Lcr	241	9.81	0.21	3	277.35		
				Ql	8	3.06	0.36	3	32.82		
				Qc	7	3.89	0.26	3	5.64		
		Total Sand							**315.82**	**21.5%**	
	Total grS								**1467.93**	100.0%	**2.15%**
	lfS	**Loam**	6.10	Jc	201	19.49	0.54	3	543.16		
				Xy	19	34.26	0.86	3	379.05		
				Bk	126	22.26	0.60	3	258.60		
				Bk	127	23.69	0.66	3	146.95		
		Total Loam							**1327.76**	**96.0%**	
		Clay	4.92	Lv	37	35.37	0.76	3	55.05		
				Vc	14	45.63	0.72	3	0.69		
		Total Clay							**55.74**	**3.8%**	
	Total lfS								**1383.50**	100.0%	**2.03%**
	nlF	**Loam**	4.59	Bk	128	23.88	0.57	4	322.84		
				Xk	117	23.55	0.45	4	205.75		
				Xk	118	16.11	0.44	4	194.68		
				Be	21	16.68	0.38	4	127.86		
				Bk	126	22.26	0.60	3	100.99		
				Bk	127	23.69	0.66	3	57.32		
				E	203	20.64	0.52	4	47.72		
				Jc	201	19.49	0.54	3	46.41		
				Lg	238	12.85	0.33	4	44.24		
				Xy	19	34.26	0.86	3	41.14		
				Re	206	15.53	0.34	4	5.32		
				Rd	202	13.24	0.31	4	3.54		
				Bk	129	26.89	0.56	4	2.66		
		Total Loam							**1200.46**	**100.0%**	
	Total nlF								**1200.46**	100.0%	**1.76%**
	ocA	**Loam**	6.83	Ic	5	17.07	0.62	2	885.48		
		Total Loam							**885.48**	**100.0%**	
	Total ocA								**885.48**	100.0%	**1.30%**
	lyL	**Loam**	5.40	Jc	201	19.49	0.54	3	333.75		
				Bk	126	22.26	0.60	3	181.19		
				Xy	19	34.26	0.86	3	93.20		
				Bk	127	23.69	0.66	3	36.12		
		Total Loam							**644.27**	**100.0%**	
	Total lyL								**644.27**	100.0%	**0.94%**
	wtF	**Sand**	3.80	Bh	24	12.88	0.30	5	506.29		
				Lga	38	10.30	0.10	5	32.14		
				Phf	39	10.58	0.36	4	13.09		
		Total Sand							**551.52**	**100.0%**	
	Total wtF								**551.52**	100.0%	**0.81%**
	rcR	**Loam**	4.49	Bk	128	23.88	0.57	4	47.25		
				Jc	201	19.49	0.54	3	28.82		
				E	203	20.64	0.52	4	22.35		
				Be	21	16.68	0.38	4	22.24		
		Total Loam							**120.66**	**100.0%**	
	Total rcR								**120.66**	100.0%	**0.18%**

Rad. Vuln. Index I_RV	Crop group (IAEA, 2010) ID_C	Soil texture	Transfer Factor Index I_TF	Soil class. (FAO-UNESCO, 1974)	No. soil group	Clay content (%)	K content (cmol·kg^{-1})	RCs Reserv. Index I_Cs	Surface area of the soil groups (km^2)	Crop Group area grown in each soil texture (%)	Crop group area with each I_RV (%)
3	**tbT**	**Loam**	4.65	Jc	201	19.49	0.54	3	71.61		
				Bk	128	23.88	0.57	4	37.37		
				Bk	127	23.69	0.66	3	3.06		
				Bk	126	22.26	0.60	3	1.71		
				Bk	129	26.89	0.56	4	1.21		
				E	203	20.64	0.52	4	0.39		
				Re	206	15.53	0.34	4	0.34		
		Total Loam							**115.70**	**100.0%**	
	Total tbT								**115.70**	100.0%	**0.17%**
	lvS	**Loam**	4.09	Be	21	16.68	0.38	4	12.94		
				Lo	132	14.21	0.33	4	8.85		
				Bh	124	17.13	0.33	4	0.81		
		Total Loam							**22.59**	**100.0%**	
	Total lvS								**22.59**	100.0%	**0.03%**
Total 3									**68285.51**		100.0%

Agricultural areas surface within the *Medium Radiological Vulnerability* considering the *representative crop*, in km^2 and in percentage:

Affected crops in areas within I_RV = 3				
Crop code	**Crop**	**Crop group code**	**Surface (km^2)**	**Surface percentage**
a11020da	Rainfed barley total	ceG	35545.26	52.05
a11010da	Rainfed wheat total	ceG	17175.98	25.15
a11020fia	Irrigated barley total	ceG	4905.81	7.18
a12020fia	Irrigated maize	maG	3562.50	5.22
a62010fia	Irrigated lucerne	lfS	1093.21	1.60
a61010da	Rainfed winter cereals	grS	893.02	1.31
w15010drap	Rainfed almond	ocA	885.48	1.30
a44010fia	Irrigated garlic	nlF	705.41	1.03
a42070sia	Sheltered tomato	nlF	495.05	0.72
a11010fia	Irrigated wheat total	ceG	488.20	0.71
a41050fia	Irrigated lettuce	lyL	431.25	0.63
w21020drap	Rainfed wine grapes	wtF	348.06	0.51
a63000dga	Rainfed grazed meadows	grS	308.14	0.45
a12010ta	Total rice	ceG	215.33	0.32
a62030dga	Rainfed grazed sainfoin	lfS	167.97	0.25
w12010drap	Rainfed apple	wtF	135.06	0.20
a62050da	Rainfed vetch	lfS	122.32	0.18
a51020fia	Irrigated sugar beet	rcR	120.66	0.18
a31010fia	Irrigated potatoes total	tbT	115.70	0.17
a41030fia	Irrigated asparagus	lyL	105.62	0.15
a63000iga	Irrigated grazed meadows	grS	104.21	0.15
a63000da	Rainfed meadows	grS	65.85	0.10
a61020fia	Irrigated maize for stock feeding	grS	56.34	0.08
w12020irap	Irrigated pear	wtF	44.05	0.06
a65030da	Rainfed other crops for stock feeding	lyL	37.26	0.05
a43020fia	Irrigated broccoli	lyL	26.48	0.04
a61050da	Rainfed other gramineous	grS	25.15	0.04
a46030fia	Irrigated other vegetables	lyL	23.27	0.03
a22010da	Rainfed dry beans	lvS	22.59	0.03
a43010fia	Irrigated artichoke	lyL	20.39	0.03
w31020drap	Rainfed olives for oil	wtF	19.68	0.03
a61050iga	Irrigated grazed other gramineous	grS	15.22	0.02
w14080irap	Irrigated kiwi	wtF	2.33	<0.01
w13030irap	Irrigated peach	wtF	2.22	<0.01
a12020da	Rainfed maize	maG	0.32	<0.01
w13030drap	Rainfed peach	wtF	0.13	<0.01
Total			68285.51	100%

Agricultural areas surface within the *Medium Radiological Vulnerability* considering the crop group to which the *representative crop* of the *basic cartographic units* belongs to, in km^2 and in percentage:

Affected crops groups in areas within I_RV = 3			
Crop group code	**Crop group – Plant compartment**	**Surface (km^2)**	**Surface percentage**
ceG	Cereals' grain	58330.58	85.42%
maG	Maize's grain	3562.82	5.22%
grS	Grasses' stems and shoots	1467.93	2.15%
lfS	Legume fodder's stems and shoots	1383.50	2.03%
nlF	Non-leafy vegetables' fruit, heads, berries and buds	1200.46	1.76%
ocA	Other crops (all plant's compartments)	885.48	1.30%
lyL	Leafy vegetables' leaves	644.27	0.94%
wtF	Woody trees' fruits	551.52	0.81%
rcR	Root crops' roots	120.66	0.18%
tbT	Tubers	115.70	0.17%
lvS	Legume vegetables' seeds and pods	22.59	0.03%

Surface of the agricultural areas affected by the *Low Radiological Vulnerability Index* (*I_RV* equal to 2), disaggregated by crop group, topsoil texture and soil group according to the soil type (FAO-UNESCO 1974):

Rad. Vuln. Index I_RV	Crop group (IAEA, 2010) ID_C	Soil texture	Transfer Factor Index I_TF	Soil class. (FAO-UNESCO, 1974)	No. soil group	Clay content (%)	K content (cmol·kg^{-1})	RCs Reserv. Index I_Cs	Surface area of the soil groups (km^2)	Crop Group area grown in each soil texture (%)	Crop group area with each I_RV (%)
2	**wtF**	**Loam**	2.35	Bk	128	23.88	0.57	4	20324.65		
				Rd	202	13.24	0.31	4	6143.14		
				Re	206	15.53	0.34	4	6036.91		
				Bk	126	22.26	0.60	3	5406.20		
				Jc	201	19.49	0.54	3	3309.81		
				Bk	127	23.69	0.66	3	3264.88		
				Ag	204	21.75	0.19	5	1907.82		
				Xk	117	23.55	0.45	4	1211.22		
				E	203	20.64	0.52	4	943.03		
				Lcr	242	20.55	0.38	5	939.16		
				Be	21	16.68	0.38	4	697.31		
				Bh	124	17.13	0.33	4	621.79		
				Ie	3	15.59	0.34	4	412.61		
				Lc	240	23.92	0.55	4	336.41		
				Lc	239	17.33	0.28	5	269.60		
				Lg	238	12.85	0.33	4	249.92		
				U	9	14.64	0.32	4	198.31		
				Xk	116	20.11	0.36	5	187.83		
				Bk	129	26.89	0.56	4	180.67		
				Lo	132	14.21	0.33	4	99.93		
				Zo	205	19.65	0.31	4	65.48		
				Xy	19	34.26	0.86	3	59.13		
				Lo	133	12.17	0.31	4	52.15		
				Lkc	245	26.70	0.47	4	33.27		
				Bd	23	16.54	0.41	4	23.01		
				Lkcr	246	23.86	0.59	4	12.16		
				Lkc	244	21.65	0.47	4	8.26		
				Zg	15	17.02	0.39	4	2.38		
				Rc	207	20.53	0.45	4	2.06		
				Xk	118	16.11	0.44	4	0.10		
		Total Loam							**52999.19**	**98.8%**	
		Sand	3.80	Lcr	241	9.81	0.21	3	316.73		
				Ql	8	3.06	0.36	3	314.60		
				Qc	7	3.89	0.26	3	26.79		
		Total Sand							**658.12**	**1.2%**	
	Total wtF								**53657.31**	100.0%	**51.59%**
	ceG	**Loam**	4.09	Bk	126	22.26	0.60	3	11226.16		
				Jc	201	19.49	0.54	3	10110.36		
				Bk	127	23.69	0.66	3	9183.40		
				Ic	5	17.07	0.62	2	3479.96		
				Xy	19	34.26	0.86	3	1895.44		
				Je	1	14.45	0.61	2	149.61		
		Total Loam							**36044.94**	**84.8%**	
		Clay	3.49	Lv	37	35.37	0.76	3	4652.69		
				Vc	14	45.63	0.72	3	1813.96		
		Total Clay							**6466.66**	**15.2%**	
	Total ceG								**42511.60**	100.0%	**40.88%**
	maG	**Loam**	3.86	Jc	201	19.49	0.54	3	2624.42		
				Bk	127	23.69	0.66	3	992.96		
				Bk	126	22.26	0.60	3	204.59		
				Je	1	14.45	0.61	2	153.42		
				Xy	19	34.26	0.86	3	90.34		
				Ic	5	17.07	0.62	2	21.22		
		Total Loam							**4086.96**	**93.8%**	
		Clay	3.58	Lv	37	35.37	0.76	3	269.07		
		Total Clay							**269.07**	**6.2%**	
	Total maG								**4356.03**	100.0%	**4.19%**

Rad. Vuln. Index I_RV	Crop group (IAEA, 2010) ID_C	Soil texture	Transfer Factor Index I_TF	Soil class. (FAO-UNESCO, 1974)	No. soil group	Clay content (%)	K content (cmol·kg^{-1})	RCs Reserv. Index I_Cs	Surface area of the soil groups (km^2)	Crop Group area grown in each soil texture (%)	Crop group area with each I_RV (%)
2	**grS**	**Clay**	3.58	Lv	37	35.37	0.76	3	939.86		
				Vc	14	45.63	0.72	3	271.46		
		Total Clay							**1211.32**	**67.4%**	
		Loam	4.96	Ic	5	17.07	0.62	2	311.97		
				Je	1	14.45	0.61	2	273.27		
		Total Loam							**585.24**	**32.6%**	
	Total grS								**1796.56**	100.0%	**1.73%**
	ocA	**Clay**	6.83	Vp	12	55.77	1.31	1	738.65		
		Total Clay							**738.65**	**80.6%**	
		Sand	6.83	Id	6	14.09	0.99	1	177.88		
		Total Sand							**177.88**	**19.4%**	
	Total ocA								**916.53**	100.0%	**0.88%**
	lyL	**Loam**	5.40	Ic	5	17.07	0.62	2	259.49		
		Total Loam							**259.49**	**90.9%**	
		Clay	3.98	Vc	14	45.63	0.72	3	25.93		
		Total Clay							**25.93**	**9.1%**	
	Total lyL								**285.42**	100.0%	**0.27%**
	hpF	**Sand**	2.53	Ql	8	3.06	0.36	3	168.67		
		Total Sand							**168.67**	**100.0%**	
	Total hpF								**168.67**	100.0%	**0.16%**
	nlF	**Loam**	4.59	Ic	5	17.07	0.62	2	145.52		
		Total Loam							**145.52**	**90.9%**	
		Clay	3.30	Vc	14	45.63	0.72	3	14.52		
		Total Clay							**14.52**	**9.1%**	
	Total nlF								**160.04**	100.0%	**0.15%**
	lfS	**Loam**	6.10	Ic	5	17.07	0.62	2	124.47		
				Je	1	14.45	0.61	2	0.55		
		Total Loam							**125.02**	**100.0%**	
	Total lfS								**125.02**	100.0%	**0.12%**
	tbT	**Loam**	4.65	Ic	5	17.07	0.62	2	21.89		
		Total Loam							**21.89**	**100.0%**	
	Total tbT								**21.89**	100.0%	**0.02%**
	lvS	**Loam**	4.09	Jc	201	19.49	0.54	3	0.44		
		Total Loam							**0.44**	**100.0%**	
	Total lvS								**0.44**	100.0%	**0.0004%**
	rcR	**Loam**	4.49	Ic	5	17.07	0.62	2	0.39		
		Total Loam							**0.39**	**100.0%**	
	Total rcR								**0.39**	100.0%	**0.0004%**
Total 2									**103999.90**		100.0%

Agricultural areas surface within the Low Radiological Vulnerability considering the *representative crop*, in km^2 and in percentage:

Affected crops in areas within I_RV = 2				
Crop code	**Crop**	**Crop group code**	**Surface (km^2)**	**Surface percentage**
w31020drap	Rainfed olives for oil	wtF	34897.29	33.56
a11020da	Rainfed barley total	ceG	23854.42	22.94
w21020drap	Rainfed wine grapes	wtF	12707.89	12.22
a11010da	Rainfed wheat total	ceG	11957.93	11.50
a11020fia	Irrigated barley total	ceG	4885.34	4.70
a12020fia	Irrigated maize	maG	4356.03	4.19
w11010trap	Total sweet orange	wtF	2935.59	2.82
a11010fia	Rainfed winter cereals	ceG	1116.42	1.07
a61010da	Irrigated cotton seed	grS	711.94	0.68
a52010fia	Total rice	ocA	706.01	0.68
a12010ta	Total mandarin oranges	ceG	697.47	0.67
w11030trap	Rainfed cherry	wtF	655.40	0.63
w13020drap	Irrigated grazed meadows	wtF	552.45	0.53
a63000iga	Irrigated wine grapes	grS	546.70	0.53
w21020irap	Rainfed winter cereals	wtF	478.65	0.46
w31020irap	Irrigated olives for oil	wtF	411.67	0.40
a61050da	Rainfed other gramineous	grS	332.47	0.32
w13030irap	Irrigated peach	wtF	280.28	0.27
w12010drap	Rainfed apple	wtF	223.44	0.21
w14040irap	Irrigated avocado	wtF	186.49	0.18
w15010drap	Rainfed almond	ocA	177.88	0.17
w12020irap	Irrigated pear	wtF	169.10	0.16
a42090sia	Sheltered strawberry	hpF	168.67	0.16
a44010fia	Irrigated garlic	nlF	160.04	0.15
a46030fia	Irrigated other vegetables	lyL	109.99	0.11
a63000da	Rainfed meadows	grS	101.52	0.10
a41050fia	Irrigated lettuce	lyL	76.53	0.07
a62010fia	Irrigated lucerne	lfS	65.45	0.06
w12010irap	Irrigated apple	wtF	64.74	0.06
a63000dga	Rainfed grazed meadows	grS	63.47	0.06
a62030dga	Rainfed grazed sainfoin	lfS	58.04	0.06
w14010drap	Rainfed fig tree	wtF	42.26	0.04
a43010fia	Irrigated artichoke	lyL	35.73	0.03
w40000drap	Rainfed other woody crops	wtF	35.40	0.03
a53020da	Rainfed sunflower seed	ocA	32.65	0.03
a43020fia	Irrigated broccoli	lyL	31.53	0.03
a61020da	Rainfed maize for stock feeding	grS	29.75	0.03
a65030da	Rainfed other crops for stock feeding	lyL	29.26	0.03
a31010fia	Irrigated potatoes total	tbT	21.89	0.02
w40000irap	Irrigated other woody crops	wtF	8.99	0.01
a61020fia	Irrigated maize for stock feeding	grS	8.73	0.01

Affected crops in areas within I_RV = 2				
Crop code	**Crop**	**Crop group code**	**Surface (km^2)**	**Surface percentage**
w14080irap	Irrigated kiwi	wtF	4.36	<0.01
a41030fia	Irrigated asparagus	lyL	2.38	<0.01
w11040trap	Total lemon	wtF	1.61	<0.01
a63000fia	Irrigated meadows	grS	1.58	<0.01
a62050da	Rainfed vetch	lfS	1.53	<0.01
w14060irap	Irrigated date palm	wtF	0.59	<0.01
w31010drap	Rainfed table olives	wtF	0.58	<0.01
a22010da	Rainfed dry beans	lvS	0.44	<0.01
a61050iga	Irrigated grazed other gramineous	grS	0.39	<0.01
a51020fia	Irrigated sugar beet	rcR	0.39	<0.01
w13030drap	Rainfed peach	wtF	0.27	<0.01
w12020drap	Rainfed pear	wtF	0.25	<0.01
Total			103999.90	100%

Agricultural areas surface within the *Low Radiological Vulnerability* considering the crop group to which the *representative crop* of the *basic cartographic units* belongs to, in km^2 and in percentage:

Affected crops groups in areas within I_RV = 2			
Crop group code	**Crop group – Plant compartment**	**Surface (km^2)**	**Surface percentage**
wtF	Woody trees' fruits	53657.31	51.59%
ceG	Cereals' grain	42511.60	40.88%
maG	Maize's grain	4356.03	4.19%
grS	Grasses' stems and shoots	1796.56	1.73%
ocA	Other crops (all plant's compartments)	916.53	0.88%
lyL	Leafy vegetables' leaves	285.42	0.27%
hpF	Herbaceous plants' fruits	168.67	0.16%
nlF	Non-leafy vegetables' fruit, heads, berries and buds	160.04	0.15%
lfS	Legume fodder's stems and shoots	125.02	0.12%
tbT	Tubers	21.89	0.02%
lvS	Legume vegetables' seeds and pods	0.44	<0.01%
rcR	Root crops' roots	0.39	<0.01%

Surface of the agricultural areas affected by the *Minimum Radiological Vulnerability Index* (*I_RV* equal to 2), disaggregated by crop group, topsoil texture and soil group according to the soil type (FAO-UNESCO 1974):

Rad. Vuln. Index I_RV	Crop group (IAEA, 2010) ID_C	Soil texture	Transfer Factor Index I_TF	Soil class. (FAO-UNESCO, 1974)	No. soil group	Clay content (%)	K content (cmol·kg^{-1})	RCs Reserv. Index I_Cs	Surface area of the soil groups (km^2)	Crop Group area grown in each soil texture (%)	Crop group area with each I_RV (%)
1	**wtF**	**Clay**	1.19	Vc	14	45.63	0.72	3	1187.52		
				Lv	37	35.37	0.76	3	871.24		
				Vp	12	55.77	1.31	1	198.20		
		Total Clay							**2256.96**	**47.6%**	
		Loam	2.35	Ic	5	17.07	0.62	2	1883.02		
				Je	1	14.45	0.61	2	86.35		
		Total Loam							**1969.37**	**41.5%**	
		Sand	3.80	Id	6	14.09	0.99	1	517.34		
		Total Sand							**517.34**	**10.9%**	
	Total wtF								**4743.66**	100.0%	**66.34%**
	ceG	**Clay**	3.49	Vp	12	55.77	1.31	1	1771.08		
		Total Clay							**1771.08**	**96.7%**	
		Sand	4.76	Id	6	14.09	0.99	1	59.71		
		Total Sand							**59.71**	**3.3%**	
	Total ceG								**1830.79**	100.0%	**25.60%**
	grS	**Sand**	5.52	Id	6	14.09	0.99	1	403.61		
		Total Sand							**403.61**	**89.4%**	
		Clay	3.58	Vp	12	55.77	1.31	1	47.68		
		Total Clay							**47.68**	**10.6%**	
	Total grS								**451.29**	100.0%	**6.31%**
	hpF	**Loam**	0.99	Bk	128	23.88	0.57	4	20.80		
				Bk	126	22.26	0.60	3	14.67		
				Bk	127	23.69	0.66	3	8.72		
				Re	206	15.53	0.34	4	4.47		
		Total Loam							**48.66**	**74.6%**	
		Clay	0.99	Vc	14	45.63	0.72	3	12.50		
				Vp	12	55.77	1.31	1	4.04		
		Total Clay							**16.54**	**25.4%**	
	Total hpF								**65.20**	100.0%	**0.91%**
	lyL	**Sand**	5.88	Id	6	14.09	0.99	1	51.69		
		Total Sand							**51.69**	**100.0%**	
	Total lyL								**51.69**	100.0%	**0.72%**
	maG	**Sand**	4.98	Id	6	14.09	0.99	1	5.50		
		Total Sand							**5.50**	**100.0%**	
	Total maG								**5.50**	100.0%	**0.08%**
	nlF	**Sand**	4.65	Id	6	14.09	0.99	1	2.07		
		Total Sand							**2.07**	**100.0%**	
	Total nlF								**2.07**	100.0%	**0.03%**
Total 1									**7150.21**		100.0%

Agricultural areas surface within the *Minimum Radiological Vulnerability* considering the *representative crop*, in km^2 and in percentage:

Affected crops in areas within I_RV = 1				
Crop code	**Crop**	**Crop group code**	**Surface (km^2)**	**Surface percentage**
w31020drap	Rainfed olives for oil	wtF	2640.345	36.93
a11010da	Rainfed wheat total	ceG	1447.794	20.25
w21020drap	Rainfed wine grapes	wtF	960.174	13.43
w11010trap	Total sweet orange	wtF	601.280	8.41
a12010ta	Total rice	ceG	331.144	4.63
a63000iga	Irrigated grazed meadows	grS	298.347	4.17
w13020drap	Rainfed cherry	wtF	164.822	2.31
w11030trap	Total mandarin oranges	wtF	158.151	2.21
a61010da	Rainfed winter cereals	grS	142.588	1.99
w14010drap	Rainfed fig tree	wtF	98.627	1.38
a42090sia	Sheltered strawberry	hpF	65.201	0.91
a41050fia	Irrigated lettuce	lyL	51.314	0.72
w31020irap	Irrigated olives for oil	wtF	45.133	0.63
a11020da	Rainfed barley total	ceG	30.007	0.42
w21020irap	Irrigated wine grapes	wtF	28.171	0.39
a11010fia	Irrigated wheat total	ceG	17.139	0.24
w12020irap	Irrigated pear	wtF	14.012	0.20
w40000drap	Rainfed other woody crops	wtF	13.673	0.19
w14040irap	Irrigated avocado	wtF	9.851	0.14
a63000dga	Rainfed grazed meadows	grS	6.707	0.09
a12020fia	Irrigated maize	maG	5.501	0.08
a11020fia	Irrigated barley total	ceG	4.708	0.07
w12010irap	Irrigated apple	wtF	4.008	0.06
a63000fia	Irrigated meadows	grS	3.648	0.05
w12010drap	Rainfed apple	wtF	3.006	0.04
a42070sia	Sheltered tomato	nlF	2.069	0.03
w13030irap	Irrigated peach	wtF	1.859	0.03
w11040trap	Total lemon	wtF	0.551	0.01
a41030fia	Irrigated asparagus	lyL	0.380	0.01
Total			7150.21	100%

Agricultural areas surface within the *Minimum Radiological Vulnerability* considering the crop group to which the *representative crop* of the *basic cartographic units* belongs to, in km^2 and in percentage:

Affected crops groups in areas within I_RV = 1			
Crop group code	**Crop group – Plant compartment**	**Surface (km^2)**	**Surface percentage**
wtF	Woody trees' fruits	4743.66	66.34%
ceG	Cereals' grain	1830.79	25.60%
grS	Grasses' stems and shoots	451.29	6.31%
hpF	Herbaceous plants' fruits	65.20	0.91%
lyL	Leafy vegetables' leaves	51.69	0.72%
maG	Maize's grain	5.50	0.08%
nlF	Non-leafy vegetables' fruit, heads, berries and buds	2.07	0.03%

ANNEXE XI: AGRICULTURAL SURFACE AREA AFFECTED BY THE FIVE DEPOSITION INDEXES (I_D) FOR ANNUAL AND SEASONAL AVERAGE METEOROLOGICAL CONDITIONS IN EACH SPANISH PENINSULAR PROVINCE

Peninsular Spain Province	Province Code	Surface affected by each Deposition Index value in the Annual Average Deposition map (km^2)				
		I_D = 1	I_D = 2	I_D = 3	I_D = 4	I_D = 5
Álava	1			1146.96		
Albacete	2		3824.42	4128.35	505.00	
Alicante	3	241.26	2248.22			
Almería	4	1395.31	1473.27			
Ávila	5			2321.42	337.49	
Badajoz	6		23.96	13363.90	1094.35	
Barcelona	8	17.88	1895.91			
Burgos	9		67.23	7070.77		
Cáceres	10		255.13	3368.63	4659.56	799.44
Cádiz	11	3865.80	455.97			
Castellón	12		1345.41	432.08		
Ciudad real	13			7726.98	3624.49	
Córdoba	14	25.08	6298.70	3740.27		
A Coruña	15	1967.82	661.17			
Cuenca	16			2660.32	5955.80	
Girona	17	1276.60	81.98			
Granada	18	980.17	5390.92			
Guadalajara	19			10.95	3936.27	
Guipúzcoa	20		53.96	353.86		
Huelva	21	0.70	2400.29	1570.65		
Huesca	22		5907.84	182.42		
Jaén	23		6485.16	1343.91		
León	24	217.35	4580.84	91.92		
Lleida	25	49.70	4625.95			
La Rioja	26			1833.36		
Lugo	27	3262.51				
Madrid	28				2907.40	
Málaga	29	3121.92	627.48			
Murcia	30	2089.41	3902.11			
Navarra	31		442.86	3897.41		
Ourense	32	1303.43	214.15			
Asturias	33	1255.87	1349.58			
Palencia	34		1199.31	4241.63		
Pontevedra	36	1052.67	222.93			
Salamanca	37		3621.36	2875.47		
Cantabria	39		1429.09	73.93		
Segovia	40			2226.21	1113.64	
Sevilla	41	430.00	9297.33	813.91		
Soria	42			1459.35	2692.04	
Tarragona	43		2812.95			
Teruel	44		379.60	4778.90	205.05	
Toledo	45				8716.20	1132.33
Valencia	46		3087.29	1042.40		
Valladolid	47		715.84	5255.26	495.25	
Vizcaya	48		19.14	467.26		
Zamora	49		3755.50	1864.17		
Zaragoza	50		1210.51	6440.28	2246.92	
Total surface (km^2)		22553.46	82363.36	86782.97	38489.46	1931.76

Blank cells mean no affected surface.

Only agricultural areas, to which a *representative crop* and their corresponding topsoil texture are assigned, are considered.

Peninsular Spain Province	Province code	Surface affected by each Deposition Index value in the Spring Average Deposition map (km²)				
		I_D = 1	I_D = 2	I_D = 3	I_D = 4	I_D = 5
Álava	1		178.64	968.33		
Albacete	2		818.11	6523.64	1116.022	
Alicante	3		2489.48			
Almería	4	192.00	2450.68	225.90		
Ávila	5		50.79	2009.11	599.015	
Badajoz	6		153.04	12039.05	2290.130	
Barcelona	8	25.23	1888.56			
Burgos	9	27.73	2830.17	4280.10		
Cáceres	10		290.02	4282.10	3966.452	544.19
Cádiz	11	3626.60	695.18			
Castellón	12		411.78	1365.70		
Ciudad real	13			4279.04	7072.442	
Córdoba	14		2416.80	7647.25		
A Coruña	15	2556.75	72.24			
Cuenca	16		33.64	3359.94	5222.548	
Girona	17	1111.61	246.97			
Granada	18		4274.04	2097.05		
Guadalajara	19			14.30	3932.918	
Guipúzcoa	20		38.76	369.06		
Huelva	21	0.70	401.86	3569.07		
Huesca	22		5903.59	186.66		
Jaén	23		734.60	7048.79	45.685	
León	24	249.58	4308.20	332.32		
Lleida	25	7.44	4668.21			
La Rioja	26		73.68	1725.82	33.859	
Lugo	27	3187.63	74.88			
Madrid	28				2907.397	
Málaga	29	1520.35	2229.05			
Murcia	30	799.96	4132.69	1058.87		
Navarra	31		0.24	4197.01	143.015	
Ourense	32	1302.66	214.92			
Asturias	33	1445.36	1160.08			
Palencia	34	51.92	1476.95	3912.07		
Pontevedra	36	1243.39	32.20			
Salamanca	37		3458.38	3038.45		
Cantabria	39	1327.30	175.73			
Segovia	40			1053.44	2286.407	
Sevilla	41	59.35	5682.35	4799.54		
Soria	42			2819.33	1332.058	
Tarragona	43	430.76	2369.74	12.46		
Teruel	44		387.10	4078.32	898.127	
Toledo	45			78.86	9537.093	232.58
Valencia	46		2524.34	1602.58	2.770	
Valladolid	47		223.23	5911.14	331.980	
Vizcaya	48		182.95	303.45		
Zamora	49	55.64	2299.29	3264.75		
Zaragoza	50		1654.85	7212.09	1030.781	
Total surface (km²)		**19221.95**	**63708.01**	**105665.58**	**42748.70**	**776.77**

Blank cells mean no affected surface.

Only agricultural areas, to which a *representative crop* and their corresponding topsoil texture are assigned, are considered.

Peninsular Spain Province	Province code	Surface affected by each Deposition Index value in the Summer Average Deposition map (km^2)				
		I_D = 1	I_D = 2	I_D = 3	I_D = 4	I_D = 5
Álava	1			827.47	319.50	
Albacete	2		1568.49	4828.07	2061.21	
Alicante	3	512.90	1976.58			
Almería	4	2627.19	241.39			
Ávila	5			948.65	1710.26	
Badajoz	6		15.49	7350.20	7116.53	
Barcelona	8	2.52	1911.27			
Burgos	9			3197.71	3940.29	
Cáceres	10	0.01	865.23	3104.35	4599.13	514.04
Cádiz	11	4321.78				
Castellón	12		410.96	1336.74	29.78	
Ciudad real	13			3423.64	7905.19	22.65
Córdoba	14	1075.80	4364.23	4429.96	194.06	
A Coruña	15	2629.00				
Cuenca	16			612.28	6902.90	1100.94
Girona	17	1120.64	237.93			
Granada	18	3343.31	3027.78			
Guadalajara	19				2007.78	1939.44
Guipúzcoa	20		53.96	353.86		
Huelva	21	1.60	2138.73	1831.31		
Huesca	22		4059.23	2031.02		
Jaén	23	667.66	6317.33	844.08		
León	24	945.00	3853.18	91.92		
Lleida	25		2822.37	1853.28		
La Rioja	26			65.91	1767.45	
Lugo	27	3262.51				
Madrid	28				1085.99	1821.41
Málaga	29	3749.40				
Murcia	30	4494.50	1055.23	441.79		
Navarra	31		346.42	2483.44	1510.40	
Ourense	32	1517.58				
Asturias	33	1732.36	873.09			
Palencia	34		700.83	4232.09	508.03	
Pontevedra	36	1275.59				
Salamanca	37	68.04	4178.12	2250.67		
Cantabria	39		709.92	793.10		
Segovia	40				3339.84	
Sevilla	41	2411.19	6621.93	1508.12		
Soria	42				4151.39	
Tarragona	43	0.49	2651.27	161.19		
Teruel	44			484.50	4879.05	
Toledo	45				3514.14	6334.39
Valencia	46		2599.02	1427.48	103.19	
Valladolid	47		421.27	4374.63	1670.45	
Vizcaya	48		181.24	305.16		
Zamora	49	818.60	2956.13	1844.94		
Zaragoza	50		351.72	4358.13	5187.87	
Total surface (km^2)		36577.66	57510.36	61795.68	64504.45	11732.87

Blank cells mean no affected surface.

Only agricultural areas, to which a *representative crop* and their corresponding topsoil texture are assigned, are considered.

Peninsular Spain Province	Province code	Surface affected by each Deposition Index value in the Autumn Average Deposition map (km^2)				
		I_D = 1	I_D = 2	I_D = 3	I_D = 4	I_D = 5
Álava	1			1132.50	14.46	
Albacete	2		6349.35	1990.15	118.27	
Alicante	3	784.52	1704.96			
Almería	4	1722.44	1146.13			
Ávila	5			1795.13	863.77	
Badajoz	6		2684.37	11360.01	437.84	
Barcelona	8	1041.85	871.94			
Burgos	9			7020.32	117.69	
Cáceres	10		4.26	3247.00	4721.79	1109.71
Cádiz	11	3536.27	785.51			
Castellón	12	0.82	1186.36	590.30		
Ciudad real	13		2785.67	7400.88	1164.93	
Córdoba	14	983.20	8445.96	634.89		
A Coruña	15	1664.29	964.70			
Cuenca	16		574.72	5421.09	2620.31	
Girona	17	1358.58				
Granada	18	1514.17	4856.92			
Guadalajara	19			783.74	3163.48	
Guipúzcoa	20		34.96	372.86		
Huelva	21	276.71	3296.91	398.02		
Huesca	22	2461.53	3550.52	78.20		
Jaén	23		7829.08			
León	24		2231.27	2658.83		
Lleida	25	1518.58	3157.07			
La Rioja	26			1767.45	65.91	
Lugo	27	2892.22	370.28			
Madrid	28			61.47	2845.92	
Málaga	29	1842.74	1906.66			
Murcia	30	2382.11	3609.41			
Navarra	31	6.28	834.42	3499.57		
Ourense	32	257.94	1259.64			
Asturias	33	362.50	2242.95			
Palencia	34		394.78	4961.86	84.31	
Pontevedra	36	55.34	1220.25			
Salamanca	37		157.73	6321.43	17.66	
Cantabria	39		144.89	1358.13		
Segovia	40			2865.21	474.64	
Sevilla	41	2862.49	7678.75			
Soria	42			1398.93	2752.46	
Tarragona	43	1061.55	1751.41			
Teruel	44	177.90	1956.11	3229.54		
Toledo	45			2813.77	6499.60	535.15
Valencia	46		3520.43	609.26		
Valladolid	47		377.94	4492.21	1596.20	
Vizcaya	48			486.40		
Zamora	49		640.39	4979.28		
Zaragoza	50	54.69	2442.95	5345.57	2054.50	
Total surface (km^2)		28818.71	82969.67	89074.02	29613.75	1644.86

Blank cells mean no affected surface.

Only agricultural areas, to which a *representative crop* and their corresponding topsoil texture are assigned, are considered.

Peninsular Spain Province	Province code	Surface affected by each Deposition Index value in the Winter Average Deposition map (km^2)				
		I_D = 1	I_D = 2	I_D = 3	I_D = 4	I_D = 5
Álava	1		832.69	314.28		
Albacete	2	9.97	7346.12	1101.69		
Alicante	3	740.61	1748.87			
Almería	4	2868.57				
Ávila	5		501.76	1956.23	200.93	
Badajoz	6	185.63	3781.55	9899.19	615.86	
Barcelona	8	636.99	1276.80			
Burgos	9		1529.85	5608.15		
Cáceres	10	7.09	845.64	3846.64	3742.52	640.89
Cádiz	11	3020.99	1300.78			
Castellón	12	494.22	1283.26			
Ciudad real	13		4379.89	6969.17	2.41	
Córdoba	14	1711.98	8148.19	203.87		
A Coruña	15	179.56	2449.44			
Cuenca	16		441.06	7401.59	773.48	
Girona	17	1355.47	3.11			
Granada	18	4453.98	1917.11			
Guadalajara	19		285.98	859.24	2802.00	
Guipúzcoa	20		375.42	32.40		
Huelva	21	288.50	3522.78	160.36		
Huesca	22	1261.42	4109.78	719.06		
Jaén	23	636.31	7146.39	46.38		
León	24	128.19	4761.92			
Lleida	25	753.40	3922.25			
La Rioja	26		1512.36	321.00		
Lugo	27	2715.84	546.67			
Madrid	28			137.11	2770.29	
Málaga	29	3604.42	144.98			
Murcia	30	2769.79	3221.73			
Navarra	31	3.11	4116.64	220.51		
Ourense	32	772.02	745.56			
Asturias	33	1684.76	920.69			
Palencia	34		2479.20	2961.75		
Pontevedra	36	240.09	1035.50			
Salamanca	37	48.87	6348.13	99.84		
Cantabria	39		1503.02			
Segovia	40		951.17	2388.68		
Sevilla	41	2508.17	8033.07			
Soria	42		805.44	2908.51	437.44	
Tarragona	43	1056.57	1756.39			
Teruel	44	1254.47	3925.56	183.52		
Toledo	45		149.79	4976.83	4267.61	454.30
Valencia	46		3292.59	837.10		
Valladolid	47		2797.24	3669.11		
Vizcaya	48		477.58	8.82		
Zamora	49		5519.89	99.78		
Zaragoza	50	344.76	3622.38	5891.15	39.42	
Total surface (km^2)		35735.74	115816.20	63821.93	15651.96	1095.19

Blank cells mean no affected surface.

Only agricultural areas, to which a *representative crop* and their corresponding topsoil texture are assigned, are considered.

ANNEXE XII: ANNUAL AND SEASONAL MATRIXES WITH THE AGRICULTURAL SURFACE AREA (IN KM^2 AND IN PERCETAGE) CORRESPONDING TO ALL THE POSSIBLE COMBINATIONS BETWEEN THE RADIOLOGICAL VULNERABILITY INDEX (I_RV) AND THE DEPOSITION INDEX (I_D), TO OBTAIN THE PRIORITISATION INDEX

Period	Rad. Vulnerability Index / Deposition Index		Surface area (km²) Minimum I_RV	Low I_RV	Medium I_RV	High I_RV	Maximum I_RV	Total by I_D	Percentage of the agricultural areas (%) Minimum I_RV	Low I_RV	Medium I_RV	High I_RV	Maximum I_RV	Total by I_D
			1	2	3	4	5		1	2	3	4	5	
Annual average	Minimum I_D	1	703.334	5236.694	3997.621	12176.881	438.934	22553.464	0.303%	2.256%	1.722%	5.246%	0.189%	9.716%
	Low I_D	2	4345.222	35276.723	21360.527	20646.358	734.529	82363.359	1.872%	15.198%	9.202%	8.895%	0.316%	35.483%
	Medium I_D	3	909.335	43686.623	29553.774	12565.739	67.497	86782.968	0.392%	18.821%	12.732%	5.413%	0.029%	37.387%
	High I_D	4	939.243	18753.166	13119.982	5618.838	58.227	38489.456	0.405%	8.079%	5.652%	2.421%	0.025%	16.582%
	Maximum I_D	5	253.079	1046.692	253.609	371.924	6.460	1931.764	0.109%	0.451%	0.109%	0.160%	0.003%	0.832%
	Total by I_RV		7150.213	103999.898	68285.513	51379.740	1305.647	232121.01	3.081%	44.805%	29.417%	22.135%	0.562%	100.00%
Spring average	Minimum I_D	1	491.459	3904.600	2645.605	11811.866	368.418	19221.948	0.212%	1.682%	1.140%	5.089%	0.159%	8.282%
	Low I_D	2	2969.080	24656.923	19398.229	16091.477	592.305	63708.014	1.279%	10.622%	8.357%	6.932%	0.255%	27.445%
	Medium I_D	3	2465.153	53413.817	31107.097	18395.166	284.349	105665.582	1.062%	23.011%	13.401%	7.925%	0.123%	45.522%
	High I_D	4	1197.013	21605.819	15009.048	4876.465	60.352	42748.697	0.516%	9.308%	6.466%	2.101%	0.026%	18.417%
	Maximum I_D	5	27.507	418.740	125.533	204.766	0.224	776.770	0.012%	0.180%	0.054%	0.088%	0.0001%	0.334%
	Total by I_RV		7150.212	103999.899	68285.512	51379.740	1305.648	232121.01	3.081%	44.803%	29.418%	22.135%	0.563%	100.00%
Summer average	Minimum I_D	1	1114.730	11148.571	6908.562	16832.464	573.335	36577.662	0.480%	4.803%	2.976%	7.252%	0.247%	15.758%
	Low I_D	2	3650.054	25435.142	14455.037	13401.364	568.758	57510.355	1.572%	10.958%	6.227%	5.773%	0.245%	24.775%
	Medium I_D	3	868.322	27908.482	20123.281	12850.278	45.315	61795.678	0.374%	12.023%	8.669%	5.536%	0.020%	26.622%
	High I_D	4	939.337	33250.039	22409.257	7811.548	94.265	64504.446	0.405%	14.324%	9.654%	3.365%	0.041%	27.789%
	Maximum I_D	5	577.770	6257.664	4389.374	484.087	23.973	11732.868	0.249%	2.696%	1.891%	0.209%	0.010%	5.055%
	Total by I_RV		7150.213	103999.898	68285.511	51379.741	1305.646	232121.01	3.080%	44.804%	29.417%	22.135%	0.563%	100.00%
Autumn average	Minimum I_D	1	1713.543	8726.854	6872.481	11196.493	309.343	28818.714	0.738%	3.760%	2.961%	4.824%	0.133%	12.416%
	Low I_D	2	3321.884	37546.201	20355.569	20947.852	798.163	82969.669	1.431%	16.175%	8.769%	9.025%	0.344%	35.744%
	Medium I_D	3	811.698	42267.079	31617.116	14208.209	169.915	89074.017	0.350%	18.209%	13.621%	6.121%	0.073%	38.374%
	High I_D	4	1122.774	14620.443	9287.062	4555.290	28.179	29613.748	0.484%	6.299%	4.001%	1.962%	0.012%	12.758%
	Maximum I_D	5	180.313	839.321	153.284	471.898	0.047	1644.863	0.078%	0.362%	0.066%	0.203%	0.00002%	0.709%
	Total by I_RV		7150.212	103999.898	68285.512	51379.742	1305.647	232121.01	3.081%	44.805%	29.418%	22.135%	0.562%	100.00%
Winter average	Minimum I_D	1	1209.832	13759.208	7854.963	12346.163	565.569	35735.735	0.521%	5.928%	3.384%	5.319%	0.244%	15.396%
	Low I_D	2	4101.219	47846.770	34354.641	28884.158	629.410	115816.198	1.767%	20.613%	14.800%	12.444%	0.271%	49.895%
	Medium I_D	3	731.841	34353.147	21679.930	6972.496	84.514	63821.928	0.315%	14.800%	9.340%	3.004%	0.036%	27.495%
	High I_D	4	1009.285	7526.464	4272.294	2823.132	20.784	15651.959	0.435%	3.242%	1.841%	1.216%	0.009%	6.743%
	Maximum I_D	5	98.034	514.310	123.684	353.791	5.369	1095.188	0.042%	0.222%	0.053%	0.152%	0.002%	0.471%
	Total by I_RV		7150.212	103999.899	68285.513	51379.741	1305.647	232121.01	3.080%	44.805%	29.418%	22.135%	0.562%	100.00%

Prioritisation Index (I_P) Legend

Minimum Priority. I_P = 1 | Low Priority. I_P = 2 | Medium Priority. I_P = 3 | High Priority. I_P = 4 | Maximum Priority. I_P = 5

ANNEXE XIII: TABLES AND GRAPHS OF THE SURFACE AFFECTED IN THE AGRICULTURAL AREAS IN EACH PENINSULAR SPAIN PROVINCE, BY PRIORITISATION INDEX (I_P) (IN KM^2 AND IN PERCETAGE)

Peninsular Spain Province	Province Code	Surface affected by each Prioritisation Index value in the Annual Average Prioritisation map (km²)				
		I_P = 1	I_P = 2	I_P = 3	I_P = 4	I_P = 5
Álava	1	38.93	345.87	627.79	134.37	
Albacete	2	67.81	5118.34	2861.69	409.93	
Alicante	3	422.46	1767.78	299.25		
Almería	4	892.47	1323.76	652.35		
Ávila	5	134.77	1521.72	633.52	368.90	
Badajoz	6	90.41	9916.35	3704.88	770.58	
Barcelona	8	78.97	1574.77	260.05		
Burgos	9	90.69	3104.49	3413.23	529.60	
Cáceres	10	375.89	1322.62	2058.96	5015.01	310.28
Cádiz	11	3213.76	1096.45	11.56		
Castellón	12	209.69	1056.22	385.88	125.69	
Ciudad real	13	8.18	3199.15	5621.98	2522.16	
Córdoba	14	493.96	4951.91	1825.37	2792.82	
A Coruña	15		1967.82	661.17		
Cuenca	16	37.84	1684.40	2786.17	4107.72	
Girona	17	1253.38	95.65	9.54		
Granada	18	453.02	5031.37	886.71		
Guadalajara	19		6.25	2264.21	1676.77	
Guipúzcoa	20		52.55	79.97	275.29	
Huelva	21	111.31	2927.46	769.16	163.70	
Huesca	22	4.42	5254.16	815.78	15.90	
Jaén	23	341.50	7072.70	382.58	32.30	
León	24	149.13	3263.39	1470.91	6.67	
Lleida	25	49.75	3837.24	788.66		
La Rioja	26	16.12	1173.03	421.43	222.78	
Lugo	27	9.12	3253.38			
Madrid	28		44.45	1942.80	920.14	
Málaga	29	2624.02	1094.91	30.48		
Murcia	30	550.84	3347.10	2093.59		
Navarra	31	0.52	2132.07	2068.07	139.60	
Ourense	32	360.51	1028.13	128.93		
Asturias	33	88.22	1410.88	1106.35		
Palencia	34		2282.52	2720.62	437.81	
Pontevedra	36	7.04	1047.06	221.48		
Salamanca	37	48.27	2800.91	2764.80	882.85	
Cantabria	39	1.59	384.83	1060.87	55.73	
Segovia	40	9.09	1753.51	1071.75	505.49	
Sevilla	41	2034.05	5040.18	2841.66	625.35	
Soria	42	2.28	962.64	2007.57	1178.90	
Tarragona	43	277.32	1916.30	619.34		
Teruel	44	9.10	2249.01	2444.81	660.63	
Toledo	45		662.08	5224.33	3836.39	125.73
Valencia	46	609.39	2842.29	562.89	115.12	
Valladolid	47	26.40	3701.39	2511.45	227.11	
Vizcaya	48		31.69	31.61	423.10	
Zamora	49		3566.08	1990.87	62.73	
Zaragoza	50		3915.13	3597.44	2385.15	
Total surface (km²)		15192.21	114132.01	70734.52	31626.27	436.01

Blank cells mean no affected surface.

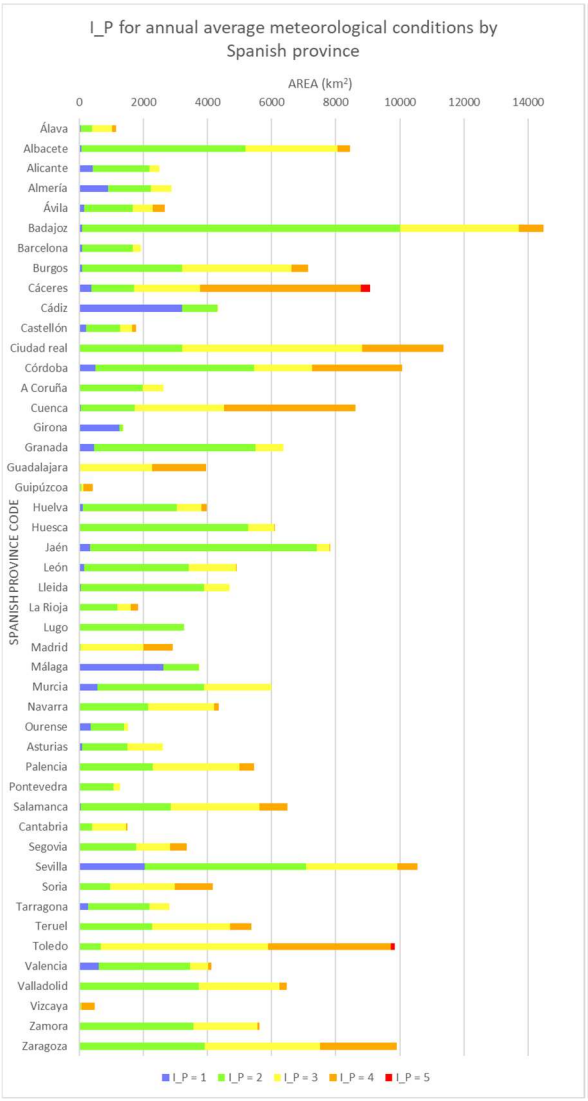
I_P for annual average meteorological conditions by Spanish province
AREA (km²)
0
2000
4000
6000
8000
10000
12000
14000
SPANISH PROVINCE CODE
Álava
Albacete
Alicante
Almería
Ávila
Badajoz
Barcelona
Burgos
Cáceres
Cádiz
Castellón
Ciudad real
Córdoba
A Coruña
Cuenca
Girona
Granada
Guadalajara
Guipúzcoa
Huelva
Huesca
Jaén
León
Lleida
La Rioja
Lugo
Madrid
Málaga
Murcia
Navarra
Ourense
Asturias
Palencia
Pontevedra
Salamanca
Cantabria
Segovia
Sevilla
Soria
Tarragona
Teruel
Toledo
Valencia
Valladolid
Vizcaya
Zamora
Zaragoza
I_P = 1
I_P = 2
I_P = 3
I_P = 4
I_P = 5

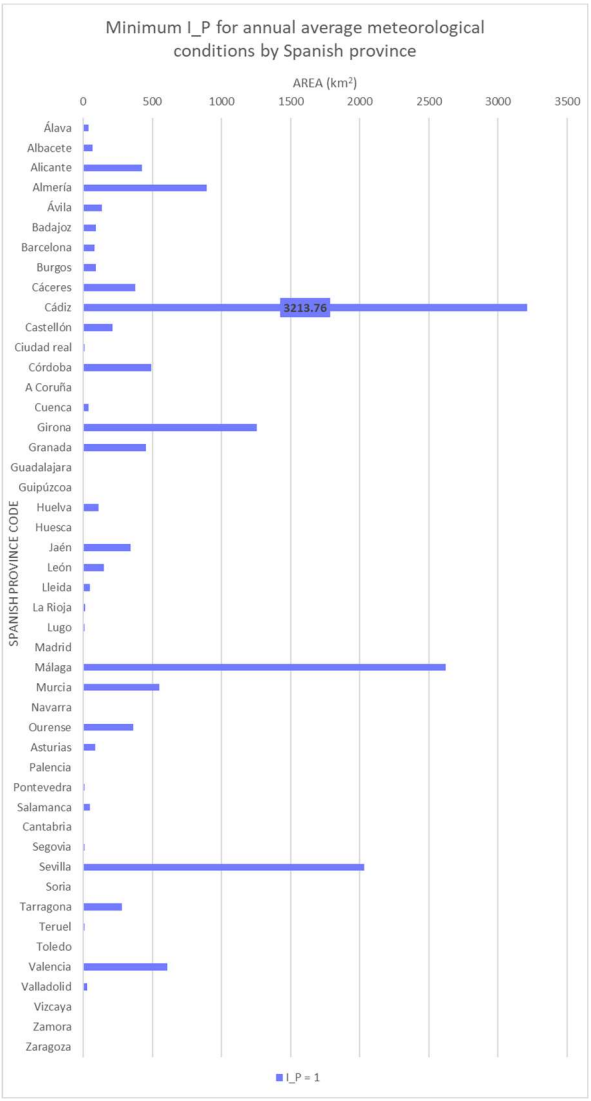
Minimum I_P for annual average meteorological conditions by Spanish province
AREA (km²)
0
500
1000
1500
2000
2500
3000
3500
SPANISH PROVINCE CODE
Álava
Albacete
Alicante
Almería
Ávila
Badajoz
Barcelona
Burgos
Cáceres
Cádiz
3213.76
Castellón
Ciudad real
Córdoba
A Coruña
Cuenca
Girona
Granada
Guadalajara
Guipúzcoa
Huelva
Huesca
Jaén
León
Lleida
La Rioja
Lugo
Madrid
Málaga
Murcia
Navarra
Ourense
Asturias
Palencia
Pontevedra
Salamanca
Cantabria
Segovia
Sevilla
Soria
Tarragona
Teruel
Toledo
Valencia
Valladolid
Vizcaya
Zamora
Zaragoza
I_P = 1

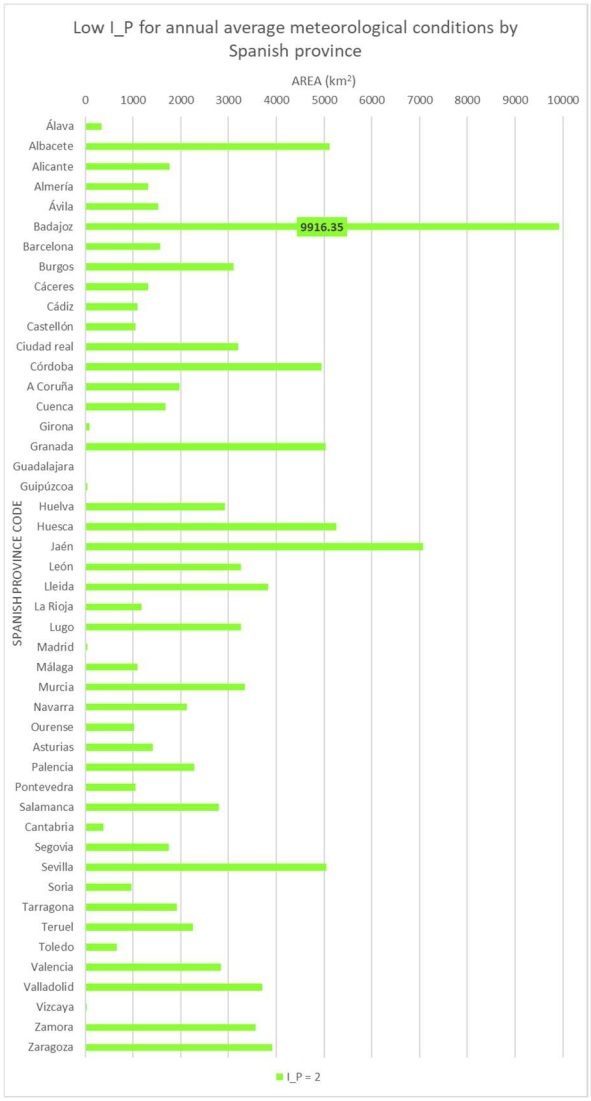
Low I_P for annual average meteorological conditions by Spanish province
AREA (km²)
0
1000
2000
3000
4000
5000
6000
7000
8000
9000
10000
SPANISH PROVINCE CODE
Álava
Albacete
Alicante
Almería
Ávila
Badajoz
9916.35
Barcelona
Burgos
Cáceres
Cádiz
Castellón
Ciudad real
Córdoba
A Coruña
Cuenca
Girona
Granada
Guadalajara
Guipúzcoa
Huelva
Huesca
Jaén
León
Lleida
La Rioja
Lugo
Madrid
Málaga
Murcia
Navarra
Ourense
Asturias
Palencia
Pontevedra
Salamanca
Cantabria
Segovia
Sevilla
Soria
Tarragona
Teruel
Toledo
Valencia
Valladolid
Vizcaya
Zamora
Zaragoza
I_P = 2

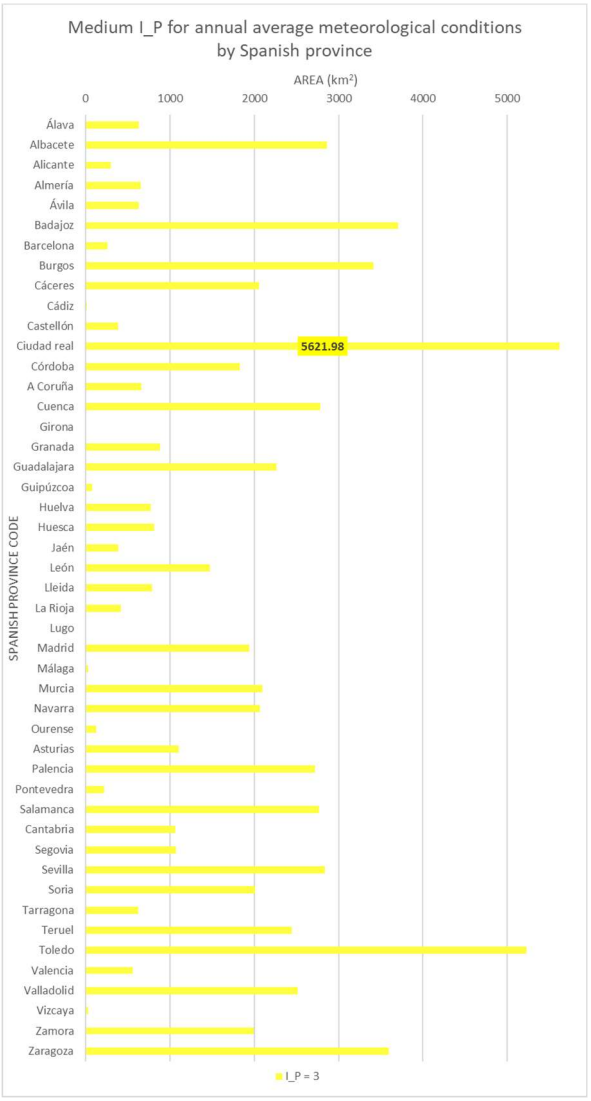
Medium I_P for annual average meteorological conditions by Spanish province
AREA (km²)
0
1000
2000
3000
4000
5000
SPANISH PROVINCE CODE
Álava
Albacete
Alicante
Almería
Ávila
Badajoz
Barcelona
Burgos
Cáceres
Cádiz
Castellón
Ciudad real
5621.98
Córdoba
A Coruña
Cuenca
Girona
Granada
Guadalajara
Guipúzcoa
Huelva
Huesca
Jaén
León
Lleida
La Rioja
Lugo
Madrid
Málaga
Murcia
Navarra
Ourense
Asturias
Palencia
Pontevedra
Salamanca
Cantabria
Segovia
Sevilla
Soria
Tarragona
Teruel
Toledo
Valencia
Valladolid
Vizcaya
Zamora
Zaragoza
I_P = 3

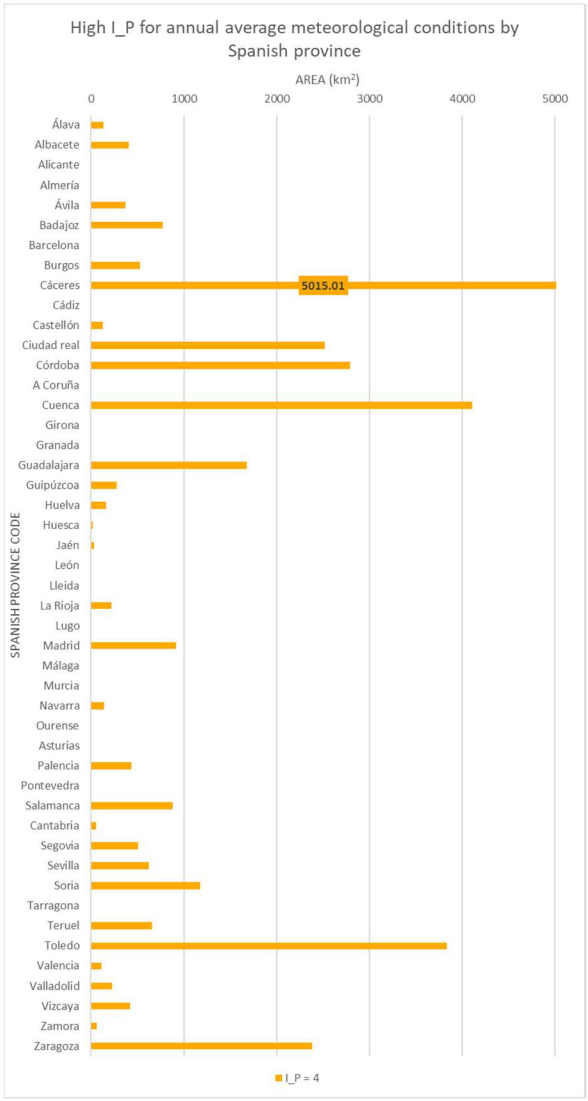
High I_P for annual average meteorological conditions by Spanish province
AREA (km²)
0
1000
2000
3000
4000
5000
SPANISH PROVINCE CODE
Álava
Albacete
Alicante
Almería
Ávila
Badajoz
Barcelona
Burgos
Cáceres
Cádiz
Castellón
Ciudad real
Córdoba
A Coruña
Cuenca
Girona
Granada
Guadalajara
Guipúzcoa
Huelva
Huesca
Jaén
León
Lleida
La Rioja
Lugo
Madrid
Málaga
Murcia
Navarra
Ourense
Asturias
Palencia
Pontevedra
Salamanca
Cantabria
Segovia
Sevilla
Soria
Tarragona
Teruel
Toledo
Valencia
Valladolid
Vizcaya
Zamora
Zaragoza
5015.01
I_P = 4

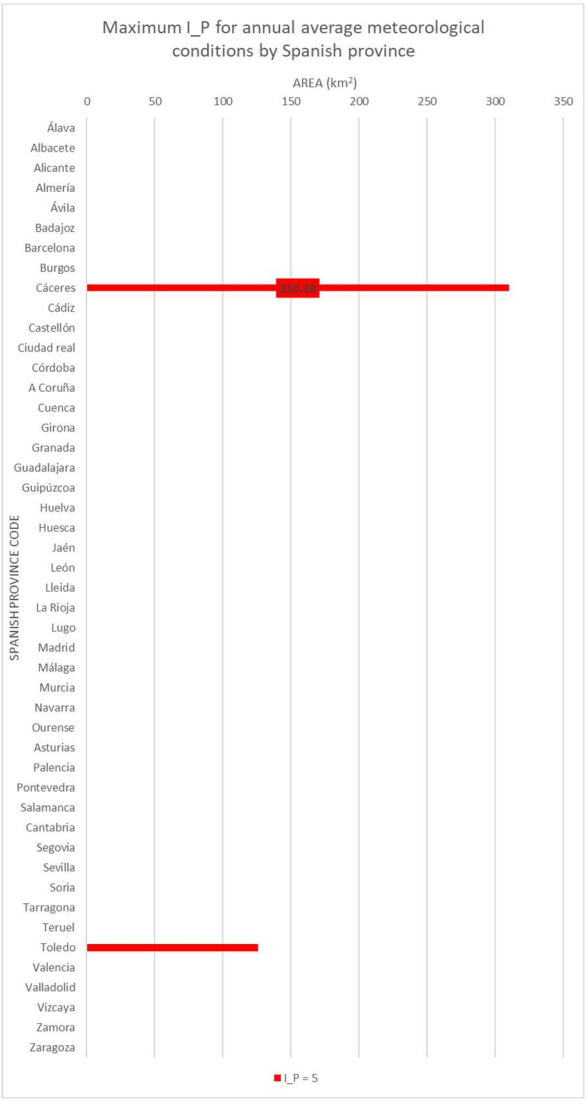
Maximum I_P for annual average meteorological conditions by Spanish province
AREA (km²)
0
50
100
150
200
250
300
350
SPANISH PROVINCE CODE
Álava
Albacete
Alicante
Almería
Ávila
Badajoz
Barcelona
Burgos
Cáceres
Cádiz
Castellón
Ciudad real
Córdoba
A Coruña
Cuenca
Girona
Granada
Guadalajara
Guipúzcoa
Huelva
Huesca
Jaén
León
Lleida
La Rioja
Lugo
Madrid
Málaga
Murcia
Navarra
Ourense
Asturias
Palencia
Pontevedra
Salamanca
Cantabria
Segovia
Sevilla
Soria
Tarragona
Teruel
Toledo
Valencia
Valladolid
Vizcaya
Zamora
Zaragoza
310.28
I_P = 5

Peninsular Spain Province	Province Code	Surface percentage by I_P for annual average meteorological conditions in the agricultural areas, in each province (%)				
		I_P = 1	I_P = 2	I_P = 3	I_P = 4	I_P = 5
Álava	1	3.39	30.16	54.73	11.72	
Albacete	2	0.80	60.52	33.84	4.85	
Alicante	3	16.97	71.01	12.02		
Almería	4	31.11	46.15	22.74		
Ávila	5	5.07	57.23	23.83	13.87	
Badajoz	6	0.62	68.47	25.58	5.32	
Barcelona	8	4.13	82.29	13.59		
Burgos	9	1.27	43.49	47.82	7.42	
Cáceres	10	4.14	14.56	22.67	55.21	3.42
Cádiz	11	74.36	25.37	0.27		
Castellón	12	11.80	59.42	21.71	7.07	
Ciudad real	13	0.07	28.18	49.53	22.22	
Córdoba	14	4.91	49.20	18.14	27.75	
A Coruña	15		74.85	25.15		
Cuenca	16	0.44	19.55	32.34	47.67	
Girona	17	92.26	7.04	0.70		
Granada	18	7.11	78.97	13.92		
Guadalajara	19		0.16	57.36	42.48	
Guipúzcoa	20		12.89	19.61	67.50	
Huelva	21	2.80	73.71	19.37	4.12	
Huesca	22	0.07	86.27	13.39	0.26	
Jaén	23	4.36	90.34	4.89	0.41	
León	24	3.05	66.73	30.08	0.14	
Lleida	25	1.06	82.07	16.87		
La Rioja	26	0.88	63.98	22.99	12.15	
Lugo	27	0.28	99.72			
Madrid	28		1.53	66.82	31.65	
Málaga	29	69.98	29.20	0.81		
Murcia	30	9.19	55.86	34.94		
Navarra	31	0.01	49.12	47.65	3.22	
Ourense	32	23.76	67.75	8.50		
Asturias	33	3.39	54.15	42.46		
Palencia	34		41.95	5	8.05	
Pontevedra	36	0.55	82.08	17.36		
Salamanca	37	0.74	43.11	42.56	13.59	
Cantabria	39	0.11	25.60	70.58	3.71	
Segovia	40	0.27	52.50	32.09	15.14	
Sevilla	41	19.30	47.81	26.96	5.93	
Soria	42	0.05	23.19	48.36	28.40	
Tarragona	43	9.86	68.12	22.02		
Teruel	44	0.17	41.93	45.58	12.32	
Toledo	45		6.72	53.05	38.95	1.28
Valencia	46	14.76	68.83	13.63	2.79	
Valladolid	47	0.41	57.24	38.84	3.51	
Vizcaya	48		6.51	6.50	86.99	
Zamora	49		63.46	35.43	1.12	
Zaragoza	50		39.56	36.35	24.10	

Blank cells mean no affected surface.

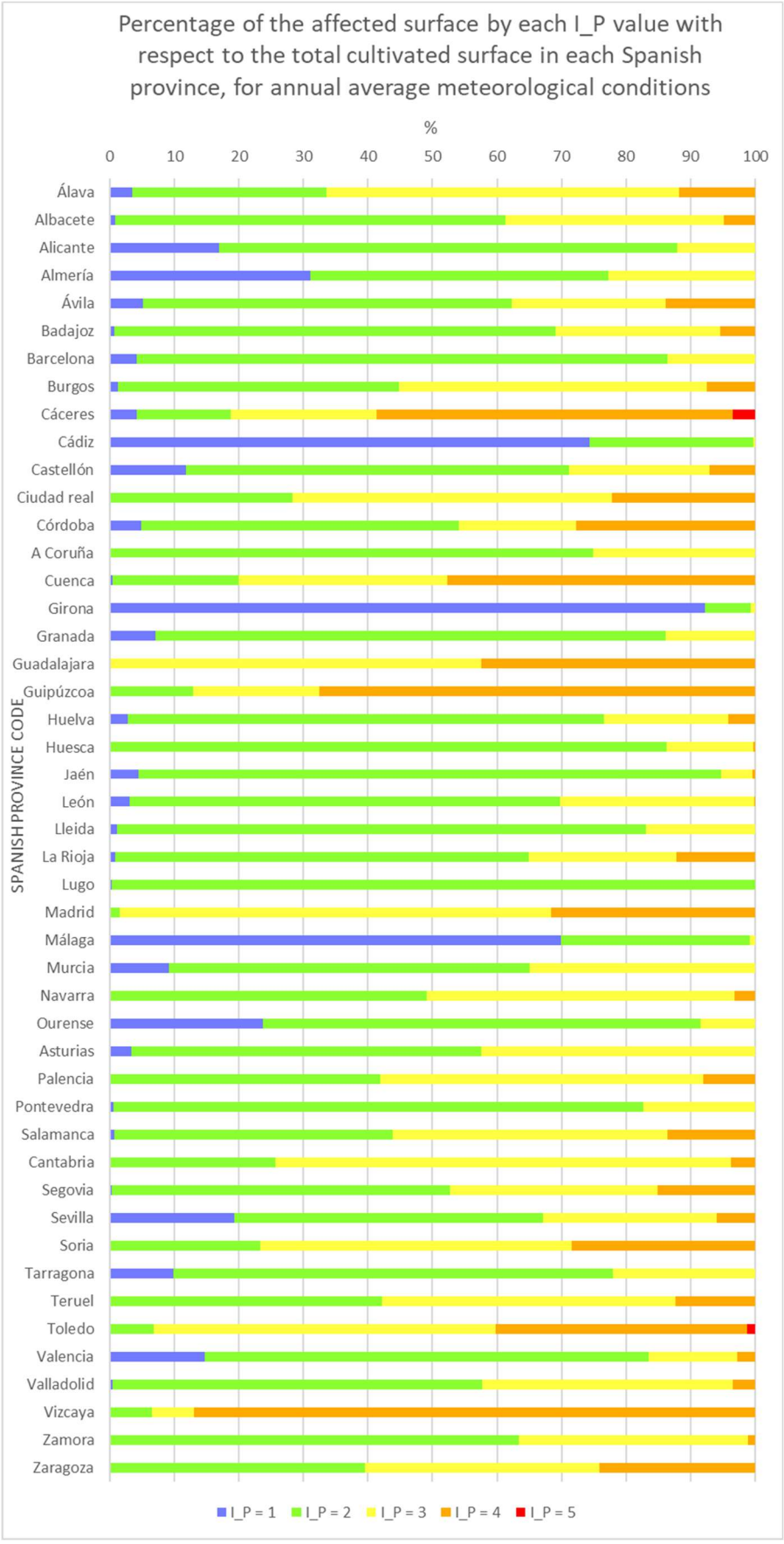
Percentage of the affected surface by each I_P value with respect to the total cultivated surface in each Spanish province, for annual average meteorological conditions
%
0
10
20
30
40
50
60
70
80
90
100
SPANISH PROVINCE CODE
Álava
Albacete
Alicante
Almería
Ávila
Badajoz
Barcelona
Burgos
Cáceres
Cádiz
Castellón
Ciudad real
Córdoba
A Coruña
Cuenca
Girona
Granada
Guadalajara
Guipúzcoa
Huelva
Huesca
Jaén
León
Lleida
La Rioja
Lugo
Madrid
Málaga
Murcia
Navarra
Ourense
Asturias
Palencia
Pontevedra
Salamanca
Cantabria
Segovia
Sevilla
Soria
Tarragona
Teruel
Toledo
Valencia
Valladolid
Vizcaya
Zamora
Zaragoza
I_P = 1
I_P = 2
I_P = 3
I_P = 4
I_P = 5

Peninsular Spain Province	Province Code	Surface percentage by I_P for annual average meteorological conditions in the agricultural areas, with respect all the cultivated surface (%)				
		I_P = 1	I_P = 2	I_P = 3	I_P = 4	I_P = 5
Álava	1	0.017	0.149	0.270	0.058	
Albacete	2	0.029	2.205	1.233	0.177	
Alicante	3	0.182	0.762	0.129		
Almería	4	0.384	0.570	0.281		
Ávila	5	0.058	0.656	0.273	0.159	
Badajoz	6	0.039	4.272	1.596	0.332	
Barcelona	8	0.034	0.678	0.112		
Burgos	9	0.039	1.337	1.470	0.228	
Cáceres	10	0.162	0.570	0.887	2.161	0.134
Cádiz	11	1.385	0.472	0.005		
Castellón	12	0.090	0.455	0.166	0.054	
Ciudad real	13	0.004	1.378	2.422	1.087	
Córdoba	14	0.213	2.133	0.786	1.203	
A Coruña	15		0.848	0.285		
Cuenca	16	0.016	0.726	1.200	1.770	
Girona	17	0.540	0.041	0.004		
Granada	18	0.195	2.168	0.382		
Guadalajara	19		0.003	0.975	0.722	
Guipúzcoa	20		0.023	0.034	0.119	
Huelva	21	0.048	1.261	0.331	0.071	
Huesca	22	0.002	2.264	0.351	0.007	
Jaén	23	0.147	3.047	0.165	0.014	
León	24	0.064	1.406	0.634	0.003	
Lleida	25	0.021	1.653	0.340		
La Rioja	26	0.007	0.505	0.182	0.096	
Lugo	27	0.004	1.402			
Madrid	28		0.019	0.837	0.396	
Málaga	29	1.130	0.472	0.013		
Murcia	30	0.237	1.442	0.902		
Navarra	31		0.919	0.891	0.060	
Ourense	32	0.155	0.443	0.056		
Asturias	33	0.038	0.608	0.477		
Palencia	34		0.983	1.172	0.189	
Pontevedra	36	0.003	0.451	0.095		
Salamanca	37	0.021	1.207	1.191	0.380	
Cantabria	39	0.001	0.166	0.457	0.024	
Segovia	40	0.004	0.755	0.462	0.218	
Sevilla	41	0.876	2.171	1.224	0.269	
Soria	42	0.001	0.415	0.865	0.508	
Tarragona	43	0.119	0.826	0.267		
Teruel	44	0.004	0.969	1.053	0.285	
Toledo	45		0.285	2.251	1.653	0.054
Valencia	46	0.263	1.224	0.242	0.050	
Valladolid	47	0.011	1.595	1.082	0.098	
Vizcaya	48		0.014	0.014	0.182	
Zamora	49		1.536	0.858	0.027	
Zaragoza	50		1.687	1.550	1.028	

Blank cells mean no affected surface.

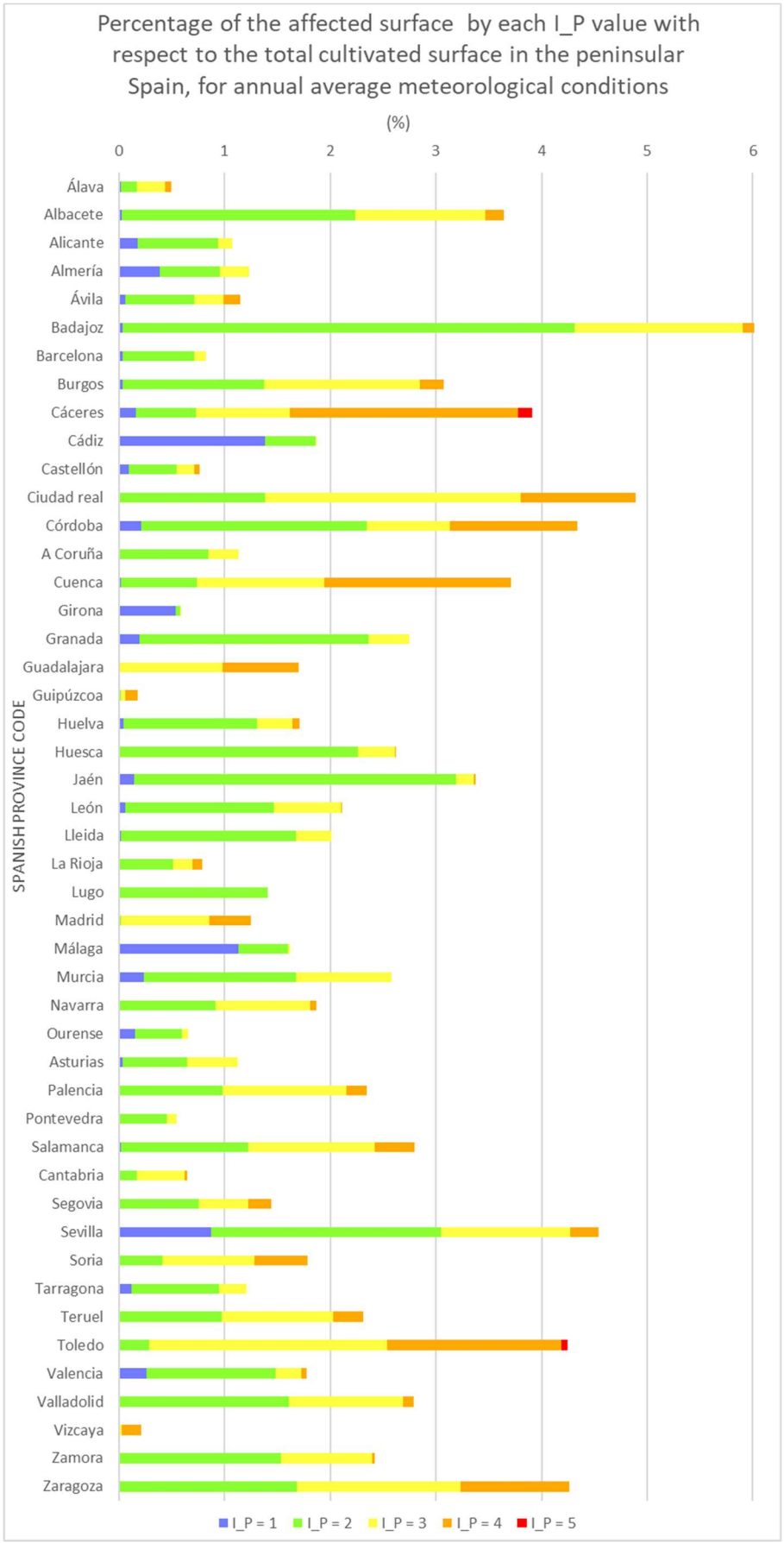
Percentage of the affected surface by each I_P value with respect to the total cultivated surface in the peninsular Spain, for annual average meteorological conditions
(%)
0
1
2
3
4
5
6
SPANISH PROVINCE CODE
Álava
Albacete
Alicante
Almería
Ávila
Badajoz
Barcelona
Burgos
Cáceres
Cádiz
Castellón
Ciudad real
Córdoba
A Coruña
Cuenca
Girona
Granada
Guadalajara
Guipúzcoa
Huelva
Huesca
Jaén
León
Lleida
La Rioja
Lugo
Madrid
Málaga
Murcia
Navarra
Ourense
Asturias
Palencia
Pontevedra
Salamanca
Cantabria
Segovia
Sevilla
Soria
Tarragona
Teruel
Toledo
Valencia
Valladolid
Vizcaya
Zamora
Zaragoza
I_P = 1
I_P = 2
I_P = 3
I_P = 4
I_P = 5

Peninsular Spain Province	Province Code	Surface affected by each Prioritisation Index value in the Spring Average Prioritisation map (km^2)				
		I_P = 1	I_P = 2	I_P = 3	I_P = 4	I_P = 5
Álava	1	38.93	474.14	512.47	121.43	
Albacete	2	67.81	3326.77	3854.41	1208.79	
Alicante	3	271.41	1828.62	389.46		
Almería	4	205.21	1376.14	1270.70	16.52	
Ávila	5	78.30	1428.43	777.50	374.67	
Badajoz	6	90.80	9203.05	3980.24	1208.13	
Barcelona	8	84.02	1572.02	257.75		
Burgos	9	99.85	4450.38	2523.43	64.34	
Cáceres	10	410.30	1468.08	1952.19	5066.96	185.23
Cádiz	11	3117.38	1167.67	36.73		
Castellón	12	209.69	985.00	267.33	315.46	
Ciudad real	13	8.18	1827.05	5212.72	4303.52	
Córdoba	14	469.34	4742.72	1082.22	3769.77	
A Coruña	15		2556.75	72.24		
Cuenca	16	38.86	1817.14	3265.28	3494.84	
Girona	17	1109.81	217.96	30.81		
Granada	18	44.86	4178.82	1865.75	281.66	
Guadalajara	19		11.14	2257.78	1678.31	
Guipúzcoa	20		54.73	62.42	290.66	
Huelva	21	111.31	2878.58	143.04	838.70	
Huesca	22	4.42	5224.64	832.89	28.31	
Jaén	23	341.50	6673.90	470.75	342.93	
León	24	168.15	3223.62	1328.33	17	
Lleida	25	20.38	3853.73	801.54		
La Rioja	26	13.03	1206.56	381.73	232.04	
Lugo	27	9.12	3178.50	74.88		
Madrid	28		44.45	1942.80	920.14	
Málaga	29	1289.92	2165.64	293.85		
Murcia	30	161.81	2433.85	3148.80	247.07	
Navarra	31	0.23	1886.73	2181.59	271.71	
Ourense	32	381.12	986.14	150.32		
Asturias	33	170.19	1435.59	999.66		
Palencia	34	18.21	2498.42	2545.42	378.90	
Pontevedra	36	8.22	1235.43	31.94		
Salamanca	37	48.27	2872.96	2279.85	1295.75	
Cantabria	39	348.27	1017.17	137.58		
Segovia	40	0.04	936.96	1604.70	798.15	
Sevilla	41	1771.14	5079.70	1448.54	2241.87	
Soria	42	2.28	1789.93	1712.98	646.20	
Tarragona	43	605.99	1655.04	551.28	0.65	
Teruel	44	9.10	1878.97	2542.27	933.22	
Toledo	45		669.55	5252.88	3849.71	76.39
Valencia	46	609.39	2744.15	574.21	201.94	
Valladolid	47	26.40	3427.53	2777.68	234.74	
Vizcaya	48		38.68	155.39	292.33	
Zamora	49	11.77	2768.93	2477.96	361.01	
Zaragoza	50	0.86	4381.80	3301.19	2210.74	3.12
Total surface (km^2)		12475.90	110873.77	69815.44	38691.16	**264.74**

Blank cells mean no affected surface.

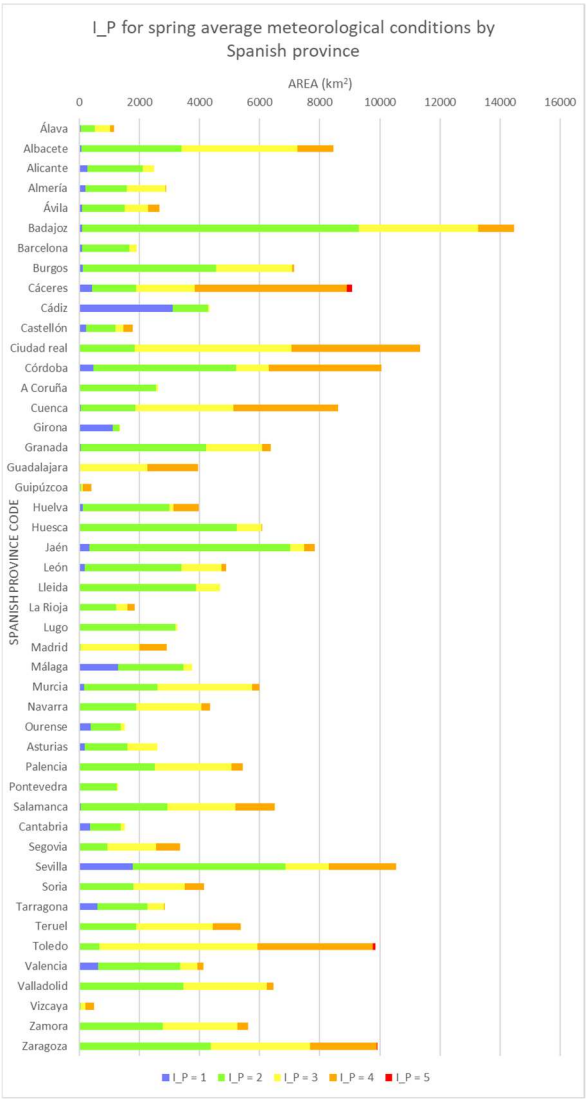
I_P for spring average meteorological conditions by Spanish province
AREA (km²)
0
2000
4000
6000
8000
10000
12000
14000
16000
SPANISH PROVINCE CODE
Álava
Albacete
Alicante
Almería
Ávila
Badajoz
Barcelona
Burgos
Cáceres
Cádiz
Castellón
Ciudad real
Córdoba
A Coruña
Cuenca
Girona
Granada
Guadalajara
Guipúzcoa
Huelva
Huesca
Jaén
León
Lleida
La Rioja
Lugo
Madrid
Málaga
Murcia
Navarra
Ourense
Asturias
Palencia
Pontevedra
Salamanca
Cantabria
Segovia
Sevilla
Soria
Tarragona
Teruel
Toledo
Valencia
Valladolid
Vizcaya
Zamora
Zaragoza
I_P = 1
I_P = 2
I_P = 3
I_P = 4
I_P = 5

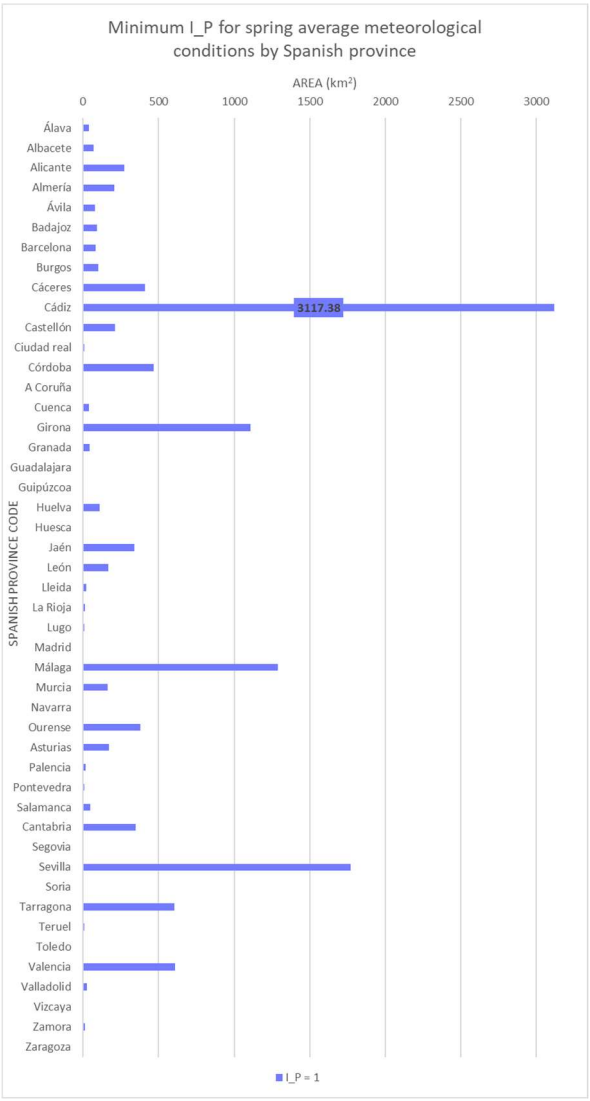
Minimum I_P for spring average meteorological conditions by Spanish province
AREA (km²)
0
500
1000
1500
2000
2500
3000
SPANISH PROVINCE CODE
Álava
Albacete
Alicante
Almería
Ávila
Badajoz
Barcelona
Burgos
Cáceres
Cádiz
3117.38
Castellón
Ciudad real
Córdoba
A Coruña
Cuenca
Girona
Granada
Guadalajara
Guipúzcoa
Huelva
Huesca
Jaén
León
Lleida
La Rioja
Lugo
Madrid
Málaga
Murcia
Navarra
Ourense
Asturias
Palencia
Pontevedra
Salamanca
Cantabria
Segovia
Sevilla
Soria
Tarragona
Teruel
Toledo
Valencia
Valladolid
Vizcaya
Zamora
Zaragoza
I_P = 1

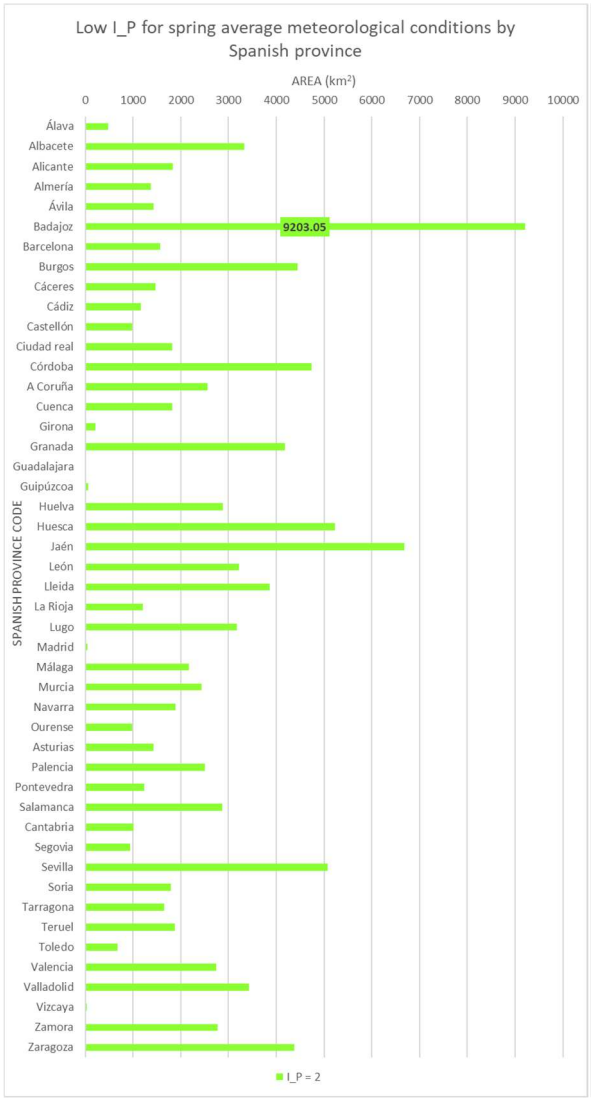
Low I_P for spring average meteorological conditions by Spanish province
AREA (km²)
0 1000 2000 3000 4000 5000 6000 7000 8000 9000 10000
SPANISH PROVINCE CODE
Álava
Albacete
Alicante
Almería
Ávila
Badajoz
9203.05
Barcelona
Burgos
Cáceres
Cádiz
Castellón
Ciudad real
Córdoba
A Coruña
Cuenca
Girona
Granada
Guadalajara
Guipúzcoa
Huelva
Huesca
Jaén
León
Lleida
La Rioja
Lugo
Madrid
Málaga
Murcia
Navarra
Ourense
Asturias
Palencia
Pontevedra
Salamanca
Cantabria
Segovia
Sevilla
Soria
Tarragona
Teruel
Toledo
Valencia
Valladolid
Vizcaya
Zamora
Zaragoza
I_P = 2

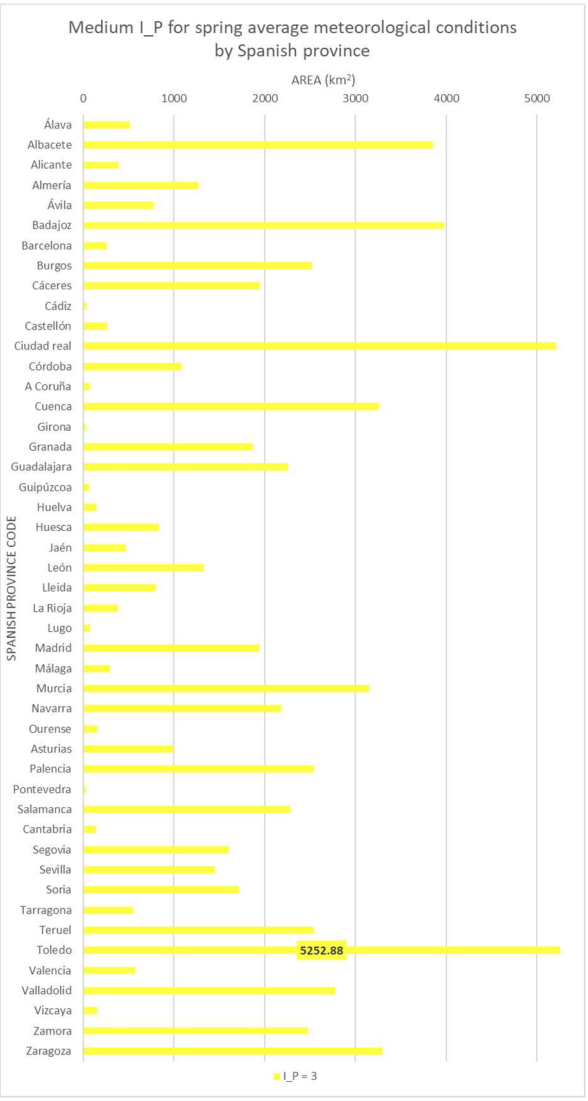
Medium I_P for spring average meteorological conditions by Spanish province
AREA (km²)
0 1000 2000 3000 4000 5000
SPANISH PROVINCE CODE
Álava
Albacete
Alicante
Almería
Ávila
Badajoz
Barcelona
Burgos
Cáceres
Cádiz
Castellón
Ciudad real
Córdoba
A Coruña
Cuenca
Girona
Granada
Guadalajara
Guipúzcoa
Huelva
Huesca
Jaén
León
Lleida
La Rioja
Lugo
Madrid
Málaga
Murcia
Navarra
Ourense
Asturias
Palencia
Pontevedra
Salamanca
Cantabria
Segovia
Sevilla
Soria
Tarragona
Teruel
Toledo
5252.88
Valencia
Valladolid
Vizcaya
Zamora
Zaragoza
I_P = 3

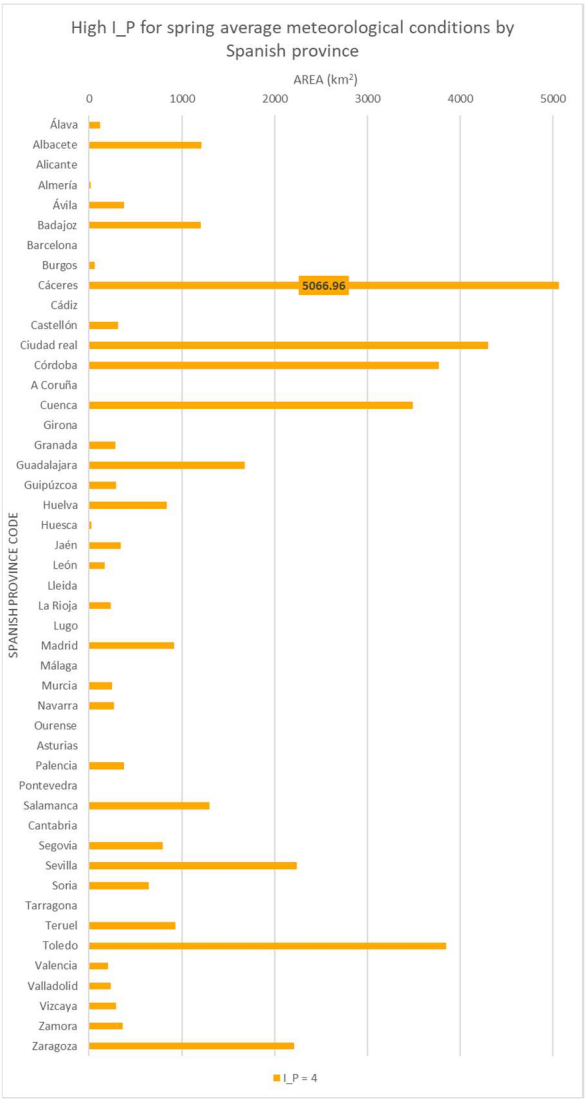
High I_P for spring average meteorological conditions by Spanish province
AREA (km²)
0
1000
2000
3000
4000
5000
SPANISH PROVINCE CODE
Álava
Albacete
Alicante
Almería
Ávila
Badajoz
Barcelona
Burgos
Cáceres
5066.96
Cádiz
Castellón
Ciudad real
Córdoba
A Coruña
Cuenca
Girona
Granada
Guadalajara
Guipúzcoa
Huelva
Huesca
Jaén
León
Lleida
La Rioja
Lugo
Madrid
Málaga
Murcia
Navarra
Ourense
Asturias
Palencia
Pontevedra
Salamanca
Cantabria
Segovia
Sevilla
Soria
Tarragona
Teruel
Toledo
Valencia
Valladolid
Vizcaya
Zamora
Zaragoza
I_P = 4

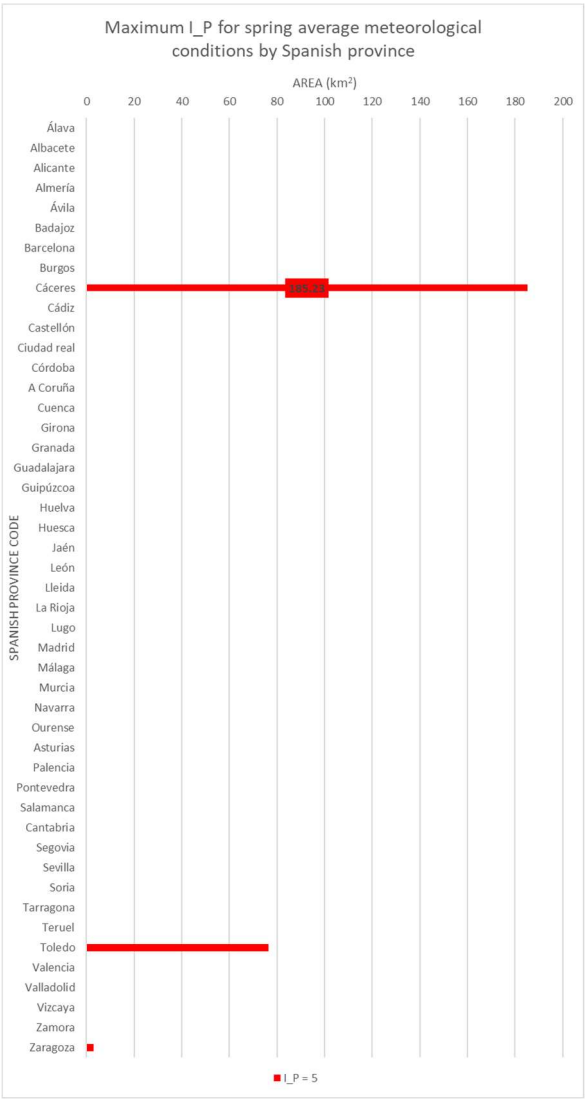
Maximum I_P for spring average meteorological conditions by Spanish province
AREA (km²)
0
20
40
60
80
100
120
140
160
180
200
SPANISH PROVINCE CODE
Álava
Albacete
Alicante
Almería
Ávila
Badajoz
Barcelona
Burgos
Cáceres
185.23
Cádiz
Castellón
Ciudad real
Córdoba
A Coruña
Cuenca
Girona
Granada
Guadalajara
Guipúzcoa
Huelva
Huesca
Jaén
León
Lleida
La Rioja
Lugo
Madrid
Málaga
Murcia
Navarra
Ourense
Asturias
Palencia
Pontevedra
Salamanca
Cantabria
Segovia
Sevilla
Soria
Tarragona
Teruel
Toledo
Valencia
Valladolid
Vizcaya
Zamora
Zaragoza
I_P = 5

Peninsular Spain Province	Province Code	Surface percentage by I_P for spring average meteorological conditions in the agricultural areas, in each province (%)				
		I_P = 1	I_P = 2	I_P = 3	I_P = 4	I_P = 5
Álava	1	3.39	41.34	44.68	10.59	
Albacete	2	0.80	39.33	45.57	14.29	
Alicante	3	10.90	73.45	15.64		
Almería	4	7.15	47.97	44.30	0.58	
Ávila	5	2.94	53.72	29.24	14.09	
Badajoz	6	0.63	63.55	27.48	8.34	
Barcelona	8	4.39	82.14	13.47		
Burgos	9	1.40	62.35	35.35	0.90	
Cáceres	10	4.52	16.16	21.49	55.79	2.04
Cádiz	11	72.13	27.02	0.85		
Castellón	12	11.80	55.42	15.04	17.75	
Ciudad real	13	0.07	16.10	45.92	37.91	
Córdoba	14	4.66	47.13	10.75	37.46	
A Coruña	15		97.25	2.75		
Cuenca	16	0.45	21.09	37.90	40.56	
Girona	17	81.69	16.04	2.27		
Granada	18	0.70	65.59	29.28	4.42	
Guadalajar	19		0.28	57.20	42.52	
Guipúzcoa	20		13.42	15.31	71.27	
Huelva	21	2.80	72.48	3.60	21.12	
Huesca	22	0.07	85.79	13.68	0.46	
Jaén	23	4.36	85.25	6.01	4.38	
León	24	3.44	65.92	27.16	3.48	
Lleida	25	0.44	82.42	17.14		
La Rioja	26	0.71	65.81	20.82	12.66	
Lugo	27	0.28	97.43	2.30		
Madrid	28		1.53	66.82	31.65	
Málaga	29	34.40	57.76	7.84		
Murcia	30	2.70	40.62	52.55	4.12	
Navarra	31	0.01	43.47	50.26	6.26	
Ourense	32	25.11	64.98	9.90		
Asturias	33	6.53	55.10	38.37		
Palencia	34	0.33	45.92	46.78	6.96	
Pontevedr	36	0.64	96.85	2.50		
Salamanca	37	0.74	44.22	35.09	19.94	
Cantabria	39	23.17	67.68	9.15		
Segovia	40		28.05	48.05	23.90	
Sevilla	41	16.80	48.19	13.74	21.27	
Soria	42	0.05	43.12	41.26	15.57	
Tarragona	43	21.54	58.84	19.60	0.02	
Teruel	44	0.17	35.03	47.40	17.40	
Toledo	45		6.80	53.34	39.09	0.78
Valencia	46	14.76	66.45	13.90	4.89	
Valladolid	47	0.41	53.01	42.96	3.63	
Vizcaya	48		7.95	31.95	60.10	
Zamora	49	0.21	49.27	44.09	6.42	
Zaragoza	50	0.01	44.27	33.35	22.34	0.03

Blank cells mean no affected surface.

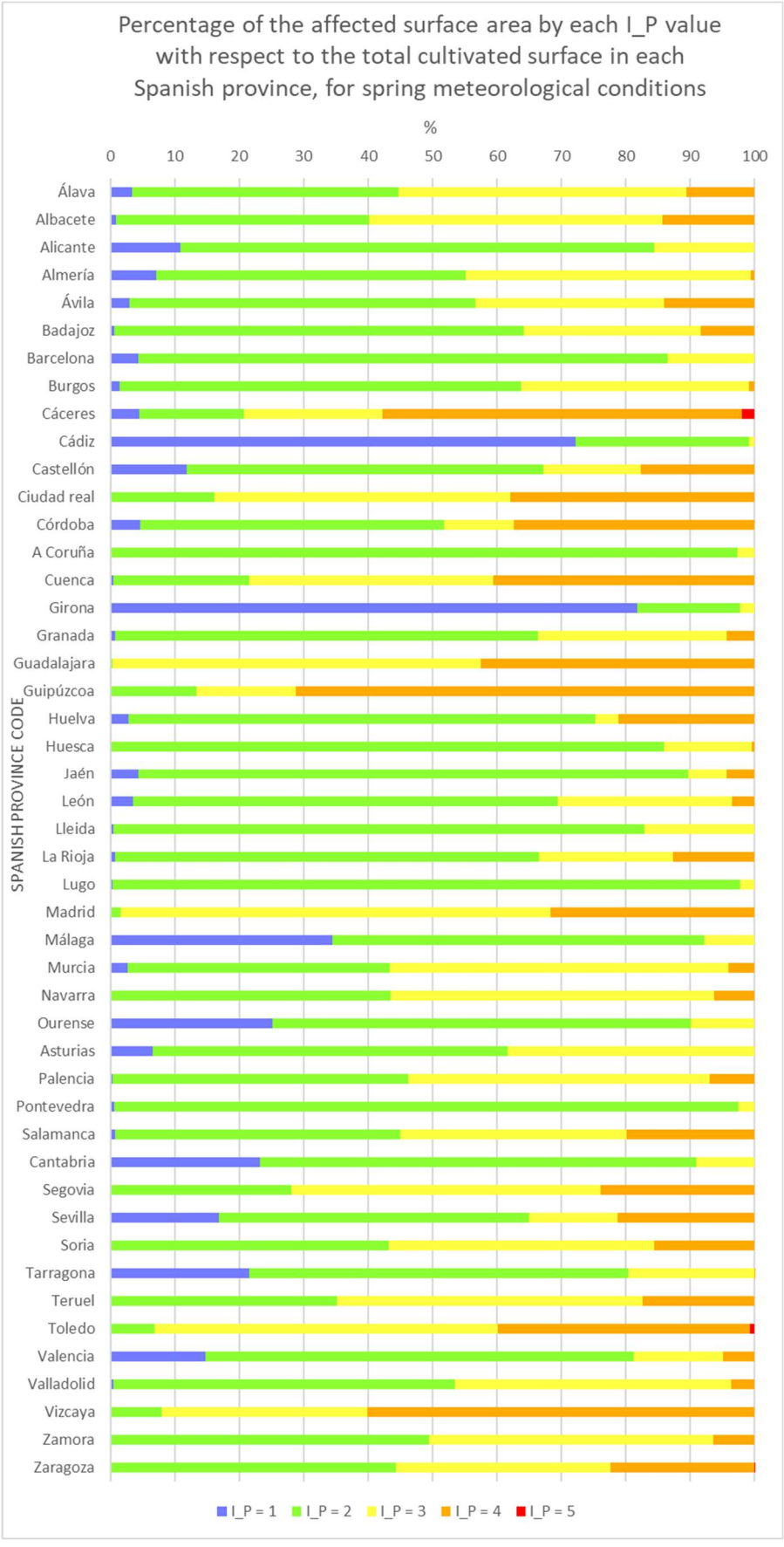
Percentage of the affected surface area by each I_P value with respect to the total cultivated surface in each Spanish province, for spring meteorological conditions
%
0
10
20
30
40
50
60
70
80
90
100
SPANISH PROVINCE CODE
Álava
Albacete
Alicante
Almería
Ávila
Badajoz
Barcelona
Burgos
Cáceres
Cádiz
Castellón
Ciudad real
Córdoba
A Coruña
Cuenca
Girona
Granada
Guadalajara
Guipúzcoa
Huelva
Huesca
Jaén
León
Lleida
La Rioja
Lugo
Madrid
Málaga
Murcia
Navarra
Ourense
Asturias
Palencia
Pontevedra
Salamanca
Cantabria
Segovia
Sevilla
Soria
Tarragona
Teruel
Toledo
Valencia
Valladolid
Vizcaya
Zamora
Zaragoza
I_P = 1
I_P = 2
I_P = 3
I_P = 4
I_P = 5

Peninsular Spain Province	Province Code	Surface percentage by I_P for spring average meteorological conditions in the agricultural areas, with respect all the cultivated surface (%)				
		I_P = 1	I_P = 2	I_P = 3	I_P = 4	I_P = 5
Álava	1	0.017	0.204	0.221	0.052	
Albacete	2	0.029	1.433	1.661	0.521	
Alicante	3	0.117	0.788	0.168		
Almería	4	0.088	0.593	0.547	0.007	
Ávila	5	0.034	0.615	0.335	0.161	
Badajoz	6	0.039	3.965	1.715	0.520	
Barcelona	8	0.036	0.677	0.111		
Burgos	9	0.043	1.917	1.087	0.028	
Cáceres	10	0.177	0.632	0.841	2.183	0.080
Cádiz	11	1.343	0.503	0.016		
Castellón	12	0.090	0.424	0.115	0.136	
Ciudad real	13	0.004	0.787	2.246	1.854	
Córdoba	14	0.202	2.043	0.466	1.624	
A Coruña	15		1.101	0.031		
Cuenca	16	0.017	0.783	1.407	1.506	
Girona	17	0.478	0.094	0.013		
Granada	18	0.019	1.800	0.804	0.121	
Guadalajara	19		0.005	0.973	0.723	
Guipúzcoa	20		0.024	0.027	0.125	
Huelva	21	0.048	1.240	0.062	0.361	
Huesca	22	0.002	2.251	0.359	0.012	
Jaén	23	0.147	2.875	0.203	0.148	
León	24	0.072	1.389	0.572	0.073	
Lleida	25	0.009	1.660	0.345		
La Rioja	26	0.006	0.520	0.164	0.100	
Lugo	27	0.004	1.369	0.032		
Madrid	28		0.019	0.837	0.396	
Málaga	29	0.556	0.933	0.127		
Murcia	30	0.070	1.049	1.357	0.106	
Navarra	31		0.813	0.940	0.117	
Ourense	32	0.164	0.425	0.065		
Asturias	33	0.073	0.618	0.431		
Palencia	34	0.008	1.076	1.097	0.163	
Pontevedra	36	0.004	0.532	0.014		
Salamanca	37	0.021	1.238	0.982	0.558	
Cantabria	39	0.150	0.438	0.059		
Segovia	40		0.404	0.691	0.344	
Sevilla	41	0.763	2.188	0.624	0.966	
Soria	42	0.001	0.771	0.738	0.278	
Tarragona	43	0.261	0.713	0.237		
Teruel	44	0.004	0.809	1.095	0.402	
Toledo	45		0.288	2.263	1.658	0.033
Valencia	46	0.263	1.182	0.247	0.087	
Valladolid	47	0.011	1.477	1.197	0.101	
Vizcaya	48		0.017	0.067	0.126	
Zamora	49	0.005	1.193	1.068	0.156	
Zaragoza	50		1.888	1.422	0.952	0.001

Blank cells mean no affected surface.

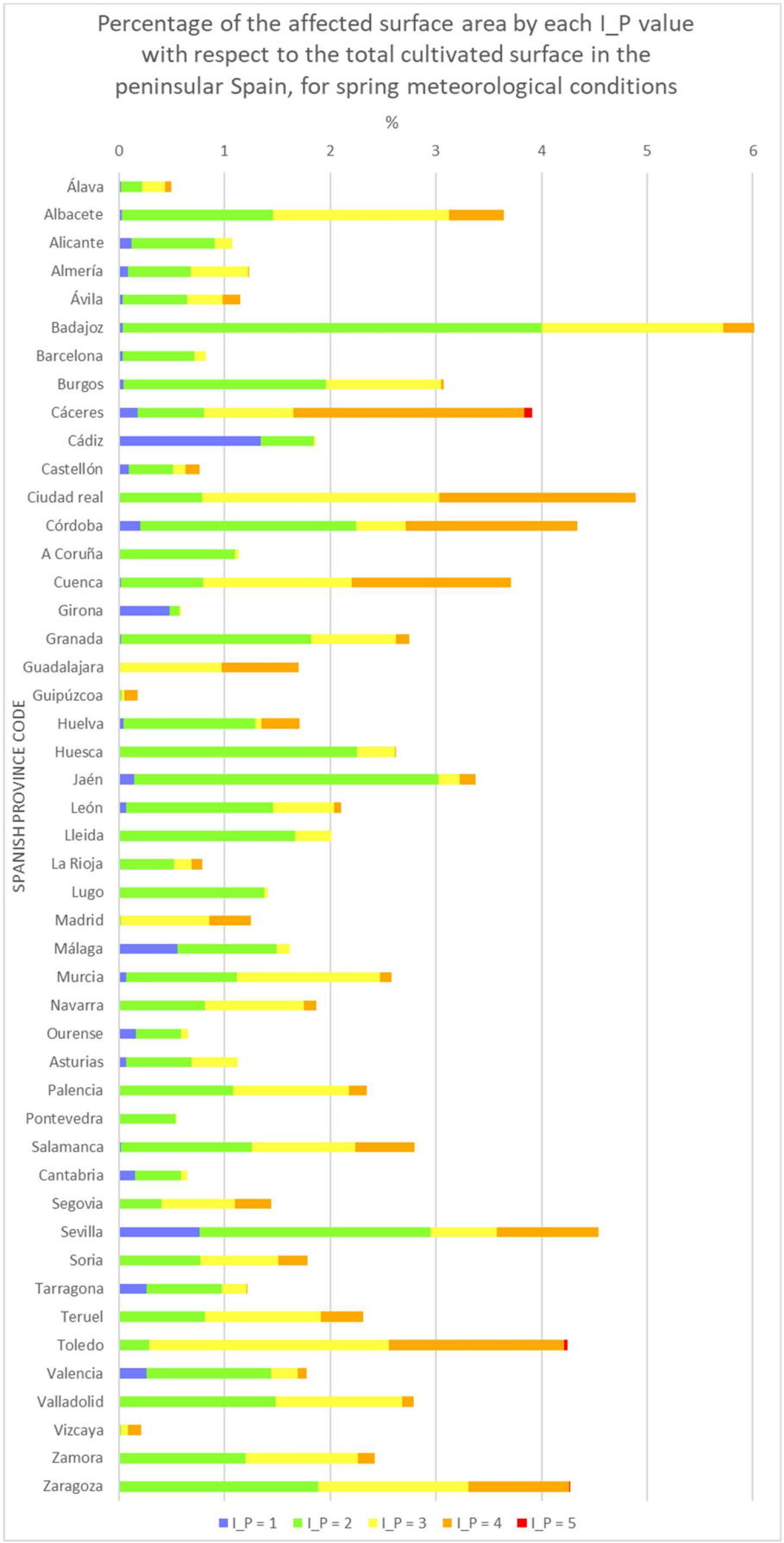
Percentage of the affected surface area by each I_P value with respect to the total cultivated surface in the peninsular Spain, for spring meteorological conditions
%
0
1
2
3
4
5
6
SPANISH PROVINCE CODE
Álava
Albacete
Alicante
Almería
Ávila
Badajoz
Barcelona
Burgos
Cáceres
Cádiz
Castellón
Ciudad real
Córdoba
A Coruña
Cuenca
Girona
Granada
Guadalajara
Guipúzcoa
Huelva
Huesca
Jaén
León
Lleida
La Rioja
Lugo
Madrid
Málaga
Murcia
Navarra
Ourense
Asturias
Palencia
Pontevedra
Salamanca
Cantabria
Segovia
Sevilla
Soria
Tarragona
Teruel
Toledo
Valencia
Valladolid
Vizcaya
Zamora
Zaragoza
I_P = 1
I_P = 2
I_P = 3
I_P = 4
I_P = 5

Peninsular Spain Province	Province Code	Surface affected by each Prioritisation Index value in the Summer Average Prioritisation map (km²)				
		I_P = 1	I_P = 2	I_P = 3	I_P = 4	I_P = 5
Álava	1	1.22	178.36	757.74	209.64	
Albacete	2	67.54	3060.17	3857.22	1472.84	
Alicante	3	666.88	1544.87	277.74		
Almería	4	1487.02	1301.45	80.10		
Ávila	5	77.04	631.09	1318.48	632.30	
Badajoz	6	16.99	5753.55	6372.19	2339.48	
Barcelona	8	65.08	1587.18	261.53		
Burgos	9	59.24	1418.23	2911.26	2749.27	
Cáceres	10	344.83	1667.69	2019.59	4853.44	197.21
Cádiz	11	3579.00	742.78			
Castellón	12	209.69	984.00	254.73	329.06	
Ciudad real	13	8.18	1392.94	5427.32	4523.04	
Córdoba	14	1523.64	3855.67	1346.54	3338.19	
A Coruña	15		2629.00			
Cuenca	16	0.54	471.52	3286.70	4857.02	0.34
Girona	17	1112.80	221.02	24.77		
Granada	18	2563.85	3154.57	652.68		
Guadalajara	19			2265.75	1681.48	
Guipúzcoa	20		52.55	79.97	275.29	
Huelva	21	112.21	2924.05	722.21	213.16	
Huesca	22	4.42	4097.67	1865.21	122.96	
Jaén	23	985.72	6458.92	372.84	11.60	
León	24	592.38	3104.55	1186.51	6.67	
Lleida	25	19.27	3130.31	1139.77	386.30	
La Rioja	26	0.11	38.76	1192.69	601.79	
Lugo	27	9.12	3253.38			
Madrid	28		44.45	1942.80	896.87	23.28
Málaga	29	3217.89	531.52			
Murcia	30	1397.90	3941.92	550.68	101.03	
Navarra	31	0.23	1231.00	2315.91	793.12	
Ourense	32	445.73	1071.85			
Asturias	33	141.11	1781.60	682.74		
Palencia	34		1944.20	2672.21	824.54	
Pontevedra	36	8.49	1267.10			
Salamanca	37	97.09	2890.70	3021.11	487.93	
Cantabria	39	1.59	351.53	504.84	645.06	
Segovia	40		12.00	2403.01	924.83	
Sevilla	41	3596.82	3567.03	2322.77	1054.62	
Soria	42		2.28	2475.79	1673.32	
Tarragona	43	277.81	1910.75	589.59	34.81	
Teruel	44	2.73	278.82	2156.93	2914.11	10.96
Toledo	45		662.08	5224.33	3634.77	327.34
Valencia	46	592.54	2764.88	543.16	229.12	
Valladolid	47	21.43	2734.04	3066.23	644.65	
Vizcaya	48		36.28	180.72	269.40	
Zamora	49	382.10	3640.81	1515.11	81.65	
Zaragoza	50		2402.46	3759.64	3693.02	42.59
Total surface (km²)		23690.24	86721.57	73601.11	47506.37	601.73

Blank cells mean no affected surface.

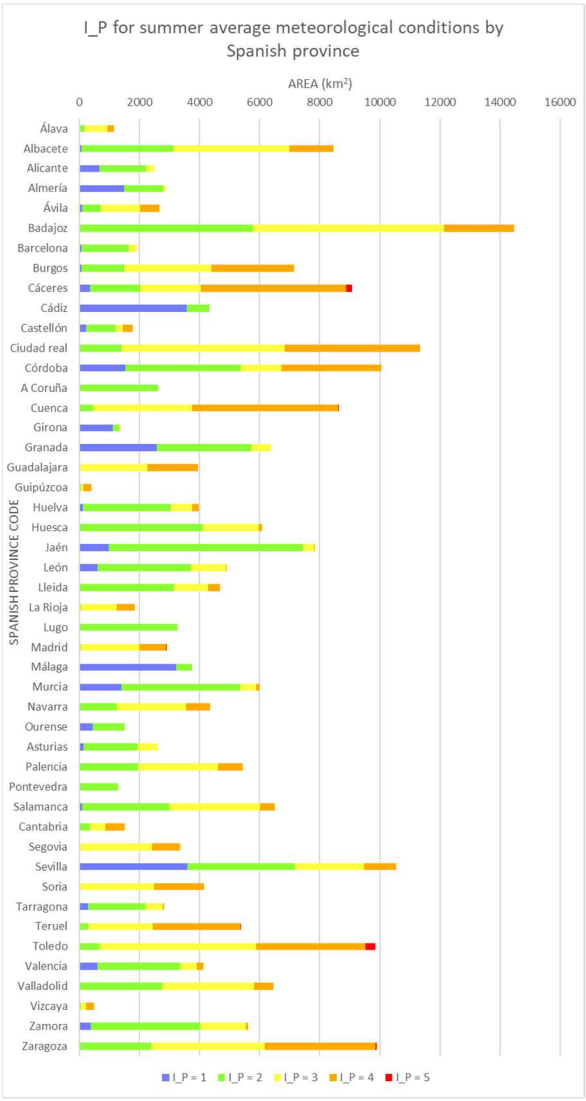
I_P for summer average meteorological conditions by Spanish province
AREA (km²)
0
2000
4000
6000
8000
10000
12000
14000
16000
SPANISH PROVINCE CODE
Álava
Albacete
Alicante
Almería
Ávila
Badajoz
Barcelona
Burgos
Cáceres
Cádiz
Castellón
Ciudad real
Córdoba
A Coruña
Cuenca
Girona
Granada
Guadalajara
Guipúzcoa
Huelva
Huesca
Jaén
León
Lleida
La Rioja
Lugo
Madrid
Málaga
Murcia
Navarra
Ourense
Asturias
Palencia
Pontevedra
Salamanca
Cantabria
Segovia
Sevilla
Soria
Tarragona
Teruel
Toledo
Valencia
Valladolid
Vizcaya
Zamora
Zaragoza
I_P = 1
I_P = 2
I_P = 3
I_P = 4
I_P = 5

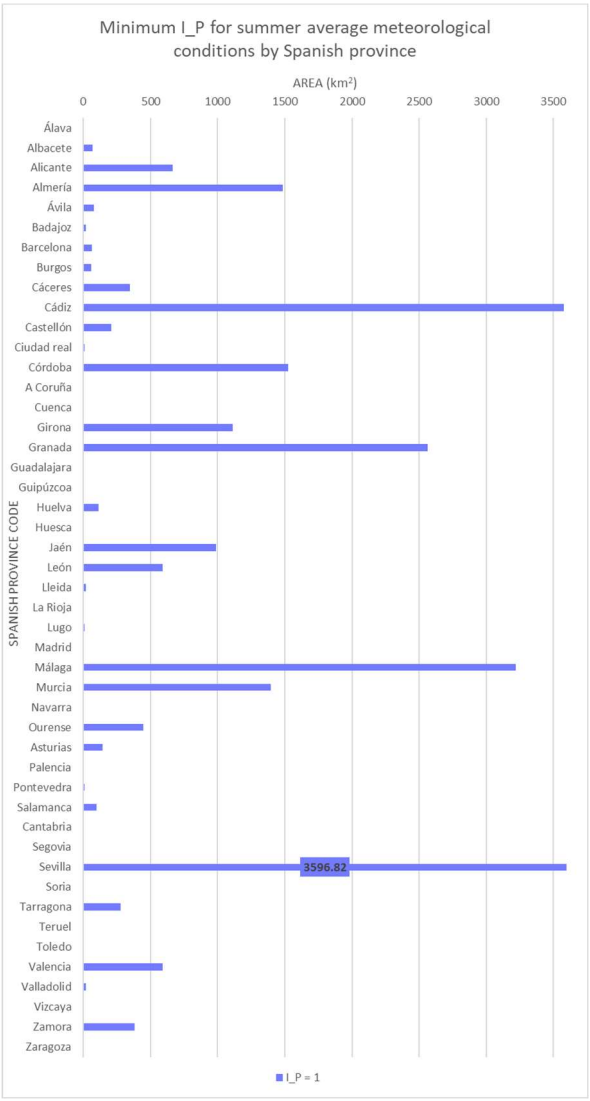
Minimum I_P for summer average meteorological conditions by Spanish province
AREA (km²)
0
500
1000
1500
2000
2500
3000
3500
SPANISH PROVINCE CODE
Álava
Albacete
Alicante
Almería
Ávila
Badajoz
Barcelona
Burgos
Cáceres
Cádiz
Castellón
Ciudad real
Córdoba
A Coruña
Cuenca
Girona
Granada
Guadalajara
Guipúzcoa
Huelva
Huesca
Jaén
León
Lleida
La Rioja
Lugo
Madrid
Málaga
Murcia
Navarra
Ourense
Asturias
Palencia
Pontevedra
Salamanca
Cantabria
Segovia
Sevilla
3596.82
Soria
Tarragona
Teruel
Toledo
Valencia
Valladolid
Vizcaya
Zamora
Zaragoza
I_P = 1

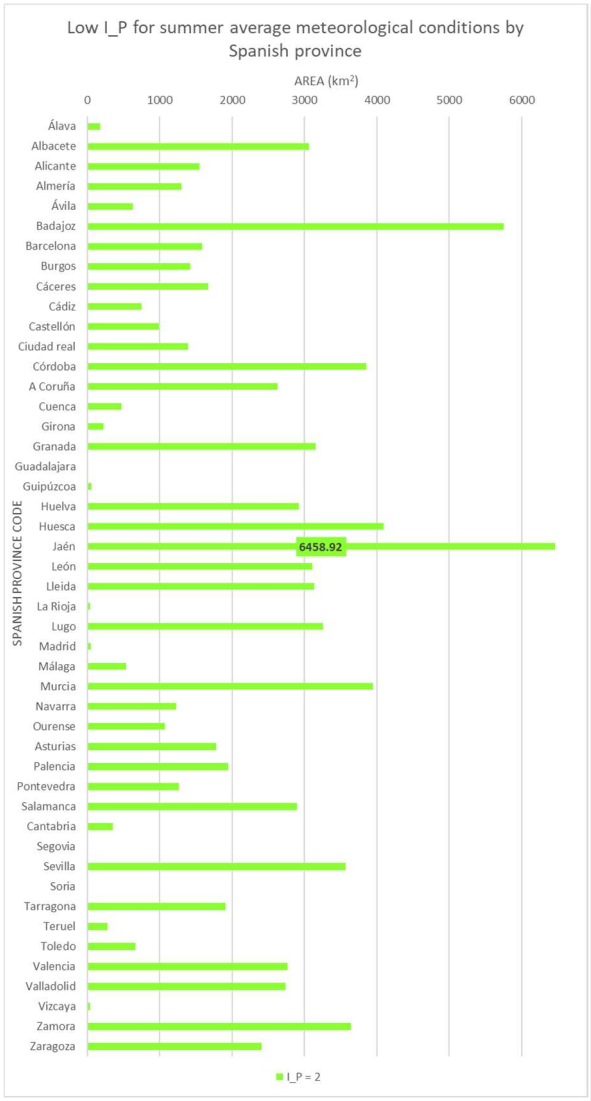
Low I_P for summer average meteorological conditions by Spanish province
AREA (km²)
0
1000
2000
3000
4000
5000
6000
SPANISH PROVINCE CODE
Álava
Albacete
Alicante
Almería
Ávila
Badajoz
Barcelona
Burgos
Cáceres
Cádiz
Castellón
Ciudad real
Córdoba
A Coruña
Cuenca
Girona
Granada
Guadalajara
Guipúzcoa
Huelva
Huesca
Jaén
6458.92
León
Lleida
La Rioja
Lugo
Madrid
Málaga
Murcia
Navarra
Ourense
Asturias
Palencia
Pontevedra
Salamanca
Cantabria
Segovia
Sevilla
Soria
Tarragona
Teruel
Toledo
Valencia
Valladolid
Vizcaya
Zamora
Zaragoza
I_P = 2

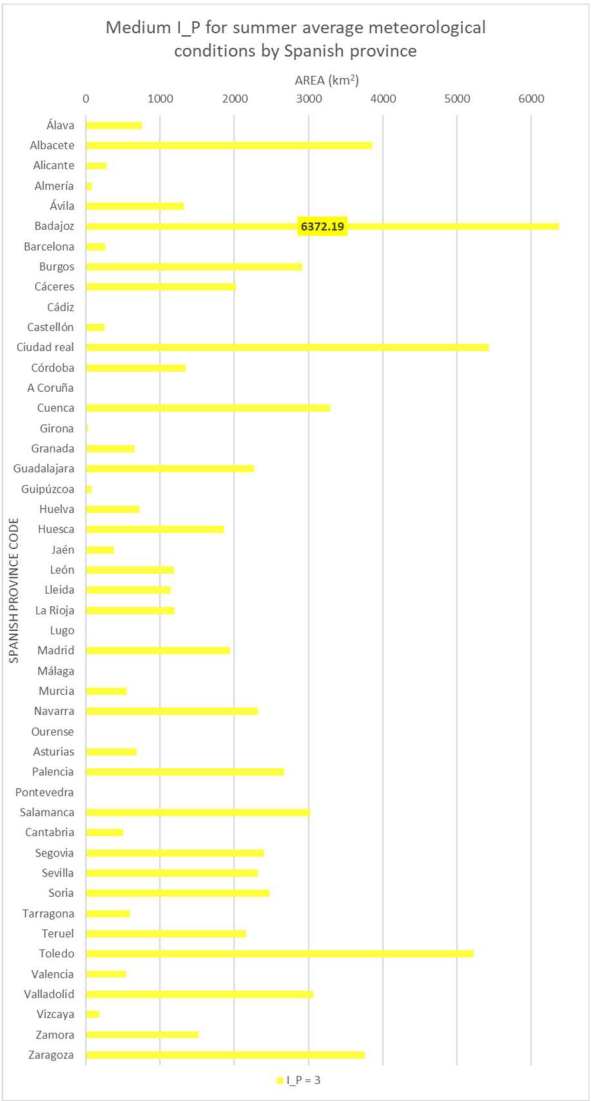
Medium I_P for summer average meteorological conditions by Spanish province
AREA (km²)
0
1000
2000
3000
4000
5000
6000
SPANISH PROVINCE CODE
Álava
Albacete
Alicante
Almería
Ávila
Badajoz
6372.19
Barcelona
Burgos
Cáceres
Cádiz
Castellón
Ciudad real
Córdoba
A Coruña
Cuenca
Girona
Granada
Guadalajara
Guipúzcoa
Huelva
Huesca
Jaén
León
Lleida
La Rioja
Lugo
Madrid
Málaga
Murcia
Navarra
Ourense
Asturias
Palencia
Pontevedra
Salamanca
Cantabria
Segovia
Sevilla
Soria
Tarragona
Teruel
Toledo
Valencia
Valladolid
Vizcaya
Zamora
Zaragoza
I_P = 3

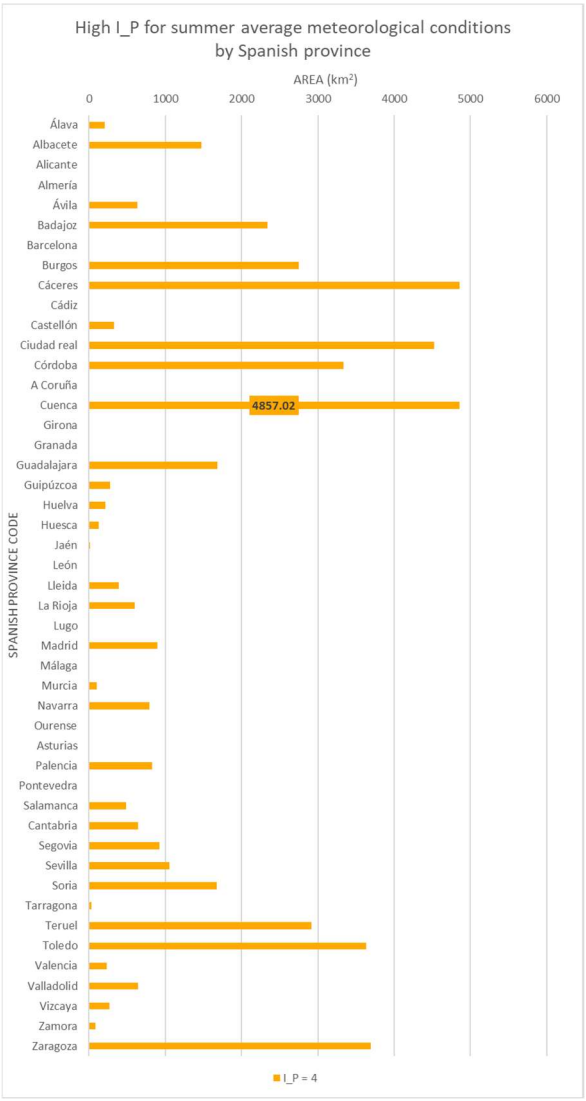
High I_P for summer average meteorological conditions by Spanish province
AREA (km²)
0
1000
2000
3000
4000
5000
6000
SPANISH PROVINCE CODE
Álava
Albacete
Alicante
Almería
Ávila
Badajoz
Barcelona
Burgos
Cáceres
Cádiz
Castellón
Ciudad real
Córdoba
A Coruña
Cuenca
Girona
Granada
Guadalajara
Guipúzcoa
Huelva
Huesca
Jaén
León
Lleida
La Rioja
Lugo
Madrid
Málaga
Murcia
Navarra
Ourense
Asturias
Palencia
Pontevedra
Salamanca
Cantabria
Segovia
Sevilla
Soria
Tarragona
Teruel
Toledo
Valencia
Valladolid
Vizcaya
Zamora
Zaragoza
4857.02
I_P = 4

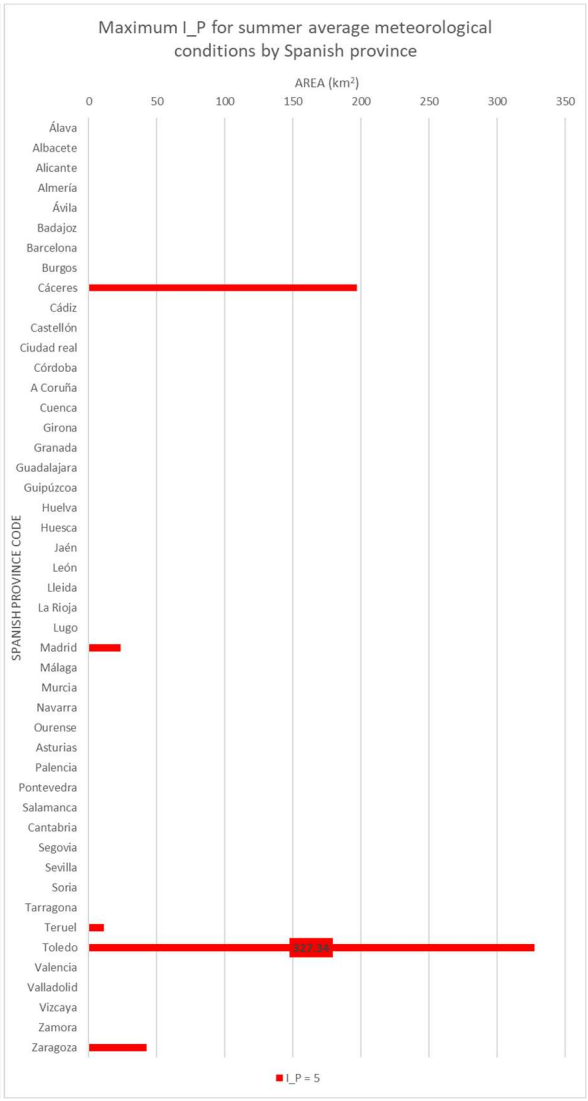
Maximum I_P for summer average meteorological conditions by Spanish province
AREA (km²)
0
50
100
150
200
250
300
350
SPANISH PROVINCE CODE
Álava
Albacete
Alicante
Almería
Ávila
Badajoz
Barcelona
Burgos
Cáceres
Cádiz
Castellón
Ciudad real
Córdoba
A Coruña
Cuenca
Girona
Granada
Guadalajara
Guipúzcoa
Huelva
Huesca
Jaén
León
Lleida
La Rioja
Lugo
Madrid
Málaga
Murcia
Navarra
Ourense
Asturias
Palencia
Pontevedra
Salamanca
Cantabria
Segovia
Sevilla
Soria
Tarragona
Teruel
Toledo
Valencia
Valladolid
Vizcaya
Zamora
Zaragoza
327.34
I_P = 5

Peninsular Spain Province	Province Code	Surface percentage by I_P for summer average meteorological conditions in the agricultural areas, in each province (%)				
		I_P = 1	I_P = 2	I_P = 3	I_P = 4	I_P = 5
Álava	1	0.11	15.55	66.07	18.28	
Albacete	2	0.80	36.18	45.61	17.41	
Alicante	3	26.79	62.06	11.16		
Almería	4	51.84	45.37	2.79		
Ávila	5	2.90	23.73	49.59	23.78	
Badajoz	6	0.12	39.73	44.00	16.15	
Barcelona	8	3.40	82.93	13.67		
Burgos	9	0.83	19.87	40.79	38.52	
Cáceres	10	3.80	18.36	22.24	53.44	2.17
Cádiz	11	82.81	17.19			
Castellón	12	11.80	55.36	14.33	18.51	
Ciudad real	13	0.07	12.27	47.81	39.85	
Córdoba	14	15.14	38.31	13.38	33.17	
A Coruña	15		10			
Cuenca	16	0.01	5.47	38.15	56.37	
Girona	17	81.91	16.27	1.82		
Granada	18	40.24	49.51	10.24		
Guadalajara	19			57.40	42.60	
Guipúzcoa	20		12.89	19.61	67.50	
Huelva	21	2.83	73.62	18.18	5.37	
Huesca	22	0.07	67.28	30.63	2.02	
Jaén	23	12.59	82.50	4.76	0.15	
León	24	12.11	63.49	24.26	0.14	
Lleida	25	0.41	66.95	24.38	8.26	
La Rioja	26	0.01	2.11	65.06	32.82	
Lugo	27	0.28	99.72			
Madrid	28		1.53	66.82	30.85	0.80
Málaga	29	85.82	14.18			
Murcia	30	23.33	65.79	9.19	1.69	
Navarra	31	0.01	28.36	53.36	18.27	
Ourense	32	29.37	70.63			
Asturias	33	5.42	68.38	26.20		
Palencia	34		35.73	49.11	15.15	
Pontevedra	36	0.67	99.33			
Salamanca	37	1.49	44.49	46.50	7.51	
Cantabria	39	0.11	23.39	33.59	42.92	
Segovia	40		0.36	71.95	27.69	
Sevilla	41	34.12	33.84	22.04	1	
Soria	42		0.05	59.64	40.31	
Tarragona	43	9.88	67.93	20.96	1.24	
Teruel	44	0.05	5.20	40.21	54.33	0.20
Toledo	45		6.72	53.05	36.91	3.32
Valencia	46	14.35	66.95	13.15	5.55	
Valladolid	47	0.33	42.28	47.42	9.97	
Vizcaya	48		7.46	37.15	55.39	
Zamora	49	6.80	64.79	26.96	1.45	
Zaragoza	50		24.27	37.98	37.31	0.43

Blank cells mean no affected surface.

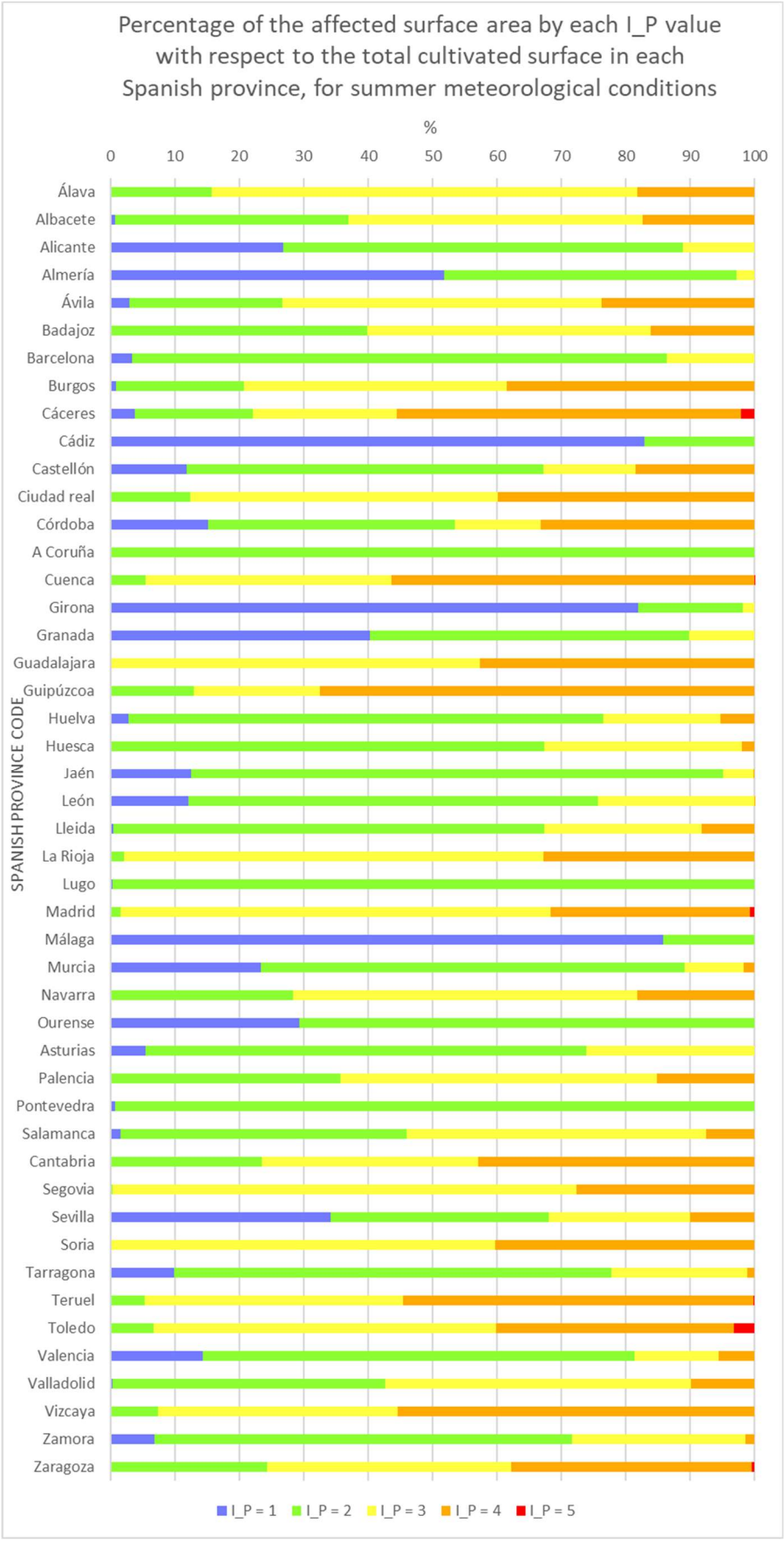
Percentage of the affected surface area by each I_P value with respect to the total cultivated surface in each Spanish province, for summer meteorological conditions
%
0
10
20
30
40
50
60
70
80
90
100
SPANISH PROVINCE CODE
Álava
Albacete
Alicante
Almería
Ávila
Badajoz
Barcelona
Burgos
Cáceres
Cádiz
Castellón
Ciudad real
Córdoba
A Coruña
Cuenca
Girona
Granada
Guadalajara
Guipúzcoa
Huelva
Huesca
Jaén
León
Lleida
La Rioja
Lugo
Madrid
Málaga
Murcia
Navarra
Ourense
Asturias
Palencia
Pontevedra
Salamanca
Cantabria
Segovia
Sevilla
Soria
Tarragona
Teruel
Toledo
Valencia
Valladolid
Vizcaya
Zamora
Zaragoza
I_P = 1
I_P = 2
I_P = 3
I_P = 4
I_P = 5

Peninsular Spain Province	Province Code	Surface percentage by I_P for summer average meteorological conditions in the agricultural areas, with respect all the cultivated surface (%)				
		I_P = 1	I_P = 2	I_P = 3	I_P = 4	I_P = 5
Álava	1	0.001	0.077	0.326	0.090	
Albacete	2	0.029	1.318	1.662	0.635	
Alicante	3	0.287	0.666	0.120		
Almería	4	0.641	0.561	0.035		
Ávila	5	0.033	0.272	0.568	0.272	
Badajoz	6	0.007	2.479	2.745	1.008	
Barcelona	8	0.028	0.684	0.113		
Burgos	9	0.026	0.611	1.254	1.184	
Cáceres	10	0.149	0.718	0.870	2.091	0.085
Cádiz	11	1.542	0.320			
Castellón	12	0.090	0.424	0.110	0.142	
Ciudad real	13	0.004	0.600	2.338	1.949	
Córdoba	14	0.656	1.661	0.580	1.438	
A Coruña	15		1.133			
Cuenca	16		0.203	1.416	2.092	
Girona	17	0.479	0.095	0.011		
Granada	18	1.105	1.359	0.281		
Guadalajara	19			0.976	0.724	
Guipúzcoa	20		0.023	0.034	0.119	
Huelva	21	0.048	1.260	0.311	0.092	
Huesca	22	0.002	1.765	0.804	0.053	
Jaén	23	0.425	2.783	0.161	0.005	
León	24	0.255	1.337	0.511	0.003	
Lleida	25	0.008	1.349	0.491	0.166	
La Rioja	26		0.017	0.514	0.259	
Lugo	27	0.004	1.402			
Madrid	28		0.019	0.837	0.386	0.010
Málaga	29	1.386	0.229			
Murcia	30	0.602	1.698	0.237	0.044	
Navarra	31		0.530	0.998	0.342	
Ourense	32	0.192	0.462			
Asturias	33	0.061	0.768	0.294		
Palencia	34		0.838	1.151	0.355	
Pontevedra	36	0.004	0.546			
Salamanca	37	0.042	1.245	1.302	0.210	
Cantabria	39	0.001	0.151	0.217	0.278	
Segovia	40		0.005	1.035	0.398	
Sevilla	41	1.550	1.537	1.001	0.454	
Soria	42		0.001	1.067	0.721	
Tarragona	43	0.120	0.823	0.254	0.015	
Teruel	44	0.001	0.120	0.929	1.255	0.005
Toledo	45		0.285	2.251	1.566	0.141
Valencia	46	0.255	1.191	0.234	0.099	
Valladolid	47	0.009	1.178	1.321	0.278	
Vizcaya	48		0.016	0.078	0.116	
Zamora	49	0.165	1.568	0.653	0.035	
Zaragoza	50		1.035	1.620	1.591	0.018

Blank cells mean no affected surface.

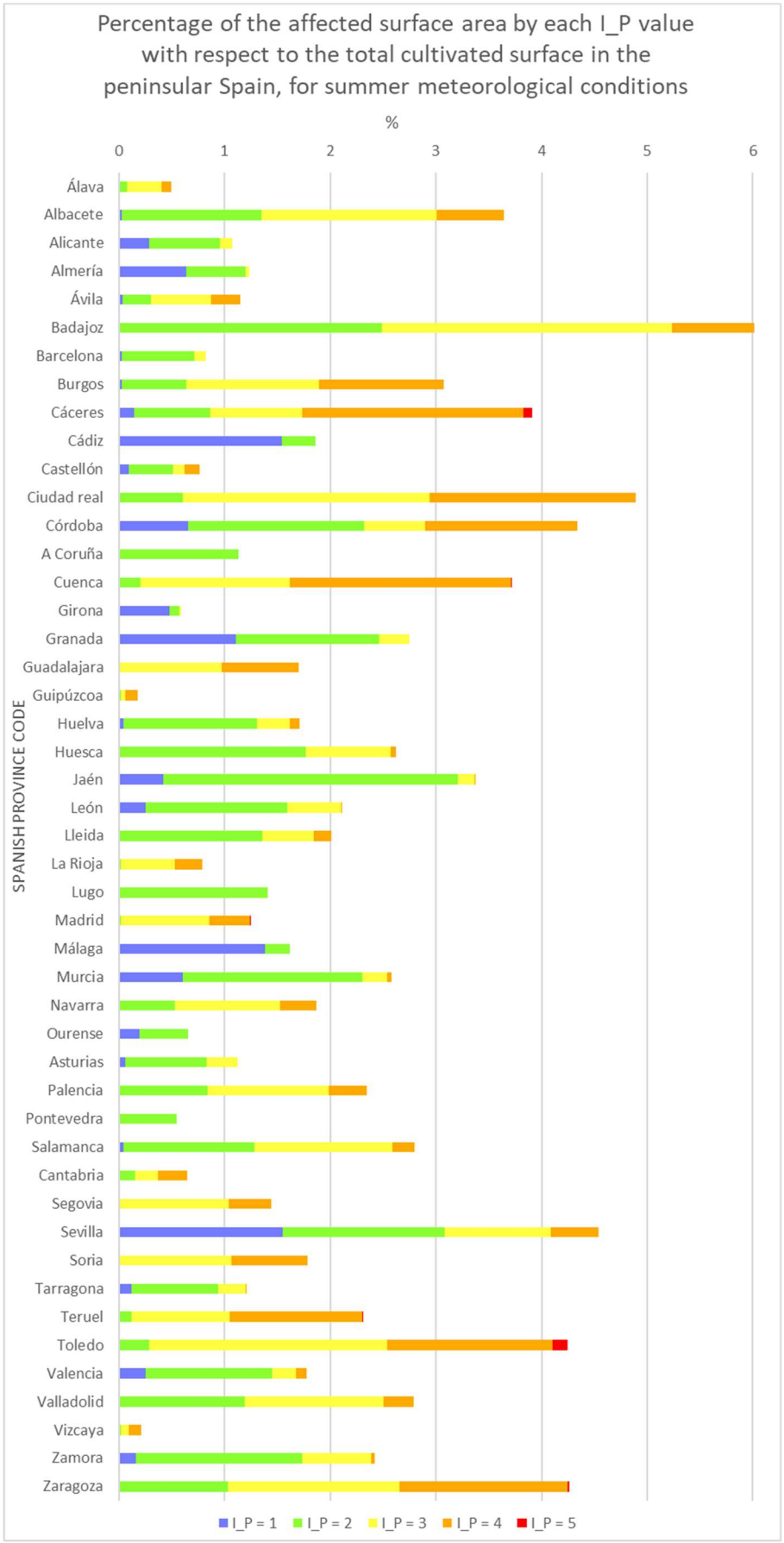
Percentage of the affected surface area by each I_P value with respect to the total cultivated surface in the peninsular Spain, for summer meteorological conditions
%
0
1
2
3
4
5
6
SPANISH PROVINCE CODE
Álava
Albacete
Alicante
Almería
Ávila
Badajoz
Barcelona
Burgos
Cáceres
Cádiz
Castellón
Ciudad real
Córdoba
A Coruña
Cuenca
Girona
Granada
Guadalajara
Guipúzcoa
Huelva
Huesca
Jaén
León
Lleida
La Rioja
Lugo
Madrid
Málaga
Murcia
Navarra
Ourense
Asturias
Palencia
Pontevedra
Salamanca
Cantabria
Segovia
Sevilla
Soria
Tarragona
Teruel
Toledo
Valencia
Valladolid
Vizcaya
Zamora
Zaragoza
I_P = 1
I_P = 2
I_P = 3
I_P = 4
I_P = 5

Peninsular Spain Province	Province Code	Surface affected by each Prioritisation Index value in the Autumn Average Prioritisation map (km²)				
		I_P = 1	I_P = 2	I_P = 3	I_P = 4	I_P = 5
Álava	1	38.93	339.19	626.69	142.15	
Albacete	2	67.81	6484.89	1765.58	139.49	
Alicante	3	851.96	1451.36	186.16		
Almería	4	1018.44	1394.95	455.19		
Ávila	5	129.55	1167.21	830.33	531.82	
Badajoz	6	90.80	11084.14	2611.94	695.33	
Barcelona	8	945.22	866.23	102.34		
Burgos	9	89.74	3064.61	3381.80	601.85	
Cáceres	10	288.21	1266.15	2046.57	5045.62	436.21
Cádiz	11	2930.85	1348.74	42.19		
Castellón	12	210.52	1107.84	347.26	111.87	
Ciudad real	13	8.18	5793.00	3975.12	1575.18	
Córdoba	14	1198.62	5091.63	3340.83	432.98	
A Coruña	15		1664.29	964.70		
Cuenca	16	38.86	2734.70	4163.78	1678.77	
Girona	17	1325.82	32.76			
Granada	18	910.39	4649.24	811.47		
Guadalajara	19		460.01	2110.55	1376.66	
Guipúzcoa	20		51.66	66.96	289.19	
Huelva	21	228.19	2966.08	757.46	19.91	
Huesca	22	1995.35	3736.32	342.69	15.90	
Jaén	23	341.50	7135.15	352.43		
León	24	0.28	2227.13	1827.24	835.45	
Lleida	25	1354.44	2679.86	641.36		
La Rioja	26	16.01	1150.39	401.77	265.19	
Lugo	27	6.02	2889.31	367.18		
Madrid	28		46.14	1944.19	917.06	
Málaga	29	1530.12	2021.20	198.08		
Murcia	30	661.85	3417.76	1911.91		
Navarra	31	4.60	2277.14	2003.33	55.20	
Ourense	32	88.41	526.85	902.32		
Asturias	33	41.89	610.18	1953.38		
Palencia	34		2106.84	2590.64	743.47	
Pontevedra	36		63.83	1211.76		
Salamanca	37	48.24	1758.01	1852.08	2838.51	
Cantabria	39	1.59	338.81	163.58	999.04	
Segovia	40	11.97	2187.08	781.18	359.61	
Sevilla	41	3255.73	4298.62	2986.89		
Soria	42	2.28	951.53	1969.37	1228.21	
Tarragona	43	913.29	1537.85	361.82		
Teruel	44	139.55	3230.16	1677.16	316.68	
Toledo	45		2327.56	4407.06	3050.60	63.32
Valencia	46	609.39	2897.28	550.76	72.26	
Valladolid	47	5.32	2813.41	3020.72	626.90	
Vizcaya	48		31.69	12.49	442.22	
Zamora	49		2107.07	2704.44	808.17	
Zaragoza	50	46.57	4591.92	3100.13	2159.10	
Total surface (km²)		21446.46	112977.77	68822.89	28374.36	499.52

Blank cells mean no affected surface.

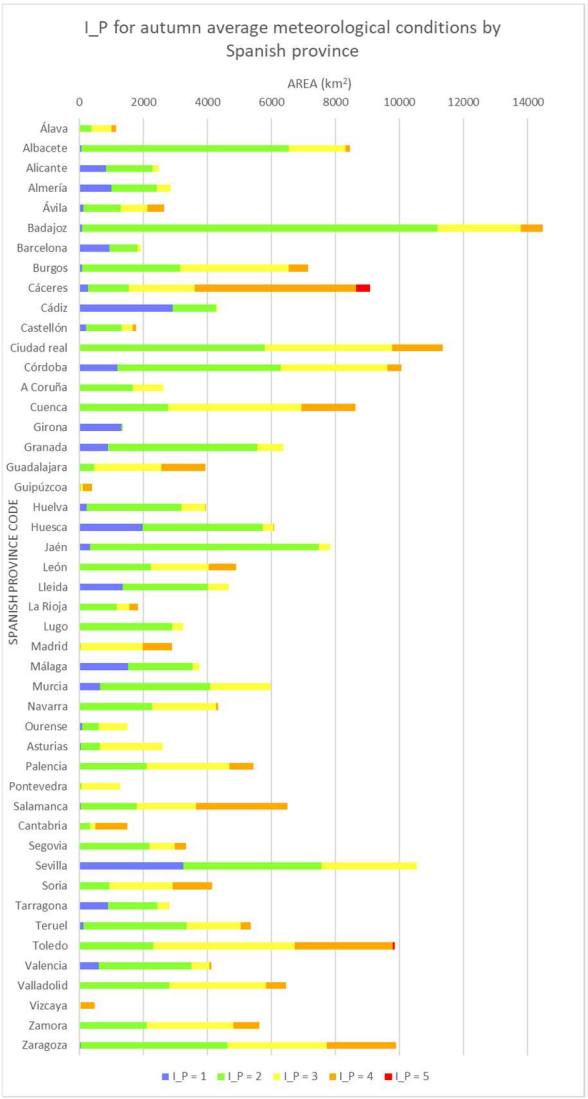
I_P for autumn average meteorological conditions by Spanish province
AREA (km²)
0
2000
4000
6000
8000
10000
12000
14000
SPANISH PROVINCE CODE
Álava
Albacete
Alicante
Almería
Ávila
Badajoz
Barcelona
Burgos
Cáceres
Cádiz
Castellón
Ciudad real
Córdoba
A Coruña
Cuenca
Girona
Granada
Guadalajara
Guipúzcoa
Huelva
Huesca
Jaén
León
Lleida
La Rioja
Lugo
Madrid
Málaga
Murcia
Navarra
Ourense
Asturias
Palencia
Pontevedra
Salamanca
Cantabria
Segovia
Sevilla
Soria
Tarragona
Teruel
Toledo
Valencia
Valladolid
Vizcaya
Zamora
Zaragoza
I_P = 1
I_P = 2
I_P = 3
I_P = 4
I_P = 5

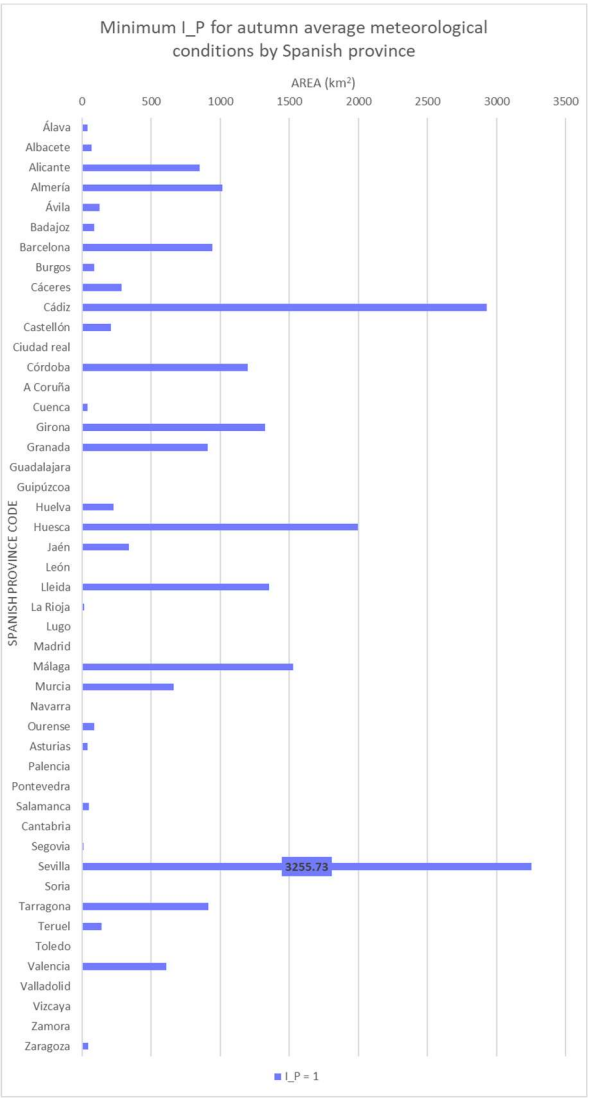
Minimum I_P for autumn average meteorological conditions by Spanish province
AREA (km²)
0
500
1000
1500
2000
2500
3000
3500
SPANISH PROVINCE CODE
Álava
Albacete
Alicante
Almería
Ávila
Badajoz
Barcelona
Burgos
Cáceres
Cádiz
Castellón
Ciudad real
Córdoba
A Coruña
Cuenca
Girona
Granada
Guadalajara
Guipúzcoa
Huelva
Huesca
Jaén
León
Lleida
La Rioja
Lugo
Madrid
Málaga
Murcia
Navarra
Ourense
Asturias
Palencia
Pontevedra
Salamanca
Cantabria
Segovia
Sevilla
3255.73
Soria
Tarragona
Teruel
Toledo
Valencia
Valladolid
Vizcaya
Zamora
Zaragoza
I_P = 1

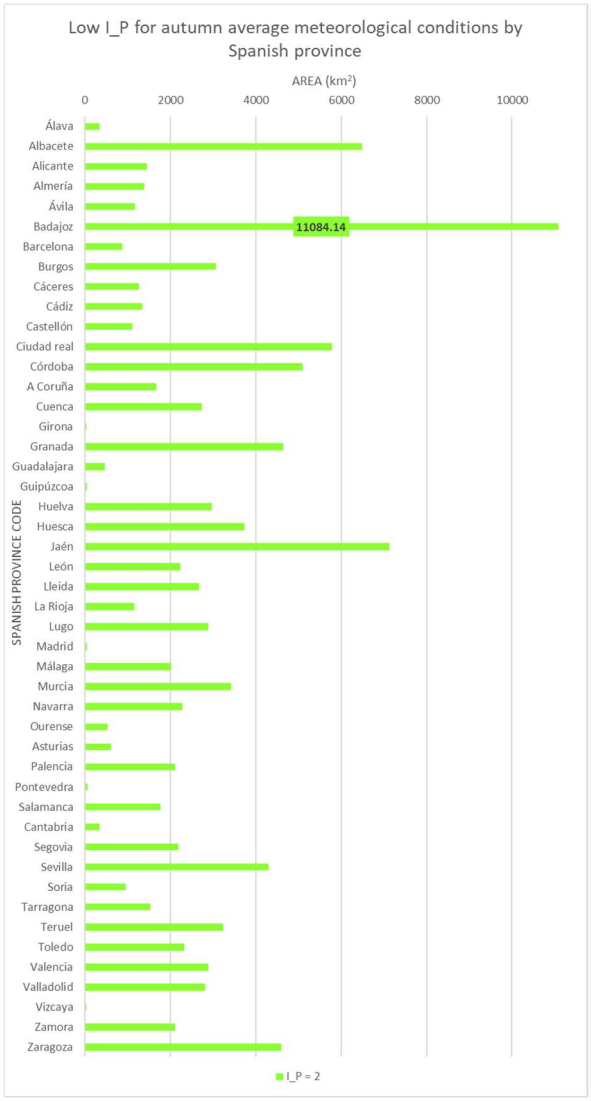
Low I_P for autumn average meteorological conditions by Spanish province
AREA (km²)
0
2000
4000
6000
8000
10000
SPANISH PROVINCE CODE
Álava
Albacete
Alicante
Almería
Ávila
Badajoz
11084.14
Barcelona
Burgos
Cáceres
Cádiz
Castellón
Ciudad real
Córdoba
A Coruña
Cuenca
Girona
Granada
Guadalajara
Guipúzcoa
Huelva
Huesca
Jaén
León
Lleida
La Rioja
Lugo
Madrid
Málaga
Murcia
Navarra
Ourense
Asturias
Palencia
Pontevedra
Salamanca
Cantabria
Segovia
Sevilla
Soria
Tarragona
Teruel
Toledo
Valencia
Valladolid
Vizcaya
Zamora
Zaragoza
I_P = 2

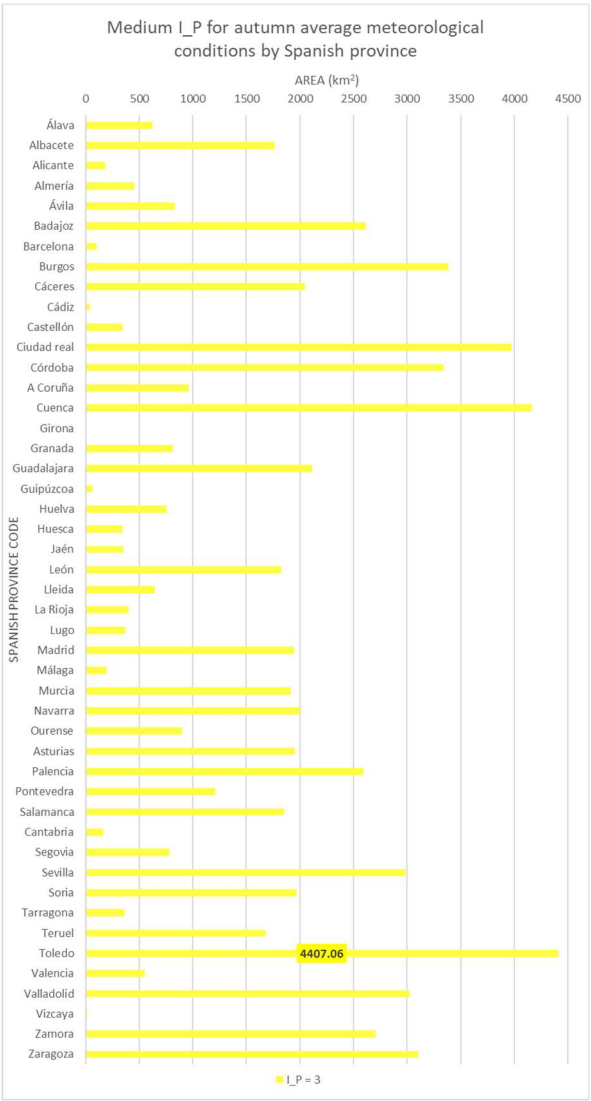
Medium I_P for autumn average meteorological conditions by Spanish province
AREA (km²)
0
500
1000
1500
2000
2500
3000
3500
4000
4500
SPANISH PROVINCE CODE
Álava
Albacete
Alicante
Almería
Ávila
Badajoz
Barcelona
Burgos
Cáceres
Cádiz
Castellón
Ciudad real
Córdoba
A Coruña
Cuenca
Girona
Granada
Guadalajara
Guipúzcoa
Huelva
Huesca
Jaén
León
Lleida
La Rioja
Lugo
Madrid
Málaga
Murcia
Navarra
Ourense
Asturias
Palencia
Pontevedra
Salamanca
Cantabria
Segovia
Sevilla
Soria
Tarragona
Teruel
Toledo
4407.06
Valencia
Valladolid
Vizcaya
Zamora
Zaragoza
I_P = 3

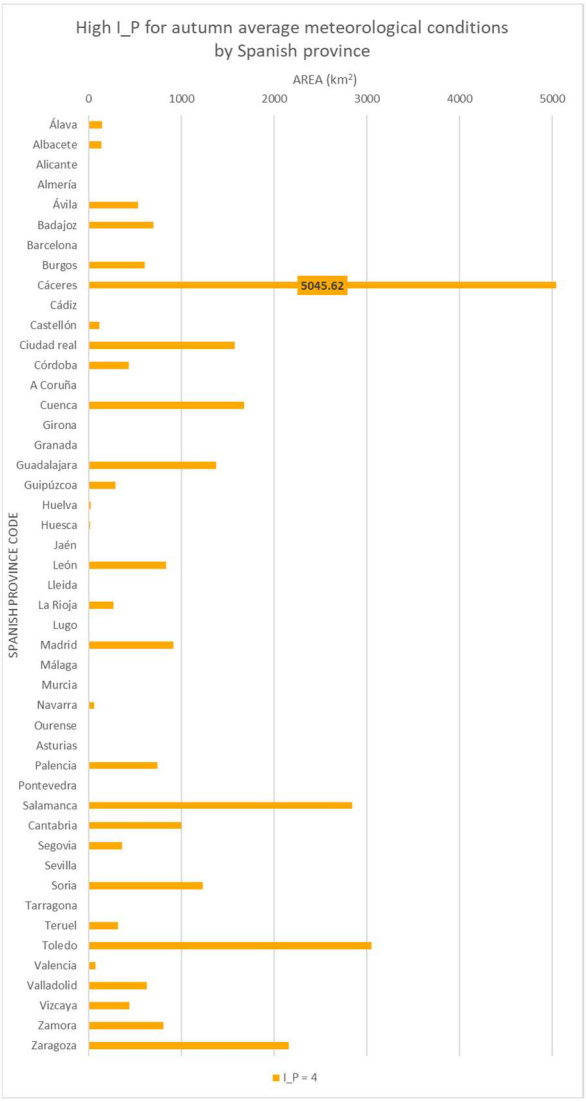
High I_P for autumn average meteorological conditions by Spanish province
AREA (km²)
0
1000
2000
3000
4000
5000
SPANISH PROVINCE CODE
Álava
Albacete
Alicante
Almería
Ávila
Badajoz
Barcelona
Burgos
Cáceres
Cádiz
Castellón
Ciudad real
Córdoba
A Coruña
Cuenca
Girona
Granada
Guadalajara
Guipúzcoa
Huelva
Huesca
Jaén
León
Lleida
La Rioja
Lugo
Madrid
Málaga
Murcia
Navarra
Ourense
Asturias
Palencia
Pontevedra
Salamanca
Cantabria
Segovia
Sevilla
Soria
Tarragona
Teruel
Toledo
Valencia
Valladolid
Vizcaya
Zamora
Zaragoza
5045.62
I_P = 4

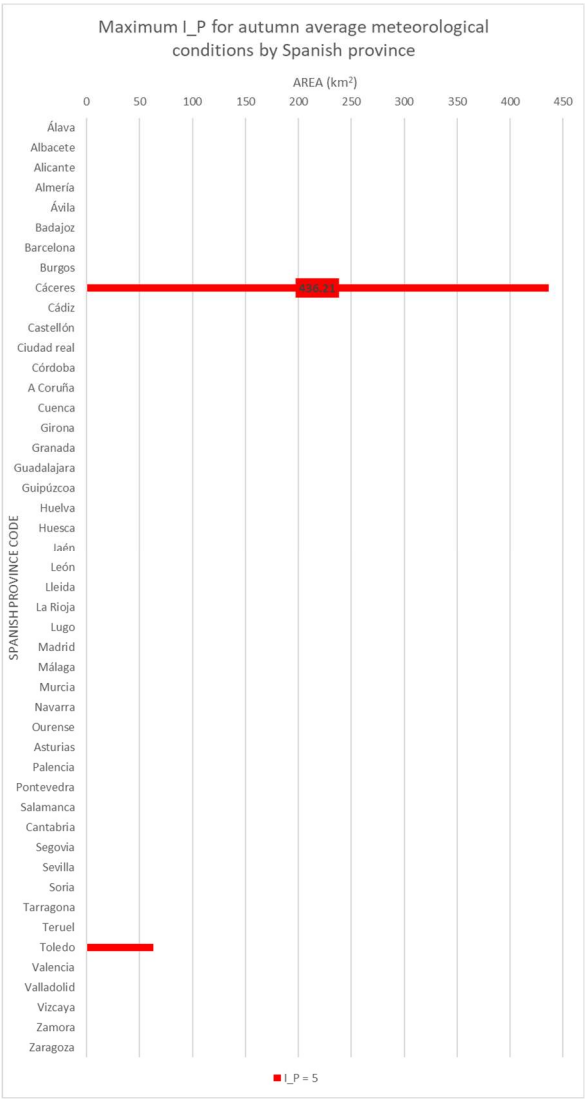
Maximum I_P for autumn average meteorological conditions by Spanish province
AREA (km²)
0
50
100
150
200
250
300
350
400
450
SPANISH PROVINCE CODE
Álava
Albacete
Alicante
Almería
Ávila
Badajoz
Barcelona
Burgos
Cáceres
Cádiz
Castellón
Ciudad real
Córdoba
A Coruña
Cuenca
Girona
Granada
Guadalajara
Guipúzcoa
Huelva
Huesca
León
Lleida
La Rioja
Lugo
Madrid
Málaga
Murcia
Navarra
Ourense
Asturias
Palencia
Pontevedra
Salamanca
Cantabria
Segovia
Sevilla
Soria
Tarragona
Teruel
Toledo
Valencia
Valladolid
Vizcaya
Zamora
Zaragoza
I_P = 5

Peninsular Spain Province	Province Code	Surface percentage by I_P for autumn average meteorological conditions in the agricultural areas, in each province (%)				
		I_P = 1	I_P = 2	I_P = 3	I_P = 4	I_P = 5
Álava	1	3.39	29.57	54.64	12.39	
Albacete	2	0.80	76.67	20.88	1.65	
Alicante	3	34.22	58.30	7.48		
Almería	4	35.50	48.63	15.87		
Ávila	5	4.87	43.90	31.23	2	
Badajoz	6	0.63	76.54	18.04	4.80	
Barcelona	8	49.39	45.26	5.35		
Burgos	9	1.26	42.93	47.38	8.43	
Cáceres	10	3.17	13.94	22.53	55.55	4.80
Cádiz	11	67.82	31.21	0.98		
Castellón	12	11.84	62.33	19.54	6.29	
Ciudad real	13	0.07	51.03	35.02	13.88	
Córdoba	14	11.91	50.59	33.20	4.30	
A Coruña	15		63.31	36.69		
Cuenca	16	0.45	31.74	48.33	19.48	
Girona	17	97.59	2.41			
Granada	18	14.29	72.97	12.74		
Guadalajara	19		11.65	53.47	34.88	
Guipúzcoa	20		12.67	16.42	70.91	
Huelva	21	5.75	74.68	19.07	0.50	
Huesca	22	32.76	61.35	5.63	0.26	
Jaén	23	4.36	91.14	4.50		
León	24	0.01	45.54	37.37	17.08	
Lleida	25	28.97	57.32	13.72		
La Rioja	26	0.87	62.75	21.91	14.46	
Lugo	27	0.18	88.56	11.25		
Madrid	28		1.59	66.87	31.54	
Málaga	29	40.81	53.91	5.28		
Murcia	30	11.05	57.04	31.91		
Navarra	31	0.11	52.47	46.16	1.27	
Ourense	32	5.83	34.72	59.46		
Asturias	33	1.61	23.42	74.97		
Palencia	34		38.72	47.61	13.66	
Pontevedra	36		5.00	95.00		
Salamanca	37	0.74	27.06	28.51	43.69	
Cantabria	39	0.11	22.54	10.88	66.47	
Segovia	40	0.36	65.48	23.39	10.77	
Sevilla	41	30.89	40.78	28.34		
Soria	42	0.05	22.92	47.44	29.59	
Tarragona	43	32.47	54.67	12.86		
Teruel	44	2.60	60.22	31.27	5.90	
Toledo	45		23.63	44.75	30.98	0.64
Valencia	46	14.76	70.16	13.34	1.75	
Valladolid	47	0.08	43.51	46.71	9.69	
Vizcaya	48		6.51	2.57	90.92	
Zamora	49		37.49	48.12	14.38	
Zaragoza	50	0.47	46.39	31.32	21.81	

Blank cells mean no affected surface.

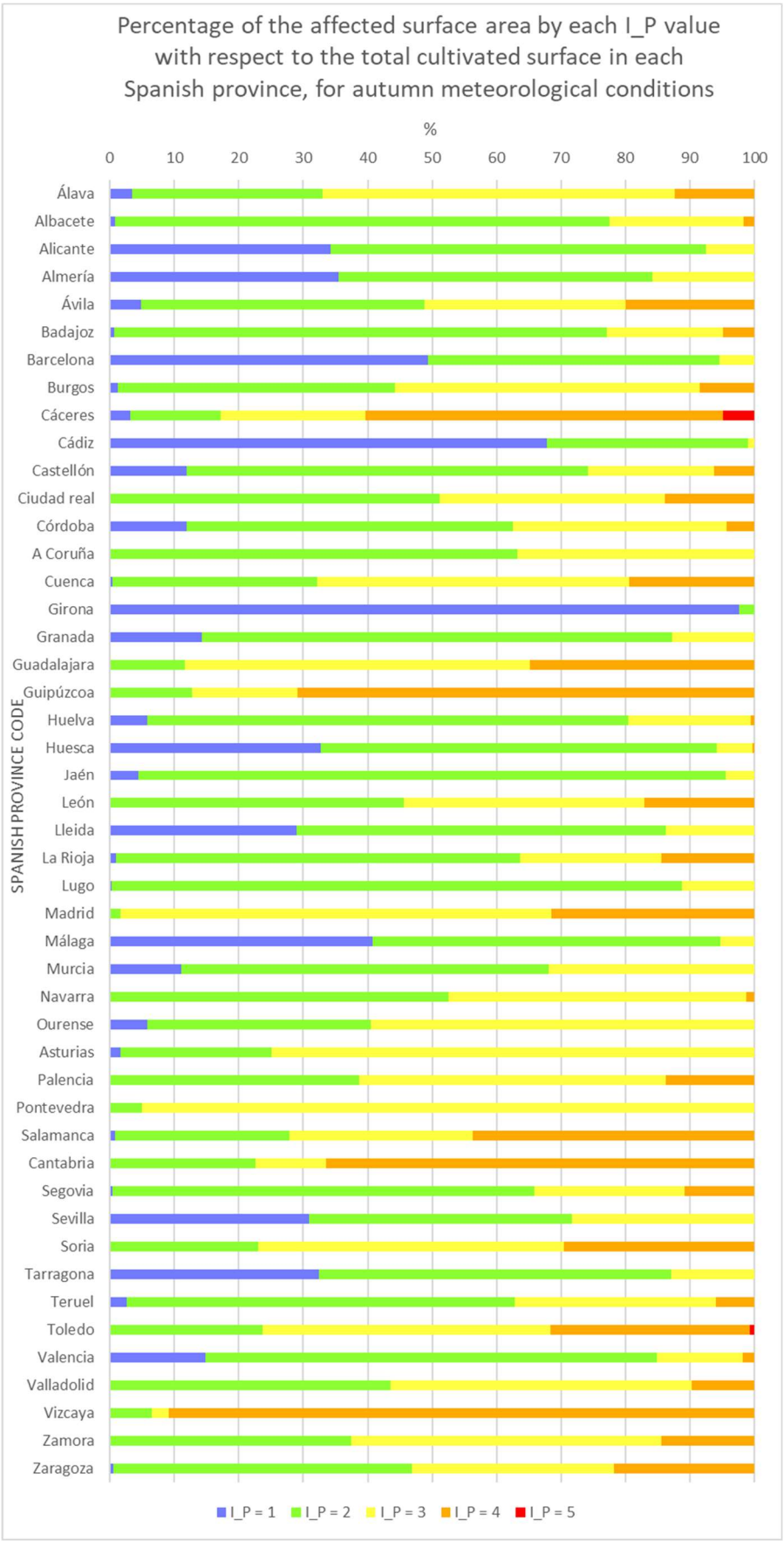
Percentage of the affected surface area by each I_P value with respect to the total cultivated surface in each Spanish province, for autumn meteorological conditions
%
0
10
20
30
40
50
60
70
80
90
100
SPANISH PROVINCE CODE
Álava
Albacete
Alicante
Almería
Ávila
Badajoz
Barcelona
Burgos
Cáceres
Cádiz
Castellón
Ciudad real
Córdoba
A Coruña
Cuenca
Girona
Granada
Guadalajara
Guipúzcoa
Huelva
Huesca
Jaén
León
Lleida
La Rioja
Lugo
Madrid
Málaga
Murcia
Navarra
Ourense
Asturias
Palencia
Pontevedra
Salamanca
Cantabria
Segovia
Sevilla
Soria
Tarragona
Teruel
Toledo
Valencia
Valladolid
Vizcaya
Zamora
Zaragoza
I_P = 1
I_P = 2
I_P = 3
I_P = 4
I_P = 5

Peninsular Spain Province	Province Code	Surface percentage by I_P for autumn average meteorological conditions in the agricultural areas, with respect all the cultivated surface (%)				
		I_P = 1	I_P = 2	I_P = 3	I_P = 4	I_P = 5
Álava	1	0.017	0.146	0.270	0.061	
Albacete	2	0.029	2.794	0.761	0.060	
Alicante	3	0.367	0.625	0.080		
Almería	4	0.439	0.601	0.196		
Ávila	5	0.056	0.503	0.358	0.229	
Badajoz	6	0.039	4.775	1.125	0.300	
Barcelona	8	0.407	0.373	0.044		
Burgos	9	0.039	1.320	1.457	0.259	
Cáceres	10	0.124	0.545	0.882	2.174	0.188
Cádiz	11	1.263	0.581	0.018		
Castellón	12	0.091	0.477	0.150	0.048	
Ciudad real	13	0.004	2.496	1.713	0.679	
Córdoba	14	0.516	2.194	1.439	0.187	
A Coruña	15		0.717	0.416		
Cuenca	16	0.017	1.178	1.794	0.723	
Girona	17	0.571	0.014			
Granada	18	0.392	2.003	0.350		
Guadalajara	19		0.198	0.909	0.593	
Guipúzcoa	20		0.022	0.029	0.125	
Huelva	21	0.098	1.278	0.326	0.009	
Huesca	22	0.860	1.610	0.148	0.007	
Jaén	23	0.147	3.074	0.152		
León	24		0.959	0.787	0.360	
Lleida	25	0.584	1.155	0.276		
La Rioja	26	0.007	0.496	0.173	0.114	
Lugo	27	0.003	1.245	0.158		
Madrid	28		0.020	0.838	0.395	
Málaga	29	0.659	0.871	0.085		
Murcia	30	0.285	1.472	0.824		
Navarra	31	0.002	0.981	0.863	0.024	
Ourense	32	0.038	0.227	0.389		
Asturias	33	0.018	0.263	0.842		
Palencia	34		0.908	1.116	0.320	
Pontevedra	36		0.027	0.522		
Salamanca	37	0.021	0.757	0.798	1.223	
Cantabria	39	0.001	0.146	0.070	0.430	
Segovia	40	0.005	0.942	0.337	0.155	
Sevilla	41	1.403	1.852	1.287		
Soria	42	0.001	0.410	0.848	0.529	
Tarragona	43	0.393	0.663	0.156		
Teruel	44	0.060	1.392	0.723	0.136	
Toledo	45		1.003	1.899	1.314	0.027
Valencia	46	0.263	1.248	0.237	0.031	
Valladolid	47	0.002	1.212	1.301	0.270	
Vizcaya	48		0.014	0.005	0.191	
Zamora	49		0.908	1.165	0.348	
Zaragoza	50	0.020	1.978	1.336	0.930	

Blank cells mean no affected surface.

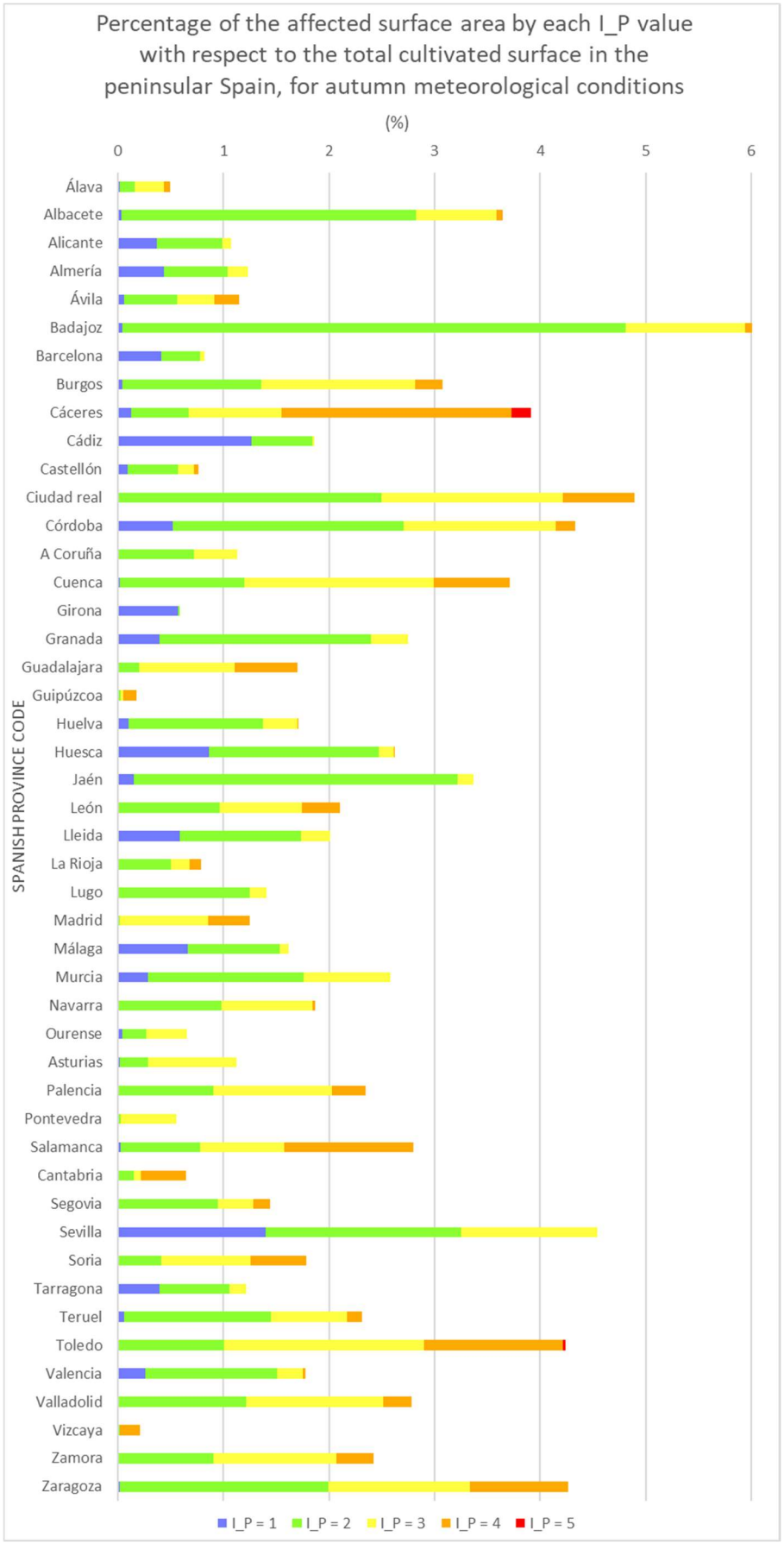
Percentage of the affected surface area by each I_P value with respect to the total cultivated surface in the peninsular Spain, for autumn meteorological conditions
(%)
0
1
2
3
4
5
6
SPANISH PROVINCE CODE
Álava
Albacete
Alicante
Almería
Ávila
Badajoz
Barcelona
Burgos
Cáceres
Cádiz
Castellón
Ciudad real
Córdoba
A Coruña
Cuenca
Girona
Granada
Guadalajara
Guipúzcoa
Huelva
Huesca
Jaén
León
Lleida
La Rioja
Lugo
Madrid
Málaga
Murcia
Navarra
Ourense
Asturias
Palencia
Pontevedra
Salamanca
Cantabria
Segovia
Sevilla
Soria
Tarragona
Teruel
Toledo
Valencia
Valladolid
Vizcaya
Zamora
Zaragoza
I_P = 1
I_P = 2
I_P = 3
I_P = 4
I_P = 5

Peninsular Spain Province	Province Code	Surface affected by each Prioritisation Index value in the Winter Average Prioritisation map (km²)				
		I_P = 1	I_P = 2	I_P = 3	I_P = 4	I_P = 5
Álava	1	38.93	804.18	262.41	41.44	
Albacete	2	77.24	7051.85	1270.82	57.86	
Alicante	3	816.08	1479.87	193.53		
Almería	4	1641.69	1226.88			
Ávila	5	135.77	1662.03	577.29	283.82	
Badajoz	6	274.90	11229.80	2371.05	606.47	
Barcelona	8	607.79	1136.23	169.77		
Burgos	9	90.69	3848.83	2892.60	305.88	
Cáceres	10	453.34	1787.88	1943.11	4586.07	312.36
Cádiz	11	2773.48	1290.83	257.47		
Castellón	12	557.96	923.34	296.19		
Ciudad real	13	8.18	7204.63	3136.31	1002.36	
Córdoba	14	2015.16	4109.46	3844.72	94.70	
A Coruña	15		179.56	2449.44		
Cuenca	16	41.67	3484.27	4453.67	636.52	
Girona	17	1322.71	35.87			
Granada	18	3208.38	2959.57	203.15		
Guadalajara	19		808.22	1895.11	1243.89	
Guipúzcoa	20		84.80	293.00	30.02	
Huelva	21	274.42	289	802.49	4.73	
Huesca	22	956.32	4231.51	841.86	60.56	
Jaén	23	944.14	6562.78	322.16		
León	24	64.62	3388.61	1436.88		
Lleida	25	669.68	3295.98	709.99		
La Rioja	26	16.12	1465.12	338.30	13.82	
Lugo	27	6.68	2711.61	544.22		
Madrid	28		54.82	1938.65	913.93	
Málaga	29	3073.30	675.72	0.39		
Murcia	30	1142.82	2844.06	2004.65		
Navarra	31	3.63	3997.28	328.99	10.36	
Ourense	32	165.39	886.97	465.22		
Asturias	33	177.80	1660.62	767.03		
Palencia	34		3253.77	1828.51	358.67	
Pontevedra	36		248.57	1027.02		
Salamanca	37	55.93	3592.46	2829.83	18.61	
Cantabria	39	1.59	384.83	1116.61		
Segovia	40	12.00	2464.29	818.82	44.73	
Sevilla	41	3200.24	4683.08	2657.92		
Soria	42	2.28	2623.83	1245.10	280.17	
Tarragona	43	1003.36	1362.66	446.94		
Teruel	44	1027.77	3722.51	597.47	15.79	
Toledo	45		3564.36	4208.36	2008.82	66.98
Valencia	46	609.39	2902.65	525.93	91.72	
Valladolid	47	26.40	5120.71	1254.83	64.41	
Vizcaya	48		43.86	434.04	8.50	
Zamora	49		4437.23	1170.49	11.95	
Zaragoza	50	159.21	6195.65	2061.94	1480.91	
Total surface (km²)		27657.06	130573.61	59234.27	14276.72	379.34

Blank cells mean no affected surface.

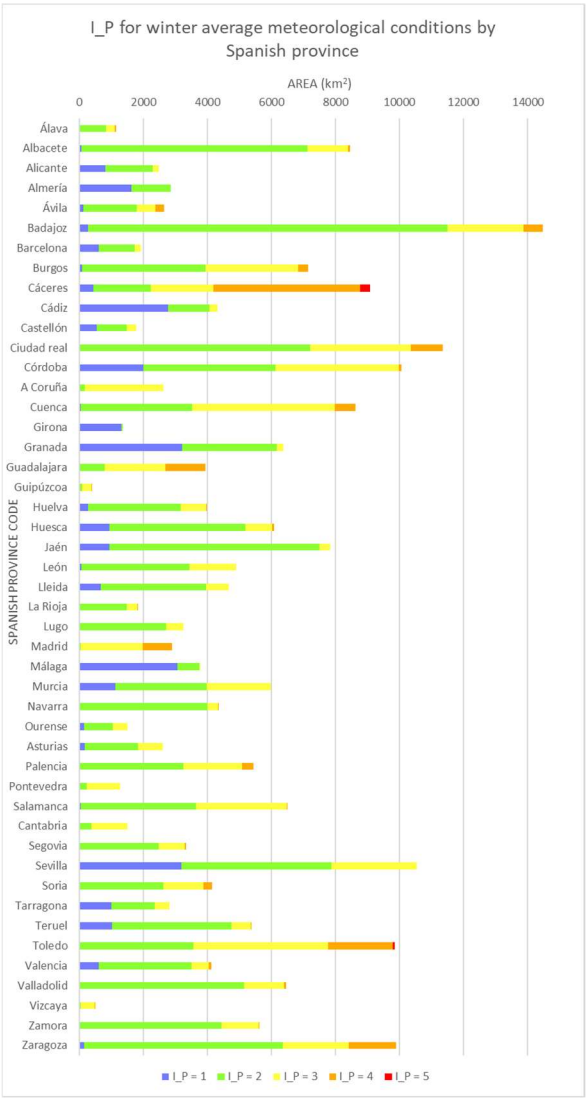
I_P for winter average meteorological conditions by Spanish province
AREA (km²)
0
2000
4000
6000
8000
10000
12000
14000
SPANISH PROVINCE CODE
Álava
Albacete
Alicante
Almería
Ávila
Badajoz
Barcelona
Burgos
Cáceres
Cádiz
Castellón
Ciudad real
Córdoba
A Coruña
Cuenca
Girona
Granada
Guadalajara
Guipúzcoa
Huelva
Huesca
Jaén
León
Lleida
La Rioja
Lugo
Madrid
Málaga
Murcia
Navarra
Ourense
Asturias
Palencia
Pontevedra
Salamanca
Cantabria
Segovia
Sevilla
Soria
Tarragona
Teruel
Toledo
Valencia
Valladolid
Vizcaya
Zamora
Zaragoza
I_P = 1
I_P = 2
I_P = 3
I_P = 4
I_P = 5

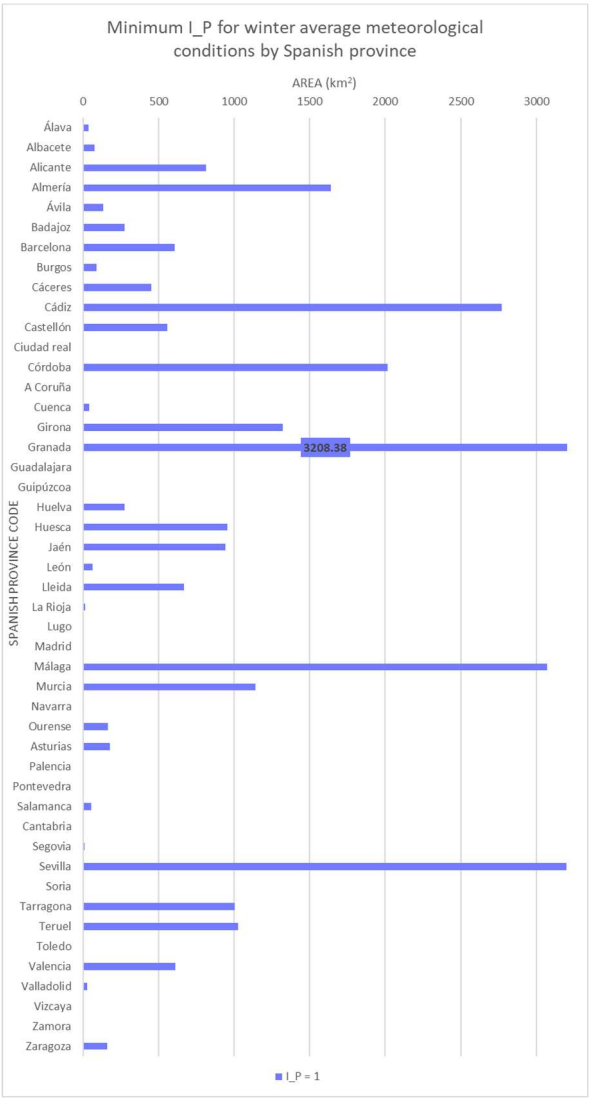
Minimum I_P for winter average meteorological conditions by Spanish province
AREA (km²)
0
500
1000
1500
2000
2500
3000
SPANISH PROVINCE CODE
Álava
Albacete
Alicante
Almería
Ávila
Badajoz
Barcelona
Burgos
Cáceres
Cádiz
Castellón
Ciudad real
Córdoba
A Coruña
Cuenca
Girona
Granada
3208.38
Guadalajara
Guipúzcoa
Huelva
Huesca
Jaén
León
Lleida
La Rioja
Lugo
Madrid
Málaga
Murcia
Navarra
Ourense
Asturias
Palencia
Pontevedra
Salamanca
Cantabria
Segovia
Sevilla
Soria
Tarragona
Teruel
Toledo
Valencia
Valladolid
Vizcaya
Zamora
Zaragoza
I_P = 1

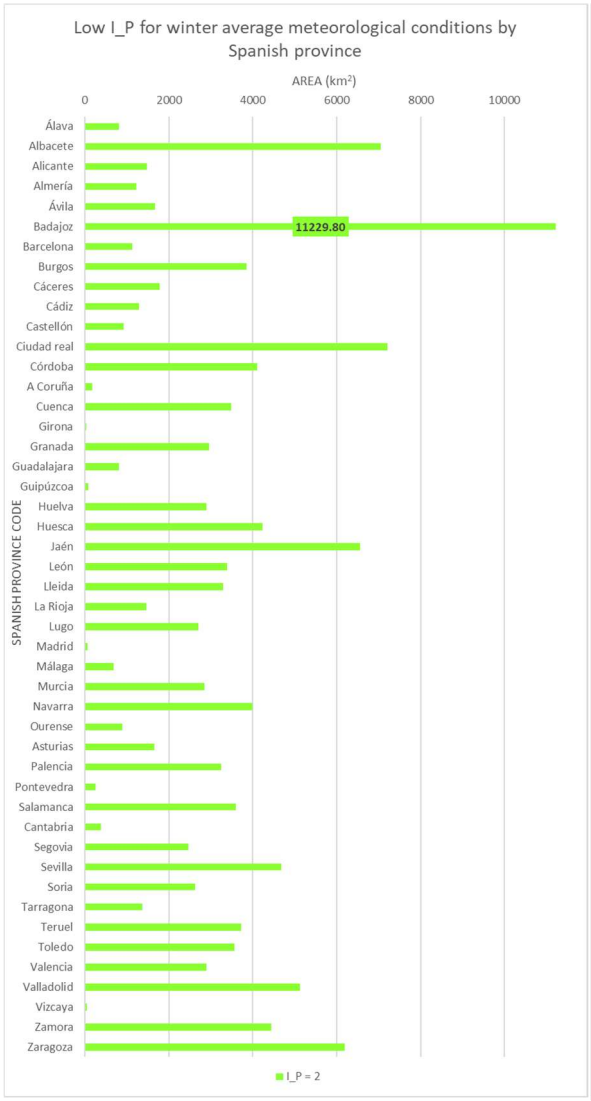
Low I_P for winter average meteorological conditions by Spanish province
AREA (km²)
0
2000
4000
6000
8000
10000
SPANISH PROVINCE CODE
Álava
Albacete
Alicante
Almería
Ávila
Badajoz
11229.80
Barcelona
Burgos
Cáceres
Cádiz
Castellón
Ciudad real
Córdoba
A Coruña
Cuenca
Girona
Granada
Guadalajara
Guipúzcoa
Huelva
Huesca
Jaén
León
Lleida
La Rioja
Lugo
Madrid
Málaga
Murcia
Navarra
Ourense
Asturias
Palencia
Pontevedra
Salamanca
Cantabria
Segovia
Sevilla
Soria
Tarragona
Teruel
Toledo
Valencia
Valladolid
Vizcaya
Zamora
Zaragoza
I_P = 2

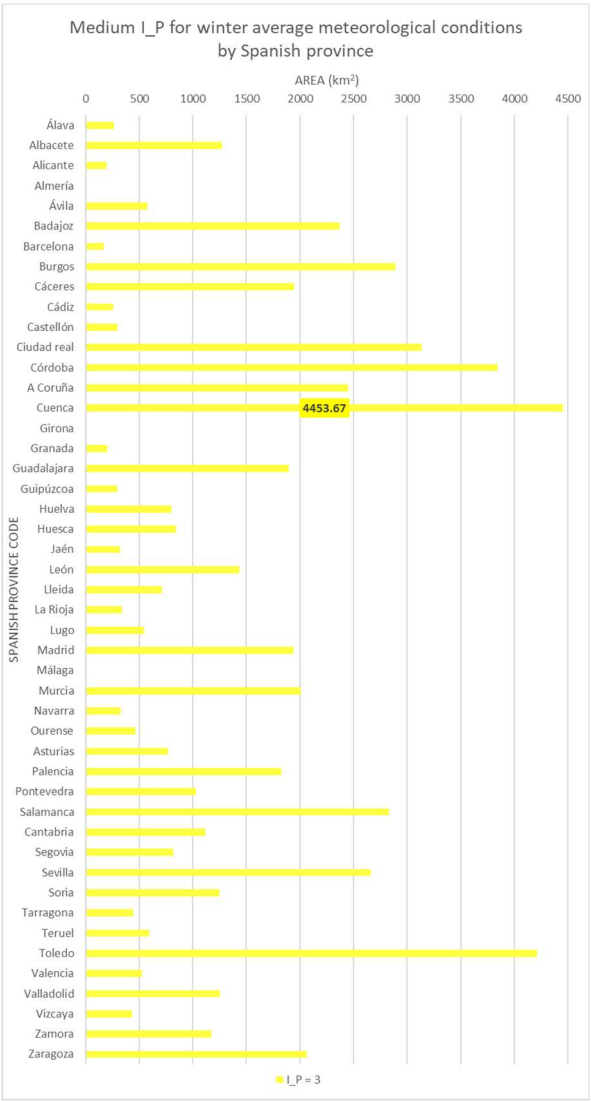
Medium I_P for winter average meteorological conditions by Spanish province
AREA (km²)
0
500
1000
1500
2000
2500
3000
3500
4000
4500
SPANISH PROVINCE CODE
Álava
Albacete
Alicante
Almería
Ávila
Badajoz
Barcelona
Burgos
Cáceres
Cádiz
Castellón
Ciudad real
Córdoba
A Coruña
Cuenca
4453.67
Girona
Granada
Guadalajara
Guipúzcoa
Huelva
Huesca
Jaén
León
Lleida
La Rioja
Lugo
Madrid
Málaga
Murcia
Navarra
Ourense
Asturias
Palencia
Pontevedra
Salamanca
Cantabria
Segovia
Sevilla
Soria
Tarragona
Teruel
Toledo
Valencia
Valladolid
Vizcaya
Zamora
Zaragoza
I_P = 3

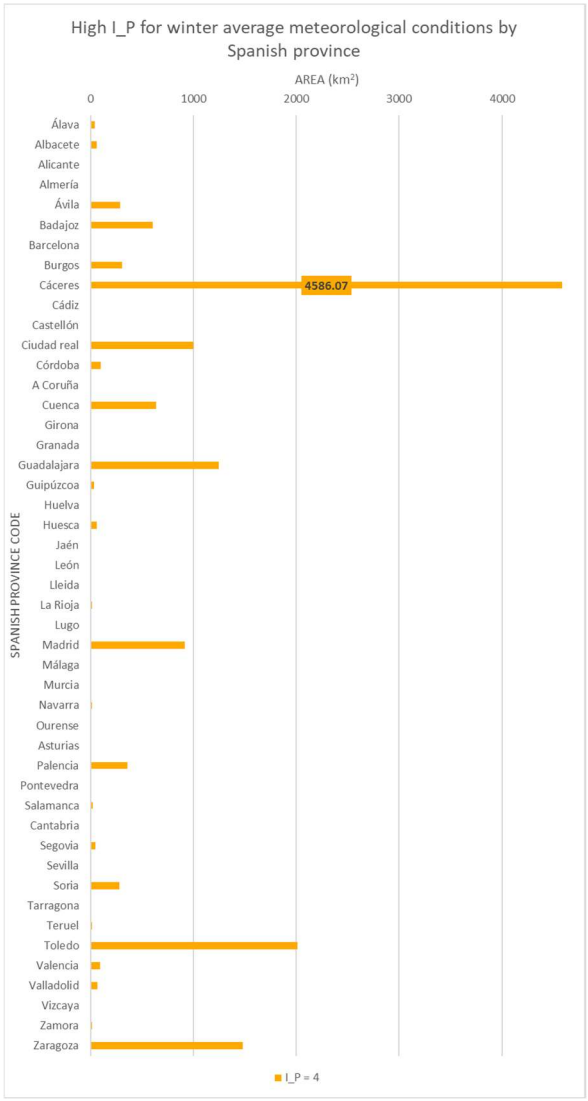
High I_P for winter average meteorological conditions by Spanish province
AREA (km²)
0
1000
2000
3000
4000
SPANISH PROVINCE CODE
Álava
Albacete
Alicante
Almería
Ávila
Badajoz
Barcelona
Burgos
Cáceres
Cádiz
Castellón
Ciudad real
Córdoba
A Coruña
Cuenca
Girona
Granada
Guadalajara
Guipúzcoa
Huelva
Huesca
Jaén
León
Lleida
La Rioja
Lugo
Madrid
Málaga
Murcia
Navarra
Ourense
Asturias
Palencia
Pontevedra
Salamanca
Cantabria
Segovia
Sevilla
Soria
Tarragona
Teruel
Toledo
Valencia
Valladolid
Vizcaya
Zamora
Zaragoza
4586.07
I_P = 4

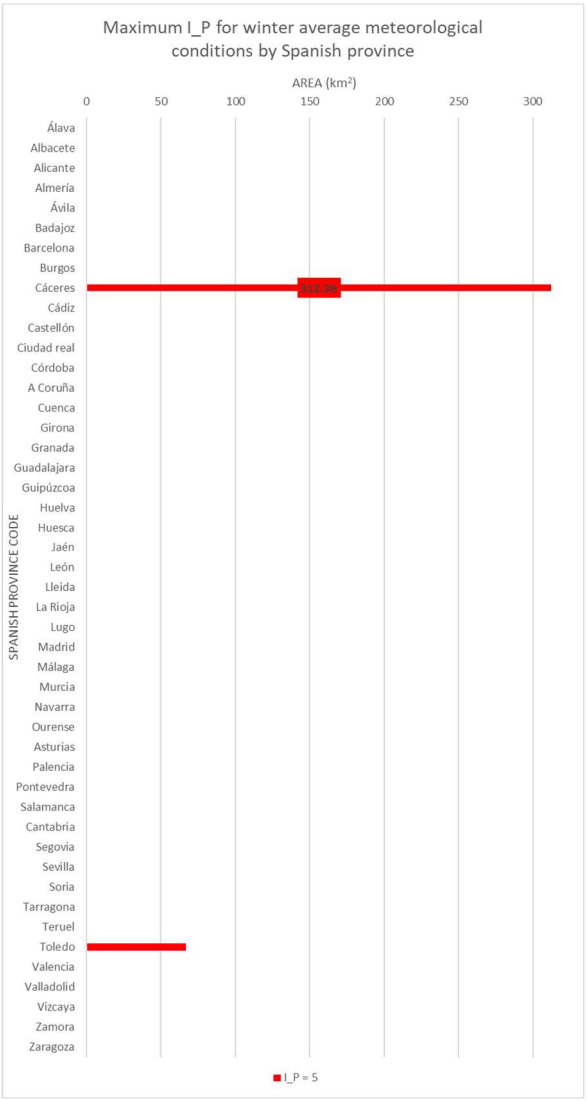
Maximum I_P for winter average meteorological conditions by Spanish province
AREA (km²)
0
50
100
150
200
250
300
SPANISH PROVINCE CODE
Álava
Albacete
Alicante
Almería
Ávila
Badajoz
Barcelona
Burgos
Cáceres
Cádiz
Castellón
Ciudad real
Córdoba
A Coruña
Cuenca
Girona
Granada
Guadalajara
Guipúzcoa
Huelva
Huesca
Jaén
León
Lleida
La Rioja
Lugo
Madrid
Málaga
Murcia
Navarra
Ourense
Asturias
Palencia
Pontevedra
Salamanca
Cantabria
Segovia
Sevilla
Soria
Tarragona
Teruel
Toledo
Valencia
Valladolid
Vizcaya
Zamora
Zaragoza
I_P = 5

Peninsular Spain Province	Province Code	Surface percentage by I_P for winter average meteorological conditions in the agricultural areas, in each province (%)				
		I_P = 1	I_P = 2	I_P = 3	I_P = 4	I_P = 5
Álava	1	3.39	70.11	22.88	3.61	
Albacete	2	0.91	83.38	15.03	0.68	
Alicante	3	32.78	59.44	7.77		
Almería	4	57.23	42.77			
Ávila	5	5.11	62.51	21.71	10.67	
Badajoz	6	1.90	77.54	16.37	4.19	
Barcelona	8	31.76	59.37	8.87		
Burgos	9	1.27	53.92	40.52	4.29	
Cáceres	10	4.99	19.68	21.39	50.49	3.44
Cádiz	11	64.17	29.87	5.96		
Castellón	12	31.39	51.95	16.66		
Ciudad real	13	0.07	63.47	27.63	8.83	
Córdoba	14	20.02	40.83	38.20	0.94	
A Coruña	15		6.83	93.17		
Cuenca	16	0.48	40.44	51.69	7.39	
Girona	17	97.36	2.64			
Granada	18	50.36	46.45	3.19		
Guadalajara	19		20.48	48.01	31.51	
Guipúzcoa	20		20.79	71.85	7.36	
Huelva	21	6.91	72.77	20.21	0.12	
Huesca	22	15.70	69.48	13.82	0.99	
Jaén	23	12.06	83.83	4.11		
León	24	1.32	69.30	29.38		
Lleida	25	14.32	70.49	15.18		
La Rioja	26	0.88	79.91	18.45	0.75	
Lugo	27	0.20	83.11	16.68		
Madrid	28		1.89	66.68	31.43	
Málaga	29	81.97	18.02	0.01		
Murcia	30	19.07	47.47	33.46		
Navarra	31	0.08	92.10	7.58	0.24	
Ourense	32	10.90	58.45	30.66		
Asturias	33	6.82	63.74	29.44		
Palencia	34		59.80	33.61	6.59	
Pontevedra	36		19.49	80.51		
Salamanca	37	0.86	55.30	43.56	0.29	
Cantabria	39	0.11	25.60	74.29		
Segovia	40	0.36	73.78	24.52	1.34	
Sevilla	41	30.36	44.43	25.21		
Soria	42	0.05	63.20	29.99	6.75	
Tarragona	43	35.67	48.44	15.89		
Teruel	44	19.16	69.40	11.14	0.29	
Toledo	45		36.19	42.73	20.40	0.68
Valencia	46	14.76	70.29	12.74	2.22	
Valladolid	47	0.41	79.19	19.41	1.00	
Vizcaya	48		9.02	89.23	1.75	
Zamora	49		78.96	20.83	0.21	
Zaragoza	50	1.61	62.60	20.83	14.96	

Blank cells mean no affected surface.

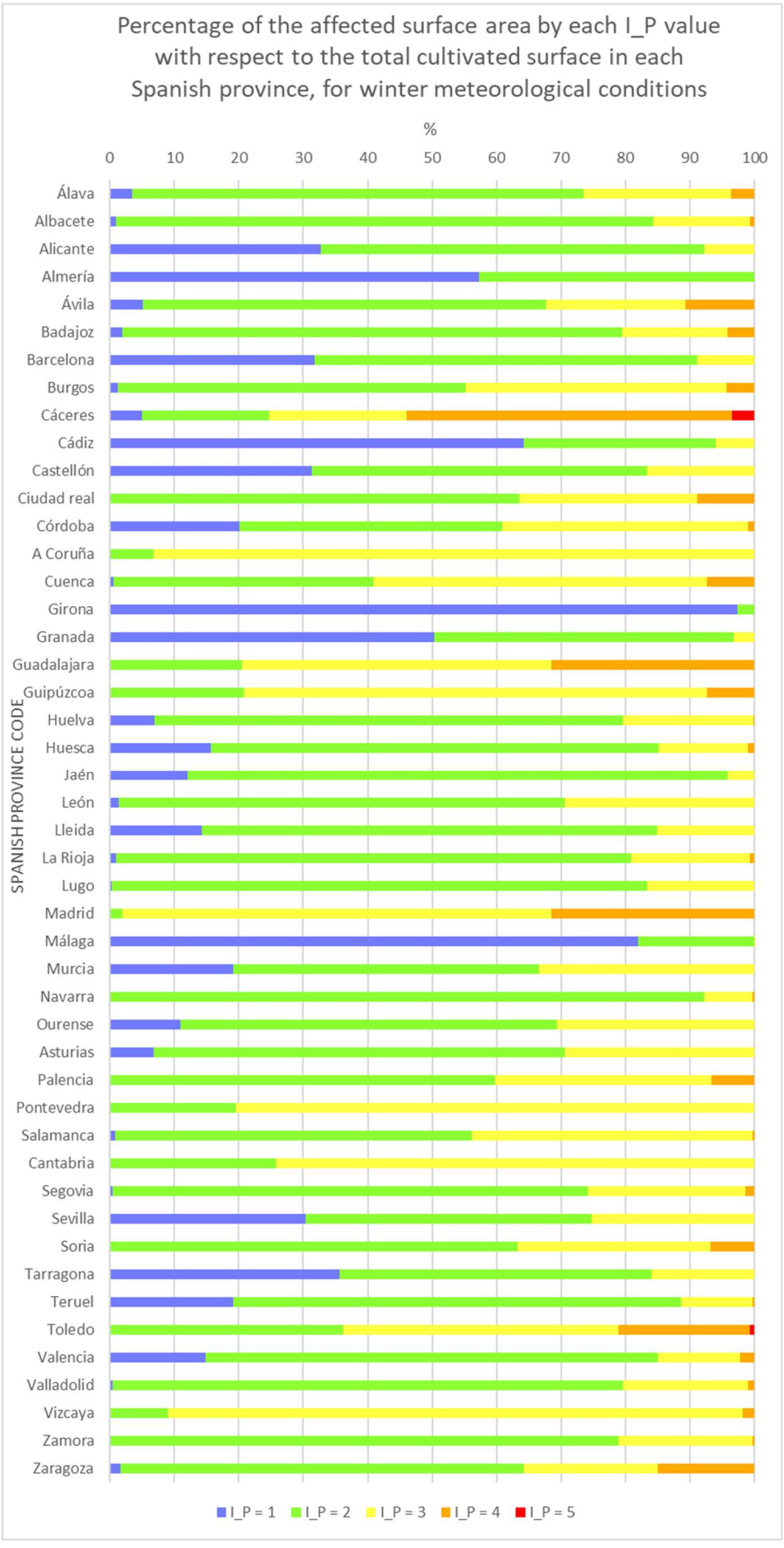
Percentage of the affected surface area by each I_P value with respect to the total cultivated surface in each Spanish province, for winter meteorological conditions
%
0
10
20
30
40
50
60
70
80
90
100
SPANISH PROVINCE CODE
Álava
Albacete
Alicante
Almería
Ávila
Badajoz
Barcelona
Burgos
Cáceres
Cádiz
Castellón
Ciudad real
Córdoba
A Coruña
Cuenca
Girona
Granada
Guadalajara
Guipúzcoa
Huelva
Huesca
Jaén
León
Lleida
La Rioja
Lugo
Madrid
Málaga
Murcia
Navarra
Ourense
Asturias
Palencia
Pontevedra
Salamanca
Cantabria
Segovia
Sevilla
Soria
Tarragona
Teruel
Toledo
Valencia
Valladolid
Vizcaya
Zamora
Zaragoza
I_P = 1
I_P = 2
I_P = 3
I_P = 4
I_P = 5

Peninsular Spain Province	Province Code	Surface percentage by I_P for winter average meteorological conditions in the agricultural areas, with respect all the cultivated surface (%)				
		I_P = 1	I_P = 2	I_P = 3	I_P = 4	I_P = 5
Álava	1	0.017	0.346	0.113	0.018	
Albacete	2	0.033	3.038	0.547	0.025	
Alicante	3	0.352	0.638	0.083		
Almería	4	0.707	0.529			
Ávila	5	0.058	0.716	0.249	0.122	
Badajoz	6	0.118	4.838	1.021	0.261	
Barcelona	8	0.262	0.489	0.073		
Burgos	9	0.039	1.658	1.246	0.132	
Cáceres	10	0.195	0.770	0.837	1.976	0.135
Cádiz	11	1.195	0.556	0.111		
Castellón	12	0.240	0.398	0.128		
Ciudad real	13	0.004	3.104	1.351	0.432	
Córdoba	14	0.868	1.770	1.656	0.041	
A Coruña	15		0.077	1.055		
Cuenca	16	0.018	1.501	1.919	0.274	
Girona	17	0.570	0.015			
Granada	18	1.382	1.275	0.088		
Guadalajara	19		0.348	0.816	0.536	
Guipúzcoa	20		0.037	0.126	0.013	
Huelva	21	0.118	1.245	0.346	0.002	
Huesca	22	0.412	1.823	0.363	0.026	
Jaén	23	0.407	2.827	0.139		
León	24	0.028	1.460	0.619		
Lleida	25	0.289	1.420	0.306		
La Rioja	26	0.007	0.631	0.146	0.006	
Lugo	27	0.003	1.168	0.234		
Madrid	28		0.024	0.835	0.394	
Málaga	29	1.324	0.291			
Murcia	30	0.492	1.225	0.864		
Navarra	31	0.002	1.722	0.142	0.004	
Ourense	32	0.071	0.382	0.200		
Asturias	33	0.077	0.715	0.330		
Palencia	34		1.402	0.788	0.155	
Pontevedra	36		0.107	0.442		
Salamanca	37	0.024	1.548	1.219	0.008	
Cantabria	39	0.001	0.166	0.481		
Segovia	40	0.005	1.062	0.353	0.019	
Sevilla	41	1.379	2.018	1.145		
Soria	42	0.001	1.130	0.536	0.121	
Tarragona	43	0.432	0.587	0.193		
Teruel	44	0.443	1.604	0.257	0.007	
Toledo	45		1.536	1.813	0.865	0.029
Valencia	46	0.263	1.250	0.227	0.040	
Valladolid	47	0.011	2.206	0.541	0.028	
Vizcaya	48		0.019	0.187	0.004	
Zamora	49		1.912	0.504	0.005	
Zaragoza	50	0.069	2.669	0.888	0.638	

Blank cells mean no affected surface.

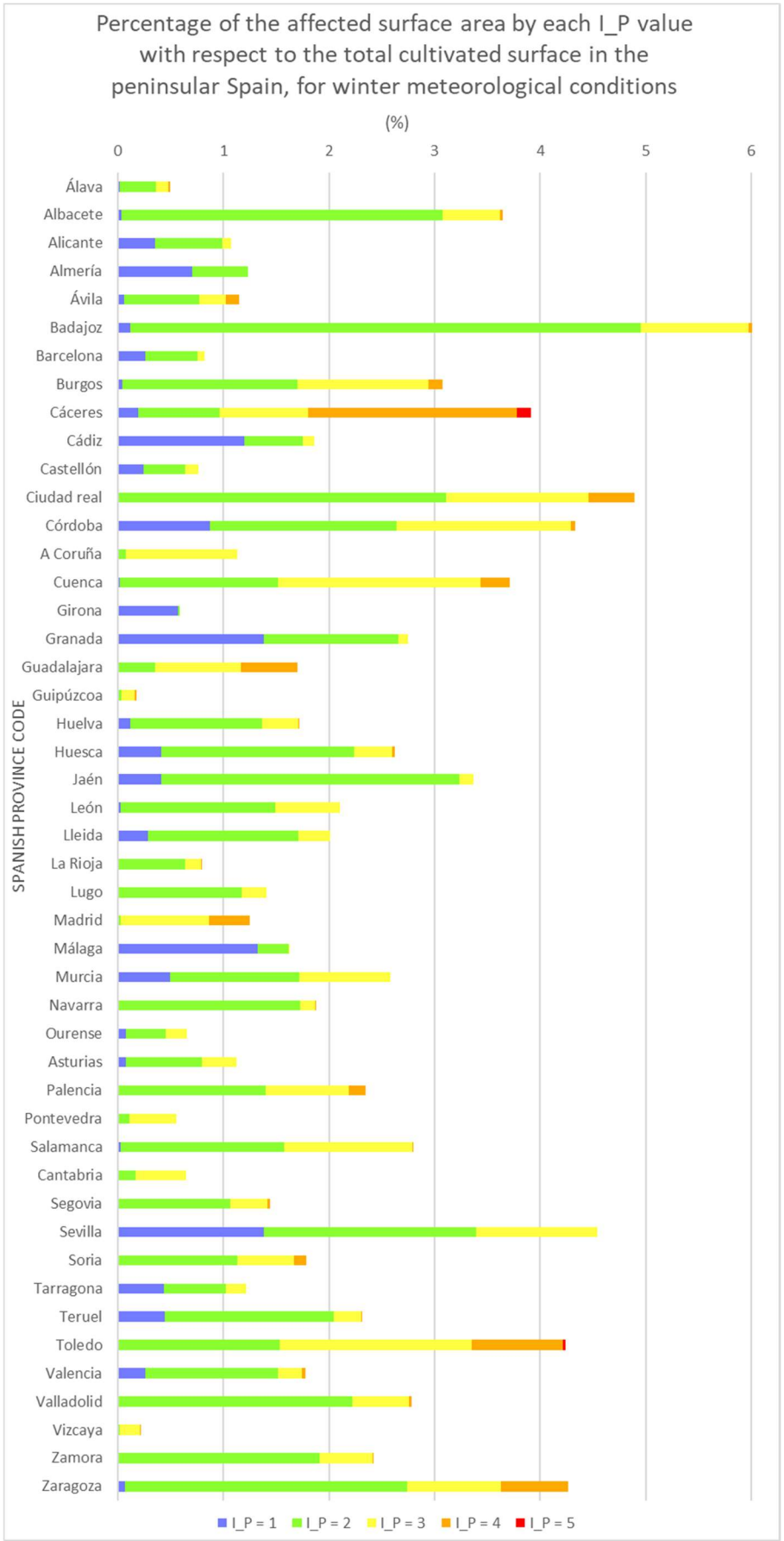
Percentage of the affected surface area by each I_P value with respect to the total cultivated surface in the peninsular Spain, for winter meteorological conditions
(%)
0
1
2
3
4
5
6
SPANISH PROVINCE CODE
Álava
Albacete
Alicante
Almería
Ávila
Badajoz
Barcelona
Burgos
Cáceres
Cádiz
Castellón
Ciudad real
Córdoba
A Coruña
Cuenca
Girona
Granada
Guadalajara
Guipúzcoa
Huelva
Huesca
Jaén
León
Lleida
La Rioja
Lugo
Madrid
Málaga
Murcia
Navarra
Ourense
Asturias
Palencia
Pontevedra
Salamanca
Cantabria
Segovia
Sevilla
Soria
Tarragona
Teruel
Toledo
Valencia
Valladolid
Vizcaya
Zamora
Zaragoza
I_P = 1
I_P = 2
I_P = 3
I_P = 4
I_P = 5

ANNEXE XIV: SURFACE OF THE AGRICULTURAL AREAS INCLUDED IN EACH PRIORITY INDEX CLASS, DISAGGREGATED BY CROP GROUP (IAEA, 2010), CONSIDERING THE AVERAGE METEOROLOGICAL CONDITIONS (ANNUAL AND SEASONAL)

Surface of the crop groups (IAEA, 2010) included in each *Prioritisation Index* class considering the annual meteorological conditions:

Prioritisation Index I_P	Crop group (IAEA, 2010) ID_C	Surface area occupied by the soil crop groups (km^2)
5	grS	310.28
	lfS	102.32
	ceG	20.20
	ocA	3.22
Total 5		**436.01**
4	ceG	16983.32
	grS	10467.76
	ocA	2128.42
	lfS	1520.70
	maG	393.14
	lyL	106.28
	nlF	17.90
	lvS	8.75
Total 4		**31626.27**
3	ceG	39256.09
	wtF	9039.22
	grS	8989.13
	ocA	8429.75
	maG	1943.99
	lfS	1882.27
	lyL	825.18
	nlF	208.65
	rcR	120.66
	lvS	20.90
	tbT	18.69
Total 3		**70734.52**
2	ceG	48541.85
	wtF	43297.33
	grS	9509.00
	maG	5209.19
	ocA	4549.19
	lyL	1581.67
	lfS	621.11
	nlF	530.38
	hpF	168.67
	tbT	118.90
	lvS	4.32
	rcR	0.39
Total 2		**114132.01**
1	wtF	6615.94
	ceG	6024.07
	nlF	642.81
	grS	598.00
	lyL	474.19
	maG	433.71
	ocA	336.53
	hpF	65.20
	lfS	1.77
Total 1		**15192.21**
Total		**232121.01**

Surface of the crop groups (IAEA, 2010) included in each *Prioritisation Index* class considering the spring meteorological conditions:

Prioritisation Index I_P	Crop group (IAEA, 2010) ID_C	Surface area occupied by the soil crop groups (km^2)
5	grS	185.23
	lfS	74.09
	ocA	4.55
	ceG	0.86
Total 5		**264.74**
4	ceG	19411.43
	grS	12153.69
	ocA	4623.93
	lfS	1711.34
	maG	450.47
	lyL	276.85
	nlF	57.71
	lvS	5.74
Total 4		**38691.16**
3	ceG	40037.46
	wtF	10471.00
	ocA	7749.61
	grS	5810.41
	maG	2159.63
	lfS	1656.27
	lyL	1306.38
	nlF	447.67
	rcR	118.72
	tbT	32.05
	lvS	26.24
Total 3		**69815.44**
2	ceG	46203.68
	wtF	42918.20
	grS	10797.63
	maG	4962.65
	ocA	2965.77
	lyL	1249.62
	nlF	812.62
	lfS	685.06
	hpF	168.67
	tbT	105.55
	rcR	2.33
	lvS	1.99
Total 2		**110873.77**
1	wtF	5563.29
	ceG	5172.09
	grS	927.21
	maG	407.27
	lyL	154.46
	ocA	103.24
	nlF	81.72
	hpF	65.20
	lfS	1.41
Total 1		**12475.90**
Total		**232121.01**

Surface of the crop groups (IAEA, 2010) included in each *Prioritisation Index* class considering the summer meteorological conditions:

Prioritisation Index I_P	Crop group (IAEA, 2010) ID_C	Surface area occupied by the soil crop groups (km^2)
5	grS	220.49
	lfS	194.43
	ceG	169.27
	ocA	17.54
Total 5		**601.73**
4	ceG	29878.60
	grS	11315.04
	ocA	3339.51
	lfS	2067.25
	maG	561.26
	lyL	193.34
	nlF	112.92
	rcR	21.40
	lvS	8.75
	wtF	5.64
	tbT	2.68
Total 4		**47506.37**
3	ceG	40980.31
	wtF	16217.00
	grS	6573.00
	ocA	5104.28
	maG	2730.16
	lfS	1152.35
	lyL	454.21
	nlF	237.13
	rcR	99.65
	tbT	32.12
	lvS	20.90
Total 3		**73601.11**
2	wtF	31288.03
	ceG	30919.96
	grS	11172.26
	ocA	6276.96
	maG	4086.22
	lyL	1698.98
	lfS	658.33
	nlF	345.04
	hpF	168.67
	tbT	102.80
	lvS	4.32
Total 2		**86721.57**
1	wtF	11441.81
	ceG	8877.39
	ocA	708.82
	nlF	704.64
	lyL	640.79
	maG	602.39
	grS	593.38
	hpF	65.20
	lfS	55.81
Total 1		**23690.24**
Total		**232121.01**

Surface of the crop groups (IAEA, 2010) included in each *Prioritisation Index* class considering the autumn meteorological conditions:

Prioritisation Index I_P	Crop group (IAEA, 2010) ID_C	Surface area occupied by the soil crop groups (km^2)
5	grS	436.21
	lfS	61.95
	ceG	1.01
	ocA	0.36
Total 5		**499.52**
4	ceG	14332.66
	grS	10382.27
	ocA	1711.00
	lfS	1318.01
	maG	517.33
	lyL	89.10
	lvS	10.94
	nlF	6.12
	wtF	5.66
	rcR	1.27
Total 4		**28374.36**
3	ceG	38378.67
	grS	11084.61
	ocA	8062.07
	wtF	5866.92
	maG	2582.90
	lfS	1849.11
	lyL	744.90
	rcR	119.39
	nlF	103.29
	lvS	19.09
	tbT	11.94
Total 3		**68822.89**
2	ceG	48223.88
	wtF	45006.26
	grS	7164.30
	ocA	4935.28
	maG	4284.45
	lyL	1645.15
	lfS	750.16
	nlF	680.28
	hpF	158.46
	tbT	125.22
	lvS	3.94
	rcR	0.39
Total 2		**112977.77**
1	ceG	9889.29
	wtF	8073.65
	grS	806.79
	ocA	738.39
	nlF	610.05
	maG	595.34
	lyL	508.16
	lfS	148.94
	hpF	75.41
	tbT	0.43
Total 1		**21446.46**
Total		**232121.01**

Surface of the crop groups (IAEA, 2010) included in each *Prioritisation Index* class considering the winter meteorological conditions:

Prioritisation Index I_P	Crop group (IAEA, 2010) ID_C	Surface area occupied by the soil crop groups (km²)
5	grS	312.36
	lfS	57.88
	ceG	8.75
	ocA	0.36
Total 5		**379.34**
4	ceG	6755.03
	grS	5301.43
	ocA	1203.15
	lfS	664.12
	maG	313.25
	lyL	39.73
Total 4		**14276.72**
3	ceG	29006.13
	grS	15987.86
	ocA	7221.01
	wtF	2975.99
	lfS	1981.08
	maG	1259.62
	lyL	715.19
	nlF	53.86
	rcR	16.14
	lvS	13.31
	tbT	4.08
Total 3		**59234.27**

Prioritisation Index I_P	Crop group (IAEA, 2010) ID_C	Surface area occupied by the soil crop groups (km²)
2	ceG	63310.68
	wtF	43291.98
	grS	7522.46
	ocA	6637.59
	maG	5927.48
	lyL	1631.72
	lfS	1208.61
	nlF	634.16
	hpF	168.67
	tbT	114.70
	rcR	104.90
	lvS	20.66
Total 2		**130573.61**
1	wtF	12684.52
	ceG	11744.94
	grS	750.05
	nlF	711.71
	lyL	600.68
	maG	479.68
	ocA	385.00
	lfS	216.47
	hpF	65.20
	tbT	18.82
Total 1		**27657.06**
Total		**232121.01**


VNIVERSITAS COMPLVTENSIS MATRITENSIS


GOBIERNO
DE ESPAÑA
MINISTERIO
DE CIENCIA
E INNOVACIÓN
Ciemat
Centro de Investigaciones
Energéticas, Medioambientales
y Tecnológicas